

Proteomic and Metabolomic
Analysis of Manganese Toxicity and
Tolerance in *Vigna unguiculata* L.

Von der Naturwissenschaftlichen Fakultät
der Gottfried Wilhelm Leibniz Universität Hannover
zur Erlangung des Grades
Doktor der Naturwissenschaften
Dr. rer. nat.
genehmigte Dissertation
von
Dipl.-Ing. agr. Hendrik Führs
geboren am 10. März 1978 in Papenburg

2009

Referent: Prof. Dr. Walter Johannes Horst, Leibniz Universität Hannover

Korreferent: Prof. Dr. Hans-Peter Braun, Leibniz Universität Hannover

Korreferent: Dr. Joachim Kopka, Max-Planck-Institut für Molekulare
Pflanzenphysiologie

Tag der Promotion: 18 Februar 2009

MEINER MUTTER UND MEINEM BRUDER

Zusammenfassung

Mangantoxizität äußert sich in Cowpea (*Vigna unguiculata* L.) in Form von braunen Punkten auf den Blättern, die durch apoplastische Ablagerungen von oxidierten Phenolen und Mn-Oxiden erzeugt werden. Die Reaktionen, die zur Bildung von braunen Punkten führen, werden auf eine erhöhte Aktivität von apoplastischen Peroxidasen (EC 1.11.17) zurückgeführt. Es kann davon ausgegangen werden, dass der Symplast modulierend auf apoplastische Reaktionen, die zur Ausbildung von Mn Toxizität führen, einwirkt. Ziel dieser Arbeit war es mittels proteomischer und metabolomischer Untersuchungen, Mangan- und Silizium induzierte Veränderungen im Apoplasten und Symplasten zu charakterisieren, die ursächlich für Mn-Toleranz oder Mn-Sensitivität sind. Folgende zentrale Ergebnisse wurden erzielt:

(i) Ein erhöhtes Mn-Angebot von nur einem Tag führte bereits zu einer verstärkten Synthese von apoplastischen Peroxidasen, aber auch von Proteinen, die in der Signaltransduktion und der Zellwandmodifizierung beteiligt sind. Ein längerfristig erhöhtes Mn-Angebot führte zu symplastischen proteomischen Veränderungen, die sich in drei physiologische Hauptklassen einteilen lassen: die Photosynthese, eine generelle Stressantwort und Proteinabbau. Die intensivste Reaktion zeigte dabei die Photosynthese durch eine Mn-induzierte State transition, eine reduzierte Elektronentransportrate und eine Runterregulation von Enzymen des Calvin Zyklus. Den Chloroplasten wird daher eine besondere Bedeutung in der Entwicklung von Mn Toxizität zugeschrieben.

(ii) Gelelektrophoretisch aufgetrennte Peroxidase-Isoenzyme zeigten sowohl H₂O₂-verbrauchende Guaiacol-Peroxidase Aktivität als auch H₂O₂-bildende NADH-Peroxidase Aktivität, beide jedoch mit verschiedenen pH Optima. Die Charakterisierung der Substratspezifität der als entscheidend für die apoplastische Ausprägung von Mn-Toxizität angesehenen NADH-Peroxidase Aktivität zeigte, dass spezifische Phenole allein oder in Kombination die spezifische NADH-Peroxidase Aktivität fördern oder hemmen. Es konnten im Blattapoplasten fünf Phenole identifiziert werden, die *in-vitro* die NADH-Peroxidase Aktivität unterschiedlich beeinflusst hatten. Die durch Mn-Überschuß und durch Mn-Toleranz erhöhendes Si-Angebot induzierten Unterschiede im Gehalt an diesen Phenolen im Blattapoplasten unterstützen die Hypothese, dass die apoplastische NADH-Peroxidase Aktivität und die Modulation ihrer Aktivität durch Phenole eine entscheidende Rolle in der Ausprägung von Mn Toxizität spielen. Diese wesentliche Rolle von apoplastischen Peroxidasen und ihrer Modulation durch Phenole bestätigte sich auch für genotypische Mn Toleranz.

(iii) Untersuchungen der Reaktion des Gesamtblatt Metaboloms sowie des apoplastischen wasserlöslichen und ionisch-gebundenen Metaboloms auf Mn-Überschuß mit und ohne Si-Angebot bei zwei unterschiedlich Mn-toleranten Genotypen zeigten deutliche behandlungsbedingte Unterschiede. Ein mit statistischen Verfahren durchgeführtes Screening auf relevante Metabolite erlaubte eine erste Übersicht über die involvierten biochemischen Pfade. Ein veränderter Zuckermetabolismus wurde sowohl auf eine veränderte Photosynthese als auch auf einen erhöhten Bedarf an Energie für eine Stressantwort zurückgeführt. Organische Säuren könnten als Radikalfänger oder auch als Komplexoren für Mn Spezies beginnende Mn Toxizität beschleunigen oder Mn Toleranz fördern. Veränderungen im Aminosäurepool werden hauptsächlich auf eine verminderte Nitratassimilationsleistung aufgrund zyklischen Elektronentransportes durch State transitions zurückgeführt. Der Veränderung von an der Signaltransduktion beteiligten Metaboliten wird eine Rolle in der Stresswahrnehmung und Übermittlung zugeschrieben und damit als primäre Antwort auf ein erhöhtes Mn und Si Angebot betrachtet. Zusammenfassend bestätigten die systembiologischen Untersuchungen sowohl den essentiellen Beitrag des Apoplasten als auch des Symplasten zu Mn-Sensitivität, Si-vermittelter und genotypischer Mn-Toleranz.

Schlagworte: Apoplast, Peroxidase, Silizium

Abstract

Manganese toxicity in cowpea (*Vigna unguiculata* L.) is expressed in form of brown spots on the leaves which are formed by apoplastic depositions of oxidized phenols and Mn-oxides. The reactions leading to the formation of brown spots are ascribed to an increased activity of apoplastic peroxidases (EC 1.11.17). However, it can be assumed that the symplast modulates apoplastic responses which lead to the formation of brown spots. The aim of this study was to characterize by means of proteomic and metabolomic approaches manganese and silicon-induced changes in the apoplast and symplast which are causative for Mn tolerance or Mn sensitivity. The following central results have been obtained:

(i) An increased Mn supply for only one day led to an increased synthesis of apoplastic peroxidases, but also of proteins involved in signal transduction and cell wall modification processes. Longer-termed Mn supply led to symplastic proteomic changes which can be grouped into three physiological main classes: photosynthesis, general stress response, and protein degradation. The most intense reaction was observed in the photosynthesis through Mn-induced state transitions, a reduced electron transport rate, and a down-regulation of enzymes of the Calvin cycle. Therefore, a special importance of the chloroplasts in the development of Mn toxicity is indicated.

(ii) Peroxidase isoenzymes separated by electrophoresis performed both the H₂O₂-consuming guaiacol-peroxidase activity and the H₂O₂-producing NADH-*peroxidase* activity, however, with different pH optima. The characterization of the substrate specificity of the NADH-*peroxidase* activity which is supposed to be decisive for the expression of apoplastic Mn toxicity showed that specific phenols alone or in combination enhance or inhibit the specific NADH-*peroxidase* activity. Five phenols have been identified in the leaf apoplast which had differentially affected the *in-vitro* NADH-*peroxidase* activity. The excess Mn and Mn-tolerance enhancing Si supply induced changes of these phenol contents supported the hypothesis that the apoplastic NADH-*peroxidase* activity and the modulation of its activity by phenols play a decisive role in the expression of Mn toxicity. This essential role of apoplastic peroxidases and their modulation by phenols was also proven for genotypic differences in Mn tolerance.

(iii) Investigations of changes in the bulk-leaf metabolome and the water-soluble and ionically-bound apoplastic metabolome in response to excess Mn with and without Si supply in two genotypes differing in Mn tolerance showed clear treatment-dependent differences. Using statistical methods to screen for relevant metabolites allowed a first overview over involved biochemical pathways. A changed sugar metabolism was not only reduced to changed photosynthesis but also to an increased demand for energy for a stress response. Organic acids as scavengers of oxygen radicals or as chelators of Mn species could accelerate Mn toxicity or confer Mn tolerance. Changes in the amino acid pool have been primarily attributed to a decreased nitrate assimilation due to cyclic electron transport as a consequence of state transitions. The changes of metabolites involved in signal transduction have been attributed a role in stress sensing and response and are, therefore, regarded as primary response to an increased Mn and Si supply.

In sum the “systems biology” approach confirmed the essential contribution not only of the apoplast but also of the symplast to Mn sensitivity, Si-mediated and genotypic Mn tolerance.

Keywords: apoplast, peroxidase, silicon

Contents

ZUSAMMENFASSUNG.....	IV
ABSTRACT.....	V
CONTENTS.....	VI
ABBREVIATIONS	IX
GENERAL INTRODUCTION.....	11
CHAPTER I.....	19
EARLY MANGANESE-TOXICITY RESPONSE IN <i>VIGNA UNGUICULATA</i> L. – A PROTEOMIC AND TRANSCRIPTOMIC STUDY	
ABSTRACT	20
INTRODUCTION	21
MATERIALS AND METHODS	23
Plant material.....	23
Quantification of toxicity symptoms	23
Mineral analysis.....	23
Chlorophyll fluorescence.....	24
Photosynthesis rate	24
Extraction of proteins from leaf.....	24
Isolation of chloroplasts and protein extraction for BN/SDS-PAGE.....	25
2D IEF / SDS-PAGE	25
2D Blue-native / SDS-PAGE	26
Staining of protein gels and spot detection.....	26
Mass spectrometric analysis and data interpretation	26
Generation of subtractive cDNA libraries enriched in transcripts induced by Mn stress	28
Statistical analysis	28
RESULTS	29
Effect of increased Mn supply on the Mn uptake and expression of Mn toxicity symptoms	29
Effect of increased Mn supply on the leaf proteome	30
Identification of proteins affected by increased Mn supply.....	31
Physiological changes linked to increased Mn supply	32
Manganese-induced gene expression	34
DISCUSSION	36
Proteins specifically affected by Mn stress in cowpea	36
Transcripts specifically affected by Mn stress in cowpea	39
Apoplastic versus symplastic Mn-stress response in cowpea.....	40
CHAPTER II.....	41
CHARACTERIZATION OF LEAF APOPLASTIC PEROXIDASES AND METABOLITES IN <i>VIGNA UNGUICULATA</i> IN RESPONSE TO TOXIC MANGANESE SUPPLY AND SILICON	
ABSTRACT	42
INTRODUCTION	43
MATERIALS AND METHODS	45
Plant material.....	45
Extraction of water-soluble and ionically bound apoplastic proteins and metabolites	45
Quantification of toxicity symptoms	46
Manganese analysis	46
Silicon analysis.....	46
Determination of the protein concentration in the AWF and AWF concentrates	46
Determination of specific peroxidase activities in the AWF	47
1D BN-PAGE of apoplastic proteins and POD activity staining.....	47
Electroelution of specific POD isoenzymes for further physiological characterization	48
Determination of the pH optimum of the guaiacol-peroxidase and NADH-peroxidase activity of POD isoenzymes	48
Determination of cofactor specificity for NADH-peroxidase activity of POD isoenzymes.....	49

Determination of changes in NADH- <i>peroxidase</i> activity of POD isoenzymes as affected by combining different phenols with p-coumaric acid	49
Mass spectrometric protein analysis and data interpretation	50
GC-MS-based metabolite profiling	51
Statistical analysis of GC-MS profiles	52
Statistical analysis Mn and Si concentrations and apoplastic enzyme activities	53
RESULTS	54
DISCUSSION	67
Effect of Mn and Si on apoplastic Mn fractions	67
Manganese and Si-induced changes of peroxidase activities	67
Characterization of the identified peroxidases.....	68
The role of pH in controlling apoplastic POD isoenzyme activities.....	69
The role of metabolites in controlling apoplastic POD isoenzyme activities - Metabolite profiling.....	69
The role of phenols in controlling apoplastic NADH- <i>peroxidase</i> activity	70
CHAPTER III	73
CHARACTERIZING GENOTYPIC AND SILICON-ENHANCED MANGANESE TOLERANCE IN COWPEA (<i>VIGNA UNGUICULATA</i> L.) THROUGH APOPLASTIC PEROXIDASE AND LEAF-METABOLOME PROFILING	
ABSTRACT	74
INTRODUCTION	75
MATERIALS AND METHODS	77
Plant material.....	77
Extraction of water-soluble and ionically bound apoplastic proteins	77
Quantification of toxicity symptoms	77
Manganese analysis	77
Protein preparation from AWF	78
1D Blue Native-PAGE of apoplastic proteins and POD activity staining	78
Mass spectrometric protein analysis and data interpretation	78
GC-MS-based metabolite profiling	80
Statistical analysis of GC-MS profiles	81
Statistical analysis except metabolite profiling	81
RESULTS	82
Toxicity status	82
Characterization of the apoplastic protein composition with emphasis on peroxidase isoenzyme profiling of the apoplast.....	82
Metabolite profiling – Independent component analysis.....	86
Metabolite profiling – Treatment effects on individual metabolites.....	91
DISCUSSION	104
Genotypic Mn tolerance	105
Silicon-mediated Mn tolerance.....	109
CHAPTER IV	112
PROTEOMIC CHARACTERIZATION OF THE LEAF APOPLAST OF <i>VIGNA UNGUICULATA</i> L. IN RESPONSE TO SHORT-TERM TOXIC MANGANESE SUPPLY	
ABSTRACT	113
INTRODUCTION	114
MATERIALS AND METHODS	116
Plant material.....	116
Extraction of water-soluble and ionically bound apoplastic proteins and cell wall proteins from leaves ..	116
Manganese analysis	117
Determination of the protein concentration in the AWF and AWF concentrates.....	117
Determination of the phenol concentration in the AWF	117
Determination of specific peroxidase activities in the AWF	118
Preparation of AWF proteins for IEF/SDS-PAGE	118
2D IEF / SDS-PAGE	119
Staining of protein gels and spot detection.....	119
Mass spectrometric protein analysis and data interpretation	120
Statistical analysis	121
RESULTS	122
Characterization of leaf Mn toxicity.....	122
Characterization of the water-soluble and NaCl-extractable apoplastic proteome	123

Isolation of cell walls and investigation of Mn-induced changes in the cell-wall proteome	131
DISCUSSION	134
Manganese uptake	134
Evaluation of the procedures to isolate and characterize apoplastic proteome fractions.....	135
Effect of short-term elevated Mn supply on the apoplastic proteome	137
Apoplastic peroxidases identified by IEF/SDS-PAGE.....	139
GENERAL DISCUSSION	141
THE ROLE OF DIFFERENT POD ISOENZYMES AND THEIR H ₂ O ₂ -PRODUCING NADH- <i>PEROXIDASE</i> ACTIVITY AS MODULATED BY PH AND PHENOLS	141
PHOTOSYNTHESIS IS IMPAIRED BY MN STRESS.....	143
SILICON-MEDIATED MN TOLERANCE AND GENETICALLY-BASED MN TOLERANCE.....	144
EARLY MN TOXICITY RESPONSES IN THE APOPLAST SUGGEST MN-INDUCED CHANGES IN SIGNAL PERCEPTION/SIGNAL TRANSDUCTION AND DEVELOPMENT	145
COMBINING PROTEOMIC AND METABOLOMIC DATA TO UNRAVEL A SEQUENCE OF EVENTS LEADING TO MN TOXICITY, GENOTYPIC AND SI-MEDIATED MN TOLERANCE	146
OUTLOOK	150
THE APOPLAST	150
THE SYMPLAST.....	151
DIFFERENT MECHANISMS OF MN TOLERANCE.....	151
REFERENCES	152
PROTEOMIC AND METABOLOMIC ANALYSIS OF MANGANESE TOXICITY AND TOLERANCE IN <i>VIGNA UNGUICULATA</i> : SUPPLEMENTARY MATERIAL.....	166
SUPPLEMENTARY MATERIAL FOR CHAPTER I.....	167
SUPPLEMENTARY MATERIAL FOR CHAPTER II.....	177
SUPPLEMENTARY MATERIAL FOR CHAPTER III	184
SUPPLEMENTARY MATERIAL FOR CHAPTER IV	247
DANKE	255
LEBENS LAUF	256

Abbreviations

1D	one-dimensional
2D	two-dimensional
AsA	ascorbic acid
AA	amino acid
APX	ascorbate peroxidase
ATP	adenosine-5'-triphosphate
AWF _{H₂O}	apoplastic washing fluid extracted with dH ₂ O
AWF _{NaCl}	apoplastic washing fluid extracted with NaCl
Bis-Tris	1,3-bis(tris(hydroxymethyl)methylamino)propane
BN	blue native
BP	byproduct
CAX	cation exchanger / transporter
cDNA	complementary DNA
CHAPS	3-[(3-Cholamidopropyl)-dimethylammonio]-1-propane sulfonate
DAB	3,3'-diaminobenzidine
DHA	dehydroascorbic acid
dH ₂ O, ddH ₂ O	demineralised water, double demineralised water
DTT	dithiothreitol
ECA	endoplasmic reticulum-type calcium transporting ATPase
EDTA	ethylenediaminetetraacetic acid
ETR	electron transport / transfer rate
GC-MS	gas chromatography - mass spectrometry
Gen	genotype
h	hour(s)
HPLC	high performance liquid chromatography
HR	hypersensitive response
IC	independent component
ICA	independent component analyses
ICP-OES	inductive-coupled plasma optical emission spectroscopy
IEF	isoelectric focussing
IPG	immobilized pH gradient
kDa	kilodalton
LHC	light harvesting complex
MDH	malate dehydrogenase
MDHAR	monodehydroascorbate reductase
Mn	manganese
MTP	metal transporter
MS	mass spectrometry
MWCO	molecular weight cut off

NADH	nicotineamide adenine dinucleotide
<i>n</i> LC-MS/MS	nano-liquid chromatography-mass spectrometry/mass spectrometry
NBT	nitro blue tetrazolium
n.s.	not significant
OEC	oxygen evolving complex
OEE	oxygen evolving enhancer protein
PAGE	polyacrylamide gel electrophoresis
PAR	photosynthetic active radiation
PCA	principal component analyses
POD	peroxidase
PR	pathogenesis-related
RP	reverse-phase
RubisCO	Ribulose-1,5-bisphosphate carboxylase/oxygenase
SAR	systemic acquired resistance
SDS	sodium dodecyl sulphate
Si	silicon / silicic acid / H ₄ SiO ₄
SOD	superoxide dismutase
SSH	Suppression Subtractive Hybridization
Tris	Tris (hydroxymethylamino)-methane
(Q)-TOF	(quadrupole orthogonal acceleration) time of flight
TVu	Tropical Vigna unguiculata
v	volume
w	weight

General Introduction

Manganese (Mn) as transition metal may be present in several oxidation states including the most common II (+2), III (+3), IV (+4), VI (+6), and VII (+7). This property makes Mn to an essential element in plants. Manganese is involved in reduction-oxidation (redox) processes including the oxidation of water to hydrogen and oxygen during photosynthesis as part of the oxygen-evolving complex (OEC) of photosystem II (PSII) (Burnell, 1988). Among this essential function, it also forms part of several redox enzymes such as Mn-dependent peroxidases, dehydrogenases, transferases, superoxide dismutases (SODs) etc., and is involved in lignin biosynthesis (Burnell, 1988 and citations therein). Mn^{2+} was also shown to substitute Mg^{2+} as co-factor in plant cells particularly considering the RubisCO activity (Jordan and Ogren, 1981).

The mean soil Mn concentration is 600 mg kg^{-1} , but soil Mn concentrations vary greatly depending on the parent material and the pedogenesis, and range from $200 - 3000 \text{ mg kg}^{-1}$ (Mortvedt and Cunningham, 1971). In the soil, Mn exists mainly in the oxidation states II, III, and IV. Mn^{II} is the form in the soil solution, which is also the uptake form by plants. In their work with legumes Morris and Pierre (1949) cited soil solution concentrations of Mn up to 50 mg l^{-1} . Several conditions can lead to increased soil Mn plant availability among them reducing conditions and low pH (El-Jaoual and Cox, 1998). In addition, sterilization of substrates in horticulture can lead to increased Mn availability, since this process removes Mn-oxidizing bacteria from the substrate (Sonneveldt and Voogt, 1975).

Increased plant Mn availability may lead to Mn toxicity in plants which is often accompanied by typical Mn toxicity symptoms. Particularly in cowpea (*Vigna unguiculata* L., Fig. 1) and common bean (*Phaseolus vulgaris* L.) the formation of brown spots spreading over the whole leaf, followed by chlorosis and leaf shedding finally leading to dramatic yield decline has been described. But also Mn-induced Ca^{2+} deficiency particularly in soybean (*Glycine max*), the so-called “crinkled leaf” syndrome, and Mn-induced physiological Fe deficiency have been observed and are mostly regarded as secondary symptoms (Morris and Pierre, 1949; Horst and Marschner, 1978b; Horst, 1983; Heenan and Carter, 1975, 1977).

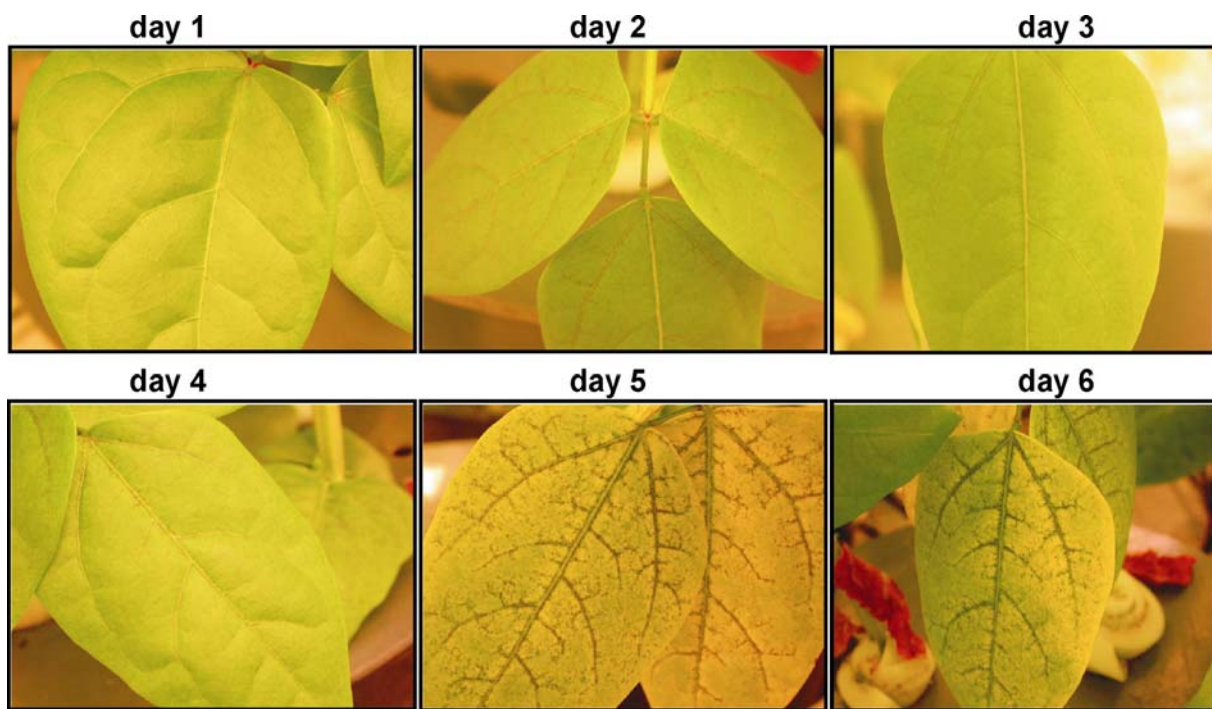


Fig. 1: Images of the time course of the development of Mn toxicity symptoms on the oldest trifoliate leaf of the Mn-sensitive cowpea cultivar TVu 91. After 14 d of preculture plants received 50 μM Mn for one to six days. Typical toxicity symptoms in form of distinct brown spots already start after 2 days of elevated Mn supply. After five days leaves show considerable chlorosis.

Worldwide Mn toxicity is a major factor limiting plant production, particularly on soils of the tropics and subtropics where naturally occurring soil conditions increase the Mn availability and increasing the soil pH by liming to reduce plant Mn availability is often not economic (Horst, 1980). Therefore, exploring biochemical pathways leading to Mn toxicity and/or tolerance particularly in crop plants may facilitate breeding programs for plant genotypes with increased yields under excess Mn concentrations in the soil.

Manganese resistance and sensitivity varies greatly between plant species (Foy et al., 1978). Based on own results (not shown) rice was able to tolerate 10 to 100-fold higher Mn tissue concentrations compared with barley. Even between cultivars within species great differences in Mn resistance have been observed. This is particularly the case for cowpea (Horst, 1982), common bean (González and Lynch, 1999; Heenan and Carter, 1975) and soybean (Morris and Pierre, 1949). The mechanisms of Mn resistance are poorly understood so far particularly because Mn resistance or Mn sensitivity may be based on different physiological responses to excess Mn depending on plant species. The present knowledge implies that several mechanisms may contribute to Mn resistance (El-Jaoual and Cox, 1998): (i) restricted absorption, (ii) restricted translocation of Mn to the shoot, (iii) tolerance of high Mn levels in the plant tissue, so-called tissue tolerance, for example through Mn chelation and, therefore,

detoxification, and/or transport into physiologically inert cell compartments and/or prevention of Mn excess-induced oxidative stress.

In cowpea, but also in common bean, soybean and particularly rice, a restricted absorption can be excluded since Mn treatments increased the Mn tissue concentrations in leaves. For cowpea it has been shown that Mn-tolerant cultivars take up even more Mn than sensitive cultivars (Horst, 1982, see also Chapters 1 and 3 of this thesis). Moreover, the second listed tolerance mechanism, restricted translocation to the shoot, can be neglected for most plants, too (Horst, 1988). One important way to reduce metal toxicities in the plant tissue is the detoxification by chelation. For non-essential metals like Cd detoxification by phytochelatins has been extensively studied (Rauser, 1995), but the chelating power for Mn is quite low. One additional possible mechanism is the chelation of Mn^{2+} by other organic compounds, most likely organic acids. However, in comparative studies of two cowpea cultivars greatly differing in Mn tolerance Maier (1997) concluded that chelation of Mn by organic acids only partly contributes to increased Mn tolerance.

By using forward and reverse genetic approaches, several transporters have been identified that could confer Mn tolerance to plants through internal sequestration into the vacuole, the ER, and the Golgi apparatus (Peiter et al., 2007; Delhaize et al., 2003, 2007; Hirschi et al., 2000; Wu et al., 2002). These transporters belong to the cation/ H^+ antiporters, natural resistance-associated macrophage protein (Nramp) transporters, zinc/iron-regulated transporter (ZRT/IRT1) related protein (ZIP) transporters, the cation diffusion facilitator (CDF) transporter family, and P-type ATPases (Pittman, 2005) mostly lacking specificity for Mn. One specific metal transporter, the MTP11 cation diffusion facilitator with high specificity for Mn, was located to a Golgi-like compartment (Peiter et al., 2007). The authors, therefore, supposed the secretory pathway to be involved in Mn tolerance processes. Very recently Li et al. (2008) provided evidence for a post-Golgi localization of a Ca^{2+}/Mn^{2+} pump that conferred Mn tolerance. Since the secretory pathway might finally lead to the exclusion from the symplast and transport into the apoplast, plants have to cope with high apoplastic Mn concentrations. Indeed, increased apoplastic Mn concentrations due to elevated Mn supply have been described for cowpea (Fecht-Christoffers et al., 2003b). However, in cowpea the Mn distribution in different cell compartments such as the vacuole and the apoplast did not show differences in the distribution of Mn between cultivars with contrasting Mn tolerance (Maier, 1997).

The fact that Mn forms part of the Mn toxicity symptoms, the characteristic brown spots in the apoplast of the leaf epidermis, led to further investigations on the role of the apoplast. Usually, apoplastic Mn is an essential factor for plant growth and developmental processes

since it plays a key role for example as co-factor in lignin formation (Halliwell, 1978). On the other hand, increased apoplastic Mn^{2+} concentrations, either from apoplastic uptake mechanisms or from the secretion into the apoplast via the secretory system of the symplast (Peiter et al., 2007; Li et al., 2008), can lead to several detrimental effects in the apoplast like lipid peroxidation and, therefore, cell desintegration. This and the brown spots first appearing on the leaves consisting of oxidized Mn and oxidized phenolic compounds (Wissemeier and Horst, 1992) led to the conclusion that the oxidation of Mn^{2+} and phenols mediated by apoplastic peroxidases (PODs) could be a key reaction leading to Mn toxicity (Horst, 1988; Fecht-Christoffers et al., 2006). Following studies focusing on apoplastic responses to increased Mn supply in cowpea have therefore been published (Fecht-Christoffers et al., 2003a, 2003b, 2005, 2006, 2007).

Fecht-Christoffers et al. (2003a, b) showed that long-term Mn toxicity response included the secretion of typically stress-induced proteins like pathogenesis-related (PR-) proteins, thaumatin-like proteins and peroxidases (PODs). Moreover, they provided evidence for the decisive involvement of the PODs in the development of Mn toxicity. On the proteome level only a Mn-sensitive cowpea cultivar showed increased abundance of so-called class III PODs after additional Mn application. This was accompanied by increased POD activities in the so-called Apoplastic Washing Fluid (AWF), namely the H_2O_2 -producing NADH-*peroxidase* activity and the H_2O_2 -consuming guaiacol-*peroxidase* activity. Both activities were already described for class III peroxidases in the pioneering work of Halliwell (1978). The multigenic family of class III apoplastic PODs (Passardi et al., 2004, EC 1.11.17) has several developmental functions during plant growth and development (Passardi et al., 2005). Numerous factors like pH (Bolwell et al., 1995, 2001; Pignocchi and Foyer, 2003), phenols as co-factors (Gross et al., 1977; Halliwell, 1978; Fecht-Christoffers et al., 2006), and Mn^{2+} concentration *in vivo* (Yamazaki and Piette, 1963; Halliwell, 1978) influencing the reaction indicate the complexity of particularly the NADH-*peroxidase* activity. Indeed, in depth investigations of the NADH-*peroxidase* activity using two cowpea genotypes with contrasting Mn tolerance revealed that Mn^{II} and phenols are necessary co-factors for the apoplastic NADH-*peroxidase* activity and, therefore, the development or avoidance of Mn toxicity (Fecht-Christoffers et al., 2006). Moreover, Pignocchi and Foyer (2003) and Pignocchi et al. (2006) pointed to the decisive role of apoplastic ascorbate in the oxidative burst phenomenon induced by various environmental stresses and in the regulation of cell signalling by the control of the apoplastic redox state. However, whereas ascorbate and its oxidized form dehydroascorbate were shown to contribute to Mn tolerance they failed to fully explain genotypic differences in Mn tolerance (Fecht-Christoffers and Horst, 2005).

Summarizing the current view of the role of the leaf apoplast in the development of Mn toxicity, Fecht-Christoffers et al. (2007) proposed the following reaction scheme (Fig. 2 next page): peroxidases are stimulated by elevated Mn concentrations in the leaf AWF leading to the formation of H_2O_2 in the peroxidase-oxidase cycle. H_2O_2 is then consumed by the peroxidase cycle producing phenoxyradicals causing the formation of Mn^{III} . Mn^{III} is instable and disproportionates to Mn^{II} which re-enters the reaction cycle, and Mn^{IV} which is precipitated as $Mn^{IV}O_2$. MnO_2 accumulates together with oxidized phenolic compounds in the cell wall causing the formation of brown spots. Ascorbic acid is oxidized by the H_2O_2 -producing NADH-*peroxidase* activity and the H_2O_2 -consuming guaiacol-*peroxidase* activity. The primary oxidation product of these reactions is monodehydroascorbate (MDHA) which is either regenerated by monodehydroascorbate reductase (MDHAR), or oxidized to dehydroascorbate (DHA), which is then regenerated in the cytoplasm. H_2O_2 in the apoplast might act as a second messenger stimulating a receptor and protein kinases, or Mn^{II} might directly stimulate a signalling pathway by activation of receptors or protein-kinases. Mn may also interact with apoplastic Ca^{2+} which induces a specific “ Ca^{2+} signature” triggering callose synthesis and the alkalization of the apoplast which additionally stimulates NADH-*peroxidase* activity. The induction of a signal cascade may then cause the activation of transcription factors and gene expression coding for PR-like proteins.

However, apoplastic responses to elevated Mn supply so far studied appeared at comparable late stages of Mn toxicity after several days of Mn supply. As supposed by the reaction scheme (Fig. 2) apoplastic responses should be accompanied or should even trigger symplastic responses and / or *vice versa* most probably already after short-term Mn supply. Considering the NADH-*peroxidase* activity that produces several Reactive Oxygen Species (ROS) including superoxide (O_2^-) and hydrogen peroxide (H_2O_2) (Halliwell, 1978, Hauser and Olsen, 1998), an induction of signaling pathways is conceivable (Mittler et al., 2004) also

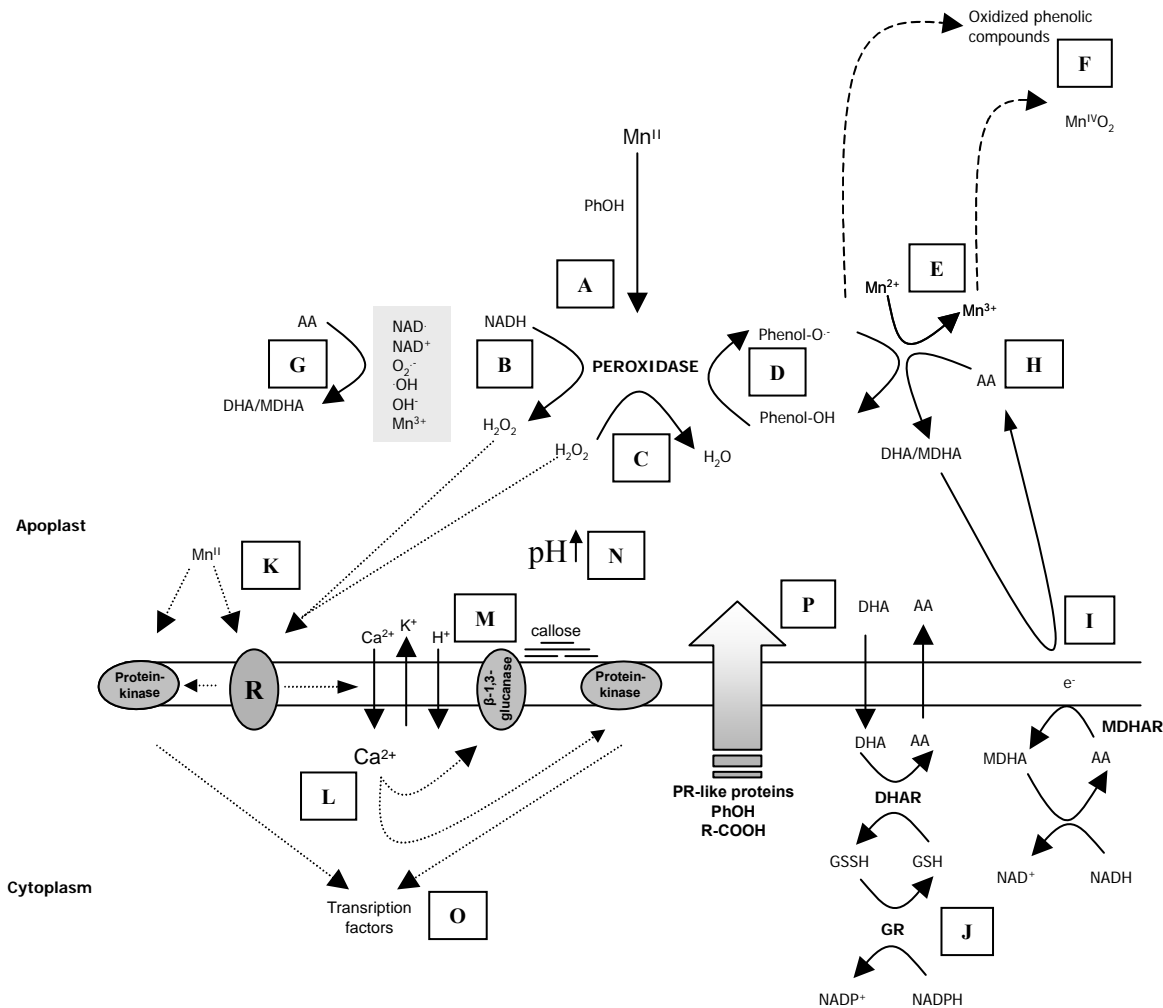


Fig. 2: Proposed reactions in the leaf apoplast of Mn-sensitive tissues of cowpea (*Vigna unguiculata*). Peroxidases (PODs) are directly stimulated by elevated Mn concentrations in the leaf AWF (A). H₂O₂ is formed during the peroxidase-oxidase cycle (B) and consumed by the peroxidatic-peroxidase cycle (C). Intermediates of phenol oxidation (phenoxyradicals) (D) are oxidizing Mn^{II} causing the formation of Mn^{III} (E). Mn^{III} is oxidized to Mn^{IV}O₂, which accumulates together with oxidized phenolic compounds in the cell wall, causing the formation of brown depositions and spots (F). Ascorbic acid is oxidized in the peroxidase-oxidase (G) and in the peroxidatic cycle of POD (H). The primary oxidation product monodehydroascorbate (MDHA) is regenerated by monodehydroascorbate reductase (MDHAR) (I), or oxidized to dehydroascorbate (DHA), which is regenerated in the cytoplasm (J). Elevated concentrations of H₂O₂ in the AWF might act as a second messenger, stimulating a receptor and protein kinases (K), or Mn^{II} might stimulate the signalling pathway by stimulating receptors or protein-kinases (K). The hypothetical induction of a “Ca²⁺ signature” (L) might cause callose synthesis (M) and the alkalization of the apoplast (N), which stimulates NADH-*peroxidase*. The induction of a signal cascade causes the activation of transcription factors (O), indicated by the expression of PR-like proteins (P). Figure from Fecht-Christoffers et al. (2004, 2007).

as part of an integrated signaling response pattern including other signal transduction mechanisms (Brenner et al., 2006). Indeed, several studies on Mn toxicity described Mn effects on symplastic biochemical pathways and compartments. Houtz et al. (1988), Nable et

al. (1988) and Macfie and Taylor (1992) reported reduced chlorophyll contents and reduced CO₂ assimilation rates in tobacco and wheat, respectively. Reduced assimilation rates for wheat were also described by Moroni et al. (1991). This and morphological changes in the chloroplastic ultrastructure have been also described in common bean (González and Lynch, 1997, 1999; González et al., 1998). In contrast, in the highly Mn-tolerant rice Lidon et al. (2004) proposed the chloroplasts as storage compartment for excess Mn. A Mn-mediated impaired photosynthesis could itself produce ROS either contributing to signaling processes or leading to oxidative damage (Mittler et al., 2004).

Silicon (Si) supply has been reported to greatly enhance plant tolerance of abiotic stresses particularly Mn toxicity (Iwasaki et al., 2002a, b; Iwasaki and Matsumara, 1999; Rogalla and Römheld, 2002; Horiguchi, 1988; Horst und Marschner 1978a) but also of biotic stresses (Fauteux et al., 2005, 2006). Therefore, Si is regarded as a beneficial element for most plants (Epstein, 1999), but only a few plant species use it as a plant nutrient (Liang et al., 2007). Liang et al. (2007) listed key mechanisms leading to the Si-mediated suppression of abiotic stresses in higher plants including the stimulation of antioxidant systems, removal of physiological active toxic metal ions by complexation or co-precipitation, modulated uptake processes, and compartmentation of metal ions in plants. In cucumber Si-mediated amelioration of Mn toxicity was thought to take place through inactivation of Mn by stonger binding to the cell wall (Rogalla and Römheld, 2002). Also in cowpea Si supply reduced apoplastic Mn concentrations due to changes in apoplastic Mn-binding properties (Horst et al., 1999). However, this only partly explained Si-enhanced Mn tolerance in cowpea. Instead, a close relationship between Mn toxicity symptoms/guaiacol-POD activities and apoplastic Si rather than apoplastic Mn concentrations was found (Iwasaki et al., 2002b). A more direct involvement of apoplastic Si was proposed for cowpea. One additional factor most likely contributing to increased Mn tolerance conferred by Si is a more homogenous distribution of Mn (Horst and Marschner, 1978a). Also, autoradiographic comparative studies with different cowpea genotypes revealed that a more homogenous Mn distribution in the leaf also could form part of the genetically-based Mn tolerance (Horst, 1983).

During the past three decades intensive studies of Horst et al. on Mn toxicity and Mn tolerance focused on cowpea (*Vigna unguiculata* L. Walp.), which is an important tropical legume for human nutrition due to its high protein contents. Cowpea spreads from Western Africa, lower elevation areas of eastern and southern Africa, to the south-eastern and south-western areas of North America and north-eastern Brazil in South America, India and parts of Middle East, and covers about 7 million ha (Ehlers and Hall, 1997).

Since former studies particularly focused on apoplastic responses to elevated Mn supply at comparable late toxicity events, this work focused on early Mn toxicity stages not only addressing Mn excess-induced apoplastic but also symplastic reactions. For the study of Mn tolerance two genotypes differing in Mn tolerance were compared, and the Mn tolerance-enhancing effect of Si supply was studied. A “systems biology” approach was chosen by using a combination of proteomic, metabolomic and physiological methodologies. The study was divided into four areas:

- (i) The effect of elevated Mn supply on the total water-soluble leaf proteome and the chloroplastic supramolecular organization of two cowpea cultivars differing in Mn tolerance (Chapter 1)
- (ii) Characterization of specific apoplastic peroxidase isoenzymes and their modulation by metabolites in a Mn-sensitive cowpea cultivar in response to Mn and Si supply (Chapter 2)
- (iii) Comparison of the apoplastic peroxidase isoenzyme composition of two cowpea genotypes differing in Mn tolerance and screening for Mn and Si supply-affected metabolites in the bulk-leaf extract and two apoplastic fractions (Chapter 3)
- (iv) Study of the apoplastic proteome after short-term exposure to toxic Mn supply in the Mn-sensitive cowpea cultivar (Chapter 4).

**Early manganese-toxicity response in *Vigna unguiculata* L. – A proteomic
and transcriptomic study**

Hendrik Führs¹, Moritz Hartwig¹, Laura Elisa Buitrago Molina¹, Dimitri Heintz², Alain Van
Dorsselaer², Hans-Peter Braun³ & Walter J. Horst¹

Proteomics (2008), 8, 149-159

¹ Institute for Plant Nutrition, Faculty of Natural Sciences, University of Hannover,
Herrenhaeuser Str.2, 30419 Hannover, Germany

² Laboratoire de Spectrométrie de Masse Bioorganique, Unité Mixte de Recherche 7509, 25
rue Becquerel, F-67087 Strasbourg cedex 2, France

³ Department for Plant Genetics, Faculty of Natural Sciences, University of Hannover,
Herrenhaeuser Str.2, 30419 Hannover, Germany

Abstract

The apoplast is known to play a predominant role in the expression of manganese (Mn) toxicity in cowpea (*Vigna unguiculata* L.) leaves. To unravel early Mn-toxicity responses after 1-3 days Mn treatment also in the leaf symplast, we studied the symplastic reactions induced by Mn in two cultivars differing in Mn tolerance on a total cellular level. Comparative proteome analyses of plants exposed to low or high Mn allowed to identify proteins specifically affected by Mn, particularly in the Mn-sensitive cowpea cultivar. These proteins are involved in CO₂ fixation, stabilization of the manganese cluster of the photosystem II, pathogenesis-response reactions and protein degradation. Chloroplastic proteins important for CO₂ fixation and photosynthesis were of lower abundance upon Mn stress suggesting scavenging of metabolic energy for a specific stress response. Transcriptome analyses supported these findings, but additionally revealed an up-regulation of genes involved in signal transduction only in the Mn-sensitive cultivar. In conclusion, a coordinated interplay of apoplastic and symplastic reactions seems to be important during the Mn-stress response in cowpea.

Introduction

Manganese (Mn) is an essential nutrient for plant growth and development (Burnell, 1988, Marschner 1995). At the same time, high Mn availability is toxic and can limit plant growth (Horst, 1988). This is especially relevant on acidic and imperfectly drained soils of the tropics and subtropics. There is a great inter- and intra-specific variability in Mn resistance (Foy et al., 1978; El-Jaoual and Cox, 1998; Horst, 1980). The cultivar-specific differences in Mn resistance in the tropical legume cowpea are due to a Mn leaf-tissue tolerance as comparable leaf Mn concentrations lead to Mn toxicity in Mn-sensitive but not in Mn-tolerant cultivars (Horst, 1983).

In common bean as well as in cowpea, typical Mn toxicity symptoms start with brown spots on old leaves, followed by chlorosis, necrosis and finally leaf shedding (Horst and Marschner, 1978b; Horst, 1982). These Mn-induced brown spots consist of oxidized Mn and oxidized phenols mainly located in the cell wall of the epidermal layer (Horst and Marschner, 1978b; Wissemeier and Horst, 1992). This and greatly enhanced activities of H₂O₂-producing and H₂O₂-consuming peroxidases suggest that the leaf apoplast is the decisive compartment for the development or avoidance of Mn toxicity in cowpea (Fecht-Christoffers et al., 2003a, 2006). Proteome analyses of the apoplastic washing fluid (AWF) confirmed an enhanced release of peroxidases into the leaf apoplast, but in addition revealed the induction of several other apoplastic stress-response proteins in response to advanced Mn stress (Fecht-Christoffers et al., 2003b). We recently provided evidence suggesting that apoplastic phenols in addition to Mn play a major role in modulating genotypic differences in Mn tolerance (Fecht-Christoffers et al., 2006).

It can be expected that changes in the proteome and metabolome of the leaf apoplast are triggered by molecular changes in the symplast and that such changes would represent a more rapid response to Mn excess. A role of the symplast in the expression of Mn toxicity is also suggested by results in other plant species that the sequestration of Mn in symplastic compartments confers enhanced Mn tolerance. In Arabidopsis, Mn tolerance is mediated by an ER-localized Ca²⁺/Mn²⁺ pump designated ECA1 (Wu et al., 2002). Recently, MTP11 cation diffusion facilitators from Arabidopsis and poplar were shown to confer tolerance to Mn-hypersensitive yeast mutants (Peiter et al., 2007). Promoter-GUS studies indicated a Golgi-based Mn accumulation resulting in Mn tolerance most likely through vesicular trafficking and exocytosis. In the tropical legume *Stylosanthes hamata* the ShMTP1 protein proved to be important for Mn tolerance (Delhaize et al., 2003, 2007). Expressed in

Arabidopsis and yeast this protein was shown to confer Mn tolerance through inner-cellular Mn sequestration. Contradictory results were obtained for the subcellular localization of ShMTP1 in these organisms because it was found in the tonoplast membrane in Arabidopsis but in the ER membrane in yeast. Another cation transporter important for Mn translocation in Arabidopsis is the CAX2 protein. Over-expressed in tobacco this transporter conferred high Mn tolerance (Hirschi et al., 2000). CAX2 was shown to be localized in the tonoplast membrane. Mn accumulation in the vacuole was also reported in cowpea but could not be related to differences in leaf Mn tolerance owing to genotype, silicon nutrition and N form (Horst et al., 1999; Maier, 1997).

There are a number of studies suggesting chloroplasts and photosynthesis as targets of Mn stress. Enrichment of Mn in the chloroplast was reported for common bean (González and Lynch, 1999) and rice (Lidon et al., 2004). In common bean this was accompanied by a decrease of the chlorophyll content and by a reduction of CO₂ assimilation rates (González et al., 1998, González and Lynch, 1997, 1999). Reduced CO₂ assimilation upon Mn stress was also reported for tobacco (Nable et al., 1988; Houtz et al., 1988) and reduced chlorophyll content for wheat (Moroni et al., 1991).

Based on our own results suggesting symplastic reactions triggering apoplastic lesions and reports on symplastic lesions of Mn toxicity we initiated a systematic investigation of Mn excess-induced changes in leaves of two cowpea cultivars differing in Mn tolerance on a cellular level using proteome and transcriptome analyses.

Materials and Methods

Plant material

Cowpea (*Vigna unguiculata* [L.] Walp. cvs TVu 91 and TVu 1987) was grown hydroponically in a growth chamber under controlled environmental conditions at 30/27°C day/night temperature, 75%±5 % relative humidity, and a photon flux density of 150 $\mu\text{mol m}^{-2}\text{s}^{-1}$ photosynthetic active radiation (PAR) at mid-plant height during a 16-h photoperiod. After germination on filter paper in 1 mM CaSO_4 for 7 days, seedlings were transferred into 5 liter pots and supplied with a constantly aerated nutrient solution with the following composition (μM): 1000 $\text{Ca}(\text{NO}_3)_2$, 100 KH_2PO_4 , 375 K_2SO_4 , 325 MgSO_4 , 20 FeEDDHA, 10 NaCl, 8 H_3BO_3 , 0.2 MnSO_4 , 0.2 CuSO_4 , 0.2 ZnSO_4 , 0.05 Na_2MoO_4 . After pre-culture for 14 days, the Mn concentration in the nutrient solution was increased to 50 μM MnSO_4 for 3 days, whereas control plants received 0.2 μM Mn continuously. The nutrient solution was changed two to three times a week to avoid nutrient deficiencies.

Quantification of toxicity symptoms

For the quantification of Mn toxicity symptoms, the density of brown spots was counted on a 1 cm^2 area at the base and tip on the upper side of the second oldest middle trifoliate leaf.

Mineral analysis

Manganese in the bulk-leaf tissue was determined after dry ashing (480°C, 8h) and dissolving the ash in 6 M HCl with 1.5% [w/v] hydroxylammonium chloride and diluted 1:10 [v/v] with water. Measurements were carried out by inductively-coupled plasma optical emission spectroscopy (Spectro Analytical Instruments GmbH, Kleve, Germany).

After isolation of chloroplasts (see below) the Mn content was determined as follows: 500 μl of isolated chloroplasts (0.1 g chloroplasts ml^{-1}) were centrifuged at 15000 g for 5 min. To 500 μl of the supernatant 500 μl 6 M HCl with 1.5% [w/v] hydroxylammonium chloride was added and diluted 1:2 [v/v] with ddH_2O . The pellet was dried at 60°C and then dry-ashed at 480°C over night. The ash was dissolved in 500 μl 6 M HCl with 1.5% [w/v]

hydroxylammonium chloride and diluted 1:4 [v/v] with ddH₂O. Manganese was measured by inductively-coupled plasma optical emission spectroscopy (Spectro Analytical Instruments GmbH, Kleve, Germany).

Chlorophyll fluorescence

Chlorophyll fluorescence of the second oldest middle trifoliolate leaf was determined using a Mini-PAM fluorometer (Waltz, Germany). Measurements were carried out on dark adapted plants using the light induction curve-program: One minute after a first saturation pulse actinic light was turned on and from then every 30 seconds a new saturation pulse was applied over a period of 6.5 minutes. The Yield, ETR, nP, nQ and NPQ values were calculated immediately by the included software and stored. All measurements were repeated four times and evaluated by statistical analyses.

Photosynthesis rate

Photosynthesis rate was measured with four replications on the second oldest middle trifoliolate leaf with the Li-Cor 6400 portable photosynthesis (Li-Cor Inc., Lincoln, NE, USA) system using a CO₂ curve programme with the following sequence: 400, 600, 800, 1000, 400 $\mu\text{mol CO}_2 \cdot \text{mol}^{-1}$ and a flux of 500 μms . Leaves received 1500 $\mu\text{mol PAR} \cdot \text{m}^{-2} \cdot \text{s}^{-1}$. Photosynthesis rate was calculated immediately by the Li-Cor control software and values were submitted to statistical analysis.

Extraction of proteins from leaf

Protein extraction for 2-D gel electrophoresis (2DE) analyses was carried out as outlined by Mihr and Braun (2003) using the second oldest trifoliolate leaf of cowpea plants. Proteins were independently extracted three times from the pooled leaf material of two plants:

Leaf tissue (0.2 g) was ground by mortar and pestle in liquid nitrogen. Homogenized leaf powder was suspended in 750 μl extraction buffer (700 mM sucrose, 500 mM Tris, 50 mM EDTA, 100 mM KCl, and 2% [v/v] mercaptoethanol) and incubated for 10 minutes on ice. Afterwards, an equal volume of water-saturated phenol was added and incubated for another 10 min. The aqueous and organic phases were separated by centrifugation for 10 min at 5,000

g and 4°C. The phenolic phase was re-extracted with extraction buffer and centrifuged once more. Phenol phases were combined, supplemented with 5 volumes of 0.1 M ammonium acetate in methanol and incubated over night at -20°C. After centrifugation at 11,000 g for 3 min at 4°C, precipitated proteins were washed three times with ammonium acetate in methanol and finally with acetone. Extracted proteins were resolved in “rehydration buffer” (see below) for 2DE analysis. Protein concentration of extracts were determined in rehydration buffer using the 2-D Quant Kit[®] (GE Healthcare, Munich, Germany) according to the manufacturer’s instructions.

Isolation of chloroplasts and protein extraction for BN/SDS-PAGE¹

Chloroplasts were isolated according to Heinemeyer et al. (2004) using about 20 g of leaf tissue. Leaf tissue was homogenized in “homogenization buffer” (330 mM mannitol, 30 mM HEPES, 2 mM EDTA, 3 mM MgCl₂ and 0.1 % [w/v] BSA, pH 7.8) using a Waring blender for 3 x 3 seconds. Purification of organelles was based on a differential centrifugation combined with a Percoll density-gradient centrifugation (for details see Heinemeyer et al., 2004). Purified chloroplasts were re-suspended in “homogenization buffer” without BSA at a protein concentration of 15 mg ml⁻¹, frozen in liquid nitrogen and stored at -80°C.

2D IEF / SDS-PAGE

For IEF, the IPGphor system (GE Healthcare, Munich, Germany) and Immobiline DryStrip gels (18 cm) with a nonlinear pH gradient (pH 3-11) were used. About 500 µg protein in “rehydration solution” (8 M urea, 2% [w/v] CHAPS, 0.5% [v/v] carrier ampholyte mixture [IPG buffer, pH 3-11 NL; GE Healthcare], 50 mM dithiothreitol, 12 µl ml⁻¹ DeStreak [GE Healthcare], and a trace of bromphenol blue) was loaded onto individual gel strips. Focussing was done according to Werhahn and Braun (2002). Afterwards, Immobiline DryStrip gels were incubated with equilibration solution (50 mM Tris-Cl [pH 8.8], 6 M urea, 30% [v/v] glycerol, 2% [w/v] SDS, and bromphenol blue) supplemented with (a) 1% [w/v] dithiothreitol and (b) 2.5% [v/w] iodacetamide each for 15 min. Finally, DryStrips were placed horizontally onto second dimension SDS gels and proteins were resolved according to Schagger and von Jagow (1987).

¹ Isolation of chloroplasts was done in collaboration with Prof. Dr. Hans-Peter Braun, Institute of Plant Genetics, Leibniz University Hannover, Herrenhäuser Str. 2, 30419 Hannover

2D Blue-native / SDS-PAGE²

Thylakoid membrane complexes were analysed by two-dimensional Blue-native PAGE (Wittig et al., 2006, Heinemeyer et al., 2007). Thylakoids of chloroplast fractions (about 1 mg protein) were sedimented by centrifugation for 10 minutes at 5000 x g and resuspended in 80 µl “solubilization solution” (30 mM HEPES, pH 7.4, 150 mM potassium acetate, 10% glycerol, 2 mM PMSF and 1.5% [w/v] digitonin [Fluka, Buchs, Switzerland]). Samples were centrifuged for 30 minutes; the supernatants were supplemented with “Coomassie-blue solution” (5% [w/v] Serva Blue G, 750 mM aminocaproic acid) and directly loaded onto the native gel. Gel electrophoresis conditions for the first and second dimensions were as described in Heinemeyer et al. (2007).

Staining of protein gels and spot detection

All protein gels were stained with colloidal Coomassie-blue according to Neuhoff et al. (1985, 1990). Spot detection and the calculation of master gels was carried out using the ImageMaster™ 2D Platinum Software 6.0 (GE Healthcare, Munich, Germany).

Mass spectrometric analysis and data interpretation³

Each SDS-PAGE gel spot was dried under vacuum. In-gel digestion was performed with an automated protein digestion system, MassPREP Station (Micromass, Manchester, UK). The gel slices were washed three times in a mixture containing 25 mM NH₄HCO₃:ACN [1:1, v/v]. The cysteine residues were reduced by 50 µl of 10 mM dithiothreitol at 57°C and alkylated by 50 µl of 55 mM iodoacetamide. After dehydration with acetonitrile, the proteins were cleaved in the gel with 40 µl of 12.5 ng µl⁻¹ of modified porcine trypsin (Promega, Madison, WI, USA) in 25 mM NH₄HCO₃ at room temperature for 14 hours. The resulting tryptic peptides

² 2D Blue-native / SDS-PAGE was done in collaboration with Prof. Dr. Hans-Peter Braun, Institute of Plant Genetics, Leibniz University Hannover, Herrenhäuser Str. 2, 30419 Hannover

³ Mass spectrometric analysis and data interpretation was done in collaborations with Dr. Dimitri Heintz, Institut de Biologie Moléculaire des Plantes (IBMP) CNRS-UPR2357,ULP, 67083 Strasbourg, France, and Prof. Dr. Alain Van Dorsselaer, Laboratoire de Spectrométrie de Masse Bio-Organique, IPHC-DSA, ULP, CNRS, UMR7178; 25 rue Becquerel, 67 087 Strasbourg, France

were extracted with 60% acetonitrile in 5% formic acid, followed by a second extraction with 100% [v/v] acetonitrile.

Nano-LC-MS/MS analysis of the resulting tryptic peptides was performed using a CapLC capillary LC system (Micromass) coupled to a hybrid quadrupole orthogonal acceleration time-of-flight tandem mass spectrometer (Q-TOF II, Micromass). Chromatographic separations were conducted on a Pepmap_ C18 75 μm i.d. x 15 cm length, reverse-phase (RP) capillary column (LC Packings, Sunnyvale, CA, USA) with a flow rate of 200 nl min^{-1} , accomplished by a pre-column split. An external calibration was performed using a 2 pmol l^{-1} GFP ([Glu1]-Fibrinopeptide B) solution. Mass data acquisition was piloted by MassLynx 4 software (Micromass) using automatic switching between MS and MS/MS modes. Classical protein database searches were performed on a local Mascot_ (Matrix Science, London, UK) server. To be accepted for the identification, an error of less than 100 p.p.m. on the parent ion mass was tolerated and the sequences of the peptides were manually checked. One missed cleavage per peptide was allowed and some modifications were taken into account: carbamidomethylation for cysteine, and oxidation for methionine. In addition, the searches were performed without constraining protein Mr and pI, and without any taxonomic specifications. These searches did not always lead to a positive identification since the cowpea (*Vigna unguiculata*) genome has not yet been sequenced. In such cases, the use of a *de novo* sequencing approach was necessary for a successful identification. For this purpose, the interpretation of the MS/MS spectra was performed with the PepSeq tool from the MassLynx 4 (Micromass) software, as well as the PEAKS Studio software (Bioinformatics Solutions, Waterloo, Canada v.3). The resulting peptide sequences were submitted to the BLAST program provided at the EMBL site (<http://dove.embl-heidelberg.de/Blast2/msblast.html>) in order to identify them by homology with proteins present in the databases. We used the MS-BLAST specifically modified PAM30MS scoring matrix, no filter was set and the nrdb95 database was used for the searches as described by Castro et al. (2005). The statistical evaluation of the results and the validation of the matches was performed according to Shevchenko et al. (2001).

Protein identifications by mass spectrometry only were carried for one of the three gel replicates, because gels obviously were very similar. Also, all analyses allowed to unambiguously identify proteins of the expected molecular mass range.

Generation of subtractive cDNA libraries enriched in transcripts induced by Mn stress⁴

The cDNA libraries were constructed by “suppressive subtractive hybridization” (SSH) (Diatchenko et al., 1996) as outlined in Wulf et al. (2003):

After 7 days of germination in 1 mM CaSO₄ solution cowpea plants of the Mn-sensitive cultivar TVu 91 and the Mn-tolerant cultivar TVu 1987 were transferred into 5 liter plastic pots containing nutrient solution (composition see “Plant material” section). To avoid shading and interactions between individual plants only one plant per pot was cultivated. The nutrient solution was changed every two to three days to prevent nutrient deficiencies. After 14 days of preculture under controlled environmental conditions in a growth chamber the Mn supply was either increased to 50 µM Mn for three days or kept at 0.2 µM Mn continuously. The second oldest trifoliolate leaves from individual plants were harvested, petioles were removed, and remaining material was directly frozen in liquid nitrogen. Samples from five individual plants were pooled and homogenized with mortar and pestle under permanent supply of liquid nitrogen. Leaf powder was transferred into Eppendorf tubes and stored at -80°C until further analysis.

RNA was extracted with the LiCl method as described earlier (Franken und Gnädinger, 1994). Total RNA (3 µg) was used to produce cDNA using the SMART cDNA synthesis kit (Clontech, Palo Alto, CA). This cDNA was used to perform an SSH using the PCR select cDNA subtractive kit (Clontech). Amplification products were cloned into the pGEM-Teasy vector (Promega, Madison, WI, USA). Selected clones were analysed by DNA sequencing.

Statistical analysis

Statistical analysis, unless otherwise mentioned, was carried out using the SAS software package (Release v8.0, SAS Institute, Cary, NC, USA). Results from analysis of variance are given according to their level of significance as ***, **, * and ⁺ for $p < 0.001$, 0.01, 0.05, and 0.1, respectively.

⁴ Generation of subtractive cDNA libraries enriched in transcripts induced by Mn stress was done in collaboration with Prof. Dr. Hans-Peter Braun, Institute of Plant Genetics, Leibniz University Hannover, Herrenhäuser Str. 2, 30419 Hannover

Results

Effect of increased Mn supply on the Mn uptake and expression of Mn toxicity symptoms

Increasing the Mn supply from 0.2 μM (control) to 50 μM (Mn treatment) for three days led to an about 10-fold increase of Mn leaf-tissue concentrations in both investigated cowpea cultivars (Fig. 1). The leaf Mn concentration of the Mn-tolerant cultivar TVu 1987 was 30% higher than of the Mn-sensitive cultivar TVu 91. Nevertheless, Mn toxicity symptoms (brown spots) were only visible on the leaves of the Mn-sensitive cultivar. The toxicity level was moderate as it was in the range of twenty spots per cm^{-2} (for a detailed evaluation of Mn toxicity symptoms see Fecht-Christoffers et al., 2003b) The chloroplast Mn content, which was estimated to account for about 2% of the bulk-leaf Mn after elevated Mn supply, did not show differences neither between the Mn treatments nor between cultivars ($0.85 \mu\text{mol Mn [g chloroplast dry matter]}^{-1}$ corresponding to $0.14 \mu\text{mol Mn [g chloroplast fresh matter]}^{-1}$).

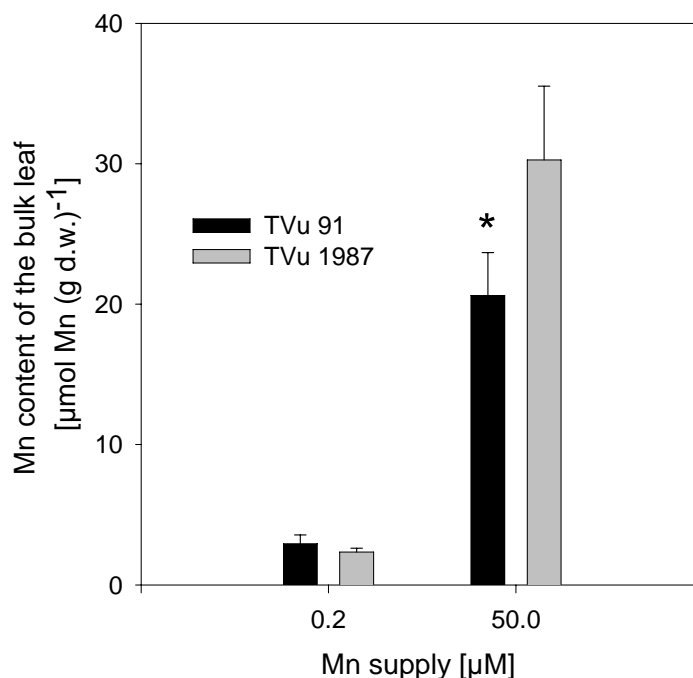


Fig. 1: Manganese tissue-concentrations of leaves as affected by Mn supply in the cowpea cultivars TVu 91 (Mn-sensitive) and TVu 1987 (Mn-tolerant). Plants were pre-cultured for 14 days and afterwards cultured at 0.2 μM or 50 μM Mn for 3 days. * Toxicity symptoms (20 brown spots cm^{-2}) appearing only on the leaves of the Mn-treated Mn-sensitive cultivar TVu 91. Bars represent standard deviations of the means.

Effect of increased Mn supply on the leaf proteome

Proteome analysis was carried out to systematically identify proteins affected by Mn supply. Total proteins of both cultivars treated with 0.2 or 50 μM Mn for three days were extracted from leaves and resolved by 2D IEF / SDS PAGE (Fig. 2). Careful comparison of the protein patterns on the resulting four 2D gels by visual inspection allowed identifying several differences in protein abundance between the two genotypes or the two Mn treatments. More than 25 proteins clearly exhibited differential abundance due to the Mn treatment. Protein extractions for 2D IEF / SDS PAGE were repeated three times independently using the pooled leaf material of two plants. The obtained gels were evaluated by the ImageMaster™ 2D Platinum Software 6.0 (GE Healthcare, Munich, Germany). Master gels were calculated for both genotypes and Mn treatments and then compared. 540 and 464 spots were included into the statistical analysis (Tab. S1). Using rigorous threshold parameters (spot ratio on the two compared master gels < 0.5 or > 2 , p-value of the difference in abundance in individual experiments < 0.01) eight proteins were identified exhibiting differential abundance due to the Mn treatment (indicated by arrows on Fig. 2 and Fig. 3). Seven of these proteins showed changes in abundance in the Mn-sensitive cultivar (five had lower and two had higher abundance, Figure 2, upper gels) and one protein showed a change in the Mn-tolerant cowpea cultivar (increased abundance, Fig. 2, lower gels). Close-ups of the gel regions containing proteins of differential abundance are shown in Figure 3.

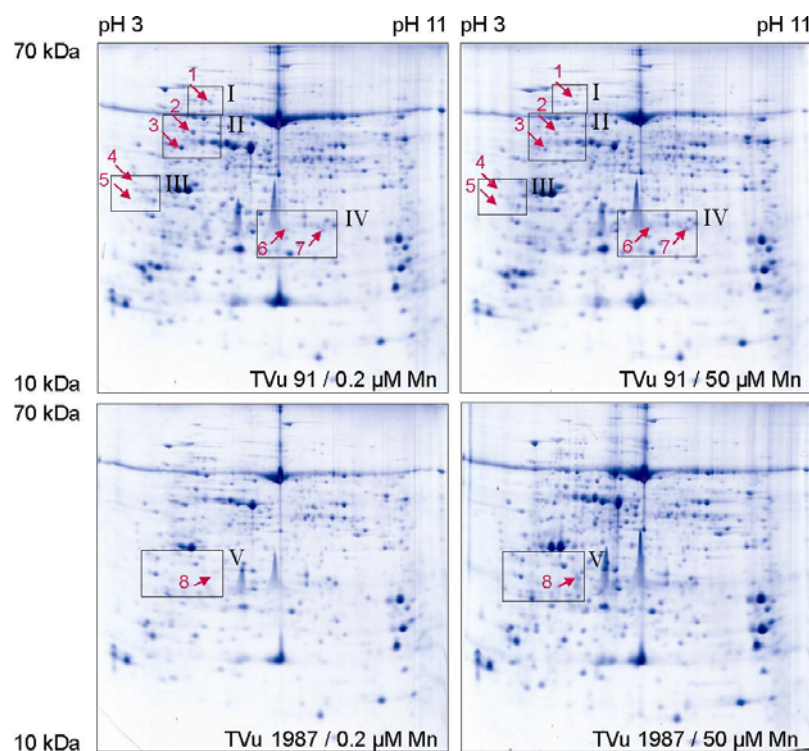


Fig. 2: 2-D resolution of the total leaf proteome of the Mn-sensitive cowpea cultivar TVu 91 and the Mn-tolerant cultivar TVu 1987 after treatment with 0.2 μ M or with 50 μ M Mn. Treatment of plants was for 3 days after 14 days of pre-culture. Leaf material was homogenized in liquid N₂ and proteins were extracted as described in the Materials and Methods section. IEF was carried out on broad range pH gradient gels (pH 3-11). Differentially expressed spots are marked by arrows and numbered consecutively (see Tab. 1 for identities). The boxes indicate gel regions used for the detailed comparisons shown in Fig. 3.

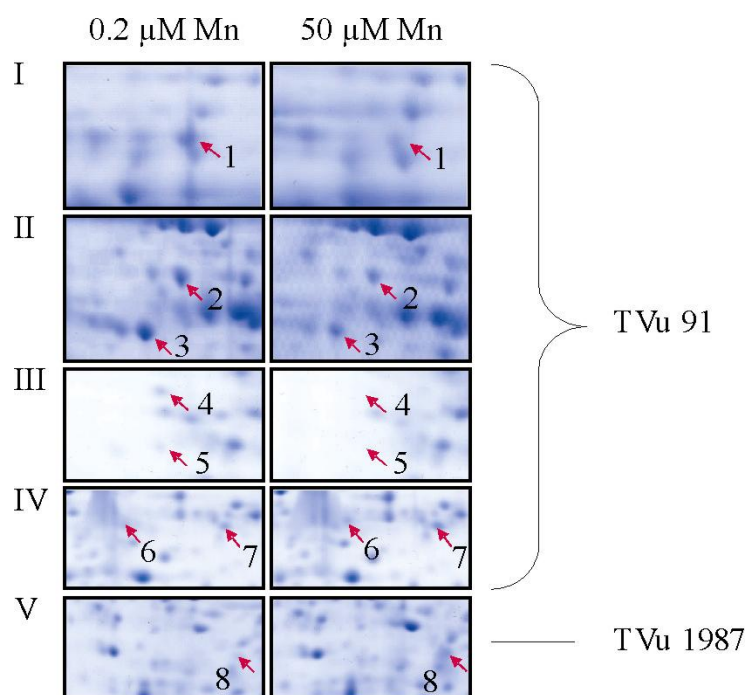


Fig. 3: Close ups of regions of the 2D gels shown in Fig. 2 including differentially expressed proteins of the two cowpea cultivars TVu 91 and TVu 1987. Treatment of plants was for 3 days after 14 days of pre-culture. Leaf material was homogenized in liquid N₂ and proteins were extracted as described in the Materials and Methods section. Differentially expressed spots are marked by arrows (for identifications see Tab. 1).

Identification of proteins affected by increased Mn supply

The eight proteins clearly affected by Mn treatment were analysed by *de novo* peptide sequencing using ESI tandem mass spectrometry and identified by sequence comparisons using the NCBI protein database (Tab. 1). Three of the proteins reduced at high Mn treatment in the Mn-sensitive genotype represent enzymes involved in primary carbon fixation (RubisCO-binding protein, RubisCO activase, phosphoribulokinase; Fig. 2, spots 1, 2 and 3). Two proteins of changed abundance (higher, spot 7; lower, spot 5, Fig. 2) in the Mn-sensitive genotype are pathogenesis-related proteins. Another protein reduced in the Mn-sensitive cultivar upon Mn treatment is homologous to an “Oxygen-evolving enhancer protein, type 1” (also termed OEC33 protein) from *Arabidopsis thaliana* (Fig. 2, spot 4). Finally, the β -6 subunit of the proteasome is of increased abundance in Mn-treated plants of the Mn-sensitive

cowpea cultivar (Fig. 2, spot 6). The only clearly Mn-affected (up-regulated) protein of the Mn-tolerant cowpea genotype represents another type of “oxygen-evolving enhancer protein (type 2)” (also termed OEC23 protein).

Tab. 1. Leaf proteins of cowpea cultivars TVu 91 and TVu 1987 affected by treatment with 50 μ M Mn for 3 days.

Spot ^a	Identity ^b	Acc. No ^b	MW (Da) / No. of amino acids	Fold induction / reduction ^c
1	RubisCO-binding protein, beta subunit (pea)	P08927	62984 / 595	0.38
2	RubisCO activase (rice)	Q7XXR6	51454 / 466	0.48
3	Phosphoribulokinase (pea)	P93681	39026 / 352	0.49
4	Oxygen-evolving enhancer protein 1 (<i>A. thaliana</i>)	Q9S841	35019 / 331	n.d.
5	Pathogenesis-related protein P4 (tomato)	Q04108	17439 / 159	n.d.
6	Putative beta6 proteasome subunit (tobacco)	Q93X30	20864 / 192	2.03
7	Pathogenesis-related protein 5-1 (sunflower)	Q8LSM9	23953 / 222	2.46
8	Oxygen-evolving enhancer protein 2 (<i>B. gymnorhiza</i>)	Q9MAW2	17537 / 160	3.80

^a The numbers correspond to numbers given in Figures 2 and 3. Spots 1-7 are from the Mn-sensitive cultivar TVu 91 and spot 8 from the Mn-tolerant cultivar TVu 1987. For statistical evaluation and peptide sequences see supplementary material, Tables S1 and S2.

^b Identities are based on sequence comparisons using the NCBI protein database.

^c Fold induction / reduction in plants cultivated at 50 μ M Mn in relation to plants cultivated at 0.2 μ M. For further details see Table S1. Spots 4 and 5 completely disappeared during Mn treatment and, therefore, could not be quantified (n.d.)

Physiological changes linked to increased Mn supply

Two of the Mn-affected proteins are indirectly involved in the photosynthetic water splitting process. This was assumed to have consequences for the electron transfer rate (ETR) and photosynthesis of the studied leaves. Indeed, ETR was significantly reduced in the Mn-sensitive cultivar exposed to high Mn supply as early as after one day (Fig. 4). In contrast, the ETR of the Mn-tolerant cultivar was not affected by the elevated Mn supply even after 3 days of Mn treatment.

Net CO₂ fixation rate measured in parallel was not affected by Mn treatment for up to 3 days and did not differ between the Mn treatments in either cultivar (data not shown).

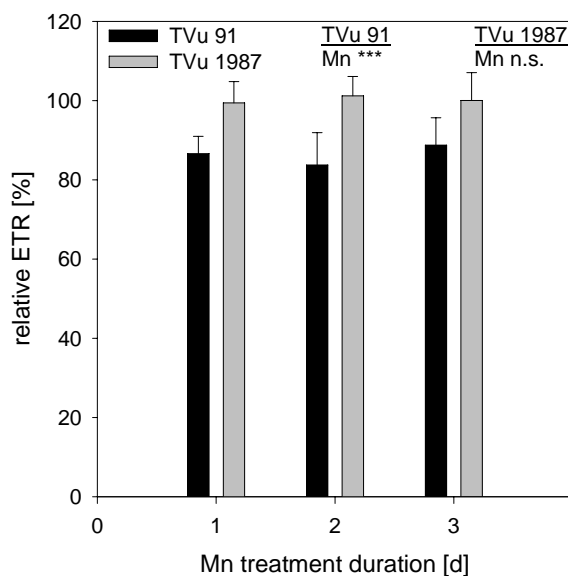


Fig. 4: Relative electron-transport rate (ETR) of the cowpea cultivars TVu 91 and TVu 1987 after enhanced Mn supply relative to the ETR at optimum Mn supply. Plants pre-cultivated for 14 days were supplied with 0.2 μM or 50 μM Mn for 0 – 3 days. ETR was measured using a Mini-PAM fluorometer. Means were calculated on the basis of four independent experiments and evaluated for each cultivar separately. Results of the analysis of variance are given according to their level of significance as *** for $P < 0.001$. Bars represent standard deviations of the means.

Since the water splitting complex forms part of the photosystem II supercomplex, two-dimensional Blue native / SDS PAGE was carried out to analyse the photosystem II subunit composition and abundance. For this approach, chloroplasts were isolated from leaves of plants of both cowpea cultivars cultivated at low (0.2 μM) or high Mn (50 μM) supply. Thylakoid protein complexes proved to have a similar structure in all four samples analysed. A representative example out of three replicates is shown in Fig. 5. In particular, structure and abundance of the photosystem II was similar in both cowpea cultivars independent of Mn treatment. However, a slightly enlarged form of the photosystem I, which runs at about 650 kDa on the native gel dimension (Heinemeyer et al., 2004), was enriched 1.7-fold in the plants exposed to high Mn supply for 3 days in the Mn-sensitive cultivar TVu 91. A 1.2-fold enrichment could also be found in the Mn-tolerant cultivar TVu 1987. This larger form of the photosystem I is known to arise by attachment of trimeric LHCII during transition from state 1 to state 2 photosynthesis (Haldrup et al., 2001).

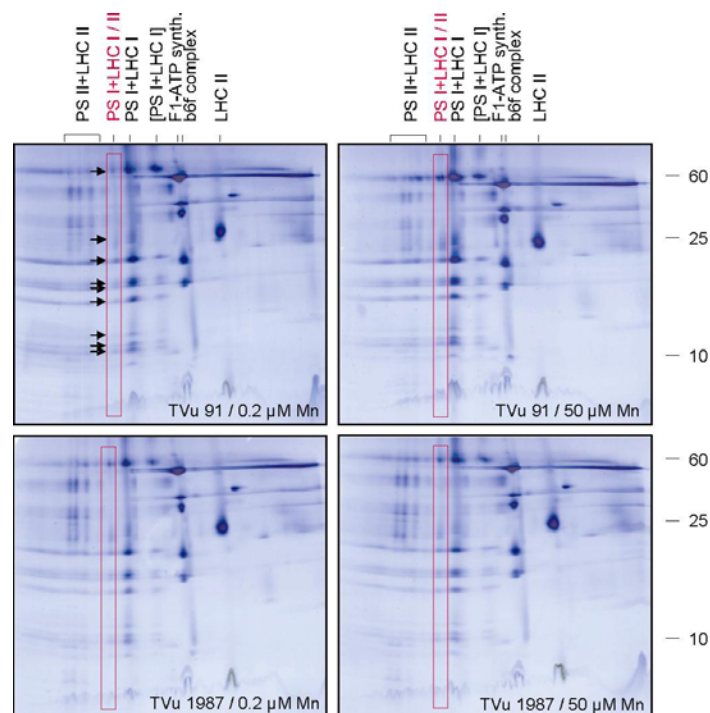


Fig. 5: Two-dimensional resolution of the chloroplast protein complexes of the cowpea cultivars TVu 91 and TVu 1987 by 2D Blue-native / SDS PAGE. Plants pre-cultivated for 14 days were supplied with 0.2 μM or 50 μM Mn for 3 days. Total leaf protein was extracted as described in the Materials and Methods section. Resolved protein complexes were identified on the basis of their subunit compositions according to Heinemeyer et al. (2004). Molecular masses of standard proteins are given to the right and the identities of the resolved protein complexes above the gels. Abbreviations: PS II + LHC II – supercomplex of dimeric photosystem II + light-harvesting II complexes; PS I + LHC I / II – photosystem I + light-harvesting proteins I + light-harvesting complex II; PS I + LHC I – photosystem I + light-harvesting proteins I, [PS I + LHC I] – subcomplex of PS I + LHC I; F1-ATP synthase – F1 part of the ATP synthase complex; b6f complex – cytochrome b6f complex; LHC II – light-harvesting complex II. Marked spots were analysed by ImageMaster 2D Platinum to quantify differences between the Mn treatments within each genotype. The PS I + LHC I / II complex was enhanced at high Mn 1.7-fold and 1.2-fold in the Mn-sensitive cultivar TVu 91 and the Mn-tolerant cultivar TVu 1987, respectively.

Manganese-induced gene expression

Changes of the cowpea-leaf proteome in response to Mn stress are assumed to be preceded by changes in gene expression. The Suppression Subtractive Hybridization (SSH) strategy (Diatchenko et al., 1996) was chosen to systematically monitor Mn stress-induced changes in gene expression in the leaves. For this approach, total mRNA of both cowpea cultivars grown for one day in the presence of normal or enhanced Mn supply was isolated and used to generate two subtractive cDNA libraries. Enrichment of the obtained libraries in transcripts specifically induced by enhanced Mn supply was verified by Northern blotting experiments

for 20 randomly selected clones (data not shown). For preliminary analyses of the two cDNA libraries, 100 clones per library were selected on a random basis and subjected to DNA sequence analyses. The corresponding genes were identified on the basis of sequence comparisons and assigned to functional categories (Fig. 6). The number of transcripts involved in photosynthesis and respiration declined upon enhanced Mn supply in the Mn-sensitive TVu 91 cultivar if compared to the Mn-tolerant cultivar TVu 1987. At the same time, the number of transcripts involved in signal transduction increased in the Mn-sensitive cultivar. These preliminary results point to a rapid broad-range transcriptomic response of the Mn-sensitive cowpea cultivar upon Mn stress.

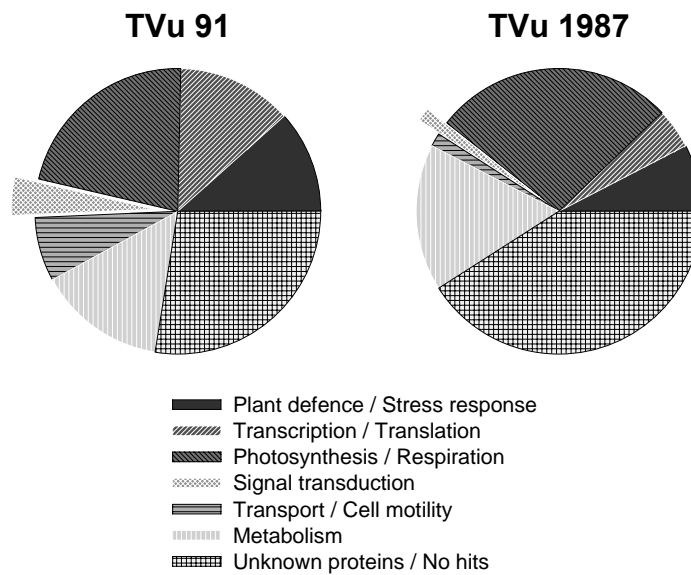


Fig. 6: Manganese-induced gene expression in the cowpea cultivars TVu 91 and TVu 1987. Treatment of plants was 0.2 μM versus 50 μM Mn for 1 day after 14 days of pre-culture. Transcripts were isolated by Suppression Subtractive Hybridization (SSH) as described in the Material and Methods section. 100 clones were selected for both cultivars on a random basis, sequenced and classified into functional categories on the basis of sequence homology (for details see supplementary material, Tab. S3).

Discussion

Previous studies in cowpea revealed that the leaf apoplast represents the most important compartment involved in the expression of Mn toxicity (Fecht-Christoffers et al., 2007) which is characterised by formation of brown spots, induction of callose formation, and an enhanced release into the apoplast of phenols, peroxidases and other stress-related proteins (Fecht-Christoffers et al., 2003a, 2003b, 2006). These Mn stress-induced physiological changes in the older leaves can be measured after two to three days after exposure of the plants to toxic Mn supply. It is conceivable that these apoplastic changes involved in Mn toxicity are triggered by excess Mn through molecular events in the symplast. This assumption is addressed in the present study through a transcriptomic and proteomic analysis of total leaves of cowpea genotypes differing in Mn tolerance as affected by toxic Mn supply.

Proteins specifically affected by Mn stress in cowpea

The RubisCO-binding subunit, the RubisCO activase and the phosphoribulokinase (Spots 1-3 in Figures 2, 3 and Tab. 1) all are essential for efficient CO₂ fixation in plants. Phosphoribulokinase catalyses the formation of ribulose-1,5-bisphosphate, which represents the acceptor molecule for CO₂ fixation of the Calvin cycle (Miziorko, 2000). The RubisCO binding subunit is important for folding of the large subunit of RubisCO (Boston et al., 1996). RubisCO activase promotes and maintains the catalytic activity of RubisCO (Portis, 2003). It removes inhibitors from catalytic sites of RubisCO, prevents changes in conformation, and activates RubisCO. The amount of all three proteins in the Mn-sensitive cowpea genotype TVu 91 was reduced to less than half when treated with high Mn supply. Therefore, Mn stress specifically induces a down-regulation of the key enzymes responsible for CO₂ fixation of the Calvin cycle. This process might be important to save energy for the Mn-stress response. A direct regulation of RubisCO possibly would be less efficient because of the large quantities of this enzyme present in chloroplasts. However, measurable reduction of CO₂ fixation seems to be delayed compared to the reduction of the levels of RubisCO-binding protein and RubisCO activase, which most likely also is a consequence of the huge excess of RubisCO in relation to its regulating proteins.

Two cowpea proteins specifically affected by Mn-treatment form part of the “Oxygen Evolving complex” (OEC) of the photosystem II (PSII). This complex is composed of three proteins, the Psb O (OEC33), the Psb P (OEC23) and the Psb Q (OEC16) protein (Raymond and Blankenship, 2004). All three proteins are attached to the photosystem II on the luminal side of the thylakoids and are believed to be important for the stabilisation of the Mn cluster of PSII, for efficient water splitting, and overall PSII stability (Ifuku et al., 2005, Yi et al., 2005). Recently, homologous PSII subunits also were identified in cyanobacteria (Thornton et al., 2004, Summerfield et al., 2005). The precise function of the three proteins in cyanobacteria and higher plants is not known. Interestingly, abundance of OEC23 (spot 8 in Fig. 2, 3 and Tab. 1) is four-fold increased by Mn treatment in the Mn-tolerant cowpea cultivar TVu 1987. Possibly, the expression of the corresponding gene is Mn-regulated. In contrast, the Mn-stabilizing OEC33 protein (spot 4 in Fig. 2, 3 and Tab. 1) is drastically reduced in the Mn-sensitive cultivar TVu 91 upon Mn stress. This could contribute to growth reduction of this cultivar at toxic Mn supply because the water-splitting process of photosynthesis is impeded. Indeed, electron transfer-rates (ETR) decreased in the Mn-sensitive cultivar upon Mn stress in comparison to normal Mn conditions (Fig. 4). This decrease cannot be interpreted as a consequence of reduced leaf area of Mn-stressed plants due to the development of the characteristic brown spots, because the decrease in ETR occurred before these spots became visible. However, conclusions on the functional relevance of the observed changes in abundance of the OEC proteins should be treated with caution, because they are encoded by small gene families. The precise regulation of the abundances of OEC isoforms so far is unknown.

Also, a state 1 to state 2 transition of photosynthesis was observed in Mn-stressed cowpea leaves (Fig. 5). During this state transition, light harvesting proteins are detached from the photosystem II and bind to the photosystem I (Haldrup et al., 2001). As a consequence, light absorption at photosystem II decreases and increases at photosystem I. This leads to an overall reduction of linear photosynthetic electron transfer, but an induction of cyclic electron transfer, which is especially important for ATP synthesis in chloroplasts (Finazzi et al., 2002). State I – state II transitions of photosynthesis were previously reported to form part of a plant-stress response towards varying light conditions. Both cultivars responded principally similarly to Mn treatment, although less marked in the Mn-tolerant cultivar as calculated by ImageMaster™ 2D Platinum Software 6.0 (GE Healthcare, Munich, Germany).

The changes in the chloroplast proteome (Fig. 2, Fig. 3, Fig. 5) and in the photosynthetic performance (Fig. 4) cannot be explained by differences in the Mn contents of the isolated chloroplasts as they did not differ between Mn treatments and cultivars. However,

chloroplasts were isolated in the presence of EDTA to inhibit metalloproteases. As a consequence, large amounts of free and labile-bound Mn might have been lost during the organelle isolation procedure. Indeed, Keren et al. (2002) showed that they could remove a substantial labile Mn fraction by washing photosynthetic *Synechocystis* cells with EDTA. Also, using a non-aqueous isolation technique, a positive linear relationship between bulk-leaf and chloroplast Mn concentrations was shown in common bean (González and Lynch, 1999). We thus cannot exclude the possibility that the Mn-tolerant cultivar is able to exclude Mn from the chloroplasts more effectively than the Mn-sensitive cultivar.

Two further cowpea proteins affected by Mn-stress represent pathogenesis-related (PR) proteins (spots 5 and 6 in Figures 2, 3 and Tab. 1). Both proteins only were identified in the Mn-sensitive cultivar. One PR protein belongs to the PR-4 family and is of reduced abundance in Mn-stressed plants; the other is similar to proteins of the PR-5 family and is of increased abundance. PR-like proteins were also detected by a proteome analysis of Mn-inducible proteins of the apoplast of cowpea (Fecht-Christoffers et al., 2003b) at an advanced stage of Mn toxicity. However, these proteins were not identical to the newly identified PR proteins. In general, a large number of PR proteins are known and most of them are induced by biotic and/or abiotic stress factors (van Loon and Strien, 1999; van Loon et al., 2006). The role of the up and down regulation of the two identified PR proteins in Mn tolerance is not yet understood.

Finally, a β -6 type proteasome subunit was specifically induced in the Mn-sensitive cowpea cultivar upon Mn stress. Proteasomes in general are responsible for the main protein degradation pathway in eukaryotic cells (Moon et al., 2004). The substitution of α - and β -subunits of the 20S proteasome was previously suggested to be responsible for the specific proteolysis of proteins as part of defence reactions (Dahan et al., 2001). However, the specific role of the β -6 subunit in proteolysis is currently not known.

The apoplast proteins important for the Mn-stress response in cowpea (Fecht-Christoffers et al., 2003b) were not detected on the total leaf proteome level, most likely due to their comparatively low abundance. Also, Mn membrane transporters were not identified, which certainly play an important role in Mn compartmentation in plant cells (hydrophobic proteins such as ion transporters are known to be only poorly resolved during isoelectric focussing for 2D gel electrophoresis; also, enrichment of hydrophobic proteins would need a different extraction procedure than used in the current study).

Transcripts specifically affected by Mn stress in cowpea

An investigation of transcripts induced in the Mn-sensitive and the Mn-tolerant cowpea cultivars upon Mn-stress was carried out by the SSH technology (Fig. 6). Using this procedure, transcripts induced by Mn stress were specifically enriched. Systematic sequencing of 2 x 100 clones of the resulting cDNA libraries on the basis of random clone selection gave first insights into the rapid (one day treatment) transcriptomic Mn-stress response: (1) Compared to the Mn-tolerant cowpea cultivar, the number of transcripts coding for proteins involved in photosynthesis, respiration and primary metabolisms were reduced in the Mn-sensitive genotype. (2) At the same time, transcripts encoding for proteins involved in signal transduction were increased. (3) All other functional categories of proteins were more or less unchanged between the Mn-tolerant and the sensitive cultivar upon Mn stress. (4) In both cultivars, several PR proteins were induced by Mn treatment. (5) Some of the induced transcripts identified in a cDNA library for the Mn-sensitive cowpea genotype after 3 days of Mn stress encode for PR proteins previously identified in this cultivar in the course of an investigation of the apoplast proteome (Fecht-Christoffers et al., 2003b, Fig. 7).

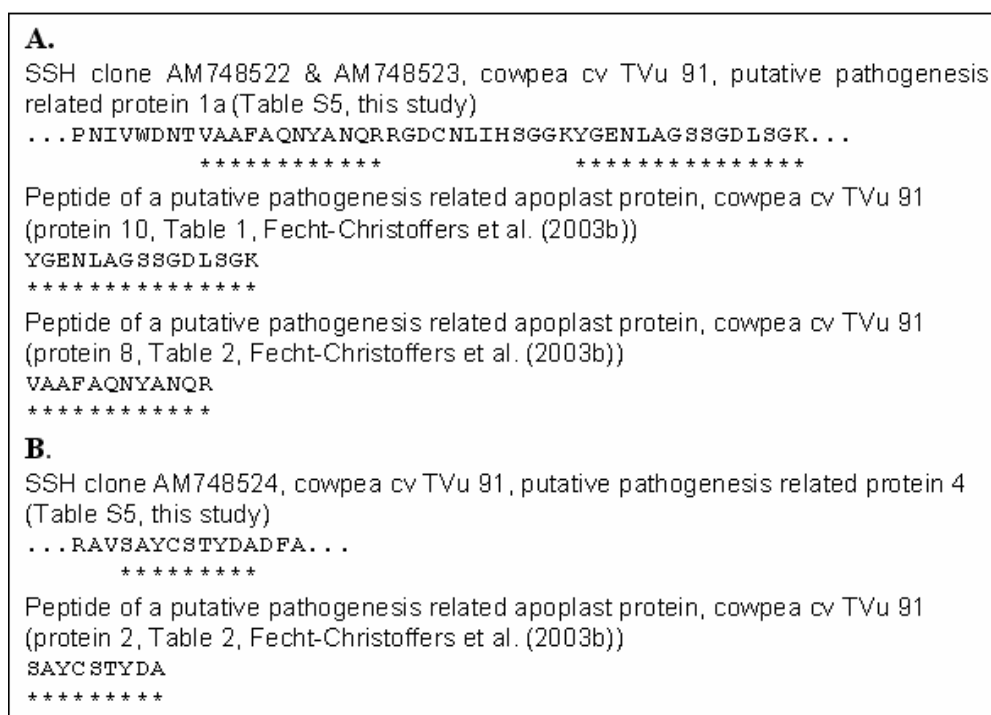


Fig. 7: Detailed sequence comparisons between two Mn-induced proteins of the cowpea cultivar TVu 91 identified by SSH and proteins identified by direct proteome analyses of the total leaf proteome (this study) or the apoplast proteome (Fecht-Christoffers et al., 2003b). Stars beneath the sequences indicate identical residues. Used clones were named according to their accession numbers at the EMBL database.

Apoplastic versus symplastic Mn-stress response in cowpea

The results generally reveal an involvement of proteins of symplastic compartments in the Mn-stress response. Using stringent threshold criteria, proteins which are related to photosynthetic water splitting were shown to be clearly affected by Mn excess, CO₂ fixation, the pathogen defence-response, and the protein degradation-pathway. This can be attributed to modified transcription of genes as early as 1 day after transfer of the plants to excessive Mn supply. This is in agreement with our expectations and appears to corroborate conclusions made by some authors (see introduction for references) that Mn toxicity primarily affects chloroplast functions in other plant species. However, it needs to be considered that in these plant species young leaves have been studied, whereas in cowpea Mn toxicity expresses strictly primarily in old leaves. This could be one of the reasons why for Mn toxicity in cowpea apoplastic lesions are more important than symplastic lesions after longer Mn treatment.

In conclusion, the Mn-stress response still is only partially understood. This is especially true for the initial symplastic molecular events induced by Mn excess which are presumed to induce signal transduction pathways leading to apoplastic stress reactions. Overall, the Mn-stress response seems to be a specific interplay of apoplastic and symplastic reactions, which in concert result in the expression of Mn toxicity and Mn tolerance. Future research will be necessary to further clarify the molecular details of the Mn-stress response in cowpea and other plant species.

Characterization of leaf apoplastic peroxidases and metabolites in *Vigna unguiculata* in response to toxic manganese supply and silicon

Hendrik Führs¹, Stefanie Götze¹, André Specht¹, Alexander Erban², Sébastien Gallien³, Dimitri Heintz⁴, Alain Van Dorsselaer³, Joachim Kopka², Hans-Peter Braun⁵ & Walter J. Horst¹

Journal of Experimental Botany (2009), doi:10.1093/jxb/erp034

¹ Institute of Plant Nutrition, Faculty of Natural Sciences, Leibniz University Hannover, Herrenhäuser Str. 2, 30419 Hannover, Germany

² Max Planck Institute of Molecular Plant Physiology, Am Mühlenberg 1, 14476 Potsdam-Golm, Germany

³ Laboratoire de Spectrométrie de Masse Bio-Organique, IPHC-DSA, ULP, CNRS, UMR7178 ; 25 rue Becquerel, 67 087 Strasbourg, France

⁴ Institut de Biologie Moléculaire des Plantes (IBMP) CNRS-UPR2357,ULP, 67083 Strasbourg, France

⁵ Institute of Plant Genetics, Faculty of Natural Sciences, Leibniz University Hannover, Herrenhäuser Str. 2, 30419 Hannover, Germany

Abstract

Previous work (Fecht-Christoffers et al., 2006) suggested that the apoplastic phenol composition and its interaction with apoplastic class III peroxidases (PODs) are decisive in the development or avoidance of manganese (Mn) toxicity in cowpea (*Vigna unguiculata* L.). This study characterizes apoplastic PODs with particular emphasis on the activities of specific isoenzymes and their modulation by phenols in the Mn-sensitive cowpea cultivar TVu 91 as affected by Mn and silicon (Si) supply. Si reduced Mn-induced toxicity symptoms without affecting the Mn uptake. Blue Native-PAGE combined with Nano-LC-MS/MS allowed identification of a range of POD isoenzymes in the Apoplastic Washing Fluid (AWF). In Si-treated plants Mn-mediated induction of POD activity was delayed. Four POD isoenzymes eluted from the BN gels catalysed both H₂O₂-consuming and H₂O₂-producing activity with pH optima at 6.5 and 5.5, respectively. Four phenols enhanced NADH-*peroxidase* activity of these isoenzymes in presence of Mn²⁺ (*p*-coumaric = vanillic > benzoic >> ferulic acid). *P*-coumaric acid-enhanced NADH-*peroxidase* activity was inhibited by ferulic acid (50%) and five other phenols (50-90%). An independent component analysis (ICA) of the total and apoplastic GC-MS-based metabolome profile showed that Mn, Si supply, and the AWF fraction (AWF_{H2O}, AWF_{NaCl}) significantly changed the metabolite composition. Extracting non-polar metabolites from the AWF allowed the identification of phenols. Predominantly NADH-*peroxidase* activity-inhibiting ferulic acid appeared to be down-regulated in Mn-sensitive (+Mn, -Si) and upregulated in Mn-tolerant (+Si) leaf tissue. The results presented here support the previously hypothesized role of apoplastic NADH-*peroxidase* and its activity-modulating phenols in Mn toxicity and Si-enhanced Mn tolerance.

Introduction

Manganese (Mn) in plants is an essential micronutrient (Marschner, 1995). However, at supra-optimum supply Mn readily becomes toxic to plants. Mn toxicity in crops is a widely distributed plant disorder mainly on acidic and insufficiently drained soils with low redox potentials thus leading to high amounts of plant-available Mn (Horst, 1988).

In cowpea Mn-resistant cultivars do not differ in Mn accumulation from Mn-sensitive cultivars (Horst, 1980; Chapter 1). Therefore, in this species Mn resistance is regarded as Mn tolerance (Horst, 1983). Typical Mn stress-induced toxicity symptoms in cowpea develop primarily on older leaves as distinct brown spots located in the leaf apoplast of the epidermis starting at the leaf base, then spreading to the tip, followed by chlorosis, and finally leaf shedding (Horst and Marschner, 1978b; Horst, 1982).

The brown spots consist of oxidized Mn and oxidized phenolic compounds (Wissemeier and Horst, 1992). Hence, the oxidation of Mn^{2+} and phenols mediated by apoplastic PODs was proposed to be a key reaction leading to Mn toxicity (Fecht-Christoffers et al., 2006). Class III apoplastic PODs (EC 1.11.17) belong to multigenic families (Passardi et al., 2004) with various functions in plant growth (for more information see Passardi et al., 2005). PODs are polyfunctional enzymes that undergo two reaction cycles: the peroxidase-oxidase cycle (with NADH as substrate also called NADH-*peroxidases*) resulting in H_2O_2 production (Halliwell, 1978) and the peroxidase cycle (with guaiacol as phenol substrate also called guaiacol-*peroxidase*) leading to H_2O_2 consumption (Fecht-Christoffers et al., 2003a, b). H_2O_2 -producing POD activity was intensively studied with respect to numerous exogenous factors like ambient pH (Bolwell et al., 1995, 2001), phenol composition (Halliwell, 1978; Fecht-Christoffers et al., 2006), and Mn^{2+} concentration *in vivo* (Yamazaki and Piette; 1963; Halliwell, 1978).

Fecht-Christoffers et al. (2006, 2007) investigated H_2O_2 -producing activity of apoplastic peroxidases of cowpea *in vitro* and found that not only Mn^{2+} but also phenols are required to induce NADH-*peroxidase* activity. Increasing Mn concentrations in the leaf tissue and the AWF affected the total apoplastic phenol concentration and composition. Crosswise combining of AWF metabolites with AWF proteins from cultivars differing in Mn tolerance revealed a significant effect on NADH-*peroxidase* activity. They concluded that the apoplastic phenol composition and its interaction with PODs are decisive in the development or avoidance of Mn toxicity.

Silicon is a beneficial element for most plants (Epstein, 1999), and alleviates heavy metal toxicities, e.g. aluminium and Mn toxicity. The alleviative effect of Si on Mn toxicity was described for common bean and cowpea (Horst and Marschner 1978a; Iwasaki et al., 2002a, b), cucumber (Rogalla and Römheld, 2002; Shi et al., 2005), and pumpkin (Iwasaki and Matsumura, 1999). For cowpea, Horst and Marschner (1978a) found that leaf Mn was more evenly distributed in Si-treated cowpea plants. Horst et al. (1999) demonstrated a reduction in apoplastic Mn concentrations due to Si supply and concluded that Si changes apoplastic Mn-binding properties, even though this could only partly explain Si-mediated alleviation of Mn toxicity (Iwasaki et al., 2002b). It was found that toxicity symptoms and guaiacol-peroxidase activities were more closely related to apoplastic Si concentrations than to apoplastic Mn concentrations, indicating a more direct involvement of Si nutrition in detoxification of apoplastic Mn.

The presented work specifically addressed the hypothesis that the activities of specific apoplastic peroxidases and their modulation by metabolites are decisive for Mn toxicity and Si-induced enhanced Mn tolerance in the Mn-sensitive cowpea cultivar TVu 91.

Materials and Methods

Plant material

Cowpea (*Vigna unguiculata* [L.] Walp., cv TVu 91) was grown hydroponically in a growth chamber under controlled environmental conditions at 30/27°C day/night temperatures, 75% ±5 % relative humidity, and a photon flux density of 150 $\mu\text{mol m}^{-2}\text{s}^{-1}$ photosynthetic active radiation (PAR) at mid-plant height during a 16-h photoperiod. After germination in 1 mM CaSO_4 for 7 d, seedlings were transferred to a constantly aerated nutrient solution with 4 plants in one 5-L pot. The composition of the nutrient solution was [μM]: $\text{Ca}(\text{NO}_3)_2$ 1000, KH_2PO_4 100, K_2SO_4 375, MgSO_4 325, FeEDDHA 20, NaCl 10, H_3BO_3 8, MnSO_4 0.2, CuSO_4 0.2, ZnSO_4 0.2, Na_2MoO_4 0.05. Silicon-treated plants (+Si) received Si in form of Aerosil (Horst and Marschner, 1978a; chemically clean silicic acid, solubility in water: 0.6 – 0.75 mg L^{-1} or 20-26.5 μM). After preculture for 14 d, the Mn concentration in the nutrient solution was increased from 0.2 μM (-Mn) to 50 μM (+Mn) for 4 or 6 days. The nutrient solution was changed two to three times per week to avoid nutrient deficiencies.

Extraction of water-soluble and ionically bound apoplastic proteins and metabolites

Apoplastic washing fluid (AWF) was extracted by a vacuum infiltration/centrifugation technique according to Fecht-Christoffers et al. (2003a, b). Leaves were infiltrated with chilled dH_2O by reducing the pressure to -35 hPa followed by a slow relaxation. $\text{AWF}_{\text{H}_2\text{O}}$ was recovered by centrifugation at 1324 g for 5 min at 4°C. Afterwards the same leaves were infiltrated with chilled 0.5 M NaCl solution and AWF_{NaCl} was recovered as described above. Malate dehydrogenase (MDH) activity in both AWF fractions showed a cytoplasmic contamination of less than 1% (data not shown). Until further analysis the AWF was stored at -80°C.

Quantification of toxicity symptoms

For the quantification of Mn toxicity symptoms, the density of brown spots was counted on a 1.54 cm² area at the base and tip on the upper side of the second oldest middle trifoliolate leaf and calculated on 1 cm² base.

Manganese analysis

Manganese in the bulk-leaf tissue was determined in the second oldest middle trifoliolate leaf after dry ashing at 480°C for 8h, dissolving the ash in 6 M HCl with 1.5% (w/v) hydroxylammonium chloride, and then diluting (1:10) with double demineralised water. Apoplastic Mn concentrations were measured in 1:10 dilutions of the AWF. Both measurements were carried out by optical inductively-coupled plasma-emission spectroscopy (Spectro Analytical Instruments GmbH, Kleve, Germany).

Silicon analysis

Monomeric Si concentration in the AWF was determined according to Iwasaki et al. (2002a, b). AWF and a standard solution [0 to 100 µg Si (ml AWF)⁻¹] were mixed with 250 µl of staining solution (1:1 mix of 0.08 M H₂SO₄ and 20 g L⁻¹ (NH₄)₆Mo₇O₂₄*4 H₂O). After 30 min of incubation 250 µl of freshly prepared ascorbic acid (0.1 g 25 ml⁻¹) and 250 µl tartaric acid (0.85 g 25 ml⁻¹) were added. Samples were measured at λ=811 nm in a Microplate-Reader (µQuant, BioTek Instruments, Germany).

Determination of the protein concentration in the AWF and AWF concentrates

The protein concentration in the AWF for the calculation of specific enzyme activities was determined according to Bradford (1976). The protein concentration of AWF concentrates was measured for 1D BN-PAGE using the 2-D Quant Kit[®] (GE Healthcare, USA) according to the manufacturer's instructions.

Determination of specific peroxidase activities in the AWF

For the measurement of H₂O₂-consuming guaiacol-peroxidase activities in the AWF, the oxidation of the substrate guaiacol was determined spectrophotometrically at $\lambda=470$ nm (UVIKON 943, BioTek Instruments GmbH, Neufahrn, Germany). Samples were mixed with guaiacol solution (20 mM guaiacol in 10 mM Na₂HPO₄ buffer [pH 6]) and 0.03% (v/v) H₂O₂. For calculation of enzyme activities the molar extinction coefficient 26.6 L (mmol cm)⁻¹ was used.

For the measurement of the H₂O₂-producing NADH-*peroxidase* activity in the AWF, samples were mixed with MnCl₂ (16 mM), *p*-coumaric acid (1.6 mM) and NADH (0.22 mM). The NADH oxidation-dependent decline in absorption at $\lambda = 340$ nm was determined. For calculation of enzyme activities the molar extinction coefficient 1.13 L (mmol cm)⁻¹ was used.

1D BN-PAGE of apoplastic proteins and POD activity staining

For protein separation by electrophoresis under native conditions, the proteins of the AWF were concentrated at 4°C by using centrifugal concentrators with a molecular mass cut off at 5kDa (Vivaspin 6, Vivascience, Hannover, Germany). Running conditions were used according to the manufacturer's instructions.

Proteins were separated via BN-PAGE according to Jänsch et al. (1996). Protein samples were combined with Coomassie Blue solution (5% [w/v] Serve Blue G and 750 mM aminocaproic acid) and 10% (v/v) glycerol (100%). Samples were loaded onto a native acrylamid gel with a 4% (w/v) stacking gel and a 12% to 20% (w/v) gradient separation gel. Electrophoresis was carried out at 100 V and 6 to 8 mA for 45 min followed by 13 h at 15 mA (max. 500V).

NADH-*peroxidase* activity in the gel was determined by NBT staining to detect O₂^{*-} radicals (Fig. 3) or by DAB staining (data not shown) to detect H₂O₂. Staining solution finally consisted of 16 mM MnCl₂, 1.6 mM *p*-coumaric acid, 0.22 mM NADH, and 2.5 (mg ml⁻¹) NBT in order to detect O₂^{*-} radicals, that are proposed to be produced during the NADH-*peroxidase* activity of PODs (Halliwell, 1978) because a direct detection of H₂O₂ by DAB staining was difficult due to the high gel background caused by coomassie. Gels were stained

for 30 min at room temperature. The gels were afterwards soaked in 20 mM guaiacol (in 10 mM Na₂HPO₄) and 0.03% (v/v) H₂O₂ for 3 min to detect guaiacol-peroxidase activity.

For preparative BN-PAGE guaiacol-peroxidase staining was carried out only for a few seconds in order to reduce enzyme damage by product-enzyme interaction.

Electroelution of specific POD isoenzymes for further physiological characterization⁵

Four POD isoenzymes (P1, P3, P5 and P6 in Fig. 3C) were chosen for electroelution from BN gels that was carried out according to Wehrhahn and Braun (2002). POD isoenzymes were cut from the gel and incubated for 30 min in cathodic buffer (50 mM Tricine, 15 mM Bis-Tris, 0.1 % [w/v] Coomassie 250 G, pH 7 [adjusted at 4°C]) and transferred into the chambers of an electroeluter (C.B.S. SCIENTIFIC, Del Mar, USA). The gel pieces containing the POD isoenzymes were filled into the electroeluter containing elution buffer (25 mM Tricine, 7.5 mM Bis-Tris, pH 7.0 [adjusted at 4°C]). Electroelution was carried out for 5 h and 4°C at 350 V and 6 to 10 mA, using dialysis membranes (Medicell, Kleinfeld) with a MWCO of 12 to 14 kDa under constant buffer circulation (Econopump, BioRad Laboratories, CA, USA). Until further characterization eluates were stored at -80°C.

Determination of the pH optimum of the guaiacol-peroxidase and NADH-peroxidase activity of POD isoenzymes

For guaiacol-peroxidase measurements 6 µl eluate was mixed with guaiacol (20 mM) in 0.1 M succinate buffer with the pH values 5, 5.5, 6, 6.5, and 7. The reaction was started by adding 0.3% (v/v) H₂O₂. The increase in absorption was measured at $\lambda = 470$ nm using a Microplate Reader. For calculation of enzyme activities the molar extinction coefficient 26.6 L (mmol cm)⁻¹ was used.

NADH-peroxidase activity measurements were made by combining MnCl₂, *p*-coumaric acid, and NADH in final concentrations of 16 mM, 1.6 mM and 0.66 mM, respectively, with 7.5 µl protein eluate in 0.1 M succinate buffer (as described above). The decline in absorption was

⁵ Electroelution of specific POD isoenzymes for further physiological characterization was done in collaboration with Prof. Dr. Hans-Peter Braun, Institute of Plant Genetics, Leibniz University Hannover, Herrenhäuser Str. 2, 30419 Hannover

determined using a Microplate Reader at $\lambda = 340$ nm. For calculation of enzyme activities the molar extinction coefficient $1.13 \text{ L (mmol cm)}^{-1}$ was used.

Determination of cofactor specificity for NADH-*peroxidase* activity of POD isoenzymes

The same experimental setup as for the determination of the pH optimum was followed using succinate buffer (pH 5.5). *p*-Coumaric acid was substituted with benzoic acid, caffeic acid, chlorogenic acid, ferulic acid, gallic acid, protocatechuic acid, syringic acid, vanillic acid, and *p*-hydroxybenzoic acid in four different concentrations (1.66 mM, 0.166 mM, 0.0166 mM, and 0.00166 mM) in the measuring solution. In order to simplify this report benzoic acid as aromatic carboxylic acid is termed as phenolic acid, too. For each phenol concentration specific extinction coefficients were determined and used for enzyme activity calculation (see Tab. S1).

Determination of changes in NADH-*peroxidase* activity of POD isoenzymes as affected by combining different phenols with *p*-coumaric acid

To detect the effects of different phenols on *p*-coumaric acid-stimulated NADH-*peroxidase* activity of different isoenzymes separated by BN-PAGE 0.166 mM *p*-coumaric acid was combined with benzoic acid, caffeic acid, chlorogenic acid, ferulic acid, gallic acid, protocatechuic acid, syringic acid, vanillic acid, and *p*-hydroxybenzoic acid each in a concentration of 0.0166 mM. All other factors were kept as described for the measurement of cofactor specificity. Activity was expressed as percentage of *p*-coumaric acid induced NADH-*peroxidase* activity. For each phenol concentration specific extinction coefficients were determined and used for enzyme activity calculation (see Tab. S1).

Mass spectrometric protein analysis and data interpretation⁶

Marked BN-PAGE bands stained for guaiacol-peroxidase activity were cut and dried under vacuum. In-gel digestion was performed with an automated protein digestion system, MassPREP Station (Micromass, Manchester, UK). The gel slices were washed three times in a mixture containing 25 mM NH_4HCO_3 : acetonitrile [1:1, v/v]. The cysteine residues were reduced by 50 μl of 10 mM dithiothreitol at 57 °C and alkylated by 50 μl of 55 mM iodacetamide. After dehydration with acetonitrile, the proteins were cleaved in the gel with 40 μl of 12.5 ng μl^{-1} of modified porcine trypsin (Promega, Madison, WI, USA) in 25 mM NH_4HCO_3 at room temperature for 14 hours. The resulting tryptic peptides were extracted with 60% acetonitrile in 0.5% formic acid, followed by a second extraction with 100% (v/v) acetonitrile.

Nano-LC-MS/MS analysis of the resulting tryptic peptides was performed using using an Agilent 1100 series HPLC-Chip/MS system (Agilent Technologies, Palo Alto, USA) coupled to an HCT Ultra ion trap (Bruker Daltonics, Bremen, Germany). Chromatographic separations were conducted on a chip containing a Zorbax 300SB-C18 (75 μm inner diameter \times 150 mm) column and a Zorbax 300SB-C18 (40 nL) enrichment column (Agilent Technologies).

HCT Ultra ion trap was externally calibrated with standard compounds. The general mass spectrometric parameters were as follows: capillary voltage, -1750V; dry gas, 3 liters min^{-1} ; dry temperature, 300 °C. The system was operated with automatic switching between MS and MS/MS modes using. The MS scanning was performed in the standard-enhanced resolution mode at a scan rate of 8,100 m/z per second with an aimed ion charge control of 100,000 in a maximal fill time of 200 ms and a total of 4 scans were averaged to obtain MS spectrum. The three most abundant peptides and preferentially doubly charged ions were selected on each MS spectrum for further isolation and fragmentation. The MS/MS scanning was performed in the ultrascan resolution mode at a scan rate of 26,000 m/z per second with an aimed ion charge control of 300,000 and a total of 6 scans were averaged to obtain MS/MS spectrum. The complete system was fully controlled by ChemStation Rev. B.01.03 (Agilent Technologies) and EsquireControl 6.1 Build 78 (Bruker Daltonics) softwares. Mass data collected during LC-MS/MS analyses were processed using the software tool DataAnalysis

⁶ Mass spectrometric protein analysis and data interpretation was done in collaborations with Dr. Dimitri Heintz, Institut de Biologie Moléculaire des Plantes (IBMP) CNRS-UPR2357,ULP, 67083 Strasbourg, France, and Prof. Dr. Alain Van Dorsselaer and Sébastien Gallien, Laboratoire de Spectrométrie de Masse Bio-Organique, IPHC-DISA, ULP, CNRS, UMR7178; 25 rue Becquerel, 67 087 Strasbourg, France

3.4 Build 169 and converted into *.mgf files. The MS/MS data were analyzed using the MASCOT 2.2.0. algorithm (Matrix Science, London, UK) to search against a in-house generated protein database composed of protein sequences of Viridiplantae downloaded from <http://www.ncbi.nlm.nih.gov/sites/entrez> (on March 6, 2008) concatenated with reversed copies of all sequences ($2 \times 478,588$ entries). Spectra were searched with a mass tolerance of 0.5 Da for MS and MS/MS data, allowing a maximum of 1 missed cleavage by trypsin and with carbamidomethylation of cysteines, oxidation of methionines and N-terminal acetylation of proteins specified as variable modifications. Protein identifications were validated when at least two peptides with high quality MS/MS spectra (Mascot ion score greater than 31) were detected. In the case of one-peptide hits, the score of the unique peptide must be greater (minimal “difference score” of 6) than the 95% significance Mascot threshold (Mascot ion score >51). For the estimation of the false positive rate in protein identification, a target-decoy database search was performed (Elias and Gygi, 2007).

GC-MS-based metabolite profiling⁷

For GC-MS analysis, polar metabolite fractions were extracted from 60 mg \pm 10 % (FW) frozen plant material, ground to a fine powder, with methanol/chloroform. The fraction of polar metabolites was prepared by liquid partitioning into water/methanol (polar fraction) and chloroform (non-polar fraction) as described earlier (Roessner et al., 2000; Wagner et al., 2003). Metabolite samples were derivatized by methoxyamination, using a 20 mg ml⁻¹ solution of methoxyamine hydrochloride in pyridine, and subsequent trimethylsilylation, with N-methyl-N-(trimethylsilyl)-trifluoroacetamide (Fiehn et al., 2000; Roessner et al., 2000). A C₁₂, C₁₅, C₁₉, C₂₂, C₂₈, C₃₂, and C₃₆ n-alkane mixture was used for the determination of retention time indices (Wagner et al., 2003). Ribitol and deuterated alanine were added for internal standardization. Samples were analyzed using GC-TOF-MS (ChromaTOF software, Pegasus driver 1.61; LECO, <http://www.leco.com>). 4 sample types (-/+ Mn and -/+ Si), each with 5 replicates, comprised an experimental data set of 20 chromatograms. The chromatograms and mass spectra were evaluated using the TagFinder software (Luedemann et al., 2008).

⁷ GC-MS analyses of samples were done in collaboration with Dr. Joachim Kopka and Alexander Erban, Max-Planck-Institute of Molecular Plant Physiology, Am Mühlenberg 1, 14476 Potsdam-Golm

Sample preparation for the metabolite profiling of the AWF was adapted to the respective volumes and metabolite concentrations. In this case 200 μl of $\text{AWF}_{\text{H}_2\text{O}}$ and AWF_{NaCl} were extracted to obtain a polar metabolite fraction, without further addition of water. The volume of methanol/chloroform was reduced to 50% as were the reagents for methoxyamination and silylation. Four sample types (two Mn treatments, and two Si treatments), each with four to five replications, in total 35 chromatograms, were analyzed as described above.

In parallel free phenols (in the following termed non-polar apoplastic fraction) were extracted from $\text{AWF}_{\text{H}_2\text{O}}$ and AWF_{NaCl} . First AWF was alkalized with 0.5 N NaOH (ratio 1:1) overnight. Afterwards samples were acidified by adding 5 N HCl (ratio 0.1125:1). Phenols were then extracted by shaking with diethylether (ratio 1:1). Samples were then dried under nitrogen atmosphere and prepared for GC-MS analysis as described for AWF. Four sample types (two Mn treatments and two Si treatments), each with five to six replications, resulted in 48 chromatograms, which were processed as described.

GC-MS metabolite profiles were processed after conversion into NetCDF file format using the TagFinder (Luedemann et al., 2008) and NIST05 software (<http://www.nist.gov/srd/mslist.htm>). The mass spectral and retention index (RI) collection of the Golm metabolome database (Kopka et al., 2005; Schauer et al., 2005) was used for manually supervised metabolite identification. Yet non-identified metabolic components were disregarded for the present study. Peak height representing a mass specific arbitrary detector response was used for screening the relative changes of metabolite pools. The initial mass specific responses were normalized by leaf fresh weight and ribitol recovery. AWF metabolite profiles were normalized to ribitol recovery and AWF total volume of partitioned polar (water/methanol) and non-polar (chloroform) AWF fractions.

Statistical analysis of GC-MS profiles

Prior to statistical data assessment response ratios were calculated based on the mean response of each metabolic feature from all samples of an experimental data set. Response ratios were subsequently \log_{10} -transformed. Independent component analysis (ICA) and missing value substitution was as described earlier (Scholz et al., 2005). ICA was carried out using the first 5 principal components obtained from a set of manually identified metabolites represented by at least 3 specific mass fragments each. Basic calculations of relative changes in abundance of specific metabolites due to Mn and Si treatment were made with the

Microsoft Excel 2000 software program and respective embedded algorithms. For pairwise comparisons thresholds of 2-fold change in pool size and $P < 0.05$ (t test,) were applied or levels of significance indicated, namely ***, **, and * representing $p < 0.001$, 0.01, and 0.05, respectively. Logarithmic transformation of response ratios approximated required Gaussian normal distribution of metabolite profiling data (Schaarschmidt et al., 2007).

Statistical analysis Mn and Si concentrations and apoplastic enzyme activities

Statistical analysis, if not mentioned otherwise, was carried out using SAS Release v8.0 (SAS Institute, Cary, NC). Results from analysis of variance are given according to their level of significance as ***, **, and * for $p < 0.001$, 0.01, and 0.05, respectively. Pairwise comparisons were by using Student's t test.

Results

Exposing the plants to 50 μM Mn supply rapidly increased the Mn tissue concentration in the second oldest trifoliolate leaf over the four days treatment period (Fig. 1A). This led to typical Mn toxicity symptoms (brown spots) after 2 days increasing up to 70 spots cm^{-2} after 4 d of Mn treatment (Fig. 1B). Silicon supply did not affect leaf Mn accumulation (Fig. 1A). However, in contrast to plants cultivated without Si, Si-treated plants developed only slight Mn toxicity symptoms (2-5 spots cm^{-2}) after 4 d of Mn treatment (Fig. 1B).

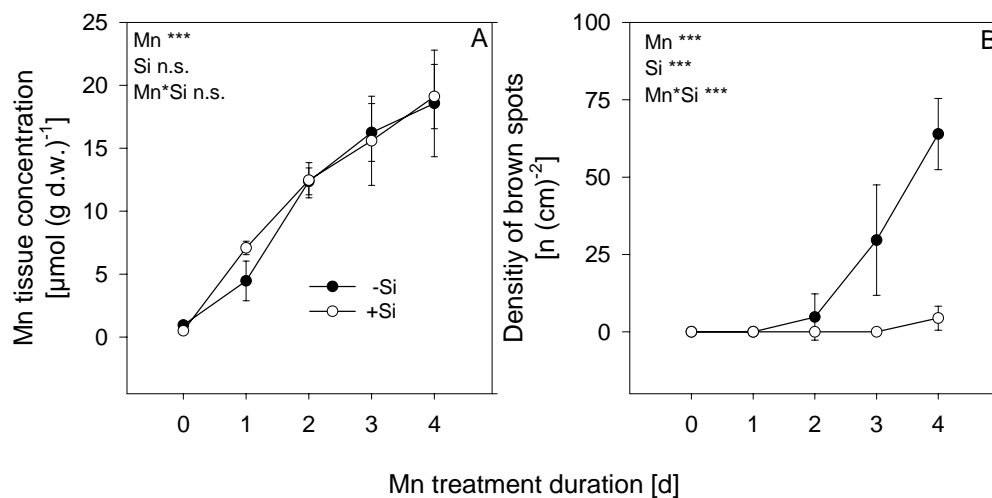


Fig. 1: Effect of Mn treatment duration and Si supply on (A) the Mn tissue concentration and (B) the density of brown spots of the second oldest trifoliolate leaves of the Mn-sensitive cowpea cultivar TVu 91. After 2 weeks of preculture at 0.2 μM Mn the Mn supply was increased to 50 μM for four days. Silicon was supplied throughout plant culture. Results of the analysis of variance are given according to their level of significance as ***, ** or * for $P < 0.001$, 0.01, 0.05, respectively. Values are means \pm SD with $n = 16$.

Since our previous work indicated a particular role of the apoplast in the expression of Mn toxicity and Mn tolerance in cowpea, we focused our studies particularly on the AWF. In this study we submitted the leaves to a fractionated AWF extraction procedure yielding a free water-soluble ($\text{AWF}_{\text{H}_2\text{O}}$) and an ionically bound NaCl-extractable (AWF_{NaCl}) fraction. The Mn concentration in the $\text{AWF}_{\text{H}_2\text{O}}$ increased rapidly after 1 day of toxic Mn supply and then it tended to decrease again (Fig. 2A). Silicon application consistently enhanced the monomeric Si concentration in the $\text{AWF}_{\text{H}_2\text{O}}$ (Fig. 2B) compared with non Si-treated plants without consistently affecting the apoplastic Mn concentration (Fig. 2A). In the AWF_{NaCl} the Mn concentration of the second trifoliolate leaf steeply increased after one day Mn treatment and remained stable at a higher level than in the $\text{AWF}_{\text{H}_2\text{O}}$ (Fig. 2C). In Si-treated plants the Mn

concentrations were slightly higher. Silicon treatment enhanced the monomeric Si concentration (Fig. 2D), but with Mn treatment duration this difference disappeared.

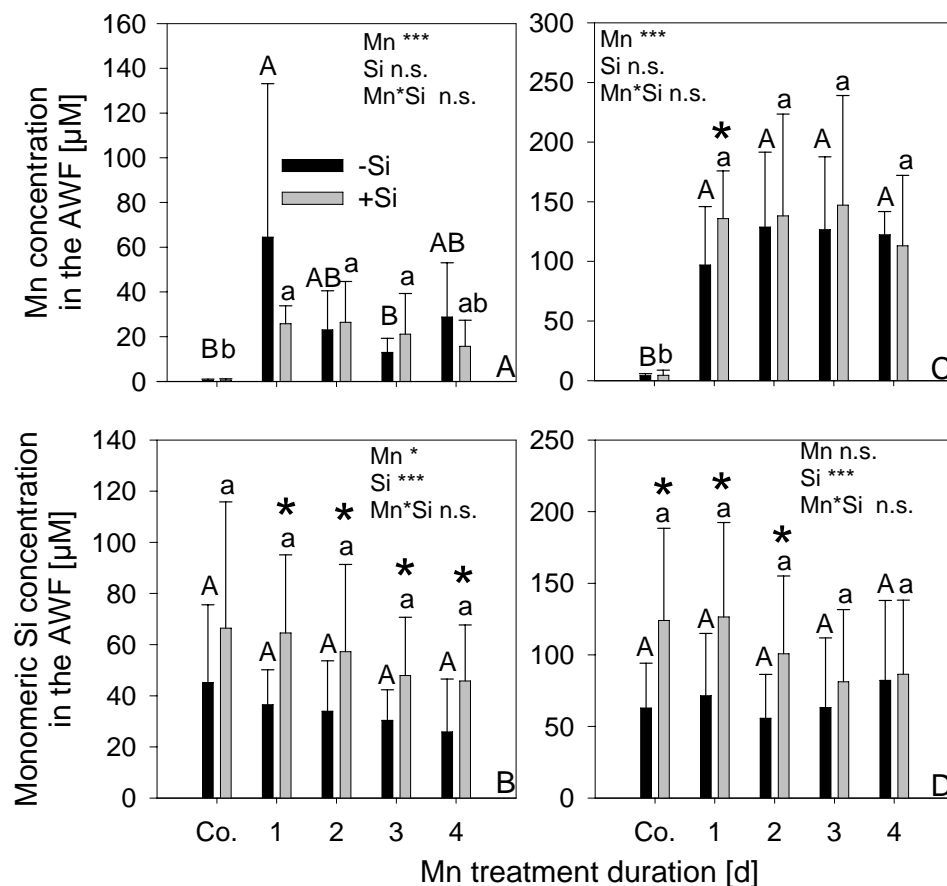


Fig. 2: Effect of Mn treatment duration and Si supply on the Mn concentration (A,C) and the monomeric Si concentration (B,D) in the water-soluble apoplasmic fraction (A,B), and in the ionically bound apoplasmic fraction (C,D) of the second oldest trifoliolate leaves of the Mn-sensitive cowpea cultivar TVu 91. After 2 weeks of preculture at $0.2 \mu\text{M}$ Mn, the Mn supply was increased to $50 \mu\text{M}$ for four days. Silicon was supplied throughout plant culture. Results of the analysis of variance are given according to their level of significance as ***, ** or * for $P < 0.001$, 0.01 , 0.05 , respectively. Upper case and lower case letters indicate significant differences between Mn treatment duration of -Si and +Si-treated plants, respectively, at $P < 0.05$. * on top of the columns indicate significant differences between the Si treatments for at least $P < 0.05$ according to Tukey. Values are means \pm SD with $n = 16$.

In order to demonstrate the capability of the POD isoenzymes to catalyze both H_2O_2 -producing and consuming POD activities AWF_{NaCl} was separated by BN-PAGE and PODs in-gel stained first for NADH-*peroxidase* followed by staining for guaiacol-*peroxidase* activity (Fig. 3A, B). Despite the quite low NADH-*peroxidase* activity staining-intensity the gels revealed that each isoenzyme showed both activities. Staining with guaiacol visualized major isoenzymes more clearly: one isoenzyme smaller than P1 and 4 isoenzymes greater than P1,

all with low activity levels (Fig. 3B). After six days of Mn treatment, three additional guaiacol-peroxidase bands appeared around greater than the P6 isoenzyme and one with a MW smaller than P1. One isoenzyme with a MW greater than P1 disappeared owing to elevated Mn supply. An extensive study of in-gel activity-stained BN gels loaded rigorously with the same protein quantities comparing Mn treatments with and without Si supply and differentiating between AWF_{H_2O} and AWF_{NaCl} proteins revealed that all isoenzymes were qualitatively present in both Mn treatments, but elevated Mn supply led to an increased abundance of especially isoenzymes P3 and P5 in the water-soluble fractions (Figs. S1 and S2). In Mn-control plants Si-treatment did not affect the POD isoenzyme pattern. Silicon delayed but not suppressed the Mn-mediated increase in the number of POD isoenzymes in the AWF_{H_2O} (Fig. S1).

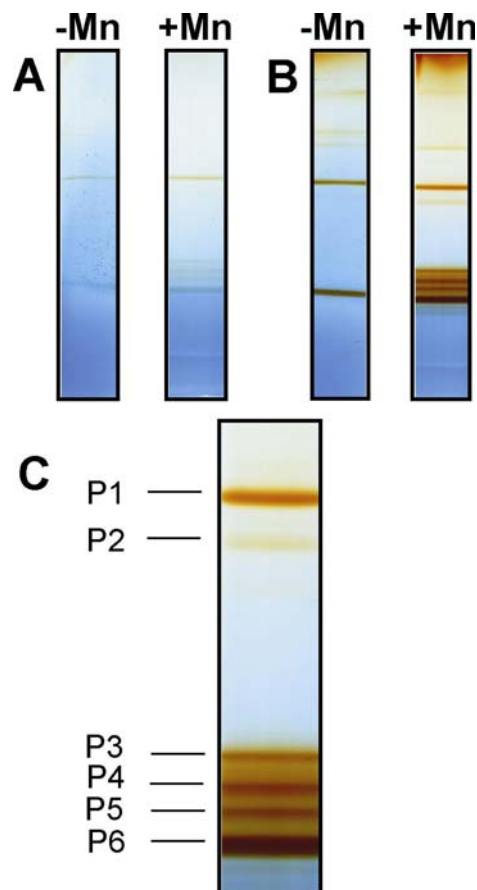


Fig. 3: AWF_{NaCl} -proteins of the second oldest trifoliolate leaf of the Mn-sensitive cultivar TVu 91 stained for (A) NADH-*peroxidase* and (B) guaiacol-*peroxidase* activity after separation by BN-PAGE. After preculture with 0.2 μ M Mn (-Mn) for 14 d, plants received 50 μ M (+Mn) Mn for 6 d. Fifty μ l of concentrated AWF_{NaCl} containing ionically bound proteins (-Mn 60 μ g, +Mn 112 μ g) were loaded onto the gels. Proteins were NBT stained for NADH-*peroxidase* (A) at pH 5.0 with 16 mM $MnCl_2$, 1.66 mM *p*-coumaric acid, 0.625 mg ml^{-1} NBT and 0.22 mM NADH. For Guaiacol-*peroxidase*, proteins were stained (B) in 18 mM guaiacol (in 9 mM Na_2HPO_4) and 0.03% H_2O_2 at pH 6.0. Close up (C) shows marked isoenzymes (P1, P3, P5, P6) that were chosen for elution and further characterization of pH optima and substrate specificity.

Fig. 3C shows a close-up of those POD isoenzymes (clearly appearing after 4 d of Mn treatment), which were chosen for further characterization after elution of the proteins from the gels: P1, P3, P5, and P6, whereas P2 and P4 were only sequenced. The eluted isoenzymes P3, P5, and P6, showed both NADH-*peroxidase* and guaiacol-*peroxidase* activities (Fig. 4A, B). The specific activity was highest for P6 followed by P5. The POD isoenzyme P1 had very little guaiacol-*peroxidase* activity. The pH optimum for all isoenzymes showing activity was consistently 6.5 for guaiacol-*peroxidase* activity (Fig. 4A) and pH 5.5 for NADH-*peroxidase* activity (Fig. 4B).

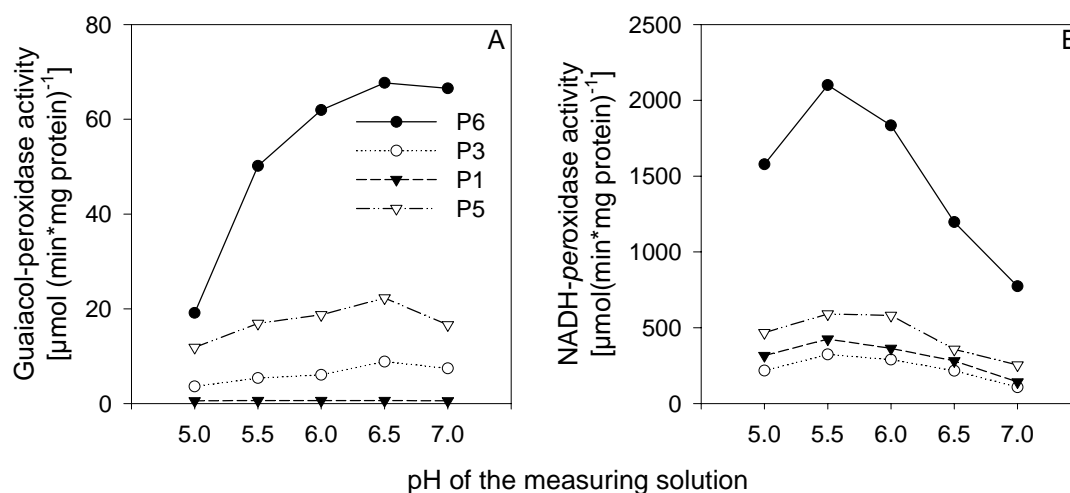


Fig. 4: Determination of the pH optimum of (A) the guaiacol-*peroxidase* activity and of (B) the NADH-*peroxidase* activity of four POD isoenzymes of the Mn-sensitive cowpea cultivar TVu 91. POD isoenzymes were eluted from BN gels that separated a mixture of AWF_{H₂O} and AWF_{NaCl} extracted from the second oldest trifoliolate leaf of Mn-treated (4 d) and ±Si treated (as described in “Materials and Methods”) plants. Measurements were done in succinate buffer with pH values between 5.0 and 7.0 using 0.5 steps between the pH values. Measuring solution (0.1 M succinate buffer) for the determination of NADH-*peroxidase* activity consisted of 16 mM MnCl₂, 1.66 mM *p*-coumaric acid, and 0.22 mM NADH, measuring solution for guaiacol-*peroxidase* activity consisted of 18 mM guaiacol (in 90 mM succinate buffer) and 0.03% H₂O₂.

All marked POD activity-stained protein bands (Fig. 3) were cut; proteins were digested and analyzed by liquid chromatography-coupled mass spectrometry (LC-MS/MS). MS/MS searches did not always lead to a positive identification in cowpea (*Vigna unguiculata*) since its genome has not yet been sequenced, but can lead to the identification of peptides in related sequences of green plants (Viridiplantae) downloaded from <http://www.ncbi.nlm.nih.gov/sites/entrez>. Forty-four unique proteins were identified in green plants database. To estimate false positive rate of identification, a target-decoy database was performed (Elias and Gygi, 2007), and no additional protein was identified in reversed

sequences suggesting that our dataset contained very few or no false-positive identifications. A list of all resulting peptides as well as their identities is given as supplementary material (Tab. S2). Among these peptides eleven peptides belonging to class III peroxidases could be identified (Fig. 5). At least three overlapping peptides provide evidence for at least three distinct gene products. Three peptides with amino acid substitutions were exclusively found in POD isoenzyme P1 when extracted with NaCl from Mn-treated plants (Figs. 3 and 5, Tab. S2).

		c1	
		1	60
FBP 1	(1)	-----VVGVVIGALPFSSDAQLDPSFYRNTCPVSVHSIVREV	
P 49 (A. t.)	(1)	-----MARLTSFLLLSLICFVPLCLCDKSYGGKLFPGYYAHSCPQVNEIVRSV	
PPOD	(1)	-----MGSAKFFVTLICIVPLLASSFCSAQLSATFYASTCPNLQTVIRNA	
VvPOD	(1)	-----MASHHSSSSVFTFKLCFCLLLSFIGMASAQLTTNFYAKTCPNALSIIKSA	
VaPOD	(1)	MASISSNKNAIFSFLLLSIILSVSVIKVCEAQRPPVTRGLSYTFYSKTCPTLKSIVRTE	
P 45 (A. t.)	(1)	-----MEKNTSQTIFFSNFLLLSLSSCVSAQLRTGFYQNSCPNVETIVRNA	
SoPOD	(1)	-----IIILAYLACLSNAQLSSKHAYSSCPNLEKIVRKT	
SiPOD	(1)	-----MGQSSFLMTLFTLSLGVIVFSGSVSAQLKQNYANI CPDVENIVRQA	
MsPOD	(1)	-----MGR-YNVILVWSLALTCLIPYTTFAQLSPNHAYNICPNVQSVIRSA	
VuPOD		-----	
		i Hdc2 c3 *****	
		61	120
FBP 1	(37)	IRNVSKSDPRMLASLIRLHFHDFVQGCDAIILLNNTDTIVSEQEALPNIN-SIRGLDVV	
P 49 (A. t.)	(50)	VAKAVARETRMAASLLRHLHFHDFVQGCDSLLLDSSGRVATEKNSNPNSK-SARGFDVV	
PPOD	(45)	MTGAVNGQPRLAASILRHLHFHDFVNGCDGSIILLDDTATFTGEKNANPNRN-SARGFEVI	
VvPOD	(53)	VNSAVKSEARMGASLLRHLHFHDFG--CDASILLDDTSNFTGEKTAGPNAN-SVRGYEVV	
VaPOD	(61)	LKKVFQSDIAQAAGLLRHLHFHDFVQGCDSVLLDGSASGSPSEKDAPPNLTLRAEAFRII	
P 45 (A. t.)	(47)	VRQKFQQTFTVPATLRLHFHDFVRCDAIIMIASP----SERDHPDDMSLAGDGFDTV	
SoPOD	(34)	MKQAVQKEQRMGASILRHLHFHDFVNGCDASLLLDSTFTGEKTAISNRNNSVARGFEVI	
SiPOD	(48)	VTAKFKQTFVTPATLRLYFHDFVSGCDASVI IASTPGNTAEKDHDPNLSLAGDGFDTV	
MsPOD	(47)	VQKKFQQTFTVPATLRLYFHDFVQGCDAIIVASSGNNAEKDHPENLSLAGDGFDTV	
VuPOD		-----MGASILR-----DHPDNLSLAGDGFDTV	
			GYEVV GFEVI
		c4 c5 II *****	
		121	180
FBP 1	(96)	NQIKTAVEN--ACPGVVCADILTLAAEISSVLAQGPDKWVPLGRKDSL-TANRTLANQN	
P 49 (A. t.)	(109)	DQIKAELEK--QCPGTVSCADVLTLAARDSSVLTGGPSWVPLGRRDSR-SASLSQSNNN	
PPOD	(104)	DTIKTRVEA--ACNATVSCADILALAARDGVVLLGGPSWTVPLGRRDAR-TASQSAANSQ	
VvPOD	(110)	DTIKSQLEA--SCPGVVCADILVAARDSVVALRGPSWVRLGRRDST-TASLSAANSN	
VaPOD	(121)	ERIRGLLEK--SCGRVVCSDITALAARDAVFLSGGPDYEIPLGRRDGLTFASRQVTLDN	
P 45 (A. t.)	(103)	VKAKQAVDSNPNCRNKVCADILALATREVVVLTGGPSYPVELGRRDGR-ISTKASVQSQ	
SoPOD	(94)	DSIKTNVEA--SCKATVSCADILALAARDGVFLLGGPSWKVPLGRRDAR-TASLTAATNN	
SiPOD	(108)	IKAKAAVDAVPRCRNKVSCADILALATRDVINLAGGPSYPVELGRLDGL-KSTAASVNGN	
MsPOD	(107)	IKAKAALDAVPOCRNKVSCADILALATRDVINLAGGPSYTVELGRFDGL-VSRSSDVNGR	
VuPOD		IK-----VSCADILALATR-----FDGL-VSR-----	
		DTIK	
		DTIK	
		III hp c6 *****	
		181	240
FBP 1	(153)	LPAPFFNLTLLKAAFVAVQGLNNTDLVALSGAHTFGRAQCSTFVNRLYNFSNTGNPDPPTLN	
P 49 (A. t.)	(166)	IPAPNNTFQTIILSKFNROGLDITDLVALSGSHTIGFSRCTSFRQRLYNQSGNGSPDMTLE	
PPOD	(161)	IPSPASSLATLISMFSAKGLSAGDMTALSGGHTIGFARCTTFRNRIYN-----DTNID	
VvPOD	(167)	IPAPTLNLSGLISAF TNKGFNAREMVALSGSHTIGQARCTTFRTRIYN-----EANID	
VaPOD	(179)	LPPPSNNTTILNSLATKNLDPTDVVLSGGHTIGISHCSSFNRLYP-----TQDPVMD	
P 45 (A. t.)	(162)	LPQPEFNLNQNGMFSRHGLSQTDMIALSAGHTIGFAHCGKMSKRIYNFSPTRIDPSIN	
SoPOD	(151)	LPPASSLSNLTTLFNNKGLSPKDMTALSGAHTIGLARCVSFRHHIYN-----DTDID	
SiPOD	(167)	LPQPTFNLDQLNKMFAASRGLSQADMIALSAGHTLGFSHCSKFSNRIYNFSRQNPVDPPTLN	
MsPOD	(166)	LPQPSFNLNQNLTLFANNGLTQTDMIALSAGHTSGFSHCDRFSNRIQ----T-PVDPTLN	
VuPOD		-----	

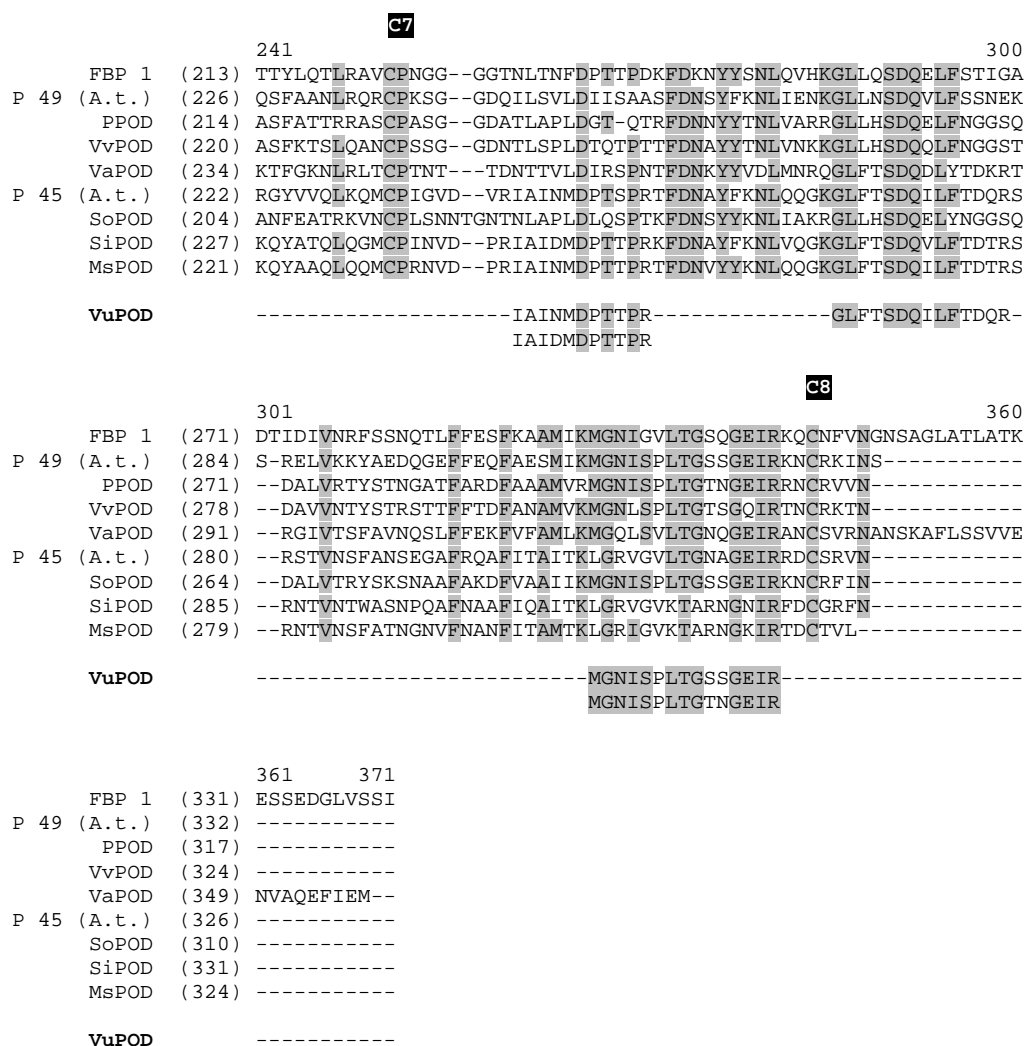


Fig. 5: Alignment of determined and deduced amino acid (aa) sequences of peroxidases of various plant species and all eleven nano LC-MS/MS-identified peroxidase peptide sequences from cowpea. Amino acid positions conserved in at least 50% of the sequences are underlayed in gray. Stars (*) indicate the conserved distal heme-binding domain (I), the central conserved domain of unknown function (II), and the proximal heme binding domain. The eight cysteines (C1-C8) and the distal (Hd) and proximal (Hp) histidines are indicated, too. Abbreviations: FBP1 French Bean Peroxidase 1 (Acc no.: AF149277), P49 (A.t.) POD isoenzyme 49 from *Arabidopsis thaliana* (Acc. no. O23237), PPOD from *Populus ssp.* (Acc. no.: AAX53172), VvPOD from *Vitis vinifera* (Acc. no.: CAO48839), VaPOD from *Vigna angularis* (Acc. no.: BAA01950), P45 (A.t.) POD isoenzyme 45 from *Arabidopsis thaliana* (Acc. no. Q96522), SoPOD from *Spinacia oleracea* (Acc. no.: CAA71493), SiPOD from *Sesamum indicum* (Acc. no.: ABB89209), MsPOD from *Medicago sativa* (Acc. no.: CAC38106), VuPOD POD peptide sequences of *Vigna unguiculata* (this study).

Since apoplasmic NADH-peroxidase proved to react most sensitively to toxic Mn supply and this enzyme has been attributed a key role in the expression of Mn toxicity (Fecht-Christoffers et al., 2006, 2007), we further characterized the NADH-peroxidase activity of the isoenzymes for interaction with different commercially available phenols (Fig. 6) at the optimum pH

identified above with *p*-coumaric acid and Mn as a cofactors. Among the ten phenols tested, *p*-coumaric acid and vanillic acid proved to be the most effective cofactors for all isoenzymes particularly at the highest concentration level. Benzoic acid showed only little activity at the higher concentrations even though the response pattern was similar, whereas ferulic acid activated NADH-*peroxidase* activity only at a lower concentration. All other phenols did not induce NADH-*peroxidase* activity. As shown above (Fig. 4A, B) the isoenzyme P6 showed by far the highest activity.

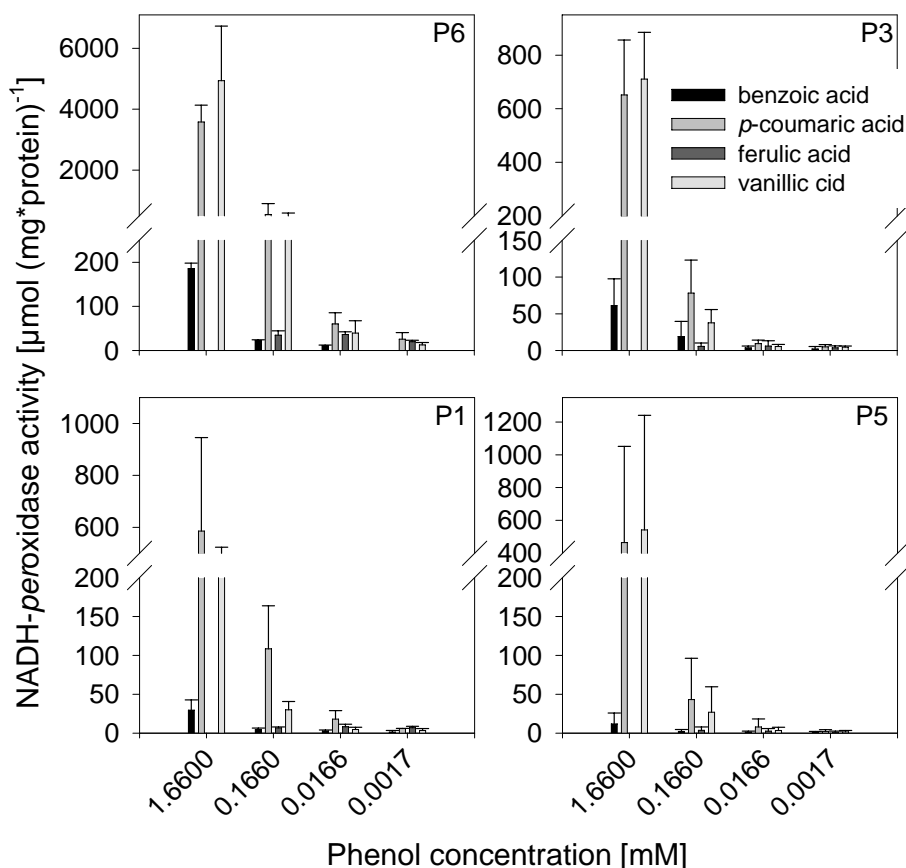


Fig. 6: Effect of different phenols on NADH-*peroxidase* activity of four POD isoenzymes. POD isoenzymes were eluted from BN-gels (see Fig. 4 and “Materials and Methods”). Measuring solution (0.1 M succinate buffer, pH 5.5) consisted of 16 mM MnCl₂, 0.22 mM NADH and phenols (benzoic acid, *p*-coumaric acid, ferulic acid, caffeic acid, chlorogenic acid, gallic acid, protocatechuic acid, syringic acid, and vanillic acid) in different concentrations (1.6 mM, 0.166 mM, 0.016 mM and 0.0016 mM). Only the four displayed phenols induced NADH-*peroxidase* activity. For calculation of enzyme activities, extinction coefficients were adapted (Supplementary material Tab. S1). Results are from two independent experiments including plant growth and protein separation.

The potential inhibitory effect of phenols on NADH-*peroxidase* activity was studied by adding eight phenols to the reaction mixture monitoring their effect on *p*-coumaric acid-stimulated enzyme activity (Fig. 7). Benzoic acid and vanillic acid did not reduce the *p*-

coumaric acid-stimulated NADH-*peroxidase* activity and even enhanced it. All other phenols inhibited NADH-*peroxidase* activity by about 50% (ferulic and syringic acid) and by > 90% for the other phenols. This was true for all isoenzymes.

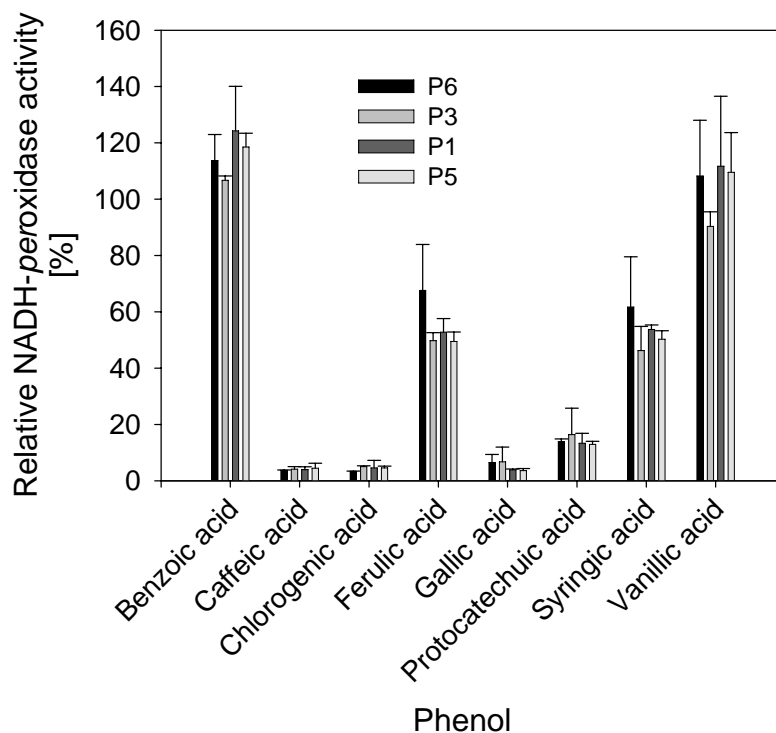


Fig. 7: Effect of combining different phenols with *p*-coumaric acid as control phenol on the induction capability for NADH-*peroxidase* activity of four POD isoenzymes. POD isoenzymes were eluted from BN gels (see Fig. 3 and Materials and Methods). Measuring solution (0.1 M succinate buffer, pH 5.5) consisted of 0.166 mM *p*-coumaric acid, 16 mM MnCl₂, 0.22 mM NADH and 0.0166 mM of one of the following phenols to examine interactions between phenols: benzoic acid, ferulic acid, caffeic acid, chlorogenic acid, gallic acid, protocatechuic acid, syringic acid or vanillic acid. Activities are expressed as relative values in relation to activities when *p*-coumaric acid was applied alone (in the same concentration). For calculation of enzyme activities, extinction coefficients were adapted (Supplementary material Tab. S1). Results are from two independent experiments including plant growth and protein separation.

Since metabolites were shown to strongly affect apoplastic PODs (see above and Fecht-Christoffers et al., 2006) we studied in a broad range approach the bulk-leaf metabolome using GC-MS and independent component analyses (ICA) (Scholz et al., 2004). Applying ICA we investigated sample clusters according to the major variances due to the treatment-induced qualitative and quantitative changes of metabolite pools. This variance criterion was augmented by subsequent pairwise or multiple probability-based statistical significance testing.

In our factorial experimental designs both Mn and Si treatment proved to be among the most important independent components (Fig. 8A) of our data sets resulting from the bulk-leaf tissue. The analysis revealed that Mn (IC01) and Si (IC04) treatments induced significant changes in the metabolome. Silicon treatment clearly induced significant conditional differences among the Mn control treatment but only slight differences in Mn-treated plants. The Mn effect was mainly caused by changes in the concentrations of amino acids (serine, threonine, asparagine, aspartic acid), phenylalcohols (coniferylalcohol), organic acids (gluconic acid), and sugar alcohols (sorbitol) as revealed by ICA loadings. The Si effect was mainly due to differences in sugars (galactose) and organic acids (gluconic acid).

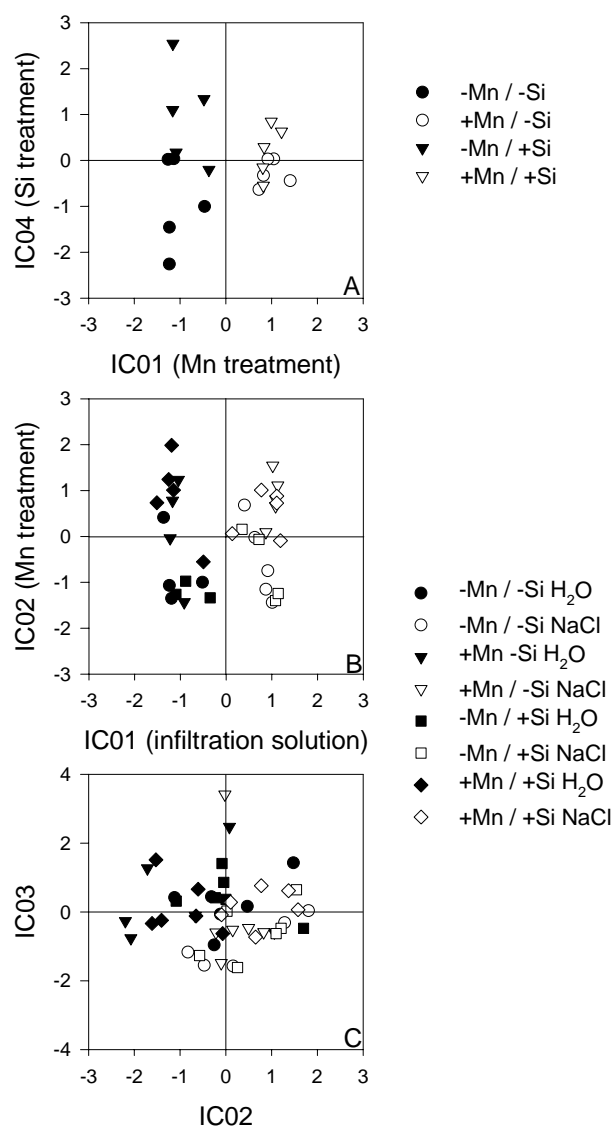


Fig. 8: ICA plot of the GC-MS-accessible (A) bulk-leaf metabolome, (B) the polar AWF metabolites, and (C) the non-polar metabolites extracted from the AWF. The second oldest trifoliolate leaf of the Mn-sensitive cultivar TVu 91 was tested for Mn- and Si- effects. After 14 d of preculture with or without Si plants received 50 μM Mn (+Mn) for 3 d or 0.2 μM Mn (-Mn) continuously. Bulk-leaf, AWF- and non-polar apoplastic metabolites were extracted (n=5 and 6, respectively) as described in "Materials and Methods". ICA was conducted using MetaGeneAlyse at <http://metagenealyse.mpimp-golm.mpg.de>.

In view of the particular role of the activity of apoplastic peroxidases in Mn toxicity additionally the $\text{AWF}_{\text{H}_2\text{O}}$ and the AWF_{NaCl} were subjected to a metabolomic analysis. The ICA showed clear differences between the AWF fractions (IC01, Fig. 8B). Also, manganese treatment induced separate clustering in both AWF fractions (IC02). In this approach Si did not affect the sample clustering according to treatment-mediated metabolite differences. As revealed by ICA loadings, metabolites mainly responsible for the differential clustering of $\text{AWF}_{\text{H}_2\text{O}}$ and AWF_{NaCl} were GABA, organic acids (malic acid, ribonic acid, gluconic acid), amino acids (threonine), and sugars (xylose, erythrose, fucose) among many currently not identified metabolites. The clustering according to the Mn treatment was mainly caused by organic acids (maleic acid, malic acid, nicotinic acid, itaconic acid), amino acids (threonine, alanine), sugars (xylose, fructose, tagatose) and phenols (3-hydroxybenzoic acid).

Further fractionation of the leaf apoplastic metabolome by an extraction method specifically yielding non-polar metabolites revealed a clustering of samples according to the infiltration solution confirming the strong experimental impact of the AWF fraction on the result (Fig. 8C). Loadings derived from ICA showed that among other currently unknown metabolites mainly organic acids (fumaric acid, malic acid, succinic acid, citric acid, 3-oxoglutaric acid) and phenylpropanoids (*cis*- and *trans*-cinnamic acid, *p*-hydroxybenzoic acid) were responsible for this clustering.

Quantification of relative changes between treatments yielded five different phenols in this non-polar extract (Tab. 1) among them ferulic acid, *p*-hydroxybenzoic acid, and *p*-coumaric acid which had shown considerable inhibiting or enhancing effects, respectively, on *in-vitro* NADH-*peroxidase* activity. Ferulic acid and *p*-coumaric acid were analytically separated into respective *cis*- and *trans*-isomers, whereas in the *in-vitro* NADH-*peroxidase* activity-enhancing/inhibiting tests (Figs. 6 and 7) commercially available isomer mixture were used. Both ferulic acid isomers showed a significant two to four-fold reduction in abundance in Mn-treated plants compared with control plants in the $\text{AWF}_{\text{H}_2\text{O}}$ fraction. A comparison of $\pm\text{Si}$ treatments revealed a significantly increased abundance of benzoic acid and of ferulic acid isomers (more than three-fold) in Si-treated plants only in the AWF_{NaCl} fraction. In Si-treated

plants, high Mn supply led to increased concentrations of benzoic acid in the AWF_{H2O} fraction and to decreased abundance of ferulic acid compared with plants grown at low Mn supply. A comparison of +Mn/+Si with +Mn/-Si (Mn toxicity-showing) plants showed significantly decreased *p*-hydroxybenzoic acid concentrations. A major, however not significant, increase in abundance of *cis*-ferulic acid is indicated in the +Mn/+Si plants not showing Mn toxicity symptoms. NADH-*peroxidase* activity enhancing *p*-coumaric acid showed no changes in abundance in each of the comparisons.

A three-factorial ANOVA showed benzoic acid, *p*-hydroxybenzoic acid and ferulic acid to be significantly affected by Mn (Tab. 2). Silicon treatment significantly affected *p*-hydroxybenzoic acid and *cis*-ferulic acid. Highly significant differences between the apoplastic fractions were found for all identified phenylpropanoids except ferulic acid and benzoic acid. Also the infiltration solution had a clear impact on *p*-hydroxybenzoic acid, *p*-coumaric acid, and *trans*-sinapic acid. None of the two or three way interactions were significant (not presented).

Tab. 1: Identified phenols (GC-MS) in the non-polar fraction of the leaf AWF recovered after infiltration with H₂O or NaCl. Displayed are the relative pool-size changes of each phenol calculated on the basis of response ratios. The effects of these phenols on the NADH-*peroxidase* activity (see Figs. 6 and 7) of apoplastic peroxidase isoenzymes are also shown. After 14 d of preculture, \pm Si-treated plants of the Mn-sensitive cowpea cultivar TVu 91 received 50 μ M Mn for three days or 0.2 μ M Mn continuously. Statistical testing of changes in metabolite abundance were calculated using log₁₀-transformed response ratios. * denote significant differences at least at $P < 0.05$ (n = 6), respectively (t test).

Detected metabolites	+Mn / -Mn		+Si / -Si		+Mn +Si / -Mn +Si		+Mn +Si / +Mn -Si		Effect of phenol on NADH- <i>peroxidase</i> activity ^a
	AWF _{H₂O}	AWF _{NaCl}	AWF _{H₂O}	AWF _{NaCl}	AWF _{H₂O}	AWF _{NaCl}	AWF _{H₂O}	AWF _{NaCl}	
benzoic acid	1.41 ^c	1.35	0.91	1.32*	1.49*	1.14	0.97	1.12	weak induction / no inhibition
<i>p</i> -hydroxybenzoic acid ^b	1.47	1.61	0.87	0.65	1.03	1.23	0.61*	0.50*	no induction / 50% inhibition
<i>cis-p</i> -coumaric acid	1.00	0.81	0.95	1.13	1.06	0.62	1.00	0.86	strong induction
<i>cis</i> -ferulic acid	0.24*	0.30*	1.03	3.77*	0.70	0.35*	2.96	4.37	weak induction / 50 % inhibition
<i>trans-p</i> -coumaric acid	0.88	0.82	0.84	0.95	0.97	0.59	0.92	0.68	strong induction
<i>trans</i> -ferulic acid	0.44*	2.31	1.34	3.61*	0.50	0.37*	1.52	0.57	weak induction / 50 % inhibition
<i>trans</i> -sinapic acid	2.39	0.81	n.d. ^{+d}	0.72	n.d. ⁺⁺	0.90	n.d. ⁺⁺	0.80	not examined

^a from Figs. 6 and 7

^b after identification of *p*-hydroxybenzoic acid, this phenol was additionally tested with respect to NADH-*peroxidase* activity. In addition to the 50% inhibitory effect it showed no induction capability for NADH-*peroxidase* activity for each isoenzyme tested.

^c Numbers are calculated ratios of the response ratios (not log₁₀-transformed) within the individual comparison. ANOVA did not reveal a significant Mn*Si interaction.

^d + and ++ were not detected (n.d.) in +Si and +Mn+Si treatments, respectively.

Tab. 2: Identified phenols (GC-MS) in the non-polar fraction of the leaf AWF recovered after infiltration with H₂O or NaCl (Inf.). Displayed are the *p*-values derived from analysis of variance based on log₁₀-transformed response ratios (n=6). For the effects of these phenols on the NADH-*peroxidase* activity of apoplastic peroxidase isoenzymes see Figs. 6 and 7 as well as Tab. 1. After 14 d of preculture, ±Si-treated plants of the Mn-sensitive cowpea cultivar TVu 91 received 50 µM Mn for three days or 0.2 µM Mn, continuously.

metabolite	Mn	Si	Inf.
benzoic acid	0.0032	0.2786	0.2615
4-hydroxybenzoic acid ^a	0.0093	<0.0001	<0.0001
<i>cis</i> -4-hydroxycinnamic acid	0.4236	0.5636	<0.0001
<i>cis</i> -ferulic acid	<0.0001	0.0012	0.4433
<i>trans</i> -4-hydroxycinnamic acid	0.1269	0.1057	<0.0001
<i>trans</i> -ferulic acid	0.0129	0.2470	0.3870
<i>trans</i> -sinapic acid	0.4671	0.1685	0.0039

^a after identification of *p*-hydroxybenzoic acid, this phenol was additionally tested with respect to NADH-*peroxidase* activity. In addition to the 50% inhibitory effect it showed no induction capability for NADH-*peroxidase* activity for each isoenzyme tested.

Discussion

Effect of Mn and Si on apoplastic Mn fractions

Manganese is readily taken up by plants independent of the Si supply, but the expression of toxicity symptoms was suppressed by Si treatment (Fig. 1A, B) which is in line with results previously published for cowpea (Horst et al., 1999; Iwasaki et al., 2002 a, b). This Si-enhanced Mn tolerance has been explained entirely in cucumber (Rogalla and Römheld, 2002) or partly in cowpea (Iwasaki et al., 2002a, b) by a reduction of the free Mn in the apoplast through enhanced strong binding of Mn by the cell walls in Si-treated plants. However, in the present study neither the AWF_{H_2O} (Fig. 2A) nor the five-fold higher AWF_{NaCl} (Fig. 2C) Mn concentrations differed clearly owing to Si treatment. This might be explained by different growing conditions of the plants and Mn extraction procedures. Nevertheless, this clearly shows that in cowpea, the expression of Mn toxicity cannot be explained just on the basis of the free and exchangeable Mn concentration in the leaf apoplast in agreement with the conclusion drawn by Iwasaki et al. (2002 a, b). They postulated a particular role of the monomeric Si in enhancing Mn tolerance. Indeed, also in our study the monomeric Si concentration was consistently higher in Si-treated plants in the AWF_{H_2O} (Fig. 2B) and initially also in the AWF_{NaCl} (Fig. 2D) fraction. The decreasing concentration of monomeric Si with increasing Mn treatment duration in the latter fraction possibly due to polymerization and/or strong binding in the cell walls (incrustation) may explain why Si treatment did not prevent but only delayed the formation of brown spots (Fig. 1B) with extended Mn treatment duration.

Manganese and Si-induced changes of peroxidase activities

All isoenzymes were shown to perform both reaction cycles (Figs. 3, 4). Mn treatment led to an increased abundance of POD isoenzymes (Fig. 3, Fig. S1, Fecht-Christoffers et al., 2003b) thus explaining enhanced apoplastic POD activities (Fecht-Christoffers et al., 2006). Silicon treatment only delayed but not suppressed the Mn-mediated increased abundance of POD isoenzymes (Fig. S1), which is in line with the delayed but not prevented development of Mn toxicity symptoms (Fig. 1B). Using higher protein loadings BN-PAGE separation of AWF_{H_2O} and AWF_{NaCl} protein did not reveal qualitative but only quantitative differences in POD

isoenzyme patterning between the infiltration solutions indicating that all detected isoenzymes are principally water-soluble (Fig. S2), even though a low protein loading could lead to the opposite conclusion (Figs. 3 and S1). The results confirm a particular role of PODs in the AWF_{H_2O} in the modulation of Mn toxicity (Fecht-Christoffers et al., 2006, 2007).

Characterization of the identified peroxidases

The sequencing of the POD activity-showing 1D-BN protein bands P1 to P6 revealed that each band was composed of more than one protein (Tab. S2) confirming BN/SDS-PAGE results previously published by Fecht-Christoffers et al. (2003b). All bands led to the identification of at least one peptide with high sequence homology to peroxidases in the NCBI green plants database. In total, eleven different peptides have been identified belonging to the class III secretory peroxidase family including sequences for the conserved so-called “domain II” [Hiraga et al., 2001] / “domain D” [Delannoy et al., 2003] (Figure 5, Table S2). Three overlapping peptide sequences provide evidence for the presence of at least 3 distinct genes encoding for class III secretory peroxidases (Fig.5). Three peptides with amino acid substitutions (including the overlapping peptide sequences (Fig.5)) were exclusively found in AWF_{NaCl} extracted isoenzyme P1 from Mn-treated plants (Figs. 3 and 5, Tab. S2) indicating specific apoplastic binding properties.

As MS analyses did not result in complete POD sequences, one can only speculate about the total number of distinct class III secretory peroxidases in *Vigna unguiculata*. Based on *in gel* activity stainings, peroxidases of a wide range of MW were detected (Figs. 3, S1 and S2). There are several possibilities leading to such great differences in the MW of the isoenzymes: (i) class III peroxidases belong to a large multigenic family even though they are distinct proteins (Passardi et al., 2004) with MWs ranging 28 kDa up to 60 kDa (Hiraga et al., 2001). (ii) A protein oligomer showing peroxidase activity is conceivable, such as a peroxidase dimer. (iii) Depending on the degree of *N*-glycosylation the native MW may vary thus leading to changes in the MW in the order of P3-P6 (Fig. 3). (iv) Other apoplastic proteins than class III peroxidases might also have peroxidative activity, i.e. oxidoreductase and/or auxin-binding (germin-like) proteins even though the sequencing results did not identify proteins that could perform a peroxidative reaction (Tab. S2)

The role of pH in controlling apoplastic POD isoenzyme activities

A pH optimum seems to be necessary for POD self-protection (Olsen et al., 2003). In addition, the pH could be an important regulatory factor for the relative performance of either the peroxidative or the peroxidative-oxidative reaction cycle of the enzyme. If an apoplastic pH of about 5.0 to 6.0 as shown for *Vicia faba* (Mühling and Läuchli, 2000) is assumed, both POD cycles are expected to have high activities within this range (Fig. 5), indicating that the apoplastic pH is not decisive in regulating the relative contribution of each reaction cycle in response to toxic Mn supply. The determined pH optimum for both POD activities is precisely in the range of the recommended pH of the measuring solutions for POD activity determination *in vitro* in studies investigating lignin formation (Kärkönen et al., 2002). However, in studies on the hypersensitive stress response to leaf pathogens, NADH-peroxidase-mediated H₂O₂ production proved to be related to an alkalization of the apoplast (Bolwell et al., 1995, 1998, 2001; Pignocchi and Foyer, 2003) suggesting differences between biotic and abiotic stress responses.

The role of metabolites in controlling apoplastic POD isoenzyme activities - Metabolite profiling

In a broad range metabolomic approach we could show that Mn toxicity induced changes in the bulk-leaf metabolome according to ICA (Fig. 8A, IC01) consistent with our recent results showing that Mn toxicity also affects symplastic reactions using a combined proteomic/transcriptomic and physiological approach (Chapter 1). The involvement of the symplast in Mn toxicity is in line with studies using other plant species showing Mn toxicity-induced reduced CO₂ assimilation capacity (González and Lynch, 1997, 1999; González et al., 1998 [common bean]; Nable et al., 1988; Houtz et al., 1988 [tobacco]) accompanied by reduced chlorophyll contents (Gonzalez and Lynch 1999, 1998 [common bean], Moroni et al., 1991 [wheat]), and high Mn-accumulation rates in chloroplasts (Lidon et al., 2004 [rice]). Our metabolomic approach also showed that Si supply led to a particular clustering of the total leaf metabolome as revealed by ICA (Fig. 8A, IC04). This is in agreement with the work of Maksimović et al. (2007) on Si/Mn-toxicity interaction in cucumber who concluded that Si supply modulates the phenol metabolism.

A closer investigation of the apoplastic metabolome using AWF_{NaCl} and AWF_{H₂O} revealed that the infiltration solution (IC01, Fig. 8B) was the most important factor explaining

differences between the extracted metabolome fractions. Manganese (IC02) but not Si treatment affected both AWF metabolome fractions. The ICA loadings identified organic acids, amino acids, and sugars to be responsible for Mn and infiltration solution-related clusterings (Fig. 8B), whereas phenolic compounds were unexpectedly low since Fecht-Christoffers et al. (2006, 2007) reported a Mn-induced change in the apoplastic water-soluble phenol composition (and at later toxicity stages even in phenol concentration) using HPLC separation of leaf AWF_{H₂O} in cowpea (see discussion below). However, GC-MS based metabolite profiling typically covers mostly primary metabolites explaining the relative low abundance of phenolic compounds.

To overcome this problem, an additional special AWF-extraction procedure was applied yielding non-polar metabolites. This resulted in clustering only according to the infiltration solution (Fig. 8C, IC02, see discussion below). ICA loadings revealed in addition to organic acids mainly phenylpropanoids to be responsible for the clustering. Among other detected aromatic compounds we identified ferulic acid as a clearly Mn and Si-affected phenol (Tabs. 1 and 2, see discussion below).

Overall, the broad-range metabolite profiling in the bulk-leaf extract (Fig. 8A, ICA01) and the AWF (Fig. 8B, ICA02) revealed a clear difference related to the Mn treatment. The Si effect was less clearly expressed. A preliminary metabolite-specific evaluation of the metabolites indicates alterations of metabolic pathways mainly related to organic acids, amino acids, and sugars/sugar alcohols. A detailed evaluation and discussion of the qualitative changes in polar apoplastic metabolites is beyond the scope of this paper and will be subject of a subsequent paper.

The role of phenols in controlling apoplastic NADH-*peroxidase* activity

Analyzing the AWF_{H₂O} using HPLC, Fecht-Christoffers et al. (2006) separated water-soluble phenols in the apoplast. A Mn treatment not only increased the peak size but also led to at least two additional peaks which supported their conclusion that the presence of phenols in the apoplast is decisive for the expression of Mn toxicity/Mn tolerance in cowpea leaf tissue. However, they failed to identify the phenols. Our gas chromatography – mass spectrometry approach allowed us to identify five phenols. However, the method does not allow determining absolute concentrations but only relative treatment-related concentration changes. Also, we were unable to identify most phenols directly in the AWF. Therefore, we extracted the aqueous AWF with diethylether which led to a concentration of the phenols but at the

same time only yielded non-polar metabolites. Thus, the applied technique did not allow us to identify and quantify all phenols present in the apoplast which is a major focus of ongoing research. Nevertheless, among the identified phenols (Tabs. 1 and 2) four were found which had been tested for their effect on NADH-*peroxidase* activity *in vitro*. Only *p*-coumaric acid had a strong activity-enhancing effect. Ferulic acid and *p*-hydroxybenzoic acid had only a weak or lacking stimulating but a strong inhibiting effect when combined with *p*-coumaric acid. Benzoic acid only weakly enhanced and did not inhibit NADH-*peroxidase* activity (Figs. 6 and 7, Tab. 1).

The 3-factorial analysis of variance of the treatment-induced changes in the abundance of the phenols (Tab. 2) revealed that Mn treatment significantly affected the concentrations of benzoic, *p*-hydroxybenzoic and most clearly ferulic acid, whereas Si treatment affected *p*-hydroxybenzoic and again most clearly *cis*-ferulic acid. Looking at the comparison of means of the treatment-specific relative pool-size changes of the individual phenols (Tab. 1) it appears that the change in the concentration in the apoplast of particularly ferulic acid plays a key role in the expression of Mn toxicity symptoms: a reduction of the concentration leading to a reduced inhibition of NADH-*peroxidase* activity is characteristic for leaves showing Mn toxicity symptoms (+Mn/-Si), while Mn-tolerant leaf tissue (-Mn/+Si; +Mn/+Si) is characterized by an enhanced accumulation. The constitutive effect of Si on an enhanced abundance of ferulic acid seems to be strong enough to counteract the Mn-induced reducing effect (comparison +Mn +Si/-Mn +Si, Tab. 1). Also, it appears that Si affects more the phenol concentration in the AWF_{NaCl} (as indicated by the high infiltration solution-effect on the phenols in Tab. 2) than in the AWF_{H₂O} corroborating results demonstrating Si-mediated changes of apoplastic Mn-binding properties (Iwasaki et al., 2002a; Rogalla and Römheld, 2002). However, especially ferulic acid and benzoic acid were not affected by the infiltration solution, indicating specific apoplastic binding properties in the apoplast for each phenol regardless of Si nutrition (Tab. 1). The Si-induced significantly higher abundance of benzoic acid might be of minor importance given the only weak NADH-*peroxidase* activity-enhancing effect (Figs. 6 and 7, Tab. 1). However, the lowered concentration of NADH-*peroxidase* activity-inhibiting *p*-hydroxybenzoic acid in presence of Si at high Mn supply is not in line with the above expressed line of thinking. Thus it appears a more detailed and quantitative inventory of the phenols present in the leaf apoplast is necessary to fully understand Mn toxicity and Mn tolerance.

In conclusion, the results presented here confirm the hypothesized role of apoplastic NADH-*peroxidase* and its activity-modulating phenols in Mn toxicity and Si-enhanced Mn tolerance. Isoenzyme BN gel-profiling of POD enzymes and their characterization after elution from the

gels, and metabolite profiling of the bulk-leaf and the AWF appear to be powerful tools in enhancing the physiological and molecular understanding of Mn toxicity and Mn tolerance.

Characterizing genotypic and silicon-enhanced manganese tolerance in cowpea (*Vigna unguiculata* L.) through apoplastic peroxidase and leaf-metabolome profiling

Hendrik Führs¹, André Specht¹, Joachim Kopka², Sébastien Gallen³, Dimitri Heintz⁴, Alain Van Dorsselaer³, Hans-Peter Braun⁵ & Walter J. Horst¹

to be submitted

¹ Institute of Plant Nutrition, Faculty of Natural Sciences, Leibniz University Hannover, Herrenhäuser Str. 2, 30419 Hannover, Germany

² Max Planck Institute of Molecular Plant Physiology, Am Mühlenberg 1, 14476 Potsdam-Golm, Germany

³ Laboratoire de Spectrométrie de Masse Bio-Organique, IPHC-DSA, ULP, CNRS, UMR7178 ; 25 rue Becquerel, 67 087 Strasbourg, France

⁴ Institut de Biologie Moléculaire des Plantes (IBMP) CNRS-UPR2357,ULP, 67083 Strasbourg, France

⁵ Institute of Plant Genetics, Faculty of Natural Sciences, Leibniz University Hannover, Herrenhäuser Str. 2, 30419 Hannover, Germany

Abstract

Previous studies characterized genotypic differences in manganese (Mn) tolerance and silicon (Si)-enhanced Mn tolerance in cowpea (*Vigna unguiculata* L.) either in the symplast or in the apoplast. To relate apoplastic to symplastic responses and to compare genotypic and Si-enhanced Mn tolerance, the bulk-leaf and two apoplastic metabolome fractions (free and ionically bound) were comparatively analysed using a metabolite-profiling approach. Supervised and unsupervised statistical analyses of the metabolome profiles allowed a screening for metabolites highly significantly responding to Mn and Si supply. The analysis yielded metabolites involved in stress sensing and signaling. This is regarded as a primary response to excess Mn and Si supply. A number of organic acids may play a role as mediators of Mn stress through their antioxidant activity and through their proposed function as scavengers and chelators of Mn^{III} either accelerating Mn-stress responses or enhancing Mn tolerance. A Mn stress-induced rebalancing of carbohydrates in the Mn-sensitive cultivar TVu 91 could reflect an increased demand for C-skeletons for fuelling stress responses. Manganese excess-induced changes in the carbohydrate as well as amino acid metabolism may be related to an impaired nitrogen assimilation of TVu 91 compared with Mn-tolerant TVu 1987 most probably in response to impaired photosynthesis. Considerable differences between the cultivars in the apoplastic peroxidase isoenzyme profile as revealed by Blue Native-(BN-) PAGE in relation to the dynamics of NADH-*peroxidase* activity enhancing and inhibiting phenols further confirmed the decisive role of peroxidases and activity-modulating phenols for Mn toxicity and genotypic and Si-induced Mn tolerance.

Introduction

Manganese (Mn) toxicity is a plant disorder appearing on acid and insufficiently drained soils with low redox potential, therefore leading to high concentrations of plant-available Mn. Not only in cowpea a great inter- and intra-specific variability in Mn resistance has been observed (Foy et al., 1978; El-Jaoual and Cox, 1998; Horst, 1980). In cowpea, Mn-resistant cultivars do not differ from Mn-sensitive cultivars in Mn accumulation (Horst, 1980, Chapter 1). Therefore, in this species Mn resistance is regarded as Mn tissue tolerance (Horst, 1983). Toxicity symptoms in cowpea first appear on older leaves as distinct brown spots. They are located in the leaf epidermal apoplast. In the further development of Mn toxicity leaves are shedded thus leading to yield decline (Horst and Marschner, 1978b; Horst, 1982).

The brown spots contain oxidized Mn and oxidized phenolic compounds (Wissemeier and Horst, 1992). Hence, the oxidation of Mn^{2+} and phenols mediated by apoplastic peroxidases (PODs) was proposed to be a key reaction leading to Mn toxicity (Horst, 1988; Fecht-Christoffers et al., 2006, 2007). Characterization of peroxidase isoenzymes from a Mn-sensitive cowpea cultivar with respect to pH optimum and response to phenols supported this hypothesis. The H_2O_2 -producing cycle of apoplastic peroxidases also requires Mn^{2+} and phenols as cofactors (Chapter 2). Furthermore, it has been shown that the phenol identity rather than the phenol concentration is decisive for the activation of the H_2O_2 -producing peroxidase cycle (Chapter 2). Increasing Mn concentrations in the leaf tissue and the Apoplastic Washing Fluid (AWF) affected the total apoplastic phenol concentration as well as the phenol composition (Fecht-Christoffers et al., 2006) indicating that the interaction of metabolites with apoplastic peroxidases rather than the peroxidases themselves are responsible for the expression of Mn toxicity.

In a range of plant species symplastic rather than apoplastic reactions appear to play an important role in the development of Mn toxicity and/or tolerance. This is indicated by the role of specific and unspecific transporters in sequestering Mn in different symplastic compartments thus conferring enhanced Mn tolerance (Delhaize et al. 2003, 2007; Peiter et al., 2007; Hirschi et al., 2000; Wu et al., 2002). Also, a significant impact of Mn excess on chloroplasts and photosynthesis has been reported in common bean (González and Lynch, 1997, 1999, González et al., 1998), tobacco (Houtz et al., 1988; Nable et al., 1988) and wheat (Moroni et al., 1991). But also in cowpea, it has been shown that elevated Mn supply lead to a state I to state II transition of photosynthesis more clearly in a Mn-sensitive compared with a Mn-tolerant genotype (Chapter 1). In line with this result, the photosynthetic electron

transport was impaired in the Mn-sensitive cultivar TVu 91 already after 1 day of high Mn supply. Therefore, even though the role of the apoplast in the expression of Mn toxicity is well established (Fecht-Christoffers et al., 2007) it appears that also in cowpea, it cannot be excluded that Mn toxicity stress is perceived in the symplast/chloroplast triggering subsequent reactions in the apoplast. Preliminary results on the transcriptome level revealed an enhanced abundance of transcripts involved in signal transduction in the Mn-sensitive compared with the Mn-tolerant cultivar after short-term Mn application (Chapter 1, data not shown). Long-term Mn excess induced transcripts involved in plant defence (Chapter 1). Furthermore, Mn toxicity did not only induce significant changes in the metabolite composition of the AWF but also in the whole leaf extract (Chapter 2).

Silicon is a beneficial element for plants (Epstein, 1999), since it alleviates heavy metal toxicities including Mn toxicity. Liang et al. (2007) described several key mechanisms leading to the suppression of abiotic stresses by Si in higher plants including Mn compartmentation within the cell. Horst and Marschner (1978a) found a more evenly distribution of Mn in Si-treated cowpea plants. Silicon-enhanced Mn tolerance could be related to a reduction in apoplastic Mn concentrations due to reduction of the free Mn concentration in the apoplast by stronger binding to the cell wall (Iwasaki et al., 2002a; Rogalla and Römheld, 2002). Iwasaki et al. (2002b) concluded from their results with cowpea that in addition to Si-mediated stronger binding of Mn by the cell walls, Si contributed to maintaining a reduced state of the apoplast, thought to be a prerequisite for Mn tolerance. Such an additional role of Si is supported by results showing that Si affects both the bulk-leaf as well as the apoplastic metabolome (Chapter 2).

The work presented here further characterizes apoplastic peroxidases and the metabolite composition of the total leaf and the leaf apoplast as affected by genotype and Si in order to better understand genotypic differences in Mn tolerance and the role of Si in the alleviation of Mn toxicity.

Materials and Methods

Plant material

Cowpea (*Vigna unguiculata* L. Walp., Mn-sensitive cultivar TVu 91 and Mn-tolerant cultivar TVu 1987) was grown hydroponically in a growth chamber as described in Chapters 1 and 2. Silicon-treated plants received Si in form of Aerosil (Horst and Marschner, 1978a; chemically clean silicic acid, yielding a Si concentration of 20-26.5 μM , in the following mentioned as +Si). After preculture for 14 d, the Mn concentration in the nutrient solution was increased from 0.2 μM (-Mn) to 50 μM (+Mn) for 3 or 4 days.

Extraction of water-soluble and ionically bound apoplastic proteins

Apoplastic washing fluid (AWF) was extracted by a vacuum infiltration/centrifugation technique according to Chapter 2. Malate dehydrogenase (MDH) activity in the AWF showed a cytoplasmic contamination of both AWF fractions by less than 1% (data not shown). Until further analysis the AWF was stored at -80°C .

Quantification of toxicity symptoms

For the quantification of Mn toxicity symptoms, the density of brown spots was counted on a 1.54 cm^2 area at the base and tip on the upper side of the second oldest middle trifoliate leaf and calculated on a cm^2 base.

Manganese analysis

Manganese in the bulk-leaf tissue was determined in the second oldest middle trifoliate leaf after dry ashing at 480°C for 8h and dissolving the ash in 6 M HCl with 1.5% (w/v) hydroxylammonium chloride, and then dilution (1:10) with double demineralised water. Measurements were carried out by optical inductively-coupled plasma-emission spectroscopy (Spectro Analytical Instruments GmbH, Kleve, Germany).

Protein preparation from AWF

For protein separation by electrophoresis under native conditions, the proteins of the AWF were concentrated at 4°C by using centrifugal concentrators with a molecular mass cut off at 5kD (Vivaspin 6, Vivascience, Hannover, Germany). Running conditions were used according to the manufacturer's instructions. The protein concentration of the AWF was then measured for Blue Native (BN)-PAGE in the protein concentrate of the AWF using the 2-D Quant Kit[®] (GE Healthcare) according to the manufacturers instructions.

1D Blue Native-PAGE of apoplastic proteins and POD activity staining

Proteins were separated by BN-PAGE according to Jänsch et al. (1996) as described in Chapter 2. After scanning the gels, in a first approach specific POD activity stained bands were cut from the gel and sequenced (see Materials and Methods section below). In a second sequencing run POD-stained gels were stained with colloidal Coomassie-blue according to Neuhoff et al. (1985, 1990) prior to sequencing.

For staining, the gels were soaked in 20 mM guaiacol (in 10 mM Na₂HPO₄) and 0.03% (v/v) H₂O₂ for 3 min to detect in-gel guaiacol-peroxidase activity.

Mass spectrometric protein analysis and data interpretation⁸

Marked BN-PAGE bands stained for guaiacol-peroxidase activity were cut and dried under vacuum. In-gel digestion was performed with an automated protein digestion system, MassPREP Station (Micromass, Manchester, UK). The gel slices were washed three times in a mixture containing 25 mM NH₄HCO₃ : acetonitrile [1:1, v/v]. The cysteine residues were reduced by 50 µl of 10 mM dithiothreitol at 57°C and alkylated by 50µl of 55 mM iodacetamide. After dehydration with acetonitrile, the proteins were cleaved in the gel with 40 µl of 12.5 ng µl⁻¹ of modified porcine trypsin (Promega, Madison, WI, USA) in 25 mM NH₄HCO₃ at room temperature for 14 hours. The resulting tryptic peptides were extracted

⁸ Mass spectrometric protein analysis and data interpretation was done in collaborations with Dr. Dimitri Heintz, Institut de Biologie Moléculaire des Plantes (IBMP) CNRS-UPR2357,ULP, 67083 Strasbourg, France, and Prof. Dr. Alain Van Dorsselaer and Sébastien Gallien, Laboratoire de Spectrométrie de Masse Bio-Organique, IPHC-DNA, ULP, CNRS, UMR7178; 25 rue Becquerel, 67 087 Strasbourg, France

with 60% acetonitrile in 0.5% formic acid, followed by a second extraction with 100% (v/v) acetonitrile.

Nano-LC-MS/MS analysis of the resulting tryptic peptides was performed using using an Agilent 1100 series HPLC-Chip/MS system (Agilent Technologies, Palo Alto, USA) coupled to an HCT Ultra ion trap (Bruker Daltonics, Bremen, Germany). Chromatographic separations were conducted on a chip containing a Zorbax 300SB-C18 (75 μm inner diameter \times 150 mm) column and a Zorbax 300SB-C18 (40 nL) enrichment column (Agilent Technologies).

HCT Ultra ion trap was externally calibrated with standard compounds. The general mass spectrometric parameters were as follows: capillary voltage, -1750V; dry gas, 3 liters min^{-1} ; dry temperature, 300°C. The system was operated with automatic switching between MS and MS/MS modes using. The MS scanning was performed in the standard-enhanced resolution mode at a scan rate of 8,100 m/z per second with an aimed ion charge control of 100,000 in a maximal fill time of 200 ms and a total of 4 scans were averaged to obtain MS spectrum. The three most abundant peptides and preferentially doubly charged ions, were selected on each MS spectrum for further isolation and fragmentation. The MS/MS scanning was performed in the ultrascan resolution mode at a scan rate of 26,000 m/z per second with an aimed ion charge control of 300,000 and a total of 6 scans were averaged to obtain MS/MS spectrum. The complete system was fully controlled by ChemStation Rev. B.01.03 (Agilent Technologies) and EsquireControl 6.1 Build 78 (Bruker Daltonics) softwares. Mass data collected during LC-MS/MS analyses were processed using the software tool DataAnalysis 3.4 Build 169 and converted into *.mgf files. The MS/MS data were analyzed using the MASCOT 2.2.0. algorithm (Matrix Science, London, UK) to search against a in-house generated protein database composed of protein sequences of Viridiplantae downloaded from <http://www.ncbi.nlm.nih.gov/sites/entrez> (on March 6, 2008) concatenated with reversed copies of all sequences ($2 \times 478,588$ entries). Spectra were searched with a mass tolerance of 0.5 Da for MS and MS/MS data, allowing a maximum of 1 missed cleavage by trypsin and with carbamidomethylation of cysteines, oxidation of methionines and N-terminal acetylation of proteins specified as variable modifications. Protein identifications were validated when at least two peptides with high quality MS/MS spectra (Mascot ion score greater than 31) were detected. In the case of one-peptide hits, the score of the unique peptide must be greater (minimal “difference score” of 6) than the 95% significance Mascot threshold (Mascot ion score >51). For the estimation of the false positive rate in protein identification, a target-decoy database search was performed (Elias and Gygi, 2007).

GC-MS-based metabolite profiling⁹

For GC-MS analysis, polar metabolite fractions were extracted from 60 mg \pm 10 % (FW) frozen plant material, ground to a fine powder, with methanol/chloroform. The fraction of polar metabolites was prepared by liquid partitioning into water/methanol (polar fraction) and chloroform (non-polar fraction) as described earlier (Roessner et al., 2000; Wagner et al., 2003). Metabolite samples were derivatized by methoxyamination, using a 20 mg ml⁻¹ solution of methoxyamine hydrochloride in pyridine, and subsequent trimethylsilylation, with N-methyl-N-(trimethylsilyl)-trifluoroacetamide (Fiehn et al., 2000; Roessner et al., 2000). A C₁₂, C₁₅, C₁₉, C₂₂, C₂₈, C₃₂, and C₃₆ n-alkane mixture was used for the determination of retention time indices (Wagner et al., 2003). Ribitol and deuterated alanine were added for internal standardization. Samples were analyzed using GC-TOF-MS (ChromaTOF software, Pegasus driver 1.61; LECO, <http://www.leco.com>). Six sample types (two genotypes, two Mn treatments, and two Si treatments), each with 5 replicates, comprised an experimental data set of 40 chromatograms. The chromatograms and mass spectra were evaluated using the TagFinder software (Luedemann et al., 2008).

Sample preparation for the metabolite profiling of the AWF was adapted to the respective volumes and metabolite concentrations. In this case 200 μ l of AWF_{H₂O} and AWF_{NaCl} were extracted to obtain a polar metabolite fraction, without further addition of water. The volume of methanol/chloroform was reduced to 50% as were the reagents for methoxyamination and silylation. For the apoplastic metabolome fractions eight sample types (two genotypes, two Mn treatments, two infiltration solutions, and two Si treatments), each with four to five replications, in total 75 chromatograms, were analyzed as described above.

In parallel free phenols (in the following termed non-polar apoplastic fraction) were extracted from AWF_{H₂O} and AWF_{NaCl}. First AWF was alkalized with 0.5 N NaOH (ratio 1:1) overnight. Afterwards samples were acidified by adding 5 N HCl (ratio 0.1125:1). Phenols were then extracted by shaking with diethylether (ratio 1:1). Samples were then dried under nitrogen atmosphere and prepared for GC-MS analysis as described for AWF. Eight sample types (two genotypes, two Mn treatments, two infiltration solutions, and two Si treatments), each with five to six replications, yielding 93 chromatograms which were processed as described.

GC-MS metabolite profiles were processed after conversion into NetCDF file format using the TagFinder (Luedemann et al., 2008) and NIST05 software (<http://www.nist.gov/srd/mslist.htm>). The mass spectral and retention index (RI) collection of

⁹ GC-MS analyses of samples were done in collaboration with Dr. Joachim Kopka and Alexander Erban, Max-Planck-Institute of Molecular Plant Physiology, Am Mühlenberg 1, 14476 Potsdam-Golm

the Golm metabolome database (Kopka et al., 2005; Schauer et al., 2005) was used for manually supervised metabolite identification. Yet non-identified metabolic components were disregarded for the present study. Peak height representing a mass specific arbitrary detector response was used for screening the relative changes of metabolite pools. The initial mass specific responses were normalized by leaf fresh weight and ribitol recovery. AWF metabolite profiles were normalized to ribitol recovery and AWF total volume of partitioned polar (water/methanol) and non-polar (chloroform) AWF fractions.

Statistical analysis of GC-MS profiles

Prior to statistical data assessment response ratios were calculated based on the mean response of each metabolic feature from all samples of an experimental data set. Response ratios were subsequently \log_{10} -transformed. Independent component analysis (ICA) and missing value substitution was as described earlier (Scholz et al., 2005). ICA was carried out using the first 5 principal components obtained from a set of manually identified metabolites represented by at least 3 specific mass fragments each. Basic calculations of relative changes in abundance of specific metabolites due to Mn and Si treatment were made with the Microsoft Excel 2000 software program and respective embedded algorithms. For pairwise comparisons thresholds of 2-fold change in pool size and $P < 0.05$ (t test) were applied or levels of significance indicated, namely ***, **, and * representing $p < 0.001$, 0.01, and 0.05, respectively. Logarithmic transformation of response ratios approximated required Gaussian normal distribution of metabolite profiling data (Schaarschmidt et al., 2007).

Statistical analysis except metabolite profiling

Statistical analysis, if not mentioned otherwise, was carried out using SAS Release v8.0 (SAS Institute, Cary, NC) or MeV (Saeed et al., 2003). Results from analysis of variance are given according to their level of significance as ***, **, and * for $p < 0.001$, 0.01, and 0.05, respectively.

Results

Toxicity status

Elevated Mn supply for 4 d resulted in a consistent increase of the bulk-leaf Mn concentration in both cultivars independent of the Si supply (Fig. 1). The Mn-tolerant cultivar TVu 1987 had slightly higher Mn concentrations compared with the sensitive cultivar TVu 91. Also Si treatment enhanced Mn tissue concentrations. However, Mn concentrations led to moderate toxicity symptoms (10-15 brown spots cm^{-2}) only in the Mn-sensitive cultivar not treated with Si already after 2 d and in Si-treated plants after 4 d of elevated Mn supply.

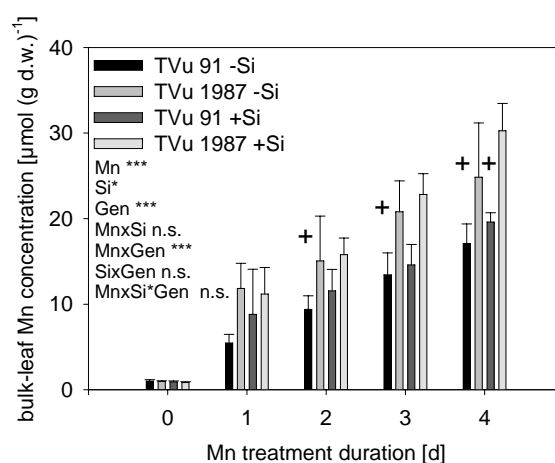


Fig. 1: Effect of Mn treatment duration and Si supply on the Mn tissue concentrations of the second oldest trifoliolate leaves of the Mn-sensitive cowpea cultivar TVu 91 and the Mn-tolerant cultivar TVu 1987. After 2 weeks of preculture at $0.2 \mu\text{M}$ Mn, the Mn supply was increased to $50 \mu\text{M}$ for four days. Silicon treatments received Aerosil (as described in “Materials and Methods”) throughout plant culture. + indicate toxicity symptoms (10-15 brown spots cm^{-2}) appearing only on the leaves of the Mn-sensitive cultivar already after 2 d (-Si) or 4 d (+Si) of elevated Mn supply.

Characterization of the apoplastic protein composition with emphasis on peroxidase isoenzyme profiling of the apoplast

Since apoplastic PODs have been shown to be critical in terms of Mn sensitivity or tolerance (Chapter 2; Fecht-Christoffers et al., 2006), apoplastic PODs of the two cowpea cultivars were separated by BN-PAGE. The apoplastic POD isoenzyme pattern differed not only between both genotypes but also between the infiltration solutions as indicated by guaiacol-POD activity-stained BN-gels (Fig. 2). In line with results for TVu 91 (Chapter 2), POD

isoenzymes around P6 appeared in control plants and in Mn-treated plants of TVu 91 (Fig. 2). Isoenzyme P6 appeared also to be present in TVu 1987, whereas all isoenzymes appearing around P6 in the Mn-sensitive cultivar hardly appeared in the Mn-tolerant cultivar even when plants were supplied with excess Mn. A comparison of the infiltration solutions revealed a lower abundance in the AWF_{NaCl} with no major qualitative differences indicating that all isoenzymes are water-soluble. Subsequent Coomassie-blue colloidal staining of previously POD activity-stained BN gels visualized mainly the same protein bands. However, several protein bands additionally appeared with a higher MW than P1 in both cultivars in the water-soluble fraction. One protein band smaller than P1 appeared most prominently in the AWF_{H_2O} of the Mn-sensitive cultivar independent of the Mn supply but also in the Mn-tolerant cultivar and the AWF_{NaCl} fractions of both cultivars. One protein, smaller than P6, showed a higher abundance in the AWF_{H_2O} in the Mn-tolerant cultivar compared with the sensitive cultivar. This protein disappeared in the AWF_{NaCl} .

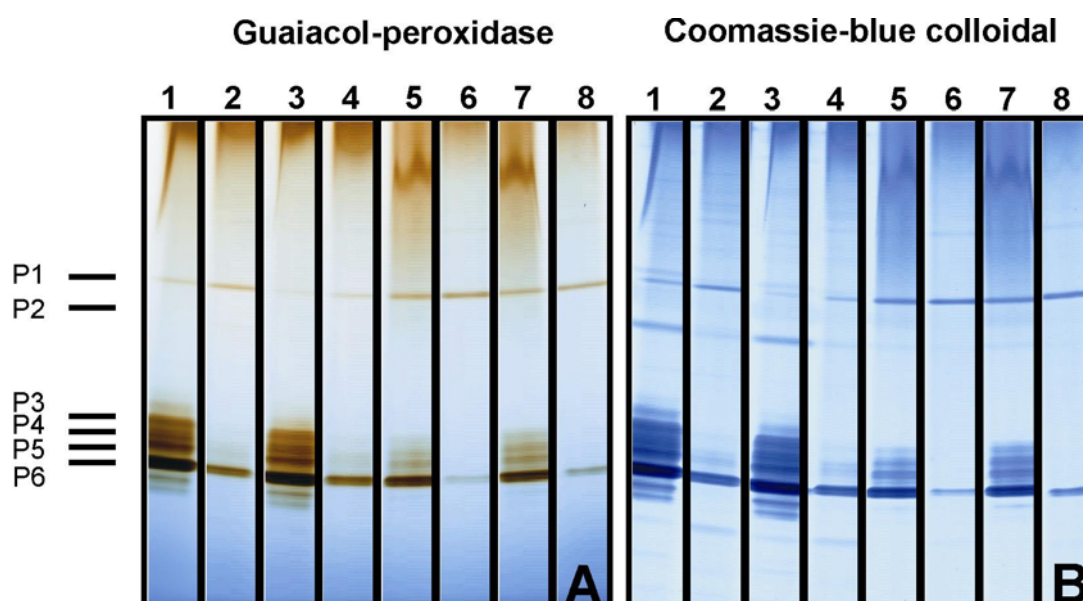


Fig. 2: AWF_{H_2O} and AWF_{NaCl} proteins of the second oldest trifoliolate leaves of the Mn-sensitive cultivar TVu 91 and the Mn-tolerant cultivar TVu 1987 stained for (A) guaiacol-peroxidase activity and (B) afterwards stained with Coomassie-blue colloidal after separation by BN-PAGE. After preculture with $0.2 \mu\text{M}$ Mn (-Mn) for 14 d plants received $50 \mu\text{M}$ (+Mn) Mn for 4 d. Lanes one to eight are as follows: 1) TVu 91 AWF_{H_2O} -Mn; 2) TVu 1987 AWF_{H_2O} -Mn; 3) TVu 91 AWF_{H_2O} +Mn; 4) TVu 1987 AWF_{H_2O} +Mn; 5) TVu 91 AWF_{NaCl} -Mn; 6) TVu 1987 AWF_{NaCl} -Mn; 7) TVu 91 AWF_{NaCl} +Mn; 8) TVu 1987 AWF_{NaCl} +Mn, $67.5 \mu\text{g}$ protein were loaded onto each lane. P1-P6 mark POD isoenzymes previously characterized in the sensitive cv. TVu 91 (Chapter 2). Guaiacol-peroxidase was stained with 18 mM guaiacol (in 9 mM Na_2HPO_4) and 0.03% H_2O_2 at pH 6.0.

Fig. 3 shows the protein bands which were chosen for sequencing and subsequent identification. In summary, 51 bands from both cultivars and both infiltration solutions were cut (Fig. 3); proteins were digested and analyzed by liquid chromatography-coupled mass spectrometry (LC-MS/MS) as already described in Chapter 2 including estimation of false

positive rate of identification (Elias and Gygi, 2007). No additional protein was identified in reversed sequences suggesting that our dataset contained very few or no false-positive identifications. Protein bands of the BN gel contained generally more than one protein. A list of all resulting peptides as well as their identities is given as supplementary material (Tab. S3, see also Chapter 2). Among these peptides 11 peptides belonging to class III peroxidases could be identified (Fig. S1, Green plants (Viridiplantae) database at NCBI). At least three overlapping peptides provide evidence for at least three distinct gene products (Fig. S1). Those bands that led to at least one peptide belonging to class III peroxidases are marked and corresponding database hits are displayed (Fig. 3).

All protein bands in control plants also appeared in Mn-treated plants (data not shown). Comparison of POD peptides / peptide composition of AWF_{H2O} from \pm Mn treatments of TVu 91 (corresponding to protein bands 12 to 18, data not shown) did not show differences between the Mn treatments. Therefore, bands were cut exclusively from Mn-treated samples.

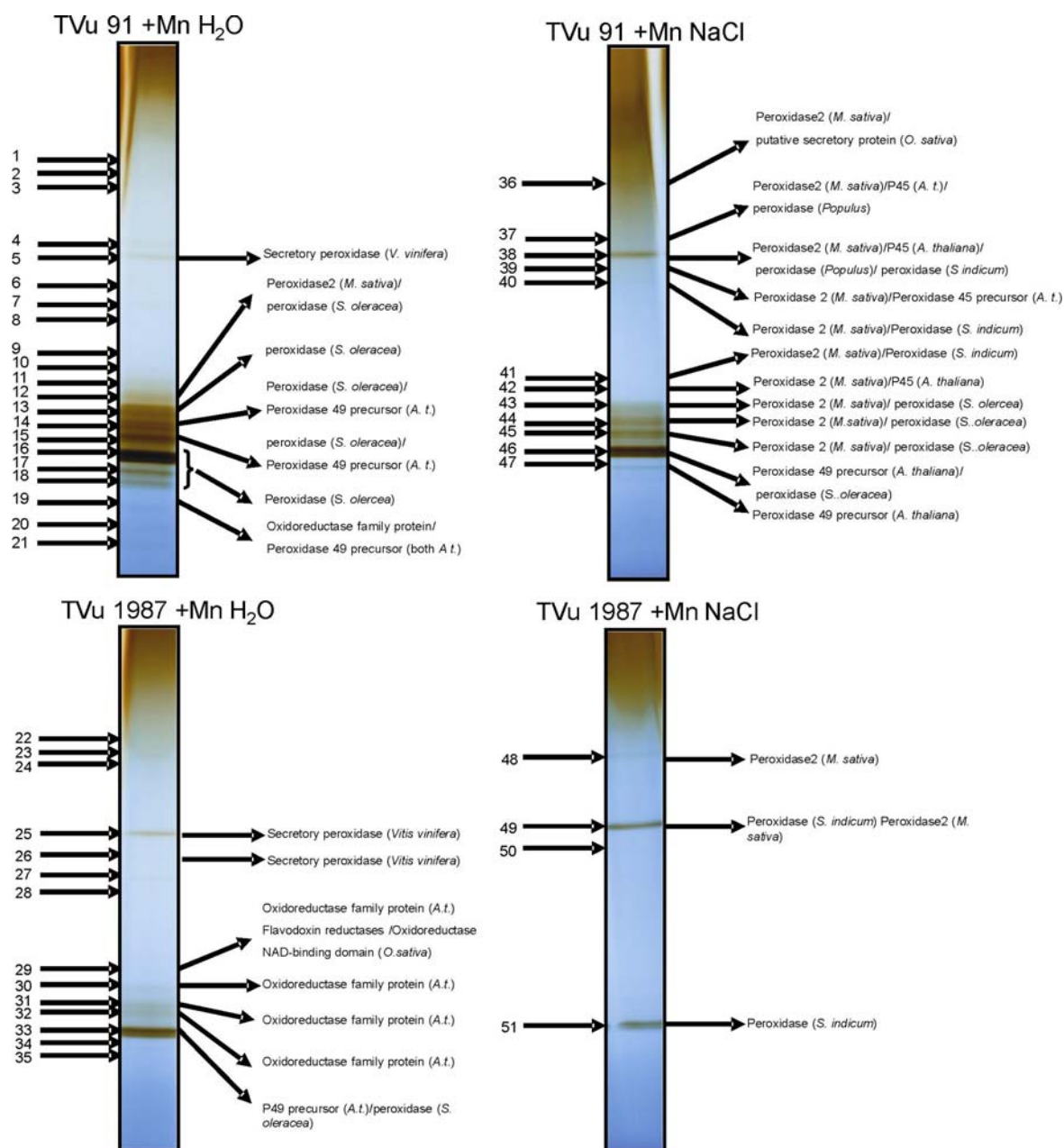


Fig. 3: Representative 1D BN-PAGE resolution of AWF_{H_2O} and AWF_{NaCl} proteins from the apoplast of the Mn-sensitive cowpea cultivar TVu 91 and the Mn-tolerant cultivar TVu 1987 stained for guaiacol-POD activity. AWF_{H_2O} and AWF_{NaCl} proteins were concentrated using centrifugal concentrators. 180 μ g and 67.5 μ g protein were applied to each lane for the first and second sequencing, respectively. After guaiacol-peroxidase activity-staining of the gels, all visible protein bands were cut, eluted, and sequenced by means of *nano*LC-MS/MS (materials and methods). Numbers in the graph correspond to the numbers in Tab. S4 given as supplementary material. POD identities are related to sequences of green plants (Viridiplantae) downloaded from <http://www.ncbi.nlm.nih.gov/sites/entrez>. Numbers 5, 25, 38, and 49 correspond to P1, numbers 13, 29, and 43 correspond to P3, numbers 15, 32, and 45 correspond to P5, and numbers 16, 33, 46, and 51 correspond to P6, all in Fig. 2 (see also Chapter 2).

In addition to peroxidases, other enzymes involved in the regulation of the redox status of the apoplast could be identified. Ascorbate peroxidases (APX) were found seven times in the

AWF_{H₂O} proteome of the Mn-tolerant cultivar (lanes no. 27, 29, 30, 31, 32, 34, and 35), but only one time in TVu 91 (lane no. 12). (Iron-) Superoxide dismutases (SOD) have been identified in both apoplastic fractions of the Mn-sensitive cultivar and the AWF_{H₂O} of the tolerant cultivar (lanes no. 6-10, 16, 27-29, 40, and 41). (Quinone-) Oxidoreductases were present only in the AWF_{H₂O} in both cultivars (lanes no. 12, 14, 19, 29, and 31), and a isoflavonoreductase-like protein and a peroxiredoxin-like protein in the water-soluble fraction of TVu 1987 (lanes no. 30, 31 and 32). Ferredoxin-NADP⁺ reductase enzyme was exclusively found in the water-soluble fraction of TVu 91 (lanes no. 11 and 12). A monodehydroascorbate reductase (MDHAR) was identified one time in both cultivars in the AWF_{H₂O} (lanes no. 9 and 28) and thioredoxin one time in the AWF_{H₂O} and the AWF_{NaCl} from TVu 1987 (lanes no. 28 and 51), but 4 times in the AWF_{NaCl} of TVu 91 (lanes no. 39, 42, 43, 47).

Metabolite profiling – Independent component analysis

Metabolite profiling of the bulk-leaf metabolome, the AWF, and the non-polar apoplastic fraction was carried out using the GC-MS technique. ICA following PCA was performed (Fig. 4A-C) and appearing sample clusters refer to the major variances due to treatment-induced qualitative and quantitative changes in metabolite pools. The first two most important independent components of the bulk-leaf metabolome were the genotype (IC01) and the Mn treatment (IC02). Within Mn-treated plants a slight effect of Si was visible. Hence, all experimental factors contributed to the variation between the samples.

The variation in the AWF metabolome was mainly caused by the infiltration solution (IC01) and the genotype (IC02).

An additional extraction procedure from the AWF yielding non-polar metabolites did not reveal a clear clustering according to the experimental design. However, the clustering of the samples from the same treatment indicates that the variation within the experiment is mainly explained by biological and not technical variations.

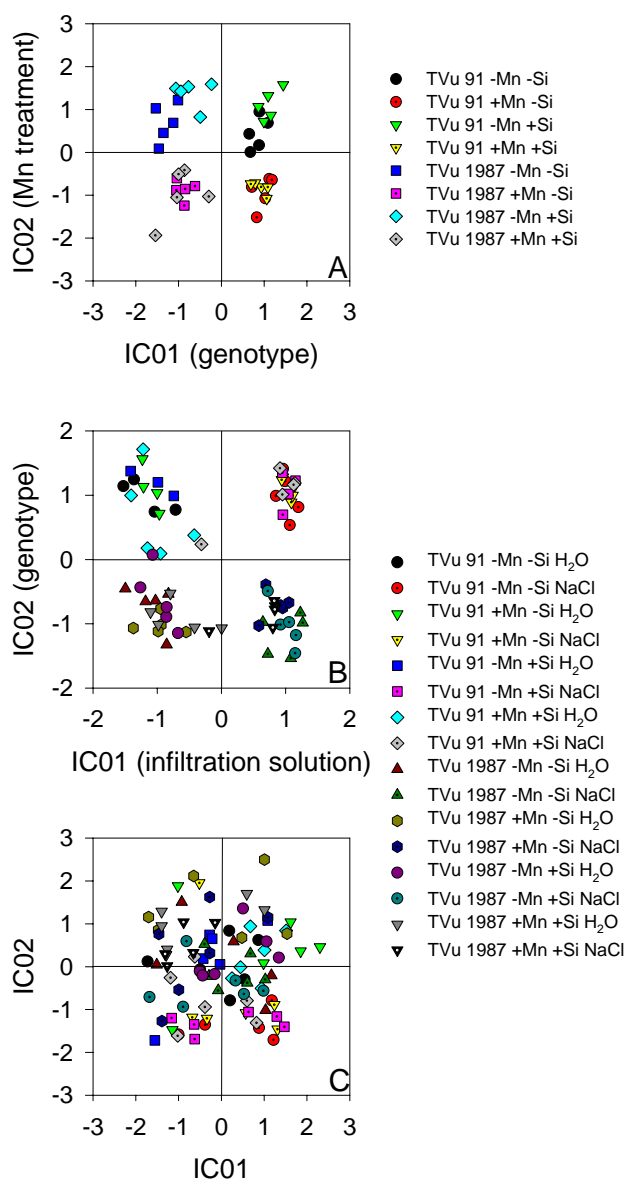


Fig. 4: ICA plot of the (A) total metabolome, (B) the apoplastic AWF_{H2O} and AWF_{NaCl}-metabolites, and (C) non-polar apoplastic metabolites extracted from the AWF_{H2O} and AWF_{NaCl} of the second oldest trifoliate leaves of the Mn-sensitive cultivar TVu 91 and the Mn-tolerant cultivar TVu 1987 as affected by Mn and Si treatments. After 14 d of preculture with or without Si (as described in “Materials and Methods”) plants received 50 μ M Mn (+Mn) for 3 d or 0.2 μ M Mn (-Mn) continuously. Bulk-leaf (n=5), AWF- and non-polar apoplastic metabolites (n=6) were extracted and measured as described in “Materials and Methods”. ICA was conducted using MetaGeneAlyse at <http://metagenealyse.mpimp-golm.mpg.de>.

In order to understand Mn sensitivity-specific changes in the different metabolome fractions, metabolic profiling results for the Mn-sensitive cultivar TVu 91 have been described earlier (Chapter 2). In this study we focussed on the Mn-tolerant genotype TVu 1987 in order to identify Mn tolerance-specific changes in the metabolome. The results of the ICA are presented in Fig. 5A-C. The first most important independent component (IC01) of the bulk-leaf metabolome was the Mn treatment. The second IC (IC04) was the Si effect. Silicon only

induced changes in the metabolome in Mn-control plants which disappeared with elevated Mn treatment.

The variation in the AWF metabolome was mainly caused by the infiltration solution (IC01) and the Mn treatment (IC02). The clustering was less clear in the AWF_{H₂O}.

The ICA of non-polar metabolites extracted from the AWF using diethylether did not only lead to a clustering of the samples according to the Mn treatments (IC02) but also, though less clear, according to the infiltration solution (IC04) indicating that the variation within the experiment is mainly explained by biological rather than technical variation.

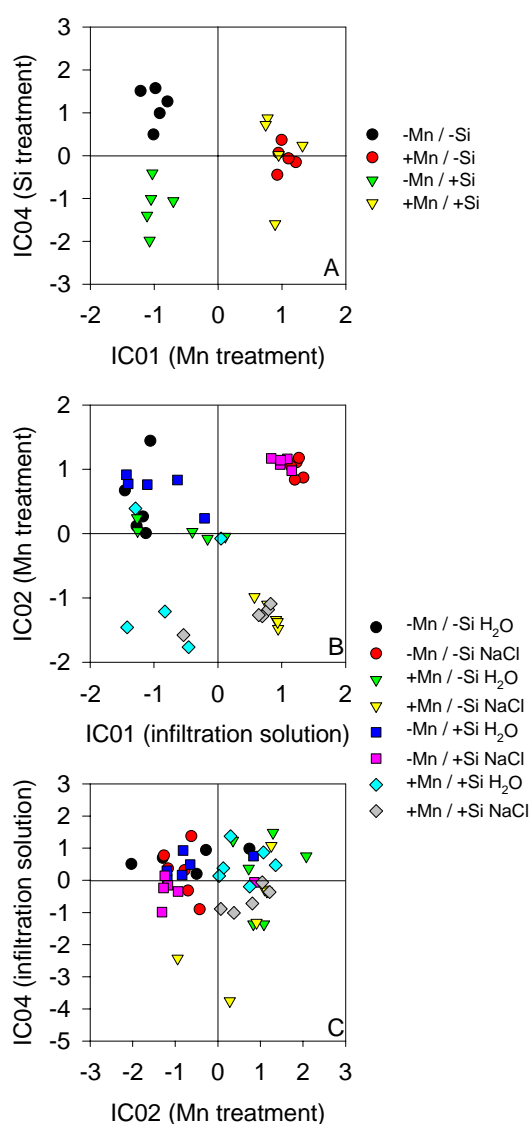


Fig. 5: ICA plot of the (A) total metabolome, (B) the apoplastic AWF_{H₂O} and AWF_{NaCl} metabolites, and (C) non-polar apoplastic metabolites extracted from the AWF_{H₂O} and AWF_{NaCl} of the second oldest trifoliolate leaf of the Mn-tolerant cultivar TVu 1987 as affected by Mn and Si treatment. After 14 d of preculture with or without Si (as described in “Materials and Methods”) plants received 50 μ M Mn (+Mn) for 3 d or 0.2 μ M Mn (-Mn) continuously. Bulk-leaf, AWF- and non-polar apoplastic metabolites were extracted and measured (n=5 and 6, respectively) as described in “Materials and Methods”. ICA was conducted using MetaGeneAlyse at <http://metagenealyse.mpimp-golm.mpg.de>.

Tab. 1 presents a list of metabolites responsible for the ICA clusterings according to the experimental factors for each cowpea genotype separately and for both genotypes together in order to get a better comparative overview. Briefly, considering the individual ICAs, ICs are the same in both cultivars, except for the non-polar apoplastic fraction. Responsible metabolites of the bulk-leaf and apoplastic metabolome differ between the cultivars with few exceptions (ascorbic acid, gluconic acid, malic acid). In the AWF metabolome the number of metabolites responsible especially for the clustering according to IC02 was higher in TVu 91 than in TVu 1987 (10 versus 3), whereas the metabolite composition responsible for clusterings in the non-polar apoplastic fraction was similar between the genotypes independent of the IC. Comparing the genotypes, the metabolites responsible for the clustering in the bulk leaf metabolome due to IC01 or IC02 differed. The role of tartaric acid in the bulk-leaf (IC01) and the AWF metabolome (IC02) for the genotype-specific clustering is particularly conspicuous. Clustering according to IC01 was due to malic acid and GABA. In the non-polar fraction IC01 was mainly formed by succinic acid and *p*-coumaric acid. The same metabolites plus several organic acids formed IC02.

Tab. 1. Metabolites responsible for clusterings in the three different leaf metabolome fractions received from ICA loadings when ICA was performed for each genotype (TVu 91 in Chapter 2, TVu 1987 in this study) and in a genotypical comparison (TVu 91 vs TVu 1987 in this study). Analyses and ICA were performed as described in the Materials and Methods section.

Bulk-leaf metabolome	TVu 1987		TVu 91		TVu 91 vs TVu 1987	
	IC01	IC04	IC01	IC04	IC01	IC02
	quinic acid gluconic acid galactinol ascorbic acid	glucose ononitol	serine threonine asparagine aspartic acid coniferylalcohol gluconic acid sorbitol ascorbic acid	galactose gluconic acid	aspartic acid glutamic acid tartaric acid quinic acid	asparagines gluconic acid ascorbic acid
AWF metabolome	IC01	IC02	IC01	IC02	IC01	IC02
	malonic acid malic acid erythronic acid-1,4-lactone galactosylglycerol isomaltose BP1 alanine BP1 threonine BP1	malonic acid shikimic acid galactosylglycerol	malic acid ribonic acid gluconic acid threonine xylose erythrose fucose	maleic acid malic acid nicotinic acid itaconic acid threonine alanine xylose fructose tagatose 3-hydroxybenzoic acid	malic acid GABA	tartaric acid
Non-polar apoplatic metabolome	IC02	IC04	IC02	IC03	IC01	IC02
	3-oxoglutaric acid <i>p</i> -coumaric acid	malonic acid fumaric acid malic acid <i>cis</i> -aconitic acid citric acid <i>p</i> -coumaric acid	3-oxoglutaric acid	malonic acid succinic acid fumaric acid citric acid 3-oxoglutaric acid <i>p</i> -coumaric acid <i>p</i> -hydroxybenzoic acid	succinic acid <i>p</i> -coumaric acid	malonic acid succinic acid fumaric acid malic acid citric acid <i>p</i> -coumaric acid

Metabolite profiling – Treatment effects on individual metabolites

General comments

The variance criterion was set more stringently by subsequent 3-factorial-ANOVA. Displayed are the fold changes calculated as main effects of the treatments (Mn, Si, and Gen) without taking significant interactions into account (Figs. 6-8). Only metabolites that showed at least either a two-fold change in abundance with $P < 0.05$ or a less than two-fold change but with $P < 0.001$ were considered.

In order to identify changes between the individual experimental factors and to evaluate and justify the display of changes between the experimental main factors despite interactions, pairwise comparisons (t-test) followed by the application of specific threshold criteria (t-test, $P < 0.05$ and fold induction / reduction > 2) were performed and are given as supplementary material (Tab. S1).

For further simplifying the presentation of the results, the discussion of the huge dataset is reduced to metabolites which are considered as particularly important for the understanding of Mn toxicity and/or tolerance. Hence, this section focuses on metabolites with high treatment-dependent responses (see also Tab. S2 to find a complete list of detected metabolites) and should, therefore, be regarded as a screening for particular metabolites. Metabolites responsible for ICA clusterings as revealed by ICA loadings (when not covered by ANOVA results) are included as well. The phenylpropanoids of the non-polar apoplasmic fraction is given particular attention with an own section in order to refer to their POD modulating function in terms of Mn toxicity development.

General results

The data are presented according the effects of the main experimental factors (ANOVA) Mn treatment, Si supply, and genotype (Figs 6-8). Based on the number of metabolites and their magnitude of change it appears that the relative importance of the individual factors is genotype \geq Mn $>$ Si. A list of the ANOVA results for all detected and annotated metabolites is given as supplementary material (Tab. S2).

In **the bulk leaf extract** (Fig. 6) 42 metabolites were identified (and 32 currently not annotated, see also supplementary material Tab. S2) which were affected at least by one of the

main factors. The metabolites were grouped into five subgroups: organic acids, (sugar-) alcohols, amino acids, sugars, and others (including spermidine as amine and *cis*- and *trans*-4-hydroxycinnamic acid in order to simplify the figure). Ascorbic acid and dehydroascorbic acid (dimer) were added to the organic acid fraction in order to simplify the results and the discussion section.

In the **AWF_{H2O}** and **AWF_{NaCl}** (Figs. 7A, B) the same selection criteria for ANOVA results as already used for the bulk-leaf metabolome led to in sum 19 metabolites in the AWF_{H2O} and 29 metabolites in the AWF_{NaCl} differing in abundance. AWF_{H2O} metabolites were grouped into organic acids, amino acids, sugars, and other metabolites (galactinol and mannitol as (sugar-) alcohols were added to subgroup “others” for simplification Fig. 7A). The AWF_{NaCl} metabolites have been grouped into organic acids, amino acids, sugars, (sugar-) alcohols, and other metabolites. Here, ascorbic acid and dehydroascorbic acid (dimer) were added to the organic acid fraction in order to simplify the results and discussion section, too.

Despite two extraction procedures for **non-polar apoplastic metabolites** (AWF extraction and extraction of non-polar metabolites from the AWF) in sum 8 metabolites have been identified from the AWF_{H2O} and 12 metabolites from the AWF_{NaCl} which revealed significant responses according to the experimental main factors (Fig. 8A, B). They could be grouped into two subgroups in the non-polar fraction of the AWF_{H2O}, namely others and phenylpropanoids, and into three subgroups in the non-polar fraction of the AWF_{NaCl}, namely organic acids, phenylpropanoids, and others.

The bulk-leaf metabolite profile

Considering the threshold criteria mentioned above, in the **bulk-leaf metabolome** (Fig. 6) Si had an increasing effect only on the synthesis of GABA (Fig. 6a), whereas all other identified amino acids decreased independent of the applied experimental main factor. GABA showed a significant Mn*Si*Gen interaction because it was enhanced by Mn more in TVu 91 than in TVu 1987 and in plants that received a combined Mn and Si treatment (Tab. S1.1c). Asparagine was more than 2-fold downregulated by increased Mn supply, whereas serine BP, threonine BP, and aspartic acid BP2 showed a more than 2-fold lower content in TVu 91.

In the group of (sugar-) alcohols (Fig. 6b) coniferylalcohol showed a 5-fold Mn-induced increase and was more than 2-fold lower abundant in TVu 91. Galactinol and myo-inositol were slightly reduced by Mn, slightly increased by Si and less abundant in TVu 91. Galactitol was strongly decreased by Mn and less abundant in the Mn-sensitive cultivar.

The organic acid fraction contributed the highest number of treatment-affected metabolites (Fig. 6c) with two very conspicuous metabolites. Gluconic acid was more than 7-fold increased by Mn showing the stress responsiveness of this metabolite, and the tartaric acid concentration was about 80-fold lower in TVu 91 than in Mn-tolerant TVu 1987 indicating that this metabolite is a Mn tolerance factor. TVu 91 had more than 2-fold higher malonic acid contents than TVu 1987. Quinic acid, ascorbic acid, and dehydroascorbic acid were lower in TVu 91 compared with TVu 1987, decreased in Mn treatments and increased in Si treatments.

Most sugars are highly abundant metabolites in plants (Fig. 6d). Thus, small changes may reflect major alterations in basic metabolic functions. Fructose, galactose, and glucose showed the same response pattern, namely a Mn-induced downregulation, a Si-induced upregulation, and a lower abundance in TVu 91 compared with TVu 1987. The significant Mn*Si*Gen interaction for glucose (Fig. 6) is explained by a higher abundance in Si-treated plants of TVu 91 compared with TVu 1987 (Tab. S1.1a-c). Sucrose was both increased by Mn and Si supply, and together with raffinose was less abundant in TVu 91. The most striking difference between the genotypes showed the xylobiose concentration (BP1) which was nearly 10-fold higher in TVu 91 than in TVu 1987.

Fig. 6e displays all remaining significantly affected metabolites. Among them the Mn-mediated more than 2-fold downregulation of spermidine has to be mentioned. Additionally, Mn reduced and Si increased threonic acid-1,4-lactone, and TVu 91 had higher contents than TVu 1987.

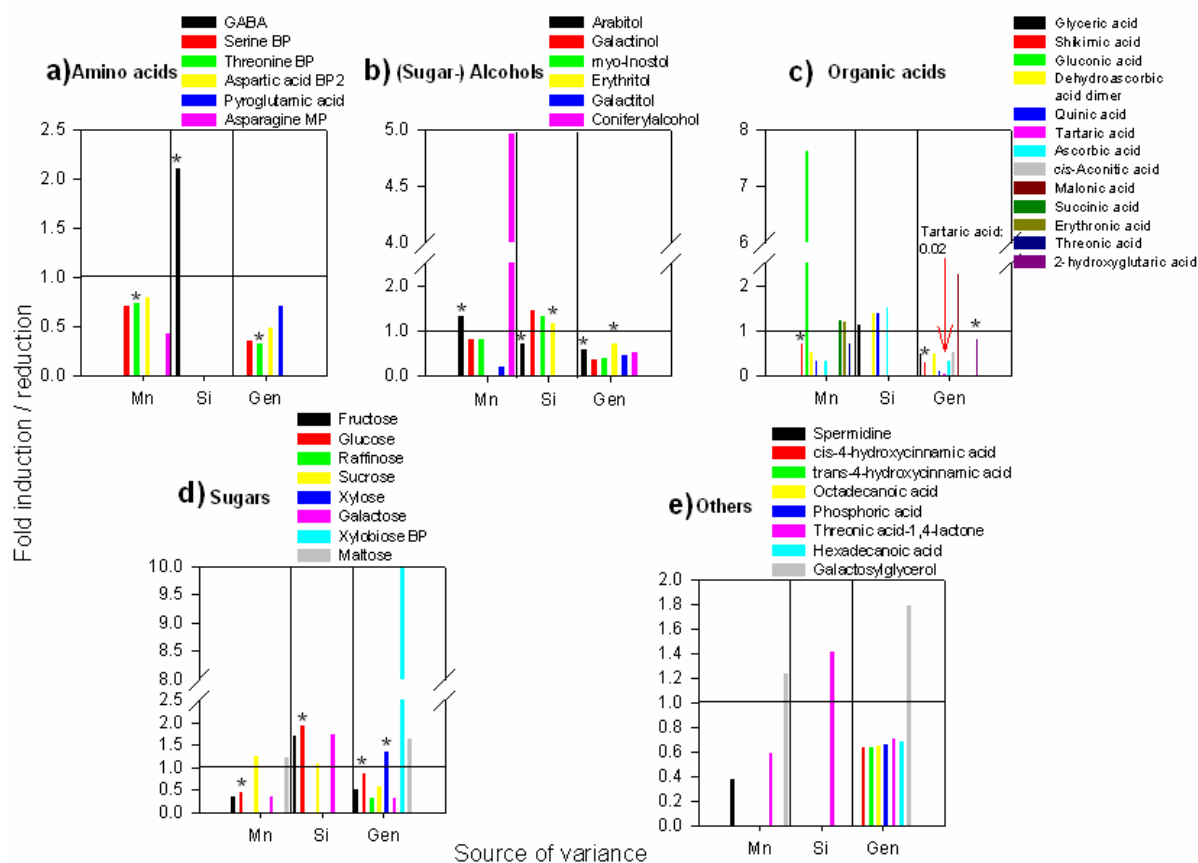


Fig. 6: Identified and significantly affected (by Mn/Si/genotype treatments) **bulk-leaf metabolites** of the second oldest trifoliolate leaves of the Mn-sensitive cultivar TVu 91 and the Mn-tolerant cultivar TVu 1987 grouped into five different metabolite groups: organic acids, (sugar-) alcohols, amino acids, sugars, and others. Displayed are fold inductions / reductions of each metabolite within the comparison of the statistical main factors listed on the x-axis: Mn (+Mn vs -Mn), Si (+Si vs -Si) and Gen (TVu 91 vs TVu 1987). * Stars indicate significant Mn*Si*Gen interactions. Only those metabolites were taken into account, which showed a significant change in abundance (more than 2-fold induction / reduction with $P < 0.05$ and/or $P < 0.001$) within the comparison (Mn: +Mn vs -Mn, Si: +Si vs -Si, Gen: TVu 91 vs TVu 1987). Bulk-leaf metabolites were extracted ($n=5$) and measured as described in “Materials and Methods”.

The apoplastic metabolite profile

In the $\text{AWF}_{\text{H}_2\text{O}}$ containing the water-soluble apoplastic metabolites, the organic acids (Fig. 7Aa) dehydroascorbic acid dimer and *cis*-aconitic acid responded with an increase to elevated Mn supply (Fig. 7A), whereas tartaric acid was nearly 50-fold lower in abundance in TVu 91 than in TVu 1987. Silicon did not influence organic acids.

Manganese did not affect water-soluble apoplastic sugars (Fig. 6Ab), but Si increased the sugars isomaltose BP1 and erythrose. Xylobiose BP1 was the only sugar with drastically higher abundance in TVu 91. All other significantly affected sugars (ribose BP1, fucose BP1, isomaltose BP1, and xylose) were lower abundant in TVu 91

Among the amino acids (Fig. 7Ac) GABA was increased by Si. Threonine BP1 concentration was enhanced by Mn and as well as alanine (BP1) and pyroglutamic acid lower in TVu 91. Galactinol increased by Mn treatment and was higher in TVu 1987 as was mannitol (Fig 7Ad). Only 3-deoxyglucose responded with an increase to Si supply.

Also in the AWF_{NaCl} Si did not affect organic acids (Fig. 7Ba). However, Mn supply increased the concentrations of maleic, tartaric, gluconic, itaconic, dehydroascorbic, and *cis*-aconitic acid, whereas shikimic, lactic, and malonic acids were decreased. Again, tartaric acid was nearly 40-fold lower abundant in TVu 91.

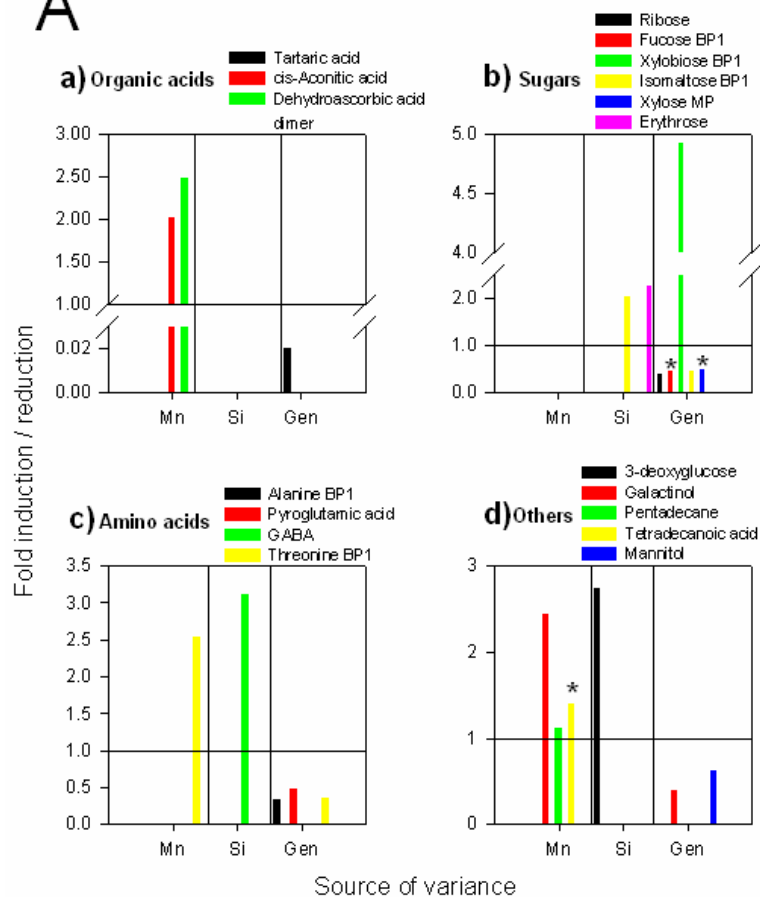
In the ionically-bound sugar fraction (Fig. 7Bb) a more than 8-fold higher xylobiose (BP1) content in TVu 91 (as shown above for the AWF_{H_2O}) was particularly prominent. Also gentiobiose BP1 was higher in TVu 91. Altrose was upregulated by Mn and lower in TVu 91 than in TVu 1987. The significant Mn*Si*Gen interaction for altrose was mainly due to a Mn-mediated increase, a Si-mediated decrease only in Mn-treated plants in TVu 91, and a higher abundance in TVu 1987 only in control plants and in a combined Mn and Si treatment (Tab. S1.2.a-c). 3-deoxyglucose and tagatose were upregulated by Mn supply. Silicon increased only isomaltose BP1 by a factor of two.

Among the amino acids ornithine showed a positive Mn treatment-response, whereas β -alanine concentration was enhanced by Si supply (Fig. 7Bc).

In the sugaralcohols fraction (Fig. 7Bd), erythritol was increased in response to excess Mn and ononitol was higher in TVu 91 compared with TVu 1987.

None of the metabolites listed in subgroup “others” (Fig. 7Be) was affected by Si and only adenosine was less abundant in TVu 91. There were many metabolites which showed responsiveness to elevated Mn supply: 3-hydroxybenzoic acid, 2-oxoglutaric acid, undecane, 2-desoxyribose-3-lyxose BP1, and tetradecanoic acid were increased, whereas octacosane, dotriacontane, hexatriacontane and hydroxylamine were decreased.

A



B

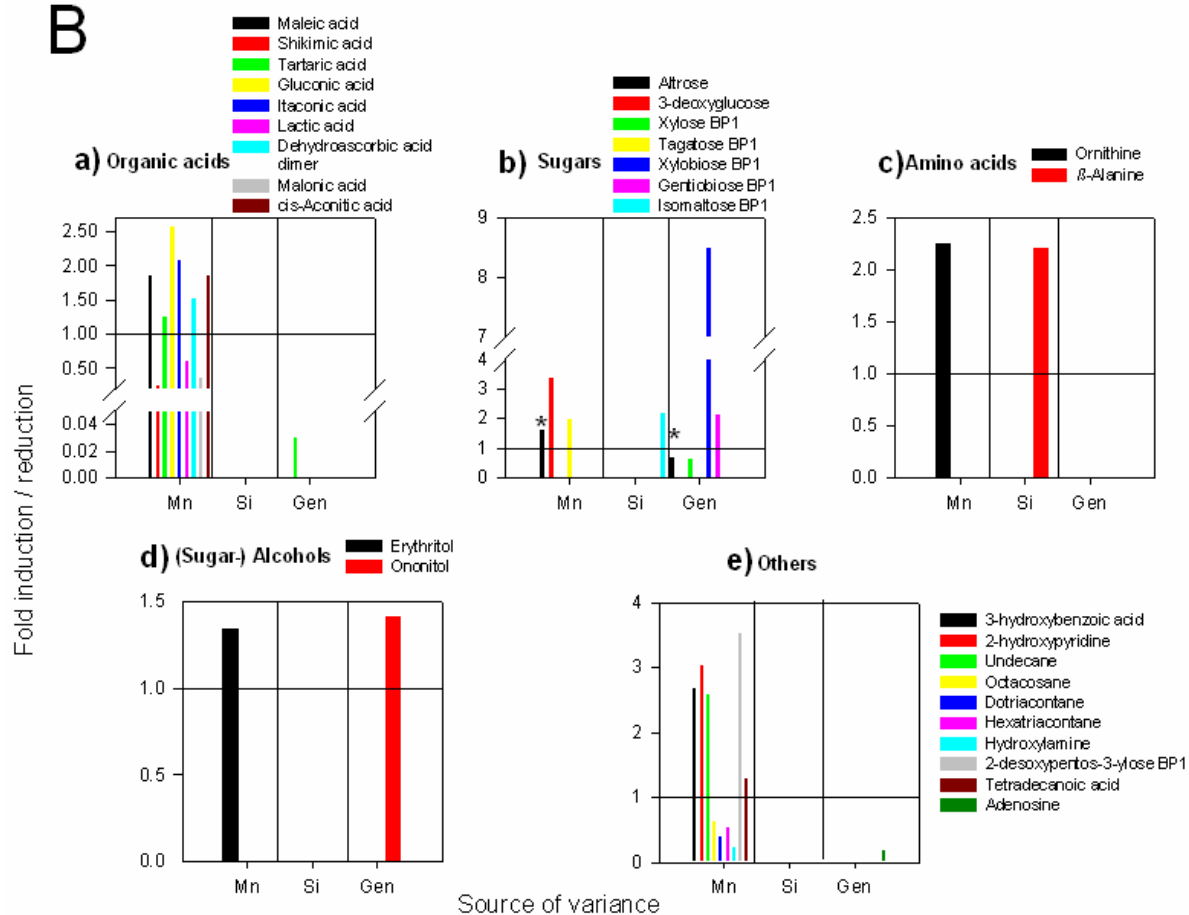


Fig. 7: Identified and significantly affected (by Mn/Si/genotype treatments) **AWF_{H₂O}** (A) and **AWF_{NaCl}** (B) **metabolites** of the second oldest trifoliolate leaves of the Mn-sensitive cultivar TVu 91 and the Mn-tolerant cultivar TVu 1987 grouped into different metabolite groups: organic acids, amino acids, sugars, (sugar-) alcohols, and others. Displayed are fold inductions / reductions of each metabolite within the comparison of the statistical main factors listed on the x-axis: Mn (+Mn vs –Mn), Si (+Si vs –Si) and Gen (TVu 91 vs TVu 1987). * Stars indicate significant Mn*Si*Gen interactions. Only those metabolites were taken into account, which showed a significant change in abundance (more than 2-fold induction / reduction with $P < 0.05$ and/or $P < 0.001$) within the comparison (Mn: +Mn vs –Mn, Si: +Si vs –Si, Gen: TVu 91 vs TVu 1987). Apoplastic metabolites were extracted (n=5) and measured as described in “Materials and Methods”.

The non-polar apoplastic metabolite profile

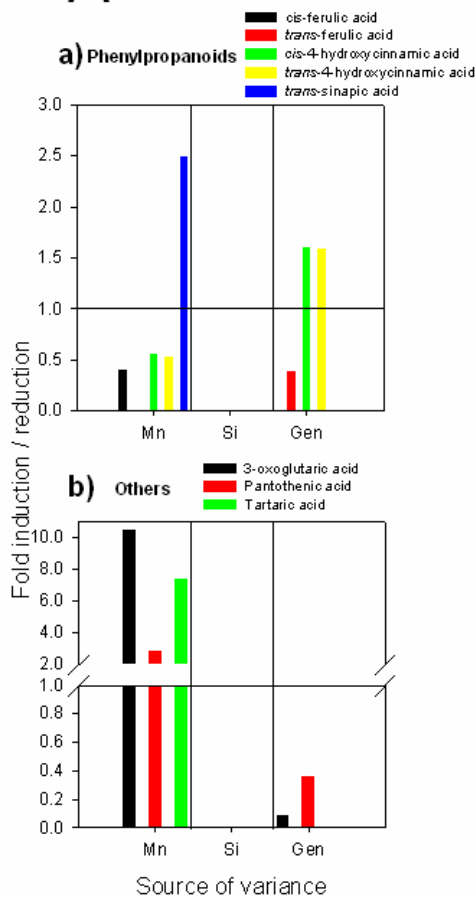
Phenylpropanoids of the **non-polar fraction of the AWF_{H₂O} and AWF_{NaCl}** (Figs. 8Aa, 8Ba) will be discussed in detail in the following “*Phenylpropanoids in the non-polar apoplastic fraction*” section.

In the fraction “others” (Fig. 8Ab) Mn treatment increased the concentrations of 3-oxoglutaric acid, an analog of 2-oxoglutaric acid known from the TCA cycle, tartaric acid and pantothenic acid. 3-oxoglutaric acid and pantothenic acid were less abundant in TVu 91 than in TVu 1987.

Among the organic acids in the **non-polar metabolite fraction of the AWF_{NaCl}** (Fig. 8Bb) succinic acid, malic acid, malonic acid, and fumaric acid were higher abundant in TVu 91. Tartaric acid and succinic acid concentrations were reduced by Si supply, the latter also by Mn supply.

3-oxoglutaric acid was strongly increased by Mn but was nearly 10-fold lower in abundance in TVu 91 as well as laminaribiose BP1 (Fig 8Bc). Pantothenic acid was increased in response to Mn and higher in TVu 91 than in TVu 1987.

A



B

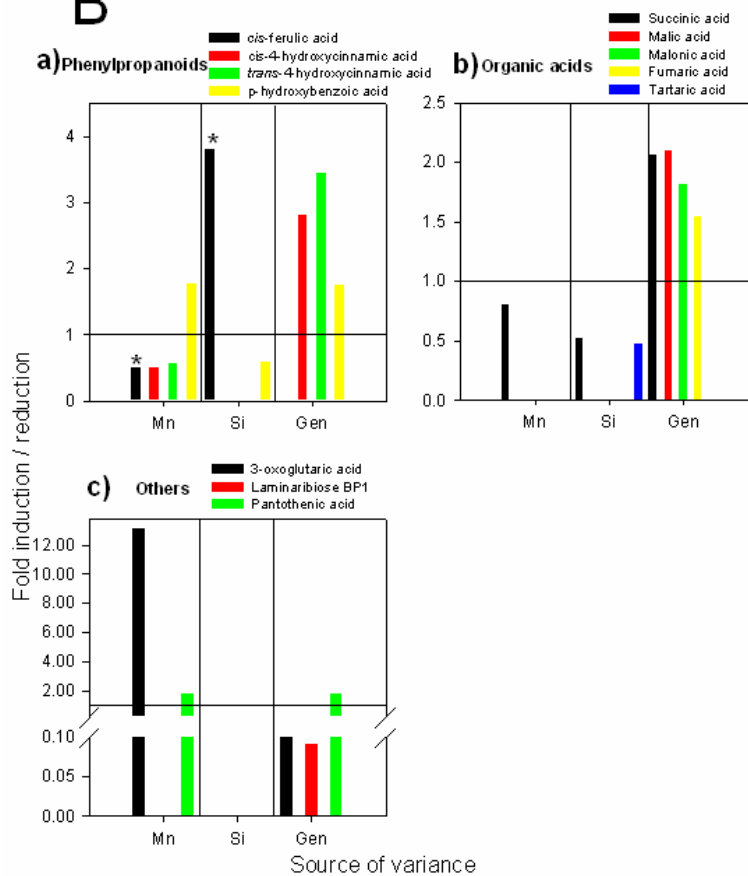


Fig. 8: Identified and significantly affected (by Mn/Si/genotype treatments) AWF_{H₂O} (A) or AWF_{NaCl} (B) **non-polar apoplastic metabolites** of the second oldest trifoliolate leaves of the Mn-sensitive cultivar TVu 91 and the Mn-tolerant cultivar TVu 1987 grouped into different metabolite groups: organic acids and phenylpropanoids. Displayed are fold inductions / reductions of each metabolite within the comparison of the statistical main factors listed on the x-axis: Mn (+Mn vs -Mn), Si (+Si vs -Si) and Gen (TVu 91 vs TVu 1987). * Stars in (B) indicate that *cis*-ferulic acid was only present in Mn-treated TVu 1987. Only those metabolites were taken into account, which showed a significant change in abundance (more than 2-fold induction / reduction with $P < 0.05$ and/or $P < 0.001$) within the comparison (Mn: +Mn vs -Mn, Si: +Si vs -Si, Gen: TVu 91 vs TVu 1987). Unpolar apoplastic metabolites were extracted (n=6) and measured as described in “Materials and Methods”.

Phenylpropanoids in the non-polar apoplastic fraction

This section describes the relative changes in abundance of identified phenols in the non-polar leaf AWF fractions of the AWF_{H₂O} and the AWF_{NaCl} for each individual comparison of the experimental setup. In order to link phenols and peroxidases here are also displayed (but not described) the abilities of the phenols to induce / inhibit NADH-*peroxidase* activity of four different apoplastic peroxidase isoenzymes as examined in Chapter 2. Only those phenols showing a significant difference in abundance (as indicated by stars) in the individual comparisons are considered in this section, even though for all phenols relative changes are shown (Tab. 2). For simplification the aromatic carboxylic acid benzoic acid is considered as phenol, too.

In the Mn-tolerant cultivar TVu 1987 Mn treatment reduced both *cis* and *trans-p*-coumaric acid concentrations about 10-fold in both apoplastic fractions (Tab. 2a). *Cis*-ferulic acid was only present in Mn-control plants which did not allow the calculation of a fold induction / reduction rate. In contrast *trans*-sinapic acid in both apoplastic fractions was higher abundant in Mn-treated compared with control plants. TVu 91 responded to Mn treatment with a significant downregulation of *cis*- and *trans*-ferulic acid (*trans*-ferulic acid only in the AWF_{H₂O}).

Si treatments significantly increased the abundance of ferulic acid exclusively in the AWF_{NaCl} (Tab. 2b). Benzoic acid was slightly but significantly increased in the AWF_{H₂O} and *trans*-sinapic acid was only present in the AWF_{H₂O} of Si-control plants.

Regarding the Si-effect in Mn-treated plants no statistically significant changes in phenol abundance have been observed in TVu 1987 (Tab. 2c), but *cis*-ferulic acid was neither present in Mn-treated nor in Mn and Si-treated plants and *trans*-ferulic acid only occurred in Mn-treated plants. *Trans*-sinapic acid has been detected only in the AWF_{NaCl} extracted from Mn-treated plants. The same was true for TVu 91. Moreover, *p*-hydroxybenzoic acid was

significantly downregulated in both apoplastic fractions of TVu 91 due to additional Si supply to Mn-treated plants compared with only Mn-treated plants.

In Si-treated plants (Tab. 2d) of TVu 1987, Mn treatment induced a significant 4 to 6-fold downregulation of the *p*-coumaric acid isomers in both apoplastic fractions, whereas *p*-hydroxybenzoic acid was significantly enhanced in the AWF_{NaCl}. *Cis* and *trans*-ferulic acid in both apoplastic fractions and *trans*-sinapic acid only in the AWF_{H₂O} could be identified only in the plants not treated with Mn. In TVu 91 only benzoic acid increased significantly in Mn-treated plants in the AWF_{H₂O}. As in TVu 1987, *trans*-sinapic acid could not be identified in the AWF_{H₂O} of Mn-treated plants.

A comparison of the cowpea cultivars in the control treatment (-Mn, -Si) (Tab. 2e) revealed significant differences only in the AWF_{NaCl}. The concentrations of all phenylpropanoids were increased (significant for *p*-hydroxybenzoic acid, *cis* and *trans*-*p*-coumaric acid, *trans*-sinapic acid), whereas benzoic acid was decreased. When the cultivars were compared at high Mn without Si supply (Tab. 2e) *cis* and *trans*-*p*-coumaric acid were much higher in both apoplastic fractions in TVu 91, whereas *trans*-ferulic acid was nearly 10-fold lower in the AWF_{H₂O}. *Cis*-ferulic acid was only present in both apoplastic fractions of TVu 91.

When the plants were Si but not Mn-treated (Tab. 2f), again most prominent differences between the cultivars appeared in the AWF_{NaCl}. Only benzoic acid in the AWF_{H₂O} was significantly lower in TVu 91. *p*-Hydroxybenzoic acid, and both isomers of *p*-coumaric acid and ferulic acid were more abundant in the AWF_{NaCl} of TVu 91 compared to TVu 1987. *Trans*-sinapic acid was only present in in the AWF_{H₂O} of TVu 1987. Comparison of the cultivars treated with Mn and Si (Tab. 2f) showed a 3 to 6-fold increased abundance of *cis* and *trans*-*p*-coumaric acid in TVu 91 compared with TVu 1987 in both AWF fractions. *Cis* and *trans*-ferulic acid could be detected only in TVu 91. *Trans*-sinapic acid was not present in the AWF_{H₂O} of both cultivars.

Tab. 2: Identified phenols (GC-MS) in the non-polar leaf AWF fraction of the AWF_{H₂O} and the AWF_{NaCl} and their relative changes in abundance for each individual comparison (based on response ratios) as well as their effect on the NADH-*peroxidase* activity of four different apoplastic peroxidase isoenzymes (Chapter 2). After 14 d of preculture ±Si (as described in “Materials and Methods”) plants of the Mn-sensitive cowpea cultivar TVu 91 and the Mn-tolerant cowpea cultivar TVu 1987 received 50 μM Mn for 3 d or 0.2 μM Mn continuously. ***, **, * indicate significant changes in metabolite abundance at $p < 0.001$, 0.01 and 0.05, respectively (t test with log₁₀-transformed response ratios, n=6).

a.)

Detected phenol	TVu 1987 ratio +Mn -Si / -Mn -Si		TVu 91 ratio +Mn -Si / -Mn -Si		Substrate specificity / interaction ^a
	dH ₂ O	NaCl	dH ₂ O	NaCl	
<i>p</i> -hydroxybenzoic acid	0.76	1.91	1.50	1.49	no induction / 50% inhibition ^b
<i>cis</i> - <i>p</i> -coumaric acid	0.079**	0.14**	1.06	0.84	Strong induction / control phenol
<i>cis</i> -ferulic acid	+	+	0.27**	0.34*	little induction / 50 % inhibition
<i>trans</i> - <i>p</i> -coumaric acid	0.048**	0.16**	0.94	0.78	Strong induction / control phenol
<i>trans</i> -ferulic acid	2.58	4.08	0.44*	1.34	little induction / 50 % inhibition
<i>trans</i> -sinapic acid	4.67*	1.52*	1.95	0.80	not examined
benzoic acid	1.47	1.17	1.40	1.28	induction / no effect

- + only present in 0.2 μM Mn

b.)

Detected phenol	TVu 1987 ratio -Mn +Si / -Mn -Si		TVu 91 ratio -Mn +Si / -Mn -Si		Substrate specificity / interaction ^a
	dH ₂ O	NaCl	dH ₂ O	NaCl	
<i>p</i> -hydroxybenzoic acid	1.22	0.65	0.88	0.61*	no induction / 50% inhibition ^b
<i>cis</i> - <i>p</i> -coumaric acid	0.77	1.17	0.85	1.12	Strong induction / control phenol
<i>cis</i> -ferulic acid	1.29	3.17**	1.19	4.13**	little induction / 50 % inhibition
<i>trans</i> - <i>p</i> -coumaric acid	0.69	0.81	0.76	0.92	Strong induction / control phenol
<i>trans</i> -ferulic acid	1.33	2.31*	1.10	3.78**	little induction / 50 % inhibition
<i>trans</i> -sinapic acid	+	1.10	+	0.72	not examined
benzoic acid	1.26*	0.91	0.96	1.31**	induction / no effect

- + only present in 0 μM Si

c.)

Detected phenol	TVu 1987 ratio +Mn +Si / +Mn -Si		Tvu 91 +Mn +Si / +Mn -Si		Substrate specificity / interaction ^a
	dH ₂ O	NaCl	dH ₂ O	NaCl	
<i>p</i> -hydroxybenzoic acid	1.69	0.69	0.61*	0.53*	no induction / 50% inhibition ^b
<i>cis</i> - <i>p</i> -coumaric acid	2.41	1.21	1.04	0.69	Strong induction / control phenol
<i>cis</i> -ferulic acid	+	+	2.48	1.97	little induction / 50 % inhibition
<i>trans</i> - <i>p</i> -coumaric acid	4.20	1.25	0.80	0.59	Strong induction / control phenol
<i>trans</i> -ferulic acid	++	++	1.29	0.63	little induction / 50 % inhibition
<i>trans</i> -sinapic acid	++	0.78	++	0.79	not examined
benzoic acid	0.79	1.00	1.01	1.14	induction / no effect

- + not present in both treatments
- ++ only present in +Mn -Si

d.)

Detected phenol	TVu 1987 ratio +Mn +Si / -Mn +Si		Tvu 91 +Mn +Si / -Mn +Si		Substrate specificity / interaction ^a
	dH ₂ O	NaCl	dH ₂ O	NaCl	
<i>p</i> -hydroxybenzoic acid	1.05	2.04**	1.04	1.29	no induction / 50% inhibition ^b
<i>cis</i> - <i>p</i> -coumaric acid	0.25***	0.15***	1.30	0.51	Strong induction / control phenol
<i>cis</i> -ferulic acid	+	+	0.56	0.16	little induction / 50 % inhibition
<i>trans</i> - <i>p</i> -coumaric acid	0.29**	0.24*	1.00	0.49	Strong induction / control phenol
<i>trans</i> -ferulic acid	+	+	0.52	0.22	little induction / 50 % inhibition
<i>trans</i> -sinapic acid	+	1.07	+	0.87	not examined
benzoic acid	0.93	1.27	1.48**	1.11	induction / no effect

- + only present in -Mn +Si

e.)

Detected phenol	-Mn -Si ratio TVu 91/TVu 1987		+Mn -Si ratio TVu 91/TVu 1987		Substrate specificity / interaction ^a
	dH ₂ O	NaCl	dH ₂ O	NaCl	
<i>p</i> -hydroxybenzoic acid	1.16	2.35**	2.30	1.83	no induction / 50% inhibition ^b
<i>cis</i> - <i>p</i> -coumaric acid	0.74	1.90*	9.95**	10.92**	Strong induction / control phenol
<i>cis</i> -ferulic acid	0.77	2.23	+	+	little induction / 50 % inhibition
<i>trans</i> - <i>p</i> -coumaric acid	0.83	2.71**	16.21*	13.34***	Strong induction / control phenol
<i>trans</i> -ferulic acid	0.72	1.95	0.12*	0.64	little induction / 50 % inhibition
<i>trans</i> -sinapic acid	1.22	2.19**	0.51	1.15	not examined
benzoic acid	1.03	0.82**	0.98	0.90	induction / no effect

- +only present in TVu 91

f.)

Detected phenol	-Mn +Si ratio TVu 91/TVu 1987		+Mn +Si ratio TVu 91/TVu 1987		Substrate specificity / interaction ^a
	dH ₂ O	NaCl	dH ₂ O	NaCl	
<i>p</i> -hydroxybenzoic acid	0.83	2.19**	0.82	1.39	no induction / 50% inhibition ^b
<i>cis</i> - <i>p</i> -coumaric acid	0.82	1.82*	4.31***	6.24**	Strong induction / control phenol
<i>cis</i> -ferulic acid	0.71	2.91**	++	++	little induction / 50 % inhibition
<i>trans</i> - <i>p</i> -coumaric acid	0.91	3.08*	3.10*	6.28**	Strong induction / control phenol
<i>trans</i> -ferulic acid	0.60	3.19**	++	++	little induction / 50 % inhibition
<i>trans</i> -sinapic acid	+	1.44	+++	1.16	not examined
benzoic acid	0.79**	1.17	1.25	1.02	induction / no effect

- +only present in TVu 1987
- ++only present in TVu 91
- +++ not present in both treatments

^a Substrate specificity and interaction results are from Chapter 2

^b after identification of *p*-hydroxybenzoic acid, this phenol was additionally tested with respect to NADH-*peroxidase* activity. Among the inhibitory effect shown in this table, it showed no induction capability for NADH-*peroxidase* activity for each isozyme tested.

Discussion

The apoplast is considered the decisive leaf compartment for the development or avoidance of Mn toxicity based on the deposition of oxidized Mn and phenols (brown spots) and related physiological and biochemical changes in the leaf apoplast (Horst et al., 1999; Fecht-Christoffers et al., 2006; Chapter 2). In this study the Mn-sensitive cowpea cultivar TVu 91 exhibited 10-15 brown spots cm⁻² leaf area typical for a medium severe expression of Mn toxicity (Chapter 2) whereas the Mn-tolerant cultivar TVu 1987 and Si-treated plants of the Mn-sensitive cultivar did not show any toxicity symptoms throughout the 3 days Mn treatment (Fig. 1). Therefore, the presented changes in the proteome and metabolome may be regarded as early effects directly linked to a Mn response rather than secondary effects induced by Mn toxicity-enhanced leaf senescence as supposed by Fecht-Christoffers et al. (2006, 2007). The development of the typical symptoms correlates with the activity of apoplastic class III secretory peroxidases (Fecht-Christoffers et al., 2003b, 2006). The activity of these peroxidases is modulated by apoplastic Mn and metabolites (Fecht-Christoffers et al., 2006). Indeed, Chapter 2 describes a successful identification of apoplastic phenols and the quantification of their treatment dependent changes in abundance which could be correlated to their capability to induce NADH-*peroxidase* activity in specific apoplastic peroxidase isoenzymes in a Mn-sensitive cultivar.

In cowpea Mn toxicity also induces symplastic responses. One major symplastic compartment affected by excess Mn is the chloroplast (Chapter 1, see also literature cited therein). In the light-driven part of photosynthesis, Mn toxicity reduced the electron transport rates and induced state I to state II transitions of photosynthesis, and in the Calvin cycle three proteins involved in the provision of physiologically active RubisCO were reduced. Since photosynthesis is a central process in plant life, it could be expected that Mn treatment-dependent alterations of photosynthesis and the integrity of the photosynthetic apparatus also affect various metabolic pathways. Indeed, in this study ICA clusterings particularly of the bulk-leaf but also of the AWF fractions revealed that all experimental factors (genotype > Mn treatment > Si treatment) lead to significant changes in the leaf metabolome (Figs. 4, 5 Chapter 2). Unfortunately, the analyses of non-polar apoplastic metabolites with metabolite profiling tools did not lead to clear clusterings (Chapter 2, Figs. 4 and 5 of this study). Nevertheless, it was possible to identify and quantify treatment-dependent changes of specific phenols obtained from the non-polar fraction and to correlate them with the phenols' ability to induce NADH-*peroxidase* activity (Tab. 2, see discussion below).

In conclusion, the screening for metabolites yielded several metabolites which were strongly affected by either of the experimental factors (Mn, Si, Gen). These are discussed in the following sections with special emphasis on genotypic and Si-mediated leaf-tissue Mn tolerance.

Genotypic Mn tolerance

In this study, protein-sequencing results substantiated the presence of the same class III peroxidases in both genotypes (Fig. 3, Tab. S3). But there is a genotypical difference in the apoplastic peroxidase isoenzyme profile (Fig. 2). Moreover, Mn excess treatment induced an increase of POD abundance in TVu 91 (Chapter 2).

In TVu 91 Mn toxicity development was discussed with respect to apoplastic phenols and their individual capacity to induce NADH-*peroxidase* activity (Chapter 2). Particularly the downregulation of activity-inhibiting ferulic acid appeared to play a key role (Chapter 2, Tab. 2a, b). In this study, in TVu 1987 the strong Mn-mediated downregulation of peroxidase activity-enhancing *p*-coumaric acid was conspicuous (Tab. 2a, d). Moreover, the role of phenols in peroxidase-mediated toxicity development is corroborated (i) by higher phenol contents in the AWF_{NaCl} of TVu 91 of plants not treated with Mn and (ii) particularly by the higher *p*-coumaric acid contents in Mn-treated plants of TVu 91 independent of the Si supply (Tab. 2e, f). It appears that a reduction of NADH-*peroxidase* activity-inducing phenols may increase the effect of NADH-*peroxidase* activity inhibiting phenols and *vice versa*. In conclusion, it appears that genotypic Mn tolerance is due to constitutive lower abundance and number of apoplastic peroxidase isoenzymes in combination with a lower abundance of peroxidase activity-inducing phenols particularly at excess Mn supply.

The modulation of apolastic peroxidase activities is only one quality of phenols, but phenylpropanoids/flavonoids are also involved in a wide range of biotic and abiotic stress responses (Dixon and Paiva, 1995), especially in their function as naturally occurring antioxidants (Aaby et al., 2004; Pietta, 2000; Rice-Evans et al., 1996). Since leaf-tissue injury by excess Mn has been related to oxidative stress (González et al., 1998), a specific symplastic composition and Mn-induced changes in antioxidant-acting phenylpropanoids may contribute to Mn tolerance. Compared to the Mn-sensitive cultivar TVu 91, the Mn-tolerant cultivar TVu 1987 showed 10-fold higher quinic acid contents (Fig. 6c). In the symplastic phenylpropanoid and flavonoid biosynthesis pathway, quinic acid is utilized by *p*-coumaryl-CoA:quinic acid hydroxycinnamoyltransferase (HCT) to yield *p*-coumaryl quinate (Hoffmann et al., 2003). Silencing HCT led to quantitative and qualitative changes in the soluble phenylpropanoid pool and lignin content (Hoffmann et al., 2004). Therefore, higher quinic

acid contents in TVu 1987 (Fig. 6c) may be indicative of a constitutive Mn tolerance-specific difference in the phenylpropanoid metabolism compared with TVu 91. A Mn excess-induced and Si-enhanced abundance of quinic acid (Fig. 6c) in the bulk-leaf extract support the view that maintaining a high quinic acid content thus fuelling the phenylpropanoid biosynthesis contributes to genotypic but also Si-mediated Mn tolerance.

Fecht-Christoffers et al. (2003a) presented evidence for the contribution of symplastic and apoplastic ascorbate and its regeneration system to Mn tolerance in cowpea. In this study ascorbic acid and its oxidized form dehydroascorbic acid were higher in the bulk-leaf extract in TVu 1987 than in TVu 91 and excess Mn downregulated both metabolites (Fig. 6c). In contrast to Fecht-Christoffers et al. (2003a) we were not able to identify ascorbic acid in the apoplast (not shown), but its oxidized equivalent, dehydroascorbic acid has been shown to be more abundant in Mn-treated compared to Mn-control plants (Fig. 7, Tab. S2) indicating Mn-induced oxidation of apoplastic ascorbic acid. This is supported by protein sequencing results which yielded more APX peptides in the AWF_{H₂O} of Mn-treated TVu 1987 compared with Mn-treated TVu 91 (Fig. 3, Tab. S3). An in depth APX isoenzyme characterizations appears to be necessary and promising.

The role of other organic acids in Mn toxicity and tolerance is ambivalent. One possible role of organic acids in genotypic Mn tolerance could be based on their ability to scavenge reaction intermediates of the peroxidase-oxidase cycle of peroxidases. From an in-depth comparison of the apoplastic and vacuolar compartmentation of organic acids in leaf tissues differing in Mn tolerance, Maier (1997) and Fecht-Christoffers et al., (2007) concluded that the formation of Mn^{II}-organic acid complexes could not explain Mn tolerance. However, in this study (Fig. 6c) three organic acids appeared to be strongly though inconsistently affected by the experimental factors (Mn, Si, Gen): gluconic acid, tartaric acid and malonic acid.

Gluconic acid is involved in the formation of tartaric acid particularly in legumes (Loewus, 1999), and both tartaric acid (Podgornik et al., 2001) and malonic acid (Wariishi et al., 1992) are known as Mn^{III}-chelators. Following the proposed reaction scheme for peroxidase-mediated Mn toxicity development (see Fecht-Christoffers et al., 2007 and General Introduction) scavenging of Mn^{III} by complexation would terminate the recycling of Mn^{II} and remove an essential reaction intermediate of the NADH-*peroxidase* activity thus preventing oxidative stress. On the other hand Mn^{III}-organic acid complexes themselves can act as oxidants (Podgornik et al., 2001). This is an essential non-enzymatic step in the depolymerization of lignin: Mn-dependent peroxidases from fungi first oxidize Mn^{II} to Mn^{III} and subsequently formed Mn^{III}-organic acid complexes then themselves act as oxidants. Additional oxidant activity could then accelerate Mn toxicity development and could,

therefore, be regarded as mediators of Mn sensitivity rather than as tolerance promoting metabolites.

Thus it is difficult to draw final conclusions about the role of the changes in the content of the three identified organic acids. Further investigations particularly on the Mn^{2+} and Mn^{3+} chelating power of the identified organic acids and their effect on the NADH-*peroxidase* activity are necessary.

Amino acids and amines play an important role in the response to abiotic e.g. heavy metal stress (Sharma and Dietz, 2006; Less and Galili, 2008). In this study, ICA loadings pointed to several amino acids that were responsible for the excess Mn-induced clustering. Especially aspartate and asparagine were reduced by Mn supply and lower contents were found in TVu 91 (Fig. 6a). Both amino acids are involved in nitrogen assimilation and especially transport. The Mn-stress induced state I to state II transitions of photosynthesis particularly in TVu 91 (Chapter 1) may be regarded as flexible energy converter mechanism balancing the demand for ATP and/or reducing capacity (Wollman, 2001). Moreover, the state I is regarded as provider of reducing equivalents allowing the reduction of nitrate in addition to CO_2 , whereas in state II ATP production is preferred decreasing the available pool of reduced ferredoxin and thus nitrate reduction (Sheremeti et al., 2002). Therefore, it appears not surprising that the main nitrogen storage and transport forms, aspartic acid and asparagine, are negatively affected by Mn especially in the Mn-sensitive cultivar since in our experiments only nitrate was supplied to the nutrient solution. In conclusion the changes in the amino acid pool could be regarded as secondary Mn effect mainly caused by Mn-induced changes in photosynthesis. Polyamines in general are metabolites induced by various stresses (Galston and Sawhney, 1990) and are essential for growth and development of plants through their involvement in the synthesis of DNA, RNA, and proteins. In this study, two metabolites have been detected which could be interesting: Ornithine, which is involved in the polyamine biosynthesis (Galston and Sawhney, 1990), and sperimidine. Unfortunately, not only the leaf compartments, in which they were detected, but also the response particularly to Mn treatments differed between both metabolites without apparent linkage between them. Nevertheless, recently Moschou et al. (2008) showed that polyamines play a significant role in the apoplastic polyamine oxidase-derived H_2O_2 -signalling under salt stress. Therefore, in view of the proposed decisive role of H_2O_2 in the development of Mn toxicity (Chapter 2; Fecht-Christoffers et al., 2006), an in depth analysis of apoplastic polyamine dynamics including ornithine decarboxylase and polyamine oxidase activity appears to be promising.

Also the sugar metabolism was affected by Mn excess. Glucose and fructose contents decreased in response to excess Mn (Fig. 6). This could be linked to the negative effect of Mn on photosynthesis (Chapter 1) and to a higher demand for carbon sources and energy for stress responses. The higher stress level of the Mn-sensitive genotype TVu 91 may be underlined by higher sugar contents in the Mn-tolerant genotype TVu 1987. Moreover, the content of sucrose the main sugar transport form in the phloem of plants was increased by Mn excess (Fig. 6). This additionally points to an overall higher demand and redistribution of carbon to the mature leaf sampled for stress responses. The determined responses of the sugars to excess Mn may also explain the described higher tolerance of NO_3^- compared with NH_4^+ -fed plants (Horst et al., 1999), since NH_4^+ nutrition induced a higher demand for C-skeletons for the assimilation of NH_4^+ in the roots (Gazzarini et al., 1999) thus further reducing the C pool for the Mn stress response. In conclusion, the changes in the sugar pool could be regarded on the one hand as a secondary Mn effect mainly caused by a Mn-induced reduction in photosynthesis but on the other hand as a primary effect through the provision of energy for the Mn stress response.

Recently a function of galactinol and raffinose as scavengers of hydroxyl radicals has been shown (Nishizawa et al., 2008). Both galactinol and raffinose were higher abundant in in the bulk-leaf of TVu 1987 (Fig. 6) and a Mn treatment increased the galactinol concentration in the $\text{AWF}_{\text{H}_2\text{O}}$ (Fig. 7Ad). Therefore, particularly galactinol might detoxify hydroxylradicals that are produced as reaction intermediates in the peroxidase-oxidase cycle of peroxidases (Schweikert et al., 2000) and in this way protect plant cells from oxidative damage. This may contribute to the enhanced Mn tolerance of TVu 1987.

Recently, extracellular ATP (eATP) has been shown to be involved in several physiological processes as signaling molecule in stress responses (Jeter et al., 2004). Very recently Riewe et al. (2008) provided evidence for a cell wall-bound adenosine nucleosidase activity that converts apoplastic adenosine to D-ribose and adenine as part of an eATP salvage pathway. In this study in the AWF_{NaCl} adenosine (Fig. 7Be) and in the $\text{AWF}_{\text{H}_2\text{O}}$ ribose (Fig. 7Ab) as product of the adenosine nucleosidase activity were higher in TVu 1987. In view of the proposed eATP salvage pathway the higher apoplastic adenosine and ribose concentrations in TVu 1987 may indicate an apoplastic involvement of eATP in terms of successful stress response

Silicon-mediated Mn tolerance

A direct effect of Si on metabolic pathways has not been shown so far. In their transcriptomic study of the role of Si in the resistance of Arabidopsis against powdery mildew, Fauteux et al. (2006) showed that in absence of biotic stress only two out of about 40,000 investigated genes were affected by Si supply. However, in line with the alleviation of disease stress Si affected more than 4,000 genes, many of them related to biotic stress defence.

Indeed, the contribution of Si treatment to metabolomic changes appeared comparable small which was underlined by ICA results sorting the sample clusters in the order of importance with genotype > Mn treatment > Si treatment (see discussion above, Fig. 4, 5, Chapter 2). Nevertheless, in this study, the samples of Si-treated plants did cluster in Mn-control plants but not in Mn excess-stressed plants. The Si-induced changes in the leaf metabolome of both cultivars may have enhanced the (contrasting) constitutive Mn tolerance of the leaf tissue of both cultivars which is then masked by Mn-induced changes. The comparable small effect of Si on the leaf metabolome of Mn-treated plants may thus explain that Si only delays but not prevents Mn toxicity (Fig.1).

The particular role of apoplastic phenols in modulation NADH-*peroxidase* activity considered as a key step in the development or avoidance of Mn toxicity has been demonstrated earlier in Chapter 2 and above in this chapter. Considering the apoplastic peroxidase isoenzyme profile evidence was provided that in the Mn-sensitive cultivar TVu 91 Si had no direct impact on the peroxidase isoenzyme pattern, but Si delayed the Mn-mediated upregulation of peroxidase isoenzyme abundance (Chapter 2, supplementary material Fig. S1). Regarding phenols as co-factors of peroxidases Si strongly increased the abundance of NADH-*peroxidase* activity-inhibiting ferulic acid independent of the genotype (Tab. 2b). One factor of Si-mediated Mn tolerance in the Mn-sensitive cultivar TVu 91 could be the Si-mediated upregulation of ferulic acid at excess Mn supply compensating for the decrease in absence of Si (Tab. 2a) thus preventing enhanced peroxidase activities. The upregulation of ferulic acid appears to be a general Si effect in cowpea since it was also upregulated in TVu 1987. Furthermore, the effect of Si on ferulic acid abundance was only visible in the AWF_{NaCl} fraction supporting the view that Si modifies apoplastic binding properties (Chapter 2, Iwasaki et al., 2002a, b; Rogalla and Römheld 2002). In conclusion, the results suggest that the physiological and molecular mechanisms underlying Si-enhanced Mn tolerance differ from genotypic Mn tolerance. It appears that Si-mediated Mn tolerance is due to a suppression of Mn excess-induced increases in peroxidase abundance in combination with a Si-mediated higher abundance of peroxidase activity-inhibiting phenols independent of the genotype.

A number of other metabolites were significantly affected by Si nutrition and may contribute to the clarification of the role of Si in Mn tolerance. Glucose and fructose were upregulated by Si (Fig. 6). Silicon seems to enhance sugar synthesis which is supported by transcriptomic analyses revealing an impact of Si on transcripts encoding proteins facilitating photosynthesis (data not shown). Sucrose was also upregulated by Si (Fig. 6). This upregulation was damped by excess Mn supply independent of the genotype (Tab. S1.1a, b) reflecting a Mn-induced higher demand for carbon/energy for stress responses (see above).

Silicon treatment also increased the abundance of ascorbic acid in the bulk-leaf extract (Fig. 6, Tab. S2) thus enhancing the capacity of the plants to meet oxidative stress imposed by Mn toxicity. In-depth individual comparison of both genotypes (Tab. S1.1a, b) showed that Si increased ascorbic acid concentrations which are nevertheless consumed with ongoing Mn treatments. Ascorbic acid could therefore be one metabolite contributing to the ICA cluster results shown for Si in individual genotypes (Chapter 2 [TVu 91] and Fig. 5a [TVu 1987]) (see above).

Another metabolite greatly affected by Si nutrition was GABA which was increased by Si supply in the bulk-leaf of Mn-treated plants (Fig. 6a) of particularly TVu 91 (Tab. S1.1a, b). Moreover, Si increased the abundance of GABA in both apoplastic fractions (Fig. 7A) particularly in TVu 1987 independent of the Mn supply (Tab. S1.2b). Moreover, GABA was higher in TVu 91 than in TVu 1987 (Tab. S1.1c). GABA has several physiological functions not only in the nitrogen metabolism (see previous section) but also in regulating the cytosolic pH and particularly in the protection against oxidative stress and in cell signalling (see review of Bouché and Fromm, 2004). Especially apoplastic GABA is known to function in cell-signalling processes (Shelp et al., 2006). Therefore, on the one hand in view of the physiological functions and symplastic responses of (symplastic) GABA in TVu 91 it appears that GABA could be involved in a Si-mediated symplastic re-coordination of pathways thus increasing the stress tolerance. On the other hand Si constitutively modulates the apoplastic signaling system particularly in TVu 1987

β -alanine was an apoplastically localized amino acid which was upregulated in the apoplast by Si. It is involved as intermediate in the biosynthesis of coenzyme A (CoA) via pantothenic acid (White et al., 2001; Broeckling et al., 2005). Pantothenic acid itself was also upregulated by Si and also Mn supply in the non-polar apoplastic fraction of the AWF_{NaCl}. Moreover, it showed a higher abundance in TVu 1987 in the non-polar fraction of the AWF_{H₂O} but in the non-polar fraction of the AWF_{NaCl} it was higher in TVu 91 (Fig. 8). Pantothenic acid is involved in lipid biosynthesis and secondary metabolite biosynthesis, e.g. lignin biosynthesis (Smith et al., 2007). Both metabolites may act as modulators in the fatty acid, carbohydrate

and protein metabolism by the provision of CoA particularly in Mn tolerance due to the consistent higher abundance in Si treatments, but a possible specific role of β -alanine and pantothenic acid in the apoplast remains speculative without further investigations.

In conclusion, the comparative peroxidase isoenzyme profile study confirmed the decisive role of apoplastic peroxidases in Mn toxicity and tolerance. Their role is further underlined by the dynamics of activity modulating phenylpropanoids particularly in the leaf apoplast. However, the metabolomic analysis suggests that other metabolites not only in the apoplast but also in the bulk leaf are involved in the modulation of Si-mediated and genotypic Mn tolerance. The role of metabolites in stress sensing and signal transduction processes can particularly be regarded as **primary responses to Mn and Si**. The role of organic acids can be regarded as **mediators of the excess Mn effects** through their function as antioxidants, scavengers of reactive oxygen species and NADH-*peroxidase* reaction intermediates, and as complexors for Mn species. Changes in metabolites related to the primary metabolism (sugars, amino acids) may be regarded as **responses to Mn excess** stress reflecting its disturbance and need for rebalancing. Future work is necessary to more specifically address the demonstrated affected pathways in order to better understand genotypic and Si-mediated Mn tolerance.

Proteomic characterization of the leaf apoplast of *Vigna unguiculata* L. in response to short-term toxic manganese supply

Hendrik Führs¹, Mareike Vorholt¹, Sébastien Gallien², Dimitri Heintz³, Alain Van Dorsselaer², Hans-Peter Braun⁴ & Walter J. Horst¹

to be submitted

¹ Institute of Plant Nutrition, Faculty of Natural Sciences, Leibniz University Hannover, Herrenhäuser Str. 2, 30419 Hannover, Germany

² Laboratoire de Spectrométrie de Masse Bio-Organique, IPHC-DSA, ULP, CNRS, UMR7178 ; 25 rue Becquerel, 67 087 Strasbourg, France

³ Institut de Biologie Moléculaire des Plantes (IBMP) CNRS-UPR2357,ULP, 67083 Strasbourg, France

⁴ Institute of Plant Genetics, Faculty of Natural Sciences, Leibniz University Hannover, Herrenhäuser Str. 2, 30419 Hannover, Germany

Abstract

Previous studies investigating the leaf apoplastic water-soluble proteome after longer term Mn treatment in cowpea (*Vigna unguiculata* L.) suggested that the leaf apoplast is the decisive leaf compartment for the development or avoidance of Mn toxicity. To study the short-term effect of excess Mn supply apoplastic proteins were extracted from leaves of the Mn-sensitive cowpea cultivar TVu 91 and the apoplastic proteome characterized by means of IEF/SDS-PAGE and peptide mass spectrometry. Two Apoplastic Washing Fluid fractions (AWF_{H_2O} and AWF_{NaCl}) and a cell-wall fraction released from isolated cell walls were analysed. The suitability of these techniques was tested by determining the activity of malate dehydrogenase as cytoplasmic contamination marker-enzyme. The cell-wall isolation-procedure proved to be inappropriate for the investigation of strongly bound cell-wall proteins owing to a symplastic contamination of 4% and the identification of mainly typical symplastic proteins. The AWF extraction procedures yielded low contaminations (<0.5 %) and only few peptides assigned to typical symplastic proteins. One day of excess Mn allowed to identify two AWF_{H_2O} and three AWF_{NaCl} extracted protein spots on the 2D gels. The identification of Mn-induced basic POD isoenzyme in the AWF_{NaCl} fraction in addition to acidic POD isoenzymes in the AWF_{H_2O} further supports the proposed decisive role of H_2O_2 -producing and consuming PODs for the development of Mn toxicity. Further proteins significantly affected by Mn treatment (PGIPs and α -galactosidases) suggest Mn excess-induced modification of cell-wall development and functions, whereas others (acetylcholinesterase and GDSL-lipase 1) indicate changes in broad-sense signal transduction processes.

Introduction

Manganese (Mn) is an essential plant micronutrient affecting a range of physiological processes such as photosynthesis and redox homeostasis (Burnell, 1988; Marschner, 1995). Under conditions of increased plant Mn availability typical for acid and insufficiently drained soils of the tropics and subtropics, Mn becomes toxic to plants. Hence, Mn toxicity in crops is a widely distributed plant disorder mainly in the tropics and subtropics (Horst, 1988). There is a great inter- and intra-specific variability in Mn tolerance in plants (Foy et al., 1978; El-Jaoual and Cox; 1998; Horst, 1980).

In cowpea, Mn-sensitive and tolerant cultivars do not differ in Mn uptake (Chapter 1). Hence, in this plant species Mn resistance is due to Mn leaf-tissue tolerance (Horst, 1983). Typical Mn toxicity symptoms in cowpea are distinct brown spots starting at the leaf base. With increasing Mn treatment duration the brown spots spread to the tip, followed by chlorosis, and finally leaf shedding (Horst and Marschner, 1978; Horst, 1982).

The localization of the brown spots in the apoplast of epidermal cells points to the apoplast as the decisive compartment for the development of Mn toxicity. The spots consist of oxidized Mn and oxidized phenolic compounds (Wissemeier and Horst, 1992). Therefore, the recently published apoplastic proteome and peroxidase characterization studies of cowpea investigated the water-soluble Apoplastic Washing Fluid (AWF_{H₂O}) which was extracted by an infiltration/centrifugation technique (Fecht-Christoffers et al., 2003, 2006). Here, evidence was provided that the H₂O₂-producing peroxidase-oxidase cycle of apoplastic peroxidases responded most sensitively to increasing Mn supply (Fecht-Christoffers et al., 2006). Therefore, this reaction was regarded as key and initial step triggering apoplastic and symplastic processes leading to Mn toxicity. These authors also provided evidence that Mn²⁺ and phenols are decisive co-factors for the induction of the H₂O₂-producing peroxidase cycle.

Chapters 2 and 3 of this thesis showed first results on apoplastic in-depth comparative investigations of apoplastic isoenzymes of two different apoplastic proteome fractions. The different AWF fractions were harvested in two subsequent infiltration/centrifugation steps first yielding water-soluble proteins (AWF_{H₂O}) followed by ionically-bound proteins (AWF_{NaCl}). Based on the number and induction of apoplastic peroxidase isoenzymes differences the peroxidase isoenzyme pattern clearly showed differences between both fractions and also between the two genotypes with contrasting Mn tolerance. Moreover, protein sequencing of separated peroxidase bands gave several hints for different binding properties of specific peroxidase isoenzymes.

In view of the applied methods for extracting the different AWF fractions it was possible to get reliable results for the water-soluble proteome and the characterization of the water-soluble and ionically bound apoplastic peroxidase pattern (Fecht-Christoffers et al., 2003b, 2006; Chapters 2 and 3). In general, the suitability of the infiltration/centrifugation technique as tool for the isolation and investigation of plant apoplastic solutes was extensively evaluated (see for example Lohaus et al., 2001; Jamet et al., 2006).

Depending on the objectives another possibility for the investigation of apoplastic proteomes often used is the cultivation of cell suspension cultures (Borderies et al., 2003; Ndimba et al., 2003; Chivasa et al., 2005, 2006) either in response to specific treatments or to fundamentally clarify the apoplastic protein composition. For the investigation of the apoplastic secretome cell suspension cultures are especially suitable since only the culture medium has to be submitted to proteomic analysis without disturbing the cultured cells (Tran and Plaxton, 2008) thus avoiding cytoplasmic contaminations.

The addressed AWF-yielding procedures do not include the comparable strongly bound so-called cell-wall protein-fraction. It comprises less than 10% of the cell wall (Fry, 1988) but fulfils a number of developmental and regulatory functions (Jamet et al., 2006) and could, therefore, also contribute to the understanding of apoplastic responses to Mn toxicity.

All proteomic results on Mn toxicity and tolerance took place in response to advanced Mn toxicity stages (Fecht-Christoffers et al., 2003b, 2006). They revealed an increased abundance of especially pathogenesis-related proteins, thaumatin-like proteins, chitinases, and also peroxidases in the leaf apoplast thus indicating a more general stress response. Therefore, in order to better understand specific apoplastic Mn toxicity events, our work presented here further characterized the apoplastic proteome after only one day of elevated Mn supply. The study focused on the Mn-sensitive cowpea cultivar TVu 91 differentiating between three apoplastic protein fractions, a free and an ionically bound AWF and a strongly bound cell-wall fraction. In addition to the Mn-induced changes in the different proteomic fractions with respect to beginning Mn toxicity also the suitability of the applied apoplast protein isolation-methods are discussed.

Materials and Methods

Plant material

Cowpea (*Vigna unguiculata* [L.] Walp., cv TVu 91) was grown hydroponically in a growth chamber under controlled environmental conditions at 30/27°C day/night temperatures, 75% ±5 % relative humidity, and a photon flux density of 150 $\mu\text{mol m}^{-2}\text{s}^{-1}$ photosynthetic active radiation (PAR) at mid-plant height during a 16-h photoperiod. After germination in 1 mM CaSO_4 for 7 d, seedlings were transferred to a constantly aerated nutrient solution with 4 plants in one 5-L pot. The composition of the nutrient solution was [μM]: $\text{Ca}(\text{NO}_3)_2$ 1000, KH_2PO_4 100, K_2SO_4 375, MgSO_4 325, FeEDDHA 20, NaCl 10, H_3BO_3 8, MnSO_4 0.2, CuSO_4 0.2, ZnSO_4 0.2, Na_2MoO_4 0.05. After preculture for 14 d, the Mn concentration in the nutrient solution was increased from 0.2 μM (-Mn) to 50 μM (+Mn) for 1 day. The nutrient solution was changed two to three times per week to avoid nutrient deficiencies.

Extraction of water-soluble and ionically bound apoplastic proteins and cell wall proteins from leaves

Apoplastic washing fluid (AWF) was extracted by a vacuum infiltration/centrifugation technique according to Fecht-Christoffers et al. (2003a, b). In previous studies the second oldest trifoliate leaf was either infiltrated with $\text{AWF}_{\text{H}_2\text{O}}$ (Fecht-Christoffers et al., 2003b, 2006) or in two subsequent steps first with $\text{AWF}_{\text{H}_2\text{O}}$ followed by an infiltration of the same leaves with AWF_{NaCl} (0.5 M NaCl) (Chapters 2 and 3). In this study the second oldest trifoliate leaves were infiltrated either with chilled dH_2O or with chilled 0.25 M NaCl (in the following termed AWF_{NaCl}) by reducing the pressure to -35 hPa followed by a slow relaxation. $\text{AWF}_{\text{H}_2\text{O}}$ and AWF_{NaCl} were recovered by centrifugation at 1324 g for 5 min at 4°C. Malate dehydrogenase (MDH) activity in both AWF fractions showed a cytoplasmic contamination of less than 0.5 % (data not shown). Until further analysis the AWF was stored at -80°C.

The isolation of cell walls from the leaf material was an additional approach to extract strongly ionically-bound cell wall proteins. Frozen leaf material harvested from plants either treated with additional Mn for one day or continuous optimum Mn supply were ground in liquid nitrogen. 2.5 g of the homogenized material was transferred to centrifugal devices (Oak

RidgeCentrifuge Tube, PPCO, 50 ml, Nalgene Company, USA) and supplied with 30 ml ethanol. Samples were mixed and incubated on a test tube roller at 4°C for 15 min. Samples were subsequently centrifuged at 20000 g and 4°C for 5 min. These steps were repeated until the supernatant was colourless and the remaining pellet white indicating the complete removal of cytoplasmic contamination. The white pellet was then washed two times with 30 ml ddH₂O for 15 min at 4°C on a test tube roller in order to remove excess EtOH. The actual exchange of ionically-bound apoplastic proteins took place over night in HEPES-buffer (20mM, pH 7.4, containing 1 M NaCl) on a test tube roller. After centrifugation the resulting supernatant (subsequently named isolated cell wall fraction or strongly ionically bound cell wall fraction) was frozen and stored at -80 °C until further analyses. Malate dehydrogenase (MDH) activity in the isolated cell wall fraction showed a cytoplasmic contamination of less than 4% (data not shown). Until further analysis the AWF was stored at -80°C.

Manganese analysis

Manganese in the bulk-leaf tissue was determined in the second oldest middle trifoliolate leaf after dry ashing at 480°C for 8h, dissolving the ash in 6 M HCl with 1.5% (w/v) hydroxylammonium chloride, and then diluting (1:10) with double demineralised water. Apoplastic Mn concentrations were measured in 1:10 dilutions of the AWF containing 0.6 M HCl with 1.5% (w/v) hydroxylammonium chloride. Both measurements were carried out by optical inductively-coupled plasma-emission spectroscopy (Spectro Analytical Instruments GmbH, Kleve, Germany).

Determination of the protein concentration in the AWF and AWF concentrates

The protein concentration in the AWF for the calculation of specific enzyme activities was determined according to Bradford (1976).

Determination of the phenol concentration in the AWF

The phenol concentration in the AWF was determined by adding 50 µl Folin-Denis solution (Merck, Darmstadt) and 350 µl double demineralized water to 50 µl AWF. After 3 min 100 µl saturated Na₂CO₃ solution was added and the mixture incubated for 1 h in the dark.

Afterwards the samples were centrifuged for 1 min at 5000 g and then measured at $\lambda=725$ nm in a Microplate Reader. Phenol concentration was calculated using a 0 to 1000 μM *p*-coumaric acid standard curve.

Determination of specific peroxidase activities in the AWF

For the measurement of H_2O_2 -consuming guaiacol-peroxidase activities in the AWF, the oxidation of the substrate guaiacol was determined spectrophotometrically at $\lambda=470$ nm (UVIKON 943, BioTek Instruments GmbH, Neufahrn, Germany). Samples were mixed with guaiacol solution (20 mM guaiacol in 10 mM Na_2HPO_4 buffer [pH 6]) and 0.03% (v/v) H_2O_2 . For calculation of enzyme activities the molar extinction coefficient $26.6 \text{ L (mmol cm)}^{-1}$ was used.

For the measurement of the H_2O_2 -producing NADH-*peroxidase* activity in the AWF, samples were mixed with MnCl_2 (16 mM), *p*-coumaric acid (1.6 mM) and NADH (0.22 mM). Measurements were done in a photometer (Multiplate Reader, μQuant , Bio-Tek Instruments, Inc., USA) following the NADH oxidation-dependent decline in absorption at $\lambda = 340$ nm. For calculation of enzyme activities the molar extinction coefficient $1.13 \text{ L (mmol cm)}^{-1}$ was used.

Preparation of AWF proteins for IEF/SDS-PAGE

Proteins of all three apoplastic and cell wall fractions were concentrated at 4°C by using centrifugal concentrators with a MWCO of 5 kDa (Vivaspin 6, Vivascience, Hannover, Germany) according to the manufacturer's instructions.

Afterwards, AWF and cell wall protein concentrates were supplied with 500 μl extraction buffer (700 mM sucrose, 500 mM Tris, 50 mM EDTA, 100 mM KCl, and 2% [v/v] mercaptoethanol) and incubated for 10 minutes on ice. Afterwards, an equal volume of water-saturated phenol was added and shaken for 30 min at room temperature. The aqueous and organic phases were separated by centrifugation for 10 min at $5,000 \times g$ and 4°C . The phenolic phase was re-extracted with extraction buffer and centrifuged once more. Phenol phases were combined, supplemented with 5 volumes of 0.1 M ammonium acetate in methanol and incubated over night at -20°C . After centrifugation at 11,000 g for 3 min at 4°C , precipitated proteins were washed three times with ammonium acetate in methanol and finally with acetone. Precipitated proteins were resolved in "rehydration buffer" (see below)

for 2DE analysis. Protein concentration of extracts were determined in rehydration buffer using the 2-D Quant Kit[®] (GE Healthcare, Munich, Germany) according to the manufacturer's instructions.

2D IEF / SDS-PAGE

For IEF, the IPGphor system (GE Healthcare, Munich, Germany) and Immobiline DryStrip gels (18 cm) with a nonlinear pH gradient (pH 3-11) were used. Protein resolubilized in "rehydration solution" (8 M urea, 2% [w/v] CHAPS, 0.5% [v/v] carrier ampholyte mixture [IPG buffer, pH 3-11 NL; GE Healthcare], 50 mM dithiothreitol, 12 $\mu\text{l ml}^{-1}$ DeStreak [GE Healthcare], and a trace of bromphenol blue) was loaded onto individual gel strips (amount of protein loaded on individual gel see gel description). Focussing was done according to Werhahn and Braun (2002). Afterwards, Immobiline DryStrip gels were incubated with equilibration solution (50 mM Tris-Cl [pH 8.8], 6 M urea, 30% [v/v] glycerol, 2% [w/v] SDS, and bromphenol blue) supplemented with (a) 1% [w/v] dithiothreitol and (b) 2.5% [v/w] iodacetamide each for 15 min. Finally, DryStrips were placed horizontally onto second dimension SDS gels and proteins were resolved according to Schagger and von Jagow (1987). For each Mn treatment six ($\text{AWF}_{\text{H}_2\text{O}}$) and three (AWF_{NaCl} , strongly ionically bound cell wall fraction) biological replicates, each containing AWF from 16 individual plants or leaf material for cell wall isolation from two individual plants, were carried out.

Staining of protein gels and spot detection

All protein gels were stained with colloidal Coomassie-blue according to Neuhoff et al. (1985, 1990). The leaf apoplastic proteome (water-soluble [$\text{AWF}_{\text{H}_2\text{O}}$] and slightly ionically bound [AWF_{NaCl}] of cowpea plants cultivated in the presence of normal (0.2 μM) or enhanced (50 μM) Mn for 1 day was analysed by 2D IEF / SDS PAGE. Since the infiltration of the leaves with $\text{AWF}_{\text{H}_2\text{O}}$ was the same for both described infiltration / centrifugation methods (see "Extraction of water-soluble and ionically bound apoplastic proteins and cell wall proteins from leaves" section) all sample gels were combined and finally yielded six independent replicas. The adapted method for the investigation of ionically-bound apoplastic proteins as well as for the investigation of isolated cell wall proteins finally yielded three replicas. Therefore, three to six replicas were run for each condition and used for the calculation of master gels by the ImageMasterTM 2D Platinum Software 6.0 (GE Healthcare).

Proteins of significantly different abundance ($P < 0.05$ for AWF fractions and $P < 0.01$ for cell wall fraction [t-test incorporated in the Image Master software]) were identified by comparison of the master gels. Calculations based on %Vol values in order to reduce effects of protein loading differences between individual gels. Number of detected spots were: 0.2 μM Mn, AWF_{H₂O}: replica 1-6: 192, 127, 203, 136, 126, 92; 50 μM Mn, AWF_{H₂O}: replica 1-6: 157, 86, 128, 168, 157, 116; 0.2 μM Mn, AWF_{NaCl}: replica 1-3: 100, 123, 169; 50 μM Mn, AWF_{NaCl}: replica 1-3: 111, 146, 200; 0.2 μM Mn, isolated cell wall fraction: replica 1-3: 469, 423, 375; 50 μM Mn, isolated cell wall fraction: replica 1-3: 375, 394, 437. Statistical analyses (Tabs. 1, 3 and S2) included 218, 200, and 376 proteinspots in the AWF_{H₂O}, the AWF_{NaCl}, and the isolated cell wall fraction, respectively.

Mass spectrometric protein analysis and data interpretation ¹⁰

Marked protein spots on the gels were cut and dried under vacuum. In-gel digestion was performed with an automated protein digestion system, MassPREP Station (Micromass, Manchester, UK). The gel slices were washed three times in a mixture containing 25 mM NH₄HCO₃ : acetonitrile [1:1, v/v]. The cysteine residues were reduced by 50 μl of 10 mM dithiothreitol at 57°C and alkylated by 50 μl of 55 mM iodacetamide. After dehydration with acetonitrile, the proteins were cleaved in the gel with 40 μl of 12.5 ng μl^{-1} of modified porcine trypsin (Promega, Madison, WI, USA) in 25 mM NH₄HCO₃ at room temperature for 14 hours. The resulting tryptic peptides were extracted with 60% acetonitrile in 0.5% formic acid, followed by a second extraction with 100% (v/v) acetonitrile.

Nano-LC-MS/MS analysis of the resulting tryptic peptides was performed using using an Agilent 1100 series HPLC-Chip/MS system (Agilent Technologies, Palo Alto, USA) coupled to an HCT Ultra ion trap (Bruker Daltonics, Bremen, Germany). Chromatographic separations were conducted on a chip containing a Zorbax 300SB-C18 (75 μm inner diameter \times 150 mm) column and a Zorbax 300SB-C18 (40 nl) enrichment column (Agilent Technologies).

HCT Ultra ion trap was externally calibrated with standard compounds. The general mass spectrometric parameters were as follows: capillary voltage, -1750V; dry gas, 3 liter min^{-1} ; dry temperature, 300°C. The system was operated with automatic switching between MS and MS/MS modes using. The MS scanning was performed in the standard-enhanced resolution

¹⁰ Mass spectrometric protein analysis and data interpretation was done in collaborations with Dr. Dimitri Heintz, Institut de Biologie Moléculaire des Plantes (IBMP) CNRS-UPR2357, ULP, 67083 Strasbourg, France, and Prof. Dr. Alain Van Dorsselaer and Sébastien Gallien, Laboratoire de Spectrométrie de Masse Bio-Organique, IPHC-DSA, ULP, CNRS, UMR7178; 25 rue Becquerel, 67 087 Strasbourg, France

mode at a scan rate of 8,100 m/z per second with an aimed ion charge control of 100,000 in a maximal fill time of 200 ms and a total of 4 scans were averaged to obtain MS spectrum. The three most abundant peptides and preferentially doubly charged ions, were selected on each MS spectrum for further isolation and fragmentation. The MS/MS scanning was performed in the ultrascan resolution mode at a scan rate of 26,000 m/z per second with an aimed ion charge control of 300,000 and a total of 6 scans were averaged to obtain MS/MS spectrum. The complete system was fully controlled by ChemStation Rev. B.01.03 (Agilent Technologies) and EsquireControl 6.1 Build 78 (Bruker Daltonics) softwares. Mass data collected during LC-MS/MS analyses were processed using the software tool DataAnalysis 3.4 Build 169 and converted into *.mgf files. The MS/MS data were analyzed using the MASCOT 2.2.0. algorithm (Matrix Science, London, UK) to search against a in-house generated protein database composed of protein sequences of Viridiplantae downloaded from <http://www.ncbi.nlm.nih.gov/sites/entrez> (on March 6, 2008) concatenated with reversed copies of all sequences ($2 \times 478,588$ entries). Spectra were searched with a mass tolerance of 0.5 Da for MS and MS/MS data, allowing a maximum of 1 missed cleavage and with carbamidomethylation of cysteines, oxidation of methionines and N-terminal acetylation of proteins specified as variable modifications. Protein identifications were validated when at least two peptides with high quality MS/MS spectra (Mascot ion score greater than 31) were detected. In the case of one-peptide hits, the score of the unique peptide must be greater (minimal “difference score” of 6) than the 95% significance Mascot threshold (Mascot ion score > 51). For the estimation of the false positive rate in protein identification, a target-decoy database search was performed (Elias and Gygi, 2007).

Mass spectrometric protein analysis and data interpretation for the isolated cell wall fraction was different from the AWF fractions as described in Chapter 1.

Statistical analysis

Statistical analysis, if not mentioned otherwise, was carried out using SAS Release v8.0 (SAS Institute, Cary, NC). Results from analysis of variance are given according to their level of significance as ***, **, and * for $p < 0.001$, 0.01, and 0.05, respectively.

Results

Characterization of leaf Mn toxicity

In order to characterize the Mn toxicity level, typical apoplastic parameters as suggested by previous studies (Fecht-Christoffers et al., 2003b, 2006, 2007) were evaluated after 1 d elevated Mn supply. Manganese was readily taken up by cowpea plants shown by a significant increase in the bulk-leaf Mn concentrations (Fig. 1A) and in both AWF fractions (Fig. 1B). The ionically bound Mn fraction was 3-4-fold higher than the water-soluble fraction. Apoplastic protein as well as phenol concentrations did not respond to elevated Mn supply for 1 d (Fig. 1C, D). Both the protein and phenol concentration showed about 2-fold higher concentrations in the AWF_{NaCl} compared with the AWF_{H₂O}.

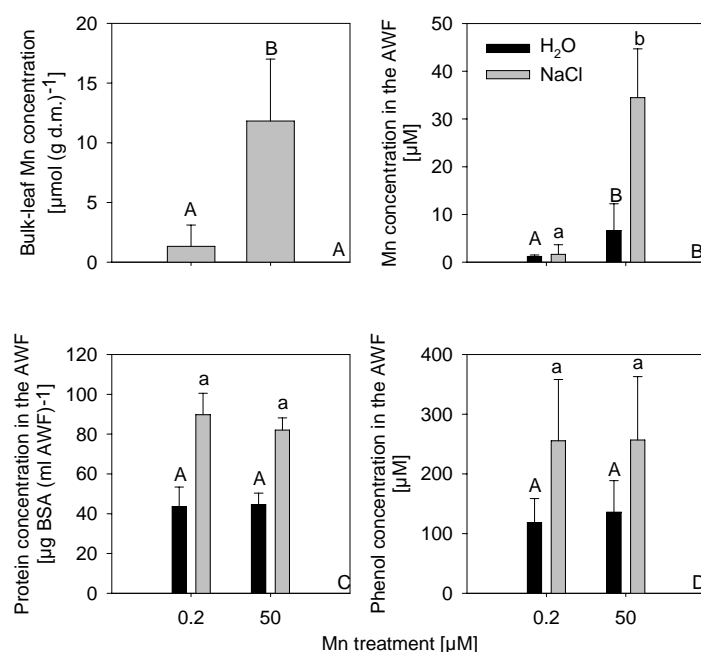


Fig. 1: Effect of elevated Mn supply on the bulk-leaf Mn concentration (A), and the Mn concentration (B), the protein concentration (C), and the phenol concentration (D) of two AWF fractions. After 14 days of preculture, plants received 50 μM Mn for 1 d or 0.2 μM Mn continuously. Displayed are means ± SD of 38 samples each (A, B) or means ± SD of 9 samples (C, D). Upper and lower case letters indicate significant differences between the Mn treatments of the bulk leaf and the AWF_{H₂O}, and the AWF_{NaCl}, respectively at $P < 0.05$ (t-test).

The H₂O₂-consuming guaiacol-peroxidase and the H₂O₂-producing NADH-*peroxidase* activities were not affected by 1 d elevated Mn supply (Fig. 2A-D) independent of the calculation on a protein (specific activity) or an AWF volume basis. Compared to the AWF_{H₂O}, both POD activities of the AWF_{NaCl} were higher on an AWF volume basis.

However, the specific NADH-*peroxidase* activity of the AWF_{NaCl} was higher than the in the AWF_{H₂O}, whereas the specific guaiacol-*peroxidase* activity did not differ between the two AWF fractions.

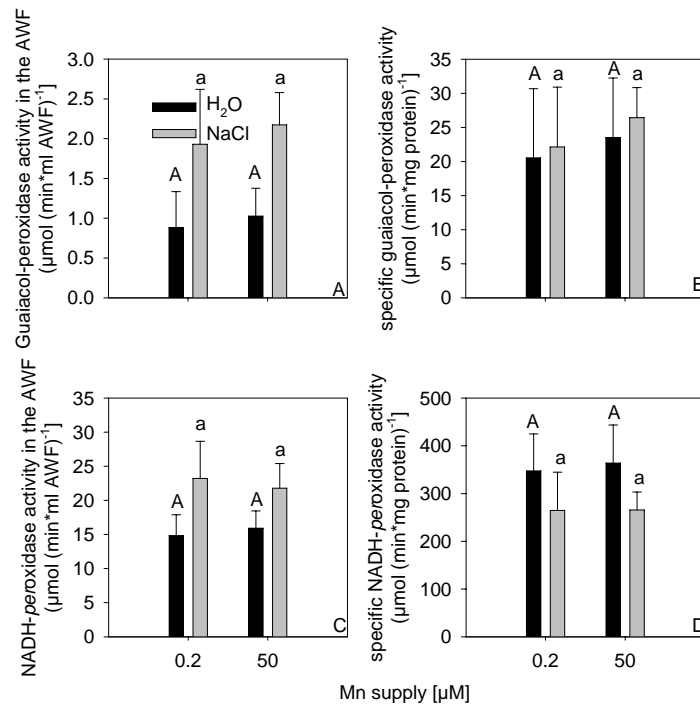


Fig.2: Effect of elevated Mn supply on the apoplastic guaiacol-*peroxidase* activity (A), on its specific activity (B), on the apoplastic NADH-*peroxidase* activity (C), and on its specific activity (D) of two AWF fractions. After 14 days of preculture, plants received 50 μM Mn for 1 d or 0.2 μM Mn continuously. Displayed are means ± SD of 38 samples each (A, B) or means ± SD of 9 samples (C, D). Upper and lower case letters indicate significant differences between the Mn treatments of the AWF_{H₂O} and the AWF_{NaCl}, respectively at P < 0.05 (t-test).

Characterization of the water-soluble and NaCl-extractable apoplastic proteome

Figs. 3 and 4 show 2D resolutions of the AWF_{H₂O} and AWF_{NaCl}, respectively, as well as close ups of gel regions containing Mn stress-affected proteins. Results of statistical analyses of protein abundance and estimated isoelectric points (pI) and MW are shown in Tab. 1. Identities of protein spots as revealed by peptide sequencing analyses are shown in Tab. 2. Alignment of peptide sequences to corresponding database hits are given as supplementary material (Tab. S1).

In the AWF_{H₂O}, analyses revealed two proteins to be significantly affected by elevated Mn supply. Protein spot 1 showed a 60% lower whereas spot 2 showed a 3-fold higher abundance of Mn-treated plants compared with control plants (Fig. 3, Tab. 1).

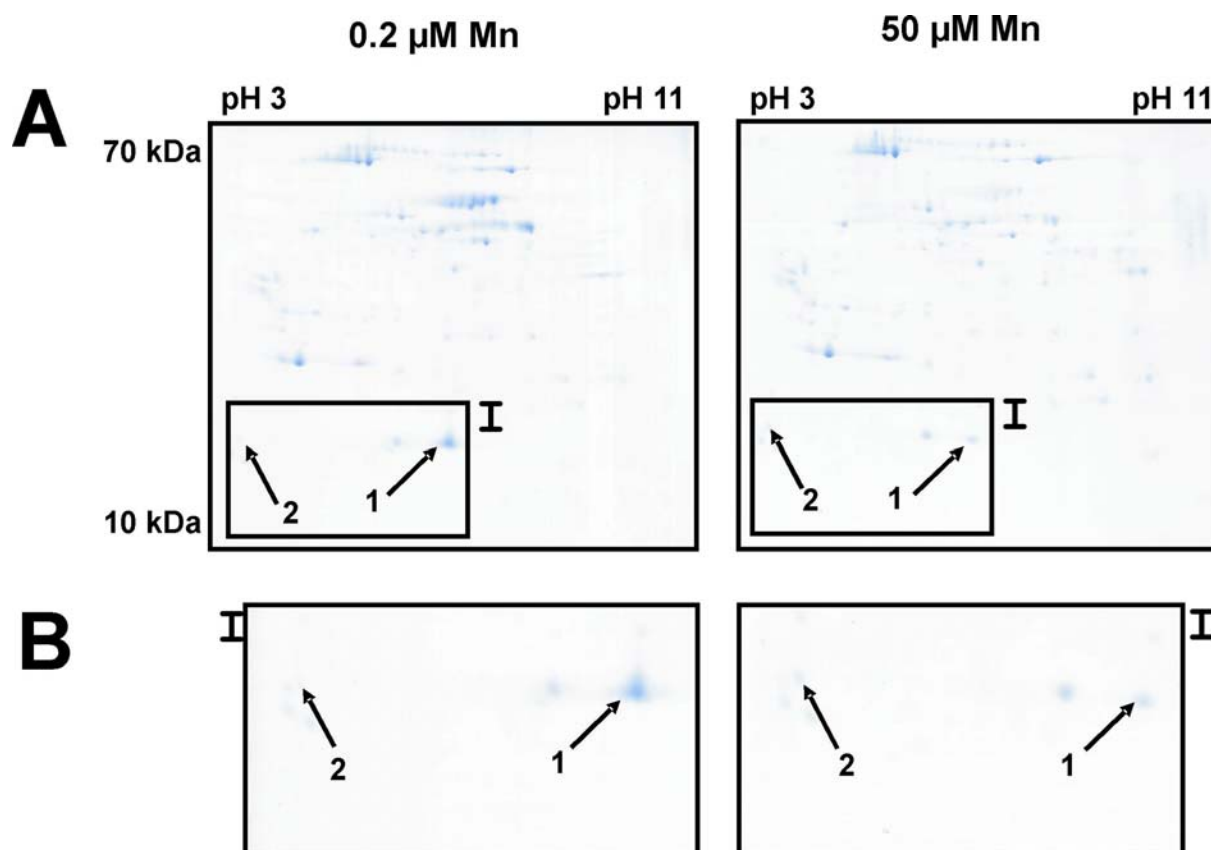


Fig. 3: 2-D resolution of (A) the AWF_{H_2O} proteome and (B) close ups of regions (B) of the 2D resolutions including differentially expressed proteins of the cowpea cultivar TVu 91 after treatment with 0.2 μM or with 50 μM Mn for 1 day after 14 days of pre-culture. Proteins were extracted from the AWF as described in the Materials and Methods section. About 40 μg protein was loaded onto each gel. IEF was carried out on broad range pH gradient gels (pH 3-11). Differentially expressed spots are marked by arrows (for identifications see Tab. 2).

In the AWF_{NaCl} , three proteins differed significantly in abundance when Mn-treated plants were compared with control plants (Fig. 4, Tab. 1). Protein spots 3 and 5 were about 1.2-fold upregulated, whereas spot 4 showed a 0.66-fold lower abundance.

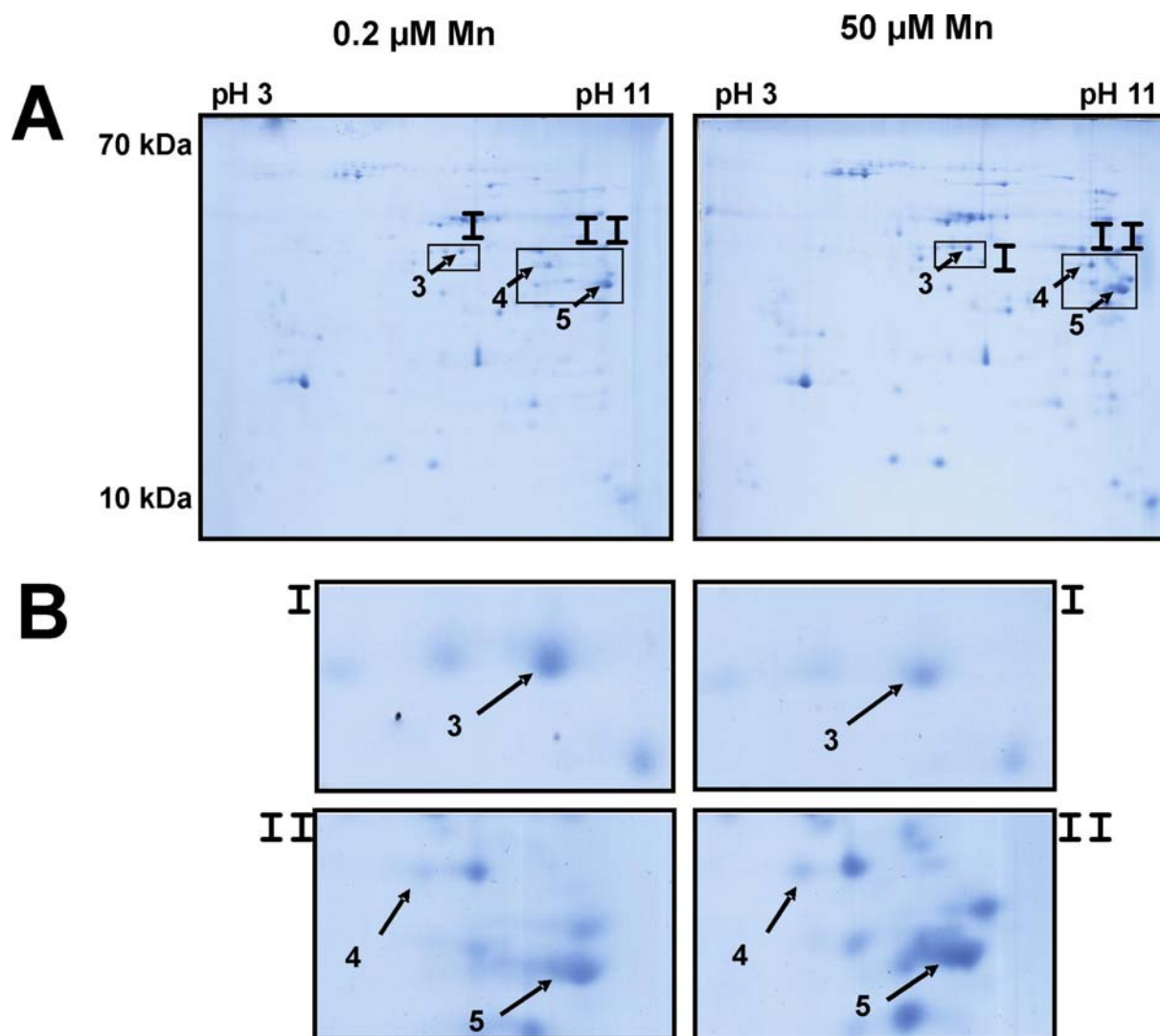


Fig. 4: 2-D resolution of (A) the AWF_{NaCl} proteome and (B) close ups of regions (B) of the 2D resolutions including differentially expressed proteins of the cowpea cultivar TVu 91 after treatment with $0.2 \mu\text{M}$ or with $50 \mu\text{M}$ Mn for 1 day after 14 days of pre-culture. Proteins were extracted from the AWF as described in the Materials and Methods section. About $120 \mu\text{g}$ protein was loaded onto each gel. IEF was carried out on broad range pH gradient gels (pH 3-11). Differentially expressed spots are marked by arrows (for identifications see Tab. 2).

All five marked protein spots (Figs. 3 and 4) were cut and submitted to protein sequence analysis using liquid chromatography-coupled mass spectrometry (LC-MS/MS). Blast searches did not always lead to a positive identification in cowpea since its genome has not yet been sequenced, but led to the identification of peptides in related sequences of green plants (Viridiplantae) downloaded from <http://www.ncbi.nlm.nih.gov/sites/entrez>. Seventeen unique proteins were identified in the green plants database. The false positive rate of identification was estimated as described by Elias and Gygi (2007). Moreover, no additional proteins were identified in reversed sequences suggesting that our dataset contained no false-positive identifications. A list of all resulting peptides as well as their identities is given in Tab. 2.

In the AWF_{H₂O} peptide sequencing yielded several peptides for each protein spot (Tab. 2). Database searches using the listed peptides (blastp) then resulted in different protein identities. Spot 1 contained peptides belonging to class III secretory peroxidases and the RubisCO small subunit. The same is true for spot 2.

In the AWF_{NaCl} more than two proteins have been identified per protein spot (Tab. 2). Spot 3 contained several peptides leading to currently unknown, predicted or hypothetical protein hits in the database (Tab. 2). However, an acetylcholinesterase as well as a typical apoplastic α -galactosidase have been indentified, too. In spot 4 a polygalacturonase-inhibiting protein, an α -galactosidase, and a symplastic 41 kDa chloroplast nucleoid DNA binding protein, but also currently unnamed or unknown protein products were identified by database searches. Spot 5 contained several peptides belonging to the class III peroxidase family, as a GDSL-lipase 1, and again peptides belonging to proteins currently unnamed or unknown in the databases.

Tab. 1. Data of evaluated protein spots from the AWF_{H₂O} and AWF_{NaCl} of the sensitive cowpea cultivar TVu 91 after 1 day of elevated Mn supply.

No. ^a	Mean spot volume on individual gels ^b		Ratio ^c	<i>p</i> -value ^d	pI ^e	MW (kDa) ^e
	0.2 μ M Mn	50 μ M Mn				
AWF_{H₂O}						
1	3.39	2.39	0.60	<0.05	5.8	25
2	0.17	0.51	3.00	<0.05	4.5	25
AWF_{NaCl}						
3	0.71	0.84	1.18	<0.05	6.0	45
4	0.65	0.43	0.66	<0.05	7.9	43
5	3.35	4.04	1.21	<0.05	9.2	40

^a Numbers correspond to the spot numbers given in gels.

^b Values indicate mean % volume of the spots in relation to the total volume of all proteins calculated from three gel replicates.

^c calculated fold induction / reduction of proteins of Mn-treated (1 d 50 μ M Mn) in relation to control (0.2 μ M Mn) plants (ratio) using by using the % volume values of three to six independent gels.

^d *P*-values were calculated using an algorithm incorporated into ImageMaster™ 2D Platinum Software 6.0.

^e pI (isoelectric point) and MW (molecular weight) values were estimated according to the spot position in the gels and “pH as function of distance” graphs (GE Healthcare)

Tab. 2. Leaf apoplastic proteins of cowpea cultivar TVu 91 affected by treatment with 50 μ M Mn for 1 day.

Spot no. ^a	Protein name ^b	Protein accession numbers	Protein molecular weight (Da)	Number of unique peptides	Percentage sequence coverage	Peptide sequence	Best Mascot Ion score	Best Mascot Identity score	Difference score	Number of identified +1H spectra	Number of identified +2H spectra	Number of identified +3H spectra	Number of identified +4H spectra	Number of enzymatic termini	Calculated +1H Peptide Mass (AMU)	estimated pI ^c	calculated pI ^c	estimated MW ^d	calculated MW ^d
spot 1	peroxidase [Sesamum indicum]	ABB89209.1	35 838.4	1	3.64%	VSCADILALATR	72.3	47.1	25.2	0	1	0	0	2	1 289,6889	5.8	9.19	25	35.86
spot 1	Peroxidase 45 precursor (Aterox P45)	Q96522.1	35 811.1	1	8.00%	GLFTSDQLFTDQR	84.8	45.3	39.5	0	1	1	0	2	1 640,8287	5.8	9.3	25	35.84
spot 1	Peroxidase 45 precursor (Aterox P45)	Q96522.1	35 811.1	1	8.00%	VSCADILALATR	72.3	47.1	25.2	0	1	0	0	2	1 289,6889	5.8	9.3	25	35.84
spot 1	rubisco small subunit [Coffea arabica]	CAD11991.1	20 373.9	3	12.70%	EIDVLR	37.6	47.8	-10.2	1	0	0	0	2	921,5047	5.8	8.25	25	20.39
spot 1	rubisco small subunit [Coffea arabica]	CAD11991.1	20 373.9	3	12.70%	IIGFDNVR	61.5	47.2	14.3	0	3	0	0	2	933,516	5.8	8.25	25	20.39
spot 1	rubisco small subunit [Coffea arabica]	CAD11991.1	20 373.9	3	12.70%	SPGYDGR	45.8	47.4	-1.6	0	1	0	0	2	914,4008	5.8	8.25	25	20.39
spot 2	peroxidase [Sesamum indicum]	ABB89209.1	35 838.4	1	3.64%	VSCADILALATR	85.9	47.1	38.8	0	1	0	0	2	1 289,6889	4.5	9.19	25	35.86
spot 2	rubisco small subunit [Coffea arabica]	CAD11991.1	20 373.9	2	8.84%	IIGFDNVR	42.4	47.2	-4.8	0	1	0	0	2	933,516	4.5	8.25	25	20.39
spot 2	rubisco small subunit [Coffea arabica]	CAD11991.1	20 373.9	2	8.84%	SPGYDGR	48	47.4	0.6	0	1	0	0	2	914,4008	4.5	8.25	25	20.39
spot 2	Peroxidase 45 precursor (Aterox P45)	Q96522.1	35 811.1	1	8.00%	GLFTSDQLFTDQR	89.3	45.3	44	0	1	0	0	2	1 640,8287	4.5	9.3	25	35.84
spot 2	Peroxidase 45 precursor (Aterox P45)	Q96522.1	35 811.1	1	8.00%	VSCADILALATR	85.9	47.1	38.8	0	1	0	0	2	1 289,6889	4.5	9.3	25	35.84
spot 3	predicted protein [Physcomitrella patens subsp. patens]	XP_001755457.1	50 463.6	1	1.48%	IADAVGR	58.1	47.5	10.6	0	1	0	0	2	701,3947	6	5.45	45	50.49
spot 3	acetylcholinesterase [Macropitium atropurpureum]	BAG09557.1	42 760.3	2	5.24%	DQNEATEFNK	59.2	45.9	13.3	0	1	0	0	2	1 326,5636	6	6.32	45	42.78
spot 3	acetylcholinesterase [Macropitium atropurpureum]	BAG09557.1	42 760.3	2	5.24%	TEGFVDPMK	51	46.5	4.5	0	1	0	0	2	1 023,4823	6	6.32	45	42.78
spot 3	unnamed protein product [Senna occidentalis]	CAA03733.1	44 295.1	1	8.37%	ALADYVHSK	57.3	46.7	10.6	0	2	0	0	2	1 003,5213	6	5.2	45	44.32
spot 3	unnamed protein product [Senna occidentalis]	CAA03733.1	44 295.1	1	8.37%	EVIAVNQDSLGVQGK	108	46.4	61.6	0	13	1	0	2	1 556,8285	6	5.2	45	44.32
spot 3	acid alpha galactosidase 1 [Cucumis sativus]	CAA03733.1	45 680.3	2	8.47%	ETADALVSTGLSK	86.6	47.1	39.5	0	10	0	0	2	1 291,6746	6	5.5	45	45.7
spot 3	acid alpha galactosidase 1 [Cucumis sativus]	CAA03733.1	45 680.3	2	8.47%	IGYSDAGYFTCSK	84.7	45.8	38.9	0	1	0	0	2	1 581,7259	6	5.5	45	45.7
spot 3	acid alpha galactosidase 1 [Cucumis sativus]	CAA03733.1	45 680.3	2	8.47%	VAVVLLNR	71.7	45.6	26.1	0	1	0	0	2	883,5728	6	5.5	45	45.7
spot 3	alpha-galactosidase 1 [Pisum sativum]	CAF34023.1	44 946.6	8	22.00%	ALADYVHSK	57.3	46.7	10.6	0	2	0	0	2	1 003,5213	6	6.55	45	44.97
spot 3	alpha-galactosidase 1 [Pisum sativum]	CAF34023.1	44 946.6	8	22.00%	APLLLGCDVR	48.5	45.9	2.6	0	2	0	0	2	1 113,6093	6	6.55	45	44.97
spot 3	alpha-galactosidase 1 [Pisum sativum]	CAF34023.1	44 946.6	8	22.00%	LGYS DAGYFTCSK	84.7	45.8	38.9	0	1	0	0	2	1 581,7259	6	6.55	45	44.97
spot 3	alpha-galactosidase 1 [Pisum sativum]	CAF34023.1	44 946.6	8	22.00%	LGYYVNIIDCWAE LNR	87.4	44.6	42.8	0	6	1	0	2	2 101,9654	6	6.55	45	44.97
spot 3	alpha-galactosidase 1 [Pisum sativum]	CAF34023.1	44 946.6	8	22.00%	MYVLKPA	66.3	46.7	19.6	2	2	0	0	2	920,528	6	6.55	45	44.97
spot 3	alpha-galactosidase 1 [Pisum sativum]	CAF34023.1	44 946.6	8	22.00%	QMPGSLGHEFDQAK	49.4	46.1	3.3	0	1	0	0	2	1 544,7169	6	6.55	45	44.97
spot 3	alpha-galactosidase 1 [Pisum sativum]	CAF34023.1	44 946.6	8	22.00%	TFASWGIDY LK	69.3	46.5	22.8	0	1	0	0	2	1 300,6578	6	6.55	45	44.97
spot 3	alpha-galactosidase 1 [Pisum sativum]	CAF34023.1	44 946.6	8	22.00%	VGN SWR	32.8	47	-14.2	0	1	0	0	2	718,3636	6	6.55	45	44.97
spot 3	hypothetical protein [Vitis vinifera]	CAN75822.1	45 399.0	2	14.50%	ALADYVHSK	57.3	46.7	10.6	0	2	0	0	2	1 003,5213	6	5.48	45	39.54
spot 3	hypothetical protein [Vitis vinifera]	CAN75822.1	45 399.0	2	14.50%	APLLLGCDVR	48.5	45.9	2.6	0	2	0	0	2	1 113,6093	6	5.48	45	39.54
spot 3	hypothetical protein [Vitis vinifera]	CAN75822.1	45 399.0	2	14.50%	KSTFP SGIK	47.5	46.8	0.7	0	1	0	0	2	964,5468	6	5.48	45	39.54
spot 3	hypothetical protein [Vitis vinifera]	CAN75822.1	45 399.0	2	14.50%	LGYS DAGYFTCSK	84.7	45.8	38.9	0	1	0	0	2	1 581,7259	6	5.48	45	39.54
spot 3	hypothetical protein [Vitis vinifera]	CAN75822.1	45 399.0	2	14.50%	STFP SGIK	37.5	47	-9.5	0	2	0	0	2	836,4519	6	5.48	45	39.54
spot 3	hypothetical protein [Vitis vinifera]	CAN75822.1	45 399.0	2	14.50%	TFASWGIDY LK	69.3	46.5	22.8	0	1	0	0	2	1 300,6578	6	5.48	45	39.54
spot 3	hypothetical protein [Vitis vinifera]	CAN75822.1	45 399.0	2	14.50%	VGN SWR	32.8	47	-14.2	0	1	0	0	2	718,3636	6	5.48	45	39.54
spot 4	unnamed protein product [Senna occidentalis]	CAA03733.1	44 295.1	1	3.69%	EVIAVNQDSLGVQGK	82.5	46.4	36.1	0	1	1	0	2	1 556,8285	7.9	5.2	43	44.32
spot 4	unknown [Populus trichocarpa]	ABK95990.1	37 757.7	1	3.69%	LATDFAETLGFK	85.1	46.2	38.9	0	1	0	0	2	1 379,7424	7.9	7.44	43	37.78
spot 4	polygalacturonase-inhibiting protein [Phaseolus vulgaris]	AAR92038.1	37 086.3	2	7.02%	FVSSVANNK	62.1	48.9	13.2	0	1	0	0	2	1 144,5274	7.9	8.97	43	37.08
spot 4	polygalacturonase-inhibiting protein [Phaseolus vulgaris]	AAR92038.1	37 086.3	2	7.02%	ISGAIPSSVGSFSK	45.8	45.8	0	0	1	0	0	2	1 428,7010	7.9	8.97	43	37.08
spot 4	41 kD chloroplast nucleoid DNA binding protein (CND41) [Nicotiana sylvestris]	BAC22609.1	53 617.6	2	4.58%	DLSLIFDTGSDLTWTQCPCVK	72.6	44	28.6	0	0	1	0	2	2 584,2069	7.9	8.68	43	53.64
spot 4	41 kD chloroplast nucleoid DNA binding protein (CND41) [Nicotiana sylvestris]	BAC22609.1	53 617.6	2	4.58%	KDLSLIFDTGSDLTWTQCPCVK	38.4	43.6	-5.2	0	0	2	0	2	2 712,3018	7.9	8.68	43	53.64
spot 4	Os08g0505900 [Oryza sativa (japonica cultivar-group)]	NP_001062185.1	38 776.4	1	2.63%	LSSLILADWK	54.2	46.3	7.9	0	1	0	0	2	1 145,6572	7.9	5.82	43	38.8
spot 4	alpha-galactosidase 1 [Pisum sativum]	CAF34023.1	44 946.6	1	4.20%	LGYYVNIIDCWAE LNR	70.7	44.6	26.1	0	1	0	0	2	2 101,9654	7.9	6.55	43	44.97

Tab. 2. Leaf proteins of cowpea cultivar TVu 91 affected by treatment with 50 μ M Mn for 1 day. (continued)

Spot no. ^a	Protein name ^b	Protein accession numbers	Protein molecular weight (Da)	Number of unique peptides	Percentage sequence coverage	Peptide sequence	Best Mascot Ion score	Best Mascot Identity score	Difference score	Number of identified +1H spectra	Number of identified +2H spectra	Number of identified +3H spectra	Number of identified +4H spectra	Number of enzymatic termini	Calculated +1H Peptide Mass (AMU)	estimated pI ^c	calculated pI ^c	estimated MW ^c	calculated MW ^c
spot 5	peroxidase [Sesamum indicum]	ABB89209.1	35 838,4	4	16.40%	DHPDNLFLAGDGFDTVIK	119	45,3	73,7	0	1	1	0	2	1 913,9248	9,2	9,19	40	35,86
spot 5	peroxidase [Sesamum indicum]	ABB89209.1	35 838,4	4	16.40%	EKQTFVTVPATLR	83,7	46	37,7	0	2	0	0	2	1 507,8639	9,2	9,19	40	35,86
spot 5	peroxidase [Sesamum indicum]	ABB89209.1	35 838,4	4	16.40%	IAIDMDPTTFR	89,3	46,6	42,7	0	2	0	0	2	1 229,6203	9,2	9,19	40	35,86
spot 5	peroxidase [Sesamum indicum]	ABB89209.1	35 838,4	4	16.40%	VSCADILALATR	59,8	47,1	12,7	0	2	2	0	2	1 289,6889	9,2	9,19	40	35,86
spot 5	GDSL-lipase 1 [Capsicum annuum]	AAZ23955.1	40 237,4	4	13.20%	FALIGVQIGGCPNALAQNSPDGR	53,4	43,9	9,5	0	0	1	0	2	2 442,2203	9,2	8,73	40	40,26
spot 5	GDSL-lipase 1 [Capsicum annuum]	AAZ23955.1	40 237,4	4	13.20%	GVNYASAAAGIR	119	46,3	72,7	0	1	0	0	2	1 149,6016	9,2	8,73	40	40,26
spot 5	GDSL-lipase 1 [Capsicum annuum]	AAZ23955.1	40 237,4	4	13.20%	KFALIGVQIGGCPNALAQNSPDGR	40,4	44,1	-3,7	0	0	1	0	2	2 570,3153	9,2	8,73	40	40,26
spot 5	GDSL-lipase 1 [Capsicum annuum]	AAZ23955.1	40 237,4	4	13.20%	VTNAGCCGVGR	33,3	46,2	-12,9	0	1	0	0	2	1 150,5099	9,2	8,73	40	40,26
spot 5	peroxidase2 [Medicago sativa]	CAC38106.1	35 992,3	2	13.10%	FDGLVSR	52,5	47,7	4,8	0	5	0	0	2	793,4209	9,2	9,07	40	35,42
spot 5	peroxidase2 [Medicago sativa]	CAC38106.1	35 992,3	2	13.10%	FQQTFVTVPATLR	83,7	46	37,7	0	2	0	0	2	1 507,8275	9,2	9,07	40	35,42
spot 5	peroxidase2 [Medicago sativa]	CAC38106.1	35 992,3	2	13.10%	IAINMDPTTFR	95,8	46,5	49,3	0	3	0	0	2	1 244,6311	9,2	9,07	40	35,42
spot 5	peroxidase2 [Medicago sativa]	CAC38106.1	35 992,3	2	13.10%	VSCADILALATR	59,8	47,1	12,7	0	2	2	0	2	1 289,6889	9,2	9,07	40	35,42
spot 5	unnamed protein product [Vitis vinifera]	CAO71984.1	35 939,4	1	13.30%	DHPDNLFLAGDGFDTVIK	119	45,3	73,7	0	1	1	0	2	1 913,9248	9,2	8,52	40	35,96
spot 5	unnamed protein product [Vitis vinifera]	CAO71984.1	35 939,4	1	13.30%	FDVYVYQNLQQGK	61,2	46	15,2	0	1	1	0	2	1 616,7710	9,2	8,52	40	35,96
spot 5	unnamed protein product [Vitis vinifera]	CAO71984.1	35 939,4	1	13.30%	EKQTFVTVPATLR	83,7	46	37,7	0	2	0	0	2	1 507,8639	9,2	8,52	40	35,96
spot 5	unknown [Populus trichocarpa]	ABK94318.1	37 787,6	2	6.21%	IGASLR	52,8	46,9	5,9	0	1	0	0	2	729,4624	9,2	4,65	40	37,81
spot 5	unknown [Populus trichocarpa]	ABK94318.1	37 787,6	2	6.21%	MGNISPLTGTDGEIR	72,8	45,9	26,9	0	1	0	0	2	1 576,7644	9,2	4,65	40	37,81
spot 5	Peroxidase 45 precursor (Atperox P45)	Q96522.1	35 811,1	1	8.00%	GLFTSDQILFTDQR	99,8	45,3	54,5	0	6	5	0	2	1 640,8287	9,2	9,3	40	35,84
spot 5	Peroxidase 45 precursor (Atperox P45)	Q96522.1	35 811,1	1	8.00%	VSCADILALATR	59,8	47,1	12,7	0	2	2	0	2	1 289,6889	9,2	9,3	40	35,84

^a The numbers correspond to numbers given in Figs 3 and 4. For statistical evaluation and peptide sequences see Table 1.

^b Identities are based on sequence comparisons using the NCBI protein database.

^c estimated pI (isoelectric point) and MW (molecular weight) values were estimated according to the spot position in the gels and “pH as function of distance” graphs (GE Healthcare), pI and MW calculation were made by using <http://www.embl-heidelberg.de/cgi/pi-wrapper.pl> and <http://www.sciencegateway.org/tools/proteinmw.htm> web based calculation tools, respectively.

Regarding the identified peroxidase peptides of protein spots 1, 2 and 5 (Tab. 2), in sum eleven peptides could be aligned to class III peroxidases from several plant species (Fig. 5). Five of the eleven peptides have been newly identified (red typed peptides in alignment of VuPOD in Fig. 5) whereas six peptides (blue typed peptides in alignment of VuPOD in Fig. 5) had already previously been identified (Chapter 2). The five black typed peptides in the VuPOD sequence (Fig. 5) were identified in previous studies investigating the apoplastic peroxidase isoenzyme profile (Chapters 2 and 3) but were not detected in this study.

All detected peptides leading to a class III POD database hit have been identified in spot 5 (Tab. 2), three peptides including one peptide belonging to a conserved domain (VSCADILALATR) were also detected in spots 1 and 2. At least four overlapping peptides provide evidence for at least four distinct peroxidase gene products.

			c1	
		1		60
FBP 1	(1)	-----VVGVVVIGALPFSSDAQLDPSFYRNTCPVSHSIVREV		
P 49 (A. t.)	(1)	-----MARLTSFLLLLSLICFVPLCLCDKSYGGKLFPGYYAHSCPQVNEIVRSV		
PPOD	(1)	-----MGSAKFFVTLICIVPLLASSFCSAQLSATFYASTCPNLQTVIRNA		
VvPOD	(1)	-----MASHHSSSSVFTTFKLCFCLLLSFIGMASAQLTTNFYAKTCPNALSIIKSA		
VaPOD	(1)	MASISSNKNAIFSFLLLSIILSVSVIKVCEAQRPPTRVGLSYTFYSKTCPTLKSIVRTE		
P 45 (A. t.)	(1)	-----MEKNSTQITFSNFFLLLSLSSCVSAQLRTGFYQNSCPNVETIVRNA		
SoPOD	(1)	-----IILAYLAACLNSAQLSSKHAYSSCPNLEKIVRKT		
SiPOD	(1)	-----MGQSSFMLTFLTSLGLVIVFSGSVSAQLKQNYANI CPDVENIVRQA		
MsPOD	(1)	-----MGR-YNVILVWSLALTCLIPYTTFAQLSPNHYANICPNVQSI VRSA		
VuPOD		-----		
			i hdC2 c3	
		61	*****	120
FBP 1	(37)	IRNVSKSDPRMLASLIRLHFHDCFVQGCDA ILLNNTDTIVSEQEALPNIN-SIRGLDVV		
P 49 (A. t.)	(50)	VAKAVARETRMAASLLRHLHFHDCFVQGCDSLLLDSSGRVATEKNSNPNSK-SARGFDVV		
PPOD	(45)	MTGAVNGQPRLAASILRHLHFHDCFVNGCDGSILLDDTATFTGKNNANPNRN-SARGFEVI		
VvPOD	(53)	VNSAVKSEARMGASLLRHLHFHDCFG--CDASILLDDTSTNFTGKTAGPNAN-SVRGYEVV		
VaPOD	(61)	LKKVFQSDIAQAAGLLRHLHFHDCFVQGCDSVLLDGSASGPSEKDAPPNLTAEAFRII		
P 45 (A. t.)	(47)	VRQKFQQTFTVPATLRLRFHDCFVRCGDASIMIASP----SERDHPDDMSLAGDGFDTV		
SoPOD	(34)	MKQAVQKEQRMGASILRHLHFHDCFVNGCDASLLLDSTFTGKTAISNRNNSVRGFEVI		
SiPOD	(48)	VTAKFKQTFVTPATLRLYFHDCFVSGCDASVIASTPGNTAEKDHDPNLSLAGDGFDTV		
MsPOD	(47)	VQKKFQQTFTVPATLRLRFHDCFVQGCDA SVLVASSGNNKAEKDHPENLSLAGDGFDTV		
VuPOD		-----MGASILR-----DHPDNLSLAGDGFDTV		
		IGASLIR		GYEVV
		FKQTFVTPATLR		GFEVI
		FQQTFVTPATLR		
			c4 c5 ii	
		121	*****	180
FBP 1	(96)	NQIKTAVEN--ACPGVVSCADILTLAAEISSVLAQGPDWKVP LGRKDSL-TANRTLANQN		
P 49 (A. t.)	(109)	DQIKAELEK--QCPGTVSCADVLT LAARDSSVLTGGPSWVPLGRDRS-SASLSQSNNN		
PPOD	(104)	DTIKTRVEA--ACNATVSCADILALAARDGVLLGGPSWVPLGRRDAR-TASQSAANSQ		
VvPOD	(110)	DTIKSQLEA--SCPGVVSCADILAVARDVVALRGP SWVPLGRRDST-TASLSAANSN		
VaPOD	(121)	ERIRGLLEK--SCGRVSCSDITALAARDAVFLSGGPDYEIPLGRRDGLTFASRQVTLDN		
P 45 (A. t.)	(103)	VKAKQAVDSNPNCRNK VSCADILALATREVVVLTGGPSYPVELGRRDGR-ISTKASVQSQ		
SoPOD	(94)	DSIKTNVEA--SCKATVSCADILALAARDGVLLGGPSWVPLGRRDAR-TASLTAAATNN		
SiPOD	(108)	IKAKAAVDVAVPRCNK VSCADILALATRDVINLAGGPSYPVELGRLDGL-KSTAASVNGN		
MsPOD	(107)	IKAKAALDAVPQCRNK VSCADILALATRDVINLAGGPSYTVELGRFDGL-VSRSSDVNGR		
VuPOD		IK-----VSCADILALATR-----FDGL-VSR-----		
		DTIK		
		DTIK		

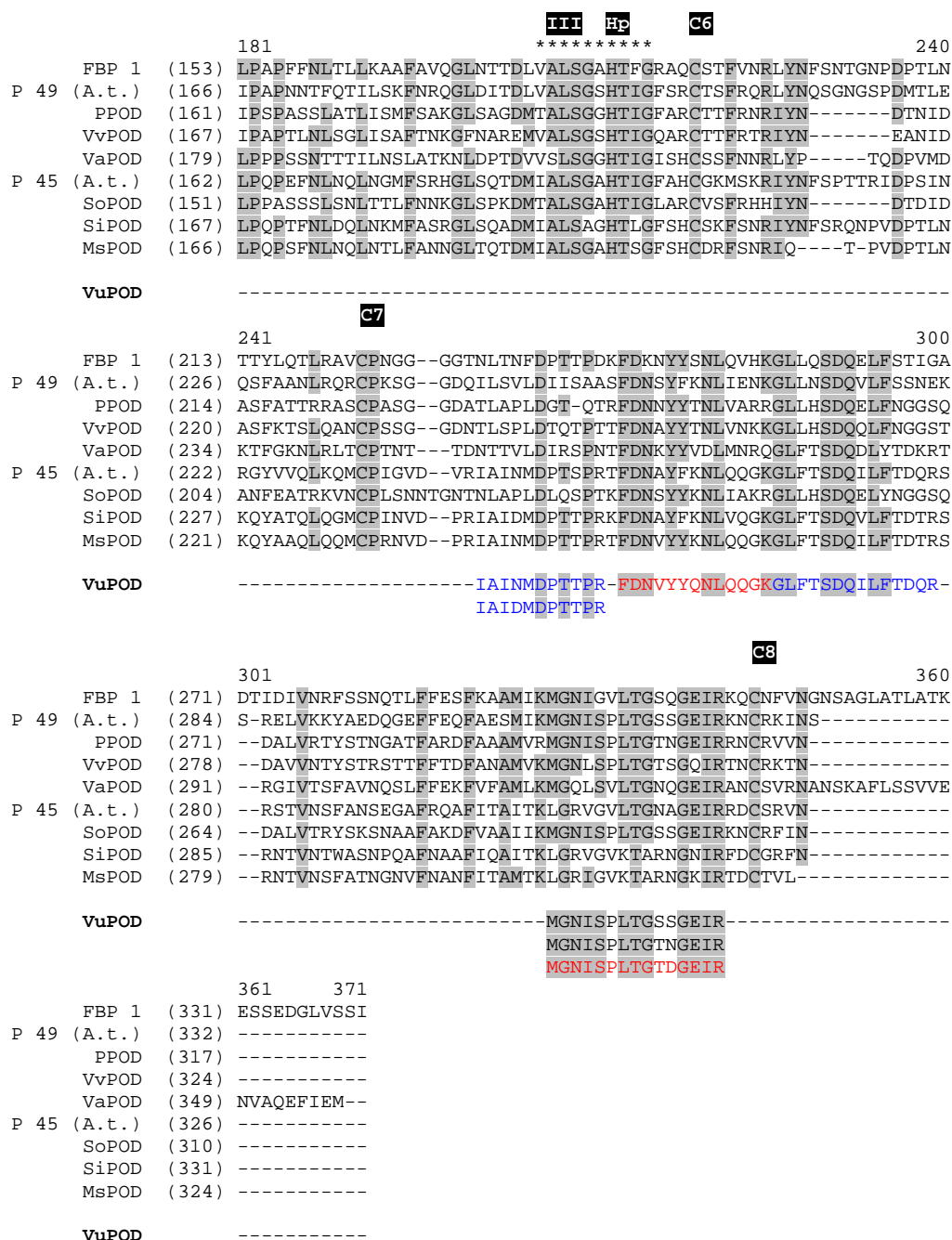


Fig. 5: Alignment of determined and deduced amino acid (aa) sequences of peroxidases of various plant species and nano LC-MS/MS-identified peroxidase peptide sequences from cowpea. Five newly identified aa of this study belonging to a peroxidase (VuPOD) are typed in red letters, the eleven remaining aa (six blue and five black typed) were already described in Chapters 2 and 3. Amino acid positions conserved in at least 50% of the sequences are underlayed in gray. Stars (*) indicate the conserved distal heme-binding domain (I), the central conserved domain of unknown function (II), and the proximal heme binding domain. The eight cysteines (C1-C8) and the distal (Hd) and proximal (Hp) histidines are indicated, too. Abbreviations: FBP1 French Bean Peroxidase 1 (Acc no.: AF149277), P49 (A.t.) POD isoenzyme 49 from *Arabidopsis thaliana* (Acc. no. O23237), PPOD from *Populus ssp.* (Acc. no.: AAX53172), VvPOD from *Vitis vinifera* (Acc. no.: CAO48839), VaPOD from *Vigna angularis* (Acc. no.: BAA01950), P45 (A.t.) POD isoenzyme 45 from *Arabidopsis thaliana* (Acc. no. Q96522), SoPOD from *Spinacia oleracea* (Acc. no.: CAA71493), SiPOD from *Sesamum indicum* (Acc. no.: ABB89209), MsPOD from *Medicago sativa* (Acc. no.: CAC38106), VuPOD POD peptide sequences of *Vigna unguiculata*.

Isolation of cell walls and investigation of Mn-induced changes in the cell-wall proteome

The applied procedure to investigate Mn-induced changes in the cell-wall proteome allowed the identification of in sum seven proteins affected by excess Mn for 1 d (Fig. 6). Results of the statistical analyses of the cell wall proteome fraction is given as supplementary material (Tab. S2), and alignment of peptide sequences to corresponding database hits are given as in Tab. S3. Plastocyanine, a protein typically located in the lumen of chloroplasts, was about 1.8-fold upregulated in Mn-treated plants (Spot 1, Fig 6, Tabs. 3, S2 and S3). An additional chloroplastic RNA binding ribonucleoprotein was more than 1.3-fold upregulated by excess Mn as well (Spot 2). Spot 3 contained several proteins: two different phosphatases, a phosphoglycolate phosphatase and a nitrophenylphosphatase, and a putative glyoxalase. Spot 4 was identified as a putative thioredoxin type m typical for chloroplasts which was 1.2-fold upregulated. A nearly 1.5-fold increased abundance of a cyclophilin-like protein was detected in spot 5. Spots 6 and 7 contained peptides with homology to malate dehydrogenase. Spot 6 was downregulated by less than 30% whereas spot 7 was 1.7-fold upregulated by excess Mn supply.

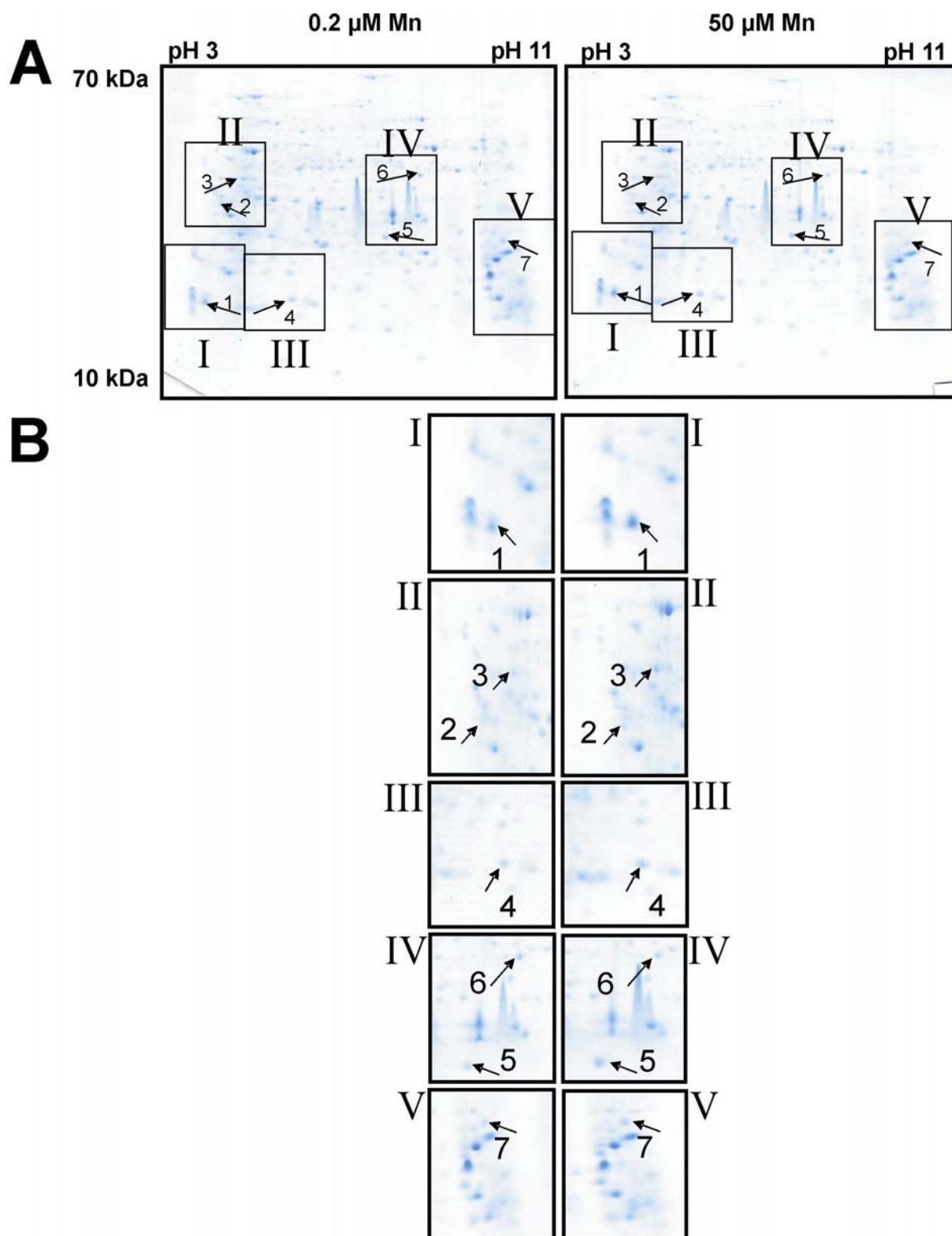


Fig. 6: 2-D resolution of (A) the strongly ionically bound cell wall proteome and (B) close ups of regions (B) of the 2D resolutions including differentially expressed proteins of the cowpea cultivar TVu 91 after treatment with 0.2 μM or with 50 μM Mn for 1 day after 14 days of pre-culture. Proteins were extracted from isolated cell walls as described in the Materials and Methods section. About 510 μg protein was loaded onto each gel. IEF was carried out on broad range pH gradient gels (pH 3-11). Differentially expressed spots are marked by arrows (for identifications see Tab. 3).

Tab. 3. Strongly ionically bound leaf apoplastic proteins of cowpea cultivar TVu 91 affected by treatment with 50 μ M Mn for 1 days.

Spot ^a	Identity ^b	Acc. No ^b	No. of amino acids ^b	estimated pI ^c	calculated pI ^c	estimated MW ^c (kDa)	calculated MW ^c (kDa)	Fold induction / reduction ^d
1	Plastocyanine (<i>P. vulgaris</i>)	P00287	99	4.2	4.1	26	10.5	1.8
2	28 kDa ribonucleoprotein, chloroplast (<i>S. oleracea</i>)	CAA41023	233	4.45	4.2	45	25.2	1.3
3	putative phosphoglycolate phosphatase (<i>A. thaliana</i>)	NP_198495	362	4.8	7.0	50	39.8	1.5
	4-nitrophenolphosphatase-like protein (<i>A. thaliana</i>)	BAA98057	389	4.8	8.6	50	43.1	1.5
	putative glyoxalase (<i>O. sativa</i>)	Q75GB0	263	4.8	4.8	50	29.6	1.5
4	putative thioredoxin m2 (<i>P. sativum</i>)	Q95AH9	180	5.4	9.3	26.5	19.9	1.2
5	cyclophilin-like protein (<i>T. aestivum</i>)	AAP44537	245	6.0	9.9	40	25.9	1.5
6	putative malate dehydrogenase (<i>P. aestivum</i>)	AAO27260	356	6.4	7.2	52	37.1	0.7
7	malate dehydrogenase precursor (<i>M. sativa</i>)	O48903	358	8.8	8.4	39.5	38.1	1.7

^a The numbers correspond to numbers given in Fig. 6. For statistical evaluation and peptide sequences see supplementary material, Tabs. S2 and S3.

^b Identities are based on sequence comparisons using the NCBI protein database.

^c estimated pI (isoelectric point) and MW (molecular weight) values were estimated according to the spot position in the gels and “pH as function of distance” graphs (GE Healthcare), pI and MW calculation were made by using <http://www.embl-heidelberg.de/cgi/pi-wrapper.pl> and <http://www.sciencegateway.org/tools/proteinmw.htm> web based calculation tools, respectively.

^d Fold induction / reduction in plants cultivated at 50 μ M Mn in relation to plants cultivated at 0.2 μ M. For further details see materials and methods section and Table S2.

Discussion

Previous studies (Chapter 1-3) focused on plants, which already showed visible even though moderate toxicity symptoms. Hence, very early (apoplastic) processes leading to Mn toxicity might have been masked by secondary toxicity mechanisms. The aim of this work was, therefore, to study early proteomic events leading to the development of Mn toxicity. Two apoplastic fractions of a Mn-sensitive cultivar were investigated by using an infiltration/centrifugation technique yielding apoplastic washing fluid (AWF). Moreover, this Chapter provides results on a methodological approach to isolate cell walls in order to determine also Mn-induced changes in the strongly bound cell-wall proteome.

Manganese uptake

A Mn treatment for one day appears to be suitable for the investigation of early apoplastic Mn toxicity responses, as Mn is readily taken up by plants (Fig. 1A) without having an effect on apoplastic parameters (Figs. 1C, D, 2A-D) typically linked to Mn toxicity (Fecht-Christoffers et al., 2003a, b, 2005, 2006, 2007).

The apoplastic Mn concentrations were significantly increased (Fig. 1B). In control plants a homogenous distribution of the apoplastic Mn between AWF_{H_2O} and the AWF_{NaCl} has been observed. The 2 to 3-fold increase in the Mn concentration of the AWF_{H_2O} was within the range published earlier by Fecht-Christoffers (2004). The 10-fold increase of the Mn concentration of the AWF_{NaCl} may reflect the strong binding capacity of the cell walls for Mn (Horst et al., 1999). Obviously, a higher proportion of the additional Mn is ionically bound to the cell wall. The amount of extractable apoplastic Mn positively correlates with the ionic strength of the extraction solution: compared with this study using a 0.25 M NaCl solution, in Chapter 2 a sequential extraction of leaf AWF with first water followed by 0.5 M NaCl solution yielded up to 3-fold more extractable Mn ($150 \mu\text{mol Mn g}^{-1} \text{dm}$).

Only 3-5% of the total Mn taken up was localized in the apoplast. In experiments with longer Mn treatment periods Fecht-Christoffers (2004) could show that the absolute water-soluble apoplastic Mn concentration increased with treatment time but finally levelled off. Thus the ratio of apoplastic to bulk-leaf Mn reached a peak after 24 h and decreased with ongoing Mn treatment. This indicates a limited Mn binding capacity of the apoplast. However, the

identified apoplastic Mn concentrations were thought to trigger the Mn toxicity response through enhancing apoplastic peroxidase activities (Fecht-Christoffers et al., 2006).

Evaluation of the procedures to isolate and characterize apoplastic proteome fractions

An infiltration/centrifugation technique yielding AWF always also modifies apoplastic protein and metabolite concentrations and thus their equilibrium, and may contain symplastic contaminations strongly depending on the infiltration medium (Sattelmacher, 2001; Lohaus et al., 2001). The *in-vivo* occurring protein and metabolite compositions and concentrations may, therefore, not be reflected by the AWF harvesting procedures but it is, nevertheless, an accepted method for the investigation of the apoplast (Sattelmacher, 2001; Lohaus et al., 2001).

The symplastic contamination of the AWF is usually evaluated by the determination of symplastic marker-enzyme activities like malate dehydrogenase (MDH). The existence of an apoplastic MDH providing apoplastic NADH has been proposed (Gross et al., 1977; Gross 1977; Kärkönen et al., 2002). This would question the suitability as AWF contamination marker-enzyme. In this study, the symplastic contamination determined using MDH activity assay was below 0.5% in both AWF fractions. A concentration of both AWF fractions and subsequent separation and identification of differentially formed protein spots yielded peptides belonging to proteins typically located in the symplast (e.g. RubisCO, spots 1 and 2, and a 41 kDa chloroplast nucleotide DNA-binding protein, spot 4) confirming a slight contamination of the AWF. However, no MDH has been found. This is underlined by the fact that also in the literature an apoplastic MDH (Kärkönen et al., 2002; Kwon et al., 2005) has not yet unequivocally been identified. Also, there are no reports about the identification of NAD in the apoplast except Shinkle et al. (1992). Unfortunately, the applied GC-MS-based metabolite-profiling approach is also not capable of detecting NAD⁺/NADH (Chapters 2 and 3). Therefore, the apoplastic localization of MDH and the presence of NAD/NADH in the apoplast remains speculative. However, in the strongly bound cell-wall protein fraction MDH has been identified (spots 6 and 7). But in view of the comparatively high symplastic contamination of the fraction of about 4% (data not shown) and the identification of several typical symplastic proteins (e.g. plastocyanine, spot 1, ribonucleoprotein, spot 2, phosphatases, spot 3, thioredoxin, spot 4; Tab. 3) it remains questionable whether the identified MDH in the isolated cell-wall fraction is an apoplastic MDH *in vivo*: during the homogenization of leaf material *in vivo* distinct leaf compartments come into contact thus

most likely leading to a binding/trapping of symplastic proteins in the cell-wall networks (Fry, 1988; Feiz et al., 2006). The applied method for cell-wall purification with the aim of subsequent extraction of cell-wall proteins could be a critical point, too. Jamet et al. (2006) mentioned the lack of an efficient procedure to extract strongly bound cell-wall proteins from the extracellular matrix, even though a number of protocols exist for the extraction of specific cell-wall proteins. The same group recently published a paper critically comparing several currently available cell-wall extraction-methods (Feiz et al., 2006). Based on the published procedures they developed a new method. None of the methods use ethanol as an extractant. It thus appears that the applied extraction procedure may not be suitable for the extraction of cell-wall proteins reflecting the *in vivo* protein binding and distribution.

In conclusion the applied method for extracting water-soluble and ionically bound apoplastic proteins with the infiltration/centrifugation technique yielding AWF and the MDH as marker enzyme appear both to be suitable tools for the investigation and evaluation of Mn excess-induced changes in the apoplastic free and ionically bound proteome. The cell-wall isolation procedure on the other hand is critical and needs further adaptations. Therefore, in the following the identified strongly bound proteins of the cell-wall fraction are not discussed further with respect to the development of Mn toxicity.

Although one day Mn treatment lead to clear increases in the bulk-leaf and apoplastic Mn concentrations the lack of measurable physiological responses (see above) suggested that possible changes in the symplastic and particularly the apoplastic proteome would be small compared to the great changes detected in the apoplast after long-term (3 d) excess Mn treatment (Fecht-Christoffers et al., 2003b; Chapters 2 and 3). Therefore, the setting of the threshold criteria for the detection of significantly affected proteins by using Image Master Platinum Software (v. 6.0) was adapted: no threshold for the change in abundance was set but the change had to be significant at least at $P < 0.05$ (t test). This procedure led in sum to five protein spots that were changed in abundance. The identified proteins will be discussed in the following sections with respect to their possible function in the Mn stress response.

The identification of proteins which are responsible for the Mn-induced changes in abundance (Tab. 1) is complicated by the fact that even after 2D separation one protein spot may contain several proteins (Tabs. 2, S1 and S3). In order to identify the protein most likely responsible for the changes in expression level, calculated and estimated isoelectric points and molecular weights were compared (Tab. 2). Moreover, the peptides with the highest percentage sequence coverage and number of unique peptides were specifically addressed. In some cases, in view of their putative physiological roles also specific protein identities which only

contributed a comparatively low number of peptides to the whole peptide profile of a spot were discussed.

Effect of short-term elevated Mn supply on the apoplastic proteome

Simple protein quantification in the AWF showed higher protein concentrations in the AWF_{NaCl} than in the AWF_{H₂O} (Fig. 1C). Submitting both AWF fractions to 2D PAGE showed that there are major differences in spot patterning between both proteomes, even though the AWF_{NaCl} contains also the apoplastic water-soluble proteins (Figs. 3 and 4). Especially cationic, basic protein spots additionally appeared among the AWF_{NaCl} proteins. Setting the appropriate thresholds for only 1 d of elevated Mn supply (see previous section) led in sum to five proteins spots that were changed in abundance.

The sequencing results for spot 1 and spot 2 of the AWF_{H₂O} yielded nearly equal numbers of peptides for a peroxidase and for RubisCO. Unfortunately, also the calculated and estimated pIs varied greatly from each other and from calculated pIs. Therefore, it was not possible to determine the protein identity which was responsible for the Mn-induced change in abundance (Tab. 2). The question arises why both spots yielded the same protein peptides and, therefore, database hits despite differences in the isoelectric points. Unfortunately, this question cannot be satisfactorily answered here. Nevertheless, the possible physiological role of the typically apoplastically localized class III peroxidase is discussed in a later section.

Two proteins involved in cell-wall modification and, therefore, in plant development in the broadest sense were affected by elevated Mn supply in the AWF_{NaCl}. The downregulated spot 4 (Fig. 4) contained a polygalacturonase (PG-)-inhibiting protein (PGIP) (Tab. 2). Particularly in response to various stresses like wounding, fungal infection and elicitor treatment, plants accumulate PGIPs (Ferrari et al., 2006; Bergmann et al., 1994) which inhibit polygalacturonases and, thereby, increase stress tolerance. In contrast, after long-term Mn treatments of cowpea Fecht-Christoffers et al. (2003b) showed an enhanced release of various typical plant defence-related proteins into the apoplast suggesting a stress response in the apoplast. Mehli et al. (2004) provided evidence for a constitutive expression of developmentally regulated PGIPs, and recently Protsenko et al. (2008) in their review suggested that PGIPs are also structural components and, therefore, cell wall property-determining proteins. The lower abundance of PGIP as an initial response to Mn stress might, therefore, be regarded as developmental difference in cell-wall modification between Mn-treated and control plants. An interacting activity of PGIPs and apoplastic peroxidases is also

conceivable since the proposed apoplastic peroxidase reaction scheme leading to Mn toxicity (Fecht-Christoffers et al., 2007) forms also part of the naturally occurring lignin formation in cell walls (Halliwell, 1978). However, a role of PGIPs as Mn-sensitivity conferring apoplastic protein needs to be confirmed and substantiated.

In the AWF_{NaCl} the 1.2-fold upregulated spot 3 consisted of peptides assigned to α -galactosidase (Tab. 2). α -Galactosidases catalyse the hydrolysis of α -1,6-linked α -galactose residues from oligosaccharides. α -galactosidases greatly contribute to the dynamic behaviour of the cell wall during the development of plants (Chrost et al., 2007) and have also been shown to enhance cold tolerance of plants when downregulated (Pennycooke et al., 2003). However, a specific role of increased hydrolytic activity by α -galactosidase e.g. in terms of Mn stress perception and/or other cell-wall modification-processes also in view of increased apoplastic peroxidase activities in the Mn stress response remains so far unclear and speculative.

Two protein annotations, an acetylcholinesterase (spot 4) and a GDSL-lipase 1 (spot 5) are involved in stress perception and signal-transduction processes and, therefore, provide a more direct hint at Mn stress. The comparable low coverage of the acetylcholinesterase in spot 4 may indicate a low contribution to the Mn-induced change in spot abundance compared with the co-identified α -galactosidase. Acetylcholinesterases are involved in signal-transduction processes (Brenner et al., 2006; Sagane et al., 2005) and, therefore, an upregulation may indicate that the cowpea plant perceives a stress signal leading to broad-range biochemical changes on the whole plant level. Moreover, a response of the acetylcholine-mediated signalling system to stimuli-mediated changes of Ca^{2+} signals has been suggested (Momonoki et al., 1996). Manganese-induced changes of Ca^{2+} signals might also occur through partial substitution of apoplastic Ca^{2+} by apoplastic Mn^{2+} (Fig. 1B).

Spot 5 was 1.2-fold upregulated in response to increased Mn availability (Tab. 1). Four peptides from that spot were assigned to a GDSL-lipase 1 (Tab. 2). GDSL-lipases are known to be involved in various regulating mechanisms like plant development, morphogenesis, synthesis of secondary metabolites and/or defense responses (Ling et al., 2006; Kim et al., 2008), like salt tolerance (Naranjo et al., 2006). Hence, a slight upregulation of this protein beside the peroxidase, which is represented by a higher number of peptides (Tab. 2), seems to be also likely in terms of a general stress response.

Apoplasmic peroxidases identified by IEF/SDS-PAGE

Fecht-Christoffers et al. (2003b, 2006) showed a Mn-induced increase in so-called acidic peroxidase abundance after long-termed Mn supply. This study additionally specifically identified basic peroxidases induced by short-term elevated Mn supply (Tab. 2, spots 1, 2, 5). The large class III peroxidase gene family with more than 70 genes in Arabidopsis (Duroux and Welinder, 2003) gives rise to the expectation of highly variable isoelectric points. The presence of isoenzymes is further supported by the fact, that in the AWF_{H₂O} the acidic spot 1 was downregulated by more than 30% due to elevated Mn supply, whereas acidic spot 2 was 3-fold upregulated (Tab. 1). Also in the AWF_{NaCl} the basic spot 5 contained at least 11 peptides belonging to the class III peroxidase family indicating a stronger induction compared with the AWF_{H₂O} extracted peroxidases. Increased apoplasmic Mn concentrations may, therefore, differentially affect specific peroxidase isoenzymes. In the literature the appearance and specific roles of acidic and basic peroxidases is discussed. Acidic peroxidases show high affinity to lignin precursors and H₂O₂ and, therefore, are proposed to be important for lignification and cell-wall functioning related to plant development, whereas basic peroxidases mostly utilize NADH as substrate leading to the formation of H₂O₂ (de Souza and MacAdam, 1998; Fecht-Christoffers et al., 2006; Klotz et al., 1998; MacAdam et al., 1992; Mäder et al., 1980; Mäder and Amberg-Fischer, 1982; Mäder et al., 1986; Polle et al., 1994; Ros Barcelo, 1997). The formation of the typical Mn toxicity symptoms in form of brown spots in cowpea is supposed to be related to a fast increased activity of the H₂O₂-producing NADH-peroxidase delivering the substrate for the H₂O₂-consuming guaiacol-POD activity (Fecht-Christoffers et al., 2007). Therefore, the proposed kinetics of the reaction scheme seems to be supported by the results since the abundance of the basic NADH-producing POD is increased already after 1 d of elevated Mn supply, whereas the guaiacol-POD abundance is increased only after two to three days of elevated Mn supply (Fecht-Christoffers et al., 2003b).

On the other hand evidence was provided (Chapter 2) that all tested peroxidase isoenzyme bands obtained from BN-PAGE separations were capable of performing both reaction cycles under optimum conditions *in vitro* indicating that all peroxidase isoenzymes are able to catalyze both reaction cycles also *in vivo*. This polyfunctionality of class III peroxidases has been well characterized (Passardi et al., 2004). However, this does not agree with Mäder et al. (1980) who concluded from their results that both reaction cycles are catalyzed by distinct PODs. This view might be supported by the extraction from the apoplast of specific acidic or

basic PODs with water and NaCl solution, respectively. However, it is currently difficult to draw a final picture for the involvement of specific peroxidase isoenzymes in the development of Mn toxicity.

All peptides which could be aligned to peroxidases (Fig. 5) have been qualitatively identified in protein spot 5 (Fig. 4) which was extracted with 0.25 M NaCl solution containing not only the water-soluble but also the ionically-bound apoplastic proteome. However, evidence is provided for at least four different overlapping peroxidase isoenzymes in this protein spot 5 encoded by an equal amount of distinct peroxidase genes (Fig. 5) confirming previous results (Chapters 2 and 3) which pointed to different binding properties of specific peroxidase isoenzymes as revealed by sequential extraction with AWF_{H_2O} and AWF_{NaCl} . However, the four distinct peroxidase isoenzymes did not differ in the isoelectric point (Fig. 4, Tab. 2) indicating that the displayed amino acid substitutions do not lead to dramatic molecule charge and, therefore, pI changes.

In conclusion, the results presented in this Chapter confirm that the applied AWF protein extraction-method is suitable for the investigation of Mn excess-induced early responses of the apoplastic proteome. However, the procedure for the isolation of strongly cell wall-bound proteins appeared to be unsuitable due to the comparatively high symplastic contamination of this protein fraction. The identification of Mn-induced basic POD isoenzyme in the AWF_{NaCl} fraction in addition to acidic POD isoenzymes in the AWF_{H_2O} further supports the proposed decisive role of H_2O_2 -producing and consuming PODs for the development of Mn toxicity (Fecht-Christoffers et al., 2007). Further proteins significantly affected by Mn treatment (PGIPs and α -galactosidases) suggest Mn excess-induced modification of cell-wall development and functions, whereas others (acetylcholinesterase and GDSL-lipase 1) indicate changes in broad-sense signal transduction processes.

General Discussion

Mn toxicity is a widely distributed plant disorder occurring on soils of the tropics and subtropics. Species and cultivars within species differ considerably in their ability to tolerate high Mn tissue contents. Even though several recent studies identified various transporters conferring Mn tolerance to plants through cell internal sequestration into the vacuole, the endoplasmatic reticulum, and also the Golgi apparatus (Peiter et al., 2007; Delhaize et al., 2003, 2007, Wu et al., 2002; Korenkov et al., 2007; Li et al., 2008), in cowpea the apoplast appears to be the decisive compartment for the development or avoidance of Mn toxicity (Fecht-Christoffers et al., 2003b, 2006). Fecht-Christoffers et al. (2007) proposed a reaction scheme leading to Mn toxicity starting with peroxidases and their two reaction cycles producing and consuming H₂O₂. These peroxidases have been shown to be modulated by Mn^{II} and phenolics *in vitro*. A role of H₂O₂ in generating oxidative stress but also as inducer of signal transduction pathways, e.g. Ca²⁺ signaling, triggering symplastic responses was suggested. The presented work provides an in-depth investigation of apoplastic peroxidase functionality with respect to Mn toxicity and additionally adds new insights into proteomic and metabolomic responses of the symplast to excess Mn. Here the most important results are summarized and discussed in an integrative way.

The role of different POD isoenzymes and their H₂O₂-producing NADH-peroxidase activity as modulated by pH and phenols

Considerable constitutive differences in the peroxidase isoenzyme pattern between both cultivars were found (Chapter 3). Moreover, particularly in the sensitive cultivar excess Mn increased the abundance of constitutively expressed peroxidases (Chapter 2). Both results underline the decisive role of peroxidases for the development or avoidance of Mn toxicity.

In the Mn-sensitive cultivar, IEF/SDS-PAGE technique yielded short-term Mn-induced peptides belonging to so-called basic peroxidases (Chapter 4). In contrast, Fecht-Christoffers et al. (2003b, 2006) showed increased abundance of acidic peroxidases after long-term Mn treatments. Acidic peroxidases are thought to have high affinity to lignin precursors and H₂O₂ and therefore appear to be involved in cell wall functioning, whereas basic peroxidases (Chapter 4) can use NADH as substrate and form H₂O₂ (de Souza and MacAdam, 1998; Fecht-Christoffers et al., 2006; Klotz et al., 1998; MacAdam et al., 1992; Mäder et al., 1980;

Mäder and Amberg-Fischer, 1982; Mäder et al., 1986; Polle et al., 1994; Ros Barcelo, 1997). Following the proposed reaction scheme of Fecht-Christoffers et al. (2007) the starting and, therefore, key reaction for the development of Mn toxicity is the H₂O₂-producing activity utilizing NADH, followed by the H₂O₂-consuming POD activity. The time course of POD activity induction seems to be proven by the proteomic approach after short-term (Chapter 4) and long-term Mn treatment (Fecht-Christoffers et al., 2003b).

However, the proposed diverse functions of acidic and basic peroxidases hold not completely true for cowpea since in-depth characterization of apoplastic peroxidase isoenzymes showed that all identified isoenzymes were able to perform both reaction cycles under optimum conditions *in vitro* (Chapter 2) contradicting results of Mäder et al. (1980) who proposed that both reaction cycles are catalyzed by distinct peroxidases. Indeed, class III peroxidases are now known to perform both cycles (Passardi et al., 2005). However, the studied peroxidases appeared to have different binding properties in the apoplast of cowpea as revealed by sequencing results (Fecht-Christoffers et al., 2003b, Chapters 2 and 4) which might be related to the pI rather than to their functionality.

The origin of the substrate NADH for the NADH-*peroxidase* activity in the apoplast is still a matter of debate. An apoplastic malate dehydrogenase has been proposed by some authors (Kärkönen et al., 2002; Gross et al., 1977; Shinkle et al., 1992; Otter and Polle, 1997). Unfortunately, the used method for the GC-MS-based metabolite profiling approach is not capable to determine NAD/NADH (Chapter 3). Therefore, the origin and role of apoplastic NADH needs further clarification.

Fecht-Christoffers et al. (2006) attributed a decisive effect to the Mn concentration and particularly to concentration and nature of phenols for the specific modulation/induction of NADH-*peroxidase* activity. This conclusion was based on *in-vitro* studies including crosswise combining of AWF proteins and AWF metabolites of two cowpea cultivars differing in Mn tolerance and HPLC analytical results showing quantitative and qualitative differences of phenols present in the apoplast of the cultivars differing in Mn tolerance. In-depth characterization of specific POD isoenzymes in combination with the characterization of the non-polar apoplastic fraction confirmed these results (Chapter 2 and 3): among several identified phenolic compounds mainly *p*-coumaric acid and ferulic acid showed not only Mn and Si-induced significant changes but also genotypical differences which could be related to their enhancing or inhibiting effect on NADH-*peroxidase* activity. The chosen metabolite profiling approach only allowed the quantification of treatment-dependent changes. Therefore, a final picture is difficult to draw.

The picture gets even more complex when organic acids are additionally taken into account (Chapter 3). The comparable great group of organic acids, particularly ascorbic acid, has been proposed to contribute to an antioxidative symplastic cell state. Tartaric and particularly malonic acid may be regarded as apoplastic scavengers of Mn^{III} , a reaction intermediate of the peroxidase-oxidase activity. Fecht-Christoffers et al. (2005) suggested an inhibitory effect of ascorbate on peroxidase activities and concluded from their results, that ascorbate contributes but not fully explains Mn tolerance. However, Mn^{III} /organic acids complexes have been shown to act themselves as strong oxidants, particularly in lignin degrading fungi utilizing Mn-dependent peroxidases (Podgornik et al., 2001).

The role of the different pH optima for both POD reaction cycles is difficult to interpret. It has been argued that the pH optimum differences are not sufficient to be decisive in regulating the relative contribution of each reaction cycle to Mn toxicity (Chapter 2). Moreover, differences between biotic and abiotic stress responses have been proposed: on the one hand the pH range covers the recommended pH range for the investigation of lignin formation processes (Kärkönen et al., 2002) on the other hand the hypersensitive response (HR) to pathogens in plants was associated with an alkalization of the apoplast (Bolwell et al., 1995, 1998, 2001; Pignocchi and Foyer, 2003). However, locally restricted more important pH changes particularly in the area of appearing brown spots could give further insights into the role of the pH in controlling apoplastic peroxidases.

Photosynthesis is impaired by Mn stress

A number of studies reported symplastic responses to excess Mn. Particularly an impaired photosynthesis and morphological alterations of the chloroplasts have been reported (González and Lynch, 1997, 1999; González et al., 1998; Lidon et al., 2004; Nable et al., 1988; Houtz et al., 1988; Moroni et al., 1991). Also in cowpea, as fast as one day after elevated Mn supply a reduced electron transport rate has been identified (Chapter 1). Moreover, state I to state II transitions of photosynthesis have been observed particularly in the Mn-sensitive cultivar (Chapter 1). This was attributed to a higher energy demand for plant stress responses. This is corroborated by metabolite profiling/metabolite screening studies (Chapter 3). The changes observed in the carbohydrate but particularly the amino acid metabolism indicate that the nitrogen assimilation is reduced in the Mn-sensitive cultivar. This appears to be most likely due to changed energy provision during state I to state II transitions of photosynthesis (Sherameti et al., 2002). Specific differences and changes in the

sugar pool additionally lead to the suggestion that a Mn stress-induced rebalancing of carbohydrates particularly in the Mn-sensitive cowpea cultivar could be the effect of an increased demand for C-skeletons most likely for defense responses (Chapter 3). The creation of subtractive cDNA libraries by means of suppression subtractive hybridization (SSH) technique (Diatchenko et al., 1996) from the Mn-sensitive genotype after short-term Mn treatment for one day may corroborate the proteomic and metabolomic changes in the photosynthetic apparatus and photosynthetic performance since a Mn excess-induced reduction in the number of transcripts involved in photosynthesis and general metabolism was found (Chapter 1).

Silicon-mediated Mn tolerance and genetically-based Mn tolerance

Comparative metabolite profiling studies including cowpea cultivars differing in Mn tolerance yielded several hints for important individual metabolites involved in Mn sensitivity, Si-induced Mn tolerance, and cultivar specific Mn tolerance (Chapter 3). Nevertheless, the non-supervised independent component analysis (ICA) allowed the investigation of variance-based sample clusters which are formed by treatment-induced qualitative and quantitative changes of metabolite pools. All applied experimental sources of variance (genotype, Mn treatment, Si treatment, infiltration solution) led to clear sample clusters for bulk-leaf and apoplastic metabolite extracts strongly indicating a high responsiveness of the metabolome (Chapters 2 and 3). ICAs performed individually not only for the sensitive but also for the tolerant cultivar led to Si clusters in Mn-control plants. This clearly shows that Si induces metabolomic changes in both cultivars. However, in both cultivars the Si clusters disappeared with ongoing Mn treatments. The comparable small effect of Si on the leaf metabolome of Mn-treated plants may explain that Si only delays but not prevents Mn toxicity. From this it has been concluded that Si-mediated alleviation of Mn toxicity is different from cultivar specific genetically preformed Mn tolerance.

The lack of Si clusters in apoplastic metabolome fractions appears to be contradictory to the suggestion that the apoplast is the decisive compartment for the development of Mn toxicity/tolerance. However, Si increased the abundance particularly of ferulic acid which has been shown to inhibit the activity of apoplastic NADH-*peroxidase* (Chapter 2 and 3). This is in agreement with results by Iwasaki et al. (2002b) who found a close relation between apoplastic peroxidase activities/Mn toxicity symptoms and soluble apoplastic Si in addition to

a decreasing effect of Si on the free apoplastic Mn concentration by stronger cell-wall binding (Iwasaki et al., 2002a, b; Rogalla and Römheld, 2002; Shi et al., 2005).

Early Mn toxicity responses in the apoplast suggest Mn-induced changes in signal perception/signal transduction and development

Using a modified infiltration / centrifugation technique to harvest water-soluble and ionically-bound apoplastic proteins after short-term Mn supply for only one day it was possible to identify proteins involved in the apoplastic Mn-stress response (Chapter 4). The role of the different peroxidases identified either with IEF/SDS-PAGE or BN-PAGE technique has been discussed earlier. A number of further Mn excess-induced apoplastically localized proteins have been identified: α -galactosidase and the polygalacturonase-inhibiting protein (PGIPs) may be regarded as part of developmental difference in the second-oldest trifoliate leaves of Mn-treated and non-treated plants, since both proteins are developmentally regulated (Mehli et al., 2004; Chrost et al., 2007; Protsenko et al., 2008) even though both also show responsiveness to various biotic and abiotic stresses (Bergmann et al., 1994; Pennycooke et al., 2003; Ferrari et al., 2006).

Also, at least two indications have been found for the triggering by Mn excess of early stress perception/induction of signal transduction processes. The identification of a Mn-enhanced formation of acetylcholinesterase is indicative of the triggering of signal-transduction processes (Brenner et al., 2006; Sagane et al., 2005) leading to defense responses in agreement with the first transcriptome analyses revealing an increased number of transcripts involved in signal transduction in the Mn-sensitive cultivar compared with the Mn-tolerant cultivar (Chapter 1). Unfortunately, we were not able yet to identify also transcripts for acetylcholinesterase. The second protein in the broadest sense involved in signal perception/signal transduction processes is the GDSL-lipase 1, which is known to be involved in plant development, morphogenesis, synthesis of secondary metabolites and/or defense responses and also plays a role in systemic acquired resistance (SAR) (Ling et al., 2006; Kim et al., 2008).

The proteomic findings may also be corroborated by cDNA libraries using SSH technique made from the Mn-sensitive cultivar after 3 d of Mn treatments (Chapter 1). Some of the Mn-induced transcripts that have been identified encoded for PR proteins. Sequence comparison of the translated cDNA and and proteomic results of Fecht-Christoffers et al. (2003b) showed

that these PR proteins have been previously identified in the same cultivar in in-depth proteomic studies of apoplastic responses to long-termed excess Mn.

Combining proteomic and metabolomic data to unravel a sequence of events leading to Mn toxicity, genotypic and Si-mediated Mn tolerance

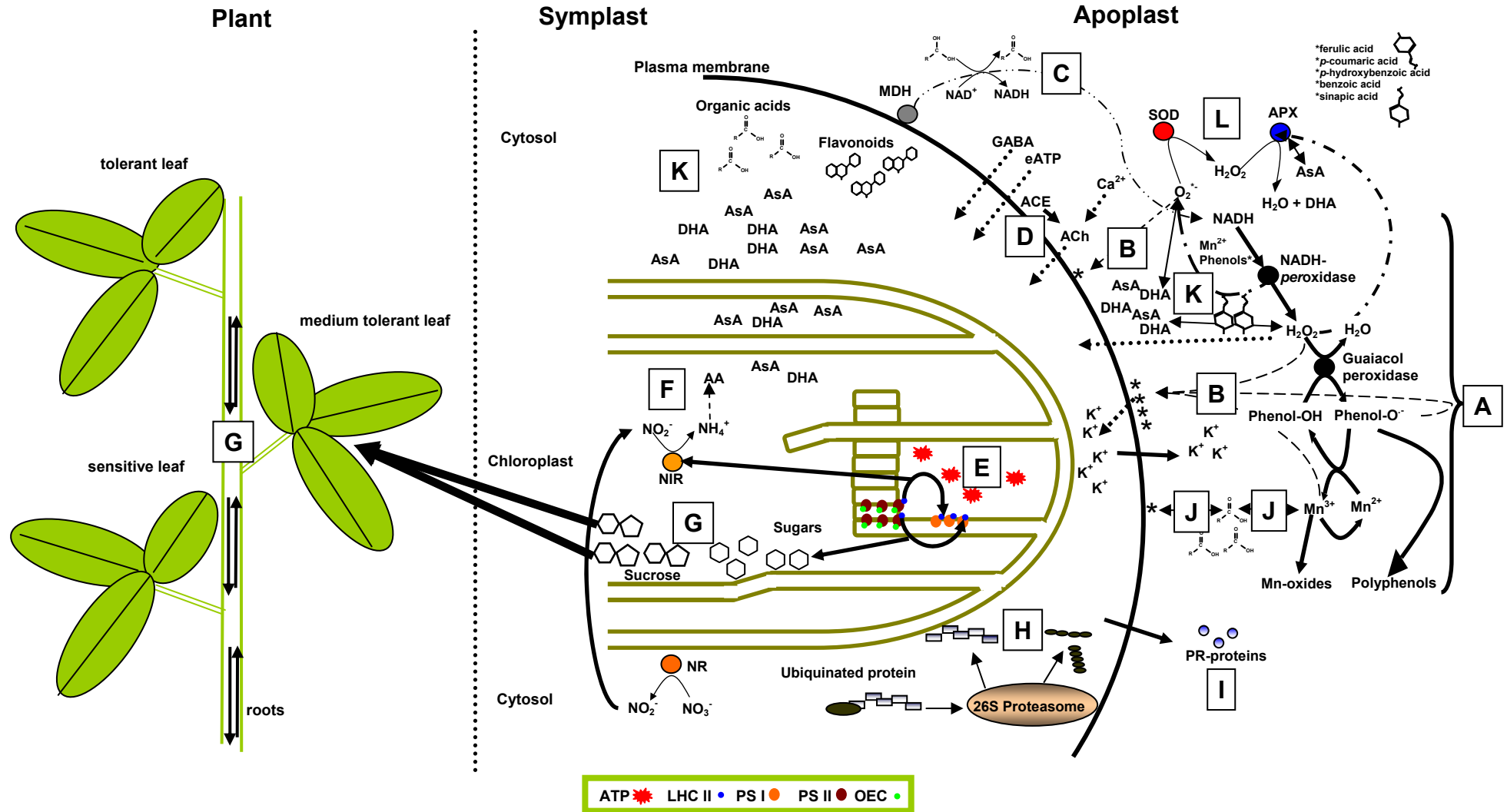
Taking together the results from metabolomic (Chapters 2 and 3) and proteomic (Chapters 1-4) analyses, these results show a sequence of events starting with signal perception/signal transduction followed by a broad range long-term Mn toxicity response on transcriptomic, proteomic and metabolomic level. Affected are several pathways including photosynthesis, phenol, sugar, and organic acid metabolism.

A picture summarizing the proposed reaction scheme leading to Mn toxicity and/or tolerance is given below (Fig. 1):

During the development of Mn toxicity at least four distinct apoplastic class III peroxidases are able to perform both the H₂O₂-peroxide-consuming guaiacol-peroxidase activity and the H₂O₂-producing NADH-*peroxidase* activity (A). The latter is regarded as starting reaction and requires Mn²⁺ and a specific activity-modulating phenol composition (indicated by *p*-coumaric acid, ferulic acid, benzoic acid, *p*-hydroxybenzoic acid, sinapic acid in the scheme) as cofactors. Formed H₂O₂ is then either consumed by the guaiacol-peroxidase activity or acts as signal transduction molecule. Reducing H₂O₂ to H₂O by guaiacol-peroxidase activity may lead to the formation of phenoxyradicals which themselves spontaneously polymerize in the cell walls and form part of the brown spots. Phenoxyradicals may also be re-reduced by Mn²⁺, which itself is oxidized to Mn^{III}. Mn^{III} is instable and disproportionates to Mn^{II} which re-enters the whole reaction cycle, or to Mn^{IV} which immediately formes Mn^{IV}-oxide as part of the brown spots. Four reaction intermediates of both peroxidase cycles may cause lipid peroxidation and increased K⁺ efflux: the reactive oxygen species H₂O₂ and superoxide (O₂^{*-}), phenoxyradicals and Mn³⁺ (B). NADH as putative substrate for NADH-*peroxidase* activity may be provided by an apoplastic malate dehydrogenase (C). Signal transduction processes may also be induced by GABA, eATP and/or an apoplastic acetylcholinesterase (ACE) which itself is modulated by changed calcium signals (D). Either increased symplastic, e.g. chloroplastidic, Mn contents or Mn-induced signal transduction processes lead then to strong modifications in the chloroplast (E). State I to state II transitions of photosynthesis resulting in higher ATP production by cyclic electron transport lead to a redistribution of energy in order to satisfy changed energy demands for a Mn-stress response. Impaired electron

transport-rates could also reflect Mn-sensitivity most likely induced by modifications/alterations of the oxygen evolving complex of PS II. Cyclic electron transport induced by state transitions on the other hand will reduce the availability of reduced ferredoxin for the nitrite reduction step following nitrate reduction in the nitrate assimilation pathway explaining reduced synthesis of amino acids through NH_4^+ assimilation (F). Moreover, state transitions lowering the linear electron flow may also lead to reduced carbon fixation and thus reduced monosugar contents in Mn-stressed plants particularly in the sensitive cultivar (G) and reduced availability of C-skeltons for the assimilation/detoxification of NH_4^+ (E, F). This could explain the reported higher Mn tolerance of NO_3^- -fed compared with NH_4^+ -fed plants. Lower sugar contents in the sensitive cultivar may also reflect an increased demand for sugar/energy for the Mn stress response. Sucrose as transport form of sugars within a plant then may point to a redistribution of sugar/energy within the whole plant (G). Advanced Mn stress leads to protein degradation by the ubiquitin-proteasome pathway (H) and secretion of stress and pathogenesis-related proteins into the apoplast (I).

Mn sensitivity, Si-mediated enhanced Mn tolerance or genetic Mn tolerance may also partially base not only on the symplastic but also the apoplastic composition and concentration of specific metabolites and proteins. Organic acids can act as apoplastic chelators of Mn^{3+} (J). Symplastic and apoplastic organic acids, phenylpropanoids / flavonoids, ascorbic acid (AsA) and its oxidized form dehydroascorbic acid (DHA) can act as scavengers of Reactive Oxygen Species (ROS) (K) thus increasing/explaining Si-enhanced and/or genotypic Mn tolerance. On the other hand particularly the Mn-chelates with organic acids may act as oxidants accelerating Mn toxicity development (J). In addition, a higher abundance of particularly two apoplastic redox level-modulating enzymes may partially explain genotypic Mn tolerance, a superoxide dismutase and (SOD) and ascorbate peroxidase (APX) (L). Apoplastic SODs may detoxify superoxide radicals formed by the NADH-peroxidase activity. APXs may reduce H_2O_2 either from the superoxide dismutase or from the NADH-peroxidase activity. Both enzymes thus may remove/reduce oxidants, putative signalling molecules, and essential reaction intermediates of the peroxidase-oxidase cycle of peroxidases leading to higher Mn tolerance.



Scheme description is given in the text, for legend see next page.

Fig. 1A. Integrated view of the involvement of the different leaf cell compartments in Mn toxicity/tolerance development. * indicates lipid peroxidation, AA amino acids, ACE acetylcholinesterase, Ach, acetylcholine, AsA ascorbic acid, APX ascorbate peroxidase, DHA dehydroascorbic acid, (e)ATP (extracellular) adenosine triphosphate, GABA γ -aminobutyric acid, LHCII light harvesting complex II, MDH malate dehydrogenase, NR nitrate reductase, NIR nitrite reductase, OEC oxygen-evolving complex, PR proteins pathogenesis-related proteins, PS I photosystem I, PS II photosystem II, SOD superoxide dismutase.

Outlook

The apoplast

One part of the present work further characterized apoplastic peroxidase isoenzymes, particularly the H₂O₂-producing NADH-*peroxidase* activity, with respect to pH optima and response to phenols. Unfortunately, the chosen method of metabolite profiling was only able to identify but not quantify metabolites so that no information currently exists on the specific qualitative and quantitative distribution of particularly phenols in the leaf apoplast of cowpea cultivars differing in Mn tolerance. Methods including HPLC measurements for the identification and quantification of phenols could substantially contribute to our knowledge, e.g. together with in depth characterization of substrate specificity also of the H₂O₂-consuming guaiacol-*peroxidase* activity of peroxidase isoenzymes. Not only phenols but also organic acids have been discussed in this study as scavengers of Mn species and should be included in future apoplastic metabolome characterization experiments. Moreover, other apoplastic redox-regulating enzymes were shown to be constitutively different between the genotypes which should be additionally subject of further comparative investigations.

IEF/SDS-PAGE of apoplastic proteins in the sensitive cultivar after short-term Mn supply led to the identification of a basic peroxidase, whereas previous studies identified acidic peroxidases after long-term Mn supply. Considering the proposed distinct roles of basic and acidic peroxidases in plant defence and cell-wall modification, respectively, a time course of the expression of the most likely peroxidase genes leading to enhanced synthesis of specific isoenzymes appears to be necessary for which the clarification of full length cDNAs of peroxidases involved in Mn toxicity development is indispensable.

In addition to peroxidases several apoplastic proteins involved in signal transduction processes have been found as early as one day after elevated Mn supply in the Mn-sensitive cultivar TVu 91 indicating that these are the first events leading to Mn toxicity. Expression analyses of these genes would be of high interest, too, particularly in a comparative study with the Mn-tolerant cultivar TVu 1987 and Si-treated plants.

The symplast

Another focus of this work were Mn and Si-mediated symplastic proteomic, metabolomic and partially also transcriptomic changes after comparable long-term Mn treatment of both cowpea cultivars.

Proteomic but also the transcriptomic studies mostly pointed to the chloroplast as mainly affected leaf cell-compartment after long-term Mn supply in the Mn-sensitive cultivar. This was further confirmed by state transitions, reduced electron transport rates and down-regulation of proteins involved in the provision of physiologically active RubisCO. Therefore, physiological studies related to photosynthesis including CO₂ assimilation rates at limited, optimal, and supra optimal CO₂ supply, 77k fluorescence, ATP production, development of Mn toxicity under PS I or PS II light or with specific state transition-inducing inhibitors etc. should be carried out in order to further clarify the effect of excess Mn on photosynthesis.

At a first glance, the comparative metabolomic studies revealed the sugar metabolism and nitrogen assimilation pathways to be affected in both cultivars most likely based on the Mn-induced changes in photosynthesis. Quantification of the different sugar and amino acid pools as well as characterization of key genes of the primary sugar and amino acid/nitrogen assimilation metabolism in time course experiments could give further insights into mechanisms leading either to Mn toxicity or Mn tolerance.

Also, it has been shown, that the amount of stable bound Mn in the chloroplasts remained unchanged by elevated Mn supply. In depth analyses especially of the labile bound apoplasmic Mn fraction that was most probably removed by EDTA in our chloroplast isolation experiments should follow, too.

Different mechanisms of Mn tolerance

Previous studies as well as this study showed differences in Mn tolerance between different leaf ages, Si treatments and genotypes. Moreover, this study provided evidence for different mechanisms underlying the Si-mediated and genetically-based Mn tolerance. In depth transcriptomic, proteomic and metabolomic analyses taking all three tolerance factors into account is necessary in order to clarify tolerance mechanisms. One starting point could be the ascorbic acid metabolism even though it has previously been shown to not decisively contribute to Mn tolerance. In depth investigations of the cellular Mn compartmentation most likely via identification of metal transporters that are known to confer Mn tolerance may be of great importance as well.

References

- Aaby K, Hvattum E, Skrede G.** 2004. Analysis of flavonoids and other phenolic compounds using High-Performance Liquid Chromatography with coulometric array detection: relationship to antioxidant activity. *Journal of Agricultural and Food Chemistry* **52**, 4595-4603.
- Bergmann CW, Ito Y, Singer D, Albersheim P, Darvill AG.** 1994. Polygalacturonase-inhibiting protein accumulates in *Phaseolus vulgaris* L. in response to wounding, elicitors and fungal infection. *The Plant Journal* **5**, 625-634.
- Bolwell GP, Butt VS, Davies DR, Zimmerlin A.** 1995. The origin of the oxidative burst in plants. *Free Radical Research* **23**, 517-532.
- Bolwell GP, Davies DR, Gerrish C, Auh C-K, Murphy TM.** 1998. Comparative biochemistry of the Oxidative Burst produced by rose and French Bean cells reveals two distinct mechanisms. *Plant Physiology* **116**, 1379-1385.
- Bolwell GP, Page A, Piślewska M, Wojtaszek.** 2001. Pathogenic infection and the oxidative defences in plant apoplast. *Protoplasma* **217**, 20-32.
- Borderies G, Jamet E, Lafitte C, Rossignol M, Jauneau A, Boudart G, Monsarrat B, Esquerré-Tugayé M-T, Boudet A, Pont-Lezica R.** 2003. Proteomics of loosely bound cell wall proteins of *Arabidopsis thaliana* cell suspension cultures: A critical analysis. *Electrophoresis* **24**, 3421-3432.
- Boston RS, Viitanen PV, Vierling E.** 1996. Molecular chaperones and protein folding in plants. *Plant Molecular Biology* **32**, 191-222.
- Bouché N, Fromm H.** 2004. GABA in plants: just a metabolite? *Trends in Plant Science* **9**, 110-115.
- Bradford MM.** 1976. A rapid and sensitive method for quantitation of microgram quantities of protein utilizing the principle of protein-dye binding. *Analytical Biochemistry* **72**, 248-254.
- Brenner ED, Stahlberg R, Mancuso S, Vivanco J, Balůška F, Van Volkenburgh E.** 2006. Plant neurobiology: an integrated view of plant signalling. *Trends in Plant Science* **11**, 413-419.
- Broeckling CD, Huhman DV, Farag MA, Smith JT, May GD, Mendes P, Dixon RA, Summer LW.** 2005. Metabolic profiling of *Medicago truncatula* cell cultures reveals the effects of biotic and abiotic elicitors on metabolism. *Journal of Experimental Botany* **56**, 323-336.

- Burnell, JN.** 1988. The biochemistry of manganese in plants. In MJ Webb, RO Nable, RD Graham, RJ Hannam, eds, *Manganese in Soil and Plants*, Kluwer Academic Publishers, Dordrecht/Boston/London, pp 125-137.
- Castro AJ, Carapito C, Zorn N, Magne C, Leize E, Van Dorsselaer A, Clement C.** 2005. Proteomic analysis of grapevine (*Vitis vinifera* L.) tissues subjected to herbicide stress. *Journal of Experimental Botany* **56**, 2783-95.
- Chivasa S, Simon WJ, Yu X-L, Yalpani N, Slabas AR.** 2005. Pathogen elicitor-induced changes in the maize extracellular matrix proteome. *Proteomics* **5**, 4894-4904.
- Chivasa S, Hamilton JM, Pringle RS, Ndimba BK, Simon WJ, Lindsey K, Slabas AR.** 2006. Proteomic analysis of differentially expressed proteins in fungal elicitor-treated *Arabidopsis* cell cultures. *Journal of Experimental Botany* **57**, 1553-1562.
- Chrost B, Kolukisaoglu U, Schulz B, Krupinska K.** 2007. An α -galactosidase with an essential function during leaf development. *Planta* **225**, 311-320.
- Dahan J, Etienne P, Petitot A-S, Houot V, Blein J-P, Suty L.** 2001. Cryptogein affects expression of $\alpha 3$, $\alpha 6$ and $\beta 1$ 20S proteasome subunits encoding genes in tobacco. *Journal of Experimental Botany* **52**, 1947-1948.
- Delannoy E, Jalloul A, Assigbetsé K, Marmey P, Geiger JP, Lherminier J, Daniel JF, Martinez C, Nicole M.** 2003. Activity of class III peroxidases in the defense of cotton to bacterial blight. *Molecular Plant-Microbe Interactions* **16**, 1030-1038.
- Delhaize E, Kataoka T, Hebb DM, White RG, Ryan P.** 2003. Genes encoding proteins of the Cation Diffusion Facilitator family that confer manganese tolerance. *The Plant Cell* **15**, 1131-1142.
- Delhaize E, Gruber BD, Pittman JK, White RG, Leung H, Miao Y, Jiang L, Ryan PR, Richardson AE.** 2007. A role for the AtMTP11 gene of *Arabidopsis* in manganese transport and tolerance. *The Plant Journal* **51**, 198-210.
- de Souza IRP, MacAdam JW.** 1998. A transient increase in apoplastic peroxidase activity precedes decrease in elongation rate of B73 maize (*Zea mays*) leaf blades. *Physiologia Plantarum* **104**, 556-562.
- Diatchenko L, Lau YF, Campbell AP, Chenchik A, Moqadam F, Huang B, Lukyanov S, Lukyanov K, Gurskaya N, Sverdlov ED, Siebert PD.** 1996. Suppression subtractive hybridization: a method for generating differentially regulated or tissue-specific cDNA probes and libraries. *Proceedings of the National Academy of Sciences of the United States of America* **93**, 6025-6030.
- Dixon RA, Paiva NL.** 2005. Stress-induced phenylpropanoid metabolism. *The Plant Cell* **7**, 1085-1097.

- Duroux L, Welinder KG.** 2003 The peroxidase gene family in plants: A phylogenetic overview. *Journal of Molecular Evolution* **57**, 397-407.
- Ehlers JD, Hall AE.** 1997. Cowpea (*Vigna unguiculata* L. Walp.). *Field Crops Research* **53**, 187-204.
- Elias JE and Gygi SP.** 2007. Target-decoy search strategy for increased confidence in large-scale protein identifications by mass spectrometry. *Nature methods* **4**, 207-214.
- El-Jaoual T, Cox DA.** 1998. Manganese toxicity in plants. *Journal of Plant Nutrition* **21**, 353-386.
- Epstein E.** 1999. Silicon. *Annual Review of Plant Physiology Plant Molecular Biology* **50**, 641-664.
- Fauteux F, Rémus-Borel W, Menzies JG, Bélanger RR.** 2005. Silicon and plant disease resistance against pathogenic fungi. *FEMS Microbiology Letters* **249**, 1-6.
- Fauteux F, Chain F, Belzile F, Menzies JG, Bélanger RR.** 2006. The protective role of silicon in the Arabidopsis-powdery mildew pathosystem. *Proceedings of the National Academy of Sciences* **103**, 17554-17559
- Fecht-Christoffers MM, Maier P, Horst WJ.** 2003a. Apoplastic peroxidase and ascorbate are involved in manganese toxicity and tolerance of *Vigna unguiculata*. *Physiologia Plantarum* **117**, 237-244.
- Fecht-Christoffers MM, Braun H-P, Lemaitre-Guillier C, VanDorsselaer A, Horst WJ.** 2003b. Effect of Manganese toxicity on the proteome of the leaf apoplast in cowpea. *Plant Physiology* **133**, 1935-1946.
- Fecht-Christoffers MM.** 2004. Manganese toxicity and tolerance in cowpea (*Vigna unguiculata* L.) – The role of the leaf apoplast. IV. Early events in the leaf apoplast of cowpea (*Vigna unguiculata*) induced by Mn excess. *PhD thesis*, University of Hannover, Germany, 107-122.
- Fecht-Christoffers MM, Horst WJ.** 2005. Does apoplastic ascorbic acid enhance manganese tolerance of *Vigna unguiculata* and *Phaseolus vulgaris*? *Journal of Plant Nutrition and Soil Science* **168**, 590-599.
- Fecht-Christoffers MM, Führs H, Braun H-P, Horst WJ.** 2006. The role of hydrogen peroxide-producing and hydrogen peroxide-consuming peroxidases in the leaf apoplast of cowpea in manganese tolerance. *Plant Physiology* **140**, 1451-1463.
- Fecht-Christoffers MM, Maier P, Iwasaki K, Braun H-P, Horst WJ.** 2007. The role of the leaf apoplast in manganese toxicity and tolerance in cowpea (*Vigna unguiculata* L., Walp). In B Sattelmacher and WJ Horst, eds, *The apoplast of higher plants:*

- compartment of storage, transport, and reactions*. Springer, Dordrecht, The Netherlands, pp 307-322.
- Feiz L, Irshad M, Pont-Lezica RF, Canut H, Jamet E.** 2006. Evaluation of cell wall preparations for proteomics: a new procedure for purifying cell walls from *Arabidopsis* hypocotyls. *Plant Methods* **2**, 10 (doi:10.1186/1746-4811-2-10).
- Ferrari S, Galletti R, Vairo D, Cervone F, De Lorenzo G.** 2006. Antisense expression of the *Arabidopsis thaliana* *AtPGIP1* gene reduces polygalacturonase-inhibiting protein accumulation and enhances susceptibility to *Botrytis cinerea*. *Molecular Plant-Microbe Interaction* **8**, 931-936.
- Fiehn O, Kopka J, Trethewey RN, Willmitzer L.** 2000. Identification of uncommon plant metabolites based on calculation of elemental compositions using gas chromatography and quadrupole mass spectrometry. *Analytical Chemistry* **72**, 3573-3580.
- Finazzi G, Rappaport F, Furia A, Fleischmann M, Rochaix JD, Zito F, Forti G.** 2002. Involvement of state transitions in the switch between linear and cyclic electron flow in *Chlamydomonas reinhardtii*. *EMBO Reports* **3**, 280-285.
- Foy DC, Chaney RL, White MC.** 1978. The physiology of metal toxicity in plants. *Annual Review of Plant Physiology* **29**, 511-566.
- Franken P, Gnädinger F.** 1994. Analysis of parsley arbuscular endomycorrhiza: infection development and mRNA levels of defense-related genes. *Molecular Plant-Microbe Interactions* **7**, 612-620.
- Fry SC.** 1988. *The growing plant cell wall: chemical and metabolic analysis*. New York, Longman Scientific and Technical, UK.
- Galston AW, Sawhney RK.** 1990. Polyamines in Plant Physiology. *Plant Physiology* **94**, 406-410.
- Gazzarrini S, Lejay L, Gojon A, Ninnemann O, Frommer WB, von Wirén N.** 1999. Three functional transporters for constitutive, diurnally regulated, and starvation-induced uptake of ammonium into *Arabidopsis* roots. *The Plant Cell* **11**, 937-947.
- González A, Lynch JP.** 1997. Effects of manganese toxicity on leaf CO₂ assimilation of contrasting common bean genotypes. *Physiologia Plantarum* **101**, 872-880.
- González A, Steffen KL, Lynch JP.** 1998. Light and excess manganese: Implications for oxidative stress in common bean. *Plant Physiology* **118**, 493-504.
- González A, Lynch JP.** 1999. Subcellular and tissue Mn compartmentation in bean leaves under Mn toxicity stress. *Australian Journal of Plant Physiology* **26**, 811-822.
- Gross GG.** 1977. Cell wall-bound malate dehydrogenase from horseradish. *Phytochemistry* **16**, 319-321

- Gross GG, Janse C, Elstner EF.** 1977. Involvement of malate, monophenols, and superoxide radical in hydrogen peroxide formation by isolated cell walls from horseradish (*Armoracia lapathifolia* Gilib.). *Planta* **136**, 271-276.
- Haldrup A, Jensen PE, Lunde C, Scheller HV.** 2001. Balance of power: a view of the mechanism of photosynthetic state transitions. *Trends Plant Science* **6**, 301-305.
- Halliwell B.** 1978. Lignin synthesis: the generation of hydrogen peroxide and superoxide by horseradish peroxidase and its stimulation by manganese (II) and phenols. *Planta* **140**, 81-88.
- Hauser MJB, Olsen LF.** 1998. The role of naturally occurring phenols in inducing oscillations in the peroxidase-oxidase reaction. *Biochemistry* **37**, 2458-2469.
- Heenan DP, Carter OG.** 1975. Response of two soya bean cultivars to manganese toxicity as affected by pH and calcium levels. *Australian Journal of Agricultural Research* **26**, 967-974.
- Heenan DP, Carter OG.** 1977. Influence of temperature on the expression of manganese toxicity by two soybean varieties. *Plant and Soil* **47**, 219-227.
- Heinemeyer J, Eubel H, Wehmhöner D, Jänsch L, Braun HP.** 2004. Proteomic approach to characterize the supramolecular organization of photosystems in higher plants. *Phytochemistry* **65**, 1683-1692.
- Heinemeyer J, Lewejohann D, Braun HP.** 2007. Blue-native gel electrophoresis for the characterization of protein complexes in plants. *Methods in Molecular Biology* **335**, 343-352.
- Hiraga S, Sasaki K, Ito H, Ohashi Y, Matsui H.** 2001. A large family of class III plant peroxidases. *Plant Cell Physiology* **42**, 462-468.
- Hirschi KD, Korenkov VD, Wilganowski NL, Wagner GJ.** 2000. Expression of *Arabidopsis* CAX2 in tobacco. Altered metal accumulation and increased manganese tolerance. *Plant Physiology* **124**, 125-133.
- Hoffmann L, Maury S, Martz F, Geoffroy P, Legrand M.** 2003. Purification, cloning, and properties of an acyltransferase controlling shikimate and quinate ester intermediates in phenylpropanoid metabolism. *The Journal of Biological Chemistry* **1**, 95-103.
- Hoffmann L, Besseau S, Geoffroy P, Ritzenthaler C, Meyer D, Lapierre C, Pollet B, Legrand M.** 2004. Silencing of hydroxycinnamoyl-coenzyme A shikimate / quinate hydroxycinnamoyltransferase affects phenylpropanoid biosynthesis. *The Plant Cell* **16**, 1446-1465.

- Horiguchi T.** 1988. Mechanism of manganese toxicity and tolerance of plants. IV. Effects of silicon on alleviation of manganese toxicity of rice plants. *Soil Science and Plant Nutrition* **34**, 65-73.
- Horst WJ, Marschner H.** 1978a. Effect of silicon on manganese tolerance of bean plants (*Phaseolus vulgaris* L.). *Plant and Soil* **50**, 287-303.
- Horst WJ, Marschner H.** 1978b. Symptome von Manganüberschuss bei Bohnen (*Phaseolus vulgaris* L.) *Zeitschrift für Pflanzenernährung und Bodenkunde* **141**, 129-142.
- Horst WJ.** 1980. Genotypische Unterschiede in der Mangan-Toleranz von Cowpea (*Vigna unguiculata*). *Angewandte Botanik* **54**, 377-392.
- Horst WJ.** 1982. Quick screening of cowpeas genotypes for manganese tolerance during vegetative and reproductive growth. *Zeitschrift für Pflanzenernährung und Bodenkunde* **145**, 423-435.
- Horst WJ.** 1983. Factors responsible for genotypic manganese tolerance in cowpea (*Vigna unguiculata*). *Plant and Soil* **72**, 213-218.
- Horst WJ.** 1988. The physiology of Mn toxicity. In MJ Webb, RO Nable, RD Graham, RJ Hannam, eds, *Manganese in Soil and Plants*, Kluwer Academic Publishers, Dordrecht/Boston/London, 175-188.
- Horst WJ, Fecht M, Naumann, A Wissemeier, AH, Maier P.** 1999. Physiology of manganese toxicity and tolerance in *Vigna unguiculata* (L.) Walp. *Journal of Plant Nutrition and Soil Science* **162**, 263-274.
- Houtz RL, Nable RO, Cheniae GM.** 1988. Evidence for effects on the *in vivo* activity of ribulose-bisphosphate carboxylase/oxygenase during development of Mn toxicity in tobacco. *Plant Physiology* **86**, 1143-1149.
- Ifuku K, Yamamoto Y, Ono TA, Ishihara S, Sato F.** 2005. PsbP protein, but not PsbQ protein, is essential for the regulation and stabilization of photosystem II in higher plants. *Plant Physiology* **139**, 1175-1184.
- Iwasaki K, Matsumura A.** 1999. Effect of silicon on alleviation of manganese toxicity in pumpkin (*Cucurbita moschata* Duch cv. Shintosa). *Soil Science and Plant Nutrition* **45**, 909-920.
- Iwasaki K, Maier P, Fecht M, Horst WJ.** 2002a. Effects of silicon supply on apoplastic manganese concentrations in leaves and their relation to manganese tolerance in cowpea (*Vigna unguiculata* (L.) Walp.). *Plant and Soil* **238**, 281-288.
- Iwasaki K, Maier P, Fecht M, Horst WJ.** 2002b. Leaf apoplastic silicon enhances manganese tolerance of cowpea (*Vigna unguiculata*). *Journal of Plant Physiology* **159**, 167-173.

- Jamet E, Canut H, Boudart G, Pont-Lezica RF.** 2006. Cell wall proteins: a new insight through proteomics. *Trends in Plant Science* **11**, 33-39.
- Jänsch L, Kruff V, Schmitz UK, Braun HP.** 1996. New insights into the composition, molecular mass and stoichiometry of the protein complexes of plant mitochondria. *The Plant Journal* **9**, 357-368.
- Jeter CR, Tang W, Henaff E, Butterfield T, Roux SJ.** 2004. Evidence of a novel signalling role for extracellular adenosine triphosphates and diphosphates in *Arabidopsis*. *The Plant Cell* **16**, 2652-2664.
- Jordan DB, Ogren WL.** 1981. A sensitive assay procedure for simultaneous determination of Ribulose-1,5-bisphosphate carboxylase and oxygenase activities. *Plant Physiology* **67**, 237-245.
- Kärkönen A, Koutaniemi S, Mustonen M, Syrjänen K, Brunow G, Kilpeläinen I, Teeri TH, Simola LK.** 2002. Lignification related enzymes in *Picea abies* suspension cultures. *Physiologia Plantarum* **114**, 343-353.
- Keren N, Kidd MJ, Penner-Hahn JE, Pakrasi HB.** 2002. A light-dependent mechanism for massive accumulation of manganese in the photosynthetic bacterium *Synechocystis* sp. PCC 6803. *Biochemistry* **41**, 15085-15092.
- Kim K-J, Lim JH, Kim MJ, Kim T, Chung HM, Paek K-H.** 2008. *GDSL-lipase1 (CaGL1)* contributes to wound stress resistance by modulation of a *CaPR-4* expression in hot pepper. *Biochemical and Biophysical Research Communications* **374**, 693-698.
- Klotz KL, Liu T-TY, Liu L, Lagrimini LM.** 1998. Expression of the tobacco anionic peroxidase gene is tissue-specific and developmentally regulated. *Plant Molecular Biology* **36**, 509-520.
- Kopka J, Schauer N, Krueger S, Birkemeyer C, Usadel B, Bergmueller E, Doermann P, Weckwerth W, Gibon Y, Stitt M, Willmitzer L, Fernie AR, Steinhauser D.** 2005. GMD@CSB.DB: the Golm Metabolome Database. *Bioinformatics* **21**, 1635-1638.
- Korenkov V, Hirschi K, Crutchfield JD, Wagner GJ.** 2007. Enhancing tonoplast Cd/H antiport activity increases Cd, Zn, and Mn tolerance, and impacts root/shoot Cd partitioning in *Nicotiana tabacum* L. *Planta* **226**, 1379-1387.
- Kwon H-K, Yokoyama R, Nishitani K.** 2005. A proteomic approach to apoplastic proteins involved in cell wall regeneration in protoplasts of *Arabidopsis* suspension-cultured cells. *Plant and Cell Physiology* **46**, 843-857.
- Less H, Galili G.** 2008. Principal transcriptional programs regulating plant amino acid in response to abiotic stresses. *Plant Physiology* **147**, 316-330.

- Li X, Chanroj S, Wu Z, Romanowsky SM, Harper JF, Sze H.** 2008. A distinct endosomal $\text{Ca}^{2+}/\text{Mn}^{2+}$ pump affects root growth through the secretory process. *Plant Physiology* **147**, 1675-1689.
- Liang Y, Sun W, Zhu Y-G, Christie P.** 2007. Mechanisms of silicon-mediated alleviation of abiotic stresses in higher plants: a review. *Environmental Pollution* **147**, 422-428.
- Lidon FC, Barreiro MG, Ramalho JC.** 2004. Manganese accumulation in rice: implications for photosynthetic functioning. *Journal of Plant Physiology* **161**, 1235-1244.
- Ling H, Zhao J, Zuo K, Qiu C, Yao H, Qin J, Sun X, Tang K.** 2006. Isolation and expression analysis of a GDSL-like lipase gene from *Brassica napus* L. *Journal of Biochemistry and Molecular Biology* **39**, 297-303.
- Loewus FA.** 1999. Biosynthesis and metabolism of ascorbic acid in plants and of analogs of ascorbic acid in fungi. *Phytochemistry* **52**, 193-210.
- Lohaus, G, Pennewiss K, Sattelmacher B, Hussmann M, Muehling KH.** 2001. Is the infiltration-centrifugation technique appropriate for the isolation of apoplastic fluid? A critical evaluation with different plant species. *Physiologia Plantarum* **111**, 457-465.
- Luedemann A, Strassburg K, Erban A, Kopka J.** 2008. TagFinder for the quantitative analysis of gas chromatography - mass spectrometry (GC-MS) based metabolite profiling experiments. *Bioinformatics* **24**, 732 -737.
- MacAdam JW, Nelson CJ, Sharp RE.** 1992. Peroxidase activity in the leaf elongation zone of tall fescue. *Plant Physiology* **99**, 872-878.
- Macfie SM, Taylor GJ.** 1992. The effect of excess manganese on photosynthetic rate and concentration of chlorophyll in *Triticum aestivum* grown in solution culture. *Plant Physiology* **85**, 467-475.
- Maier P.** 1997. Bedeutung der Kompartimentierung von Mangan und organischen Säuren für die Mangantoleranz von Cowpea (*Vigna unguiculata* (L.) Walp.). PhD thesis. University of Hannover, Hannover, Germany
- Maksimović JD, Bogdanović J, Maksimović V, Nikolic M.** 2007. Silicon modulates the metabolism and utilization of phenolic compounds in cucumber (*Cucumis sativus* L.) grown at excess manganese. *Journal of Plant Nutrition and Soil Science* **170**, 739-744.
- Marschner H.** 1995. *Mineral Nutrition in Higher Plants*, Ed 2 Academic Press, London, UK.
- Mäder M., Ungemach J., Schloß P.** 1980. The role of peroxidase isoenzyme groups of *Nicotiana tabacum* in hydrogen peroxide formation. *Planta* **147**, 467-470.
- Mäder M, Amberg-Fischer V.** 1982. Role of peroxidase in lignification of tobacco cells. I. Oxidation of nicotinamide adenine dinucleotide and formation of hydrogen peroxide by cell wall peroxidases. *Plant Physiology* **70**, 1128-1131.

- Mäder M, Nessel A, Schloss P.** 1986. Cell compartmentation and specific roles of isoenzymes. In H Greppin, C Penel, T Gaspar, eds, *Molecular and physiological Aspects of Plant Peroxidases*, University of Geneva, Geneva, 247-260.
- Mehli L, Schaart JG, Kjellsen TD, Tran DH, Salentijn EMJ, Schouten HJ, Iversen T-H.** 2004. A gene encoding a polygalacturonase-inhibiting protein (PGIP) shows developmental regulation and pathogen-induced expression in strawberry. *New Phytologist* **163**, 99-110.
- Mihr C, Braun HP.** 2003. Proteomics in Plant Biology. In Handbook of Proteomics, M Conn, ed, Humana Press, Totowa, USA, pp 409-416.
- Mittler R, Vanderauwera S, Gollery M, Van Breusegem F.** 2004. Reactive oxygen gene network of plants. *Trends in Plant Science* **9**, 490-498.
- Miziorko HM.** 2000. Phosphoribulokinase: current perspectives on the structure / function basis for regulation and catalysis. *Advances in Enzymology and Related Areas of Molecular Biology* **74**, 95-127.
- Momonoki YS, Momonoki T, Whallon JH.** 1996. Acetylcholine as a signalling system to environmental stimuli in plants. I. Contribution of Ca²⁺ in heat-stressed *Zea mays* seedlings. *Japanese Journal of Crop Science* **65**, 438-446.
- Moon J, Parry G, Estelle M.** 2004. The ubiquitin-proteasome pathway and plant development. *The Plant Cell* **16**, 3181-3195.
- Moroni JS, Briggs KG, Taylor GJ.** 1991. Chlorophyll content and leaf elongation rate in wheat seedlings as a measure of manganese tolerance. *Plant and Soil* **136**, 1-9.
- Morris HD, Pierre WH.** 1949. Minimum concentrations of manganese necessary for injury to various legumes in culture solutions. *Agronomy Journal* **41**, 107-112.
- Mortvedt JJ, Cunningham HG.** 1971. Production, marketing and use of other secondary and micronutrient fertilizer. In RA Olsen, ed, *Fertilizer Technology and Use*, Soil Science Society of America, Inc. Madison, Wisconsin, 413-454.
- Moschou PN, Paschalidis KA, Delis ID, Andriopoulou AH, Lagiotis GD, Yakoumakis DI, Roubelakis-Angelakis KA.** 2008. Spermidine exodus and oxidation in the apoplast induced by abiotic stress is responsible for H₂O₂ signatures that direct tolerance responses to tobacco. *The Plant Cell* **20**, 1708-1724.
- Mühling KH, Läuchli A.** 2000. Light-induced pH and K⁺ changes in the apoplast of intact leaves. *Planta* **212**, 9-15.
- Nable RO, Houtz RL, Cheniae GM.** 1988. Early inhibition of photosynthesis during development of Mn toxicity in tobacco. *Plant Physiology* **86**, 1136-1142.

- Naranjo MÁ, Forment J, Roldán M, Serrano R, Vicente O.** 2006. Overexpression of *Arabidopsis thaliana* *LTL1*, a salt-induced gene encoding a GDSL-motif lipase, increases salt tolerance in yeast and transgenic plants. *Plant, Cell and Environment* **29**, 1890-1900.
- Ndimba BK, Chivasa S, Hamilton JM, Simon WJ, Slabas AR.** 2003. Proteomic analysis of changes in the extracellular matrix of *Arabidopsis* cell suspension cultures induced by fungal elicitors. *Proteomics* **3**, 1047-1059.
- Neuhoff V, Stamm R, Eibl H.** 1985. Clear background and highly sensitive protein staining with Coomassie Blue dyes in polyacrylamide gels: A systematic analysis. *Electrophoresis* **6**, 427-448.
- Neuhoff V, Stamm R, Pardowitz I, Arold N, Ehrhardt W, Taube D.** 1990. Essential problems in quantification of proteins following colloidal staining with Coomassie Brilliant Blue dyes in polyacrylamide gels, and their solution. *Electrophoresis* **11**, 101-117.
- Nishizawa A; Yabuta Y, Shigeoka S.** 2008. Galactinol and raffinose constitute a novel function to protect plants from oxidative damage. *Plant Physiology* **147**, 1251-1263.
- Olsen LF, Hauser MJB, Kummer U.** 2003. Mechanism of protection of peroxidase activity by oscillatory dynamics. *European Journal of Biochemistry* **270**, 2796-2804.
- Otter T, Polle A.** 1997. Characterization of acidic and basic apoplastic peroxidases from needles of Norway spruce (*Picea abies*, L., Karsten) with respect to lignifying substrates. *Plant and Cell Physiology* **38**, 595-602.
- Passardi F, Longet D, Penel C, Dunand C.** 2004. The class III peroxidase multigenic family in rice and its evolution in land plants. *Phytochemistry* **65**, 1879-1893.
- Passardi F, Cosio C, Penel C, Dunand C.** 2005. Peroxidases have more functions than a Swiss army knife. *Plant Cell Reports* **24**, 255-265.
- Peiter E, Montanini B, Gobert A, Pedas P, Husted S, Maathuis FJ, Blaudez D, Chalot M, Sanders D.** 2007. A secretory pathway-localized cation diffusion facilitator confers plant manganese tolerance. *Proceedings of the National Academy of Sciences of the United States of America* **104**, 8532-8537.
- Pennycooke JC, Jones ML, Stushnoff C.** 2003. Down-regulating α -galactosidase enhances freezing tolerance in transgenic petunia. *Plant Physiology* **133**, 901-909.
- Pietta P-G.** 2000. Flavonoids as antioxidants. *Journal of Natural Products* **63**, 1035-1042.
- Pignocchi C, Foyer CH.** 2003. Apoplastic ascorbate metabolism and its role in the regulation of cell signalling. *Current Opinion in Plant Biology* **133**, 443-447.
- Pignocchi C, Kiddle G, Hernández I, Foster SJ, Asensi A, Taybi T, Barnes J, Foyer CH.** 2006. Ascorbate oxidase-dependent changes in the redox state of the apoplast modulate

- gene transcript accumulation leading to modified hormone signaling and orchestration of defense processes in tobacco. *Plant Physiology* **141**, 423-435.
- Pittman JK.** 2005. Managing the manganese: molecular mechanisms of manganese transport and homeostasis. *New Phytologist* **167**, 733-742.
- Podgornik H, Stegu M, Podgornik A, Perdih A.** 2001. Isolation and characterization of Mn(III) tartrate from *Phanerochaete chrysosporium* culture broth. *FEMS Microbiology Letters* **201**, 265-269.
- Polle A, Otter T, Seifert F.** 1994. Apoplastic peroxidases and lignification in needles of Norway spruce (*Picea abies* L.). *Plant Physiology* **106**, 53-60.
- Portis AR Jr.** 2003. Rubisco activase – Rubisco’s catalytic chaperone. *Photosynthesis Research* **75**, 11-27.
- Protsenko MA, Buza NL, Krinitsyna AA, Bulantseva EA, Korableva NP.** 2008. Polygalacturonase-inhibiting protein is a structural component of the plant cell wall. *Biochemistry (Moscow)* **73**, 1053-1062.
- Rausser WE.** 1995. Phytochelatins and related peptides. Structure, biosynthesis, and function. *Plant Physiology* **109**, 1141-1149.
- Raymond J, Blankenship RE.** 2004. The evolutionary development of the protein complement of photosystem 2. *Biochimica et Biophysica Acta* **1655**, 133-139.
- Rice-Evans CA, Miller NJ, Paganga G.** 1996. Structure-antioxidant activity relationships of flavonoids and phenolic acids. *Free Radical Biology and Medicine* **20**, 933-956.
- Riewe D, Grosman L, Fernie AR, Zauber H, Wucke C, Geigenberger P.** A cell wall-bound adenosine nucleosidase is involved in the salvage of extracellular ATP in *Solanum tuberosum*. *Plant and Cell Physiology* **49**, 1572-1579.
- Roessner U, Wagner C, Kopka J, Trethewey RN, Willmitzer L.** 2000. Simultaneous analysis of metabolites in potato tuber by gas chromatography-mass spectrometry. *The Plant Journal* **23**, 131-142.
- Rogalla H and Römheld V.** 2002. Role of leaf apoplast in silicon-mediated manganese tolerance of *Cucumis sativus* L. *Plant, Cell and Environment* **25**, 549-555.
- Ros Barcelo A.** 1997. Lignification in plant cell walls. *International Review of Cytology* **176**, 87-132.
- Saeed AI, Sharov V, White J, Li J, Liang W, Bhagabati N, Braisted J, Klapa M, Currier T, Thiagarajan M, Sturn A, Snuffin M, Rezantsev A, Popov D, Ryltsov A, Kostukovich E, Borisovsky I, Liu Z, Vinsavich A, Trush V, Quackenbush J.** 2003. TM4: a free, open-source system for microarray data management and analysis. *Biotechniques* **34**, 374-378.

- Sagane Y, Nakagawa T, Yamamoto K, Michikawa S, Oguri S, Momonoki YS.** 2005. Molecular characterization of maize acetylcholinesterase. A novel enzyme family in the plant kingdom. *Plant Physiology* **138**, 1359-1371.
- Sattelmacher B.** 2001. The apoplast and its significance for plant mineral nutrition. *New Phytologist* **149**, 167-192.
- Schaarschmidt S, Kopka J, Ludwig-Müller J, Hause B.** 2007. Regulation of arbuscular mycorrhization by apoplastic invertases: enhanced invertase activity in the leaf apoplast affects the symbiotic interaction. *The Plant Journal* **51**, 390-405.
- Schauer N, Steinhauser D, Strelkov S, Schomburg D, Allison G, Moritz T, Lundgren K, Roessner-Tunali U, Forbes MG, Willmitzer L, Fernie AR, Kopka J.** 2005. GC-MS libraries for the rapid identification of metabolites in complex biological samples. *FEBS Letters* **579**, 1332-1337.
- Schägger H, von Jagow G.** 1987. Tricine-sodium dodecyl sulfate-polyacrylamide gel electrophoresis for the separation of proteins in the range from 1 to 100 kDa. *Analytical Biochemistry* **166**, 368-379.
- Scholz M, Gatzek S, Sterling A, Fiehn O, Selbig J.** 2004. Metabolite fingerprinting: detecting biological features by independent component analysis. *Bioinformatics* **20**, 2447-2454.
- Scholz M, Kaplan F, Guy CL, Kopka J, Selbig J.** 2005. Non-linear PCA: a missing data approach. *Bioinformatics* **21**, 3887-3895.
- Schweikert C, Liskay A, Schopfer P.** 2000. Scission of polysaccharides by peroxidase-generated hydroxyl radicals. *Phytochemistry* **53**, 565-570.
- Sharma SS, Dietz K-F.** 2006. The significance of amino acids and amino acid-derived molecules in plant responses to heavy metal stress. *Journal of Experimental Botany* **57**, 711-726.
- Shelp BJ, Bown AW, Faure D.** 2006. Extracellular γ -aminobutyrate mediates communication between plants and other organisms. *Plant Physiology* **142**, 1350-1352.
- Sherameti I, Sopory SF, Trebicka A, Pfannschmidt T, Oelmüller R.** 2002. Photosynthetic electron transport determines nitrate reductase gene expression and activity in higher plants. *The Journal of Biological Chemistry* **277**, 46594-46600.
- Shevchenko A, Sunyaev S, Loboda A, Shevchenko A, Bork P, Ens W, Standing KG.** 2001. Charting the proteomes of organisms with unsequenced genomes by MALDI-quadrupole time-of-flight mass spectrometry and BLAST homology searching. *Analytical Chemistry* **73**, 1917-1926.

- Shi Q, Bao Z, Zhu Z, He Y, Qian Q, Yu J.** 2005. Silicon-mediated alleviation of Mn toxicity in *Cucumis sativus* in relation to activities of superoxide dismutase and ascorbate peroxidase. *Phytochemistry* **66**, 1551-1559.
- Shinkle JR, Swoap SJ, Simon P, Jones RL.** 1992. Cell wall free space of cucumis hypocotyls contains NAD and a blue light-regulated peroxidase activity. *Plant Physiology* **98**, 1336-1341.
- Smith AG, Croft MT, Moulin M, Webb ME.** 2007. Plants need their vitamins too. *Current Opinion in Plant Biology* **10**, 266-275.
- Sonneveldt C, Voogt SJ.** 1975. Studies on manganese uptake of lettuce on stream-sterilized glasshouse soils. *Plant and Soil* **42**, 49-64.
- Summerfield TC, Shand JA; Bentley FK, Eaton-Rye JJ.** 2005. PsbQ (Sl1638) in *Synechocystis* sp. PCC 6803 is required for photosystem II activity in specific mutants and in nutrient-limiting conditions. *Biochemistry* **44**, 805-815.
- Thornton LE, Ohkawa H, Roose JL, Kashino Y, Keren N, Pakrasi HB.** 2004. Homologs of plant PsbP and PsbQ proteins are necessary for regulation of photosystem II activity in the cyanobacterium *Synechocystis* 6803. *The Plant Cell* **16**, 2164-2175.
- Tran HT, Plaxton WC.** 2008. Proteomic analysis of alteration in the secretome of *Arabidopsis thaliana* suspension cells subjected to nutritional phosphate deficiency. *Proteomics* **8**, 4317-4326.
- van Loon LC, van Strien EA.** 1999. The families of pathogenesis-related proteins, their activities, and comparative analysis of PR-1 type proteins. *Physiological and Molecular Plant Pathology* **55**, 85-97.
- van Loon LC, Rep M, Pieterse CM.** 2006. Significance of inducible defense-related proteins in infected plants. *Annual Review of Phytopathology* **44**, 135-162.
- Wagner C, Sefkow M, Kopka J.** 2003. Construction and application of a mass spectral and retention time index database generated from plant GC/EI-TOF-MS metabolite profiles. *Phytochemistry* **62**, 887-900.
- Wariishi H, Valli K, Gold MH.** 1992. Manganese(II) oxidation by Manganese Peroxidase from the basidiomycete *Phanerochaete chrysosporium*. *The Journal of Biological Chemistry* **267**, 23688-23695.
- Werhahn W, Braun HP.** 2002. Biochemical dissection of the mitochondrial proteome from *Arabidopsis thaliana* by three-dimensional gel electrophoresis. *Electrophoresis* **23**, 640-646.

- White WH, Gunyuzlu PL, Toyn JH.** 2001. *Saccharomyces cerevisiae* is capable of *de novo* pantothenic acid biosynthesis involving a novel pathway of β -alanine production from spermine. *The Journal of Biological Chemistry* **276**, 10794-10800.
- Wissemeier AH, Horst WJ.** 1992. Effect of light intensity on manganese toxicity symptoms and callose formation in cowpea (*Vigna unguiculata* (L.) Walp.). *Plant and Soil* **143**, 299-309.
- Wittig I, Braun HP, Schagger H.** 2006. Blue-native PAGE. *Nature Protocols* **1**,418-428.
- Wollman F-A.** 2001. State transitions reveal dynamics and flexibility of the photosynthetic apparatus. *The EMBO Journal* **20**, 3623-3630.
- Wu Z, Liang F, Hong B, Young JC, Sussman MR, Harper JF, Sze H.** 2002. An Endoplasmatic Reticulum-bound $\text{Ca}^{2+}/\text{Mn}^{2+}$ pump, ECA1, supports plant growth and confers tolerance to Mn^{2+} stress. *Plant Physiology* **130**: 128-137.
- Wulf A, Manthey K, Doll J, Perlick AM, Linke B, Bekel T, Meyer F, Franken P, Kuster H, Krajinski F.** 2003. Transcriptional changes in response to arbuscular mycorrhiza development in the model plant *Medicago truncatula*. *Molecular Plant-Microbe Interactions* **16**: 306-14.
- Yamazaki I, Piette LH.** 1963. The mechanism of aerobic oxidase reaction catalysed by peroxidase. *Biochimica et Biophysica Acta* **77**, 47-64.
- Yi X, McChargue M, Laborde S, Frankel LK, Bricker TM.** 2005. The manganese-stabilizing protein is required for photosystem II assembly/stability and photoautotrophy in higher plants. *Journal of Biological Chemistry* **280**: 16170-16174.

**Proteomic and Metabolomic Analysis of Manganese Toxicity and Tolerance
in *Vigna unguiculata*: Supplementary material**

Supplementary material for Chapter I.

Early manganese-toxicity response in *Vigna unguiculata* L. – a proteomic and transcriptomic study

Hendrik Führs¹, Moritz Hartwig¹, Laura Elisa Buitrago Molina¹, Dimitri Heintz², Alain Van Dorsselaer², Hans-Peter Braun³ & Walter J. Horst¹

Proteomics (2008), 8, 149-159

¹ Institute for Plant Nutrition, Faculty of Natural Sciences, University of Hannover, Herrenhaeuser Str.2, 30419 Hannover, Germany

² Laboratoire de Spectrométrie de Masse Bioorganique, Unité Mixte de Recherche 7509, 25 rue Becquerel, F-67087 Strasbourg cedex 2, France

³ Department for Plant Genetics, Faculty of Natural Sciences, University of Hannover, Herrenhaeuser Str.2, 30419 Hannover, Germany

Table S1: Statistical evaluation of cowpea proteins affected by Mn toxicity stress.

No. ^a	Spot volume on the master gel ^b		Ratio ^c	Mean spot volume on individual gels ^d		<i>p</i> -value ^e
	(0.2 μ M Mn)	(50 μ M Mn)		(0.2 μ M Mn)	(50 μ M Mn)	
1	0.105	0.04	0.381	0.099	0.038	<0.01
2	0.223	0.106	0.475	0.21	0.102	<0.01
3	0.332	0.149	0.449	0.313	0.144	<0.01
6	0.113	0.229	2.026	0.107	0.224	<0.01
7	0.048	0.118	2.458	0.048	0.114	<0.01
8	0.065	0.247	3.800	0.043	0.231	<0.01

The total leaf proteome of cowpea plants cultivated in the presence of normal (0.2 μ M) or enhanced (50 μ M) Mn supply for 3 days was analysed by 2D IEF / SDS PAGE. Three replications were run for each condition and used for the calculation of master gels by the ImageMaster™ 2D Platinum Software 6.0 (GE Healthcare). Proteins of significantly different abundance (ratio >2; *p*-value < 0.01 [t test]) were identified by comparison of the master gels. Total number of detected spots were: (1) TVu 91 0.2 μ M Mn rep.1: 573; rep.2: 821; rep.3: 785, (2) TVu 91 50 μ M Mn rep. 1: 556; rep. 2: 699; rep. 3: 716, (3) TVu 1987 0.2 μ M Mn rep. 1: 525; rep. 2: 598; rep. 3: 538, (4) TVu 1987 50 μ M Mn rep. 1: 544; rep. 2: 691; rep. 3: 720. Total number of spots included into the statistical analysis was for TVu 91 540 and for TVu 1987 464.

- ^a Numbers correspond to the spot numbers given in Figures 2 and 3 and in Table 1. Spots 1-7 are from the TVu 91 cultivar; spot 8 from the TVu 1987 cultivar; spots 4 and 5 were omitted from the table because the proteins completely disappeared during Mn treatment
- ^b Values indicate % volume of the spots in relation to the total volume of all proteins on the master gels
- ^c Ratios were calculated on the basis of the values given in columns 2 and 3
- ^d Mean volumes of the proteins on the three independent gels in relation to the total volume of all proteins on the corresponding gels
- ^e *p*-values were calculated using an algorithm incorporated into ImageMaster™ 2D Platinum Software 6.0

Table S2: Peptide sequences of cowpea proteins affected by Mn toxicity stress

No. ^a	Identity ^b	Peptide sequences ^c	Coverage ^d
1	RubisCO binding protein, beta subunit (pea)	<u>EVELED</u> PVENLGAK – GYLSPYFVTDSEK – TLVGDGSTQEA>VNK – VGDGSTQEA>VNKR – VVAAGANPVLLTR – NAGVNGSVVSEK – SQYLDDIALLTG – AAVEEGLVYGGG – CCLEHAASVAK – SAENSLYVVEGMQ – LAQGLLAEGVK – LYNDGVTVAK – LADLVGVTVAPK – ESTTLVGDGST – LEAAEKDYEK – NLEEDALR – VTLEEGK – DALNATK – VGADLVK – TTSVVLA – ANPVVM PR – VGNML – NLEAAE – LADLVGVSA	25%
2	RubisCO activase (rice)	MCCLFLNDLDAGAGR – LVMSAGELESGNTGVPAK – FPGQSLDFFGALR – VTGKTFSTLYAPLLR – SFQCELVFAK – YLNEAALGDAN – EAALGDANEDSLK – EGPPTFEQPK – GLAYDLSDD – WVSNVGVEGLGK – AYDLSDDQ – EYGNMLVKE – LVKEKENVK – MTLPNLK – VPLLPGEWGGK – MLVKEKE – YSTTVGSPA – YWVPT	43%
3	Phosphoribulokinase (pea)	<u>LDELLYVESHLSNLSTK</u> – DDQTVVIGLAADSGCGK – ANDFDLMYEQVK – LTVSFGGAAEPPK – KPDFEAYLDPKK – FYGEVTKQMLK – KLTCSTYPGLK – VSVVEFDGKFDR – DLYEQLVATR – DPDSNTLL – EVLPTKLL – EGLHP – YNHGTG	36%
4	Oxygen-evolving enhancer protein 1 (<i>A. thaliana</i>)	STGYDNAVLPQG	4%
5	Pathogenesis-related protein P4 (tomato)	QPSPQDYLA>VHNDAR	9%
6	Putative beta6 proteasome subunit (tobacco)	VTPLSESNANDLVK – SPSPLLLPAK – FTYDAVG	20%
7	Pathogenesis-related protein 5-1 (sunflower)	AQGGCANNPCTVFK – LSCTADLDGQCHG – LWPR	12%
8	Oxygen-evolving enhancer protein 2 (<i>B. gymnorrhiza</i>)	SLTDYGSPEEFLS – EVEYPGQVLR – LLESATPVVDGK	21%

^a Numbers correspond to the spot numbers given in Figs. 2 and 3 and in Table 1

^b Identities are based on sequence comparisons using the NCBI protein database

^c Amino acid sequences were identified by nano LC MS/MS. Underlined residues are conserved within the proteins used for identification

^d Coverage of the peptides identified by mass spectrometry

Table S3: Genes upregulated in cowpea cultivars due to Mn treatment (50 μ M) for 1 day.

1. Mn-sensitive cultivar TVu 91

Clone No.	Length (bp)	Accession No.	Identity	Organism	Gene name / Accession No. Hit gene	Accession No. Hit protein	E-value
1	782	AM748387	putative wound-inducible carboxypeptidase	<i>Lycopersicon esculentum</i>	- / AF242849.1	AAF44708.1	1e-96
2	753	AM748388	putative wound-inducible carboxypeptidase	<i>Lycopersicon esculentum</i>	- / AF242849.1	AAF44708.1	9e-93
3	525	AM748389	putative salt-tolerance protein	<i>Glycine max</i>	- / DQ234265.1	ABB29467.1	1e-159
4	666	AM748390	putative pathogenesis-related protein	<i>Vigna unguiculata</i>	PR4.2 / X98608.1	CAA67200.1	3e-171
5	259	AM748391	putative 23S ribosomal RNA	<i>Phaseolus vulgaris</i>	rrn23 / DQ886273.1	-	7e-95
6	263	AM748392	putative 23S ribosomal RNA	<i>Phaseolus vulgaris</i>	rrn23 / DQ886273.1	-	3e-93
7	273	AM748393	putative 23S ribosomal RNA	<i>Phaseolus vulgaris</i>	rrn23 / DQ886273.1	-	8e-95
8	264	AM748394	putative 23S ribosomal RNA	<i>Phaseolus vulgaris</i>	rrn23 / DQ886273.1	-	8e-95
9	456	AM748395	putative 30S ribosomal protein S10, chloroplast	<i>Arabidopsis thaliana</i>	AT3G13120 / NM_112151.3	NP_187919.1	6e-50
10	711	AM748396	putative MYB transcription factor MYB176	<i>Glycine max</i>	MYB176 / DQ822924.1	ABH02865.1	2e-81
11	792	AM748397	unknown protein	<i>Lycopersicon esculentum</i>	- / AK246728	-	4e-57
12	279	AM748398	26S proteasome regulatory subunit S5A	<i>Mesembryanthemum crystallinum</i>	- / AF069324.2	AAC19402.1	3e-63
13	613	AM748399	putative 60S ribosomal protein	<i>Juglans regia</i>	rib 60S / AJ278460	-	1e-38
14	596	AM748400	26S proteasome regulatory subunit S5A	<i>Mesembryanthemum crystallinum</i>	- / AF069324.2	AAC19402.1	4e-128
15	711	AM748401	putative Histone 2A H2A; Histone-fold	<i>Medicago truncatula</i>	- / AC174297.1	ABO844931	2e-144
16	770	AM748402	putative rubisco activase	<i>Vigna radiata</i>	Rca / AF126870.2	AAD20019.2	0.0
17	724	AM748403	putative rubisco activase	<i>Vigna radiata</i>	Rca / AF126870.2	AAD20019.2	0.0
18	791	AM748404	putative rubisco activase	<i>Vigna radiata</i>	Rca / AF126870.2	AAD20019.2	0.0

19	644	AM748405	putative rubisco activase	<i>Vigna radiata</i>	Rca / AF126870.2	AAD20019.2	0.0
20	726	AM748406	putative rubisco activase	<i>Vigna radiata</i>	Rca / AF126870.2	AAD20019.2	0.0
21	655	AM748407	putative rubisco activase	<i>Vigna radiata</i>	Rca / AF126870.2	AAD20019.2	0.0
22	671	AM748408	putative cytochrome P450 monooxygenase CYP82E13	<i>Glycine max</i>	CYP82E13 / DQ340239.1	ABC68402.1	6e-157
23	705	AM748409	CBL-interacting protein kinase 12	<i>Populus trichcarpa</i>	CIPK12 / DQ997702.1	ABJ91219.1	2e-80
24	705	AM748410	CBL-interacting protein kinase 12	<i>Populus trichcarpa</i>	CIPK12 / DQ997702.1	ABJ91219.1	7e-79
25	653	AM748411	hypothetical protein	<i>Medicago truncatula</i>	- / AC144727.11	ABO81102.1	1e-96
26	742	AM748412	hypothetical protein	<i>Vitis vinifera</i>	- / AM463502.2	CAN68061.1	0.007
27	795	AM748413	phosphatidate cytidyltransferase, putative / CDP-diglyceride synthetase, putative	<i>Arabidopsis thaliana</i>	AT4G22340 / NM_202862.2	NBP_974591.1	9e-163
28	636	AM748414	phosphatidate cytidyltransferase, putative / CDP-diglyceride synthetase, putative	<i>Arabidopsis thaliana</i>	AT4G22340 / NM_202862.2	NBP_974591.1	2e-151
29	751	AM748415	putative proton-dependent oligopeptide transport (POT) family protein	<i>Arabidopsis thaliana</i>	AT3G54140 / NM_115274.2	NP_190982.1	2e-68
30	740	AM748416	putative proton-dependent oligopeptide transport (POT) family protein	<i>Arabidopsis thaliana</i>	AT3G54140 / NM_115274.2	NP_190982.1	2e-68
31	643	AM748417	coatamer protein complex, subunit beta 2 (beta prime), putative	<i>Arabidopsis thaliana</i>	AT3G15980 / NM_180262.2	NP_850593.1	2e-48
32	666	AM748418	putative lipid transfer protein precursor	<i>Pisum sativum</i>	LTP / AF137353.1	AAF61436.1	1e-34
33	472	AM748419	putative asparaginyl endopeptidase	<i>Vigna radiata</i>	PE1 / AF238384.1	AAK15049.1	0.0
34	478	AM748420	putative asparaginyl	<i>Vigna radiata</i>	PE1 / AF238384.1	AAK15049.1	0.0

			endopeptidase				
35	669	AM748421	putative lipoxygenase	<i>Medicago truncatula</i>	MtrDRAFT_AC146743g33v2 / AC146743.11	ABO81653.1	6e-114
36	469	AM748422	putative asparagine synthetase type II	<i>Phaseolus vulgaris</i>	as2 / AJ009952.1	CAA08913.1	4e-29
37	584	AM748423	putative cysteine proteinase precursor	<i>Phaseolus vulgaris</i>	- / Z99954.1	CAB17076.1	0.0
38	584	AM748424	putative cysteine proteinase precursor	<i>Phaseolus vulgaris</i>	- / Z99954.1	CAB17076.1	0.0
39	603	AM748425	hypothetical protein	<i>Cicer arietinum</i>	- / AJ271663.1	CAB711311	6e-38
40	603	AM748426	putative cathepsin B-like cysteine protease	<i>Arabidopsis thaliana</i>	AT1G02305 / NM_100111.2	NP_563648.1	3e-111
41	588	AM748427	putative cathepsin B-like cysteine protease	<i>Arabidopsis thaliana</i>	AT1G02305 / NM_100111.2	NP_563648.1	3e-111
42	723	AM748428	unknown protein	<i>Zea mays</i>	- / DQ246132.1	-	0.004
43	647	AM748429	hypothetical protein	<i>Cicer arietinum</i>	- / AJ131049.1	CAA10289.1	6e-176
44	725	AM748430	hypothetical protein	<i>Cicer arietinum</i>	- / AJ131049.1	CAA10289.1	0.0
45	663	AM748431	hypothetical protein	<i>Cicer arietinum</i>	- / AJ131049.1	CAA10289.1	0.0
46	776	AM748432	hypothetical protein	<i>Cicer arietinum</i>	- / AJ131049.1	CAA10289.1	0.0
47	538	AM748433	putative zinc finger (DNL type) family protein	<i>Arabidopsis thaliana</i>	AT5G27280 / NM_122610.2	NP_198080.1	3e-54
48	238	AM748434	putative 23S ribosomal RNA	<i>Phaseolus vulgaris</i>	rrn23 / DQ886273.1	-	7e-95
49	796	AM748435	putative plant disease resistance response protein family	<i>Oryza sativa</i>	Os11g0179700 / NM_001072423.1	NP_001065891.1	9e-07
50	674	AM748436	unknown protein	<i>Oryza sativa</i>	- / AC134044.4	AAX96307.1	0.035
51	550	AM748437	unknown protein	-	- / -	-	-
52	562	AM748438	unknown protein	-	- / -	-	-
53	522	AM748439	unknown protein	-	- / -	-	-
54	715	AM748440	putative thylakoid lumenal 15 kDa protein, chloroplast	<i>Arabidopsis thaliana</i>	AT2G44920 / NM_130056.5	NP_566030.1	7e-105
55	784	AM748441	putative chloroplast post-illumination chlorophyll fluorescence increase protein	<i>Nicotiana tabacum</i>	- / DQ854729.1	ABI51594.1	2e-132

56	707	AM748442	putative chloroplast post-illumination chlorophyll fluorescence increase protein	<i>Nicotiana tabacum</i>	- / DQ854729.1	ABI51594.1	1e-116
57	716	AM748443	putative thylakoid lumenal 15 kDa protein, chloroplast	<i>Arabidopsis thaliana</i>	AT2G44920 / NM_130056.5	NP_566030.1	1e-107
58	709	AM748444	putative chloroplast post-illumination chlorophyll fluorescence increase protein	<i>Nicotiana tabacum</i>	- / DQ854729.1	ABI51594.1	1e-116
59	780	AM748445	putative chloroplast post-illumination chlorophyll fluorescence increase protein	<i>Nicotiana tabacum</i>	- / DQ854729.1	ABI51594.1	2e-132
60	788	AM748446	putative chloroplast post-illumination chlorophyll fluorescence increase protein	<i>Nicotiana tabacum</i>	- / DQ854729.1	ABI51594.1	1e-130
61	261	AM748447	putative ATP synthase CF0 subunit I	<i>Cucumis sativus</i>	atpF / DQ865975.1	ABI97404.1	8e-30
62	669	AM748448	23S ribosomal RNA	<i>Phaseolus vulgaris</i>	rrn23 / DQ886273.1	-	2e-120
63	611	AM748449	unknown protein	-	- / -	-	-
64	545	AM748450	unknown protein	<i>Vitis vinifera</i>	- / AM464460.2	-	1.9
65	580	AM748451	putative S-locus glycoprotein	<i>Brassica rapa</i>	SLG9 / D88192.1	BAA21131.1	0.010
66	31	AM748452	unknown protein	<i>Populus trichocarpa x Populus deltoides</i>	- / CT028425.1	-	0.012
67	662	AM748453	unknown protein	-	- / -	-	-
68	588	AM748454	unknown protein	<i>Lycopersicon esculentum</i>	- / AP009357.1	-	2e-22
69	633	AM748455	unknown protein	-	- / -	-	-

2. Mn-tolerant cultivar TVu 1987

Clone No.	Length (bp)	Accession No.	Identity	Organism	Gene name / Accession No. Hit gene	Accession No. Hit protein	E-value
1	442	AM748456	putative aspartic proteinase	<i>Vigna unguiculata</i>	- / U61396.2	AAB03843.2	0.0
2	442	AM748457	putative aspartic proteinase	<i>Vigna unguiculata</i>	- / U61396.2	AAB03843.2	9e-100

3	598	AM748458	putative catalase	<i>Vigna radiata</i>	- / D13557.1	BAA02755.1	1e-97
4	737	AM748459	putative CLPP5 (Nuclear encoded CLP protease 1); endopeptidase Clp	<i>Arabidopsis thaliana</i>	CLPP5 / NM_100137.3	NP_563657.1	7e-176
5	737	AM748460	putative nuclear encoded precursor to chloroplast protein	<i>Pisum sativum</i>	- / L09547.1	AAA33680.1	0.0
6	179	AM748461	putative clp protease proteolytic subunit	<i>Phaseolus vulgaris</i>	clpP / DQ886273.1	ABH88110.1	0.013
7	745	AM748462	unknown protein	<i>Lotus japonicus</i>	- / AP006666.1	-	4e-55
8	744	AM748463	unknown protein	<i>Lotus japonicus</i>	- / AP006666.1	-	4e-55
9	702	AM748464	hypothetical protein	<i>Vitis vinifera</i>	VITISV_035536 / AM426893.2	CAN62489.1	3e-43
10	748	AM748565	unknown protein	<i>Lotus japonicus</i>	- / AP006666.1	-	4e-55
11	716	AM748566	putative single-stranded nucleic acid binding R3H		MtrDRAFT_AC183371g11v1 / AC183371.2	ABN09177.1	1e-88
12	383	AM748467	unknown protein	<i>Medicago truncatula</i>	- / CT485797.2	-	2e-86
13	769	AM748468	putative NADPH-cytochrome P450 reductase	<i>Pisum sativum</i>	PSC450R1 / AF002698.2	AAC09468.2	0.0
14	754	AM748469	putative LHCII type III chlorophyll a/b binding protein	<i>Vigna radiata</i>	CipLhcb3 / AF139465.2	AAD27877.1	0.0
15	771	AM748470	putative photosystem II protein I	<i>Phaseolus vulgaris</i>	psbI / DQ886273.1	ABH88094.1	2e-40
16	775	AM748471	putative photosystem II protein I	<i>Phaseolus vulgaris</i>	psbI / DQ886273.1	ABH88094.1	1e-06
17	729	AM748472	putative photosystem II protein I	<i>Phaseolus vulgaris</i>	psbI / DQ886273.1	ABH88094.1	1e-36
18	774	AM748473	putative photosystem II protein I	<i>Phaseolus vulgaris</i>	psbI / DQ886273.1	ABH88094.1	1e-06
19	793	AM748474	putative photosystem II protein I	<i>Phaseolus vulgaris</i>	psbI / DQ886273.1	ABH88094.1	9e-38
20	770	AM748475	putative photosystem II protein I	<i>Phaseolus vulgaris</i>	psbI / DQ886273.1	ABH88094.1	2e-40
21	709	AM748476	putative photosystem II protein I	<i>Phaseolus vulgaris</i>	psbI / DQ886273.1	ABH88094.1	1e-50
22	675	AM748477	unknown protein	<i>Phaseolus vulgaris</i>	trnS-GCU / DQ886273.1	-	2.9

23	633	AM748478	unknown protein	<i>Phaseolus vulgaris</i>	trnS-GCU / DQ886273.1	-	2.9
24	696	AM748479	unknown protein	<i>Phaseolus vulgaris</i>	trnS-GCU / DQ886273.1	-	2.9
25	593	AM748480	putative ATP synthase CF1 alpha subunit	<i>Phaseolus vulgaris</i>	atpA / DQ886273.1	ABH88093.1	0.0
26	598	AM748481	ATP synthase CF1 alpha subunit	<i>Phaseolus vulgaris</i>	atpA / DQ886273.1	ABH88093.1	0.0
27	713	AM748482	putative ATP synthase CF1 beta subunit	<i>Phaseolus vulgaris</i>	atpB / DQ886273.1	ABH88071.1	0.0
28	719	AM748483	putative ATP synthase CF1 beta subunit	<i>Phaseolus vulgaris</i>	atpB / DQ886273.1	ABH88071.1	1e-36
29	731	AM748484	putative ATP synthase CF1 epsilon subunit	<i>Phaseolus vulgaris</i>	atpE / DQ886273.1	ABH88072.1	4e-103
30	600	AM748485	unknown protein	<i>Medicago truncatula</i>	- / CT954236.4	-	9e-32
31	568	AM748486	unknown protein	<i>Medicago truncatula</i>	- / CT954236.4	-	9e-32
32	550	AM748487	putative ribulose-5-phosphate-3-epimerase	<i>Pisum sativum</i>	R5P3E / AF369887.1	AAM19354.1	7e-102
33	550	AM748488	putative ribulose-5-phosphate-3-epimerase	<i>Pisum sativum</i>	R5P3E / AF369887.1	AAM19354.1	7e-102
34	730	AM748489	putative photosystem I subunit IX	<i>Phaseolus vulgaris</i>	psaJ / DQ886273.1	ABH88107.1	0.0
35	564	AM748490	putative 1-aminocyclopropane-1-carboxylic acid oxidase	<i>Phaseolus lunatus</i>	ACO / AB062359.1	BAB83762.1	6e-142
36	541	AM748491	putative 1-aminocyclopropane-1-carboxylic acid oxidase	<i>Phaseolus lunatus</i>	ACO / AB062359.1	BAB83762.1	6e-142
37	736	AM748492	putative 1-aminocyclopropane-1-carboxylic acid oxidase	<i>Phaseolus lunatus</i>	ACO / AB062359.1	BAB83762.1	0.0
38	574	AM748493	unknown protein	<i>Lotus japonicus</i>	- / AP006106.1	-	2e-08
39	557	AM749494	unknown protein	<i>Lotus japonicus</i>	- / AP006106.1	-	2e-08
40	543	AM748495	unknown protein	-	- / -	-	-
41	579	AM748496	putative 23S rRNA pseudouridine synthase	<i>Escherichia coli</i>	yibC / DQ855280.1	ABK20858	1e-83
42	706	AM748497	putative aquaporin	<i>Phaseolus vulgaris</i>	PIP2;1 / AY995195.1	AAAY22203.1	3e-93
43	50	AM748498	unknown protein	-	-	-	-
44	634	AM748499	unknown protein	<i>Medicago truncatula</i>	- / AC153459.9	-	1e-21

45	633	AM748500	unknown protein	<i>Medicago truncatula</i>	- / AC153459.9	-	1e-21
46	478	AM748501	putative glyoxalase I	<i>Glycine max</i>	glxI / AJ010423.1	CAA09177.1	2e-95
47	533	AM748502	putative carbamoyl-phosphate synthase, GATase region	<i>Medicago truncatula</i>	MtrDRAFT_AC135505g12v2 / AC135505.15	ABE82026	2e-66
48	541	AM748503	putative carbamoyl-phosphate synthase, GATase region	<i>Medicago truncatula</i>	MtrDRAFT_AC135505g12v2 / AC135505.15	ABE82026	2e-68
49	543	AM748504	putative carbamoyl-phosphate synthase, GATase region	<i>Medicago truncatula</i>	MtrDRAFT_AC135505g12v2 / AC135505.15	ABE82026	2e-68
50	780	AM748505	putative fumarylacetoactase	<i>Medicago truncatula</i>	MtrDRAFT_AC150798g15v2 / AC150798.3	ABD33010.1	2e-26
51	687	AM748506	putative fumarylacetoactase	<i>Medicago truncatula</i>	MtrDRAFT_AC150798g15v2 / AC150798.3	ABD33010.1	2e-26
52	662	AM748507	putative thiamin biosynthetic enzyme	<i>Glycine max</i>	SC-03 / AB030493.1	BAA88228.1	7e-85
53	848	AM748508	unknown protein	-	- / -	-	-
54	678	AM748509	putative single-stranded nucleic acid binding R3H	<i>Medicago truncatula</i>	MtrDRAFT_AC183371g11v1 / AC183371.2	ABN09177.1	2e-72
55	675	AM748510	unknown protein	<i>Arabidopsis thaliana</i>	At1G55500 / NM_104425.1	NP_841997	9e-53
56	730	AM748511	putative protein kinase PKN/PRK1, effector	<i>Medicago truncatula</i>	MtrDRAFT_AC152348g11v2 / AC152348.7	ABE86171.1	1e-60
57	345	AM748512	unknown protein	-	- / -	-	-
58	405	AM748513	unknown protein	<i>Medicago truncatula</i>	- / DQ323045.1	-	1e-32
59	481	AM748514	unknown protein	-	- / -	-	-
60	714	AM748515	hypothetical protein	<i>Vitis vinifera</i>	VITISV_008346 / AM467898.2	CAN68216.1	0.27
61	695	AM748516	putative strictosidine synthase family protein	<i>Silene latifolia</i>	SISS / AB182104.1	BAE80094.1	0.021
62	576	AM748517	unknown protein	-	- / -	-	-
63	282	AM748518	unknown protein	<i>Medicago truncatula</i>	- / CU012050.16	-	1e-16
64	680	AM748519	unknown protein	<i>Medicago truncatula</i>	- / DQ323045.1	-	1e-32
65	322	AM748520	unknown protein	-	- / -	-	-
66	617	AM748521	unknown protein	-	- / -	-	-

^a Identifications are based on sequence comparisons using nucleotide blast at NCBI database. Sequences were submitted to the EMBL database (accession numbers AM748387 to AM748524)

Supplementary material for Chapter II.

Characterization of leaf apoplastic peroxidases and metabolites in *Vigna unguiculata* in response to toxic manganese supply and silicon

Hendrik Führs¹, Stefanie Götze¹, André Specht¹, Alexander Erban², Sébastien Gallien³,
Dimitri Heintz⁴, Alain Van Dorsselaer³, Joachim Kopka², Hans-Peter Braun⁵ & Walter J.
Horst¹

Journal of Experimental Botany (2009), doi:10.1093/jxb/erp034

¹ Institute of Plant Nutrition, Faculty of Natural Sciences, Leibniz University Hannover, Herrenhäuser Str. 2, 30419 Hannover, Germany

² Max Planck Institute of Molecular Plant Physiology, Am Mühlenberg 1, 14476 Potsdam-Golm, Germany

³ Laboratoire de Spectrométrie de Masse Bio-Organique, IPHC-DSA, ULP, CNRS, UMR7178 ; 25 rue Becquerel, 67 087 Strasbourg, France

⁴ Institut de Biologie Moléculaire des Plantes (IBMP) CNRS-UPR2357,ULP, 67083 Strasbourg, France

⁵ Institute of Plant Genetics, Faculty of Natural Sciences, Leibniz University Hannover, Herrenhäuser Str. 2, 30419 Hannover, Germany

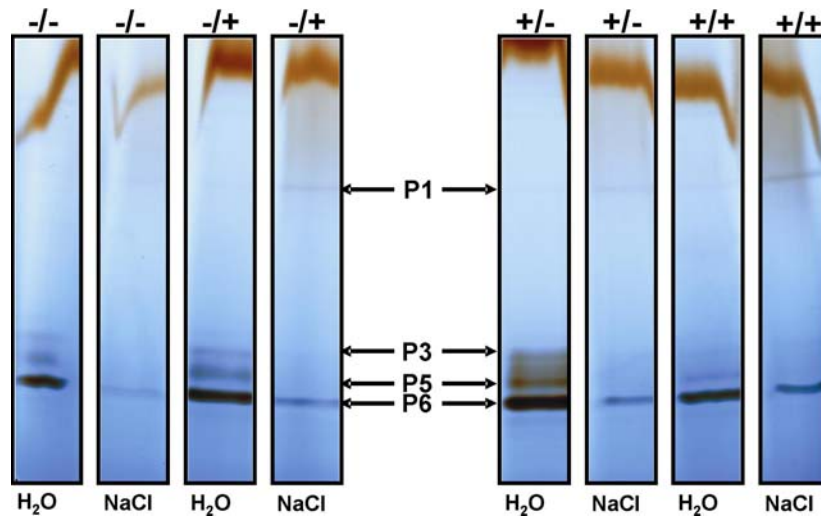


Fig. S1: Resolution of dH₂O- and NaCl-extractable AWF proteins after 0 and 4 d of Mn treatment of \pm Si treated plants (as described in “Materials and Methods”) of the Mn-sensitive cultivar TVu 91 after separation with BN-PAGE stained for guaiacol-peroxidase. The signs on the top of the lanes are as follows: -/- 0.2 μ M Mn/0 μ M Si, -/+ 0.2 μ M Mn /20 μ M Si, +/- 50 μ M Mn/0 μ M Si, +/+ 50 μ M Mn/20 μ M Si. H₂O and NaCl as indicated under the lanes describe the infiltration solution to extract AWF. 16 μ g of concentrated AWF (as determined with 2D Quant Kit) were loaded onto each lane. Guaiacol-POD staining was done in 18 mM guaiacol (in 9 mM Na₂HPO₄) and 0.03% H₂O₂ at pH 6.0.

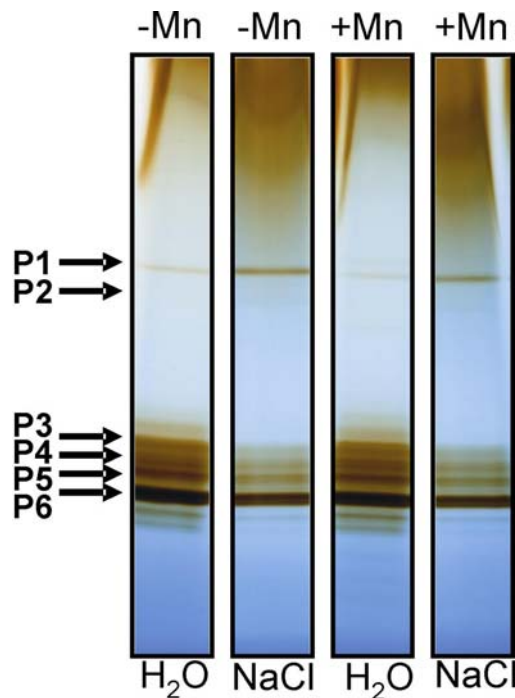


Fig. S2: Resolution of dH₂O- and NaCl-extractable AWF proteins after 0 and 4 d of Mn of the Mn-sensitive cultivar TVu 91 after separation with BN-PAGE stained for guaiacol-peroxidase. -Mn indicates 0.2 μ M Mn treatment, whereas +Mn describes 50 μ M Mn treatment for four days. H₂O and NaCl as indicated under the lanes describe the infiltration solution to extract AWF. 180 μ g of concentrated AWF (as determined with 2D Quant Kit) were loaded onto each lane. Guaiacol-POD staining was done in 18 mM guaiacol (in 9 mM Na₂HPO₄) and 0.03% H₂O₂ at pH 6.0.

Table S1: Determined extinction coefficients for the calculation of NADH-*peroxidase* activities of different POD isoenzymes supplied with different phenols in changing concentrations as shown in Fig. 4, 6 and 7.

Phenol ^a	Absorption	Phenol conc. [mM] ^b	NADH conc. [mM] ^c	Total conc. [mM] ^d	Extinction coefficient [ϵ] ^e
<i>p</i> -coumaric acid	1.979	1.66	0.22	1.88	1.13
vanillic acid	1.051	1.66	0.22	1.88	0.60
gallic acid	1.034	1.66	0.22	1.88	0.59
benzoic acid	1.026	1.66	0.22	1.88	0.58
ferulic acid	3.429	1.66	0.22	1.88	1.95
syringic acid	1.033	1.66	0.22	1.88	0.59
protocatechuic acid	1.025	1.66	0.22	1.88	0.58
caffeic acid	3.453	1.66	0.22	1.88	1.97
chlorogenic acid	3.69	1.66	0.22	1.88	2.10
<i>p</i> -hydroxybenzoic acid	0.800	1.66	0.22	1.88	0.46
<i>p</i> -coumaric acid	1.137	0.166	0.22	0.386	3.15
vanillic acid	1.046	0.166	0.22	0.386	2.90
gallic acid	1.052	0.166	0.22	0.386	2.92
benzoic acid	1.03	0.166	0.22	0.386	2.86
ferulic acid	1.484	0.166	0.22	0.386	4.12
syringic acid	1.045	0.166	0.22	0.386	2.90
protocatechuic acid	1.038	0.166	0.22	0.386	2.88
caffeic acid	1.52	0.166	0.22	0.386	4.22
chlorogenic acid	2.715	0.166	0.22	0.386	7.53
<i>p</i> -hydroxybenzoic acid	0.800	0.166	0.22	0.386	2.21
<i>p</i> -coumaric acid	1.053	0.0166	0.22	0.2366	4.77
vanillic acid	1.034	0.0166	0.22	0.2366	4.70
gallic acid	1.039	0.0166	0.22	0.2366	4.70
benzoic acid	1.04	0.0166	0.22	0.2366	4.71
ferulic acid	1.08	0.0166	0.22	0.2366	4.89
syringic acid	1.036	0.0166	0.22	0.2366	4.69
protocatechuic acid	1.032	0.0166	0.22	0.2366	4.67
caffeic acid	1.082	0.0166	0.22	0.2366	4.90
chlorogenic acid	1.195	0.0166	0.22	0.2366	5.41
<i>p</i> -hydroxybenzoic acid	0.800	0.0166	0.22	0.2366	3.62
<i>p</i> -coumaric acid	1.016	0.00166	0.22	0.22166	4.91
vanillic acid	1.017	0.00166	0.22	0.22166	4.91
gallic acid	1.021	0.00166	0.22	0.22166	4.93
benzoic acid	1.02	0.00166	0.22	0.22166	4.93
ferulic acid	1.018	0.00166	0.22	0.22166	4.92
syringic acid	1.008	0.00166	0.22	0.22166	4.87
protocatechuic acid	1.017	0.00166	0.22	0.22166	4.91
caffeic acid	0.981	0.00166	0.22	0.22166	4.74
chlorogenic acid	1.029	0.00166	0.22	0.22166	4.97
<i>p</i> -hydroxybenzoic acid	0.800	0.00166	0.22	0.22166	3.86
Phenol combination ^f	Absorption	Phenol conc. [mM] ^b	NADH conc. [mM] ^c	Total conc. [mM] ^d	Extinction coefficient [ϵ] ^e
<i>p</i> -coumaric acid [0.166mM] with:					
vanillic acid	1.079	0.0166	0.22	0.4026	2.87
gallic acid	1.078	0.0166	0.22	0.4026	2.87
benzoic acid	1.078	0.0166	0.22	0.4026	2.87
ferulic acid	1.118	0.0166	0.22	0.4026	2.97
syringic acid	1.072	0.0166	0.22	0.4026	2.85
protocatechuic acid	1.075	0.0166	0.22	0.4026	2.86
caffeic acid	1.120	0.0166	0.22	0.4026	2.98
chlorogenic acid	1.223	0.0166	0.22	0.4026	3.25
<i>p</i> -hydroxybenzoic acid		0.0166	0.22	0.4026	
- ^g	0.971	-	0.22	0.22	4.73

- ^a Phenol added to the measuring solution. Values correspond to Figs. 4, 6 and 7
- ^b Phenol concentration in the measuring solution. Values correspond to Fig. 4, 6, and 7
- ^c NADH concentration added to the measuring solution. Values correspond to Fig.4, 6, and 7
- ^d Calculated total concentration of the absorbing substances phenol and NADH based on ^b and ^c
- ^e Calculated extinction coefficient ϵ [$\text{L (mmol}\cdot\text{cm)}^{-1}$ or $\text{cm}^2 (\mu\text{mol})^{-1}$] according to the Beer-Lambert law: $\text{Abs.}=\epsilon\cdot c\cdot d$
- ^f 0.0166 mM of each phenol was added to 0.166 mM *p*-coumaric acid, so that the end concentration of absorbing substances was 0.4026. These values correspond to Fig. 7
- ^g Extinction coefficient ϵ calculated without phenol supply to the measuring solution

Tab. S2: Peptide sequences of apoplastic cowpea proteins. AWF proteins were separated by means of BN-PAGE and afterwards stained for guaiacol-peroxidase activity. Stained BN-bands were cut from the gel and sequenced with nanoLC-MS/MS. Results presented here are derived from 2 independent sequencing runs.

Band ^a	Protein name ^b	Protein accession numbers ^c	Protein molecular weight (Da) ^d	Number of unique peptides	Percentage sequence coverage ^e	Peptide sequence	Mascot Ion score	Mascot Identity score	difference score	Number of identified +1H spectra	Number of identified +2H spectra	Number of identified +3H spectra	Number of identified +4H spectra	Number of enzymatic termini	Calculated +1H Peptide Mass (AMU)
AWF _{H2O} _P1	fasciclin-like arabinogalactan protein 12 [Gossypium hirsutum]	ABV27483.1	43 894,2	1	1.88%	LADEINTR	61	47	14	0	1	0	0	2	931.4849
	Fructose-1,6-bisphosphatase, chloroplast precursor [Glycine max]	Q42796.1	43 879,4	2	7.96%	ANISNLTVGVQAVNVQGEDQK	51.5	44.8	6.7	0	0	1	0	2	2 142,0792
	Fructose-1,6-bisphosphatase, chloroplast precursor [Glycine max]	Q42796.1	43 879,4	2	7.96%	YIGSLVGFHHR	37.8	46.5	-8.7	0	0	1	0	2	1 263,6486
	fasciclin-like arabinogalactan protein FLA8 [Arabidopsis thaliana]	AAG24276.1	43 044,2	1	2.62%	VGFSAASGSK	67.5	46.1	21.4	0	1	0	0	2	967,4848
	xyloglucan endotransglucosylase/hydrolase 2 [Cucumis melo]	AB194062.1	36 316,1	1	3.88%	TDWQAPFTASYR	90.7	45.8	44.9	0	1	0	0	2	1 529,7025
	CYP1 (putative cyclophilin_ABH_like) [Vigna radiata]	BAB82452.1	18 188,7	1	6.98%	IVFELFADTTTPR	90	46	44	0	1	0	0	2	1 408,7479
	basic chitinase, chitinase [Arabidopsis thaliana]	NP_566426.1	36 196,3	1	5.67%	LPGYGVITNIINGGLECGR	128	44.9	83.1	0	1	1	0	2	2 003,0385
	Os1g0357100 [Oryza sativa (japonica cultivar-group)]	NP_001043008.1	72 385,0	1	1.65%	LADEYGSGLER	72.3	49.1	23.2	0	1	0	0	2	1 209,5752
	cytosolic malate dehydrogenase [Cicer arietinum]	CAC10208.1	41 361,4	1	2.11%	ALGQISER	61.4	47.2	14.2	0	1	0	0	2	873,4795
	cyclophilin [Phaseolus vulgaris]	CAA52414.1	18 141,5	1	8.14%	VFFDMTIGGQPAGR	75.8	45.7	30.1	0	2	0	0	2	1 511,7319
	alpha galactosidase [Glycine max]	AAA73963.1	46 378,6	4	10.40%	SVGNSWR	38.1	48.6	-10.5	0	1	0	0	2	805,3956
	alpha galactosidase [Glycine max]	AAA73963.1	46 378,6	4	10.40%	TFASWGIDYLK	64.8	46.5	18.3	0	2	0	0	2	1 300,6578
	alpha galactosidase [Glycine max]	AAA73963.1	46 378,6	4	10.40%	TMPGSLGHEEQDAK	36.8	46.1	-9.3	0	1	0	0	2	1 499,6801
	alpha galactosidase [Glycine max]	AAA73963.1	46 378,6	4	10.40%	YDNCENNNISPK	67.5	47.4	20.1	0	2	0	0	2	1 467,6175
	endochitinase precursor [Humulus lupulus]	AAD34596.1	33 511,4	1	4.11%	GFYTDALFLTAAR	75.7	46	29.7	0	1	0	0	2	1 495,7221
	unnamed protein product (putative secretory peroxidase) [Vitis vinifera]	CAO48839.1	34 372,5	1	2.79%	GVEVVDTIK	53.1	46.5	6.6	0	1	0	0	2	1 023,5363
	unnamed protein product (putative Serine carboxypeptidase) [Vitis vinifera]	CAO68876.1	57 192,0	1	2.96%	NLEVGIPDLLEDGIK	58.1	45.3	12.8	0	2	0	0	2	1 624,8801
	AWF _{H2O} _P3	fasciclin-like arabinogalactan protein 12 [Gossypium hirsutum]	ABV27483.1	43 894,2	1	1.88%	LADEINTR	73.1	47	26.1	0	1	0	0	2
pepti (ISS) (putative Cyclophilin) [Ostreococcus tauri]		CAL57205.1	38 854,4	1	3.27%	IVLGLFGDDAPR	60.6	46.3	14.3	0	2	0	0	2	1 272,6955
unnamed protein product (putative Thaumatin family) [Vitis vinifera]		CAO62993.1	26 139,4	1	4.07%	GSDGSVIGCK	77.4	46.7	30.7	0	1	0	0	2	979,452
CYP1 (putative cyclophilin_ABH_like) [Vigna radiata]		BAB82452.1	18 188,7	1	6.98%	IVFELFADTTTPR	71.7	46	25.7	0	1	0	0	2	1 408,7479
putative glycine-rich RNA-binding protein [Dianthus caryophyllus]		BAF34340.1	16 872,1	1	5.68%	SITVNEAQRS	65.3	46.4	18.9	0	1	0	0	2	1 104,5649
peroxidase [Spinacia oleracea]		CAA71493.1	33 435,5	2	7.12%	MGASILR	42.9	47.7	-4.8	0	1	0	0	2	763,4137
peroxidase [Spinacia oleracea]	CAA71493.1	33 435,5	2	7.12%	MGNISPLTGSSGEIR	79.7	45.8	33.9	0	1	0	0	2	1 534,7536	
AWF _{H2O} _P4	fasciclin-like arabinogalactan protein 12 [Gossypium hirsutum]	ABV27483.1	43 894,2	1	1.88%	LADEINTR	69.5	47	22.5	0	2	0	0	2	931.4849
	pepti (ISS) (putative Cyclophilin) [Ostreococcus tauri]	CAL57205.1	38 854,4	1	3.27%	IVLGLFGDDAPR	56.1	46.3	9.8	0	2	0	0	2	1 272,6955
	oxidoreductase family protein [Arabidopsis thaliana]	NP_188715.2	38 560,4	1	3.94%	DVAVLEAMLESQAK	96.1	46.1	50	0	1	0	0	2	1 448,7308
	CYP1 (putative cyclophilin_ABH_like) [Vigna radiata]	BAB82452.1	18 188,7	1	6.98%	IVFELFADTTTPR	76.5	46	30.5	0	1	0	0	2	1 408,7479
	hypothetical protein (putative 14-3-3 protein) [Vitis vinifera]	CAN81774.1	29 523,7	1	4.58%	TVEVELTVEER	86	46.5	39.5	0	1	0	0	2	1 432,7172
	peroxidase [Spinacia oleracea]	CAA71493.1	33 435,5	2	7.12%	MGASILR	46.2	47.7	-1.5	0	1	0	0	2	763,4137
peroxidase [Spinacia oleracea]	CAA71493.1	33 435,5	2	7.12%	MGNISPLTGSSGEIR	87.1	45.8	41.3	0	3	0	0	2	1 534,7536	
AWF _{H2O} _P5	fasciclin-like arabinogalactan protein 12 [Gossypium hirsutum]	ABV27483.1	43 894,2	1	1.88%	LADEINTR	54.4	47	7.4	0	2	0	0	2	931.4849
	unnamed protein product (putative Thaumatin family) [Vitis vinifera]	CAO62993.1	26 139,4	1	4.07%	GSDGSVIGCK	80.8	46.7	34.1	0	2	0	0	2	979,452
	CYP1 (putative cyclophilin_ABH_like) [Vigna radiata]	BAB82452.1	18 188,7	1	6.98%	IVFELFADTTTPR	73	46	27	0	1	0	0	2	1 408,7479
	Protein P21 (putative Thaumatin family) [Glycine max]	P25096.1	25 930,1	1	4.18%	TGCNFDGSGR	81.4	46	35.4	0	2	0	0	2	1 070,4326
	peroxidase [Spinacia oleracea]	CAA71493.1	33 435,5	2	7.12%	MGASILR	45.5	47.7	-2.2	0	1	0	0	2	763,4137
	peroxidase [Spinacia oleracea]	CAA71493.1	33 435,5	2	7.12%	MGNISPLTGSSGEIR	83.1	45.8	37.3	0	4	0	0	2	1 534,7536
transaldolase [Lycopersicon esculentum]	AAG16981.1	55 421,0	1	2.13%	VTSVASFVSR	59	46.2	12.8	0	1	0	0	2	1 199,6423	
AWF _{H2O} _P6	CYP1 (putative cyclophilin_ABH_like) [Vigna radiata]	BAB82452.1	18 188,7	1	6.98%	IVFELFADTTTPR	72.9	46	26.9	0	1	0	0	2	1 408,7479
	iron-superoxide dismutase precursor [Vigna unguiculata]	AAF28773.1	27 393,8	1	6.53%	ASLGLQNVAGINLLFK	83	45.4	37.6	0	1	0	0	2	1 699,9747
	peroxidase [Spinacia oleracea]	CAA71493.1	33 435,5	2	7.12%	MGASILR	51.8	47.7	4.1	0	2	0	0	2	763,4137
	peroxidase [Spinacia oleracea]	CAA71493.1	33 435,5	2	7.12%	MGNISPLTGSSGEIR	105	45.8	59.2	0	4	1	0	2	1 534,7536
	ATAM11, amidase [Arabidopsis thaliana]	NP_563831.1	45 038,6	1	3.53%	LVDFSIGDTGGSVR	91.2	45.8	45.4	0	1	0	0	2	1 523,7707
AWF _{NL-CU} _P1	peroxidase [Populus alba x Populus tremula var. glandulosa]	AAX53172.1	33 367,4	2	7.59%	GFEVIDTIK	59.6	47.7	11.9	0	1	0	0	2	1 021,5571

	peroxidase [Populus alba x Populus tremula var. glandulosa]	AAX53172.1	33 367,4	2	7.59%	MGNISPLTGTNGEIR	57.3	45.8	11.5	0	1	0	0	2	1 559,7854
	peroxidase [Sesamum indicum]	ABB89209.1	35 838,4	2	6.97%	IAIDMDPTTPR	73.6	47.7	25.9	0	1	0	0	2	1 245,6152
	peroxidase [Sesamum indicum]	ABB89209.1	35 838,4	2	6.97%	VSCADILALATR	89.5	47.1	42.4	0	2	0	0	2	1 289,6889
	pectinacetyltransferase precursor [Vigna radiata var. radiata]	CAA67728.1	43 804,9	2	8.77%	VFAAVVDDLLAK	50.7	46.6	4.1	0	1	0	0	2	1 260,7204
	pectinacetyltransferase precursor [Vigna radiata var. radiata]	CAA67728.1	43 804,9	2	8.77%	YCDGSSFTGDVEAVDPATNLHFR	78.7	44	34.7	0	0	1	0	2	2 558,1258
	Peroxidase 45 precursor [Arabisopsis thaliana]	Q96522.1	35 811,1	1	8.00%	GLFTSDQILFTDQR	86.6	45.3	41.3	0	2	0	0	2	1 640,8287
	Peroxidase 45 precursor [Arabisopsis thaliana]	Q96522.1	35 811,1	1	8.00%	VSCADILALATR	89.5	47.1	42.4	0	2	0	0	2	1 289,6889
	acid alpha galactosidase 1 [Cucumis sativus]	ABC55266.1	45 680,3	1	1.94%	VAVVLLNR	56.2	45.6	10.6	0	1	0	0	2	883,5728
	pectin acetyltransferase [Eucalyptus globulus subsp. globulus]	ABG34280.1	38 829,9	2	6.29%	AEENPDFFNWNR	81.6	45.8	35.8	0	1	0	0	2	1 538,6663
	pectin acetyltransferase [Eucalyptus globulus subsp. globulus]	ABG34280.1	38 829,9	2	6.29%	AIDCPYPCDK	53.5	48.9	4.6	0	1	0	0	2	1 238,5189
	Fructose-bisphosphate aldolase, chloroplast precursor [Oryza sativa (japonica cultivar-group)]	ABA91632.2	42 913,5	1	3.26%	LASIGLETEANR	88.3	46	42.3	0	1	0	0	2	1 387,7181
	CYP1 (putative cyclophilin_ABH_like) [Vigna radiata]	BAB82452.1	18 188,7	2	15.10%	IVFELFADTTTPR	90.4	46	44.4	0	1	0	0	2	1 408,7479
	CYP1 (putative cyclophilin_ABH_like) [Vigna radiata]	BAB82452.1	18 188,7	2	15.10%	TSRPVAIADCGQLS	40.7	46.1	-5.4	0	1	0	0	2	1 474,7326
	peroxidase2 [Medicago sativa]	CAC38106.1	35 992,3	2	9.12%	FDGLVSR	50	47.7	2.3	0	2	0	0	2	793,4209
	peroxidase2 [Medicago sativa]	CAC38106.1	35 992,3	2	9.12%	IAINMDPTTPR	89.1	46.5	42.6	0	3	0	0	2	1 244,6311
	peroxidase2 [Medicago sativa]	CAC38106.1	35 992,3	2	9.12%	VSCADILALATR	89.5	47.1	42.4	0	2	0	0	2	1 289,6889
	Polygalacturonase inhibitor 2 precursor [Phaseolus vulgaris]	P58822.1	37 086,3	1	4.09%	ISGAIPDSYGSFSK	62	45.8	16.2	0	1	0	0	2	1 428,7010
	basic chitinase, chitinase [Arabisopsis thaliana]	NP_566426.1	36 196,3	2	7.46%	IGFYQR	31.7	45.3	-13.6	0	1	0	0	2	783,4154
	basic chitinase, chitinase [Arabisopsis thaliana]	NP_566426.1	36 196,3	2	7.46%	LPGYGVITNIINGGLECGR	103	44.9	58.1	0	1	1	0	2	2 003,0385
	cyclophilin [Phaseolus vulgaris]	CAA52414.1	18 141,5	1	8.14%	VFFDMTIGGQPAGR	79.8	45.7	34.1	0	2	0	0	2	1 511,7319
	endochitinase precursor [Humulus lupulus]	AAD34596.1	33 511,4	1	6.01%	GFYTYDAFLTAAR	71.5	46	25.5	0	1	0	0	2	1 495,7221
	unnamed protein product [Populus trichocarpa]	ABK94155.1	77 435,5	1	1.28%	TCAQDEVLR	53.5	46.8	6.7	0	1	0	0	2	1 091,5157
	unnamed protein product (putative Serine carboxypeptidase) [Vitis vinifera]	CAO68876.1	57 192,0	1	2.96%	NLEVGIPDLLEDGIK	58.1	45.3	12.8	0	2	0	0	2	1 624,8801
	CYP1 (putative cyclophilin_ABH_like) [Vigna radiata]	BAB82452.1	18 188,7	1	6.98%	IVFELFADTTTPR	90	46	44	0	1	0	0	2	1 408,7479
	peroxidase [Sesamum indicum]	ABB89209.1	35 838,4	2	9.09%	DHPDNLSLAGDGFDTVIK	56.9	45.3	11.6	0	0	1	0	2	1 913,9248
	peroxidase [Sesamum indicum]	ABB89209.1	35 838,4	2	9.09%	VSCADILALATR	93.1	47.1	46	0	1	0	0	2	1 289,6889
	Probable non-specific lipid-transfer protein AKCS9 precursor [Vigna unguiculata]	Q43681.1	10 431,0	2	24.20%	KVLSNCGVITYPNC	31.6	45.7	-14.1	0	1	0	0	2	1 511,6987
	Probable non-specific lipid-transfer protein AKCS9 precursor [Vigna unguiculata]	Q43681.1	10 431,0	2	24.20%	VQEPCLCNYYK	53.9	47.5	6.4	0	1	0	0	2	1 423,6716
	peroxidase2 [Medicago sativa]	CAC38106.1	35 992,3	2	9.12%	FDGLVSR	47.7	47.7	0	0	1	0	0	2	793,4209
	peroxidase2 [Medicago sativa]	CAC38106.1	35 992,3	2	9.12%	IAINMDPTTPR	81.8	46.5	35.3	0	2	0	0	2	1 228,6362
	peroxidase2 [Medicago sativa]	CAC38106.1	35 992,3	2	9.12%	VSCADILALATR	93.1	47.1	46	0	1	0	0	2	1 289,6889
	unnamed protein product [Vitis vinifera]	CAO17011.1	42 507,9	3	6.11%	LFSPGNLR	34.6	47.3	-12.7	0	1	0	0	2	903,5053
	unnamed protein product [Vitis vinifera]	CAO17011.1	42 507,9	3	6.11%	TTYVLALK	33.9	46.4	-12.5	0	1	0	0	2	908,5457
	unnamed protein product [Vitis vinifera]	CAO17011.1	42 507,9	3	6.11%	VINNLDER	62.1	46.7	15.4	0	1	0	0	2	972,5114
	basic chitinase, chitinase [Arabisopsis thaliana]	NP_566426.1	36 196,3	1	5.67%	LPGYGVITNIINGGLECGR	114	44.9	69.1	0	1	0	0	2	2 003,0385
	cyclophilin [Phaseolus vulgaris]	CAA52414.1	18 141,5	1	8.14%	VFFDMTIGGQPAGR	71	45.7	25.3	0	1	1	0	2	1 511,7319
	iron-superoxide dismutase precursor [Vigna unguiculata]	AAF28773.1	27 393,8	2	8.98%	LVSWDVSSR	73.1	46.5	26.6	0	1	0	0	2	1 119,5798
	iron-superoxide dismutase precursor [Vigna unguiculata]	AAF28773.1	27 393,8	2	8.98%	SLEEHVTAYNK	52.9	46.2	6.7	0	1	0	0	2	1 379,7421
	pectinacetyltransferase precursor [Vigna radiata var. radiata]	CAA67728.1	43 804,9	1	3.01%	VFAAVVDDLLAK	54.2	46.6	7.6	0	1	0	0	2	1 260,7204
	endochitinase precursor [Humulus lupulus]	AAD34596.1	33 511,4	1	4.11%	GFYTYDAFLTAAR	69.8	46	23.8	0	1	0	0	2	1 495,7221
	xyloglucan endotransglucosylase/hydrolase 2 [Cucumis melo]	ABI94062.1	36 316,1	1	3.88%	TDWSQAPFTASYR	79.9	45.8	34.1	0	1	0	0	2	1 529,7025
	Phosphoglucomutase, cytoplasmic [Pisum sativum]	Q9SM60.1	63 106,2	2	4.12%	LSGTGSEGATIR	112	46.5	65.5	0	1	0	0	2	1 148,5913
	Phosphoglucomutase, cytoplasmic [Pisum sativum]	Q9SM60.1	63 106,2	2	4.12%	YDYENVDAAGAAK	62.2	47.5	14.7	0	1	0	0	2	1 315,5807
	putative pectin methyltransferase 3 [Linum usitatissimum]	AAG17110.1	69 430,1	1	1.90%	DITFQNTAGPSK	66.1	46.6	19.5	0	1	0	0	2	1 278,6333
	pectin acetyltransferase [Eucalyptus globulus subsp. globulus]	ABG34280.1	38 829,9	2	6.29%	AEENPDFFNWNR	81.8	45.8	36	0	1	0	0	2	1 538,6663
	pectin acetyltransferase [Eucalyptus globulus subsp. globulus]	ABG34280.1	38 829,9	2	6.29%	AIDCPYPCDK	48.5	46.5	2	0	1	0	0	2	1 238,5189
AWF _{NaCl} _P2	Probable non-specific lipid-transfer protein AKCS9 precursor [Vigna unguiculata]	Q43681.1	10 431,0	2	22.20%	KVLSNCGVITYPNC	51.6	45.7	5.9	0	1	0	0	2	1 511,6987
	Probable non-specific lipid-transfer protein AKCS9 precursor [Vigna unguiculata]	Q43681.1	10 431,0	2	22.20%	QYVNSPGAK	33.6	47.7	-14.1	0	1	0	0	2	963,49
	pepti (ISS) (putative Cyclophilin) [Ostreococcus tauri]	CAL57205.1	38 854,4	1	3.27%	IVLGLFGDDAPR	57.7	46.3	11.4	0	2	0	0	2	1 272,6955
	unnamed protein product (putative Thaumatin family) [Vitis vinifera]	CAO62993.1	26 139,4	1	4.07%	GSDGSVIGCK	61.2	46.7	14.5	0	1	0	0	2	979,452
	CYP1 (putative cyclophilin_ABH_like) [Vigna radiata]	BAB82452.1	18 188,7	2	10.50%	IVFELFADTTTPR	90	46	44	0	2	0	0	2	1 408,7479
	CYP1 (putative cyclophilin_ABH_like) [Vigna radiata]	BAB82452.1	18 188,7	2	10.50%	TAENFR	40	47.9	-7.9	0	1	0	0	2	737,3582
	ubiquitin/ribosomal protein 27a [Prunus avium]	AAG13985.1	85 258,5	1	1.18%	TLADYNIQK	57.2	46.4	10.8	0	20	0	0	2	1 065,5582
	peroxidase2 [Medicago sativa]	CAC38106.1	35 992,3	2	5.47%	FDGLVSR	49.4	47.7	1.7	0	1	0	0	2	793,4209
AWF _{NaCl} _P3	Probable non-specific lipid-transfer protein AKCS9 precursor [Vigna unguiculata]	Q43681.1	10 431,0	2	22.20%	KVLSNCGVITYPNC	51.6	45.7	5.9	0	1	0	0	2	1 511,6987
	Probable non-specific lipid-transfer protein AKCS9 precursor [Vigna unguiculata]	Q43681.1	10 431,0	2	22.20%	QYVNSPGAK	33.6	47.7	-14.1	0	1	0	0	2	963,49
	pepti (ISS) (putative Cyclophilin) [Ostreococcus tauri]	CAL57205.1	38 854,4	1	3.27%	IVLGLFGDDAPR	57.7	46.3	11.4	0	2	0	0	2	1 272,6955
	unnamed protein product (putative Thaumatin family) [Vitis vinifera]	CAO62993.1	26 139,4	1	4.07%	GSDGSVIGCK	61.2	46.7	14.5	0	1	0	0	2	979,452
	CYP1 (putative cyclophilin_ABH_like) [Vigna radiata]	BAB82452.1	18 188,7	2	10.50%	IVFELFADTTTPR	90	46	44	0	2	0	0	2	1 408,7479
	CYP1 (putative cyclophilin_ABH_like) [Vigna radiata]	BAB82452.1	18 188,7	2	10.50%	TAENFR	40	47.9	-7.9	0	1	0	0	2	737,3582
	ubiquitin/ribosomal protein 27a [Prunus avium]	AAG13985.1	85 258,5	1	1.18%	TLADYNIQK	57.2	46.4	10.8	0	20	0	0	2	1 065,5582
	peroxidase2 [Medicago sativa]	CAC38106.1	35 992,3	2	5.47%	FDGLVSR	49.4	47.7	1.7	0	1	0	0	2	793,4209

	peroxidase2 [Medicago sativa]	CAC38106.1	35 992.3	2	5.47%	IAINMDPTTPR	81.3	46.5	34.8	0	2	0	0	2	1 244,6311
	aldehyde reductase [Vigna radiata]	AAD53967.1	35 565.6	1	3.69%	DPQTELLDPAVK	81.5	47.6	33.9	0	1	0	0	2	1 325,6955
	putative glycine-rich RNA-binding protein [Dianthus caryophyllus]	BAF34340.1	16 872.1	1	5.68%	SITVNEAQRS	53.9	46.4	7.5	0	1	0	0	2	1 104,5649
	cyclophilin [Phaseolus vulgaris]	CAA52414.1	18 141.5	1	11.60%	VFFDMTIGGQPAGR	79.2	45.7	33.5	0	2	0	0	2	1 511,7319
	peroxidase [Spinacia oleracea]	CAA71493.1	33 435.5	1	4.85%	MGNISPLTGSSGEIR	75.2	45.8	29.4	0	1	0	0	2	1 534,7536
	unnamed protein product [Populus trichocarpa]	ABK93386.1	83 612.9	1	0.92%	HIDE TLK	63	45.7	17.3	0	2	0	0	2	855,4578
AWF _{NaCl} _P4	Os09g0537600 [Oryza sativa (japonica cultivar-group)]	NP_001063792.1	23 389.0	1	5.58%	IVIGLYGDVVPK	53.5	46.3	7.2	0	1	0	0	2	1 272,7570
	oxidoreductase family protein [Arabidopsis thaliana]	NP_188715.2	38 560.4	1	3.94%	DVAVLEAMLES GAK	107	46.1	60.9	0	1	0	0	2	1 448,7308
	CYP1 (putative cyclophilin_ABH_like) [Vigna radiata]	BAB82452.1	18 188.7	2	10.50%	IVFELFADTTTPR	72.9	46	26.9	0	2	0	0	2	1 408,7479
	CYP1 (putative cyclophilin_ABH_like) [Vigna radiata]	BAB82452.1	18 188.7	2	10.50%	TAENFR	37.2	47.9	-10.7	0	1	0	0	2	737,3582
	Cysteine proteinase inhibitor [Vigna unguiculata]	Q06445.1	10 740.0	1	16.50%	DVAGNQNSLEIDSLAR	63.4	45.2	18.2	0	1	0	0	2	1 701,8408
	peroxidase2 [Medicago sativa]	CAC38106.1	35 992.3	2	5.47%	FDGLVSR	33.4	47.7	-14.3	0	1	0	0	2	793,4209
	peroxidase2 [Medicago sativa]	CAC38106.1	35 992.3	2	5.47%	IAINMDPTTPR	65.2	46.5	18.7	0	1	0	0	2	1 244,6311
	putative glycine-rich RNA-binding protein [Dianthus caryophyllus]	BAF34340.1	16 872.1	1	5.68%	SITVNEAQRS	56.6	46.4	10.2	0	1	0	0	2	1 104,5649
	cyclophilin [Phaseolus vulgaris]	CAA52414.1	18 141.5	1	11.60%	VFFDMTIGGQPAGR	89.8	45.7	44.1	0	2	0	0	2	1 511,7319
	peroxidase [Spinacia oleracea]	CAA71493.1	33 435.5	2	7.12%	MGASILR	49.8	47.7	2.1	0	2	0	0	2	763,4137
	peroxidase [Spinacia oleracea]	CAA71493.1	33 435.5	2	7.12%	MGNISPLTGSSGEIR	56.4	45.8	10.6	0	1	0	0	2	1 534,7536
	pterocarpan reductase [Lotus japonicus]	BAF34844.1	33 974.1	1	3.23%	AGHPTFALVR	59.6	46	13.6	0	0	1	0	2	1 068,5955
	unnamed protein product [Populus trichocarpa]	ABK94155.1	77 435.5	1	1.28%	TCAQDEVLR	65.5	46.8	18.7	0	1	0	0	2	1 091,5157
	Os01g0840100 [Oryza sativa (japonica cultivar-group)]	NP_001044757.1	71 715.0	1	1.99%	TTPSYVAFTDSEIR	67.2	45.9	21.3	0	2	0	0	2	1 473,6861
pterocarpan reductase [Lotus japonicus]	BAF34842.1	36 176.4	1	3.09%	VHILGDGNPK	58.9	45.9	13	0	1	0	0	2	1 025,5998	
AWF _{NaCl} _P5	unnamed protein product (putative Thaumatin family) [Vitis vinifera]	CAO62993.1	26 139.4	1	4.07%	GSDGSVIGCK	76.2	46.7	29.5	0	2	0	0	2	979,452
	CYP1 (putative cyclophilin_ABH_like) [Vigna radiata]	BAB82452.1	18 188.7	1	6.98%	IVFELFADTTTPR	76.6	46	30.6	0	2	0	0	2	1 408,7479
	peroxidase2 [Medicago sativa]	CAC38106.1	35 992.3	1	3.34%	IAINMDPTTPR	58.7	46.5	12.2	0	1	0	0	2	1 244,6311
	putative glycine-rich RNA-binding protein [Dianthus caryophyllus]	BAF34340.1	16 872.1	1	5.68%	SITVNEAQRS	60.8	46.4	14.4	0	1	0	0	2	1 104,5649
	Protein P21 (putative Thaumatin family) [Glycine max]	P25096.1	25 930.1	1	4.18%	TGCNFDGSGR	86	46	40	0	1	0	0	2	1 070,4326
	cyclophilin [Phaseolus vulgaris]	CAA52414.1	18 141.5	1	8.14%	VFFDMTIGGQPAGR	90.1	45.7	44.4	0	2	0	0	2	1 511,7319
	peroxidase [Spinacia oleracea]	CAA71493.1	33 435.5	1	4.85%	MGNISPLTGSSGEIR	87.1	45.8	41.3	0	1	0	0	2	1 534,7536
	Os01g0840100 [Oryza sativa (japonica cultivar-group)]	NP_001044757.1	71 715.0	1	1.99%	TTPSYVAFTDSEIR	67.5	45.9	21.6	0	1	0	0	2	1 473,6861
AWF _{NaCl} _P6	CYP1 (putative cyclophilin_ABH_like) [Vigna radiata]	BAB82452.1	18 188.7	1	6.98%	IVFELFADTTTPR	76.5	46	30.5	0	1	0	0	2	1 408,7479
	putative glycine-rich RNA-binding protein [Dianthus caryophyllus]	BAF34340.1	16 872.1	1	5.68%	SITVNEAQRS	73.2	46.4	26.8	0	1	0	0	2	1 104,5649
	cyclophilin [Phaseolus vulgaris]	CAA52414.1	18 141.5	1	8.14%	VFFDMTIGGQPAGR	56.4	45.7	10.7	0	1	0	0	2	1 511,7319
	peroxidase [Spinacia oleracea]	CAA71493.1	33 435.5	1	4.85%	MGNISPLTGSSGEIR	88.6	45.8	42.8	0	2	0	0	2	1 534,7536

^a AWF_{H2O} and AWF_{NaCl} describe the apoplast extraction solution from which the BN-PAGE followed by protein sequencing was performed, respectively.

Numbers P1 to P6 correspond to the numbers given in Fig. 3

^b Identities are based on sequence comparisons using the NCBI green plants protein database

^c Accession numbers are based on sequence comparisons using the NCBI green plants protein database

^d Molecular weights (MW) are based on sequence comparisons using the NCBI green plants protein database

^e Protein sequence coverage obtained with the peptides identified by mass spectrometry

Supplementary material for Chapter III.

Characterizing genotypic and silicon-enhanced manganese tolerance in cowpea (*Vigna unguiculata* L.) through apoplastic peroxidase and leaf-metabolome profiling

Hendrik Führs¹, André Specht¹, Joachim Kopka², Sébastien Gallen³, Dimitri Heintz⁴, Alain Van Dorsselaer³, Hans-Peter Braun⁵ & Walter J. Horst¹

to be submitted

¹ Institute of Plant Nutrition, Faculty of Natural Sciences, Leibniz University Hannover, Herrenhäuser Str. 2, 30419 Hannover, Germany

² Max Planck Institute of Molecular Plant Physiology, Am Mühlenberg 1, 14476 Potsdam-Golm, Germany

³ Laboratoire de Spectrométrie de Masse Bio-Organique, IPHC-DSA, ULP, CNRS, UMR7178 ; 25 rue Becquerel, 67 087 Strasbourg, France

⁴ Institut de Biologie Moléculaire des Plantes (IBMP) CNRS-UPR2357,ULP, 67083 Strasbourg, France

⁵ Institute of Plant Genetics, Faculty of Natural Sciences, Leibniz University Hannover, Herrenhäuser Str. 2, 30419 Hannover, Germany

Tab. S1.1. Identified metabolites from bulk-leaf homogenates of the two cowpea cultivars TVu 91 and TVu 1987 and their relative changes in abundance including statistical significance as affected by Mn and Si treatments

a.) TVu 91

Metabolite	<i>p</i> -value (t-test)	
	Mn-effect	
Succinic acid	2.97E-05	1.62
Threonic acid-1,4-lactone	2.03E-04	0.58
Aspartic acid BP2	4.34E-04	0.50
Erythronic acid	4.00E-04	1.18
Fructose BP1	2.20E-04	0.57
M000000_A194007	5.19E-07	3.67
A194005 or Coniferylalcohol	9.06E-07	4.28
Gluconic acid	2.49E-05	9.66
A207009	3.29E-04	2.56
A245004_2436	1.58E-05	2.09
Sucrose MP	2.43E-04	1.55
Serine BP1	0.0036	0.31
Glyceric acid	5.24E-05	0.74
Serine MP	0.022	0.23
Aspartic acid MP	0.0012	0.54
Ascorbic acid	0.0031	0.34
Pyroglutamic acid	0.022	1.22
4-aminobutyric acid	0.014	0.55
Threonic acid	0.0011	0.74
2-hydroxyglutaric acid	0.025	0.89
M000000_A159003	0.014	1.19
Asparagine MP	0.0048	0.34
M000000_A170001	0.037	1.27
M000000_A174001	0.015	1.19
A183011	0.015	1.29
Dehydroascorbic acid dimer	0.014	0.58
Fructose MP	0.0016	0.62
M000000_A187005	0.017	1.21
M000238_A190007	0.0049	1.32
Galactose BP1	0.035	0.55
A192018	0.011	0.38
Sorbitol / Galactitol	0.003	0.39
Galactonic acid	0.0082	1.14
M000000_A201002	0.022	1.36
M000000_A207008	0.022	1.36
M000000_A211001	7.64E-04	1.23
M000000_A214003	0.0025	1.27
A223007	0.046	1.24
M000000_A225004	6.23E-04	0.64
Galactosylglycerol	0.0015	1.31
M000000_A250001	0.0018	1.39
A255001_2537	0.015	1.34
M000000_A311002	0.033	1.56
	Si-effect	
Glyceric acid	5.15E-05	2.14
M0000000_A141003	7.23E-08	2.58
2-hydroxyglutaric acid	2.50E-05	0.65
Shikimic acid	7.60E-05	1.58
Fructose MP	2.62E-06	3.60
Fructose BP1	1.32E-05	3.67
Glucose MP	4.79E-05	5.48
Glucose BP1	5.27E-06	4.47
M000000_A207008	6.60E-05	1.72
M000000_A214003	1.30E-05	1.78

M000000_A225004	1.14E-04	1.73
M000000_A248003	1.18E-04	0.53
Sucrose MP	7.86E-05	1.92
Benzoic acid	0.017	0.79
Serine BP1	7.57E-04	2.17
Threonine BP1	0.015	1.66
Succinic acid	0.044	1.10
M000000_A140003	0.0018	1.24
Threonic acid-1,4-lactone	6.21E-04	1.54
Threonic acid	0.039	1.16
M000000_A159003	0.017	1.12
Xylose MP	0.013	1.31
A183011	0.038	1.14
Dehydroascorbic acid dimer	0.011	1.32
Quinic acid	8.15E-04	1.49
A188011	5.87E-04	2.31
Gluconic acid-1,5-lactone	0.0026	1.25
M000238_A190007	0.0025	0.75
Galactose BP1	0.027	2.52
M000000_A192007	0.0074	0.64
M000000_A194007	0.0055	0.75
Galactonic acid	0.018	1.12
M000000_A201002	0.0072	1.18
<i>myo</i> -Inositol	0.0015	1.36
M000000_A211001	8.98E-04	1.23
A216006	0.014	0.82
M000000_A217004	0.017	0.85
Galactosylglycerol	0.046	0.89
M000000_A242009	0.0016	1.78
Xylobiose BP	0.038	0.77
A245004_2436	7.66E-04	1.53
M000000_A246005	0.0029	0.67
A255001_2537	0.012	1.37
M000000_A279002	5.58E-04	1.77
M000000_A291005	0.0077	1.81
Galactinol	0.0099	1.82
Si-effect in Mn-treated plants		
Glyceric acid	6.73E-05	1.62
4-aminobutyric acid	7.79E-06	3.92
Xylobiose BP	1.51E-04	0.74
Serine BP1	0.044	1.75
Phosphoric acid	0.0069	1.25
Ascorbic acid	0.0011	1.51
Succinic acid	0.014	1.15
M000000_A140003	0.011	1.11
Threonic acid-1,4-lactone	0.0058	1.28
Erythronic acid-1,4-lactone	0.023	1.15
Erythritol	0.0022	1.22
Pyroglutamic acid	0.0012	0.76
Threonic acid	0.020	1.15
2-hydroxyglutaric acid	0.030	1.11
Glutamic acid	0.031	0.72
Shikimic acid	0.0040	0.71
A183011	0.030	0.78
Dehydroascorbic acid dimer	0.026	1.53
M000238_A190007	0.0032	1.19
Galactose BP1	0.019	1.57
A192018	0.012	1.50
A194005 / Coniferylalcohol	0.029	1.09
Galactonic acid	0.0027	1.13
M000000_A207008	0.0089	1.20
A207009	0.022	1.28
<i>myo</i> -Inositol	0.0052	1.23

M000000_A214003	0.0026	1.27
M000000_A217004	0.0074	1.14
M000000_A225004	5.34E-04	1.52
Galactosylglycerol	0.0038	0.80
A255001_2537	0.034	0.85
M000000_A261006	0.049	1.25
Sucrose MP	0.0023	1.26
M000000_A291005	0.040	1.28
Mn-effect in Si-treated plants		
Benzoic acid	4.83E-04	1.56
Serine BP1	1.78E-05	0.25
Succinic acid	1.29E-04	1.70
Glyceric acid	3.00E-08	0.56
Threonic acid-1,4-lactone	1.59E-05	0.48
Aspartic acid BP1	1.43E-04	0.47
2-hydroxyglutaric acid	2.57E-05	1.51
Shikimic acid	4.42E-05	0.40
Quinic acid	2.68E-04	0.61
Fructose MP	3.35E-07	0.18
M000000_A187005	4.04E-04	1.37
Fructose BP1	2.21E-05	0.17
A188011	7.41E-05	0.42
Glucose MP	2.99E-06	0.17
M000238_A190007	3.17E-06	2.08
Glucose BP1	1.68E-05	0.21
M000000_A194007	2.63E-08	5.68
A194005 / Coniferylalcohol	2.91E-05	5.13
Gluconic acid	2.65E-05	8.70
M000000_A217004	1.66E-04	1.45
M000000_A225004	2.15E-05	0.56
A254004_2436	2.02E-05	1.28
M000000_A246005	1.49E-05	1.39
M000000_A248003	1.61E-04	2.07
Ascorbic acid	0.0081	0.34
Glycoloc acid	0.013	1.44
A113001	0.016	1.38
Benzylalcohol	0.012	1.71
Monomethylphosphate	0.024	0.71
Malonic acid	0.022	1.74
Threonine BP1	8.57E-04	0.44
A137006	0.010	1.50
M000000_A140003	0.0016	0.86
M000000_A141003	0.018	0.083
4-aminobutyric acid	0.025	2.60
Erythronic acid	0.0021	1.22
Threonic acid	0.0028	0.74
M000000_A159003	0.012	1.14
4-hydroxybenzoic acid	0.018	1.50
Asparagine MP	7.04E-04	0.23
M000000_A174001	0.0025	1.18
cis-4-hydroxycinnamic acid	0.0011	1.31
Dehydroascorbic acid dimer	0.0039	0.67
Gluconic acid-1,5-lactone	0.044	0.87
Galactose BP1	0.015	0.34
A192018	5.86E-04	0.46
M000000_A192007	0.0058	1.67
Mannitol	0.033	0.86
Sorbitol / Galactitol	0.0016	0.26
Galactonic acid	0.0010	1.15
Hexadecanoic acid	0.038	1.39
A207009	0.0013	2.75
myo-inositol	0.0034	0.83
A216006	0.0027	1.30

Octadecanoic acid	0.035	1.33
Spermidine MP	0.039	0.46
Galactosylglycerol	0.012	1.18
M000000_A242009	0.0026	0.55
M000000_A250001	0.0012	1.30
A255001_2537	0.0099	0.83
M000000_A261006	0.038	1.43
M000000_A279002	0.0086	0.62
M000000_A291005	0.0023	0.54
Galactinol	0.0060	0.48
M000000_A311002	0.027	1.58

b.) TVu 1987

Metabolite	<i>p</i> -value (t-test)	
	Mn-effect	fold induction / reduction
M000000_A141003	3.94E-05	0.37
Arabitol	2.35E-04	1.44
Quinic acid	3.79E-07	0.34
M000000_A187005	8.87E-05	1.38
A192018	1.05E-04	0.28
M000000_A192007	9.04E-07	2.09
M000000_A194007	1.43E-06	7.88
A194005 / Coniferylalcohol	4.07E-05	5.07
Gluconic acid	1.64E-04	6.83
M000000_A211001	4.71E-06	1.75
M000000_A214003	4.44E-05	2.64
M000000_A225004	2.52E-04	0.59
Hydroxylamine	0.035	0.59
Ascorbic acid	0.0022	0.26
Monomethylphosphate	0.0057	0.35
Ethanolamine MP	0.033	0.70
Phosphoric acid	0.013	0.65
Glyceric acid	0.013	1.45
M000000_A140003	9.19E-04	1.63
Threonic acid-1,4-lactone	8.31E-04	0.80
Erythronic acid-1,4-lactone	0.023	0.77
Malic acid	0.020	1.32
Erythritol	0.017	1.22
Erythronic acid	0.022	1.19
Threonic acid	0.0021	0.71
2-hydroxyglutaric acid	0.026	1.34
Citric acid	0.0041	1.26
A183011	0.047	1.41
Dehydroascorbic acid dimer	6.9E-04	0.47
M000238_A190007	0.0094	1.60
Galactose BP1	0.021	0.38
Glucose BP1	0.0031	1.42
Sorbitol / Galactitol	0.0061	0.21
M000000_A201002	0.042	0.87
A207009	5.13E-04	3.94
A216006	0.015	0.69
Spermidine MP	0.015	0.28
A245004_2436	0.0077	0.58
M000000_A248003	0.0099	2.27
A255001_2537	0.0027	0.78
M000000_261006	0.0020	0.31
Sucrose MP	0.0055	1.61
Maltose A247001 2727	0.012	1.47
	Si-effect	
Arabitol	1.93E-07	0.42
Glucose MP	5.72E-06	1.84
Glucose BP1	1.94E-04	1.97
Malonic acid MP	0.020	0.81
Ethanolamine MP	0.031	0.68
Threonic acid-1,4-lactone	0.018	1.51
Threonine MP	0.020	6.78
M000000_A141003	0.033	1.50
Aspartic acid BP2	0.0093	1.31
Erythritol	0.021	1.40
Aspartic acid MP	0.028	9.20
Glutamic acid MP	0.016	5.77
Xylose MP	0.022	0.77
Fructose MP	0.0026	1.93
M000000_A187005	0.048	0.88

Fructose BP1	0.0019	1.92
Mannitol	0.0014	0.83
Ononitol	0.0091	3.31
M000000_A207008	0.042	1.36
M000000_A211001	0.0091	1.25
M000000_A225004	0.0050	1.86
A239004	0.011	1.55
M000000_A242009	0.0040	1.85
M000000_A250001	0.015	1.49
A255001_2537	0.020	1.42
M000000_A261006	0.018	0.56
M000000_A276001	0.0035	0.82
M000000_A279002	9.64E-04	1.50
M000000_A291005	0.0053	1.49
Galactinol	0.0051	1.56
Raffinose	9.76E-04	1.88
Si-effect in Mn-treated plants		
Phosphoric acid	3.30E-04	1.48
Glyceric acid	2.88E-05	0.65
M000000_A140003	2.25E-06	0.69
Arabitol	4.15E-05	0.63
A183011	9.62E-05	0.25
M000000_A214003	2.94E-04	0.60
A223007	4.27E-04	0.72
Threonic acid-1,4-lactone	0.0027	1.12
Ascorbic acid	0.016	2.01
M000000_A141003	0.033	0.77
M000000_A146004	0.012	1.42
4-aminobutyric acid	0.020	1.71
M000000_A161002	0.033	1.47
Fructose MP	0.0017	0.56
M000000_A187005	0.0087	0.91
Fructose BP1	0.036	0.60
Glucose MP	0.0025	0.58
Galactose BP1	0.027	2.02
Glucose BP1	7.71E-04	0.59
A192018	0.0011	2.23
M000000_A192007	0.0018	0.75
<i>p</i> -Tyramine MP	0.042	1.22
M000000_A207008	0.048	1.14
<i>myo</i> -Inositol	0.0062	1.21
M000000_A211001	0.0011	0.81
M000000_A217004	0.023	1.10
Octadecanoic acid	0.044	1.26
Galactosylglycerol	0.0037	0.82
A255001_2537	0.013	0.84
Sucrose MP	0.0016	0.80
M000000_A267006	0.046	0.50
Mn-effect in Si-treated plants		
M000000_A141003	3.12E-05	0.19
Arabitol	1.16E-06	2.17
A183011	4.42E-04	0.32
Quinic acid	1.32E-04	0.31
Fructose MP	1.81E-05	0.28
Glucose BP1	2.02E-04	0.42
M000000_A194007	1.74E-06	8.70
Sorbitol / Galactitol	2.43E-04	0.17
A194005 / Coniferylalcohol	1.62E-04	4.99
Gluconic acid	1.64E-04	6.21
M000000_A225004	6.69E-05	0.32
2-hydroxypyridine	0.0072	1.64
Ascorbic acid	0.018	0.38
A104001	0.043	2.03

Threonic acid-1,4-lactone	0.0073	0.59
Threonic acid	0.010	0.66
M000000_A174001	0.0027	1.17
Dehydroascorbic acid dimer	5.14E-04	0.45
M000000_A187005	0.011	1.43
Fructose BP1	6.22E-04	0.29
Glucose MP	0.0012	0.36
M000238_A190007	0.028	1.38
Galactose BP1	0.032	0.48
A192018	0.0034	0.51
M000000_A192007	0.0038	1.59
Ononitol	0.014	0.32
Glucose BP3	0.046	0.68
A207009	0.0016	2.90
M000000_A211001	0.033	1.14
M000000_A214003	0.039	1.42
A216006	0.049	0.67
Spermidine MP	0.018	0.32
A239004	0.0085	0.60
M000000_A242009	0.0027	0.51
A255001_2537	7.01E-04	0.46
Maltose_A247001_2727	0.045	1.53
M000000_A291005	0.029	0.67

c.) TVu 91 vs TVu 1987

Metabolite	<i>p</i> -value (t-test)	
	TVu 91 / TVu1987 (0.2 μ M Mn)	
Glyceric acid	3.50E-04	0.44
M000000_A140003	1.94E-04	2.08
Tartaric acid	4.52E-07	0.012
Arabitol	1.24E-05	0.48
Shikimic acid	4.70E-05	0.25
Dehydroascorbic acid dimer	6.79E-06	0.44
Quinic acid	5.49E-09	0.077
Fructose MP	3.26E-05	0.42
M000000_A187005	2.05E-05	1.44
Fructose BP1	5.67E-05	0.41
Glucose MP	1.25E-06	0.46
M000000_A207008	1.96E-04	0.44
myo-Inositol	2.61E-04	0.38
M000000_A211001	3.18E-05	1.43
M000000_A214003	3.84E-05	3.32
M000000_A225004	4.10E-07	0.14
Xylobiose BP	2.94E-05	11.41
A245004_2436	5.32E-05	3.05
A255001_2537	1.79E-04	0.51
Sucrose MP	3.19E-04	0.44
M000000_A267006	9.02E-05	3.60
Maltose_A279002_2727	5.14E-05	2.36
M000000_A279002	3.28E-04	0.56
Galactinol	1.52E-04	0.36
Hydroxylamine	0.024	0.43
Ascorbic acid	0.0037	0.30
Monomethylphosphate	0.0059	0.36
Malonic acid MP	0.0084	1.86
Serine BP1	0.0012	0.32
Ethanolamine MP	0.0076	0.44
Phosphoric acid	0.011	0.63
Threonine BP1	6.08E-04	0.26
Serine MP	0.028	3.80
Threonic acid-1,4-lactone	0.016	0.83
M000000_A141003	6.02E-04	0.44
Aspartic acid BP2	0.0040	0.67
Malic acid	0.0070	1.49
Erythritol	0.017	0.82
Aspartic acid MP	0.046	6.99
M000000_A159003	0.015	1.57
Asparagine MP	0.0033	5.13
M000000_A170002	0.011	1.76
M000000_A174001	0.0011	1.59
Citric acid	0.035	0.81
M000238_A190007	0.0025	0.55
Galactose BP1	0.0028	0.23
Glucose BP1	7.45E-04	0.54
A192018	0.0052	0.36
M000000_A192007	0.021	1.34
M000000_A194007	0.0017	1.57
Sorbitol / Galactitol	0.037	0.38
A194005 /Coniferylalcohol	0.012	0.63
Ononitol	0.0018	1.96
Galactonic acid	0.0034	1.23
M000000_A201002	9.20E-04	1.84
Galactosylglycerol	0.0073	1.85
A239004	0.0019	8.06
M000000_A246005	0.0040	1.51
M000000_A248003	0.013	3.59

M000000_A250001	0.0044	1.54
M000000_A291005	0.0027	0.51
TVu 91 / TVu1987 (50 µM Mn)		
Malonic acid	3.32E-04	2.37
Serine BP1	4.63E-05	0.11
Glyceric acid	8.67E-07	0.23
Erythritol	4.13E-06	0.64
M000000_A159003	2.85E-05	1.77
Tartaric acid	9.18E-07	0.013
M000000_A170002	4.21E-05	2.07
Arabitol	5.63E-05	0.37
M000000_A174001	9.08E-05	1.74
Shikimic acid	1.31E-05	0.28
Quinic acid	1.79E-04	0.18
Fructose MP	4.43E-05	0.27
Fructose BP1	1.88E-05	0.25
Glucose MP	3.99E-06	0.35
M000238_A190007	5.41E-07	0.45
Glucose BP1	1.91E-05	0.37
A194005 / Coniferylalcohol	5.63E-05	0.53
Galactonic acid	4.62E-04	1.36
M000000_A201002	7.09E-05	2.90
M000000_A207008	7.88E-05	0.55
A207009	5.33E-04	0.76
<i>myo</i> -Inositol	2.12E-04	0.43
M000000_A225004	4.35E-08	0.15
Galactosylglycerol	6.36E-06	1.90
Xylobiose BP	2.17E-10	10.09
A245004_2436	8.71E-06	11.07
M000000_A250001	2.20E-04	1.73
M000000_A261006	1.62E-05	3.26
Sucrose MP	1.80E-06	0.43
M000000_A267006	1.89E-04	3.11
M000000_A279002	7.78E-05	0.45
M000000_A291005	3.52E-04	0.42
Galactinol	3.78E-05	0.31
2-hydroxypyridine	0.0089	0.53
Ascorbic acid	0.0092	0.40
Glycolic acid	0.043	0.67
Monomethylphosphate	0.049	0.62
Diethylenglycol	0.019	0.76
Phosphoric acid	0.022	0.83
Threonine BP1	0.0031	0.30
Succinic acid	8.22E-04	1.39
M000000_A140003	8.81E-04	1.22
Threonic acid-1,4-lactone	0.0012	0.61
Aspartic acid BP2	6.28E-04	0.33
M000000_A146004	0.043	0.75
4-aminobutyric acid	0.043	1.46
Erythronic acid	0.039	1.06
2-hydroxyglutaric acid	0.0013	0.71
Xylose MP	0.042	1.21
<i>cis</i> -Aconitic acid	0.0035	0.50
<i>cis</i> -4-hydroxycinnamic acid	0.034	0.76
Citric acid	8.00E-04	0.62
Dehydroascorbic acid dimer	0.0067	0.54
M000000_A187005	0.0074	1.27
Gluconic acid-1,4-lactone	0.040	1.35
Galactose BP1	0.0041	0.34
A192018	0.0023	0.49
M000000_A192007	0.0020	0.59
M000000_A194007	0.0017	0.73
Ononitol	0.0018	1.82

Gluconic acid	0.0012	1.28
M000000_A214003	7.66E-04	1.61
A216006	0.0038	1.44
Octadecanoic acid	0.047	0.77
A239004	0.0020	5.39
M000000_A246005	7.24E-04	1.43
M000000_A248003	0.028	1.68
A255001_2537	0.039	0.86
Maltose_A247001_2727	0.0031	1.65
TVu 91 / TVu1987 (0.02 μ M Si)		
Tartaric acid	1.29E-08	0.012
M000000_A174001	9.56E-06	1.76
Quinic acid	7.25E-06	0.084
M000238_A190007	7.93E-05	0.36
A192018	2.61E-04	0.36
M000000_A214003	1.67E-04	5.27
M000000_A225004	1.27E-05	0.13
Raffinose	2.33E-04	0.22
Decane	0.016	0.50
Ascorbic acid	0.011	0.36
2-hydroxypyridine	0.0047	0.70
Glycolic acid	0.039	0.58
Hydroxylamine	0.0053	0.37
Malonic acid MP	0.017	1.89
Diethylenglycol	0.050	0.68
Phosphoric acid	0.013	0.58
Threonine BP1	0.0029	0.46
M000000_A140003	0.0028	2.17
Threonine MP	0.046	0.23
Aspartic acid BP2	0.0012	0.61
M000000_A146004	0.024	0.52
Erythritol	0.0067	0.63
2-hydroxyglutaric acid	0.012	0.57
M000000_A159003	0.041	1.59
M000000_A161002	0.050	0.55
Xylose MP	8.87E-04	1.80
M000000_A170002	0.013	1.60
Arabitol	0.0019	1.26
<i>cis</i> -Aconitic acid	0.018	0.50
<i>cis</i> -4-hydroxycinnamic acid	0.0085	0.49
Shikimic acid	0.0011	0.37
Citric acid	0.040	0.74
Dehydroascorbic acid	5.36E-04	0.45
M000000_A187005	0.0064	1.54
A188011	0.023	1.97
Glucose MP	0.029	1.36
Galactose BP1	0.025	0.37
Mannitol	0.0013	1.22
Sorbitol / Galactitol	0.031	0.45
A194005 / Coniferylalcohol	0.015	0.58
<i>trans</i> -4-hydroxycinnamic acid	0.019	0.53
Galactonic acid	0.0080	1.39
M000000_A201002	0.019	1.87
Hexadecanoic acid	0.025	0.63
M000000_A207008	0.0016	0.55
<i>myo</i> -Inositol	0.0012	0.40
M000000_A211001	0.0097	1.41
Octadecanoic acid	0.0067	0.59
Galactosylglycerol	0.0051	1.61
A239004	0.021	3.63
Xylobiose BP	9.00E-04	9.87
A245005_2436	6.66E-04	4.84
A255001_2537	0.0017	0.49

M000000_A261006	0.017	1.58
Sucrose MP	0.025	0.75
M000000_A267006	0.0019	3.41
Maltose_A247001_2727	0.010	1.75
M000000_A276001	0.0042	1.39
M000000_A279002	0.0020	0.67
M000000_A291005	0.0090	0.61
Galactinol	0.0024	0.42
Hexatriacontane	0.027	0.66
TVu 91 / TVu1987 (50 µM Mn, 0.02 µM Si)		
Serine BP1	4.54E-06	0.20
Phosphoric acid	4.93E-04	0.70
Threonine BP1	3.90E-06	0.21
Succinic acid	1.04E-04	1.77
Glyceric acid	7.74E-05	0.56
M000000_A140003	7.48E-06	1.94
Threonic acid-1,4-lactone	1.50E-04	0.69
M000000_A141003	3.67E-04	0.33
Aspartic acid BP2	1.67E-04	0.31
M000000_A159003	4.33E-04	1.81
Tartaric acid	6.68E-07	0.013
M000000_A170002	4.83E-05	2.14
Arabitol	2.53E-05	0.65
M000000_A174001	5.94E-07	1.77
Shikimic acid	1.20E-07	0.19
A183011	3.99E-05	3.32
Quinic acid	1.86E-05	0.17
Fructose MP	1.97E-04	0.50
M000000_A187005	1.16E-05	1.48
Galactose BP1	3.95E-04	0.26
A192018	1.38E-04	0.33
M000000_A207008	2.09E-04	0.58
myo-Inositol	1.58E-06	0.44
M000000_A214003	1.06E-06	3.39
M000000_A225004	1.41E-05	0.23
Galactosylglycerol	1.98E-05	1.84
A239004	3.47E-05	5.31
Xylobiose BP	1.00E-04	10.29
A245004_2436	1.38E-04	9.81
M000000_A246005	4.85E-05	1.50
M000000_A250001	8.36E-06	1.79
Sucrose MP	4.85E-05	0.67
Galactinol	3.85E-04	0.27
Raffinose	4.39E-04	0.26
2-hydroxypyridine	0.0014	0.49
Ascorbic acid	6.66E-04	0.30
A104001	0.010	0.43
Glycolic acid	0.022	0.72
Hydroxylamine	0.012	0.42
A113001	0.0074	0.41
Benzylalcohol	0.0019	0.50
Malonic acid MP	7.46E-04	2.91
Diethylenglycol	0.0091	0.66
Benzoic acid	0.023	0.69
Itaconic acid	0.048	0.48
Threonine MP	0.030	0.33
M000000_A146004	0.0051	0.56
Malic acid	0.047	1.18
Erythritol	0.0010	0.80
Pyroglutamic acid	8.65E-04	0.59
4-aminobutyric acid	9.46E-04	3.36
2-hydroxyglutaric acid	0.016	0.88
M000000_A161002	0.0055	0.57

Xylose MP	0.0033	1.45
<i>cis</i> -Aconitic acid	0.0011	0.45
M000000_A177004	0.017	1.32
<i>cis</i> -4-hydroxycinnamic acid	0.011	0.69
Citric acid	0.0038	0.63
Dehydroascorbic acid dimer	0.0073	0.67
Fructose BP1	0.0065	0.45
Glucose MP	0.0064	0.64
M000238_A190007	0.0057	0.55
Glucose BP1	0.0038	0.60
<i>p</i> -Tyramine MP	0.012	0.72
M000000_A194007	0.0037	0.73
A194005 / Coniferylalcohol	0.0018	0.59
Ononitol	0.0022	1.67
<i>trans</i> -4-hydroxycinnamic acid	0.049	0.73
Glucose BP3	0.022	1.35
Galactonic acid	0.0013	1.69
Gluconic acid	8.07E-04	1.16
Hexadecanoic acid	0.011	0.66
M000000_A211001	0.0012	1.36
A216006	0.0073	1.69
A223007	7.39E-04	1.45
Octadecanoic acid	0.0053	0.69
M000000_A248003	0.014	1.58
A255001_2537	0.043	0.87
M000000_A261006	0.0028	3.64
M000000_A267006	7.96E-04	6.01
M000000_A279002	0.0011	0.49
M000000_A291005	0.0025	0.49
M000000_A311002	0.030	1.95

Tab. S1.2. Identified metabolites from AWF of the two cowpea cultivars TVu 91 and TVu 1987 and their relative changes in abundance including statistical significance as affected by Mn and Si treatments

a.) TVu 91

Metabolite	<i>p</i> -value (t-test)	fold induction / reduction
Mn-effect (H ₂ O)		
2-hydroxypyridine	0.037	1.35
M000000_A194007	0.013	2.86
Xylobiose BP1	0.044	2.24
M000000_A250001	0.032	2.97
Isomaltose MP	0.033	1.73
Mn-effect (NaCl)		
Lactic acid	2.69E-04	0.56
M000000_A165003	9.00E-05	2.96
3-deoxyglucose MP	3.98E-04	3.88
M000000_A179001	5.32E-05	2.55
Desoxypento-3-ylose BP1	1.77E-04	4.43
Shikimic acid	1.52E-04	0.27
M000000_A194007	3.24E-05	3.62
<i>myo</i> -Inositol	6.86E-05	1.70
2-hydroxypyridine	4.47E-04	3.31
Hydroxylamine	0.0095	0.18
A114002	0.0019	1.74
Diethylenglycol MP	0.036	0.92
Threonine BP1	0.039	2.30
Maleic acid	0.022	2.72
M000000_A136002	0.0021	1.64
Itaconic acid	0.0094	1.73
Threonic acid-1,4-lactone	0.041	1.30
Erythritol	0.011	1.68
4-aminobutyric acid MP	0.0078	1.89
3-hydroxybenzoic acid	0.0061	2.53
Ornithine	0.018	2.02
Tartaric acid	0.010	2.91
Xylose MP	0.023	1.41
Ribose MP	0.027	1.54
Ribose BP1	0.024	1.66
Fucose BP1	0.0028	1.64
M000000_A175004	0.039	1.35
M000000_A177004	8.76E-04	1.57
A178011	0.0084	1.57
Citric acid	0.045	1.57
M000000_A183011	0.014	2.80
Tagatose BP1	0.031	3.04
Altrose MP	5.48E-04	2.59
Glucose BP1	0.018	0.96
Gluconic acid	0.0038	3.25
M000000_A202004	6.80E-04	1.62
M000000_A203003	0.027	1.39
M000000_A211001	0.0036	1.96
A216006 / A217003	0.012	2.79
M000000_A217003	0.0079	2.59
Nonadecanoic acid methylester	0.024	0.073
A239004	0.036	2.84
M000000_A240004	0.027	1.43
Xylobiose BP1	0.0026	3.07
M000000_A250001	0.0085	3.13
M000000_A261006	0.0094	2.24
Adenosine MP	0.038	3.13
M000000_A267006	0.0075	3.68

M000000_A272011	0.032	4.91
M000000_A276001	0.029	1.62
Gentiobiose MP / M000000_A279001	0.021	2.59
Octacosane	0.0018	0.65
Gentiobiose BP1	0.021	2.71
Isomaltose BP1	0.0042	0.30
Dotriacontane	0.0093	0.43
Hexatriacontane	0.018	0.56
Si-effect (H ₂ O)		
-	-	-
Si-effect (NaCl)		
Lactic acid	0.021	0.79
Itaconic acid	0.0074	0.64
M000000_A165003	0.028	1.21
M000000_A175004	0.018	0.66
Mn-effect in Si-treated plants (H ₂ O)		
M000000_A272011	1.41E-04	0.084
Erythronic acid-1,4-lactone	0.0079	0.76
Ornithine	0.038	0.34
Xylose MP	0.046	0.23
M000000_A175004	0.037	0.32
Mannitol	0.032	0.68
M000000_A214003	0.0071	2.16
M000000_A267006	0.0035	0.12
Gentiobiose / M000000_A279007	0.0034	0.24
Gentiobiose BP1	0.0074	0.30
Mn-effect in Si-treated plants (NaCl)		
2-hydroxypyridine	0.0016	2.82
Hydroxylamine	0.018	0.21
Maleic acid	0.032	2.34
M000000_A136002	0.015	1.56
Itaconic acid	0.011	1.99
Fumaric acid	0.036	1.65
Erythritol	0.014	1.39
3-hydroxybenzoic acid	0.029	3.76
Ornithine	0.035	2.25
Tartaric acid	0.0026	3.69
M000000_A165003	0.0094	1.84
M000000_A170001	0.018	1.52
M000000_A175004	0.0049	1.87
<i>cis</i> -Aconitic acid	0.042	2.31
3-deoxyglucose MP	0.015	2.96
Desoxypentos3-lyose BP1	0.0030	4.06
Shikimic acid	0.019	0.22
Tagatose BP1	0.038	3.47
M000000_A194007	0.0028	2.74
Gluconic acid	0.015	2.93
M000000_A211001	0.044	1.68
A216006 / A217003	0.0091	2.70
M000000_A217003	0.014	2.29
M000000_A225004	0.039	0.61
A239004	0.011	3.18
M000000_A246005	0.0044	0.54
M000000_A250001	0.016	2.46
Octacosane	4.33E-04	0.60
Dotracontane	0.0019	0.32
Hexatriacontane	0.0047	0.50
Si-effect in Mn-treated plants (H ₂ O)		
M000000_A170001	0.043	0.55
Mannitol	0.0061	0.44
M000000_A267006	0.022	0.19
Gentiobiose / M000000_A279001	0.0041	0.25

Gentiobiose BP1	0.0090	0.31
Si-effect in Mn-treated plants (NaCl)		
Fucose BP1	0.029	0.67
M000000_A177004	0.022	0.80
Altrose MP	0.0052	0.77
M000000_A216006	0.016	0.84
Octadecanoic acid	0.031	1.18
M000000_A236001	0.041	0.81
M000000_A246005	0.0040	0.75

b.) TVu 1987

Metabolite	p-value (t-test)	fold induction / reduction
Mn-effect (H ₂ O)		
M000000_A194007	2.78E-06	3.92
Undecane	0.0084	2.40
Malonic acid MP	0.027	3.68
Diethylenglycol	0.028	1.27
Phosphoric acid	0.030	1.45
Threonine BP1	0.020	3.64
Pentadecane	0.010	1.31
M000000_A155003	0.0095	1.51
A160004	0.048	0.50
Ornithine	0.011	0.40
M000000_A165003	0.0046	0.42
M000000_A175004	0.049	0.32
2-desoxypentose-3-ylose BP1	0.049	0.75
Octadecane	0.014	1.30
Citric acid	0.019	1.42
Tagatose BP1	0.019	0.32
Tetradecanoic acid	0.0053	2.14
M000611_A187006	0.0089	3.48
Fructose MP	0.026	1.26
Nonadecane	0.012	1.15
M000000_A202004	0.023	1.21
Hexadecanoic acid	0.0091	1.55
M000000_A213001	0.0050	3.66
M000000_A214003	0.0015	3.07
M000000_A216006	0.0017	2.46
A216006 / A217003	0.010	2.35
M000000_A217003	0.0047	2.41
Docosane	0.0099	1.33
Nondecanoic acid methylester	0.029	10.11
Octadecanoic acid	0.0082	1.63
M000000_A225004	0.029	2.16
Zuckerphosphate	0.017	1.89
Galactosylglycerol	0.012	2.11
M000000_A236001	0.0020	2.41
M000000_A240004	0.0067	2.62
M000000_A243002	0.0050	2.68
Xylobiose BP1	0.031	1.82
M000000_A246005	0.0034	2.89
M000000_A250001	0.0029	3.20
M000000_A266002	0.050	1.89
M000000_A276001	0.031	0.62
Galactinol	0.029	1.75
Mn-effect (NaCl)		
M000000_A170001	2.63E-04	1.79
M000611_A187006	1.34E-04	5.47
M000000_A194007	7.12E-05	5.15
2-hydroxypyridine	6.55E-04	3.31
Lactic acid	0.0014	0.55
Undecane	9.84E-04	3.12
Hydroxylamine	0.0024	0.11
A114002	0.028	1.52
Threonine BP1	0.031	3.61
Maleic acid	0.028	2.40
M000000_A136002	0.0033	1.72
Itaconic acid	0.018	2.96
Erythritol	0.0012	1.41
3-hydroxybenzoic acid	0.0052	3.23
Ornithine	0.035	2.50
M000000_A165003	0.030	2.90

<i>cis</i> -Aconitic acid	0.020	2.79
3-deoxyglucose MP	0.0043	3.97
M000000_A177004	0.0052	2.34
Desoxypentos-3-lyose BP1	0.033	4.40
Shikimic acid	0.014	0.31
Dehydroascorbic acid dimer	0.0045	1.76
Fructose MP	0.0012	1.40
Ononitol	0.033	0.65
Gluconic acid	0.023	3.78
M000000_A211001	7.89E-04	2.30
A216006 / A217003	0.0015	4.40
M000000_A217003	0.0027	3.47
M000000_A236001	0.036	1.44
A239004	0.0011	1.68
M000000_A243002	0.016	1.71
M000000_A249004	9.20E-04	2.44
M000000_A250001	0.0075	2.59
M000000_A264005	0.026	7.78
M000000_A266002	0.0040	1.73
M000000_A267006	0.020	7.12
M000000_A272011	0.0090	4.71
Gentiobiose MP / M000000_A279001	0.024	3.01
Octacosane	0.0079	0.62
Dotracontane	0.028	0.44
Hexatriacontane	0.0054	0.51
Si-effect (H ₂ O)		
Threonic acid-1,4-lactone	0.0062	0.36
Ornithine	0.022	0.40
M000000_A165003	0.038	0.48
Tagatose BP1	0.010	0.35
Dehydroascorbic acid dimer	0.032	0.51
M000611_A187006	0.019	1.75
M000000_A216006	0.038	1.77
M000000_A225004	0.011	1.90
M000000_A236001	0.0095	2.03
M000000_A240004	0.028	1.95
M000000_A246005	0.0031	2.27
M000000_A264005	0.035	0.61
Si-effect (NaCl)		
M000000_A170001	2.62E-04	1.71
M000000_A217003	3.58E-04	2.33
Lactic acid	0.019	0.76
A114002	0.036	1.49
Maleic acid	0.026	2.57
Threonic acid-1,4-lactone	0.025	1.99
β -Alanine	0.0062	3.07
Erythritol	0.0040	1.71
4-aminobutyric acid	0.0041	3.39
Tartaric acid	0.044	2.20
M000611_A187006	0.026	1.96
Fructose MP	0.026	1.37
Nonadecane	0.049	0.89
Mannitol	0.011	2.13
M000000_A194007	0.018	1.73
M000000_A203003	0.021	1.94
<i>myo</i> -Inositol	0.048	1.57
M000000_A211001	0.0038	2.03
M000000_A216006	0.025	1.45
A219006 / A217003	0.0094	2.85
Spermidine BP1	0.0098	3.52
M000000_A236001	0.015	1.59
A239004	9.05E-04	2.07

M000000_A250001	5.12E-04	2.42
M000000_A272011	0.034	3.20
Mn-effect in Si-treated plants (H ₂ O)		
Succinic acid	0.028	2.44
Threonic acid-1,4-lactone	0.0098	5.03
Dehydroascorbic acid dimer	0.017	5.31
M000000_A194007	0.0043	4.79
M000000_A202004	0.016	2.31
A216006 / A217003	0.021	2.51
M000000_A217003	0.031	2.32
Xylobiose BP1	0.036	3.18
M000000_A249004	0.013	2.54
M000000_A250001	0.0054	1.81
Adenosine MP	0.014	4.26
M000000_A266002	0.0089	2.37
M000000_A286002	0.026	4.28
Galactinol	0.024	3.43
Hexatriacontane	0.020	0.52
Mn-effect in Si-treated plants (NaCl)		
Undecane	1.12E-04	2.94
3-deoxyglucose MP	3.45E-05	3.09
Octacosane	3.15E-04	0.61
2-hydroxypyridine	4.93E-04	2.40
Lactic acid	0.0039	0.69
Hydroxylamine	0.016	0.19
Monomethylphosphate	0.019	1.44
Malonic acid	0.0039	0.13
M000000_A136002	8.27E-04	1.57
Itaconic acid	0.036	2.05
Malic acid	0.0032	1.24
3-hydroxybenzoic acid	0.012	2.22
Ornithine	0.049	2.18
<i>cis</i> -Aconitic acid	0.014	1.62
M000000_A177004	0.0072	2.13
Desoxypentos-3-lyose BP1	4.11E-04	3.36
Shikimic acid	0.0011	0.19
Tetradecanoic acid	0.041	1.30
Glucose MP	0.045	0.83
Nonadecane	0.029	1.08
Mannitol	0.037	0.72
M000000_A194007	0.0047	4.29
Gluconic acid	0.0051	1.82
<i>myo</i> -Inositol	0.029	0.80
M000000_A216006	0.027	0.78
A216006 / A217003	0.014	2.20
M000000_A217003	0.0075	2.04
M000000_A236001	0.029	0.80
M000000_A246005	0.0084	0.71
M000000_A249004	0.0012	1.99
M000000_A250001	0.043	1.44
M000000_A264005	0.044	5.25
M000000_A267006	0.0016	2.72
M000000_A272011	0.018	3.37
Dotriacontane	0.0014	0.37
Hexatriacontane	0.0017	0.57
Si-effect in Mn-treated plants (H ₂ O)		
Undecane	0.024	0.54
Diethylenglycol	0.025	0.79
M000000_A155003	0.0073	0.66
M000000_A174001	0.036	0.76
Shikimic acid	0.037	0.46
Tetradecanoic acid	0.022	0.59
Nonadecane	0.025	0.86

M000000_A213001	0.0065	0.54
M000000_A214003	0.0053	0.54
Docosane	0.041	0.82
Octadecanoic acid	0.032	0.71
M000000_A249004	0.012	2.14
Adenosine	0.048	2.30
M000000_A276004	0.022	1.61
Hexatriacontane	0.035	0.47
Si-effect in Mn-treated plants (NaCl)		
Monomethylphosphate	0.014	1.49
Succinic acid	0.0031	1.93
Glyceric acid	0.028	2.52
β -Alanine MP	0.018	2.67
4-aminobutyric acid	0.032	1.97
Tartaric acid	0.018	1.52
3-deoxyglucose MP	0.0088	1.23
M000000_A177004	0.025	1.12
Mannitol	0.034	1.36
M000000_A203003	0.046	1.43
M000000_A228001	0.0081	1.54
<i>myo</i> -Inositol-1-phosphate	0.031	1.84
M000000_A243002	0.043	0.68
M000000_A246005	0.042	0.82

c.)TVu 91 vs TVu 1987

Metabolite	p-value (t-test)	fold induction / reduction
control H ₂ O		
Xylobiose BP1	1.73E-04	5.43
Itaconic acid	0.0066	1.48
β -Alanine MP	0.023	0.57
Tartaric acid	7.73E-04	0.031
Ribose MP	0.010	0.41
Fucose BP1	0.032	0.46
M000000_A194007	0.031	1.50
M000000_A202004	0.0069	0.75
M000000_A249004	0.016	2.38
M000000_A266002	0.019	0.66
Gentiobiose BP1	0.047	2.45
M000000_A286002	0.026	0.32
M000000_A311002	0.027	0.46
control NaCl		
Tartaric acid	2.40E-05	0.026
Xylobiose BP1	9.98E-05	4.30
M000000_A249004	6.70E-06	12.10
Hydroxylamine	0.039	0.76
β -Alanine MP	0.037	0.49
M000000_A155003	0.015	0.71
Xylose BP1	0.029	0.55
M000000_A170001	0.0066	1.35
M000000_A177004	0.0051	2.39
Dehydroascorbic acid dimer	0.027	1.46
Altrose MP	0.0029	0.47
Glucose BP1	0.030	1.05
M000000_A194007	0.011	1.73
M000000_A211001	0.036	1.37
M000000_A216006	0.035	2.07
A216006 / A217003	0.010	2.00
M000000_A217003	0.0032	1.83
M000000_A236001	0.0019	3.08
Galactosylglycerol	0.046	1.72
M000000_A236001	0.019	2.40
A239004	0.017	2.16
M000000_A240004	0.0089	1.74
M000000_A243002	0.019	2.29
M000000_A246005	0.013	2.79
Adenosine	7.24E-04	0.090
Gentiobiose MP /	0.013	3.42
M000000_A279001		
M000000_A287005	0.0038	3.50
Mn-treatment H ₂ O		
Tartaric acid	3.49E-05	0.022
Undecane	0.0089	0.43
Diethylenglycol	0.035	0.81
M000000_A136002	0.017	0.71
Alanine BP1	0.023	0.57
Pentadecane	0.029	0.82
M000000_A155003	0.0041	0.65
Octadecane	0.012	0.78
Tetradecanoic acid	0.010	0.53
M000611_A187006	0.020	0.39
Nonadecane	0.025	0.87
Hexadecanoic acid	0.0088	0.64
Docosane	0.012	0.76
Octadecanoic acid	0.018	0.68
Xylobiose BP1	0.0023	6.67
Gentiobiose MP /	0.0064	3.76

M000000_A279001		
Gentiobiose BP1	0.0078	3.30
M000000_A311002	0.036	0.45
Mn-treatment NaCl		
Tartaric acid	7.51E-05	0.043
Xylobiose BP1	2.10E-05	11.67
M000000_A249004	1.22E-04	2.08
Undecane	9.64E-04	0.33
A114002	0.049	1.26
Threonine BP1	0.031	0.48
Succinic acid	0.016	1.74
Erythrose MP	0.011	0.82
4-aminobutyric acid	0.049	1.78
M000000_A155003	0.0050	0.55
Xylose BP1	7.60E-04	0.73
Ribose MP	0.041	1.50
Ribose BP1	0.044	1.49
<i>cis</i> -Aconitic acid	0.043	0.67
Ribonic acid	0.024	1.75
M000000_A177004	0.0036	1.60
A178011	0.0036	1.51
M000611_A187006	0.0032	0.25
Fructose MP	0.0014	0.71
Fructose BP1	0.041	0.94
Glucose MP	0.0041	1.16
Nonadecane	0.012	0.94
Ononitol	0.0099	1.79
M000000_A216006	0.0087	1.76
Nonadecanoic acid methylester	0.0062	0.20
M000000_A236001	0.0025	1.80
A239004	0.016	3.66
M000000_A240004	7.45E-04	1.93
M000000_A243002	0.0035	2.20
M000000_A249004	0.0019	8.12
M000000_A250001	0.032	1.94
Adenosine MP	0.032	0.34
M000000_A266002	0.0036	0.69
Gentiobiose MP /	0.015	2.94
M000000_A279001		
Gentiobiose BP1	0.016	3.01
M000000_A287005	0.0087	3.78
Melibiose BP1	0.024	3.00
Si-treatment H ₂ O		
Threonic acid-1,4-lactone	0.041	1.89
Erythritol	0.047	0.68
Tartaric acid	0.0086	0.040
A239004	0.042	2.17
Xylobiose BP1	0.012	10.31
M000000_A249004	0.0034	3.99
M000000_A272011	0.017	3.24
Gentiobiose MP /	0.0038	4.09
M000000_A279001		
Gentiobiose BP1	0.0018	3.46
Si-treatment NaCl		
Tartaric acid	3.97E-06	0.0099
M000000_A246005	1.33E-04	2.48
M000000_A249004	3.72E-04	11.06
Maleic acid	0.023	0.39
Nicotinic acid	0.023	0.51
Fumaric acid	0.029	0.57
Erythronic acid-1,4-lactone	0.035	0.70
Erythritol	5.65E-04	0.53
2-hydroxyglutaric acid	0.0092	0.39

M000000_A175004	0.0087	0.64
<i>cis</i> -Aconitic acid	0.016	0.33
M000000_A177004	0.014	2.19
Mannitol	0.0065	0.43
Ononitol	0.028	1.39
Gluconic acid	0.044	0.48
M000000_A216006	0.013	1.60
Octadecanoic acid	0.049	0.66
Galactosylglycerol	0.045	1.55
M000000_A236001	0.012	1.60
M000000_A237001	0.048	1.23
M000000_A240004	0.0071	2.29
M000000_A243002	0.044	1.76
Xylobiose BP1	0.012	5.91
M000000_A250001	0.018	0.54
Adenosine MP	0.0017	0.14
M000000_A287005	8.86E-04	3.25
Galactinol	0.035	0.31
Mn and Si-treatment H ₂ O		
Tartaric acid	1.12E-05	0.0092
Oxalic acid	0.016	1.49
Threonine BP1	0.023	0.19
M000000_A136002	0.028	0.47
Erythronic acid-1,4-lactone	0.022	0.73
Erythritol	0.034	0.54
2-hydroxyglutaric acid	0.032	0.52
Xylose BP1	0.024	0.41
Xylose MP	0.030	0.15
Ribose MP	0.0052	0.25
M000000_A270001	0.033	0.54
Fucose BP1	0.036	0.30
<i>cis</i> -Aconitic acid	0.040	0.36
Fructose BP1	0.036	1.24
Altrose MP	0.043	0.41
Mannitol	0.0030	0.41
M000000_A202004	0.037	0.51
A216006 / A217003	0.041	0.47
Galactosylglycerol	0.049	0.58
Xylobiose BP1	0.041	3.05
M000000_A261006	0.030	0.52
Adenosine MP	0.042	0.30
M000000_A266002	0.0019	0.31
M000000_A267006	0.028	0.17
M000000_A272011	0.040	0.19
Maltose MP	0.013	0.39
M000000_A276004	0.0043	0.56
M000000_A286002	0.022	0.22
Galactinol	0.017	0.24
M000000_A311002	0.0055	0.25
Mn and Si-treatment NaCl		
Tartaric acid	5.84E-05	0.030
Ononitol	3.11E-04	1.64
M000000_A216006	2.76E-04	1.75
Xylobiose BP1	3.37E-04	10.69
Monomethylphosphate	0.013	0.61
Itaconic acid	0.046	0.59
Erythronic acid-1,4-lactone	0.040	0.63
Erythritol	0.035	0.73
2-hydroxyglutaric acid	0.050	0.52
Xylose BP1	0.030	0.71
<i>cis</i> -Aconitic acid	0.040	0.47
Shikimic acid	0.028	0.61
Altrose MP	0.023	0.61

Mannitol	0.024	0.61
M000000_A203003	0.027	0.63
M000000_A236001	0.0040	1.66
A239004	0.025	3.36
M000000_A240004	0.0026	1.99
M000000_A243002	0.0044	2.89
M000000_A246005	5.99E-04	1.88
M000000_A249004	0.0075	8.95
Sucrose MP	0.017	1.87
Adenosine MP	7.26E-04	0.14
M000000_A266002	0.0059	0.57
conjugate_glycosylinositol	0.034	1.89

Tab. S1.3. Identified non-polar metabolites from diethylether extracts of AWF of the two cowpea cultivars TVu 91 and TVu 1987 and their relative changes including statistical significance in abundance as affected by Mn and Si treatments

a.) TVu 91

Metabolite	<i>p</i> -value (t-test)	fold induction / reduction
Mn-effect (H ₂ O)		
Malic acid	0.014	1.43
<i>cis</i> -ferulic acid	0.0034	0.27
<i>trans</i> -ferulic acid	0.020	0.44
Mn-effect (NaCl)		
3-oxoglutaric acid	8.01E-04	8.26
Dodecanoic acid	0.0071	1.12
<i>cis</i> -ferulic acid	0.018	0.34
Pantothenic acid MP	0.030	2.26
A223009	0.036	0.81
Si-effect (H ₂ O)		
Succinic acid	0.026	0.52
<i>cis</i> -Aconitic acid	0.0016	0.57
9,12-octadecadienoic acid	0.019	0.66
Hexacosanoic acid	0.029	0.60
Si-effect (NaCl)		
Benzoic acid	0.0026	1.31
Succinic acid	0.0024	0.60
<i>p</i> -hydroxybenzoic acid	0.040	0.61
<i>cis</i> -ferulic acid	0.0044	4.13
Pantothenic acid MP	0.042	1.50
<i>trans</i> -ferulic acid	0.0035	3.78
M000000_A299007	0.035	0.74
Hexacosanoic acid	0.0085	0.65
Mn-effect in Si-treated plants (H ₂ O)		
Benzoic acid	0.0056	1.48
Triethanolamine	0.0076	4.37
A211009	0.013	2.00
Mn-effect in Si-treated plants (NaCl)		
Hydroxylamine	0.041	10.73
Phosphoric acid	0.025	0.70
M000000_A264003	0.034	1.60
Si-effect in Mn-treated plants (H ₂ O)		
Succinic acid	7.92E-04	0.28
Malic acid	0.039	0.44
<i>p</i> -hydroxybenzoic acid	0.016	0.61
Si-effect in Mn-treated plants (NaCl)		
Succinic acid	7.89E-04	0.40
<i>p</i> -hydroxybenzoic acid	0.027	0.53
A23009	0.032	1.40
M000000_A299007	0.0052	0.47
β -Sitosterol	0.021	1.33

b.) TVu 1987

Metabolite	p-value (t-test)	fold induction / reduction
Mn-effect (H ₂ O)		
M000000_A136002	0.014	0.45
3-oxoglutaric acid	0.0014	24.59
<i>cis</i> -4-hydroxycinnamic acid	0.0028	0.079
<i>trans</i> -4-hydroxycinnamic acid	0.0057	0.048
<i>trans</i> -sinapic acid	0.010	4.67
Hexacosanoic acid	0.020	0.59
Mn-effect (NaCl)		
3-oxoglutaric acid	2.99E-05	30.86
2-hydroxypyridine	0.046	1.79
Malic acid	0.049	1.47
<i>cis</i> -4-hydroxycinnamic acid	0.0070	0.15
<i>trans</i> -fourhydroxycinnamic acid	0.0033	0.16
Pantothenic acid MP	0.016	3.66
<i>trans</i> -sinapic acid	0.048	1.52
Hexatriacontane	0.047	1.36
Si-effect (H ₂ O)		
Benzoic acid	0.024	1.26
Succinic acid	0.048	0.72
M000000_A299007	0.012	0.52
Hexacosanoic acid	0.0038	0.44
Si-effect (NaCl)		
<i>cis</i> -ferulic acid	0.0015	3.17
Pantothenic acid MP	0.0091	2.53
<i>trans</i> -ferulic acid	0.029	2.31
9,12-octadecadienoic acid	0.048	1.58
A223009	0.012	1.67
M000000_A255002	0.0014	1.68
Hexatriacontane	0.0016	1.29
Mn-effect in Si-treated plants (H ₂ O)		
Succinic acid	5.42E-05	0.40
<i>cis</i> -4-hydroxycinnamic acid	3.94E-04	0.25
Hydroxylamine	0.042	3.02
A134004	0.0090	0.71
3-oxoglutaric acid MP	0.0019	10.74
Dodecanoic acid	0.013	0.76
Octadecane	0.044	0.85
Nonadecane	0.043	0.86
<i>trans</i> -4-hydroxycinnamic acid	0.0012	0.29
Pantothenic acid MP	0.0021	3.56
Docosane	0.043	0.83
A223009	0.041	0.71
M000000_A264003	0.023	1.67
Mn-effect in Si-treated plants (NaCl)		
Succinic acid	2.96E-04	0.40
<i>cis</i> -4-hydroxycinnamic acid	1.09E-04	0.15
Hydroxylamine	0.016	5.01
M000000_A136003	0.013	0.29
<i>p</i> -hydroxybenzoic acid	0.0060	5.04
<i>trans</i> -4-hydroxycinnamic acid	0.023	0.24
Pantothenic acid MP	0.035	1.65
Si-effect in Mn-treated plants (H ₂ O)		
M000000_A299007	0.0069	0.67
Si-effect in Mn-treated plants (NaCl)		
Succinic acid	5.02E-04	0.42
2-hydroxypyridine	0.028	0.47
M000000_A143002	0.0081	1.14
A188001_9	0.028	0.59
M000000_A299007	0.049	0.59

c.) TVu 91 vs TVu 1987

Metabolite	p-value (t-test)	fold induction / reduction
TVu 91 / TVu 1987 control (H ₂ O)		
Succinic acid	0.048	1.35
TVu 91 / TVu 1987 control (NaCl)		
Malic acid	3.15E-04	2.76
<i>p</i> -hydroxybenzoic acid	5.76E-04	2.35
2-hydroxypyridine	0.022	1.61
Malonic acid	0.0083	4.01
Benzoic acid	0.0071	0.82
Succinic acid	0.0058	1.88
A134004	0.021	1.50
Fumaric acid	0.034	1.86
<i>cis</i> -4-hydroxycinnamic acid	0.010	1.90
Citric acid	0.0040	3.11
<i>trans</i> -4-hydroxycinnamic acid	0.0015	2.71
Pantothenic acid MP	0.0028	3.51
A223008	0.014	1.97
A223009	0.034	1.50
<i>trans</i> -sinapic acid	0.010	2.19
Hexatriacontane	0.040	1.21
TVu 91 / TVu 1987 Mn (H ₂ O)		
3-oxoglutaric acid	0.0013	0.05
<i>cis</i> -4-hydroxycinnamic acid	0.0046	9.95
<i>trans</i> -4-hydroxycinnamic acid	0.011	16.21
<i>trans</i> -ferulic acid	0.050	0.12
A257001	0.031	1.88
TVu 91 / TVu 1987 Mn (NaCl)		
Succinic acid	6.60E-04	2.77
<i>trans</i> -4-hydroxycinnamic acid	3.99E-04	13.34
Fumaric acid	0.028	2.00
M000000_A143002	0.043	1.14
Malic acid	0.0049	2.07
3-oxoglutaric acid MP	0.029	0.33
<i>cis</i> -4-hydroxycinnamic acid	0.0029	10.92
Laminaribiose BP1	0.018	0.09
TVu 91 / TVu 1987 Si (H ₂ O)		
9,12-octadecadienoic acid	6.31E-04	0.42
Benzoic acid	0.0045	0.79
<i>cis</i> -Aconitic acid	0.045	0.65
Citric acid	0.0014	0.40
Pantothenic acid MP	0.0085	0.47
TVu 91 / TVu 1987 Si (NaCl)		
Malonic acid	0.022	1.90
Succinic acid	0.0081	1.45
Malic acid	0.0082	2.10
<i>p</i> -hydroxybenzoic acid	0.0094	2.19
<i>cis</i> -4-hydroxycinnamic acid	0.033	1.82
Nonadecane	0.048	1.08
<i>cis</i> -ferulic acid	0.0033	2.91
<i>trans</i> -4-hydroxycinnamic acid	0.046	3.08
Pantothenic acid MP	0.0063	2.08
Hexadecanoic acid	0.043	0.92
<i>trans</i> -ferulic acid	0.0084	3.19
TVu 91 / TVu 1987 Mn and Si (H ₂ O)		
3-oxoglutaric acid	2.77E-05	0.093
<i>cis</i> -4-hydroxycinnamic acid	4.24E-04	4.31
Succinic acid	0.027	1.69
Dodecanoic acid	0.013	1.23
<i>trans</i> -4-hydroxycinnamic acid	0.014	3.09
Pantothenic acid MP	0.017	0.28
A211009	0.0056	2.71

9,12octadecadienoic acid	0.031	0.51
M000000_A255002	0.039	1.61
A278009	0.038	1.59
M000000_A299007	0.0087	1.53
TVu 91 / TVu 1987 Mn and Si (NaCl)		
Succinic acid	2.73E-04	2.62
3-oxoglutaric acid MP	0.0027	0.16
<i>cis</i> -4-hydroxycinnamic acid	0.0014	6.24
<i>trans</i> -4-hydroxycinnamic acid	0.0013	6.28
9,12-octadecadienoic acid	0.025	0.69

Tab. S2. Results of the ANOVA performed for all annotated metabolites. Stars in brackets represent the result of the ANOVA for the experiment with *, **, *** for $p < 0.05$, 0.01, 0.001, respectively. In the ANOVA all experimental conditions were included (Mn and Si treatments and genotypes). Additionally, shown numbers represent fold induction / reduction in abundance between +Mn vs -Mn (Mn (+/-), +Si vs -Si (Si (+/-), TVu 91 vs TVu 1987 (Gen (TVu 91/TVu 1987), respectively, throughout the whole experiment (not taking any other experimental conditions into account, when one factor was examined). The fold-induction / reduction in the individual main comparisons were also submitted to Tukey-test. Metabolites additionally signed with s. have been shown to be significantly changed at $P < 0.05$ (Tab. S1, Tukey).

S2.1. bulk-leaf metabolome ANOVA (122 metabolites)							
metabolite	Mn (+/-)	Si (+/-)	Gen (TVu 91/TVu 1987)	Mn*Si	Mn*Gen	Si*Gen	Mn*Si*Gen
Decane	0.78 (n.s.)	1.16 (n.s.)	0.75 (n.s.)	n.s.	n.s.	n.s.	n.s.
2-hydroxypyridine	1.08 (n.s.)	0.93 (n.s.)	0.50 (n.s.) s.	n.s.	n.s.	n.s.	n.s.
A104001	1.34 (n.s.)	1.12 (n.s.)	0.55 (*)	n.s.	n.s.	n.s.	n.s.
Gylcolic acid	1.09 (n.s.)	0.98 (n.s.)	0.63 (***) s.	n.s.	n.s.	n.s.	n.s.
Hydroxylamine	0.88 (n.s.)	1.04 (n.s.)	0.50 (***) s.	n.s.	n.s.	n.s.	n.s.
A113001	1.08 (n.s.)	1.24 (n.s.)	0.48 (**)	n.s.	n.s.	n.s.	n.s.
Oxalic acid	0.85 (n.s.)	1.02 (n.s.)	0.84 (n.s.)	n.s.	n.s.	n.s.	n.s.
Benzylalcohol	1.15 (n.s.)	1.26 (n.s.)	0.51 (**)	n.s.	n.s.	n.s.	n.s.
Monomethylphosphate	0.56 (***) s.	1.00 (n.s.)	0.52 (***) s.	*	n.s.	n.s.	n.s.
Malonic acid MP	1.18 (*)	0.93 (n.s.)	2.25 (***) s.	n.s.	n.s.	n.s.	n.s.
Dodecane	0.78 (*) s.	0.90 (n.s.)	0.74 (n.s.)	n.s.	n.s.	n.s.	n.s.
Ascorbic acid	0.33 (***) s.	1.50 (***)	0.33 (***) s.	n.s.	n.s.	n.s.	n.s.
Diethyleneglycol	1.10 (n.s.)	1.00 (n.s.)	0.67 (***) s.	n.s.	n.s.	n.s.	n.s.
Benzoic acid	1.07 (n.s.)	1.12 (n.s.)	0.66 (**)	n.s.	n.s.	n.s.	n.s.
Serine BP1	0.71 (***) s.	1.06 (**)	0.35 (***) s.	n.s.	***	***	n.s.
Threonine BP1	0.74 (***)	1.08 (*)	0.32 (***) s.	n.s.	n.s.	n.s.	*
Ethanolamine MP	0.87 (n.s.)	0.93 (n.s.)	0.77 (*) s.	n.s.	n.s.	**	n.s.
Phosphoric acid	0.83 (**)	1.19 (**)	0.66 (***) s.	**	*	n.s.	n.s.
<i>cis</i> -4-hydroxycinnamic acid	1.00 (n.s.)	1.21 (n.s.)	0.64 (***) s.	n.s.	n.s.	n.s.	n.s.
Sorbitol / Galactitol	0.20 (***) s.	1.24 (n.s.)	0.44 (***) s.	n.s.	n.s.	n.s.	n.s.
<i>p</i> -Tyramine MP	1.01 (n.s.)	1.16 (*) s.	0.88 (*)	n.s.	n.s.	n.s.	n.s.
Xylobiose BP	0.92 (n.s.)	0.72 (**)	9.96 (***) s.	n.s.	n.s.	n.s.	n.s.
M000000 A246005	1.46 (n.s.)	0.96 (*)	1.57 (***) s.	n.s.	**	**	**
Maleic acid	1.13 (n.s.)	1.12 (n.s.)	0.79 (n.s.)	n.s.	n.s.	n.s.	n.s.
Itaconic acid	1.14 (n.s.)	1.23 (n.s.)	0.53 (*) s.	n.s.	n.s.	n.s.	n.s.
A137006	1.07 (n.s.)	1.19 (n.s.)	0.61 (n.s.) s.	n.s.	n.s.	n.s.	n.s.
Succinic acid	1.21 (***) s.	1.12 (n.s.)	1.15 (*)	n.s.	***	n.s.	n.s.
Glyceric acid	0.91 (**)	1.13 (***)	0.49 (***) s.	***	***	***	n.s.

Fumaric acid	0.84 (n.s.)	1.14 (n.s.)	0.95 (n.s.)	n.s.	n.s.	n.s.	n.s.
<i>cis</i> -Aconitic acid	1.22 (*)	1.14 (n.s.)	0.50 (***) s.	n.s.	n.s.	n.s.	n.s.
M000000_A194007	6.11 (***) s.	1.11 (n.s.)	0.79 (n.s.)	**	***	n.s.	n.s.
M000000_A216006	0.86 (*)	1.01 (n.s.)	1.16 (***) s.	n.s.	***	n.s.	n.s.
M000000_A291005	0.72 (***) s.	1.39 (***) s.	0.52 (***) s.	*	n.s.	n.s.	n.s.
Serine MP	0.66 (n.s.)	1.84 (n.s.)	0.78 (n.s.)	n.s.	n.s.	n.s.	n.s.
M000000_A140003	1.10 (n.s.)	1.14 (n.s.)	1.80 (***) s.	**	**	**	*
Threonic acid-1,4-lactone	0.59 (***) s.	1.41 (***) s.	0.70 (***) s.	**	**	n.s.	n.s.
Threonine MP	0.74 (n.s.)	1.98 (n.s.)	0.55 (n.s.)	n.s.	n.s.	**	n.s.
M000000_A141003	0.27 (***) s.	1.42 (***)	0.82 (***)	***	***	***	.
Aspartic acid BP2	0.79 (***) s.	1.12 (**)	0.49 (***) s.	n.s.	***	n.s.	n.s.
Erythronic acid-1,4-lactone	0.88 (*) s.	1.08 (n.s.)	0.87 (*) s.	n.s.	n.s.	n.s.	n.s.
M000000_A146004	1.03 (n.s.)	1.12 (n.s.)	0.59 (***) s.	n.s.	n.s.	n.s.	n.s.
Malic acid	1.08 (n.s.)	1.00 (n.s.)	1.20 (***) s.	n.s.	n.s.	n.s.	n.s.
Asparagine MP	0.42 (***) s.	1.28 (n.s.)	1.71 (*) s.	n.s.	*	n.s.	n.s.
Erythritol	1.01 (n.s.)	1.17 (***) s.	0.71 (***) s.	n.s.	n.s.	n.s.	***
Pentadecane	0.67 (*) s.	1.04 (n.s.)	0.73 (n.s.)	n.s.	n.s.	n.s.	n.s.
Octacosane	0.65 (*) s.	1.05 (n.s.)	0.63 (n.s.)	n.s.	n.s.	n.s.	n.s.
Aspartic acid MP	0.73 (n.s.)	1.62 (n.s.) s.	0.99 (n.s.)	n.s.	n.s.	**	n.s.
Pyroglutamic acid	0.96 (n.s.)	1.09 (n.s.)	0.70 (***) s.	n.s.	n.s.	*	n.s.
4-aminobutyric acid	0.95 (n.s.)	2.10 (***) s.	1.52 (***) s.	n.s.	*	n.s.	**
M000000_A177004	0.89 (n.s.)	1.03 (n.s.)	1.10 (n.s.)	n.s.	n.s.	n.s.	n.s.
Galactosylglycerol	1.23 (***)	0.87 (**)	1.79 (***) s.	n.s.	n.s.	n.s.	n.s.
Erythronic acid	1.19 (***) s.	0.97 (n.s.)	1.10 (*) s.	n.s.	n.s.	n.s.	n.s.
Threonic acid	0.71 (***) s.	1.04 (n.s.)	1.03 (n.s.)	n.s.	n.s.	*	n.s.
2-hydroxyglutaric acid	1.12 (**)	0.96 (n.s.)	0.80 (***) s.	n.s.	n.s.	*	***
M000000_A159003	1.11 (n.s.)	1.10 (n.s.)	1.67 (***) s.	n.s.	n.s.	n.s.	n.s.
M000000_A161002	1.02 (n.s.)	1.14 (n.s.)	0.63 (***) s.	n.s.	n.s.	n.s.	n.s.
Glutamic acid MP	0.97 (n.s.)	1.37 (*)	1.04 (n.s.)	**	n.s.	**	n.s.
Tartaric acid	0.86 (n.s.)	0.94 (n.s.)	0.012 (***) s.	n.s.	n.s.	n.s.	n.s.
4-hydroxybenzoic acid	1.07 (n.s.)	1.19 (n.s.)	0.56 (*) s.	n.s.	n.s.	n.s.	n.s.
Xylose MP	1.02 (n.s.)	1.04 (n.s.)	1.35 (***) s.	n.s.	n.s.	***	*
M000000_A170001	1.05 (n.s.)	1.09 (n.s.)	1.06 (n.s.)	n.s.	n.s.	n.s.	n.s.
M000000_A170002	0.98 (n.s.)	1.08 (n.s.)	1.82 (***) s.	n.s.	n.s.	n.s.	n.s.
1,6-anhydro-β-D-glucose MP	0.90 (n.s.)	1.01(n.s.)	0.95 (n.s.)	n.s.	n.s.	n.s.	n.s.
Arabitol	1.32 (***)	0.69 (***) s.	0.57 (***) s.	***	***	***	***
Ribitol	0.97 (n.s.)	1.00 (n.s.)	1.03 (n.s.)	n.s.	n.s.	n.s.	n.s.

M000000_A174001	1.16 (***)	0.99 (n.s.)	1.71 (***) s.	n.s.	n.s.	n.s.	n.s.
Shikimic acid	0.69 (***)	1.12 (n.s.)	0.27 (***) s.	***	**	n.s.	***
Octadecane	0.72 (n.s.)	1.18 (n.s.)	0.56 (n.s.)	n.s.	n.s.	n.s.	n.s.
Citric acid	1.16 (n.s.)	1.06 (n.s.)	0.68 (***) s.	n.s.	*	n.s.	n.s.
A183011	1.00 (**)	0.81 (***) s.	1.28 (***) s.	***	***	***	***
Dehydroascorbic acid dimer MP	0.51 (***) s.	1.41 (***) s.	0.49 (***) s.	n.s.	*	n.s.	n.s.
Quinic acid	0.32 (***) s.	1.38 (***)	0.10 (***) s.	n.s.	***	n.s.	n.s.
Fructose MP	0.36 (***) s.	1.70 (***)	0.51 (***) s.	***	***	***	n.s.
M000000_A187005	1.31 (***) s.	1.00 (**)	1.40 (***) s.	*	*	**	n.s.
Fructose BP1	0.38 (***) s.	1.63 (***)	0.50 (***) s.	***	***	***	n.s.
A188011	0.74 (**)	1.27 (*)	0.96 (n.s.)	n.s.	*	*	n.s.
Gluconic acid-1,5-lactone	0.91 (n.s.)	1.09 (n.s.)	1.23 (**)	n.s.	n.s.	n.s.	n.s.
Glucose MP	0.44 (***) s.	1.91 (***) s.	0.87 (***) s.	***	***	***	**
M000238_A190007	1.53 (***) s.	0.97 (n.s.)	0.47 (***) s.	n.s.	n.s.	n.s.	**
Galactose BP1	0.36 (***) s.	1.72 (***)	0.31 (***) s.	n.s.	n.s.	n.s.	n.s.
Glucose BP1	0.60 (***) s.	1.63 (***) s.	0.72 (***) s.	***	***	***	n.s.
Nonadecane	0.63 (n.s.) s.	1.09 (n.s.)	0.60 (n.s.)	n.s.	n.s.	n.s.	n.s.
Docosane	0.64 (n.s.) s.	1.06 (n.s.)	0.61 (n.s.)	n.s.	n.s.	n.s.	n.s.
A192018	0.45 (***) s.	1.18 (***)	0.41 (***) s.	*	n.s.	n.s.	n.s.
M000000_A192007	1.49 (***) s.	0.86 (**)	0.87 (*)	n.s.	***	n.s.	***
Mannitol	0.99 (n.s.)	0.93 (n.s.)	0.97 (n.s.)	n.s.	**	n.s.	n.s.
A194005 or Coniferylalcohol	4.96 (***) s.	1.00 (n.s.)	0.52 (***) s.	n.s.	n.s.	n.s.	n.s.
Ononitol	0.65 (**)	1.40 (*)	1.06 (**)	**	*	**	**
<i>trans</i> -4-hydroxycinnamic acid	0.90 (n.s.)	1.23 (n.s.)	0.64 (***) s.	n.s.	n.s.	n.s.	n.s.
Glucose BP3	0.83 (**)	1.09 (n.s.)	1.04 (n.s.)	n.s.	*	n.s.	n.s.
Galactonic acid	1.07 (*)	1.04 (n.s.)	1.40 (***) s.	n.s.	*	**	n.s.
Gluconic acid	7.62 (***) s.	1.04 (n.s.)	1.12 (n.s.)	n.s.	***	n.s.	n.s.
M000000_A201002	1.28 (n.s.)	1.23 (n.s.)	1.81 (***) s.	n.s.	n.s.	n.s.	n.s.
Hexadecanoic acid	1.07 (n.s.)	1.01 (n.s.)	0.68 (***) s.	*	n.s.	n.s.	n.s.
M000000_A207008	1.03 (**)	1.26 (***) s.	0.54 (***) s.	**	n.s.	n.s.	n.s.
A207009	2.86 (***) s.	1.13 (**)	0.97 (n.s.)	n.s.	n.s.	n.s.	n.s.
myo-Inositol	0.81 (***)	1.31 (***)	0.40 (***) s.	n.s.	n.s.	n.s.	n.s.
M000000_A211001	1.29 (***) s.	1.10 (**)	1.24 (***) s.	***	***	**	**
M000000_A214003	1.22 (***)	1.37 (*)	2.99 (***) s.	***	***	***	n.s.
M000000_A217004	1.25 (***) s.	1.07 (n.s.)	1.05 (n.s.)	n.s.	n.s.	n.s.	n.s.
A223007	1.08 (n.s.)	0.92 (n.s.)	1.07 (n.s.)	n.s.	n.s.	n.s.	n.s.
Octadecanoic acid	1.00 (n.s.)	0.98 (n.s.)	0.65 (***) s.	n.s.	n.s.	n.s.	n.s.

M000000_A225004	0.44 (***)	1.82 (***)	0.15 (***) s.	***	**	n.s.	*
Spermidine MP	0.38 (***) s.	1.55 (*)	0.63 (*)	n.s.	n.s.	n.s.	n.s.
Glucose-6-phosphate	1.22 (n.s.)	0.92 (n.s.)	0.91 (n.s.)	n.s.	n.s.	n.s.	n.s.
A239004	0.73 (n.s.)	0.73 (n.s.)	5.95 (***) s.	n.s.	n.s.	n.s.	n.s.
M000000_A242009	0.69 (***) s.	1.38 (***) s.	0.90 (n.s.)	***	n.s.	n.s.	n.s.
A245004_2436	1.42 (n.s.)	1.05 (n.s.)	6.28 (***) s.	n.s.	***	n.s.	n.s.
M000000_248003	1.40 (***) s.	0.96 (n.s.)	1.57 (***) s.	n.s.	n.s.	**	**
M000000_250001	1.21 (**)	1.07 (*)	1.51 (***) s.	**	**	n.s.	*
A255001_2537	0.72 (***) s.	1.16 (*)	0.62 (***) s.	***	***	n.s.	n.s.
M000000_A261006	0.71 (***) s.	0.79 (n.s.)	1.86 (***) s.	**	***	n.s.	n.s.
Sucrose MP	1.25 (***)	1.09 (***)	0.57 (***) s.	***	n.s.	***	n.s.
M000000_A267006	0.98 (n.s.)	0.84 (*)	3.73 (***) s.	n.s.	n.s.	n.s.	n.s.
Maltose_A247001_2727	1.22 (***) s.	1.07 (*)	1.63 (***) s.	n.s.	**	**	n.s.
M000000_A276001	1.07 (n.s.)	0.92 (n.s.)	1.07 (n.s.)	n.s.	*	n.s.	n.s.
M000000_A279002	0.88 (***)	1.37 (***) s.	0.57 (***) s.	*	*	n.s.	n.s.
Galactinol	0.79 (***)	1.45 (***)	0.35 (***) s.	n.s.	n.s.	n.s.	n.s.
M000000_A311002	1.30 (n.s.)	1.30 (*)	1.40 (**)	n.s.	**	n.s.	n.s.
Dotriacontane	0.87 (n.s.)	1.09 (n.s.)	0.64 (n.s.)	n.s.	n.s.	n.s.	n.s.
Raffinose	0.75 (n.s.)	1.31 (n.s.)	0.33 (***) s.	n.s.	n.s.	*	n.s.
Hexatriacontane	1.08 (n.s.)	1.00 (n.s.)	0.77 (n.s.)	n.s.	n.s.	n.s.	n.s.

S2.2a. AWF metabolome ANOVA (AWF_{H2O}), 126 metabolites

metabolite	Mn (+/-)	Si (+/-)	Gen (TVu 91/TVu 1987)	Mn*Si	Mn*Gen	Si*Gen	Mn*Si*Gen
2-hydroxypyridine	1.35 (n.s.)	1.42 (n.s.)	0.67 (*) s.	n.s.	n.s.	n.s.	*
Succinic acid	1.57 (*) s.	0.98 (n.s.)	1.16 (n.s.)	n.s.	n.s.	n.s.	n.s.
M000000_A136002	1.12 (n.s.)	1.20 (n.s.)	0.73 (*) s.	n.s.	**	n.s.	n.s.
β -Alanine MP	1.15 (n.s.)	1.70 (*) s.	0.79 (n.s.)	n.s.	n.s.	n.s.	n.s.
Erythritol	1.29 (*)	1.00 (n.s.)	0.72 (**)	n.s.	n.s.	n.s.	n.s.
2-hydroxyglutaric acid	1.37 (*) s.	0.93 (n.s.)	0.67 (*) s.	n.s.	n.s.	n.s.	n.s.
Fucose BP1	1.02 (n.s.)	1.28 (n.s.)	0.45 (***) s.	n.s.	n.s.	n.s.	*
M000000_A175004	0.85 (n.s.)	1.06 (n.s.)	0.85 (n.s.)	n.s.	n.s.	n.s.	n.s.
M000000_A177004	1.74 (**)	1.46 (n.s.)	0.92 (n.s.)	n.s.	n.s.	n.s.	n.s.
M000000_A179001	1.79 (n.s.)	2.33 (n.s.)	0.47 (n.s.)	n.s.	n.s.	n.s.	**
Tagatose BP1	2.03 (n.s.)	3.23 (n.s.)	0.35 (n.s.)	n.s.	*	n.s.	**
M000000_A211001	1.50 (**)	0.94 (n.s.)	0.87 (n.s.)	n.s.	n.s.	n.s.	n.s.
M000000_A216006	1.60 (***) s.	1.04 (n.s.)	0.90 (n.s.)	n.s.	n.s.	n.s.	n.s.
M000000_A246005	1.73 (***) s.	1.05 (n.s.)	0.93 (n.s.)	*	n.s.	n.s.	n.s.

M000000_A261006	1.44 (**)	0.98 (n.s.)	0.62 (***) s.	n.s.	n.s.	n.s.	n.s.
Sucrose MP	1.39 (n.s.)	1.52 (n.s.)	0.60 (n.s.)	n.s.	n.s.	n.s.	n.s.
Lactic acid	0.88 (n.s.)	0.81 (*) s.	0.98 (n.s.)	n.s.	n.s.	n.s.	n.s.
Undecane	1.63 (**)	1.03 (n.s.)	0.73 (*) s.	n.s.	n.s.	n.s.	n.s.
Hydroxylamine	1.34 (n.s.)	0.80 (n.s.)	0.87 (n.s.)	n.s.	n.s.	n.s.	n.s.
Oxalic acid	1.44 (n.s.) s.	1.36 (n.s.)	1.03 (n.s.)	n.s.	n.s.	n.s.	n.s.
Xylose MP	0.99 (n.s.)	1.20 (n.s.)	0.48 (*) s.	n.s.	n.s.	n.s.	**
Shikimic acid	1.46 (*)	0.79 (n.s.)	0.57 (**)	n.s.	n.s.	n.s.	n.s.
A114002	1.45 (*)	1.29 (n.s.)	0.74 (n.s.)	*	n.s.	n.s.	n.s.
Monomethylphosphate	1.28 (n.s.)	1.16 (n.s.)	0.75 (n.s.)	n.s.	n.s.	n.s.	n.s.
Malonic acid	1.70 (n.s.)	0.71 (n.s.)	1.56 (n.s.)	n.s.	n.s.	n.s.	n.s.
Dodecane	1.08 (*) s.	0.96 (n.s.)	0.93 (*)	n.s.	n.s.	n.s.	*
Diethylenglycol MP	1.11 (**)	0.94 (n.s.)	0.94 (n.s.)	n.s.	n.s.	n.s.	*
Octadecane	1.14 (**)	0.98 (n.s.)	0.91 (**)	n.s.	n.s.	n.s.	*
Phosphoric acid	1.18 (n.s.)	0.94 (n.s.)	0.87 (n.s.)	n.s.	n.s.	n.s.	n.s.
Threonine BP1	2.54 (**)	2.03 (n.s.)	0.35 (*) s.	n.s.	n.s.	n.s.	n.s.
Glyceric acid	1.40 (n.s.)	1.77 (n.s.)	0.72 (n.s.)	n.s.	n.s.	n.s.	n.s.
Galactinol	2.43 (**)	1.45 (n.s.)	0.39 (***) s.	n.s.	n.s.	n.s.	n.s.
Maleic acid	1.48 (*)	1.14 (n.s.)	0.65 (*)	n.s.	n.s.	n.s.	n.s.
Nicotinic acid	1.65 (**)	1.14 (n.s.)	0.78 (*)	n.s.	*	n.s.	n.s.
Itaconic acid	1.54 (n.s.)	1.39 (n.s.)	0.76 (n.s.)	n.s.	*	n.s.	n.s.
Fumaric acid	1.37 (n.s.)	1.29 (n.s.)	0.92 (n.s.)	n.s.	n.s.	n.s.	n.s.
M000000_A240004	1.84 (***) s.	1.06 (n.s.)	0.82 (*)	n.s.	n.s.	n.s.	n.s.
Alanine BP1	1.85 (n.s.)	1.61 (n.s.)	0.34 (*) s.	n.s.	n.s.	n.s.	n.s.
Threonic acid-1,4-lactone	1.69 (n.s.)	1.13 (n.s.)	0.74 (n.s.)	*	n.s.	n.s.	n.s.
A145001	1.49 (n.s.)	0.43 (n.s.)	0.36 (n.s.)	.	n.s.	n.s.	.
Erythronic acid-1,4-lactone	0.96 (n.s.)	1.05 (n.s.)	1.05 (n.s.)	n.s.	n.s.	n.s.	*
Erythrose MP	1.80 (n.s.)	2.24 (*) s.	0.55 (n.s.)	n.s.	n.s.	n.s.	n.s.
Malic acid	1.19 (n.s.)	0.85 (n.s.)	0.78 (*) s.	n.s.	n.s.	n.s.	n.s.
Pentadecane	1.12 (***) s.	0.99 (n.s.)	0.93 (*)	n.s.	n.s.	n.s.	*
Pyroglutamic acid	1.70 (n.s.)	1.58 (n.s.)	0.48 (*) s.	n.s.	n.s.	n.s.	n.s.
M000000_A267006	1.01 (n.s.)	1.23 (n.s.)	0.92 (n.s.)	n.s.	n.s.	n.s.	**
M000000_A272011	0.84 (*)	1.42 (n.s.)	1.05 (n.s.)	n.s.	*	n.s.	**
Maltose MP	1.36 (n.s.)	1.22 (n.s.)	0.83 (n.s.)	n.s.	n.s.	n.s.	n.s.
Gentiobiose or M000000_A279001	1.17 (n.s.)	1.00 (n.s.)	2.08 (***) s.	*	*	n.s.	**
4-aminobutyric acid	1.11 (n.s.)	3.11 (*) s.	0.81 (n.s.)	n.s.	n.s.	n.s.	n.s.
Erythronic acid	0.96 (n.s.)	1.00 (n.s.)	1.03 (n.s.)	n.s.	n.s.	n.s.	n.s.

M000000_A155003	1.26 (***) s.	0.88 (n.s.)	0.84 (**)	s.	n.s.	n.s.	**	**
Threonic acid	1.57 (*) s.	1.13 (n.s.)	1.11 (n.s.)		n.s.	n.s.	n.s.	n.s.
3-hydroxybenzoic acid	1.53 (*) s.	1.20 (n.s.)	0.60 (n.s.)		n.s.	n.s.	n.s.	n.s.
A160004	0.75 (**)	0.95 (n.s.)	0.98 (n.s.)		n.s.	n.s.	n.s.	n.s.
Ornithine	0.78 (n.s.)	1.07 (n.s.)	0.59 (n.s.)		n.s.	n.s.	n.s.	**
Tartaric acid	1.75 (n.s.)	1.46 (n.s.)	0.02 (***) s.		n.s.	*	n.s.	n.s.
M000000_A203003	1.30 (n.s.)	1.38 (n.s.)	0.77 (n.s.)		n.s.	n.s.	n.s.	n.s.
M000000_A165003	2.73 (n.s.)	3.37 (n.s.)	0.38 (n.s.)		n.s.	n.s.	n.s.	**
Xylose BP1	0.94 (n.s.)	1.16 (n.s.)	0.57 (***) s.		n.s.	n.s.	n.s.	n.s.
M000000_A194007	3.53 (***) s.	1.34 (n.s.)	0.91 (n.s.)		n.s.	*	n.s.	n.s.
Ribose MP	1.22 (n.s.)	1.26 (n.s.)	0.38 (***) s.		n.s.	n.s.	n.s.	n.s.
Ribose BP1	1.58 (n.s.) s.	1.12 (n.s.)	0.72 (n.s.)		n.s.	n.s.	n.s.	.
M000000_A170001	1.43 (*) s.	0.95 (n.s.)	0.81 (n.s.)		n.s.	n.s.	n.s.	n.s.
M000000_A174001	1.60 (**)	0.81 (n.s.)	0.88 (n.s.)		n.s.	n.s.	n.s.	n.s.
<i>cis</i> -Aconitic acid	2.02 (**)	1.05 (n.s.)	0.55 (**)	s.	n.s.	n.s.	n.s.	n.s.
Ribonic acid	1.70 (*) s.	1.26 (n.s.)	0.78 (n.s.)		n.s.	n.s.	n.s.	n.s.
3-deoxyglucose MP	2.31 (n.s.)	2.73 (*) s.	0.53 (n.s.)		n.s.	n.s.	n.s.	n.s.
A178011	1.11 (n.s.)	1.00 (n.s.)	1.12 (n.s.)		n.s.	n.s.	n.s.	n.s.
2-deoxyxypentose-3-xylose BP1	3.22 (n.s.)	3.34 (n.s.)	0.39 (n.s.)		n.s.	n.s.	n.s.	*
Citric acid	1.25 (n.s.)	0.84 (n.s.)	0.73 (*) s.		n.s.	n.s.	n.s.	n.s.
M000000_A183011	1.60 (n.s.)	1.31 (n.s.)	0.63 (n.s.)		n.s.	n.s.	n.s.	n.s.
Dehydroascorbic acid dimer MP	2.48 (**)	1.71 (n.s.)	0.56 (n.s.)		*	n.s.	n.s.	n.s.
Tetradecanoic acid	1.39 (***) s.	0.89 (n.s.)	0.73 (**)	s.	*	n.s.	n.s.	**
M000611_A187006	0.68 (n.s.)	1.84 (n.s.)	1.40 (n.s.)		*	**	n.s.	n.s.
Fructose MP	1.06 (n.s.)	1.06 (n.s.)	0.94 (n.s.)		n.s.	*	n.s.	n.s.
Isomaltose BP1	1.79 (n.s.)	2.04 (*) s.	0.46 (*) s.		n.s.	n.s.	n.s.	n.s.
Fructose BP1	1.00 (n.s.)	1.06 (n.s.)	1.07 (n.s.)		n.s.	n.s.	n.s.	n.s.
Altrose MP	1.45 (n.s.)	1.55 (*) s.	0.78 (n.s.)		n.s.	n.s.	n.s.	*
Glucose MP	1.07 (n.s.)	0.80 (*) s.	0.89 (n.s.)		n.s.	n.s.	n.s.	n.s.
Glucose BP1	1.06 (n.s.)	1.22 (n.s.) s.	1.02 (n.s.)		n.s.	n.s.	n.s.	n.s.
Nonadecane	1.07 (**)	0.98 (n.s.)	0.95 (*)		n.s.	n.s.	n.s.	**
Mannitol	1.11 (n.s.)	0.98 (n.s.)	0.63 (***) s.		*	n.s.	n.s.	n.s.
Ononitol	1.36 (n.s.)	1.15 (n.s.)	1.48 (*) s.		n.s.	n.s.	n.s.	n.s.
Gluconic acid	1.37 (n.s.)	1.86 (n.s.)	0.67 (n.s.)		n.s.	n.s.	n.s.	*
M000000_A202004	1.62 (**)	1.24 (n.s.)	0.77 (n.s.)		n.s.	n.s.	n.s.	**
Hexadecanoic acid	1.18 (**)	1.00 (n.s.)	0.82 (**)	s.	n.s.	n.s.	n.s.	n.s.
<i>myo</i> -Inositol	1.36 (n.s.)	1.73 (n.s.)	0.69 (n.s.)		n.s.	n.s.	n.s.	n.s.

M000000_A213001	2.02 (***) s.	0.93 (n.s.)	1.01 (n.s.)	n.s.	n.s.	n.s.	n.s.
M000000_A214003	1.79 (***) s.	0.94 (n.s.)	0.84 (n.s.)	n.s.	n.s.	n.s.	n.s.
A216006 od. A217003	2.09 (***) s.	1.08 (n.s.)	0.70 (*)	n.s.	n.s.	n.s.	n.s.
M000000_A311002	0.99 (n.s.)	1.54 (*)	0.40 (***) s.	n.s.	n.s.	n.s.	n.s.
M000000_A217003	2.11 (***) s.	0.96 (n.s.)	0.78 (n.s.)	n.s.	n.s.	n.s.	n.s.
Spermidine BP1
Docosane	1.13 (**) s.	0.97 (n.s.)	0.89 (**) s.	n.s.	n.s.	n.s.	*
Nonadecanoic acid methylester	3.91 (*) s.	0.99 (n.s.)	0.39 (n.s.)	n.s.	n.s.	n.s.	.
Octadecanoic acid	1.23 (*) s.	1.05 (n.s.)	0.91 (n.s.)	n.s.	n.s.	n.s.	n.s.
M000000_A225004	1.39 (*) s.	0.98 (n.s.)	0.80 (n.s.)	**	n.s.	n.s.	n.s.
Spermidine MP	0.86 (n.s.)	1.19 (**)	1.23 (*)	.	.	**	.
M000000_A228001	1.57 (*) s.	1.12 (n.s.)	0.93 (n.s.)	n.s.	n.s.	n.s.	n.s.
Sugarphosphate	1.50 (n.s.) s.	1.05 (n.s.)	1.37 (n.s.)	n.s.	n.s.	n.s.	n.s.
Galactosylglycerol	1.45 (**) s.	0.98 (n.s.)	0.85 (n.s.)	*	n.s.	n.s.	n.s.
M000000_A236001	1.56 (**) s.	1.01 (n.s.)	0.79 (*)	n.s.	n.s.	n.s.	n.s.
M000000_A237001	1.34 (n.s.)	0.89 (n.s.)	0.87 (n.s.)	n.s.	n.s.	n.s.	.
A239004	1.95 (*) s.	0.74 (n.s.)	1.83 (*) s.	n.s.	n.s.	n.s.	n.s.
<i>myo</i> -Inositol-1-phosphate MP	1.40 (n.s.)	1.18 (n.s.)	0.97 (n.s.)	n.s.	.	.	.
M000000_A243002	1.85 (***) s.	1.02 (n.s.)	0.82 (n.s.)	n.s.	n.s.	n.s.	n.s.
Xylobiose BP1	1.86 (**) s.	1.09 (n.s.)	4.93 (***) s.	n.s.	n.s.	n.s.	n.s.
M000000_A249004	1.44 (*)	1.33 (*)	2.43 (***) s.	n.s.	n.s.	n.s.	*
M000000_A250001	2.32 (***) s.	0.94 (n.s.)	0.94 (n.s.)	n.s.	n.s.	n.s.	n.s.
M000000_A264005	2.48 (**) s.	1.04 (n.s.)	0.38 (***) s.	n.s.	n.s.	n.s.	n.s.
Adenosine MP	1.37 (n.s.)	1.25 (n.s.)	0.75 (n.s.)	n.s.	n.s.	n.s.	**
M000000_A266002	1.91 (**) s.	1.22 (n.s.)	0.55 (***) s.	n.s.	*	n.s.	n.s.
M000000_A276004	1.31 (n.s.)	1.26 (n.s.)	0.78 (n.s.)	n.s.	n.s.	n.s.	n.s.
M000000_A276001	1.13 (n.s.)	1.51 (n.s.)	0.88 (n.s.)	n.s.	n.s.	n.s.	*
Octacosane	0.95 (n.s.)	0.92 (n.s.)	1.04 (n.s.)	**	n.s.	n.s.	n.s.
Gentiobiose BP1	1.19 (n.s.)	1.03 (n.s.)	1.86 (**) s.	n.s.	n.s.	n.s.	**
M000000_A286002	2.48 (*) s.	2.22 (*)	0.32 (**) s.	n.s.	n.s.	n.s.	*
Isomaltose MP	1.43 (n.s.)	1.02 (n.s.)	0.86 (n.s.)	n.s.	n.s.	n.s.	n.s.
M000000_A287005	1.34 (n.s.)	0.65 (n.s.)	1.60 (n.s.)	n.s.	n.s.	n.s.	.
Melibiose BP1	0.94 (n.s.)	1.91 (n.s.)	0.94 (n.s.)	n.s.	.	.	.
conjugate glycosylglycerol	1.22 (n.s.)	1.61 (n.s.)	0.49 (n.s.)	n.s.	n.s.	n.s.	n.s.
Dotriacontane	1.06 (n.s.)	1.01 (n.s.)	0.94 (n.s.)	n.s.	n.s.	n.s.	n.s.
M000000_A361001	1.22 (n.s.)	0.78 (n.s.)	0.70 (n.s.)	n.s.	n.s.	n.s.	n.s.
Hexatriacontane	0.96 (n.s.)	0.88 (n.s.)	1.07 (n.s.)	*	n.s.	n.s.	n.s.

S2.2b. AWF metabolome ANOVA (AWF_{NaCl}), 126 metabolites							
metabolite	Mn (+/-)	Si (+/-)	Gen (TVu 91/TVu 1987)	Mn*Si	Mn*Gen	Si*Gen	Mn*Si*Gen
2-hydroxypyridine	3.02 (***) s.	0.93 (n.s.)	1.26 (n.s.)	n.s.	n.s.	n.s.	n.s.
Lactic acid	0.61 (***) s.	0.81 (*)	0.92 (n.s.)	n.s.	n.s.	n.s.	n.s.
Undecane	2.57 (***) s.	1.12 (n.s.)	0.69 (**)	n.s.	*	n.s.	n.s.
Phosphoric acid	0.99 (n.s.)	0.94 (n.s.)	1.05 (n.s.)	n.s.	n.s.	n.s.	n.s.
Hydroxylamine	0.22 (***) s.	1.08 (n.s.)	0.80 (n.s.)	n.s.	n.s.	n.s.	n.s.
Oxalic acid	0.61 (**)	1.26 (n.s.)	0.96 (n.s.)	n.s.	n.s.	n.s.	n.s.
A114002	1.42 (***) s.	1.16 (n.s.)	1.01 (n.s.)	n.s.	n.s.	n.s.	n.s.
Monomethylphosphate	1.46 (**)	1.04 (n.s.)	0.87 (n.s.)	n.s.	n.s.	*	n.s.
Malonic acid	0.35 (***) s.	0.95 (n.s.)	0.99 (n.s.)	n.s.	n.s.	n.s.	n.s.
Dodecane	1.01 (n.s.)	1.02 (n.s.)	1.02 (n.s.)	n.s.	n.s.	n.s.	n.s.
Diethylenglycol MP	0.95 (*) s.	1.01 (n.s.)	0.99 (n.s.)	n.s.	n.s.	n.s.	n.s.
Threonine BP1	1.32 (*) s.	1.79 (n.s.)	0.51 (*) s.	n.s.	n.s.	n.s.	n.s.
Maleic acid	1.86 (***) s.	1.07 (n.s.)	0.97 (n.s.)	n.s.	n.s.	*	n.s.
Nicotinic acid	1.12 (n.s.)	1.08 (n.s.)	0.84 (*)	n.s.	*	n.s.	n.s.
Succinic acid	1.25 (*)	1.13 (n.s.)	1.04 (n.s.)	n.s.	n.s.	***	n.s.
Glyceric acid	1.11 (n.s.)	1.63 (**)	0.64 (*)	n.s.	n.s.	*	n.s.
M000000_A136002	1.63 (***) s.	0.89 (n.s.)	1.04 (n.s.)	n.s.	n.s.	n.s.	n.s.
Itaconic acid	2.08 (***) s.	1.12 (n.s.)	0.83 (n.s.)	n.s.	n.s.	**	n.s.
Fumaric acid	1.34 (*) s.	1.06 (n.s.)	1.00 (n.s.)	n.s.	n.s.	*	n.s.
M000000_A272011	4.61 (***) s.	1.09 (n.s.)	1.29 (n.s.)	n.s.	n.s.	*	n.s.
Alanine BP1	1.79 (*) s.	1.98 (n.s.)	0.54 (n.s.)	n.s.	n.s.	*	n.s.
Threonic acid-1,4-lactone	1.37 (n.s.)	1.61 (*) s.	0.76 (n.s.)	n.s.	n.s.	*	n.s.
β -Alanine MP	0.70 (n.s.)	2.21 (***) s.	0.57 (**)	n.s.	n.s.	n.s.	n.s.
A145001	1.79 (n.s.)	0.72 (n.s.)	0.41 (n.s.)	.	n.s.	n.s.	.
Erythronic acid-1,4-lactone	1.18 (*)	1.15 (n.s.)	0.77 (**)	n.s.	n.s.	*	n.s.
Erythrose MP	1.40 (*) s.	1.16 (n.s.)	0.79 (n.s.)	n.s.	n.s.	n.s.	n.s.
Malic acid	1.11 (*) s.	1.07 (n.s.)	1.03 (n.s.)	n.s.	n.s.	n.s.	n.s.
Erythritol	1.34 (***) s.	1.09 (n.s.)	0.82 (**)	*	*	***	n.s.
Pentadecane	1.07 (**)	1.03 (n.s.)	1.00 (n.s.)	n.s.	n.s.	n.s.	n.s.
Pyroglutamic acid	1.10 (n.s.)	1.04 (n.s.)	0.89 (n.s.)	n.s.	n.s.	*	n.s.
4-aminobutyric acid	0.81 (n.s.)	1.97 (**)	0.82 (n.s.)	*	n.s.	*	n.s.
Erythronic acid	0.97 (n.s.)	1.08 (n.s.)	0.90 (n.s.)	n.s.	n.s.	n.s.	n.s.
M000000_A155003	1.24 (*)	1.03 (n.s.)	0.76 (***) s.	n.s.	n.s.	*	n.s.
Threonic acid	0.75 (n.s.)	1.17 (n.s.)	0.93 (n.s.)	n.s.	n.s.	*	n.s.

2-hydroxyglutaric acid	1.16 (n.s.)	1.11 (n.s.)	0.73 (*) s.	n.s.	n.s.	**	n.s.
3-hydroxybenzoic acid	2.67 (***) s.	1.13 (n.s.)	0.81 (*)	n.s.	n.s.	*	n.s.
A160004	0.75 (*) s.	0.95 (n.s.)	0.90 (n.s.)	n.s.	n.s.	n.s.	n.s.
Ornithine	2.25 (***) s.	1.06 (n.s.)	0.94 (n.s.)	n.s.	n.s.	n.s.	n.s.
Tartaric acid	1.25 (***)	1.68 (n.s.)	0.03 (***) s.	n.s.	**	*	n.s.
M000000_A165003	2.22 (***) s.	1.07 (n.s.)	0.70 (*)	n.s.	n.s.	n.s.	n.s.
Xylose BP1	0.93 (n.s.)	0.92 (n.s.)	0.65 (***) s.	n.s.	n.s.	n.s.	n.s.
Xylose MP	1.40 (*) s.	0.89 (n.s.)	0.88 (n.s.)	n.s.	n.s.	n.s.	n.s.
Ribose MP	1.15 (n.s.)	1.05 (n.s.)	1.18 (n.s.)	n.s.	n.s.	n.s.	n.s.
Ribose BP1	1.44 (***) s.	1.08 (n.s.)	1.21 (n.s.)	n.s.	n.s.	n.s.	n.s.
M000000_A170001	1.57 (***) s.	1.04 (n.s.)	1.03 (n.s.)	n.s.	n.s.	**	n.s.
M000000_A174001	1.24 (*) s.	0.93 (n.s.)	1.28 (*) s.	n.s.	n.s.	n.s.	n.s.
Fucose BP1	1.02 (n.s.)	0.79 (n.s.)	0.81 (n.s.)	n.s.	n.s.	n.s.	n.s.
M000000_A175004	1.63 (***) s.	1.02 (n.s.)	0.83 (n.s.)	n.s.	n.s.	n.s.	n.s.
<i>cis</i> -Acontic acid	1.85 (***) s.	0.97 (n.s.)	0.63 (***) s.	n.s.	n.s.	n.s.	n.s.
Ribonic acid	1.24 (n.s.)	0.88 (n.s.)	1.33 (*)	n.s.	n.s.	n.s.	n.s.
3-deoxyglucose MP	3.35 (***) s.	1.11 (n.s.)	0.90 (n.s.)	n.s.	n.s.	n.s.	n.s.
M000000_A177004	1.63 (***) s.	1.02 (n.s.)	1.76 (***) s.	n.s.	**	n.s.	n.s.
M000000_A179001	1.79 (***) s.	1.06 (n.s.)	0.81 (n.s.)	n.s.	n.s.	n.s.	n.s.
A178011	1.33 (***) s.	0.95 (n.s.)	1.23 (***) s.	n.s.	n.s.	n.s.	n.s.
2-desoxypentose-3-xylose BP1	3.53 (***) s.	0.99 (n.s.)	0.88 (n.s.)	n.s.	n.s.	n.s.	n.s.
Shikimic acid	0.24 (***) s.	1.21 (n.s.)	0.59 (***)	n.s.	n.s.	n.s.	n.s.
Octadecane	1.07 (***) s.	1.04 (n.s.)	1.02 (n.s.)	n.s.	n.s.	n.s.	n.s.
Citric acid	1.10 (n.s.)	0.97 (n.s.)	1.04 (n.s.)	n.s.	**	n.s.	n.s.
M000000_A183011	1.49 (n.s.) s.	1.09 (n.s.)	1.00 (n.s.)	n.s.	n.s.	n.s.	n.s.
Tagatose BP1	1.96 (***) s.	1.10 (n.s.)	0.87 (n.s.)	n.s.	n.s.	n.s.	n.s.
Dehydroascorbic acid dimer MP	1.53 (***) s.	0.97 (n.s.)	1.15 (n.s.)	n.s.	n.s.	n.s.	n.s.
Tetradecanoic acid	1.28 (***) s.	1.00 (n.s.)	0.99 (n.s.)	n.s.	n.s.	n.s.	n.s.
M000611_A187006	1.72 (*)	0.79 (n.s.)	0.48 (***) s.	n.s.	n.s.	n.s.	*
Fructose MP	1.01 (n.s.)	1.15 (n.s.)	0.92 (n.s.)	n.s.	n.s.	n.s.	n.s.
Fructose BP1	1.05 (n.s.)	0.90 (***) s.	0.98 (n.s.)	n.s.	n.s.	n.s.	n.s.
Altrose MP	1.59 (***) s.	1.03 (n.s.)	0.68 (***) s.	n.s.	n.s.	n.s.	*
Glucose MP	0.95 (n.s.)	1.05 (n.s.)	1.05 (n.s.)	*	n.s.	n.s.	n.s.
Gluconic acid	2.57 (***) s.	1.16 (n.s.)	0.89 (n.s.)	n.s.	n.s.	*	n.s.
Glucose BP1	0.98 (n.s.)	0.97 (n.s.)	1.03 (*) s.	n.s.	n.s.	n.s.	n.s.
Nonadecane	1.01 (n.s.)	0.96 (n.s.)	0.98 (n.s.)	n.s.	n.s.	n.s.	n.s.
Mannitol	1.03 (n.s.)	1.19 (n.s.)	0.75 (***) s.	n.s.	n.s.	**	n.s.

M000000_A194007	3.80 (***) s.	1.12 (*)	1.05 (n.s.)	n.s.	*	**	n.s.
Ononitol	0.87 (**)	0.87 (*)	1.41 (***) s.	n.s.	*	n.s.	n.s.
M000000_A202004	1.35 (***) s.	1.04 (n.s.)	0.89 (n.s.)	n.s.	n.s.	n.s.	n.s.
M000000_A203003	1.24 (*) s.	1.26 (n.s.)	0.84 (n.s.)	n.s.	n.s.	**	n.s.
Hexadecanoic acid	1.14 (*) s.	1.06 (n.s.)	0.82 (**)	n.s.	n.s.	n.s.	n.s.
<i>myo</i> -Inositol	1.05 (n.s.)	1.17 (*)	0.82 (**)	**	n.s.	n.s.	n.s.
M000000_A211001	1.75 (***) s.	1.10 (n.s.)	1.05 (n.s.)	*	n.s.	*	n.s.
M000000_A213001	1.10 (n.s.)	1.01 (n.s.)	1.03 (n.s.)	n.s.	n.s.	n.s.	n.s.
M000000_A214003	0.98 (n.s.)	1.00 (n.s.)	1.05 (n.s.)	n.s.	n.s.	n.s.	n.s.
M000000_A216006	0.95 (n.s.)	0.96 (n.s.)	1.86 (***) s.	*	n.s.	n.s.	n.s.
A216005 od. 217003	2.73 (***) s.	1.03 (*)	0.97 (n.s.)	n.s.	n.s.	**	n.s.
M000000_A217003	2.59 (***) s.	0.99 (n.s.)	1.10 (n.s.)	n.s.	n.s.	**	n.s.
Spermidine BP1	0.73 (n.s.)	1.56 (n.s.)	1.19 (n.s.)	n.s.	n.s.	n.s.	n.s.
Docosane	1.06 (*) s.	1.04 (n.s.)	1.01 (n.s.)	n.s.	n.s.	n.s.	n.s.
Nonadecanoic acid methylester	0.19 (n.s.) s.	0.43 (n.s.)	1.08 (n.s.)	n.s.	n.s.	n.s.	n.s.
Octadecanoic acid	1.11 (*)	1.07 (n.s.)	0.82 (**)	n.s.	n.s.	n.s.	n.s.
M000000_A225004	1.03 (n.s.)	1.05 (n.s.)	1.73 (***) s.	n.s.	n.s.	n.s.	n.s.
Spermidine MP	0.32 (n.s.)	3.12 (n.s.)	0.61 (n.s.)	n.s.	n.s.	n.s.	n.s.
M000000_228001	1.50 (*) s.	0.95 (n.s.)	1.08 (n.s.)	n.s.	n.s.	*	n.s.
Zuckerphosphate	1.03 (n.s.)	0.96 (n.s.)	0.99 (n.s.)	n.s.	n.s.	n.s.	n.s.
Galactosylglycerol	1.12 (n.s.)	1.01 (n.s.)	1.40 (**)	n.s.	n.s.	n.s.	n.s.
M000000_A236001	0.96 (n.s.)	0.97 (n.s.)	1.92 (***) s.	*	n.s.	n.s.	n.s.
M000000_A237001	1.42 (*) s.	0.99 (n.s.)	1.11 (n.s.)	n.s.	n.s.	n.s.	n.s.
A239004	2.56 (***) s.	0.94 (n.s.)	2.74 (***) s.	n.s.	*	n.s.	n.s.
M000000_A240004	1.16 (n.s.)	1.02 (n.s.)	2.03 (***) s.	*	n.s.	n.s.	n.s.
<i>myo</i> -Inositol-1-phosphate	1.43 (n.s.)	1.12 (n.s.)	0.98 (n.s.)	.	n.s.	*	.
M000000_A243002	1.33 (**)	0.91 (n.s.)	2.23 (***) s.	n.s.	n.s.	n.s.	n.s.
Xylobiose BP1	2.36 (**)	1.03 (n.s.)	8.50 (***) s.	n.s.	*	n.s.	n.s.
M000000_A246005	0.73 (*)	0.91 (*)	2.45 (***) s.	*	n.s.	n.s.	n.s.
M000000_A249004	2.24 (***)	1.30 (n.s.)	11.49 (***) s.	n.s.	n.s.	n.s.	n.s.
M000000_A250001	2.19 (***) s.	1.16 (n.s.)	1.10 (n.s.)	n.s.	n.s.	***	n.s.
M000000_A261006	1.47 (**)	0.95 (n.s.)	1.10 (n.s.)	n.s.	n.s.	n.s.	n.s.
Sucrose MP	0.91 (n.s.)	1.04 (n.s.)	1.32 (**)	n.s.	n.s.	n.s.	n.s.
M000000_A264005	6.63 (***) s.	1.01 (n.s.)	0.72 (n.s.)	n.s.	n.s.	n.s.	n.s.
Adenosine MP	0.76 (n.s.)	1.26 (n.s.)	0.17 (***) s.	*	n.s.	n.s.	n.s.
M000000_A266002	1.35 (***) s.	1.17 (n.s.)	0.70 (***) s.	n.s.	n.s.	n.s.	n.s.
M000000_A267006	2.93 (***) s.	1.16 (n.s.)	1.20 (n.s.)	n.s.	n.s.	n.s.	n.s.

Maltose MP	1.27 (*) s.	1.14 (n.s.)	1.15 (n.s.)	n.s.	n.s.	n.s.	n.s.
M000000_A276004	2.33 (.)	2.33 (.)	1.11 (n.s.)
M000000_A276001	1.08 (n.s.)	1.26 (n.s.)	0.93 (n.s.)	n.s.	n.s.	n.s.	n.s.
Gentiobiose MP or M000000_A279001	1.81 (***) s.	0.83 (n.s.)	2.23 (***) s.	*	n.s.	n.s.	n.s.
Gentiobiose BP1	1.74 (***) s.	0.77 (n.s.)	2.14 (***) s.	n.s.	n.s.	n.s.	n.s.
Octacosane	0.62 (***) s.	1.03 (n.s.)	1.10 (*)	n.s.	n.s.	n.s.	n.s.
M000000_A286002	2.16 (n.s.)	2.61 (*) s.	0.35 (*) s.	n.s.	n.s.	n.s.	n.s.
Isomaltose MP	1.12 (n.s.)	0.72 (n.s.)	1.40 (*) s.	n.s.	n.s.	n.s.	n.s.
M000000_A287005	1.42 (n.s.)	0.78 (n.s.)	2.66 (***) s.	n.s.	n.s.	n.s.	n.s.
Melibiose BP1	0.80 (n.s.)	1.06 (n.s.)	1.39 (n.s.)	n.s.	n.s.	n.s.	n.s.
Isomaltose BP1	1.06 (n.s.)	2.18 (*) s.	0.75 (n.s.)	n.s.	n.s.	n.s.	n.s.
Galactinol	1.19 (n.s.)	1.38 (n.s.)	0.55 (*) s.	n.s.	n.s.	*	n.s.
conjugate glycosylinositol	1.15 (n.s.)	0.76 (n.s.)	1.36 (n.s.)	n.s.	n.s.	n.s.	n.s.
M000000_A311002	0.87 (n.s.)	1.20 (n.s.)	0.99 (n.s.)	n.s.	n.s.	n.s.	n.s.
Dotriacontane	0.38 (***) s.	1.05 (n.s.)	1.29 (n.s.)	n.s.	n.s.	n.s.	n.s.
M000000_A361001	0.64 (*) s.	0.86 (n.s.)	1.10 (n.s.)	n.s.	n.s.	n.s.	n.s.
Hexatriacontane	0.53 (***) s.	1.00 (n.s.)	1.16 (n.s.)	n.s.	n.s.	n.s.	n.s.

S2.3a. non-polar apoplastic metabolites ANOVA (AWF_{H2O}), 65 metabolites

metabolite	Mn (+/-)	Si (+/-)	Gen (TVu 91/TVu 1987)	Mn*Si	Mn*Gen	Si*Gen	Mn*Si*Gen
2-hydroxypyridine	1.36 (*) s.	0.90 (n.s.)	1.00 (n.s.)	n.s.	n.s.	n.s.	n.s.
Hydroxylamine	1.82 (n.s.)	0.87 (n.s.)	1.04 (n.s.)	n.s.	n.s.	n.s.	n.s.
Malonic acid MP	1.36 (n.s.)	0.87 (n.s.)	0.90 (n.s.)	n.s.	n.s.	n.s.	n.s.
Dodecane	1.09 (n.s.)	1.03 (n.s.)	0.98 (n.s.)	n.s.	n.s.	n.s.	n.s.
Diethylenglycol MP	1.08 (n.s.)	1.05 (n.s.)	0.98 (n.s.)	n.s.	n.s.	n.s.	n.s.
Benzoic acid	1.34 (***) s.	0.92 (n.s.)	0.99 (n.s.)	n.s.	n.s.	n.s.	n.s.
Ethanolamine MP	1.08 (n.s.)	1.03 (n.s.)	1.00 (n.s.)	n.s.	n.s.	n.s.	n.s.
Phosphoric acid	1.18 (n.s.)	0.87 (n.s.)	1.58 (n.s.)	n.s.	n.s.	n.s.	n.s.
Succinic acid	0.80 (***) s.	0.48 (***) s.	1.71 (***) s.	n.s.	*	n.s.	n.s.
Malic acid	1.02 (n.s.)	0.75 (n.s.)	1.29 (n.s.)	n.s.	n.s.	n.s.	n.s.
4-hydroxybenzoic acid	1.14 (n.s.)	0.91 (n.s.)	1.02 (n.s.)	n.s.	n.s.	n.s.	n.s.
A134004	1.18 (n.s.)	0.78 (n.s.)	0.89 (n.s.)	n.s.	n.s.	n.s.	n.s.
M000000_A136002	0.45 (*) s.	0.98 (n.s.)	1.58 (n.s.)	n.s.	n.s.	n.s.	n.s.
Fumaric acid	0.81 (n.s.)	0.89 (n.s.)	1.50 (*) s.	n.s.	n.s.	n.s.	n.s.
M000000_A143002	0.99 (n.s.)	1.13 (n.s.)	1.02 (n.s.)	n.s.	n.s.	n.s.	n.s.

M000000_A143003	0.96 (n.s.)	1.05 (n.s.)	0.97 (n.s.)	n.s.	n.s.	n.s.	n.s.
M000000_A144006	0.95 (n.s.)	1.09 (n.s.)	0.97 (n.s.)	n.s.	n.s.	n.s.	n.s.
Pentadecane	0.99 (n.s.)	1.05 (n.s.)	0.97 (n.s.)	n.s.	n.s.	n.s.	n.s.
3-hydroxyglutaric acid MP	10.42 (***) s.	0.60 (n.s.)	0.09 (***) s.	n.s.	***	n.s.	n.s.
Threonic acid	1.46 (n.s.)	0.88 (n.s.)	1.04 (n.s.)	.	.	n.s.	.
Triethanolamine	1.27 (n.s.)	0.42 (n.s.)	1.88 (n.s.)	n.s.	n.s.	n.s.	n.s.
Tartaric acid	2.66 (n.s.)	2.81 (n.s.)	7.33 (***) s.	n.s.	.	.	.
Dodecanoic acid	0.95 (n.s.)	1.07 (n.s.)	1.01 (n.s.)	n.s.	*	n.s.	n.s.
<i>cis</i> -Aconitic acid	1.06 (n.s.)	0.57 (***) s.	0.66 (*)	n.s.	n.s.	n.s.	n.s.
Tridecanoic acid	1.16 (n.s.)	0.94 (n.s.)	0.96 (n.s.)	n.s.	n.s.	.	.
<i>cis</i> -4-hydroxycinnamic acid	0.56 (***) s.	0.97 (n.s.)	1.60 (***) s.	n.s.	***	n.s.	n.s.
Octadecane	0.96 (n.s.)	1.02 (n.s.)	0.94 (n.s.)	n.s.	n.s.	n.s.	n.s.
Citric acid	1.23 (n.s.)	0.61 (n.s.)	0.56 (n.s.)	n.s.	n.s.	n.s.	n.s.
Jasmonic acid MP
Tetradecanoic acid	0.98 (n.s.)	1.05 (n.s.)	1.11 (n.s.)	n.s.	n.s.	n.s.	n.s.
A187012	2.21 (n.s.)	2.15 (n.s.)	1.71 (n.s.)
A188001_9	1.07 (n.s.)	1.01 (n.s.)	1.02 (n.s.)	n.s.	n.s.	n.s.	n.s.
Nonadecane	0.99 (n.s.)	1.04 (n.s.)	0.97 (n.s.)	*	n.s.	n.s.	n.s.
Docosane	0.98 (n.s.)	1.04 (n.s.)	0.97 (n.s.)	*	n.s.	n.s.	n.s.
<i>cis</i> -ferulic acid	0.40 (***) s.	1.24 (*)	0.52 (n.s.) s.	n.s.	.	n.s.	.
<i>trans</i> -4-hydroxycinnamic acid	0.53 (***) s.	0.89 (n.s.)	1.58 (***) s.	n.s.	***	n.s.	n.s.
Pantothenic acid MP	2.79 (***) s.	1.75 (*) s.	0.36 (***) s.	n.s.	n.s.	n.s.	n.s.
A201004	1.01 (n.s.)	1.08 (n.s.)	0.98 (n.s.)	n.s.	n.s.	n.s.	n.s.
Hexadecanoic acid	0.98 (n.s.)	1.06 (n.s.)	0.95 (n.s.)	n.s.	n.s.	n.s.	n.s.
M000000_A207002	1.15 (n.s.)	0.86 (n.s.)	1.14 (n.s.)	n.s.	n.s.	n.s.	n.s.
<i>myo</i> -Inositol	-(n.s.)	0.71 (.)	0.71 (.)
A211009	1.31 (n.s.)	0.88 (n.s.)	1.36 (n.s.)	n.s.	**	n.s.	n.s.
<i>trans</i> -ferulic acid	1.02 (n.s.)	0.80 (n.s.)	0.38 (***) s.	n.s.	*	n.s.	.
Octadecan-1-ol	0.79 (n.s.)	1.13 (n.s.)	0.81 (n.s.)	n.s.	n.s.	n.s.	n.s.
A320001	1.03 (n.s.)	1.06 (n.s.)	1.05 (n.s.)	n.s.	n.s.	n.s.	n.s.
M000000_A221004	2.30 (*) s.	1.35 (n.s.)	-(.)	n.s.	.	.	.
9,12-Octadecadienoic acid	0.92 (n.s.)	1.13 (n.s.)	0.57 (***) s.	n.s.	n.s.	n.s.	n.s.
A223008	0.77 (n.s.)	1.01 (n.s.)	1.00 (n.s.)	n.s.	n.s.	n.s.	n.s.
A223009	0.86 (n.s.)	0.87 (n.s.)	1.13 (n.s.)	n.s.	n.s.	n.s.	n.s.
M000000_A223005	0.89 (n.s.)	0.95 (n.s.)	2.85 (n.s.)	n.s.	n.s.	n.s.	n.s.
Octadecanoic acid	1.01 (n.s.)	1.05 (n.s.)	0.98 (n.s.)	n.s.	n.s.	n.s.	n.s.
<i>trans</i> -sinapic acid	2.48 (*) s.	1.68 (*)	0.66 (n.s.)	.	n.s.	.	.

M000000_A255002	1.07 (n.s.)	1.10 (n.s.)	1.14 (n.s.)	n.s.	n.s.	n.s.	n.s.
A257001	28.35 (n.s.)	24.41 (n.s.)	0.04 (n.s.)	n.s.	n.s.	n.s.	n.s.
M000000_A264003	3.03 (*) s.	0.47 (n.s.)	0.56 (n.s.)	n.s.	n.s.	n.s.	n.s.
A275004	4.15 (***) s.	0.48 (n.s.)	1.54 (*)	.	*	*	.
Laminaribiose BP1	0.74 (n.s.)	0.38 (n.s.) s.	0.56 (n.s.)	n.s.	.	.	.
A278009	0.54 (n.s.) s.	0.69 (n.s.)	1.67 (n.s.)	n.s.	n.s.	n.s.	n.s.
Octacosane	1.00 (n.s.)	1.05 (n.s.)	0.98 (n.s.)	n.s.	n.s.	n.s.	n.s.
<i>trans</i> -squalene	1.23 (n.s.)	0.90 (n.s.)	0.94 (n.s.)	n.s.	n.s.	n.s.	n.s.
M000000_A299007	0.94 (n.s.)	0.80 (***) s.	1.11 (n.s.)	n.s.	n.s.	**	n.s.
Hexacosanoic acid	0.89 (n.s.)	0.72 (*) s.	1.24 (n.s.)	*	n.s.	n.s.	n.s.
Cholesterol MP	1.01 (n.s.)	0.96 (n.s.)	1.11 (n.s.)	n.s.	n.s.	.	.
β -Sitosterol	0.82 (n.s.)	1.07 (n.s.)	0.96 (n.s.)	n.s.	n.s.	n.s.	n.s.
Hexatriacontane	0.96 (n.s.)	0.98 (n.s.)	0.98 (n.s.)	n.s.	n.s.	n.s.	n.s.

S2.3.b. non-polar apoplasmic metabolites ANOVA (AWF_{NaCl}), 65 metabolites

metabolite	Mn (+/-)	Si (+/-)	Gen (TVu 91/TVu 1987)	Mn*Si	Mn*Gen	Si*Gen	Mn*Si*Gen
2-hydroxypyridine	1.08 (n.s.)	0.82 (***) s.	0.99 (n.s.)	n.s.	n.s.	n.s.	n.s.
Hydroxylamine	2.06 (*)	0.90 (n.s.)	0.83 (n.s.)	n.s.	n.s.	n.s.	n.s.
Malonic acid MP	1.26 (n.s.)	0.73 (n.s.)	1.82 (***) s.	n.s.	n.s.	n.s.	n.s.
Dodecane	1.00 (n.s.)	0.90 (*) s.	0.97 (n.s.)	n.s.	n.s.	n.s.	n.s.
Diethylenglycol	1.03 (n.s.)	0.96 (n.s.)	1.00 (n.s.)	*	n.s.	n.s.	n.s.
Benzoic acid	1.20 (*) s.	1.04 (n.s.)	1.02 (n.s.)	n.s.	n.s.	n.s.	n.s.
Ethanolamine	1.06 (n.s.)	0.96 (n.s.)	0.97 (n.s.)	n.s.	n.s.	n.s.	n.s.
Phosphoric acid	0.59 (n.s.)	0.64 (n.s.)	1.43 (n.s.)	n.s.	n.s.	n.s.	n.s.
Succinic acid	0.81 (***) s.	0.52 (***) s.	2.06 (***) s.	**	**	n.s.	n.s.
A134004	1.10 (n.s.)	0.81 (n.s.)	1.19 (n.s.)	n.s.	n.s.	n.s.	n.s.
M000000_A136002	0.47 (***) s.	2.29 (n.s.)	1.40 (n.s.)	n.s.	n.s.	n.s.	n.s.
Fumaric acid	0.89 (n.s.)	1.20 (n.s.)	1.54 (***) s.	n.s.	n.s.	n.s.	n.s.
M000000_A143002	1.00 (n.s.)	1.10 (*) s.	1.02 (n.s.)	n.s.	n.s.	n.s.	n.s.
M000000_A143003	1.01 (n.s.)	1.07 (n.s.)	0.99 (n.s.)	n.s.	n.s.	n.s.	n.s.
M000000_A144006	1.01 (n.s.)	1.09 (n.s.)	1.03 (n.s.)	n.s.	n.s.	n.s.	n.s.
Malic acid	1.11 (n.s.)	1.00 (n.s.)	2.10 (***) s.	n.s.	n.s.	n.s.	n.s.
Pentadecane	1.03 (n.s.)	0.97 (n.s.)	1.00 (n.s.)	n.s.	n.s.	n.s.	n.s.
3-oxoglutaric acid	13.14 (***) s.	0.76 (n.s.)	0.24 (n.s.) s.	n.s.	***	n.s.	n.s.
Threonic acid	0.70 (n.s.)	0.58 (n.s.)	0.51 (n.s.)	n.s.	n.s.	n.s.	.
Triethanolamine	0.42 (n.s.)	0.56 (n.s.)	0.69 (n.s.)	n.s.	n.s.	n.s.	n.s.
Tartaric acid	0.85 (n.s.)	0.47 (***) s.	1.80 (*)	n.s.	n.s.	*	.

4-hydroxybenzoic acid	1.77 (***) s.	0.58 (***) s.	1.74 (***) s.	n.s.	n.s.	n.s.	n.s.
Dodecanoic acid	1.08 (n.s.)	1.00 (n.s.)	1.01 (n.s.)	n.s.	n.s.	n.s.	n.s.
<i>cis</i> -Aconitic acid	1.34 (n.s.)	0.64 (n.s.)	1.13 (n.s.)	n.s.	n.s.	n.s.	n.s.
Tridecanoic acid	0.98 (n.s.)	0.90 (n.s.)	0.86 (n.s.)	n.s.	n.s.	n.s.	.
<i>cis</i> -4-hydroxycinnamic acid	0.50 (***) s.	1.20 (n.s.)	2.80 (***) s.	n.s.	***	n.s.	n.s.
Octadecane	1.03 (n.s.)	0.97 (n.s.)	1.01 (n.s.)	n.s.	n.s.	n.s.	n.s.
Citric acid	1.04 (n.s.)	0.77 (n.s.)	1.56 (***) s.	n.s.	n.s.	n.s.	n.s.
Jasmonic acid MP	1.42 (n.s.)	0.51 (***) s.	- (.)	n.s.	.	.	.
Tetradecanoic acid	0.84 (n.s.)	0.99 (n.s.)	0.99 (n.s.)	n.s.	n.s.	n.s.	n.s.
A187012	0.68 (n.s.)	0.92 (n.s.)	1.78 (n.s.)	n.s.	n.s.	n.s.	.
A188001_9	1.00 (n.s.)	0.88 (n.s.)	1.19 (n.s.)	*	n.s.	n.s.	n.s.
Nonadecane	1.06 (n.s.)	0.99 (n.s.)	1.02 (n.s.)	n.s.	n.s.	n.s.	n.s.
<i>cis</i> -ferulic acid	0.50 (***) s.	3.80 (***) s.	2.18 (***)	n.s.	.	n.s.)	.
<i>trans</i> -4-hydroxycinnamic acid	0.57 (***) s.	0.98 (n.s.)	3.45 (***) s.	n.s.	**	n.s.	n.s.
Pantothenic acid	1.82 (***) s.	0.98 (n.s.)	1.82 (***) s.	*	n.s.	n.s.	n.s.
A201004	1.11 (n.s.)	1.11 (n.s.)	0.99 (n.s.)	n.s.	n.s.	n.s.	n.s.
Hexadecanoic acid	1.17 (n.s.)	0.92 (n.s.)	0.81 (n.s.)	n.s.	n.s.	n.s.	n.s.
M000000_A207002	0.90 (n.s.)	0.86 (n.s.)	1.19 (n.s.)	n.s.	n.s.	n.s.	n.s.
<i>myo</i> -Inositol	0.23 (.)	0.23 (.)	0.11 (.)
A211009	0.78 (n.s.)	0.74 (n.s.)	1.21 (n.s.)	n.s.	n.s.	n.s.	n.s.
<i>trans</i> -ferulic acid	1.42 (n.s.)	1.16 (n.s.)	1.28 (n.s.)	*	n.s.	n.s.	.
Octadecan-1-ol	1.64 (*) s.	1.55 (n.s.)	1.18 (n.s.)	n.s.	n.s.	n.s.	n.s.
M000000_A221004	1.16 (.)	- (.)	- (.)
Docosane	1.03 (n.s.)	0.97 (n.s.)	1.03 (n.s.)	n.s.	n.s.	n.s.	n.s.
9,12-Octadecadienoic acid	0.99 (n.s.)	1.30 (*) s.	0.74 (*) s.	n.s.	n.s.	n.s.	n.s.
A223008	1.17 (n.s.)	1.15 (n.s.)	1.30 (*)	n.s.	n.s.	n.s.	n.s.
A223009	0.96 (n.s.)	1.23 (n.s.)	1.15 (n.s.)	n.s.	n.s.	n.s.	n.s.
M000000_A223005	0.19 (n.s.)	1.62 (n.s.)	1.89 (n.s.)	n.s.	n.s.	n.s.	n.s.
Octadecanoic acid	1.07 (n.s.)	0.98 (n.s.)	0.94 (n.s.)	n.s.	n.s.	n.s.	n.s.
<i>trans</i> -sinapic acid	0.97 (n.s.)	0.84 (n.s.)	1.44 (*) s.	n.s.	n.s.	n.s.	n.s.
M000000_A255002	1.08 (n.s.)	1.20 (n.s.)	0.99 (n.s.)	n.s.	n.s.	n.s.	n.s.
A257001	0.89 (n.s.)	1.17 (n.s.)	0.78 (n.s.)	n.s.	n.s.	n.s.	n.s.
M000000_A264003	1.98 (***) s.	0.73 (n.s.)	1.24 (*)	n.s.	n.s.	n.s.	n.s.
A275004	0.82 (n.s.)	3.30 (n.s.)	0.97 (n.s.)	.	n.s.	.	.
Laminaribiose BP1	1.94 (n.s.)	1.03 (n.s.)	0.09 (***) s.	n.s.	n.s.	n.s.	n.s.
A278009	0.88 (n.s.)	1.00 (n.s.)	0.97 (n.s.)	n.s.	n.s.	n.s.	n.s.
Octacosane	1.08 (n.s.) s.	1.00 (n.s.)	0.99 (n.s.)	n.s.	n.s.	n.s.	n.s.

<i>trans</i> -squalene	0.64 (n.s.)	1.48 (n.s.)	1.55 (n.s.)	n.s.	n.s.	n.s.	.
M000000_A299007	1.24 (n.s.)	0.56 (***) s.	0.90 (n.s.)	n.s.	n.s.	n.s.	n.s.
Hexacosanoic acid	1.19 (n.s.)	0.64 (n.s.) s.	0.84 (n.s.)	n.s.	n.s.	n.s.	n.s.
Cholesterol MP	0.82 (n.s.)	1.66 (n.s.)	1.18 (n.s.)	.	n.s.	n.s.	
A320001	1.07 (.s.)	1.07 (n.s.)	1.06 (n.s.)	n.s.	n.s.	n.s.	n.s.
β -Sitosterol	0.83 (n.s.)	1.20 (n.s.)	0.90 (n.s.)	n.s.	n.s.	n.s.	n.s.
Hexatriacontane	0.86 (n.s.)	1.20 (n.s.)	1.25 (n.s.)	*	n.s.	n.s.	n.s.

Tab. S3: Peptide sequences of apoplastic cowpea proteins. AWF proteins were separated by means of BN-PAGE and afterwards stained for guaiacol-peroxidase activity. Stained BN-bands were cut from the gel and sequenced with nanoLC-MS/MS.

Lane No. ^a	Protein name ^b	Protein accession numbers ^c	Protein molecular weight (Da) ^d	Number of unique peptides	Percentage sequence coverage ^e	Peptide sequence	Mascot Ion score	Mascot Identity score	Difference score	+1	+2	+3	+4	Number of enzymatic termini	Calculated +1H Peptide Mass (AMU)
1	basic chitinase, chitinase [Arabidopsis thaliana]	NP_566426.1	36 196,3	1	5.67%	LPGYGVITNIINGGLECGR	65.8	44.9	20.9	0	1	1	0	2	2 003,0385
1	endochitinase precursor [Humulus lupulus]	AAD34596.1	33 511,4	1	4.11%	GFYTYDAFLTAAR	75.2	46	29.2	0	1	0	0	2	1 495,7221
1	putative cysteine protease [Glycine max]	ABR26679.1	38 963,3	1	4.51%	YNGGLETEEAYPYTGK	88.4	45.8	42.6	0	1	0	0	2	1 791,8081
2	basic chitinase, chitinase [Arabidopsis thaliana]	NP_566426.1	36 196,3	1	5.67%	LPGYGVITNIINGGLECGR	108	44.9	63.1	0	1	0	0	2	2 003,0385
2	pectin acetylsterase [Eucalyptus globulus subsp. globulus]	ABG34282.1	24 848,5	1	5.53%	CLSDAGFFLDER	90.1	46.4	43.7	0	1	0	0	2	1 429,6424
2	putative cysteine protease [Glycine max]	ABR26679.1	38 963,3	1	4.51%	YNGGLETEEAYPYTGK	76.8	45.8	31	0	1	0	0	2	1 791,8081
2	unknown [Populus trichocarpa]	ABK92766.1	35 697,9	2	6.02%	ALGQISER	58	47.2	10.8	0	1	0	0	2	873,4795
2	unknown [Populus trichocarpa]	ABK92766.1	35 697,9	2	6.02%	MELVDAAFFLLK	45.7	46.4	-0.7	0	1	0	0	2	1 346,7396
3	CYP1 (putative cyclophilin_ABH_like) [Vigna radiata]	BAB82452.1	18 188,7	1	6.98%	IVFELFADTTTPR	89.7	46	43.7	0	1	0	0	2	1 408,7479
3	acetylcholinesterase [Macroptilium atropurpureum]	BAG09557.1	42 760,3	2	4.71%	DQNEMATEFNK	56.5	45.8	10.7	0	2	0	0	2	1 342,5584
3	acetylcholinesterase [Macroptilium atropurpureum]	BAG09557.1	42 760,3	2	4.71%	MNFDQIR	39.8	46.1	-6.3	0	1	0	0	2	939,4359
3	basic chitinase, chitinase [Arabidopsis thaliana]	NP_566426.1	36 196,3	2	7.46%	IGFYQR	30.7	45.3	-14.6	0	1	0	0	2	783,4154
3	basic chitinase, chitinase [Arabidopsis thaliana]	NP_566426.1	36 196,3	2	7.46%	LPGYGVITNIINGGLECGR	98.2	44.9	53.3	0	1	1	0	2	2 003,0385
3	cyclophilin [Phaseolus vulgaris]	CAA52414.1	18 141,5	1	8.14%	VFFDMTIGGQPAGR	86.8	45.7	41.1	0	1	0	0	2	1 511,7319
3	pectin acetylsterase [Eucalyptus globulus subsp. globulus]	ABG34282.1	24 848,5	1	5.53%	CLSDAGFFLDER	90.6	46.4	44.2	0	1	0	0	2	1 429,6424
3	putative cysteine protease [Glycine max]	ABR26679.1	38 963,3	1	4.51%	YNGGLETEEAYPYTGK	94.8	45.8	49	0	1	0	0	2	1 791,8081
3	unknown [Populus trichocarpa]	ABK92766.1	35 697,9	3	9.64%	ALGQISER	55.1	47.2	7.9	0	1	0	0	2	873,4795
3	unknown [Populus trichocarpa]	ABK92766.1	35 697,9	3	9.64%	LDLTADELSEEK	74	46	28	0	1	0	0	2	1 362,6643
3	unknown [Populus trichocarpa]	ABK92766.1	35 697,9	3	9.64%	MELVDAAFFLLK	54.7	46.4	8.3	0	2	0	0	2	1 346,7396
3	Os02g0698000 [Oryza sativa (japonica cultivar-group)]	NP_001047825.1	44 848,2	1	3.23%	LTSVFGGAAEPPK	76.4	46.9	29.5	0	1	0	0	2	1 273,6794
4	Os06g0133800 [Oryza sativa (japonica cultivar-group)]	NP_001056711.1	80 012,2	1	1.88%	LAQLPGTSIEGVEK	75.5	46	29.5	0	1	0	0	2	1 441,7904
4	fasciclin-like arabinogalactan protein FLA8 [Arabidopsis thaliana]	AAG24276.1	43 044,2	1	2.62%	VGFGSAASGSK	62	46.1	15.9	0	2	0	0	2	967,4848
4	unknown [Populus trichocarpa]	ABK95670.1	33 327,4	1	4.44%	GPEFATIVNSVTSK	88.3	46	42.3	0	1	0	0	2	1 449,7590
4	unnamed protein product [Vitis vinifera]	CAO47327.1	34 358,9	1	3.74%	IEISAQNSWVGK	67.8	46.1	21.7	0	1	0	0	2	1 331,6959
4	putative cysteine protease [Glycine max]	ABR26679.1	38 963,3	1	4.51%	YNGGLETEEAYPYTGK	62.8	45.8	17	0	1	0	0	2	1 791,8081
4	hypothetical protein [Vitis vinifera]	CAN77531.1	33 023,8	1	4.39%	TDWSQAPFTASYR	76	45.8	30.2	0	1	0	0	2	1 529,7025
4	unknown [Populus trichocarpa]	ABK92766.1	35 697,9	3	9.64%	ALGQISER	51.5	47.2	4.3	0	2	0	0	2	873,4795
4	unknown [Populus trichocarpa]	ABK92766.1	35 697,9	3	9.64%	LDLTADELSEEK	66.1	46	20.1	0	2	0	0	2	1 362,6643
4	unknown [Populus trichocarpa]	ABK92766.1	35 697,9	3	9.64%	MELVDAAFFLLK	49.2	46	3.2	0	2	0	0	2	1 362,7345
4	Fructose-bisphosphate aldolase, chloroplast precursor [Oryza sativa (japonica cultivar-group)]	ABA91632.2	42 913,5	1	3.26%	LASIGLENTEANR	104	46	58	0	1	0	0	2	1 387,7181
4	CYP1 (putative cyclophilin_ABH_like) [Vigna radiata]	BAB82452.1	18 188,7	1	6.98%	IVFELFADTTTPR	73.1	46	27.1	0	1	0	0	2	1 408,7479
4	oligopeptidase A [Medicago truncatula]	ABY48141.1	79 104,5	1	1.43%	FGENVLDATK	65.1	46.3	18.8	0	1	0	0	2	1 093,5531
4	acetylcholinesterase [Macroptilium atropurpureum]	BAG09557.1	42 760,3	2	6.28%	DQNEMATEFNK	57.4	45.8	11.6	0	1	0	0	2	1 342,5584
4	acetylcholinesterase [Macroptilium atropurpureum]	BAG09557.1	42 760,3	2	6.28%	HGANFATGGSTIR	38.7	46.5	-7.8	0	1	0	0	2	1 288,6399
4	basic chitinase, chitinase [Arabidopsis thaliana]	NP_566426.1	36 196,3	2	7.46%	IGFYQR	34.7	45.3	-10.6	0	2	0	0	2	783,4154
4	basic chitinase, chitinase [Arabidopsis thaliana]	NP_566426.1	36 196,3	2	7.46%	LPGYGVITNIINGGLECGR	112	44.9	67.1	0	1	3	0	2	2 003,0385
4	cyclophilin [Phaseolus vulgaris]	CAA52414.1	18 141,5	1	8.14%	VFFDMTIGGQPAGR	75.8	45.7	30.1	0	3	0	0	2	1 511,7319
4	alpha galactosidase [Glycine max]	AAA73963.1	46 378,6	1	14.50%	ALADYVHK	55.7	46.8	8.9	0	1	1	0	2	916,4893
4	alpha galactosidase [Glycine max]	AAA73963.1	46 378,6	1	14.50%	SVGNSWR	57.9	48.6	9.3	0	2	0	0	2	805,3956
4	alpha galactosidase [Glycine max]	AAA73963.1	46 378,6	1	14.50%	TFASWGIDYK	74.3	46.5	27.8	0	2	0	0	2	1 300,6578
4	alpha galactosidase [Glycine max]	AAA73963.1	46 378,6	1	14.50%	TMPGSLGHHEEQDAK	74.2	46.1	28.1	0	2	0	0	2	1 499,6801
4	alpha galactosidase [Glycine max]	AAA73963.1	46 378,6	1	14.50%	YDNCENNISPQ	84.9	47.4	37.5	0	2	0	0	2	1 467,6175
4	endochitinase precursor [Humulus lupulus]	AAD34596.1	33 511,4	1	6.01%	GFYTYDAFLTAAR	77.3	46	31.3	0	2	0	0	2	1 495,7221
4	unnamed protein product (putative Serine carboxypeptidase) [Vitis vinifera]	CAO68876.1	57 192,0	1	2.96%	NLEVGIPDLLEDGIK	58.1	45.3	12.8	0	2	0	0	2	1 624,8801

4	alpha-galactosidase [Phaseolus vulgaris]	AAA73964	47 030,7	8	18.60%	AHFSIWALAK	50.4	46.3	4.1	0	1	0	0	2	1 143,6316
4	alpha-galactosidase [Phaseolus vulgaris]	AAA73964	47 030,7	8	18.60%	ALADYVHK	55.7	46.8	8.9	0	1	1	0	2	916.4893
4	alpha-galactosidase [Phaseolus vulgaris]	AAA73964	47 030,7	8	18.60%	ASTFPPSGMK	31	45.6	-14.6	1	1	0	0	2	925.4453
4	alpha-galactosidase [Phaseolus vulgaris]	AAA73964	47 030,7	8	18.60%	LAVILWNR	61.5	45.8	15.7	0	2	0	0	2	984.5996
4	alpha-galactosidase [Phaseolus vulgaris]	AAA73964	47 030,7	8	18.60%	SVGNSWR	57.9	48.6	9.3	0	2	0	0	2	805.3956
4	alpha-galactosidase [Phaseolus vulgaris]	AAA73964	47 030,7	8	18.60%	TFASWGIDYLK	74.3	46.5	27.8	0	2	0	0	2	1 300,6578
4	alpha-galactosidase [Phaseolus vulgaris]	AAA73964	47 030,7	8	18.60%	TMPGSLGHEEQDAK	74.2	46.1	28.1	0	2	0	0	2	1 499,6801
4	alpha-galactosidase [Phaseolus vulgaris]	AAA73964	47 030,7	8	18.60%	YDNCENKNISPK	36.3	46.6	-10.3	0	1	0	0	2	1 481,6695
5	fasciclin-like arabinogalactan protein 12 [Gossypium hirsutum]	ABV27483.1	43 894,2	1	1.88%	LADENINR	61	47	14	0	1	0	0	2	931.4849
5	Fructose-1,6-bisphosphatase, chloroplast precursor [Glycine max]	Q42796.1	43 879,4	2	7.96%	ANISNLTVQGVAVNVQGEDQK	51.5	44.8	6.7	0	0	1	0	2	2 142,0792
5	Fructose-1,6-bisphosphatase, chloroplast precursor [Glycine max]	Q42796.1	43 879,4	2	7.96%	YIGSLVGFHR	37.8	46.5	-8.7	0	0	1	0	2	1 263,6486
5	fasciclin-like arabinogalactan protein FLA8 [Arabidopsis thaliana]	AAG24276.1	43 044,2	1	2.62%	VGFGSAASGSK	67.5	46.1	21.4	0	1	0	0	2	967.4848
5	xyloglucan endotransglucosylase/hydrolase 2 [Cucumis melo]	ABI94062.1	36 316,1	1	3.88%	TDWSQAPFTASYR	90.7	45.8	44.9	0	1	0	0	2	1 529,7025
5	CYP1 (putative cyclophilin_ABH_like) [Vigna radiata]	BAB82452.1	18 188,7	1	6.98%	IVFELFADTTTPR	90	46	44	0	1	0	0	2	1 408,7479
5	basic chitinase, chitinase [Arabidopsis thaliana]	NP_566426.1	36 196,3	1	5.67%	LPGYGVITNIINGGLECGR	128	44.9	83.1	0	1	1	0	2	2 003,0385
5	Os01g0357100 [Oryza sativa (japonica cultivar-group)]	NP_001043008.1	72 385,0	1	1.65%	LADYGSSEL	72.3	49.1	23.2	0	1	0	0	2	1 209,5752
5	cytosolic malate dehydrogenase [Cicer arietinum]	CAC10208.1	41 361,4	1	2.11%	ALGQISER	61.4	47.2	14.2	0	1	0	0	2	873.4795
5	cyclophilin [Phaseolus vulgaris]	CAA52414.1	18 141,5	1	8.14%	VFFDMTIGGQPAGR	75.8	45.7	30.1	0	2	0	0	2	1 511,7319
5	alpha galactosidase [Glycine max]	AAA73963.1	46 378,6	4	10.40%	SVGNSWR	38.1	48.6	-10.5	0	1	0	0	2	805.3956
5	alpha galactosidase [Glycine max]	AAA73963.1	46 378,6	4	10.40%	TFASWGIDYLK	64.8	46.5	18.3	0	2	0	0	2	1 300,6578
5	alpha galactosidase [Glycine max]	AAA73963.1	46 378,6	4	10.40%	TMPGSLGHEEQDAK	36.8	46.1	-9.3	0	1	0	0	2	1 499,6801
5	alpha galactosidase [Glycine max]	AAA73963.1	46 378,6	4	10.40%	YDNCENNNISPK	67.5	47.4	20.1	0	2	0	0	2	1 467,6175
5	endochitinase precursor [Humulus lupulus]	AAD34596.1	33 511,4	1	4.11%	GFYTYDAFLTAAR	75.7	46	29.7	0	1	0	0	2	1 495,7221
5	unnamed protein product (putative secretory peroxidase) [Vitis vinifera]	CAO48839.1	34 372,5	1	2.79%	GYEVVDITK	53.1	46.5	6.6	0	1	0	0	2	1 023,5363
5	unnamed protein product (putative Serine carboxypeptidase) [Vitis vinifera]	CAO68876.1	57 192,0	1	2.96%	NLEVGIPDLLEDGIK	58.1	45.3	12.8	0	2	0	0	2	1 624,8801
6	Os06g0133800 [Oryza sativa (japonica cultivar-group)]	NP_001056711.1	80 012,2	1	1.88%	LAQLPGTISIEGVEK	63.3	46	17.3	0	1	0	0	2	1 441,7904
6	Phosphoglucomutase, cytoplasmic [Pisum sativum]	Q9SM60.1	63 308,1	6	11.70%	LSGTGSEGATIR	116	46.5	69.5	0	1	0	0	2	1 148,5913
6	Phosphoglucomutase, cytoplasmic [Pisum sativum]	Q9SM60.1	63 308,1	6	11.70%	MEEFTGR	32.9	45.6	-12.7	0	1	0	0	2	869.3828
6	Phosphoglucomutase, cytoplasmic [Pisum sativum]	Q9SM60.1	63 308,1	6	11.70%	SMPTSAALDVVAK	87.1	46.4	40.7	0	2	0	0	2	1 305,6724
6	Phosphoglucomutase, cytoplasmic [Pisum sativum]	Q9SM60.1	63 308,1	6	11.70%	YDYENVDAKAAK	72.9	47.5	25.4	0	1	0	0	2	1 315,5807
6	Phosphoglucomutase, cytoplasmic [Pisum sativum]	Q9SM60.1	63 308,1	6	11.70%	YLFEDGSR	34	46.5	-12.5	0	1	0	0	2	986.4583
6	Phosphoglucomutase, cytoplasmic [Pisum sativum]	Q9SM60.1	63 308,1	6	11.70%	YNMENGPAPEGITNK	61.8	45.3	16.5	0	1	0	0	2	1 707,7650
6	fasciclin-like arabinogalactan protein FLA8 [Arabidopsis thaliana]	AAG24276.1	43 044,2	1	2.62%	VGFGSAASGSK	65.1	46.1	19	0	1	0	0	2	967.4848
6	unknown [Populus trichocarpa]	ABK95047.1	42 422,0	4	9.95%	FEETLYGK	48.3	46.5	1.8	0	1	0	0	2	986.4836
6	unknown [Populus trichocarpa]	ABK95047.1	42 422,0	4	9.95%	LFSPGNLR	34.9	47.3	-12.4	0	1	0	0	2	903.5053
6	unknown [Populus trichocarpa]	ABK95047.1	42 422,0	4	9.95%	TTYVLALK	40.2	46.4	-6.2	0	1	0	0	2	908.5457
6	unknown [Populus trichocarpa]	ABK95047.1	42 422,0	4	9.95%	YTGGMVDPVNVQHVK	43.8	45.5	-1.7	0	1	0	0	2	1 649,8574
6	chloroplast fructose-1,6-bisphosphatase [Oryza sativa Indica Group]	ABY75186	43 586,8	2	6.16%	TLLYGGIYGYP	82.7	49.3	33.4	0	1	0	0	2	1 372,7268
6	chloroplast fructose-1,6-bisphosphatase [Oryza sativa Indica Group]	ABY75186	43 586,8	2	6.16%	VPLYIGSVIEVEK	44.7	46.4	-1.7	0	1	0	0	2	1 461,7841
6	CYP1 (putative cyclophilin_ABH_like) [Vigna radiata]	BAB82452.1	18 188,7	2	12.20%	FADENFVKK	34.1	45.5	-11.4	0	1	0	0	2	1 097,5632
6	CYP1 (putative cyclophilin_ABH_like) [Vigna radiata]	BAB82452.1	18 188,7	2	12.20%	IVFELFADTTTPR	73.9	46	27.9	0	1	0	0	2	1 408,7479
6	aldehyde reductase [Vigna radiata]	AAD53967.1	35 565,6	1	2.77%	TGLWYNLSK	53.5	45.9	7.6	0	1	0	0	2	1 081,5683
6	unnamed protein product [Vitis vinifera]	CAO1701.1	42 507,9	1	9.92%	VINNLDER	61.8	46.7	15.1	0	1	0	0	2	972.5114
6	basic chitinase, chitinase [Arabidopsis thaliana]	NP_566426.1	36 196,3	2	7.46%	IGFYQR	33.1	45.3	-12.2	0	1	0	0	2	783.4154
6	basic chitinase, chitinase [Arabidopsis thaliana]	NP_566426.1	36 196,3	2	7.46%	LPGYGVITNIINGGLECGR	130	44.9	85.1	0	1	0	0	2	2 003,0385
6	Os01g0357100 [Oryza sativa (japonica cultivar-group)]	NP_001043008.1	66 568,3	1	1.85%	LADYGSSEL	65.4	46.3	19.1	0	1	0	0	2	1 209,5752
6	cyclophilin [Phaseolus vulgaris]	CAA52414.1	18 141,5	1	13.40%	VFFDMTIGGQPAGR	57.4	45.7	11.7	0	1	1	0	2	1 511,7319
6	putative xyloglucan endotransglucosylase [Cucumis sativus]	ABK55722.1	33 812,4	1	4.71%	IIENGNLITLSLDK	113	45.6	67.4	0	1	0	0	2	1 542,8746
6	iron-superoxide dismutase precursor [Vigna unguiculata]	AAF28773.1	27 393,8	2	8.98%	LVSWDVAVSSR	73.7	46.5	27.2	0	1	0	0	2	1 119,5798
6	iron-superoxide dismutase precursor [Vigna unguiculata]	AAF28773.1	27 393,8	2	8.98%	SLEEIIIVTAYNK	49.8	46.2	3.6	0	1	0	0	2	1 379,7421
6	hypothetical protein [Vitis vinifera]	CAN69651.1	53 162,1	1	3.90%	SGTLFDNVLICDDPEYAK	61.4	45.2	16.2	0	1	0	0	2	1 999,9325
6	alpha galactosidase [Glycine max]	AAA73963.1	46 378,6	1	5.45%	TFASWGIDYLK	62.3	46.5	15.8	0	1	0	0	2	1 300,6578
6	alpha galactosidase [Glycine max]	AAA73963.1	46 378,6	1	5.45%	YDNCENNNISPK	79.5	47.4	32.1	0	1	0	0	2	1 467,6175
6	endochitinase precursor [Humulus lupulus]	AAD34596.1	33 511,4	1	6.01%	GFYTYDAFLTAAR	89	46	43	0	1	0	0	2	1 495,7221

6	Probable phosphoglucosyltransferase, cytoplasmic 2 [Arabidopsis thaliana]	Q9SGC1.1	63 465,5	1	7.18%	LSGTGSEGATIR	116	46.5	69.5	0	1	0	0	2	1 148,5913
6	Probable phosphoglucosyltransferase, cytoplasmic 2 [Arabidopsis thaliana]	Q9SGC1.1	63 465,5	1	7.18%	LVTVEDIVR	67.3	46.3	21	0	2	0	0	2	1 043,6102
6	Probable phosphoglucosyltransferase, cytoplasmic 2 [Arabidopsis thaliana]	Q9SGC1.1	63 465,5	1	7.18%	SMPTSAAALDVVAK	87.1	46.4	40.7	0	2	0	0	2	1 305,6724
6	14-3-3 protein [Vigna angularis]	BAB47119.1	29 342,0	2	8.08%	DSTLMQLLR	68.2	46.3	21.9	0	1	0	0	2	1 189,6617
6	14-3-3 protein [Vigna angularis]	BAB47119.1	29 342,0	2	8.08%	EAAESTLAAAYK	42.7	46.1	-3.4	0	1	0	0	2	1 153,5742
6	alpha-galactosidase [Phaseolus vulgaris]	AAA73964	47 030,7	2	4.47%	LAVILWNR	52.1	45.8	6.3	0	1	0	0	2	984,5996
6	alpha-galactosidase [Phaseolus vulgaris]	AAA73964	47 030,7	2	4.47%	TFASWGIDYLYK	62.3	46.5	15.8	0	1	0	0	2	1 300,6578
6	calreticulin-1 [Glycine max]	BAF36056.1	48 157,5	2	7.14%	AAFEEAEK	41.7	46.4	-4.7	0	1	0	0	2	894,4209
6	calreticulin-1 [Glycine max]	BAF36056.1	48 157,5	2	7.14%	APLIDNPDKDDPDLVYFPNLK	44.5	44	0.5	0	0	1	0	2	2 546,2821
7	acidic chitinase class 3 [Vigna unguiculata]	CAA61280.1	26 308,7	1	12.80%	QLFLGVPASTAAAGSGFIPANDLISQ	139	42.8	96.2	0	1	0	0	2	3 166,7513
7	fasciclin-like arabinogalactan protein FLA8 [Arabidopsis thaliana]	AAG24276.1	43 044,2	1	2.62%	VGFSAASGSK	71.4	46.1	25.3	0	2	0	0	2	967,4848
7	enolase [Glycine max]	AAS18240.1	47 701,9	2	3.60%	DGGS DYLGK	39.3	45.9	-6.6	0	1	0	0	2	911,4112
7	enolase [Glycine max]	AAS18240.1	47 701,9	2	3.60%	ISGDALK	34.5	48.1	-13.6	0	1	0	0	2	703,3991
7	Os06g0206000 [Oryza sativa (japonica cultivar-group)]	NP_001057093.1	33 451,3	1	3.58%	ITVGGSPER	67.8	45.9	21.9	0	1	0	0	2	1 141,6583
7	CYP1 (putative cyclophilin_ABH_like) [Vigna radiata]	BAB82452.1	18 188,7	2	11.60%	FADENFVK	58.8	45.8	13	0	1	0	0	2	969,4682
7	CYP1 (putative cyclophilin_ABH_like) [Vigna radiata]	BAB82452.1	18 188,7	2	11.60%	IVFELFADTTTPR	91.1	46	45.1	0	2	0	0	2	1 408,7479
7	putative xyloglucan endotransglycosylase [Cucumis sativus]	ABK55722.1	33 812,4	1	4.71%	IIENGNLITLSLDK	87.9	45.6	42.3	0	1	0	0	2	1 542,8746
7	Acidic endochitinase [Vigna angularis]	P29024.1	32 880,7	1	2.97%	YGGVMLWDR	72.5	46	26.5	0	5	0	0	2	1 096,5250
7	alpha galactosidase [Glycine max]	AAA73963.1	46 378,6	1	8.77%	TFASWGIDYLYK	53.9	46.5	7.4	0	1	0	0	2	1 300,6578
7	alpha galactosidase [Glycine max]	AAA73963.1	46 378,6	1	8.77%	YDNCENNNSPK	73.7	47.4	26.3	0	1	0	0	2	1 467,6175
7	cytosolic ascorbate peroxidase [Vigna unguiculata]	AAB03844.1	27 016,7	2	8.80%	EDKPEPPPEGR	35.6	46.5	-10.9	0	1	0	0	2	1 250,6020
7	cytosolic ascorbate peroxidase [Vigna unguiculata]	AAB03844.1	27 016,7	2	8.80%	SYPTVSADYQK	44.1	46.4	-2.3	0	1	0	0	2	1 258,5955
7	fasciclin-like arabinogalactan protein 12 [Gossypium hirsutum]	ABV27483.1	43 894,2	1	1.88%	LADEINTR	66.8	47	19.8	0	2	0	0	2	931,4849
7	unnamed protein product [Vitis vinifera]	CAO61165.1	36 739,2	2	7.29%	GDSNEVGPSIENAK	55.4	45.7	9.7	0	2	0	0	2	1 416,6607
7	unnamed protein product [Vitis vinifera]	CAO61165.1	36 739,2	2	7.29%	SLVGTPLMPGK	46	46.5	-0.5	0	1	0	0	2	1 099,6189
7	Phosphoglucosyltransferase, cytoplasmic [Pisum sativum]	Q9SM60.1	63 308,1	1	2.06%	YDYENVDAAGAAK	73.9	47.5	26.4	0	1	0	0	2	1 315,5807
7	endo-1,4-beta-mannanase [Glycine max]	ABG88068.1	44 105,4	1	2.55%	LLLSLVNWK	60.6	46.2	14.4	0	1	0	0	2	1 199,7153
7	hypothetical protein [Vitis vinifera]	CAN77531.1	33 023,8	1	4.39%	TDWSQAPFTASYR	81.1	45.8	35.3	0	1	0	0	2	1 529,7025
7	lipase [Gossypium hirsutum]	ABX75139.1	40 060,9	1	6.27%	AFFVFGDSLVDNNGNNYLATTAR	76.9	44	32.9	0	0	1	0	2	2 506,1995
7	pectin acetyltransferase [Eucalyptus globulus subsp. globulus]	ABG34280.1	38 829,9	1	3.43%	AEENPDDFNWNR	80.6	48.2	32.4	0	1	0	0	2	1 538,6663
7	unnamed protein product [Vitis vinifera]	CAO17011.1	42 507,9	1	2.04%	VINNLDER	59.3	46.7	12.6	0	2	0	0	2	972,5114
7	basic chitinase, chitinase [Arabidopsis thaliana]	NP_566426.1	36 196,3	2	7.46%	JGFYQR	41.7	45.3	-3.6	0	2	0	0	2	783,4154
7	basic chitinase, chitinase [Arabidopsis thaliana]	NP_566426.1	36 196,3	2	7.46%	LPGYGVITNIINGGLECGR	121	44.9	76.1	0	2	1	0	2	2 003,0385
7	cyclophilin [Phaseolus vulgaris]	CAA52414.1	18 141,5	1	12.80%	FADENFVK	58.8	45.8	13	0	1	0	0	2	969,4682
7	cyclophilin [Phaseolus vulgaris]	CAA52414.1	18 141,5	1	12.80%	VFFDMITGGQPAGR	65.6	45.7	19.9	0	2	1	0	2	1 511,7319
7	iron-superoxide dismutase precursor [Vigna unguiculata]	AAF28773.1	27 393,8	8	40.00%	AAAATQFGSGAWAWLAYK	104	45.4	58.6	0	2	1	0	2	1 798,8917
7	iron-superoxide dismutase precursor [Vigna unguiculata]	AAF28773.1	27 393,8	8	40.00%	ASLGLQNVAGINLLFK	114	45.4	68.6	0	3	0	0	2	1 699,9747
7	iron-superoxide dismutase precursor [Vigna unguiculata]	AAF28773.1	27 393,8	8	40.00%	LDGENAANPPSAEDDNK	61.2	45.5	15.7	0	2	2	0	2	1 756,7627
7	iron-superoxide dismutase precursor [Vigna unguiculata]	AAF28773.1	27 393,8	8	40.00%	LDGENAANPPSAEDDNKLVVVK	49	44.2	4.8	0	0	1	0	2	2 309,1624
7	iron-superoxide dismutase precursor [Vigna unguiculata]	AAF28773.1	27 393,8	8	40.00%	LVSWDVSSR	83.7	46.5	37.2	0	2	0	0	2	1 119,5798
7	iron-superoxide dismutase precursor [Vigna unguiculata]	AAF28773.1	27 393,8	8	40.00%	QVVGTELDGK	44	46.9	-2.9	0	1	0	0	2	1 045,5531
7	iron-superoxide dismutase precursor [Vigna unguiculata]	AAF28773.1	27 393,8	8	40.00%	RPDYISVEMDK	62.2	46.1	16.1	0	2	1	0	2	1 370,6779
7	iron-superoxide dismutase precursor [Vigna unguiculata]	AAF28773.1	27 393,8	8	40.00%	SLEEIHTAYNK	68	46.2	21.8	0	2	1	0	2	1 379,7421
7	endochitinase precursor [Humulus lupulus]	AAD34596.1	33 511,4	1	6.01%	GFYTYDAFLTAAR	80	46	34	0	1	0	0	2	1 495,7221
7	unnamed protein product (putative Serine carboxypeptidase) [Vitis vinifera]	CAO68876.1	57 192,0	1	2.96%	NLEVGPDLLEDGK	58.1	45.3	12.8	0	2	0	0	2	1 624,8801
7	alpha-galactosidase [Phaseolus vulgaris]	AAA73964	47 030,7	3	7.76%	LAVILWNR	57.7	45.8	11.9	0	1	0	0	2	984,5996
7	alpha-galactosidase [Phaseolus vulgaris]	AAA73964	47 030,7	3	7.76%	TFASWGIDYLYK	53.9	46.5	7.4	0	1	0	0	2	1 300,6578
7	alpha-galactosidase [Phaseolus vulgaris]	AAA73964	47 030,7	3	7.76%	TMPGSLGHEEQDAK	44.3	47.8	-3.5	0	1	0	0	2	1 515,6750
8	Os06g0133800 [Oryza sativa (japonica cultivar-group)]	NP_001056711.1	80 012,2	1	1.88%	LAQLPGTISIEGVEK	54.2	46	8.2	0	1	0	0	2	1 441,7904
8	fasciclin-like arabinogalactan protein 12 [Gossypium hirsutum]	ABV27483.1	43 894,2	1	1.88%	LADEINTR	62.1	47	15.1	0	1	0	0	2	931,4849
8	fasciclin-like arabinogalactan protein FLA8 [Arabidopsis thaliana]	AAG24276.1	43 044,2	1	2.62%	VGFSAASGSK	70.7	46.1	24.6	0	1	0	0	2	967,4848
8	hypothetical protein [Vitis vinifera]	CAN77531.1	33 023,8	1	4.39%	TDWSQAPFTASYR	85.1	45.8	39.3	0	1	0	0	2	1 529,7025
8	CYP1 (putative cyclophilin_ABH_like) [Vigna radiata]	BAB82452.1	18 188,7	2	15.10%	IVFELFADTTTPR	90	46	44	0	1	0	0	2	1 408,7479
8	CYP1 (putative cyclophilin_ABH_like) [Vigna radiata]	BAB82452.1	18 188,7	2	15.10%	TSRPVAIADCQGLS	69.9	46.1	23.8	0	1	0	0	2	1 474,7326

8	aldehyde reductase [Vigna radiata]	AAD53967.1	35 565,6	3	10.80%	DPQTELLDPAVK	66.1	47.6	18.5	0	1	0	0	2	325,6955
8	aldehyde reductase [Vigna radiata]	AAD53967.1	35 565,6	3	10.80%	SLGDIYIPLEVSLK	40.1	47.4	-7.3	0	1	0	0	2	1 546,8735
8	aldehyde reductase [Vigna radiata]	AAD53967.1	35 565,6	3	10.80%	TGLWYNLSK	52.5	45.9	6.6	0	1	0	0	2	1 081,5683
8	unnamed protein product [Vitis vinifera]	CAO17011.1	42 507,9	1	2.04%	VINNLDER	61.9	46.7	15.2	0	1	0	0	2	972,5114
8	basic chitinase, chitinase [Arabidopsis thaliana]	NP_566426.1	36 196,3	1	5.67%	LPGYGVITNIINGGLECGR	104	44.9	59.1	0	1	1	0	2	2 003,0385
8	cyclophilin [Phaseolus vulgaris]	CAA52414.1	18 141,5	1	8.14%	VFFDMTIGGQPAGR	72.5	45.7	26.8	0	1	0	0	2	1 511,7319
8	iron-superoxide dismutase precursor [Vigna unguiculata]	AAF28773.1	27 393,8	7	35.90%	AAAAATQFGSGWAWLAYK	89.1	45.4	43.7	0	1	0	0	2	1 798,8917
8	iron-superoxide dismutase precursor [Vigna unguiculata]	AAF28773.1	27 393,8	7	35.90%	ASLGLQNVAGINLLFK	105	45.4	59.6	0	1	0	0	2	1 699,9747
8	iron-superoxide dismutase precursor [Vigna unguiculata]	AAF28773.1	27 393,8	7	35.90%	LDGENAANPPSADEDNK	60.2	45.5	14.7	0	1	1	0	2	1 756,7627
8	iron-superoxide dismutase precursor [Vigna unguiculata]	AAF28773.1	27 393,8	7	35.90%	LDGENAANPPSADEDNKLVVIK	39.3	44.2	-4.9	0	0	1	0	2	2 309,1624
8	iron-superoxide dismutase precursor [Vigna unguiculata]	AAF28773.1	27 393,8	7	35.90%	LVSWDAVSSR	86	46.5	39.5	0	1	0	0	2	1 119,5798
8	iron-superoxide dismutase precursor [Vigna unguiculata]	AAF28773.1	27 393,8	7	35.90%	RPDYISVFMDK	58.1	46.1	12	0	2	0	0	2	1 370,6779
8	iron-superoxide dismutase precursor [Vigna unguiculata]	AAF28773.1	27 393,8	7	35.90%	SLEEIHVTAYNK	48.3	46.2	2.1	0	1	1	0	2	1 379,7421
8	endochitinase precursor [Humulus lupulus]	AAD34596.1	33 511,4	1	4.11%	GFYTYDAFLTAAR	79.9	46	33.9	0	1	0	0	2	1 495,7221
8	alpha-galactosidase [Phaseolus vulgaris]	AAA73964	47 030,7	2	4.47%	LAVILWNR	38.5	45.8	-7.3	0	1	0	0	2	984,5996
8	alpha-galactosidase [Phaseolus vulgaris]	AAA73964	47 030,7	2	4.47%	TFASWGIDYLYK	47.7	46.5	1.2	0	1	0	0	2	1 300,6578
9	putative glutathione S-transferase [Phaseolus acutifolius]	AAM34480.1	24 665,8	2	14.00%	LQPFVVPVIQGDYTYLESR	57.8	44.7	13.1	0	0	1	0	2	2 396,2140
9	putative glutathione S-transferase [Phaseolus acutifolius]	AAM34480.1	24 665,8	2	14.00%	SQGVYELLGR	48.2	46.8	1.4	0	1	0	0	2	958,5323
9	fasciclin-like arabinogalactan protein 12 [Gossypium hirsutum]	ABV27483.1	43 894,2	1	1.88%	LADENR	56.9	47	9.9	0	1	0	0	2	931,4849
9	unnamed protein product [Vitis vinifera]	CAO61165.1	36 739,2	2	7.29%	GDSNEVGPSIENAK	53.4	45.7	7.7	0	1	0	0	2	1 416,6607
9	unnamed protein product [Vitis vinifera]	CAO61165.1	36 739,2	2	7.29%	SLVGTPLMPGK	37.4	46.5	-9.1	0	1	0	0	2	1 099,6189
9	fasciclin-like arabinogalactan protein FLA8 [Arabidopsis thaliana]	AAG24276.1	43 044,2	1	2.62%	VFGGSAASGSK	63.3	46.1	17.2	0	1	0	0	2	967,4848
9	monodehydroascorbate reductase [Mesembryanthemum crystallinum]	CAC82727.1	51 731,5	2	3.98%	LYGELR	36	46.6	-10.6	0	1	0	0	2	750,4151
9	monodehydroascorbate reductase [Mesembryanthemum crystallinum]	CAC82727.1	51 731,5	2	3.98%	QGVQPGLAISK	38.2	46	-7.8	0	0	1	0	2	1 339,7588
9	chloroplast ribose-5-phosphate isomerase [Spinacia oleracea]	AAL77589.1	30 846,5	3	16.30%	FIVVVDITK	72.6	46.6	26	0	1	0	0	2	1 035,5727
9	chloroplast ribose-5-phosphate isomerase [Spinacia oleracea]	AAL77589.1	30 846,5	3	16.30%	IDLAIDGADEVPDLNLVK	66.3	45.1	21.2	0	1	1	0	2	2 025,0395
9	chloroplast ribose-5-phosphate isomerase [Spinacia oleracea]	AAL77589.1	30 846,5	3	16.30%	SGMVLGLGTGSTAAFAVSR	80.8	45.1	35.7	0	2	1	0	2	1 797,9168
9	hypothetical protein [Vitis vinifera]	CAN77531.1	33 023,8	2	8.11%	IIFSVDGTPIR	46.7	49	-2.3	0	1	0	0	2	1 217,6895
9	hypothetical protein [Vitis vinifera]	CAN77531.1	33 023,8	2	8.11%	TDWSQPFTASYR	69.1	45.8	23.3	0	1	0	0	2	1 529,7025
9	CYP1 (putative cyclophilin_ABH_like) [Vigna radiata]	BAB82452.1	18 188,7	1	6.98%	IVFELFADITPR	76.4	46	30.4	0	1	0	0	2	1 408,7479
9	aldehyde reductase [Vigna radiata]	AAD53967.1	35 565,6	4	14.50%	SLGDIYIPLEVSLK	53	47.4	5.6	0	1	0	0	2	1 546,8735
9	aldehyde reductase [Vigna radiata]	AAD53967.1	35 565,6	4	14.50%	SLGDIYIPLEVSLKDTVESLK	53.7	44.3	9.4	0	0	1	0	2	2 319,2701
9	aldehyde reductase [Vigna radiata]	AAD53967.1	35 565,6	4	14.50%	TGLWYNLSK	53.7	45.9	7.8	0	1	0	0	2	1 081,5683
9	aldehyde reductase [Vigna radiata]	AAD53967.1	35 565,6	4	14.50%	VVLTSIAAFAVSDRPK	33.4	45.4	-12	0	0	1	0	2	1 760,9911
9	unnamed protein product [Vitis vinifera]	CAO17011.1	42 507,9	1	4.07%	VINNLDER	59.8	46.7	13.1	0	1	0	0	2	972,5114
9	basic chitinase, chitinase [Arabidopsis thaliana]	NP_566426.1	36 196,3	2	7.46%	IGFYQR	34.2	45.3	-11.1	0	1	0	0	2	783,4154
9	basic chitinase, chitinase [Arabidopsis thaliana]	NP_566426.1	36 196,3	2	7.46%	LPGYGVITNIINGGLECGR	123	44.9	78.1	0	1	1	0	2	2 003,0385
9	cyclophilin [Phaseolus vulgaris]	CAA52414.1	18 141,5	1	8.14%	VFFDMTIGGQPAGR	65.2	46	19.2	0	2	0	0	2	1 495,7370
9	putative xyloglucan endotransglycosylase [Cucumis sativus]	ABK55722.1	33 812,4	1	4.71%	IIENGNLITLSLDK	113	45.6	67.4	0	1	0	0	2	1 542,8746
9	iron-superoxide dismutase precursor [Vigna unguiculata]	AAF28773.1	27 393,8	3	15.50%	ASLGLQNVAGINLLFK	115	45.4	69.6	0	1	0	0	2	1 699,9747
9	iron-superoxide dismutase precursor [Vigna unguiculata]	AAF28773.1	27 393,8	3	15.50%	LVSWDVSSR	37.2	46.5	-9.3	0	1	0	0	2	1 119,5798
9	iron-superoxide dismutase precursor [Vigna unguiculata]	AAF28773.1	27 393,8	3	15.50%	SLEEIHVTAYNK	57.4	46.2	11.2	0	1	0	0	2	1 379,7421
9	monodehydroascorbate reductase [Vaccinium corymbosum]	ABY49995.1	47 422,2	2	5.31%	AYLFPEPAR	38.3	46.2	-7.9	0	1	0	0	2	1 150,5897
9	monodehydroascorbate reductase [Vaccinium corymbosum]	ABY49995.1	47 422,2	2	5.31%	EIDDADKLYEAIK	83.4	46.1	37.3	0	1	0	0	2	1 522,7645
9	endochitinase precursor [Humulus lupulus]	AAD34596.1	33 511,4	1	6.01%	GFYTYDAFLTAAR	75.7	46	29.7	0	1	0	0	2	1 495,7221
9	quinone oxidoreductase [Fragaria x ananassa]	AAO22131.1	34 208,3	1	7.14%	DLSFIEAASLPLAIETAYEGLER	51.6	44	7.6	0	0	1	0	2	2 508,2874
10	chloroplast transketolase precursor [Gossypium barbadense]	ABS10814.1	18 411,0	2	16.10%	ALPTYTPEPADATR	44.8	46.2	-1.4	0	1	0	0	2	1 589,7813
10	chloroplast transketolase precursor [Gossypium barbadense]	ABS10814.1	18 411,0	2	16.10%	NLSQQLNALVK	37	45.7	-8.7	0	1	0	0	2	1 341,7490
10	fasciclin-like arabinogalactan protein 12 [Gossypium hirsutum]	ABV27483.1	43 894,2	1	1.88%	LADENR	57	47	10	0	1	0	0	2	931,4849
10	fasciclin-like arabinogalactan protein FLA8 [Arabidopsis thaliana]	AAG24276.1	43 044,2	1	2.62%	VFGGSAASGSK	58	46.1	11.9	0	1	0	0	2	967,4848
10	chloroplast ribose-5-phosphate isomerase [Spinacia oleracea]	AAL77589.1	30 846,5	3	16.30%	FIVVVDITK	53.9	46.6	7.3	0	1	0	0	2	1 035,5727
10	chloroplast ribose-5-phosphate isomerase [Spinacia oleracea]	AAL77589.1	30 846,5	3	16.30%	IDLAIDGADEVPDLNLVK	55.3	45.1	10.2	0	1	0	0	2	2 025,0395
10	chloroplast ribose-5-phosphate isomerase [Spinacia oleracea]	AAL77589.1	30 846,5	3	16.30%	SGMVLGLGTGSTAAFAVSR	60.2	45.1	15.1	0	1	0	0	2	1 797,9168
10	hypothetical protein [Vitis vinifera]	CAN77531.1	33 023,8	1	4.39%	TDWSQPFTASYR	62.7	45.8	16.9	0	1	0	0	2	1 529,7025

10	CYP1 (putative cyclophilin_ABH_like) [Vigna radiata]	BAB82452.1	18 188.7	1	6.98%	IVFELFADTTTPR	90.1	46	44.1	0	1	0	0	2	1 408,7479
10	aldehyde reductase [Vigna radiata]	AAD53967.1	35 565.6	2	7.08%	SLGIDYIPLEVSLK	49.7	47.4	2.3	0	1	0	0	2	1 546,8735
10	aldehyde reductase [Vigna radiata]	AAD53967.1	35 565.6	2	7.08%	TGLWYNLSK	49.6	45.9	3.7	0	1	0	0	2	1 081,5683
10	unnamed protein product [Vitis vinifera]	CAO17011.1	42 507.9	1	2.04%	VINNLDER	59.6	46.7	12.9	0	1	0	0	2	972.5114
10	basic chitinase, chitinase [Arabidopsis thaliana]	NP_566426.1	36 196.3	1	5.67%	LPGYGVITNIINGGLECGR	117	44.9	72.1	0	1	1	0	2	2 003,0385
10	cyclophilin [Phaseolus vulgaris]	CAA52414.1	18 141.5	1	8.14%	VFFDMTIGGQPAGR	62	45.7	16.3	0	1	0	0	2	1 511,7319
10	putative xyloglucan endotransglycosylase [Cucumis sativus]	ABK55722.1	33 812.4	1	4.71%	IIENGNLITLSLDK	116	45.6	70.4	0	1	0	0	2	1 542,8746
10	iron-superoxide dismutase precursor [Vigna unguiculata]	AAF28773.1	27 393.8	2	8.98%	LVSWDAVSSR	63.9	46.5	17.4	0	1	0	0	2	1 119,5798
10	iron-superoxide dismutase precursor [Vigna unguiculata]	AAF28773.1	27 393.8	2	8.98%	SLEEIHTAYNK	55	46.2	8.8	0	1	0	0	2	1 379,7421
10	endochitinase precursor [Humulus lupulus]	AAD34596.1	33 511.4	1	4.11%	GFYTYDAFLTAAR	75.9	46	29.9	0	1	0	0	2	1 495,7221
10	heat shock protein 70 [Cucumis sativus]	CAA52149.1	75 395.0	1	1.70%	NQADSVVYQTEK	73	45.9	27.1	0	1	0	0	2	1 381,6600
11	fasciclin-like arabinogalactan protein 12 [Gossypium hirsutum]	ABV27483.1	43 894.2	1	1.88%	LADEINTR	66.8	47	19.8	0	1	0	0	2	931.4849
11	chitinase [Brassica juncea]	ABC94640.1	17 011.3	1	12.90%	LPGYGVITNIINGGLECGGR	75	44.9	30.1	0	0	1	0	2	2 003,0385
11	chloroplast ribose-5-phosphate isomerase [Spinacia oleracea]	AAL77589.1	30 846.5	2	9.69%	FIVVDDTK	55.7	46.6	9.1	0	1	0	0	2	1 035,5727
11	chloroplast ribose-5-phosphate isomerase [Spinacia oleracea]	AAL77589.1	30 846.5	2	9.69%	SGMVLGLGTGSTAAFAVSR	91.9	45.1	46.8	0	1	0	0	2	1 797,9168
11	hypothetical protein [Vitis vinifera]	CAN77531.1	33 023.8	1	4.39%	TDWSQAPFTASYR	68.9	48.1	20.8	0	1	0	0	2	1 529,7025
11	unnamed protein product (putative Thaumatin family) [Vitis vinifera]	CAO62993.1	26 139.4	1	4.07%	GSDGSVIGCK	54.2	46.7	7.5	0	1	0	0	2	979.452
11	CYP1 (putative cyclophilin_ABH_like) [Vigna radiata]	BAB82452.1	18 188.7	1	6.98%	IVFELFADTTTPR	74.1	46	28.1	0	1	0	0	2	1 408,7479
11	aldehyde reductase [Vigna radiata]	AAD53967.1	35 565.6	1	2.77%	IGFYQR	53.2	45.9	7.3	0	1	0	0	2	1 081,5683
11	unnamed protein product [Vitis vinifera]	CAO17011.1	42 507.9	1	2.04%	VINNLDER	61.8	46.7	15.1	0	1	0	0	2	972.5114
11	basic chitinase, chitinase [Arabidopsis thaliana]	NP_566426.1	36 196.3	2	7.46%	IGFYQR	32.5	45.3	-12.8	0	1	0	0	2	783.4154
11	basic chitinase, chitinase [Arabidopsis thaliana]	NP_566426.1	36 196.3	2	7.46%	LPGYGVITNIINGGLECGR	121	44.9	76.1	0	1	0	0	2	2 003,0385
11	cyclophilin [Phaseolus vulgaris]	CAA52414.1	18 141.5	1	8.14%	VFFDMTIGGQPAGR	64.2	45.7	18.5	0	2	0	0	2	1 511,7319
11	endochitinase precursor [Humulus lupulus]	AAD34596.1	33 511.4	1	6.01%	GFYTYDAFLTAAR	75.8	46	29.8	0	1	0	0	2	1 495,7221
11	hypothetical protein OsI_024005 [Oryza sativa (indica cultivar-group)]	EAZ02773.1	41 953.8	1	3.17%	EPYTATIVSVVER	73.4	45.9	27.5	0	1	0	0	2	1 364,7061
12	fasciclin-like arabinogalactan protein 12 [Gossypium hirsutum]	ABV27483.1	43 894.2	1	1.88%	LADEINTR	67.8	47	20.8	0	2	0	0	2	931.4849
12	oxidoreductase family protein [Arabidopsis thaliana]	NP_188715.2	38 560.4	1	3.94%	DVAVLEAMLESAGAK	76.3	46.1	30.2	0	1	0	0	2	1 448,7308
12	unknown [Populus trichocarpa]	ABK92721.1	40 968.1	1	3.11%	SLGLADLAIDYTK	65.6	46.2	19.4	0	1	0	0	2	1 266,6583
12	hypothetical protein [Vitis vinifera]	CAN77531.1	33 023.8	1	4.39%	TDWSQAPFTASYR	84	45.8	38.2	0	1	0	0	2	1 529,7025
12	CYP1 (putative cyclophilin_ABH_like) [Vigna radiata]	BAB82452.1	18 188.7	1	6.98%	IVFELFADTTTPR	74	46	28	0	1	0	0	2	1 408,7479
12	rofl [Arabidopsis thaliana]	AAB82061.1	61 795.5	1	2.16%	TDEEQVVDGLDR	56.1	46	10.1	0	1	0	0	2	1 375,6344
12	peroxidase2 [Medicago sativa]	CAC38106.1	35 992.3	1	3.34%	IAINMDPTTPR	65.8	46.5	19.3	0	1	0	0	2	1 244,6311
12	aldehyde reductase [Vigna radiata]	AAD53967.1	35 565.6	1	3.69%	DPQTELLDPAVK	82.6	47.6	35	0	1	0	0	2	1 325,6955
12	basic chitinase, chitinase [Arabidopsis thaliana]	NP_566426.1	36 196.3	2	7.46%	IGFYQR	31.7	45.3	-13.6	0	1	0	0	2	783.4154
12	basic chitinase, chitinase [Arabidopsis thaliana]	NP_566426.1	36 196.3	2	7.46%	LPGYGVITNIINGGLECGR	113	44.9	68.1	0	1	1	0	2	2 003,0385
12	cyclophilin [Phaseolus vulgaris]	CAA52414.1	18 141.5	1	8.14%	VFFDMTIGGQPAGR	62.9	45.7	17.2	0	2	0	0	2	1 511,7319
12	peroxidase [Spinacia oleracea]	CAA71493.1	33 435.5	1	7.12%	MGNISPLTGSSGEIR	64	45.8	18.2	0	1	0	0	2	1 534,7536
12	endochitinase precursor [Humulus lupulus]	AAD34596.1	33 511.4	1	6.01%	GFYTYDAFLTAAR	80.7	46	34.7	0	1	0	0	2	1 495,7221
12	14-3-3 protein [Vigna angularis]	BAB47119.1	29 342.0	2	6.92%	NLLSVAYK	40	47.2	-7.2	0	1	0	0	2	907.5254
12	14-3-3 protein [Vigna angularis]	BAB47119.1	29 342.0	2	6.92%	YEEMVEFMEK	32.6	46.1	-13.5	0	1	0	0	2	1 366,5546
12	hypothetical protein OsI_024005 [Oryza sativa (indica cultivar-group)]	EAZ02773.1	41 953.8	3	7.39%	EPYTATIVSVVER	35.7	45.9	-10.2	0	1	0	0	2	1 364,7061
12	hypothetical protein OsI_024005 [Oryza sativa (indica cultivar-group)]	EAZ02773.1	41 953.8	3	7.39%	LYSIASTR	40.5	48.4	-7.9	0	1	0	0	2	910.4997
12	hypothetical protein OsI_024005 [Oryza sativa (indica cultivar-group)]	EAZ02773.1	41 953.8	3	7.39%	YGDSFDGK	41.3	47.1	-5.8	0	1	0	0	2	888.3741
12	ascorbate peroxidase [Litchi chinensis]	ABZ79406.1	27 497.2	1	4.00%	EGLIQLPSDK	62.1	46.5	15.6	0	1	0	0	2	1 099,6002
13	fasciclin-like arabinogalactan protein 12 [Gossypium hirsutum]	ABV27483.1	43 894.2	1	1.88%	LADEINTR	73.1	47	26.1	0	1	0	0	2	931.4849
13	pepti (ISS) (putative Cyclophilin) [Ostreococcus tauri]	CAL57205.1	38 854.4	1	3.27%	IVLGLFGDDAPR	60.6	46.3	14.3	0	2	0	0	2	1 272,6955
13	unnamed protein product (putative Thaumatin family) [Vitis vinifera]	CAO62993.1	26 139.4	1	4.07%	GSDGSVIGCK	77.4	46.7	30.7	0	1	0	0	2	979.452
13	CYP1 (putative cyclophilin_ABH_like) [Vigna radiata]	BAB82452.1	18 188.7	1	6.98%	IVFELFADTTTPR	71.7	46	25.7	0	1	0	0	2	1 408,7479
13	putative glycine-rich RNA-binding protein [Dianthus caryophyllus]	BIF34340.1	16 872.1	1	5.68%	SITVNEAQR	65.3	46.4	18.9	0	1	0	0	2	1 104,5649
13	peroxidase [Spinacia oleracea]	CAA71493.1	33 435.5	2	7.12%	MGASILR	42.9	47.7	-4.8	0	1	0	0	2	763.4137
13	peroxidase [Spinacia oleracea]	CAA71493.1	33 435.5	2	7.12%	MGNISPLTGSSGEIR	79.7	45.8	33.9	0	1	0	0	2	1 534,7536
14	fasciclin-like arabinogalactan protein 12 [Gossypium hirsutum]	ABV27483.1	43 894.2	1	1.88%	LADEINTR	69.5	47	22.5	0	2	0	0	2	931.4849
14	pepti (ISS) (putative Cyclophilin) [Ostreococcus tauri]	CAL57205.1	38 854.4	1	3.27%	IVLGLFGDDAPR	56.1	46.3	9.8	0	2	0	0	2	1 272,6955
14	oxidoreductase family protein [Arabidopsis thaliana]	NP_188715.2	38 560.4	1	3.94%	DVAVLEAMLESAGAK	96.1	46.1	50	0	1	0	0	2	1 448,7308

14	CYP1 (putative cyclophilin_ABH_like) [Vigna radiata]	BAB82452.1	18 188,7	1	6.98%	IVFELFADTTTPR	76.5	46	30.5	0	1	0	0	2	1 408,7479
14	hypothetical protein (putative 14-3-3 protein) [Vitis vinifera]	CAN81774.1	29 523,7	1	4.58%	TVEVEELTVEER	86	46.5	39.5	0	1	0	0	2	1 432,7172
14	peroxidase [Spinacia oleracea]	CAA71493.1	33 435,5	2	7.12%	MGASILR	46.2	47.7	-1.5	0	1	0	0	2	763.4137
14	peroxidase [Spinacia oleracea]	CAA71493.1	33 435,5	2	7.12%	MGNISPLTGSSGEIR	87.1	45.8	41.3	0	3	0	0	2	1 534,7536
15	fasciclin-like arabinogalactan protein 12 [Gossypium hirsutum]	ABV27483.1	43 894,2	1	1.88%	LADEINTR	54.4	47	7.4	0	2	0	0	2	931.4849
15	unnamed protein product (putative Thaumatin family) [Vitis vinifera]	CAO62993.1	26 139,4	1	4.07%	GSDGSVIGCK	80.8	46.7	34.1	0	2	0	0	2	979.452
15	CYP1 (putative cyclophilin_ABH_like) [Vigna radiata]	BAB82452.1	18 188,7	1	6.98%	IVFELFADTTTPR	73	46	27	0	1	0	0	2	1 408,7479
15	Protein P21 (putative Thaumatin family) [Glycine max]	P25096.1	25 930,1	1	4.18%	TGCNFDGSGR	81.4	46	35.4	0	2	0	0	2	1 070,4326
15	peroxidase [Spinacia oleracea]	CAA71493.1	33 435,5	2	7.12%	MGASILR	45.5	47.7	-2.2	0	1	0	0	2	763.4137
15	peroxidase [Spinacia oleracea]	CAA71493.1	33 435,5	2	7.12%	MGNISPLTGSSGEIR	83.1	45.8	37.3	0	4	0	0	2	1 534,7536
15	transaldolase [Lycopersicon esculentum]	AAG16981.1	55 421,0	1	2.13%	VTSVASFFVSR	59	46.2	12.8	0	1	0	0	2	1 199,6423
16	CYP1 (putative cyclophilin_ABH_like) [Vigna radiata]	BAB82452.1	18 188,7	1	6.98%	IVFELFADTTTPR	72.9	46	26.9	0	1	0	0	2	1 408,7479
16	iron-superoxide dismutase precursor [Vigna unguiculata]	AAF28773.1	27 393,8	1	6.53%	ASFLGLQNVAGINLLFK	83	45.4	37.6	0	1	0	0	2	1 699,9747
16	peroxidase [Spinacia oleracea]	CAA71493.1	33 435,5	2	7.12%	MGASILR	51.8	47.7	4.1	0	2	0	0	2	763.4137
16	peroxidase [Spinacia oleracea]	CAA71493.1	33 435,5	2	7.12%	MGNISPLTGSSGEIR	105	45.8	59.2	0	4	1	0	2	1 534,7536
16	ATAM11, amidase [Arabidopsis thaliana]	NP_563831.1	45 038,6	1	3.53%	LVDFSIGDTGGSVR	91.2	45.8	45.4	0	1	0	0	2	1 523,7707
17	unknown [Populus trichocarpa]	ABK95110.1	51 395,0	1	3.44%	AVANQPVSVAIEGGGR	55.2	45.7	9.5	0	1	0	0	2	1 524,8134
17	CYP1 (putative cyclophilin_ABH_like) [Vigna radiata]	BAB82452.1	18 188,7	1	6.98%	IVFELFADTTTPR	86	46	40	0	1	0	0	2	1 408,7479
17	basic chitinase, chitinase [Arabidopsis thaliana]	NP_566426.1	36 196,3	1	5.67%	LPGYGVITNIINGGLECGR	67.1	44.9	22.2	0	0	1	0	2	2 003,0385
17	ribulose-1,5-bisphosphate carboxylase small subunit [Glycine max]	AAA81328.1	21 181,6	1	4.28%	IIGFDNVR	58.5	47.2	11.3	0	1	0	0	2	933.516
17	putative glycine-rich RNA-binding protein [Dianthus caryophyllus]	BAF34340.1	16 872,1	1	5.68%	SITVNEAQRS	52.6	46.4	6.2	0	1	0	0	2	1 104,5649
17	cyclophilin [Phaseolus vulgaris]	CAA52414.1	18 141,5	1	8.14%	VFFDMTIGGQPAGR	66.8	48	18.8	0	1	0	0	2	1 511,7319
17	peroxidase [Spinacia oleracea]	CAA71493.1	33 435,5	1	7.12%	MGNISPLTGSSGEIR	93.9	45.8	48.1	0	3	2	0	2	1 534,7536
18	fasciclin-like arabinogalactan protein 12 [Gossypium hirsutum]	ABV27483.1	43 894,2	1	1.88%	LADEINTR	54.7	47	7.7	0	1	0	0	2	931.4849
18	pepti (ISS) (putative Cyclophilin) [Ostreococcus tauri]	CAL57205.1	38 854,4	1	3.27%	IVLGLFGDDAPR	58.1	46.3	11.8	0	1	0	0	2	1 272,6955
18	unknown [Populus trichocarpa]	ABK95110.1	51 395,0	1	3.44%	AVANQPVSVAIEGGGR	77.7	45.7	32	0	1	0	0	2	1 524,8134
18	CYP1 (putative cyclophilin_ABH_like) [Vigna radiata]	BAB82452.1	18 188,7	1	6.98%	IVFELFADTTTPR	74.2	46	28.2	0	1	0	0	2	1 408,7479
18	cyclophilin [Phaseolus vulgaris]	CAA52414.1	18 141,5	1	8.14%	VFFDMTIGGQPAGR	89	48	41	0	2	0	0	2	1 511,7319
18	peroxidase [Spinacia oleracea]	CAA71493.1	33 435,5	1	7.12%	MGNISPLTGSSGEIR	86.9	45.8	41.1	0	3	0	0	2	1 534,7536
18	HSP70 (heat shock protein 70) [Arabidopsis thaliana]	NP_187864.1	71 085,2	1	2.00%	TTPSYVAFTDSEIR	60.2	45.9	14.3	0	1	0	0	2	1 473,6861
18	isopentenyl diphosphate isomerase 2 [Nicotiana tabacum]	BAB40974.1	34 190,4	1	4.32%	ESLIEENALGVR	64	45.8	18.2	0	1	0	0	2	1 458,7440
19	CYP1 (putative cyclophilin_ABH_like) [Vigna radiata]	BAB82452.1	18 188,7	1	6.98%	IVFELFADTTTPR	76.4	46	30.4	0	1	0	0	2	1 408,7479
19	cysteine proteinase precursor [Phaseolus vulgaris]	CAB17076.1	50 235,7	1	3.08%	NSWGADWGEEGYIR	62.7	47.8	14.9	0	1	0	0	2	1 639,7141
19	basic chitinase, chitinase [Arabidopsis thaliana]	NP_566426.1	36 196,3	1	5.67%	LPGYGVITNIINGGLECGR	96.7	44.9	51.8	0	1	1	0	2	2 003,0385
19	orf [Medicago sativa]	CAA66205.1	34 663,5	1	2.56%	TPGQVALR	55	46.6	8.4	0	1	0	0	2	841.4897
19	peroxidase [Spinacia oleracea]	CAA71493.1	33 435,5	1	4.85%	MGNISPLTGSSGEIR	79	46.5	32.5	0	1	0	0	2	1 518,7588
19	unnamed protein product [Vitis vinifera]	CAO15661.1	27 624,2	2	8.70%	MADLPTVLVTGAGGR	53.4	47.8	5.6	0	1	0	0	2	1 515,7843
19	unnamed protein product [Vitis vinifera]	CAO15661.1	27 624,2	2	8.70%	TGQIVYK	36.8	47.7	-10.9	0	1	0	0	2	808.457
19	unknown [Populus trichocarpa x Populus deltoides]	ABK96272.1	35 285,3	1	2.74%	IFAGDVVPR	75.1	46.8	28.3	0	1	0	0	2	973.5472
19	aldose reductase [Digitalis purpurea]	CAC32834.1	34 862,4	1	3.17%	AMEALYDSGK	57.1	45.9	11.2	0	2	0	0	2	1 084,4985
19	cysteine proteinase [Dianthus caryophyllus]	AAA79915.1	46 700,1	1	2.81%	CGIAIEPSYPVK	58.1	46.4	11.7	0	1	0	0	2	1 333,6827
19	HSP70 (heat shock protein 70) [Arabidopsis thaliana]	NP_187864.1	71 085,2	5	8.62%	IINEPTAAAIAYGLDK	88.1	45.5	42.6	0	1	0	0	2	1 659,8961
19	HSP70 (heat shock protein 70) [Arabidopsis thaliana]	NP_187864.1	71 085,2	5	8.62%	IINEPTAAAIAYGLDKK	39.1	46.9	-7.8	0	0	1	0	2	1 787,9911
19	HSP70 (heat shock protein 70) [Arabidopsis thaliana]	NP_187864.1	71 085,2	5	8.62%	NAVVTVPAYFNDSQR	46.3	45.4	0.9	0	1	0	0	2	1 680,8343
19	HSP70 (heat shock protein 70) [Arabidopsis thaliana]	NP_187864.1	71 085,2	5	8.62%	TTPSYVAFTDSEIR	87.4	45.9	41.5	0	1	0	0	2	1 473,6861
19	HSP70 (heat shock protein 70) [Arabidopsis thaliana]	NP_187864.1	71 085,2	5	8.62%	VEIHANDQGNR	42.3	48.9	-6.6	0	1	0	0	2	1 228,6286
19	putative cysteine protease [Glycine max]	ABR26679.1	38 963,3	1	4.51%	YNGGLETEEAYPYTGK	59.2	45.8	13.4	0	1	0	0	2	1 791,8081
20	Heat shock 70 kDa protein [Zea mays]	P11143.1	70 586,9	1	6.98%	NQVAMNPTNTVFDKAK	74.7	45.4	29.3	0	1	0	0	2	1 665,7905
20	Heat shock 70 kDa protein [Zea mays]	P11143.1	70 586,9	1	6.98%	TTPSYVGFDTTER	65.1	45.9	19.2	0	1	0	0	2	1 473,6862
20	unknown [Populus trichocarpa x Populus deltoides]	ABK96272.1	35 285,3	1	2.74%	IFAGDVVPR	78.9	46.8	32.1	0	1	0	0	2	973.5472
20	unknown protein [Picea sitchensis]	ABK25518.1	12 124,6	1	11.30%	EIVSSNSVVVFSK	56.7	46	10.7	0	1	0	0	2	1 394,7530
20	putative cysteine protease [Glycine max]	ABR26679.1	38 963,3	1	4.51%	YNGGLETEEAYPYTGK	80.8	45.8	35	0	1	0	0	2	1 791,8081
20	unknown [Populus trichocarpa]	ABK95110.1	51 395,0	1	3.44%	AVANQPVSVAIEGGGR	101	45.7	55.3	0	1	0	0	2	1 524,8134
20	basic chitinase, chitinase [Arabidopsis thaliana]	NP_566426.1	36 196,3	2	7.46%	JGFYQR	33.1	45.3	-12.2	0	1	0	0	2	783.4154

20	basic chitinase, chitinase [Arabidopsis thaliana]	NP_566426.1	36 196,3	2	7.46%	LPGYGVITNIINGGLECGR	137	44.9	92.1	0	1	1	0	2	2 003,0385
20	cyclophilin [Phaseolus vulgaris]	CAA52414.1	18 141,5	1	8.14%	VFFDMTIGGQPAGR	58.1	45.7	12.4	0	1	0	0	2	1 511,7319
20	HSP70 (heat shock protein 70) [Arabidopsis thaliana]	NP_187864.1	71 085,2	2	4.92%	IINEPTAAAIAYGLDKK	42.7	46.9	-4.2	0	0	1	0	2	1 787,9911
20	HSP70 (heat shock protein 70) [Arabidopsis thaliana]	NP_187864.1	71 085,2	2	4.92%	NQVAMNPTNTVFDKAK	74.7	45.4	29.3	0	1	0	0	2	1 665,7905
20	isopentenyl diphosphate isomerase 2 [Nicotiana tabacum]	BAB40974.1	34 190,4	2	9.30%	DVNVNPNPDEVAIDIK	74.1	45.4	28.7	0	1	0	0	2	1 638,7976
20	isopentenyl diphosphate isomerase 2 [Nicotiana tabacum]	BAB40974.1	34 190,4	2	9.30%	ESELIEENALGVR	55.3	45.8	9.5	0	1	0	0	2	1 458,7440
21	basic chitinase, chitinase [Arabidopsis thaliana]	NP_566426.1	36 196,3	1	5.67%	LPGYGVITNIINGGLECGR	130	44.9	85.1	0	1	1	0	2	2 003,0385
21	endochitinase precursor [Humulus lupulus]	AAD34596.1	33 511,4	1	4.11%	GFYTYDAFLTAAR	74.9	46	28.9	0	1	0	0	2	1 495,7221
21	unknown protein [Picea sitchensis]	ABK25518.1	12 124,6	1	11.30%	EIVSSNSVVVFSK	107	46	61	0	1	0	0	2	1 394,7530
21	Basic endochitinase [Nicotiana tabacum]	P29061.1	33 244,0	1	2.98%	YGGVMLWNR	55.2	46	9.2	0	1	0	0	2	1 095,5410
21	putative cysteine protease [Glycine max]	ABR26679.1	38 963,3	1	4.51%	YNGGLETEEAYPYTGK	91.8	45.8	46	0	1	0	0	2	1 791,8081
21	isopentenyl diphosphate isomerase 2 [Nicotiana tabacum]	BAB40974.1	34 190,4	1	4.32%	ESELIEENALGVR	70.6	45.8	24.8	0	1	0	0	2	1 458,7440
22	CYP1 (putative cyclophilin_ABH_like) [Vigna radiata]	BAB82452.1	18 188,7	1	6.98%	IVFELFADTTTPR	81.7	46	35.7	0	1	0	0	2	1 408,7479
22	basic chitinase, chitinase [Arabidopsis thaliana]	NP_566426.1	36 196,3	1	5.67%	LPGYGVITNIINGGLECGR	138	44.9	93.1	0	1	0	0	2	2 003,0385
22	unnamed protein product [Vitis vinifera]	CAO65970.1	80 012,1	8	11.60%	FSYSSLR	41.7	47.1	-5.4	0	1	0	0	2	859,4312
22	unnamed protein product [Vitis vinifera]	CAO65970.1	80 012,1	8	11.60%	GDEIYTVYVIDAETR	60.2	45.4	14.8	0	1	0	0	2	1 743,8443
22	unnamed protein product [Vitis vinifera]	CAO65970.1	80 012,1	8	11.60%	IDNYYWLR	51.8	46.1	5.7	0	1	0	0	2	1 142,5634
22	unnamed protein product [Vitis vinifera]	CAO65970.1	80 012,1	8	11.60%	KEEYFYMK	50	46.5	3.5	0	2	0	0	2	1 300,5924
22	unnamed protein product [Vitis vinifera]	CAO65970.1	80 012,1	8	11.60%	LSLLDR	40.4	47.6	-7.2	0	1	0	0	2	716,4307
22	unnamed protein product [Vitis vinifera]	CAO65970.1	80 012,1	8	11.60%	LVAYAEDTKGDEIYTVYVIDAETR	53.3	43.5	9.8	0	0	1	0	2	2 734,3463
22	unnamed protein product [Vitis vinifera]	CAO65970.1	80 012,1	8	11.60%	SAGLLIGAVLNMRPDLFR	47.3	45.1	2.2	0	0	2	0	2	2 016,1067
22	unnamed protein product [Vitis vinifera]	CAO65970.1	80 012,1	8	11.60%	TDDNILLFK	66.4	47.8	18.6	0	1	0	0	2	1 078,5787
22	endochitinase precursor [Humulus lupulus]	AAD34596.1	33 511,4	1	4.11%	GFYTYDAFLTAAR	70.1	46	24.1	0	1	0	0	2	1 495,7221
22	putative cysteine protease [Glycine max]	ABR26679.1	38 963,3	1	4.51%	YNGGLETEEAYPYTGK	55.9	45.8	10.1	0	1	0	0	2	1 791,8081
22	hypothetical protein [Vitis vinifera]	CAN77531.1	33 023,8	1	4.39%	TDWSQAPFTASYR	53	45.8	7.2	0	1	0	0	2	1 529,7025
22	hypothetical protein [Vitis vinifera]	CAN67131.1	50 610,7	1	2.63%	TWELDVGGSSR	87.2	46.4	40.8	0	1	0	0	2	1 319,6596
22	methionine synthase [Beta vulgaris]	BAE07181.1	84 805,9	1	1.31%	IPTEELADR	67.2	45.9	21.3	0	1	0	0	2	1 140,5903
23	unnamed protein product [Vitis vinifera]	CAO65969.1	76 969,5	2	4.84%	IDNYYWLR	51.7	46.1	5.6	0	1	0	0	2	1 142,5634
23	unnamed protein product [Vitis vinifera]	CAO65969.1	76 969,5	2	4.84%	ILVTAGLNDPR	57.9	46.9	11	0	1	0	0	2	1 168,6692
23	unnamed protein product [Vitis vinifera]	CAO65969.1	76 969,5	2	4.84%	LSLLDR	42.3	47.6	-5.3	0	1	0	0	2	716,4307
23	unnamed protein product [Vitis vinifera]	CAO65969.1	76 969,5	2	4.84%	VMYSEPAK	33.3	45.5	-12.2	0	2	0	0	2	940,445
23	basic chitinase, chitinase [Arabidopsis thaliana]	NP_566426.1	36 196,3	1	5.67%	LPGYGVITNIINGGLECGR	67.1	44.9	22.2	0	0	1	0	2	2 003,0385
23	unnamed protein product [Vitis vinifera]	CAO65970.1	80 012,1	3	4.68%	IDNYYWLR	51.7	46.1	5.6	0	1	0	0	2	1 142,5634
23	unnamed protein product [Vitis vinifera]	CAO65970.1	80 012,1	3	4.68%	LSLLDR	42.3	47.6	-5.3	0	1	0	0	2	716,4307
23	unnamed protein product [Vitis vinifera]	CAO65970.1	80 012,1	3	4.68%	SAGLLIGAVLNMRPDLFR	46.1	45.2	0.9	0	0	2	0	2	2 000,1118
23	Os01g0357100 [Oryza sativa (japonica cultivar-group)]	NP_001043008.1	66 568,3	1	1.85%	LADYEGSGELR	87.1	46.3	40.8	0	1	0	0	2	1 209,5752
23	endo-1,4-beta-mannanase [Glycine max]	ABG88068.1	44 105,4	1	2.55%	LLLSLVNNWK	60.3	46.2	14.1	0	1	0	0	2	1 199,7153
23	pectin acetyltransferase [Eucalyptus globulus subsp. globulus]	ABG34282.1	24 848,5	1	5.53%	CLSDAGFLLDER	68.4	46.4	22	0	1	0	0	2	1 429,6424
23	putative cysteine protease [Glycine max]	ABR26679.1	38 963,3	1	4.51%	YNGGLETEEAYPYTGK	102	45.8	56.2	0	1	0	0	2	1 791,8081
23	hypothetical protein [Vitis vinifera]	CAN67131.1	50 610,7	1	2.63%	TWELDVGGSSR	104	46.4	57.6	0	1	0	0	2	1 319,6596
24	CYP1 (putative cyclophilin_ABH_like) [Vigna radiata]	BAB82452.1	18 188,7	1	6.98%	IVFELFADTTTPR	90	46	44	0	1	0	0	2	1 408,7479
24	acetylcholinesterase [Macroptilium atropurpureum]	BAG09557.1	42 760,3	1	1.83%	MNFDQIR	57.5	46.1	11.4	0	1	0	0	2	939,4359
24	Os01g0357100 [Oryza sativa (japonica cultivar-group)]	NP_001043008.1	66 568,3	1	1.85%	LADYEGSGELR	93	46.3	46.7	0	1	0	0	2	1 209,5752
24	unnamed protein product [Vitis vinifera]	CAO65970.1	80 012,1	1	2.70%	SAGLLIGAVLNMRPDLFR	55.7	45.2	10.5	0	0	1	0	2	2 000,1118
24	endo-1,4-beta-mannanase [Glycine max]	ABG88068.1	44 105,4	1	2.55%	LLLSLVNNWK	60.5	46.2	14.3	0	1	0	0	2	1 199,7153
24	pectin acetyltransferase [Eucalyptus globulus subsp. globulus]	ABG34282.1	24 848,5	1	5.53%	CLSDAGFLLDER	90.5	46.4	44.1	0	1	0	0	2	1 429,6424
24	putative cysteine protease [Glycine max]	ABR26679.1	38 963,3	1	4.51%	YNGGLETEEAYPYTGK	92.2	45.8	46.4	0	1	0	0	2	1 791,8081
24	Os02g0698000 [Oryza sativa (japonica cultivar-group)]	NP_001047825.1	44 848,2	1	3.23%	LTSVFGGAAEPPK	54.4	46.9	7.5	0	1	0	0	2	1 273,6794
25	fasciclin-like arabinogalactan protein 12 [Gossypium hirsutum]	ABV27483.1	43 894,2	1	1.88%	LADENR	69.8	47	22.8	0	1	0	0	2	931,4849
25	fasciclin-like arabinogalactan protein FLA8 [Arabidopsis thaliana]	AAG24276.1	43 044,2	1	2.62%	VGFGSAASGSK	77.4	46.1	31.3	0	1	0	0	2	967,4848
25	endo-1,4-beta-mannanase [Glycine max]	ABG88068.1	44 105,4	1	2.55%	LLLSLVNNWK	76.6	46.2	30.4	0	2	0	0	2	1 199,7153
25	hypothetical protein [Vitis vinifera]	CAN77531.1	33 023,8	2	8.11%	IIFVDTGPIR	67.8	46.7	21.1	0	1	0	0	2	1 217,6895
25	hypothetical protein [Vitis vinifera]	CAN77531.1	33 023,8	2	8.11%	TDWSQAPFTASYR	85.1	45.8	39.3	0	2	0	0	2	1 529,7025
25	unknown [Populus trichocarpa]	ABK92766.1	35 697,9	2	8.43%	ALGQISER	38	47.2	-9.2	0	1	0	0	2	873,4795

25	unknown [Populus trichocarpa]	ABK92766.1	35 697.9	2	8.43%	VLVTGAAGQIGYALVPMIAR	60.6	45.1	15.5	0	0	1	0	2	2 016,1318
25	basic chitinase, chitinase [Arabidopsis thaliana]	NP_566426.1	36 196.3	2	7.46%	IGFYQR	35.4	45.3	-9.9	0	2	0	0	2	783.4154
25	basic chitinase, chitinase [Arabidopsis thaliana]	NP_566426.1	36 196.3	2	7.46%	LPGYGVITNIINGGLECGR	103	44.9	58.1	0	1	1	0	2	2 003,0385
25	putative xyloglucan endotransglycosylase [Cucumis sativus]	ABK55722.1	33 812.4	1	4.71%	IIENGNLITLSLDK	104	45.6	58.4	0	1	0	0	2	1 542,8746
25	alpha galactosidase [Glycine max]	AAA73963.1	46 378.6	1	12.60%	SVGNSWR	55.2	48.6	6.6	0	2	0	0	2	805.3956
25	alpha galactosidase [Glycine max]	AAA73963.1	46 378.6	1	12.60%	TFASWGIDYLYK	74.3	46.5	27.8	0	2	0	0	2	1 300,6578
25	alpha galactosidase [Glycine max]	AAA73963.1	46 378.6	1	12.60%	TMPGSLGHEEQDAK	58.4	46.1	12.3	0	1	0	0	2	1 499,6801
25	alpha galactosidase [Glycine max]	AAA73963.1	46 378.6	1	12.60%	YDNCENNINISPK	67.4	47.4	20	0	2	0	0	2	1 467,6175
25	endochitinase precursor [Humulus lupulus]	AAD34596.1	33 511.4	1	6.01%	GFYTYDAFLTAAR	75.9	46	29.9	0	2	0	0	2	1 495,7221
25	alpha-galactosidase [Phaseolus vulgaris]	AAA73964	47 030.7	5	11.50%	DSQGNLVPK	49.8	46.4	3.4	0	2	0	0	2	957.5007
25	alpha-galactosidase [Phaseolus vulgaris]	AAA73964	47 030.7	5	11.50%	LAVILWNR	60.8	45.8	15	0	2	0	0	2	984.5996
25	alpha-galactosidase [Phaseolus vulgaris]	AAA73964	47 030.7	5	11.50%	SVGNSWR	55.2	48.6	6.6	0	2	0	0	2	805.3956
25	alpha-galactosidase [Phaseolus vulgaris]	AAA73964	47 030.7	5	11.50%	TFASWGIDYLYK	74.3	46.5	27.8	0	2	0	0	2	1 300,6578
25	alpha-galactosidase [Phaseolus vulgaris]	AAA73964	47 030.7	5	11.50%	TMPGSLGHEEQDAK	58.4	46.1	12.3	0	1	0	0	2	1 499,6801
25	heat shock protein 70 [Cucumis sativus]	CAAS2149.1	75 395.0	3	4.10%	IPAVQELVK	38.6	45.7	-7.1	0	1	0	0	2	996.6096
25	heat shock protein 70 [Cucumis sativus]	CAAS2149.1	75 395.0	3	4.10%	NQADSVVYQTEK	54.7	45.9	8.8	0	1	0	0	2	1 381,6600
25	heat shock protein 70 [Cucumis sativus]	CAAS2149.1	75 395.0	3	4.10%	TPVENSRLR	37.5	47	-9.5	0	1	0	0	2	915.49
26	predicted protein [Physcomitrella patens subsp. patens]	XP_001760166.1	42 477.4	1	8.33%	LLVCMGEALR	62.9	46.4	16.5	0	1	0	0	2	1 104,5910
26	predicted protein [Physcomitrella patens subsp. patens]	XP_001760166.1	42 477.4	1	8.33%	YTGGMVDPVNVQLIVK	62.5	45.5	17	0	1	0	0	2	1 649,8574
26	fasciclin-like arabinogalactan protein 12 [Gossypium hirsutum]	ABV27483.1	43 894.2	1	1.88%	LADEINTR	58.8	47	11.8	0	1	0	0	2	931.4849
26	Phosphoglucomutase, cytoplasmic [Pisum sativum]	Q9SM60.1	63 308.1	6	12.20%	GATLVVSGDGR	38.4	46.6	-8.2	0	1	0	0	2	1 031,5487
26	Phosphoglucomutase, cytoplasmic [Pisum sativum]	Q9SM60.1	63 308.1	6	12.20%	LSGTGSEGATIR	91.8	46.5	45.3	0	1	0	0	2	1 148,5913
26	Phosphoglucomutase, cytoplasmic [Pisum sativum]	Q9SM60.1	63 308.1	6	12.20%	MEEFTGR	41.8	45.6	-3.8	0	2	0	0	2	869.3828
26	Phosphoglucomutase, cytoplasmic [Pisum sativum]	Q9SM60.1	63 308.1	6	12.20%	SMPTSAAALDVVAK	77	46.4	30.6	0	2	0	0	2	1 305,6724
26	Phosphoglucomutase, cytoplasmic [Pisum sativum]	Q9SM60.1	63 308.1	6	12.20%	YDYENVDAGAAK	87.8	47.5	40.3	0	1	0	0	2	1 315,5807
26	Phosphoglucomutase, cytoplasmic [Pisum sativum]	Q9SM60.1	63 308.1	6	12.20%	YNMENGGPAPEGITNK	47.3	45.3	2	0	0	1	0	2	1 707,7650
26	fasciclin-like arabinogalactan protein FLA8 [Arabidopsis thaliana]	AAG24276.1	43 044.2	1	2.62%	VGFSAASGSK	67.6	46.1	21.5	0	1	0	0	2	967.4848
26	endo-1,4-beta-mannanase [Glycine max]	ABG88068.1	44 105.4	1	2.55%	LLLSLVNNWK	62.9	46.2	16.7	0	1	0	0	2	1 199,7153
26	unknown [Populus trichocarpa]	ABK95047.1	42 422.0	6	15.30%	DQVAAMGVYGPR	35.1	46.1	-11	0	1	0	0	2	1 334,6528
26	unknown [Populus trichocarpa]	ABK95047.1	42 422.0	6	15.30%	FEETLYGK	54	46.5	7.5	0	1	0	0	2	986.4836
26	unknown [Populus trichocarpa]	ABK95047.1	42 422.0	6	15.30%	LFSPGNLR	34.8	47.3	-12.5	0	1	0	0	2	903.5053
26	unknown [Populus trichocarpa]	ABK95047.1	42 422.0	6	15.30%	TVVAYGSK	36	48.4	-12.4	0	1	0	0	2	853.442
26	unknown [Populus trichocarpa]	ABK95047.1	42 422.0	6	15.30%	TTYVLALK	35.3	46.4	-11.1	0	1	0	0	2	908.5457
26	unknown [Populus trichocarpa]	ABK95047.1	42 422.0	6	15.30%	YTGGMVDPVNVQIHK	62.5	45.5	17	0	1	0	0	2	1 649,8574
26	hypothetical protein [Vitis vinifera]	CAN77531.1	33 023.8	1	4.39%	TDWSQLPFTASYR	64.7	45.8	18.9	0	1	0	0	2	1 529,7025
26	unnamed protein product (putative secretory peroxidase) [Vitis vinifera]	CAO48839.1	34 372.5	1	2.79%	GYEVVDTIK	53.1	46.5	6.6	0	1	0	0	2	1 023,5363
26	lipase [Gossypium hirsutum]	ABX75139.1	40 060.9	1	6.27%	AFFVFGDSLVDNNGNNYLATTAR	61.5	44	17.5	0	0	1	0	2	2 506,1995
26	chloroplast fructose-1,6-bisphosphatase [Oryza sativa Indica Group]	ABY75186	43 586.8	2	3.94%	VPLYIGSVVEEVEK	40.9	46.4	-5.5	0	1	0	0	2	1 461,7841
26	chloroplast fructose-1,6-bisphosphatase [Oryza sativa Indica Group]	ABY75186	43 586.8	2	3.94%	VPLYIGSVVEEVEKVEK	43.2	46.1	-2.9	0	0	1	0	2	1 817,9901
26	unnamed protein product [Vitis vinifera]	CAO17011.1	42 507.9	1	12.00%	VINLNDER	62.1	46.7	15.4	0	1	0	0	2	972.5114
26	unnamed protein product [Vitis vinifera]	CAO17011.1	42 507.9	1	12.00%	YTGGMVDPVNVQIHK	62.5	45.5	17	0	1	0	0	2	1 649,8574
26	basic chitinase, chitinase [Arabidopsis thaliana]	NP_566426.1	36 196.3	1	5.67%	LPGYGVITNIINGGLECGR	111	44.9	66.1	0	1	1	0	2	2 003,0385
26	endochitinase precursor [Humulus lupulus]	AAD34596.1	33 511.4	1	4.11%	GFYTYDAFLTAAR	72.1	46	26.1	0	1	0	0	2	1 495,7221
26	Probable phosphoglucomutase, cytoplasmic 2 [Arabidopsis thaliana]	Q9SGC1.1	63 465.5	1	7.69%	LSGTGSEGATIR	91.8	46.5	45.3	0	1	0	0	2	1 148,5913
26	Probable phosphoglucomutase, cytoplasmic 2 [Arabidopsis thaliana]	Q9SGC1.1	63 465.5	1	7.69%	LVTVEDIVR	78.2	46.3	31.9	0	1	0	0	2	1 043,6102
26	Probable phosphoglucomutase, cytoplasmic 2 [Arabidopsis thaliana]	Q9SGC1.1	63 465.5	1	7.69%	SMPTSAAALDVVAK	77	46.4	30.6	0	2	0	0	2	1 305,6724
27	acidic chitinase class 3 [Vigna unguiculata]	CAA61280.1	26 308.7	1	12.80%	QLFLGVPASTAAAGSGFIPANDLIQ	50.6	42.8	7.8	0	0	1	0	2	3 166,7513
27	Fructose-1,6-bisphosphatase, chloroplast precursor [Glycine max]	Q42796.1	43 879.4	1	5.22%	ANISNLTVQGVAVNVQGEDQK	76.2	44.8	31.4	0	0	1	0	2	2 142,0792
27	fasciclin-like arabinogalactan protein FLA8 [Arabidopsis thaliana]	AAG24276.1	43 044.2	1	2.62%	VGFSAASGSK	78.1	46.1	32	0	2	0	0	2	967.4848
27	unknown [Populus trichocarpa]	ABK95047.1	42 422.0	2	5.36%	DQVAAMGVYGPR	32.4	46.1	-13.7	0	1	0	0	2	1 334,6528
27	unknown [Populus trichocarpa]	ABK95047.1	42 422.0	2	5.36%	FEETLYGK	50.6	46.5	4.1	0	1	0	0	2	986.4836
27	Os06g0206000 [Oryza sativa (japonica cultivar-group)]	NP_001057093.1	33 451.3	1	3.58%	ITVGGSPER	84.1	45.9	38.2	0	1	0	0	2	1 141,6583
27	CYP1 (putative cyclophilin_ABH_like) [Vigna radiata]	BAB82452.1	18 188.7	1	6.98%	IVFELFADTTPR	75.7	46	29.7	0	1	0	0	2	1 408,7479
27	putative xyloglucan endotransglycosylase [Cucumis sativus]	ABK55722.1	33 812.4	1	4.71%	IIENGNLITLSLDK	113	45.6	67.4	0	2	0	0	2	1 542,8746

27	Acidic endochitinase [Vigna angularis]	P29024.1	32 880.7	1	2.97%	YGGVMLWDR	68.6	46	22.6	0	3	0	0	2	1 096,5250
27	alpha galactosidase [Glycine max]	AAA73963.1	46 378.6	1	7.58%	TFASVGLDYLK	52.7	46.5	6.2	0	1	0	0	2	1 300,6578
27	14-3-3 protein [Vigna angularis]	BAB47119.1	29 342.0	1	3.08%	IISSIEQK	54.9	47.1	7.8	0	1	0	0	2	917,5308
27	cytosolic glutamine synthetase GSbeta1 [Glycine max]	AAG24873.1	39 100.8	1	4.78%	SLSLDLNLNLSDTTEK	81.9	45.1	36.8	0	1	0	0	2	1 918,0023
27	ascorbate peroxidase [Litchi chinensis]	ABZ79406.1	27 497.2	1	12.00%	EGLIQLPSDK	64.9	46.5	18.4	0	2	0	0	2	1 099,6002
27	ascorbate peroxidase [Litchi chinensis]	ABZ79406.1	27 497.2	1	12.00%	SGFEGPWTSNPLIFDINSYFK	113	44.3	68.7	0	1	1	0	2	2 306,0767
27	cytosolic ascorbate peroxidase [Vigna unguiculata]	AAB03844.1	27 016.7	5	29.60%	ALLSDPVFRPLVEK	59.4	45.4	14	0	1	0	0	2	1 583,9163
27	cytosolic ascorbate peroxidase [Vigna unguiculata]	AAB03844.1	27 016.7	5	29.60%	EDKPEPPPEGR	34.7	46.5	-11.8	0	1	0	0	2	1 250,6020
27	cytosolic ascorbate peroxidase [Vigna unguiculata]	AAB03844.1	27 016.7	5	29.60%	HPAELAHGANNGLDI AVR	68.9	45.3	23.6	0	0	1	0	2	1 854,9575
27	cytosolic ascorbate peroxidase [Vigna unguiculata]	AAB03844.1	27 016.7	5	29.60%	SGFEGPWTSNPLIFDINSYFK	113	44.3	68.7	0	1	1	0	2	2 306,0767
27	cytosolic ascorbate peroxidase [Vigna unguiculata]	AAB03844.1	27 016.7	5	29.60%	SYPTVSADYQK	49.8	46.4	3.4	0	2	0	0	2	1 258,5955
27	fasciclin-like arabinogalactan protein 12 [Gossypium hirsutum]	ABV27483.1	43 894.2	1	1.88%	LADENR	62.1	47	15.1	0	2	0	0	2	931,4849
27	unnamed protein product [Vitis vinifera]	CAO61165.1	36 739.2	2	10.50%	GDSNEVGPSIENAK	50.6	45.7	4.9	0	3	0	0	2	1 416,6607
27	unnamed protein product [Vitis vinifera]	CAO61165.1	36 739.2	2	10.50%	SVDTYLFALYDEDLKPGGSR	38.3	44.1	-5.8	0	0	1	0	2	2 472,1937
27	Phosphoglucomutase, cytoplasmic [Pisum sativum]	Q9SM60.1	63 308.1	3	5.33%	LSGTGSEGATIR	109	46.5	62.5	0	1	0	0	2	1 148,5913
27	Phosphoglucomutase, cytoplasmic [Pisum sativum]	Q9SM60.1	63 308.1	3	5.33%	MEEFTGR	31.7	45.6	-13.9	0	1	0	0	2	869,3828
27	Phosphoglucomutase, cytoplasmic [Pisum sativum]	Q9SM60.1	63 308.1	3	5.33%	YDYENV D A G A A K	85.5	47.5	38	0	1	0	0	2	1 315,5807
27	Peroxidase 49 precursor [Arabidopsis thaliana]	O23237.2	36 147.0	1	2.11%	MAASLLR	55.7	47.6	8.1	0	1	0	0	2	761,4344
27	endo-1,4-beta-mannanase [Glycine max]	ABG88068.1	44 105.4	1	2.55%	LLSLVNWWK	77.2	46.2	31	0	2	0	0	2	1 199,7153
27	hypothetical protein [Vitis vinifera]	CAN77531.1	33 023.8	2	6.42%	IDMQLK	36.9	47.7	-10.8	0	1	0	0	2	747,4077
27	hypothetical protein [Vitis vinifera]	CAN77531.1	33 023.8	2	6.42%	TDWSQAPFTASYR	78.2	45.8	32.4	0	2	1	0	2	1 529,7025
27	aldehyde reductase [Vigna radiata]	AAD53967.1	35 565.6	4	14.50%	DPQTELLDPAVK	96.8	47.6	49.2	0	1	0	0	2	1 325,6955
27	aldehyde reductase [Vigna radiata]	AAD53967.1	35 565.6	4	14.50%	KVDHLLSLDGAK	40.7	46.2	-5.5	0	0	1	0	2	1 295,7325
27	aldehyde reductase [Vigna radiata]	AAD53967.1	35 565.6	4	14.50%	SLGIDYIPLVSLK	37.3	47.4	-10.1	0	1	0	0	2	1 546,8735
27	aldehyde reductase [Vigna radiata]	AAD53967.1	35 565.6	4	14.50%	TGLWYNLSK	55.6	45.9	9.7	0	1	0	0	2	1 081,5683
27	unnamed protein product [Vitis vinifera]	CAO17011.1	42 507.9	1	2.04%	VNNLDER	61.9	46.7	15.2	0	1	0	0	2	972,5114
27	basic chitinase, chitinase [Arabidopsis thaliana]	NP_566426.1	36 196.3	1	5.67%	LPYGVITNIINGGLECGR	138	44.9	93.1	0	2	1	0	2	2 003,0385
27	iron-superoxide dismutase precursor [Vigna unguiculata]	AAF28773.1	27 393.8	8	38.80%	AAAAATQFGSGWAWLAYK	102	45.4	56.6	0	1	0	0	2	1 798,8917
27	iron-superoxide dismutase precursor [Vigna unguiculata]	AAF28773.1	27 393.8	8	38.80%	ASFLGLQNVAGINLLFK	101	45.4	55.6	0	1	0	0	2	1 699,9747
27	iron-superoxide dismutase precursor [Vigna unguiculata]	AAF28773.1	27 393.8	8	38.80%	LDGENAANPPSAEDNDK	68.3	45.5	22.8	0	2	0	0	2	1 756,7627
27	iron-superoxide dismutase precursor [Vigna unguiculata]	AAF28773.1	27 393.8	8	38.80%	LDGENAANPPSAEDNKL VVIK	53.9	44.2	9.7	0	0	2	0	2	2 309,1624
27	iron-superoxide dismutase precursor [Vigna unguiculata]	AAF28773.1	27 393.8	8	38.80%	LVSWDVNSSR	72.3	46.5	25.8	0	2	0	0	2	1 119,5798
27	iron-superoxide dismutase precursor [Vigna unguiculata]	AAF28773.1	27 393.8	8	38.80%	RPDYISVFM DK	39.6	45.8	-6.2	0	1	0	0	2	1 386,6728
27	iron-superoxide dismutase precursor [Vigna unguiculata]	AAF28773.1	27 393.8	8	38.80%	SLEEHVTAYNK	59	46.2	12.8	0	2	2	0	2	1 379,7421
27	iron-superoxide dismutase precursor [Vigna unguiculata]	AAF28773.1	27 393.8	8	38.80%	TYVENLK	32.4	46.5	-14.1	0	1	0	0	2	866,4624
27	endochitinase precursor [Humulus lupulus]	AAD34596.1	33 511.4	1	4.11%	GFYTYDAFLTAAR	74.8	46	28.8	0	1	0	0	2	1 495,7221
27	alpha-galactosidase [Phaseolus vulgaris]	AAA73964	47 030.7	2	4.71%	DSQGNLVPK	38.7	46.4	-7.7	0	1	0	0	2	957,5007
27	alpha-galactosidase [Phaseolus vulgaris]	AAA73964	47 030.7	2	4.71%	TFASVGLDYLK	52.7	46.5	6.2	0	1	0	0	2	1 300,6578
28	Os06g0133800 [Oryza sativa (japonica cultivar-group)]	NP_001056711.1	80 012.2	1	1.88%	LAQLPGTSIEGVEK	53.1	46	7.1	0	1	0	0	2	1 441,7904
28	Thioredoxin M-type, chloroplast precursor [Oryza sativa subsp. Japonica]	Q9ZP20.1	79 055.6	2	2.91%	MIAPVIDELAK	55.7	46.2	9.5	0	1	0	0	2	1 199,6711
28	Thioredoxin M-type, chloroplast precursor [Oryza sativa subsp. Japonica]	Q9ZP20.1	79 055.6	2	2.91%	SIPTVLMFK	36.9	46.4	-9.5	0	1	0	0	2	1 051,5863
28	fasciclin-like arabinogalactan protein 12 [Gossypium hirsutum]	ABV27483.1	43 894.2	1	1.88%	LADENR	56.9	47	9.9	0	1	0	0	2	931,4849
28	monodehydroascorbate reductase [Brassica rapa subsp. pekinensis]	AAK72107.1	46 469.1	1	2.53%	GQVEEDKGGIK	60.1	46.3	13.8	0	1	0	0	2	1 159,5962
28	fasciclin-like arabinogalactan protein FLA8 [Arabidopsis thaliana]	AAG24276.1	43 044.2	1	2.62%	VFGGSAASGSK	66.2	46.1	20.1	0	1	0	0	2	967,4848
28	endo-1,4-beta-mannanase [Glycine max]	ABG88068.1	44 105.4	1	2.55%	LLSLVNWWK	65.9	46.2	19.7	0	2	0	0	2	1 199,7153
28	UTP--glucose-1-phosphate uridylyltransferase 1 [Arabidopsis thaliana]	P57751.1	51 902.8	1	1.91%	SGFINLVS R	54.9	46.7	8.2	0	1	0	0	2	992,5529
28	hypothetical protein [Vitis vinifera]	CAN77531.1	33 023.8	1	4.39%	TDWSQAPFTASYR	80.4	45.8	34.6	0	1	0	0	2	1 529,7025
28	aldehyde reductase [Vigna radiata]	AAD53967.1	35 565.6	4	12.00%	SLGIDYIPLVSLK	63.3	47.4	15.9	0	1	0	0	2	1 546,8735
28	aldehyde reductase [Vigna radiata]	AAD53967.1	35 565.6	4	12.00%	SLGIDYIPLVSLKDTVESLK	42	44.3	-2.3	0	0	1	0	2	2 319,2701
28	aldehyde reductase [Vigna radiata]	AAD53967.1	35 565.6	4	12.00%	TGLWYNLSK	55.5	45.9	9.6	0	1	0	0	2	1 081,5683
28	aldehyde reductase [Vigna radiata]	AAD53967.1	35 565.6	4	12.00%	TLAEDA A W K	69.6	46.9	22.7	0	1	0	0	2	1 004,5055
28	unnamed protein product [Vitis vinifera]	CAO17011.1	42 507.9	1	4.07%	VNNLDER	64.3	46.7	17.6	0	1	0	0	2	972,5114
28	basic chitinase, chitinase [Arabidopsis thaliana]	NP_566426.1	36 196.3	1	5.67%	LPYGVITNIINGGLECGR	66.7	44.9	21.8	0	1	1	0	2	2 003,0385
28	putative xyloglucan endotransglycosylase [Cucumis sativus]	ABF55722.1	33 812.4	1	4.71%	IIENGNLITLSL DK	113	45.6	67.4	0	1	0	0	2	1 542,8746

28	iron-superoxide dismutase precursor [Vigna unguiculata]	AAF28773.1	27 393,8	6	33.90%	AAAAATQFGSGWAWLAYK	85.9	45.4	40.5	0	1	0	0	2	798,8917
28	iron-superoxide dismutase precursor [Vigna unguiculata]	AAF28773.1	27 393,8	6	33.90%	ASLGLQNVAGINLLFK	101	45.4	55.6	0	1	0	0	2	1 699,9747
28	iron-superoxide dismutase precursor [Vigna unguiculata]	AAF28773.1	27 393,8	6	33.90%	LDGENAANPPSADEDNK	45.4	45.5	-0.1	0	1	1	0	2	1 756,7627
28	iron-superoxide dismutase precursor [Vigna unguiculata]	AAF28773.1	27 393,8	6	33.90%	LVSWDAVSSR	70.9	46.5	24.4	0	1	0	0	2	1 119,5798
28	iron-superoxide dismutase precursor [Vigna unguiculata]	AAF28773.1	27 393,8	6	33.90%	RPDYISVFMFK	59.3	46.1	13.2	0	2	0	0	2	1 370,6779
28	iron-superoxide dismutase precursor [Vigna unguiculata]	AAF28773.1	27 393,8	6	33.90%	SLEEIHVTAYNK	73.2	46.2	27	0	1	0	0	2	1 379,7421
28	endochitinase precursor [Humulus lupulus]	AAD34596.1	33 511,4	1	4.11%	GFYTYDAFLTAAR	71.7	46	25.7	0	1	0	0	2	1 495,7221
28	heat shock protein 70 [Cucumis sativus]	CAAS2149.1	75 395,0	1	1.70%	NQADSVVYQTEK	56.2	45.9	10.3	0	1	0	0	2	1 381,6600
29	Os06g0133800 [Oryza sativa (japonica cultivar-group)]	NP_001056711.1	80 012,2	1	1.88%	LAQLPGTSIEGVEK	61.7	46	15.7	0	1	0	0	2	1 441,7904
29	cytosolic ascorbate peroxidase [Vigna unguiculata]	AAB03844.1	27 016,7	4	21.60%	ALLSDPVFRPLVEK	48	45.4	2.6	0	1	0	0	2	1 583,9163
29	cytosolic ascorbate peroxidase [Vigna unguiculata]	AAB03844.1	27 016,7	4	21.60%	EDKPEPPPEGR	36.8	46.5	-9.7	0	1	0	0	2	1 250,6020
29	cytosolic ascorbate peroxidase [Vigna unguiculata]	AAB03844.1	27 016,7	4	21.60%	HPAELAHGANNGLDI AVR	61	45.3	15.7	0	0	1	0	2	1 854,9575
29	cytosolic ascorbate peroxidase [Vigna unguiculata]	AAB03844.1	27 016,7	4	21.60%	SYPTVSADYQK	49.2	46.4	2.8	0	1	0	0	2	1 258,5955
29	fasciclin-like arabinogalactan protein 12 [Gossypium hirsutum]	ABV27483.1	43 894,2	1	1.88%	LAD EINTR	69.6	47	22.6	0	1	0	0	2	931,4849
29	fasciclin-like arabinogalactan protein FLA8 [Arabidopsis thaliana]	AAG24276.1	43 044,2	1	2.62%	VGFSGAASGSK	73.2	46.1	27.1	0	1	0	0	2	967,4848
29	endo-1,4-beta-mannanase [Glycine max]	ABG88068.1	44 105,4	1	2.55%	LLLSLVNNWK	63.8	46.2	17.6	0	1	0	0	2	1 199,7153
29	oxidoreductase family protein [Arabidopsis thaliana]	NP_188715.2	38 560,4	1	3.94%	DVAVLEAMLESGAK	68.8	46.1	22.7	0	1	0	0	2	1 448,7308
29	unknown [Populus trichocarpa x Populus deltoides]	ABK96272.1	35 285,3	1	2.74%	IFAGDVVPR	72.3	46.8	25.5	0	1	0	0	2	973,5472
29	hypothetical protein [Vitis vinifera]	CAN77531.1	33 023,8	2	8.11%	IFSVVDGTPIR	49	49	0	0	1	0	0	2	1 217,6895
29	hypothetical protein [Vitis vinifera]	CAN77531.1	33 023,8	2	8.11%	TDWSQAPFTASYR	72.3	45.8	26.5	0	1	0	0	2	1 529,7025
29	CYP1 (putative cyclophilin_ABH_like) [Vigna radiata]	BAB82452.1	18 188,7	1	6.98%	IVFELFADTTPR	69.2	46	23.2	0	1	0	0	2	1 408,7479
29	aldehyde reductase [Vigna radiata]	AAD53967.1	35 565,6	5	15.70%	KVDHLLSLDGAK	48.2	46.2	2	0	0	1	0	2	1 295,7325
29	aldehyde reductase [Vigna radiata]	AAD53967.1	35 565,6	5	15.70%	SLGIDYIPLEVSLK	51.5	47.4	4.1	0	1	0	0	2	1 546,8735
29	aldehyde reductase [Vigna radiata]	AAD53967.1	35 565,6	5	15.70%	SLGIDYIPLEVSLKDTVESLK	41	44.3	-3.3	0	0	1	0	2	2 319,2701
29	aldehyde reductase [Vigna radiata]	AAD53967.1	35 565,6	5	15.70%	TGLWYNLSK	55.5	45.9	9.6	0	1	0	0	2	1 081,5683
29	aldehyde reductase [Vigna radiata]	AAD53967.1	35 565,6	5	15.70%	TLAEDAARK	56.5	49.5	7	0	1	0	0	2	1 004,5055
29	basic chitinase, chitinase [Arabidopsis thaliana]	NP_566426.1	36 196,3	1	5.67%	LPYGVITNIINGLECGR	132	44.9	87.1	0	1	1	0	2	2 003,0385
29	unknown [Picea sitchensis]	ABK22263.1	32 671,7	1	3.81%	ITSFLDPDGWK	52.7	46.6	6.1	0	1	0	0	2	1 278,6373
29	putative xyloglucan endotransglycosylase [Cucumis sativus]	ABK55722.1	33 812,4	1	4.71%	IIENGNLITLSLDK	114	45.6	68.4	0	1	0	0	2	1 542,8746
29	iron-superoxide dismutase precursor [Vigna unguiculata]	AAF28773.1	27 393,8	2	10.60%	ASLGLQNVAGINLLFK	113	45.4	67.6	0	1	0	0	2	1 699,9747
29	iron-superoxide dismutase precursor [Vigna unguiculata]	AAF28773.1	27 393,8	2	10.60%	LVSWDAVSSR	34.4	46.5	-12.1	0	1	0	0	2	1 119,5798
29	14-3-3 protein [Vigna angularis]	BAB47119.1	29 342,0	1	4.23%	EABESTLAAAYK	55.5	46.1	9.4	0	1	0	0	2	1 153,5742
29	hypothetical protein OsI_024005 [Oryza sativa (indica cultivar-group)]	EAZ02773.1	41 953,8	3	7.92%	EPYTATIVSVER	48	45.9	2.1	0	1	0	0	2	1 364,7061
29	hypothetical protein OsI_024005 [Oryza sativa (indica cultivar-group)]	EAZ02773.1	41 953,8	3	7.92%	IEEYSDEIFK	74.8	46.3	28.5	0	1	0	0	2	1 272,6001
29	hypothetical protein OsI_024005 [Oryza sativa (indica cultivar-group)]	EAZ02773.1	41 953,8	3	7.92%	LYSIATR	41.6	48.4	-6.8	0	1	0	0	2	910,4997
29	ascorbate peroxidase [Litchi chinensis]	ABZ79406.1	27 497,2	1	4.00%	EGLIQLPSDK	60.6	46.5	14.1	0	1	0	0	2	1 099,6002
30	unknown [Populus trichocarpa]	ABK94814.1	29 532,6	4	15.60%	SGGLGDLK	46.9	47.2	-0.3	0	1	0	0	2	746,4051
30	unknown [Populus trichocarpa]	ABK94814.1	29 532,6	4	15.60%	SGGLGDLKYLPLSDVTK	36.8	45.3	-8.5	0	0	1	0	2	1 762,9594
30	unknown [Populus trichocarpa]	ABK94814.1	29 532,6	4	15.60%	TLQALQYVQENPDEVCPAGWKPGE	72.2	43.4	28.8	0	0	2	0	2	2 857,3834
30	unknown [Populus trichocarpa]	ABK94814.1	29 532,6	4	15.60%	K	55.8	46.6	9.2	0	2	0	0	2	1 035,5727
30	Ted2 [Vigna unguiculata]	CAA69914.1	34 565,9	1	6.17%	YPLISDVTK	75.3	44.8	30.5	0	0	1	0	2	2 046,0759
30	hypothetical protein OsI_037143 [Oryza sativa (indica cultivar-group)]	EAY83184.1	18 612,3	1	6.47%	DELLEAAGELFANVASGLK	66.5	45.8	20.7	0	0	1	0	2	1 533,7385
30	allantoinase [Robinia pseudoacacia]	AAR29343.1	56 352,0	2	6.84%	ECRHYTQVWVR	42	44.5	-2.5	0	0	2	0	2	2 393,2025
30	allantoinase [Robinia pseudoacacia]	AAR29343.1	56 352,0	2	6.84%	AAAAGGVTVVDMPLNNYPTTVSK	56.7	46.1	10.6	0	1	0	0	2	1 298,5655
30	fasciclin-like arabinogalactan protein FLA8 [Arabidopsis thaliana]	AAG24276.1	43 044,2	1	2.62%	TEWEGFDTGTR	78.3	46.1	32.2	0	2	0	0	2	967,4848
30	oxidoreductase family protein [Arabidopsis thaliana]	NP_188715.2	38 560,4	1	3.94%	VGFSGAASGSK	81.7	46.1	35.6	0	1	0	0	2	1 448,7308
30	predicted protein [Physcomitrella patens subsp. patens]	XP_001753067.1	57 980,8	1	1.70%	DVAVLEAMLESGAK	71.5	46.5	25	0	2	0	0	2	1 063,5678
30	chloroplast ribose-5-phosphate isomerase [Spinacia oleracea]	AAL77589.1	30 846,5	2	9.69%	LEEGDFLK	57	46.6	10.4	0	1	0	0	2	1 035,5727
30	chloroplast ribose-5-phosphate isomerase [Spinacia oleracea]	AAL77589.1	30 846,5	2	9.69%	FIVVVDTK	59.2	45.1	14.1	0	1	0	0	2	1 797,9168
30	CYP1 (putative cyclophilin_ABH_like) [Vigna radiata]	BAB82452.1	18 188,7	2	10.50%	SGMVLGLGTGSTAAFAVSR	89.8	46	43.8	0	1	0	0	2	1 408,7479
30	CYP1 (putative cyclophilin_ABH_like) [Vigna radiata]	BAB82452.1	18 188,7	2	10.50%	IVFELFADTTPR	40	47.9	-7.9	0	1	0	0	2	737,3582
30	putative xyloglucan endotransglycosylase [Cucumis sativus]	ABK55722.1	33 812,4	1	4.71%	TAENFR	119	45.6	73.4	0	1	0	0	2	1 542,8746
30	TPA: isoflavone reductase-like protein 6 [Vitis vinifera]	CAI56335.1	33 911,9	2	5.19%	IIENGNLITLSLDK	39.2	45.6	-6.4	0	1	0	0	2	628,4399
30	TPA: isoflavone reductase-like protein 6 [Vitis vinifera]	CAI56335.1	33 911,9	2	5.19%	IIAIAIK	46.1	45.9	0.2	0	1	0	0	2	1 025,5998
30	TPA: isoflavone reductase-like protein 6 [Vitis vinifera]	CAI56335.1	33 911,9	2	5.19%	VIIIGDGNPK	46.1	45.9	0.2	0	1	0	0	2	1 025,5998

30	2-cys peroxiredoxin-like protein [Hyacinthus orientalis]	AAT08751.1	21 838,3	1	19.90%	SYGVLIPDQGIALR	78.4	46.1	32.3	0	1	0	0	2	1 501,8381
30	2-cys peroxiredoxin-like protein [Hyacinthus orientalis]	AAT08751.1	21 838,3	1	19.90%	TLQALQVYQENPDEVCPAGWKPGE	72.2	43.4	28.8	0	0	2	0	2	2 857,3834
30	ascorbate peroxidase [Litchi chinensis]	ABZ79406.1	27 497,2	1	14.80%	EGLIQLPSDK	70.2	46.5	23.7	0	2	0	0	2	1 099,6002
30	chloroplast transketolase precursor [Gossypium barbadense]	ABS10814.1	18 411,0	2	16.10%	ALPTYTPESPADATR	51.4	46.2	5.2	0	1	0	0	2	1 589,7813
30	chloroplast transketolase precursor [Gossypium barbadense]	ABS10814.1	18 411,0	2	16.10%	NLSQQNLNALVK	57.2	45.7	11.5	0	1	0	0	2	1 341,7490
30	fasciclin-like arabinogalactan protein 12 [Gossypium hirsutum]	ABV27483.1	43 894,2	1	1.88%	LADEINTR	60.9	47	13.9	0	2	0	0	2	931.4849
30	cytosolic ascorbate peroxidase [Vigna unguiculata]	AAB03844.1	27 016,7	4	25.20%	ALLSDPVFRPLVEK	58.2	45.4	12.8	0	1	0	0	2	1 583,9163
30	cytosolic ascorbate peroxidase [Vigna unguiculata]	AAB03844.1	27 016,7	4	25.20%	EDKPEPPPEGR	37.5	46.5	-9	0	1	0	0	2	1 250,6020
30	cytosolic ascorbate peroxidase [Vigna unguiculata]	AAB03844.1	27 016,7	4	25.20%	SGFEGPWTSNPLIFDINSYFKELLSGE	37.5	43.2	-5.7	0	0	1	0	2	3 062,4786
30	cytosolic ascorbate peroxidase [Vigna unguiculata]	AAB03844.1	27 016,7	4	25.20%	SYPTVSADYQK	44.3	46.4	-2.1	0	1	0	0	2	1 258,5955
30	pepti (ISS) (putative Cyclophilin) [Ostreococcus tauri]	CAL57205.1	38 854,4	1	3.27%	IVLGLFGDDAPR	57	46.3	10.7	0	2	0	0	2	1 272,6955
30	endo-1,4-beta-mannanase [Glycine max]	ABG88068.1	44 105,4	1	2.55%	LLLSLVNNWK	65.7	48.8	16.9	0	1	0	0	2	1 199,7153
30	hypothetical protein [Vitis vinifera]	CAN77531.1	33 023,8	1	4.39%	TDWSQAPFTASYR	81.5	45.8	35.7	0	2	0	0	2	1 529,7025
30	aldehyde reductase [Vigna radiata]	AAD53967.1	35 565,6	6	22.50%	DPQTELLDPAVK	86.8	47.6	39.2	0	1	0	0	2	1 325,6955
30	aldehyde reductase [Vigna radiata]	AAD53967.1	35 565,6	6	22.50%	KVDHLLSLDGAK	45.8	46.2	-0.4	0	1	1	0	2	1 295,7325
30	aldehyde reductase [Vigna radiata]	AAD53967.1	35 565,6	6	22.50%	SLGIDYIPEVSLK	73.3	47.4	25.9	0	2	0	0	2	1 546,8735
30	aldehyde reductase [Vigna radiata]	AAD53967.1	35 565,6	6	22.50%	TGLWYNLSK	59.8	45.9	13.9	0	1	0	0	2	1 081,5683
30	aldehyde reductase [Vigna radiata]	AAD53967.1	35 565,6	6	22.50%	TLAEDAANK	69.8	46.9	22.9	0	2	0	0	2	1 004,5055
30	aldehyde reductase [Vigna radiata]	AAD53967.1	35 565,6	6	22.50%	VVLTSIIAAVAFSDRPK	35.7	45.4	-9.7	0	0	1	0	2	1 760,9911
30	basic chitinase, chitinase [Arabidopsis thaliana]	NP_566426.1	36 196,3	1	5.67%	LPYGVITNIINGGLECGR	60.1	44.9	15.2	0	0	1	0	2	2 003,0385
30	iron-superoxide dismutase precursor [Vigna unguiculata]	AAF28773.1	27 393,8	1	4.08%	LVSWDVAVSSR	64.4	46.5	17.9	0	1	0	0	2	1 119,5798
30	endochitinase precursor [Humulus lupulus]	AAD34596.1	33 511,4	1	4.11%	GFYTYDAFLTAAR	62.8	46	16.8	0	1	0	0	2	1 495,7221
30	heat shock protein 70 [Cucumis sativus]	CAA52149.1	75 395,0	1	1.13%	IAGLEVLR	61.7	46.7	15	0	1	0	0	2	870.5415
31	cytosolic ascorbate peroxidase [Vigna unguiculata]	AAB03844.1	27 016,7	2	11.60%	HPAELAHGANNGLDIAVR	32.3	45.3	-13	0	0	1	0	2	1 854,9575
31	cytosolic ascorbate peroxidase [Vigna unguiculata]	AAB03844.1	27 016,7	2	11.60%	SYPTVSADYQK	38.9	46.4	-7.5	0	1	0	0	2	1 258,5955
31	fasciclin-like arabinogalactan protein 12 [Gossypium hirsutum]	ABV27483.1	43 894,2	1	1.88%	LADEINTR	69.8	47	22.8	0	2	0	0	2	931.4849
31	allantoinase [Robinia pseudoacacia]	AAR29343.1	56 352,0	1	4.69%	AAAAGGVITVDMPLNNYPTTVSK	72.5	44.5	28	0	0	2	0	2	2 393,2025
31	pepti (ISS) (putative Cyclophilin) [Ostreococcus tauri]	CAL57205.1	38 854,4	1	3.27%	IVLGLFGDDAPR	60.7	46.3	14.4	0	1	0	0	2	1 272,6955
31	fasciclin-like arabinogalactan protein FLA8 [Arabidopsis thaliana]	AAG24276.1	43 044,2	1	2.62%	VGFSGAASGSK	62.3	46.1	16.2	0	1	0	0	2	967.4848
31	oxidoreductase family protein [Arabidopsis thaliana]	NP_188715.2	38 560,4	1	3.94%	DVAVLEAMLESKAK	85	46.1	38.9	0	1	0	0	2	1 448,7308
31	unknown [Populus trichocarpa x Populus deltoides]	ABK96272.1	35 285,3	1	2.74%	IFAGDVVPR	53.1	46.8	6.3	0	2	0	0	2	973.5472
31	predicted protein [Physcomitrella patens subsp. patens]	XP_001753067.1	57 980,8	1	1.70%	LLEEGDFLK	56.1	46.5	9.6	0	2	0	0	2	1 063,5678
31	CYP1 (putative cyclophilin_ABH_like) [Vigna radiata]	BAB82452.1	18 188,7	1	6.98%	IVFELFADTTTPR	71.6	46	25.6	0	1	0	0	2	1 408,7479
31	aldehyde reductase [Vigna radiata]	AAD53967.1	35 565,6	6	22.50%	DPQTELLDPAVK	80.2	47.6	32.6	0	1	0	0	2	1 325,6955
31	aldehyde reductase [Vigna radiata]	AAD53967.1	35 565,6	6	22.50%	KVDHLLSLDGAK	61.2	46.2	15	0	0	1	0	2	1 295,7325
31	aldehyde reductase [Vigna radiata]	AAD53967.1	35 565,6	6	22.50%	SLGIDYIPEVSLK	67.4	47.4	20	0	2	0	0	2	1 546,8735
31	aldehyde reductase [Vigna radiata]	AAD53967.1	35 565,6	6	22.50%	TGLWYNLSK	55.8	45.9	9.9	0	1	0	0	2	1 081,5683
31	aldehyde reductase [Vigna radiata]	AAD53967.1	35 565,6	6	22.50%	TLAEDAANK	45.6	46.9	-1.3	0	2	0	0	2	1 004,5055
31	aldehyde reductase [Vigna radiata]	AAD53967.1	35 565,6	6	22.50%	VVLTSIIAAVAFSDRPK	36.5	45.4	-8.9	0	0	1	0	2	1 760,9911
31	putative RuBisCo activase protein [Zantedeschia hybrid cultivar]	AAT12492.1	27 671,2	1	7.79%	IPVIVTGNDFSTLYAPLIR	55.6	44.6	11	0	0	1	0	2	2 089,1703
31	unknown [Populus trichocarpa]	ABK94513.1	33 962,4	1	9.09%	ILIGGTGYIGK	81.3	47	34.3	0	1	0	0	2	1 204,7309
31	endochitinase precursor [Humulus lupulus]	AAD34596.1	33 511,4	1	4.11%	GFYTYDAFLTAAR	57.7	46	11.7	0	1	0	0	2	1 495,7221
31	14-3-3 protein [Vigna angularis]	BAB47119.1	29 342,0	2	6.15%	IISSEIQK	45.7	47.1	-1.4	0	1	0	0	2	917.5308
31	14-3-3 protein [Vigna angularis]	BAB47119.1	29 342,0	2	6.15%	NLSVAYK	33.9	47.2	-13.3	0	1	0	0	2	907.5254
31	TPA: isoflavone reductase-like protein 6 [Vitis vinifera]	CAI56335.1	33 911,9	4	16.90%	GDHTNFIEIEPESFGVEASELYPDVK	36.4	43.8	-7.4	0	0	1	0	2	2 680,2420
31	TPA: isoflavone reductase-like protein 6 [Vitis vinifera]	CAI56335.1	33 911,9	4	16.90%	IIAAIK	32.1	45.6	-13.5	0	1	0	0	2	628.4399
31	TPA: isoflavone reductase-like protein 6 [Vitis vinifera]	CAI56335.1	33 911,9	4	16.90%	ILIGGTGYIGK	81.3	47	34.3	0	1	0	0	2	1 204,7309
31	TPA: isoflavone reductase-like protein 6 [Vitis vinifera]	CAI56335.1	33 911,9	4	16.90%	VIIIGDGNPK	62.3	45.9	16.4	0	2	0	0	2	1 025,5998
31	heat shock protein 70 [Cucumis sativus]	CAA52149.1	75 395,0	2	3.82%	IAGLEVLR	53.5	46.7	6.8	0	1	0	0	2	870.5415
31	heat shock protein 70 [Cucumis sativus]	CAA52149.1	75 395,0	2	3.82%	KQDITITGASTLPSDEVER	31.3	44.8	-13.5	0	0	1	0	2	2 060,0515
31	ascorbate peroxidase [Litchi chinensis]	ABZ79406.1	27 497,2	1	4.00%	EGLIQLPSDK	62.6	46.5	16.1	0	2	0	0	2	1 099,6002
32	chloroplast transketolase precursor [Gossypium barbadense]	ABS10814.1	18 411,0	1	8.93%	ALPTYTPESPADATR	55.5	46.2	9.3	0	1	0	0	2	1 589,7813
32	fasciclin-like arabinogalactan protein 12 [Gossypium hirsutum]	ABV27483.1	43 894,2	1	1.88%	LADEINTR	66.8	47	19.8	0	2	0	0	2	931.4849

32	unknown [Picea sitchensis]	ABK26871.1	41 026,6	1	3.40%	GSPLALAQAYETR	84	46.4	37.6	0	1	0	0	2	1 376,7175
32	allantoinase [Robinia pseudoacacia]	AAR29343.1	56 352,0	1	2.15%	TEWEGFDTGTR	62.7	46.1	16.6	0	2	0	0	2	1 298,5655
32	putative rubisco activase [Vigna unguiculata]	CAO02534.1	25 409,2	1	8.30%	VPIHVTGNDFSTLYAPLIR	51.3	44.6	6.7	0	0	1	0	2	2 089,1703
32	fasciclin-like arabinogalactan protein FLA8 [Arabidopsis thaliana]	AAG24276.1	43 044,2	1	2.62%	VGFSGAASGSK	75.7	46.1	29.6	0	1	0	0	2	967,4848
32	oxidoreductase family protein [Arabidopsis thaliana]	NP_188715.2	38 560,4	1	3.94%	DVAVLEAMLESQAK	101	46.1	54.9	0	1	0	0	2	1 448,7308
32	predicted protein [Physcomitrella patens subsp. patens]	XP_001753067.1	57 980,8	1	1.70%	LLEEGDFLK	56.1	46.5	9.6	0	2	0	0	2	1 063,5678
32	unknown [Populus trichocarpa x Populus deltoides]	ABK96272.1	35 285,3	1	2.74%	IFAGDVVPR	64.8	46.8	18	0	1	0	0	2	973,5472
32	hypothetical protein [Vitis vinifera]	CAN77531.1	33 023,8	1	4.39%	TDWSQAPFTASYR	65.3	45.8	19.5	0	1	0	0	2	1 529,7025
32	ATAM11, amidase [Arabidopsis thaliana]	NP_563831.1	45 038,6	1	3.53%	LVDFSIGDTGGSVR	75.3	45.8	29.5	0	1	0	0	2	1 523,7707
32	unnamed protein product (putative Thaumatin family) [Vitis vinifera]	CAO62993.1	26 139,4	1	4.07%	GSDGSVIGCK	77.4	46.7	30.7	0	2	0	0	2	979,452
32	CYP1 (putative cyclophilin_ABH_like) [Vigna radiata]	BAB82452.1	18 188,7	1	6.98%	IVFELFADTTPR	76.4	46	30.4	0	1	0	0	2	1 408,7479
32	aldehyde reductase [Vigna radiata]	AAD53967.1	35 565,6	5	17.20%	DPQTELLDPAVK	82.8	47.6	35.2	0	1	0	0	2	1 325,6955
32	aldehyde reductase [Vigna radiata]	AAD53967.1	35 565,6	5	17.20%	KVDHLLSLDGAK	44.5	49.9	-5.4	0	0	1	0	2	1 295,7325
32	aldehyde reductase [Vigna radiata]	AAD53967.1	35 565,6	5	17.20%	SLGDIYIPLEVSLK	58.6	47.4	11.2	0	1	0	0	2	1 546,8735
32	aldehyde reductase [Vigna radiata]	AAD53967.1	35 565,6	5	17.20%	TGLWYNLSK	42.1	45.9	-3.8	0	2	0	0	2	1 081,5683
32	aldehyde reductase [Vigna radiata]	AAD53967.1	35 565,6	5	17.20%	TLAEDAANK	73.8	46.9	26.9	0	1	0	0	2	1 004,5055
32	putative RuBisCo activase protein [Zantedeschia hybrid cultivar]	AAT12492.1	27 671,2	1	7.79%	IPVIVTGNDFSTLYAPLIR	105	46.7	58.3	0	1	1	0	2	2 089,1703
32	putative glycine-rich RNA-binding protein [Dianthus caryophyllus]	BAF34340.1	16 872,1	1	5.68%	SITVNEAQSR	56.4	46.4	10	0	1	0	0	2	1 104,5649
32	Protein P21 (putative Thaumatin family) [Glycine max]	P25096.1	25 930,1	1	4.18%	TGCNFDGSGR	98.7	46	52.7	0	1	0	0	2	1 070,4326
32	peroxidase [Spinacia oleracea]	CAA71493.1	33 435,5	1	4.85%	MGNISPLTGSSGEIR	56.7	45.8	10.9	0	1	0	0	2	1 534,7536
32	HSP70 (heat shock protein 70) [Arabidopsis thaliana]	NP_187864.1	71 085,2	1	2.00%	TTPSYVAFDTSER	68.6	48.2	20.4	0	1	0	0	2	1 473,6861
32	14-3-3 protein [Vigna angularis]	BAB47119.1	29 342,0	3	10.00%	IISBIEQK	40.5	47.1	-6.6	0	1	0	0	2	917,5308
32	14-3-3 protein [Vigna angularis]	BAB47119.1	29 342,0	3	10.00%	NLLSVAYK	44.4	47.2	-2.8	0	1	0	0	2	907,5254
32	14-3-3 protein [Vigna angularis]	BAB47119.1	29 342,0	3	10.00%	YEEMVEFMEK	37	46.2	-9.2	0	1	0	0	2	1 350,5598
32	TPA: isoflavone reductase-like protein 6 [Vitis vinifera]	CAI56335.1	33 911,9	3	14.90%	GDHTNFEIEPSFGVEASELYPDVK	31.7	43.8	-12.1	0	0	1	0	2	2 680,2420
32	TPA: isoflavone reductase-like protein 6 [Vitis vinifera]	CAI56335.1	33 911,9	3	14.90%	ILIIGGTGYIGK	70.1	47	23.1	0	1	0	0	2	1 204,7309
32	TPA: isoflavone reductase-like protein 6 [Vitis vinifera]	CAI56335.1	33 911,9	3	14.90%	VILGDGNPK	64.8	45.9	18.9	0	2	0	0	2	1 025,5998
32	ascorbate peroxidase [Litchi chinensis]	ABZ79406.1	27 497,2	1	4.00%	EGLIQLPSDK	62.3	46.5	15.8	0	2	0	0	2	1 099,6002
32	heat shock protein 70 [Cucumis sativus]	CAAS2149.1	75 395,0	2	2.83%	IAGLEVLR	58	46.7	11.3	0	1	0	0	2	870,5415
32	heat shock protein 70 [Cucumis sativus]	CAAS2149.1	75 395,0	2	2.83%	NQADSVVYQTEK	55.7	45.9	9.8	0	1	0	0	2	1 381,6600
33	fasciclin-like arabinogalactan protein 12 [Gossypium hirsutum]	ABV27483.1	43 894,2	1	1.88%	LADIEINTR	60.9	47	13.9	0	2	0	0	2	931,4849
33	putative rubisco activase [Vigna unguiculata]	CAO02534.1	25 409,2	1	8.30%	VPIHVTGNDFSTLYAPLIR	89	44.6	44.4	0	1	0	0	2	2 089,1703
33	ATAM11, amidase [Arabidopsis thaliana]	NP_563831.1	45 038,6	1	3.53%	LVDFSIGDTGGSVR	74	45.8	28.2	0	1	0	0	2	1 523,7707
33	CYP1 (putative cyclophilin_ABH_like) [Vigna radiata]	BAB82452.1	18 188,7	1	6.98%	IVFELFADTTPR	90	46	44	0	1	0	0	2	1 408,7479
33	putative RuBisCo activase protein [Zantedeschia hybrid cultivar]	AAT12492.1	27 671,2	1	7.79%	IPVIVTGNDFSTLYAPLIR	89	44.6	44.4	0	1	0	0	2	2 089,1703
33	putative glycine-rich RNA-binding protein [Dianthus caryophyllus]	BAF34340.1	16 872,1	1	5.68%	SITVNEAQSR	58.6	46.4	12.2	0	2	0	0	2	1 104,5649
33	hypothetical protein (putative 14-3-3 protein) [Vitis vinifera]	CAN81774.1	29 523,7	1	7.63%	IVVEELTVEER	68.3	46.5	21.8	0	1	0	0	2	1 432,7172
33	poly(A) polymerase [Pisum sativum]	AAC50041.1	50 217,5	1	7.27%	ADGFVVQTDGPEGPAEGFIDPSTEK	60.9	44.1	16.8	0	0	1	0	2	2 563,1842
33	peroxidase [Spinacia oleracea]	CAA71493.1	33 435,5	1	7.12%	MGNISPLTGSSGEIR	79.8	45.8	34	0	2	0	0	2	1 534,7536
33	unnamed protein product [Vitis vinifera]	CAO14784.1	49 165,4	2	8.48%	ESELTPSNANILDGR	32	45.5	-13.5	0	1	0	0	2	1 615,7928
33	unnamed protein product [Vitis vinifera]	CAO14784.1	49 165,4	2	8.48%	VGDVIESIQVVSGLDNLVNPSYK	50.8	44.2	6.6	0	0	1	0	2	2 445,2874
34	unnamed protein product [Vitis vinifera]	CAO70243.1	40 212,7	2	5.48%	GVNYASAAAIR	113	46.3	66.7	0	1	0	0	2	1 149,6016
34	unnamed protein product [Vitis vinifera]	CAO70243.1	40 212,7	2	5.48%	TLVNYGAR	42.9	46.4	-3.5	0	1	0	0	2	957,4793
34	cytosolic ascorbate peroxidase [Vigna unguiculata]	AAB03844.1	27 016,7	4	29.60%	HPAELAHGANNGLDIIVR SGFEGPWTSNPLIFDNSYFKELLSGE K	58.7	45.3	13.4	0	0	1	0	2	1 854,9575
34	cytosolic ascorbate peroxidase [Vigna unguiculata]	AAB03844.1	27 016,7	4	29.60%	SYPTVSADYQK	43.7	46.4	-2.7	0	1	0	0	2	1 258,5955
34	cytosolic ascorbate peroxidase [Vigna unguiculata]	AAB03844.1	27 016,7	4	29.60%	YAADDAFFADYVAHAHQK	61.2	45.5	15.7	0	0	1	0	2	2 031,9088
34	putative rubisco activase [Vigna unguiculata]	CAO02534.1	25 409,2	2	10.50%	EENPRVPIHVTGNDFSTLYAPLIR	31.4	43.8	-12.4	0	0	1	0	2	2 714,4515
34	putative rubisco activase [Vigna unguiculata]	CAO02534.1	25 409,2	2	10.50%	VPIHVTGNDFSTLYAPLIR	117	44.6	72.4	0	1	0	0	2	2 089,1703
34	fasciclin-like arabinogalactan protein FLA8 [Arabidopsis thaliana]	AAG24276.1	43 044,2	1	2.62%	VGFSGAASGSK	64.1	46.1	18	0	1	0	0	2	967,4848
34	Heat shock 70 kDa protein [Zea mays]	P11143.1	70 586,9	1	4.34%	TTPSYVGFDTTER	65.9	45.9	20	0	1	0	0	2	1 473,6862
34	unknown [Populus trichocarpa x Populus deltoides]	ABK96272.1	35 285,3	1	2.74%	IFAGDVVPR	75.3	46.8	28.5	0	1	0	0	2	973,5472
34	chloroplast ribose-5-phosphate isomerase [Spinacia oleracea]	AAL77589.1	30 846,5	1	3.11%	FIVVDDTK	61.6	46.6	15	0	1	0	0	2	1 035,5727
34	Ribulose-phosphate 3-epimerase, chloroplast precursor [Solanum tuberosum]	Q43843.1	29 863,6	1	5.71%	SDIIVSPSILSANFSK	95.1	45.3	49.8	0	1	0	0	2	1 677,9062

34	unknown [Picea sitchensis]	ABK26251.1	25 923,8	1	4.60%	GVDFSNAVIDR	79.8	46.6	33.2	0	1	0	0	2	1 192,5963
34	putative RuBisCo activase protein [Zantedeschia hybrid cultivar]	AAT12492.1	27 671,2	1	7.79%	IPVIVTGNDFSTLYAPLIR	117	44.6	72.4	0	1	0	0	2	2 089,1703
34	unnamed protein product [Vitis vinifera]	CAO14784.1	49 165,4	3	8.48%	ESELTPSNANILDGR	91.2	45.5	45.7	0	1	0	0	2	1 615,7928
34	unnamed protein product [Vitis vinifera]	CAO14784.1	49 165,4	3	8.48%	HFYDGMIEIQR	40.5	45.8	-5.3	0	1	0	0	2	1 311,5792
34	unnamed protein product [Vitis vinifera]	CAO14784.1	49 165,4	3	8.48%	LPFNAFGTMMAMAR	31	45.8	-14.8	0	1	0	0	2	1 458,6875
34	unknown [Picea sitchensis]	ABK22378.1	33 595,4	1	6.09%	VIEAGANALVAGSAVFGAK	98.8	45.5	53.3	0	1	0	0	2	1 744,9598
34	heat shock protein 70 [Cucumis sativus]	CAA52149.1	75 395,0	3	4.95%	AVVTVPAYFNDSQR	55.3	45.5	9.8	0	1	0	0	2	1 566,7915
34	heat shock protein 70 [Cucumis sativus]	CAA52149.1	75 395,0	3	4.95%	IAGLEVLR	53.4	46.7	6.7	0	1	0	0	2	870.5415
34	heat shock protein 70 [Cucumis sativus]	CAA52149.1	75 395,0	3	4.95%	QFAAEIISAQVLR	86.6	46.4	40.2	0	1	0	0	2	1 461,7702
35	cytosolic ascorbate peroxidase [Vigna unguiculata]	AAB03844.1	27 016,7	2	8.80%	EDKPEPPPEGR	35.6	46.5	-10.9	0	1	0	0	2	1 250,6020
35	cytosolic ascorbate peroxidase [Vigna unguiculata]	AAB03844.1	27 016,7	2	8.80%	SYPTVSADYQK	48.6	46.4	2.2	0	1	0	0	2	1 258,5955
35	pepti (ISS) (putative Cyclophilin) [Ostreococcus tauri]	CAL57205.1	38 854,4	1	3.27%	IVLGLFGDDAPR	62.9	46.3	16.6	0	1	0	0	2	1 272,6955
35	putative rubisco activase [Vigna unguiculata]	CAO02534.1	25 409,2	1	10.00%	MGINPIVMSAGELESGNAGEPAK	65.8	44.5	21.3	0	0	1	0	2	2 304,0853
35	fasciclin-like arabinogalactan protein FLA8 [Arabidopsis thaliana]	AAG24276.1	43 044,2	1	2.62%	VGFSGAASGSK	60.9	46.1	14.8	0	1	0	0	2	967.4848
35	Heat shock 70 kDa protein [Zea mays]	P11143.1	70 586,9	1	2.02%	TTPSYVGFDTTER	68.4	45.9	22.5	0	1	0	0	2	1 473,6862
35	unknown [Populus trichocarpa x Populus deltoides]	ABG96272.1	35 285,3	1	2.74%	IFAGDVVPR	86.9	46.8	40.1	0	1	0	0	2	973.5472
35	chloroplast ribose-5-phosphate isomerase [Spinacia oleracea]	AAL77589.1	30 846,5	2	9.69%	FIVVVDITK	53	46.6	6.4	0	1	0	0	2	1 035,5727
35	chloroplast ribose-5-phosphate isomerase [Spinacia oleracea]	AAL77589.1	30 846,5	2	9.69%	SGMVLGLGTGSTAAFAVSR	67.3	45.1	22.2	0	1	0	0	2	1 797,9168
35	aldose reductase [Digitalis purpurea]	CAC32834.1	34 862,4	2	5.71%	AMEALYDSGK	50.5	45.9	4.6	0	1	0	0	2	1 084,4985
35	aldose reductase [Digitalis purpurea]	CAC32834.1	34 862,4	2	5.71%	TPAQVALR	55.5	45.7	9.8	0	1	0	0	2	855.5053
35	Ribulose-phosphate 3-epimerase, chloroplast precursor [Solanum tuberosum]	Q43843.1	29 863,6	1	5.71%	SDIIVPSILSANFSK	88.2	45.3	42.9	0	1	0	0	2	1 677,9062
35	CYP1 (putative cyclophilin_ABH_like) [Vigna radiata]	BAB82452.1	18 188,7	1	6.98%	IVFELFADTTTPR	73.8	46	27.8	0	1	0	0	2	1 408,7479
35	hypothetical protein [Vitis vinifera]	CAN69876.1	27 324,2	1	5.93%	HVVFGHVIDGMDVVR	56.7	45.2	11.5	0	0	1	0	2	1 695,8641
35	poly(A) polymerase [Pisum sativum]	AAC50041.1	50 217,5	1	8.37%	ADGFVVQTDGPEGPAEGFIDPSTEK	57.3	44.1	13.2	0	0	1	0	2	2 563,1842
35	CPRD14 protein [Vigna unguiculata]	BAA12161.1	35 629,7	4	15.70%	DPQTELLDPALK	67	46	21	0	1	0	0	2	1 339,7113
35	CPRD14 protein [Vigna unguiculata]	BAA12161.1	35 629,7	4	15.70%	DVAIAHVLAYENASANGR	40.8	45.1	-4.3	0	0	1	0	2	1 870,9410
35	CPRD14 protein [Vigna unguiculata]	BAA12161.1	35 629,7	4	15.70%	SLGLEFTPLEVSIK	62.8	46.7	16.1	0	1	0	0	2	1 532,8576
35	CPRD14 protein [Vigna unguiculata]	BAA12161.1	35 629,7	4	15.70%	SLGLEFTPLEVSIKDTVESLK	39.8	44.3	-4.5	0	0	1	0	2	2 305,2542
35	HSP70 (heat shock protein 70) [Arabidopsis thaliana]	NP_187864.1	71 085,2	1	2.00%	TTPSYVVAFTDSEK	67.9	45.9	22	0	1	0	0	2	1 473,6861
35	Stromal 70 kDa heat shock-related protein, chloroplast precursor^Agi 871515^Agi 169023	Q02028.1	75 739,5	1	5.37%	IAGLEVLR	59.8	46.7	13.1	0	1	0	0	2	870.5415
35	Stromal 70 kDa heat shock-related protein, chloroplast precursor [Pisum sativum]	Q02028.1	75 739,5	1	5.37%	IINEPTAASLAYGFER	106	45.4	60.6	0	1	0	0	2	1 751,8969
35	heat shock protein 70 [Cucumis sativus]	CAA52149.1	75 395,0	2	3.11%	AVVTVPAYFNDSQR	46.5	45.5	1	0	1	0	0	2	1 566,7915
35	heat shock protein 70 [Cucumis sativus]	CAA52149.1	75 395,0	2	3.11%	IAGLEVLR	59.8	46.7	13.1	0	1	0	0	2	870.5415
36	CYP1 (putative cyclophilin_ABH_like) [Vigna radiata]	BAB82452.1	18 188,7	1	6.98%	IVFELFADTTTPR	72.8	46	26.8	0	1	0	0	2	1 408,7479
36	peroxidase [Populus alba x Populus tremula var. glandulosa]	AAX53172.1	33 367,4	2	7.59%	GFEVIDTIK	61.9	47.7	14.2	0	1	0	0	2	1 021,5571
36	peroxidase [Populus alba x Populus tremula var. glandulosa]	AAX53172.1	33 367,4	2	7.59%	MGNISPLTGTNGEIR	83.3	45.8	37.5	0	2	0	0	2	1 559,7854
36	peroxidase2 [Medicago sativa]	CAC38106.1	35 992,3	2	5.47%	FDGLVSR	43.9	47.7	-3.8	0	1	0	0	2	793.4209
36	peroxidase2 [Medicago sativa]	CAC38106.1	35 992,3	2	5.47%	IAINMDPTTPR	76.2	46.5	29.7	0	2	0	0	2	1 244,6311
36	Polygalacturonase inhibitor 2 precursor [Phaseolus vulgaris]	P58822.1	37 086,3	2	6.43%	ISGAIPDSYGSFSK	38.5	45.8	-7.3	0	1	0	0	2	1 428,7010
36	Polygalacturonase inhibitor 2 precursor [Phaseolus vulgaris]	P58822.1	37 086,3	2	6.43%	NLNGLDLR	34.9	47.4	-12.5	0	1	0	0	2	914.5061
36	basic chitinase, chitinase [Arabidopsis thaliana]	NP_566426.1	36 196,3	2	7.46%	IGFYQR	34.2	45.3	-11.1	0	1	0	0	2	783.4154
36	basic chitinase, chitinase [Arabidopsis thaliana]	NP_566426.1	36 196,3	2	7.46%	LPGYGVITNIINGGLECGR	61.9	44.9	17	0	0	1	0	2	2 003,0385
36	cyclophilin [Phaseolus vulgaris]	CAA52414.1	18 141,5	1	8.14%	VFFDMTIGQPAGR	71.5	45.7	25.8	0	1	0	0	2	1 511,7319
36	putative secretory protein [Oryza sativa (japonica cultivar-group)]	AAG13529.1	28 687,5	1	3.85%	WDQGYDVTAR	74.2	46.4	27.8	0	1	0	0	2	1 210,5494
36	Aminomethyltransferase, mitochondrial precursor[Pisum sativum]	P49364.2	44 273,1	2	5.88%	AEGFGLGADVILK	77.1	47.1	30	0	1	0	0	2	1 289,7108
36	Aminomethyltransferase, mitochondrial precursor[Pisum sativum]	P49364.2	44 273,1	2	5.88%	VGFISSGPPPR	43	45.9	-2.9	0	1	0	0	2	1 113,6058
36	At5g07030 [Arabidopsis thaliana]	ABG25087.1	48 676,8	2	4.62%	SSLYYVNLVAIR	80.2	45.8	34.4	0	1	0	0	2	1 397,7791
36	At5g07030 [Arabidopsis thaliana]	ABG25087.1	48 676,8	2	4.62%	SVVPIASGR	41.3	46.1	-4.8	0	1	0	0	2	885.5157
36	endochitinase precursor [Humulus lupulus]	AAD34596.1	33 511,4	1	6.01%	GFTYDAFLTAAR	79.6	46	33.6	0	1	0	0	2	1 495,7221
37	CYP1 (putative cyclophilin_ABH_like) [Vigna radiata]	BAB82452.1	18 188,7	1	6.98%	IVFELFADTTTPR	90	46	44	0	1	0	0	2	1 408,7479
37	peroxidase [Populus alba x Populus tremula var. glandulosa]	AAX53172.1	33 367,4	2	7.59%	GFEVIDTIK	56.5	47.7	8.8	0	1	0	0	2	1 021,5571
37	peroxidase [Populus alba x Populus tremula var. glandulosa]	AAX53172.1	33 367,4	2	7.59%	MGNISPLTGTNGEIR	85.7	45.8	39.9	0	2	0	0	2	1 559,7854
37	peroxidase [Sesamum indicum]	ABB89209.1	35 838,4	1	3.64%	VSCADILALATR	81.4	47.1	34.3	0	1	0	0	2	1 289,6889
37	peroxidase2 [Medicago sativa]	CAC38106.1	35 992,3	2	9.12%	FDGLVSR	45.8	47.7	-1.9	0	1	0	0	2	793.4209

37	peroxidase2 [Medicago sativa]	CAC38106.1	35 992,3	2	9.12%	IAINMDPTTPR	95.6	46.5	49.1	0	2	0	0	2	1 244,6311
37	peroxidase2 [Medicago sativa]	CAC38106.1	35 992,3	2	9.12%	VSCADILALATR	81.4	47.1	34.3	0	1	0	0	2	1 289,6889
37	cyclophilin [Phaseolus vulgaris]	CAA52414.1	18 141,5	1	8.14%	VFFDMTIGGQPAGR	68.8	45.7	23.1	0	1	0	0	2	1 511,7319
37	Aminomethyltransferase, mitochondrial precursor[Pisum sativum]	P49364.2	44 273,1	1	2.70%	VGFSSGPPPR	79.9	45.9	34	0	1	0	0	2	1 113,6058
37	pectinacetyltransferase precursor [Vigna radiata var. radiata]	CAA67728.1	43 804,9	2	8.77%	VFAAVVDDLLAK	71.9	46.6	25.3	0	1	0	0	2	1 260,7204
37	pectinacetyltransferase precursor [Vigna radiata var. radiata]	CAA67728.1	43 804,9	2	8.77%	YCDGSSFTGDVEAVDPATNLHFR	73.2	44	29.2	0	0	1	0	2	2 558,1258
37	At5g07030 [Arabidopsis thaliana]	ABG25087.1	48 676,8	2	4.62%	SSLYYVNLVAIR	93.9	45.8	48.1	0	1	0	0	2	1 397,7791
37	At5g07030 [Arabidopsis thaliana]	ABG25087.1	48 676,8	2	4.62%	SVVPIASGR	39.9	46.1	-6.2	0	1	0	0	2	885.5157
37	endochitinase precursor [Humulus lupulus]	AAD34596.1	33 511,4	1	4.11%	GFYTYDAFLTAAR	83.3	46	37.3	0	1	0	0	2	1 495,7221
37	Peroxidase 45 precursor [Arabidopsis thaliana]	Q96522.1	35 811,1	1	8.00%	GLFTSDQILFTDQR	78.6	45.3	33.3	0	1	0	0	2	1 640,8287
37	Peroxidase 45 precursor [Arabidopsis thaliana]	Q96522.1	35 811,1	1	8.00%	VSCADILALATR	81.4	47.1	34.3	0	1	0	0	2	1 289,6889
37	Glycosyl hydrolase family 3 N terminal domain containing protein, expressed [Oryza sativa (japonica cultivar-group)]	ABF98889.1	76 787,5	1	1.41%	IGAATALEVR	55.7	49.2	6.5	0	1	0	0	2	1 000,5792
37	unnamed protein product [Vitis vinifera]	CA040802.1	39 845,1	2	4.89%	ESAIQVLR	65.2	46.5	18.7	0	1	0	0	2	986.5636
37	unnamed protein product [Vitis vinifera]	CA040802.1	39 845,1	2	4.89%	TCAQDEVLR	55.3	46.8	8.5	0	1	0	0	2	1 091,5157
37	unknown [Populus trichocarpa]	ABK92766.1	35 697,9	1	2.41%	ALGQISER	55.5	47.2	8.3	0	1	0	0	2	873.4795
37	pectin acetyltransferase [Eucalyptus globulus subsp. globulus]	ABG34280.1	38 829,9	2	6.29%	AEENPDDFFNWR	81.5	45.8	35.7	0	1	0	0	2	1 538,6663
37	pectin acetyltransferase [Eucalyptus globulus subsp. globulus]	ABG34280.1	38 829,9	2	6.29%	AIDCPYPCDK	39.9	46.5	-6.6	0	1	0	0	2	1 238,5189
37	Fructose-bisphosphate aldolase, chloroplast precursor [Oryza sativa (japonica cultivar-group)]	ABA91632.2	42 913,5	1	3.26%	LASIGLENTEANR	56.1	46	10.1	0	1	0	0	2	1 387,7181
38	peroxidase [Populus alba x Populus tremula var. glandulosa]	AAX53172.1	33 367,4	2	7.59%	GFEVIDTIK	59.6	47.7	11.9	0	1	0	0	2	1 021,5571
38	peroxidase [Populus alba x Populus tremula var. glandulosa]	AAX53172.1	33 367,4	2	7.59%	MGNISPLTGTNGEIR	57.3	45.8	11.5	0	1	0	0	2	1 559,7854
38	peroxidase [Sesamum indicum]	ABB89209.1	35 838,4	2	6.97%	IAIDMDPTTPR	73.6	47.7	25.9	0	1	0	0	2	1 245,6152
38	peroxidase [Sesamum indicum]	ABB89209.1	35 838,4	2	6.97%	VSCADILALATR	89.5	47.1	42.4	0	2	0	0	2	1 289,6889
38	pectinacetyltransferase precursor [Vigna radiata var. radiata]	CAA67728.1	43 804,9	2	8.77%	VFAAVVDDLLAK	50.7	46.6	4.1	0	1	0	0	2	1 260,7204
38	pectinacetyltransferase precursor [Vigna radiata var. radiata]	CAA67728.1	43 804,9	2	8.77%	YCDGSSFTGDVEAVDPATNLHFR	78.7	44	34.7	0	0	1	0	2	2 558,1258
38	Peroxidase 45 precursor [Arabidopsis thaliana]	Q96522.1	35 811,1	1	8.00%	GLFTSDQILFTDQR	86.6	45.3	41.3	0	2	0	0	2	1 640,8287
38	Peroxidase 45 precursor [Arabidopsis thaliana]	Q96522.1	35 811,1	1	8.00%	VSCADILALATR	89.5	47.1	42.4	0	2	0	0	2	1 289,6889
38	acid alpha galactosidase 1 [Cucumis sativus]	ABC55266.1	45 680,3	1	1.94%	VAVVLLNR	56.2	45.6	10.6	0	1	0	0	2	883.5728
38	pectin acetyltransferase [Eucalyptus globulus subsp. globulus]	ABG34280.1	38 829,9	2	6.29%	AEENPDDFFNWR	81.6	45.8	35.8	0	1	0	0	2	1 538,6663
38	pectin acetyltransferase [Eucalyptus globulus subsp. globulus]	ABG34280.1	38 829,9	2	6.29%	AIDCPYPCDK	53.5	48.9	4.6	0	1	0	0	2	1 238,5189
38	Fructose-bisphosphate aldolase, chloroplast precursor [Oryza sativa (japonica cultivar-group)]	ABA91632.2	42 913,5	1	3.26%	LASIGLENTEANR	88.3	46	42.3	0	1	0	0	2	1 387,7181
38	CYP1 (putative cyclophilin_ABH_like) [Vigna radiata]	BAB82452.1	18 188,7	2	15.10%	IVFELFADTTTPR	90.4	46	44.4	0	1	0	0	2	1 408,7479
38	CYP1 (putative cyclophilin_ABH_like) [Vigna radiata]	BAB82452.1	18 188,7	2	15.10%	TSRPVAIADCQGSL	40.7	46.1	-5.4	0	1	0	0	2	1 474,7326
38	peroxidase2 [Medicago sativa]	CAC38106.1	35 992,3	2	9.12%	FDGLVSR	50	47.7	2.3	0	2	0	0	2	793.4209
38	peroxidase2 [Medicago sativa]	CAC38106.1	35 992,3	2	9.12%	IAINMDPTTPR	89.1	46.5	42.6	0	3	0	0	2	1 244,6311
38	peroxidase2 [Medicago sativa]	CAC38106.1	35 992,3	2	9.12%	VSCADILALATR	89.5	47.1	42.4	0	2	0	0	2	1 289,6889
38	Polygalacturonase inhibitor 2 precursor [Phaseolus vulgaris]	P58822.1	37 086,3	1	4.09%	ISGAIPDSYGSFSK	62	45.8	16.2	0	1	0	0	2	1 428,7010
38	basic chitinase, chitinase [Arabidopsis thaliana]	NP_566426.1	36 196,3	2	7.46%	IGFYQR	31.7	45.3	-13.6	0	1	0	0	2	783.4154
38	basic chitinase, chitinase [Arabidopsis thaliana]	NP_566426.1	36 196,3	2	7.46%	LPGYGVITNIINGGLECGR	103	44.9	58.1	0	1	1	0	2	2 003,0385
38	cyclophilin [Phaseolus vulgaris]	CAA52414.1	18 141,5	1	8.14%	VFFDMTIGGQPAGR	79.8	45.7	34.1	0	2	0	0	2	1 511,7319
38	endochitinase precursor [Humulus lupulus]	AAD34596.1	33 511,4	1	6.01%	GFYTYDAFLTAAR	71.5	46	25.5	0	1	0	0	2	1 495,7221
38	unnamed protein product [Populus trichocarpa]	ABK94155.1	77 435,5	1	1.28%	TCAQDEVLR	53.5	46.8	6.7	0	1	0	0	2	1 091,5157
38	unnamed protein product (putative Serine carboxypeptidase) [Vitis vinifera]	CA068876.1	57 192,0	1	2.96%	NLEVGPDLLEDGIK	58.1	45.3	12.8	0	2	0	0	2	1 624,8801
39	peroxidase [Sesamum indicum]	ABB89209.1	35 838,4	1	3.64%	VSCADILALATR	92.8	47.1	45.7	0	1	0	0	2	1 289,6889
39	actin [Zea mays]	AB40103.1	37 117,1	2	8.33%	AGFAGDDAPR	64.1	46.9	17.2	0	1	0	0	2	976.4489
39	actin [Zea mays]	AB40103.1	37 117,1	2	8.33%	VAPEEHPDLLTEAPLNPK	47.6	45.2	2.4	0	0	1	0	2	1 956,0446
39	Phosphoglucomutase, cytoplasmic [Pisum sativum]	Q9SM60.1	63 308,1	1	2.06%	YDYENVDAAGAK	74.2	47.5	26.7	0	1	0	0	2	1 315,5807
39	Actin [Mesostigma viride]	O65316.1	41 572,2	1	6.90%	AGFAGDDAPR	64.1	46.9	17.2	0	1	0	0	2	976.4489
39	Actin [Mesostigma viride]	O65316.1	41 572,2	1	6.90%	SYELPDGQVITIGNER	73	46.1	26.9	0	1	0	0	2	1 790,8925
39	pectinacetyltransferase precursor [Vigna radiata var. radiata]	CAA67728.1	43 804,9	2	6.77%	QIDCAYCNPCTCHNR	58.9	45.3	13.6	0	0	1	0	2	1 905,7795
39	pectinacetyltransferase precursor [Vigna radiata var. radiata]	CAA67728.1	43 804,9	2	6.77%	VFAAVVDDLLAK	59.2	46.6	12.6	0	1	0	0	2	1 260,7204
39	Peroxidase 45 precursor [Arabidopsis thaliana]	Q96522.1	35 811,1	1	8.00%	GLFTSDQILFTDQR	79.9	45.3	34.6	0	1	0	0	2	1 640,8287
39	Peroxidase 45 precursor [Arabidopsis thaliana]	Q96522.1	35 811,1	1	8.00%	VSCADILALATR	92.8	47.1	45.7	0	1	0	0	2	1 289,6889

39	pectin acetyltransferase [Eucalyptus globulus subsp. globulus]	ABG34280.1	38 829,9	2	6.29%	AEENPDFFNWNR	77.6	45.8	31.8	0	1	0	0	2	1 538,6663
39	pectin acetyltransferase [Eucalyptus globulus subsp. globulus]	ABG34280.1	38 829,9	2	6.29%	AIDCPYPYCDK	54	46.5	7.5	0	1	0	0	2	1 238,5189
39	Peroxioredoxin Q, chloroplast precursor (Thioredoxin reductase) [Sedum lineare]	Q9MB35.1	20 633,9	1	3.76%	HIDETLK	57.2	45.7	11.5	0	1	0	0	2	855,4578
39	CYP1 (putative cyclophilin_ABH_like) [Vigna radiata]	BAB82452.1	18 188,7	2	15.10%	IVFELFADTTTPR	86.3	46	40.3	0	1	0	0	2	1 408,7479
39	CYP1 (putative cyclophilin_ABH_like) [Vigna radiata]	BAB82452.1	18 188,7	2	15.10%	TSRPVAIADCGQLS	55.7	46.1	9.6	0	1	0	0	2	1 474,7326
39	peroxidase2 [Medicago sativa]	CAC38106.1	35 992,3	2	9.12%	FDGLVSR	45.9	47.7	-1.8	0	1	0	0	2	793,4209
39	peroxidase2 [Medicago sativa]	CAC38106.1	35 992,3	2	9.12%	IAINMDPTTTPR	85.2	46.5	38.7	0	2	0	0	2	1 244,6311
39	peroxidase2 [Medicago sativa]	CAC38106.1	35 992,3	2	9.12%	VSCADILALATR	92.8	47.1	45.7	0	1	0	0	2	1 289,6889
39	basic chitinase, chitinase [Arabidopsis thaliana]	NP_566426.1	36 196,3	1	5.67%	LPYGVVITNIINGGLECGR	67.7	44.9	22.8	0	1	1	0	2	2 003,0385
39	cyclophilin [Phaseolus vulgaris]	CAA52414.1	18 141,5	1	8.14%	VFFDMTIGGQPAGR	75.4	45.7	29.7	0	1	1	0	2	1 511,7319
39	unnamed protein product [Vitis vinifera]	CAO46584.1	35 610,8	1	4.91%	LPAAYEDGVEALKWIK	61.8	47.6	14.2	0	1	0	0	2	1 802,9696
40	CYP1 (putative cyclophilin_ABH_like) [Vigna radiata]	BAB82452.1	18 188,7	2	6.98%	IVFELFADTTTPR	90	46	44	0	1	0	0	2	1 408,7479
40	peroxidase [Sesamum indicum]	ABB89209.1	35 838,4	2	9.09%	DHPDNLSLAGDGFDTVIK	56.9	45.3	11.6	0	0	1	0	2	1 913,9248
40	peroxidase [Sesamum indicum]	ABB89209.1	35 838,4	2	9.09%	VSCADILALATR	93.1	47.1	46	0	1	0	0	2	1 289,6889
40	Probable non-specific lipid-transfer protein AKCS9 precursor [Vigna unguiculata]	Q43681.1	10 431,0	2	24.20%	KVLSNCGVITYPNC	31.6	45.7	-14.1	0	1	0	0	2	1 511,6987
40	Probable non-specific lipid-transfer protein AKCS9 precursor [Vigna unguiculata]	Q43681.1	10 431,0	2	24.20%	VQEPCLCNVIK	53.9	47.5	6.4	0	1	0	0	2	1 423,6716
40	peroxidase2 [Medicago sativa]	CAC38106.1	35 992,3	2	9.12%	FDGLVSR	47.7	47.7	0	0	1	0	0	2	793,4209
40	peroxidase2 [Medicago sativa]	CAC38106.1	35 992,3	2	9.12%	IAINMDPTTTPR	81.8	46.5	35.3	0	2	0	0	2	1 228,6362
40	peroxidase2 [Medicago sativa]	CAC38106.1	35 992,3	2	9.12%	VSCADILALATR	93.1	47.1	46	0	1	0	0	2	1 289,6889
40	unnamed protein product [Vitis vinifera]	CAO17011.1	42 507,9	3	6.11%	LFSPGNLR	34.6	47.3	-12.7	0	1	0	0	2	903,5053
40	unnamed protein product [Vitis vinifera]	CAO17011.1	42 507,9	3	6.11%	TTYVLAK	33.9	46.4	-12.5	0	1	0	0	2	908,5457
40	unnamed protein product [Vitis vinifera]	CAO17011.1	42 507,9	3	6.11%	VINLDER	62.1	46.7	15.4	0	1	0	0	2	972,5114
40	basic chitinase, chitinase [Arabidopsis thaliana]	NP_566426.1	36 196,3	1	5.67%	LPYGVVITNIINGGLECGR	114	44.9	69.1	0	1	0	0	2	2 003,0385
40	cyclophilin [Phaseolus vulgaris]	CAA52414.1	18 141,5	1	8.14%	VFFDMTIGGQPAGR	71	45.7	25.3	0	1	1	0	2	1 511,7319
40	iron-superoxide dismutase precursor [Vigna unguiculata]	AAF28773.1	27 393,8	2	8.98%	LVSWDAVSSR	73.1	46.5	26.6	0	1	0	0	2	1 119,5798
40	iron-superoxide dismutase precursor [Vigna unguiculata]	AAF28773.1	27 393,8	2	8.98%	SLEEIHVTAYNK	52.9	46.2	6.7	0	1	0	0	2	1 379,7421
40	pectinacetyltransferase precursor [Vigna radiata var. radiata]	CAA67728.1	43 804,9	1	3.01%	VFAAVVDDLAK	54.2	46.6	7.6	0	1	0	0	2	1 260,7204
40	endochitinase precursor [Humulus lupulus]	AAD34596.1	33 511,4	1	4.11%	GFYTYDAFLTAAR	69.8	46	23.8	0	1	0	0	2	1 495,7221
40	xyloglucan endotransglucosylase/hydrolase 2 [Cucumis melo]	ABI94062.1	36 316,1	1	3.88%	WFSQAPFTASYR	79.9	45.8	34.1	0	1	0	0	2	1 529,7025
40	Phosphoglucomutase, cytoplasmic [Pisum sativum]	Q9SM60.1	63 106,2	2	4.12%	LSGTGSEGATIR	112	46.5	65.5	0	1	0	0	2	1 148,5913
40	Phosphoglucomutase, cytoplasmic [Pisum sativum]	Q9SM60.1	63 106,2	2	4.12%	YDYENVDAAGAAK	62.2	47.5	14.7	0	1	0	0	2	1 315,5807
40	putative pectin methyltransferase 3 [Linum usitatissimum]	AAG17110.1	69 430,1	1	1.90%	DITFQNTAGPSK	66.1	46.6	19.5	0	1	0	0	2	1 278,6333
40	pectin acetyltransferase [Eucalyptus globulus subsp. globulus]	ABG34280.1	38 829,9	2	6.29%	AEENPDFFNWNR	81.8	45.8	36	0	1	0	0	2	1 538,6663
40	pectin acetyltransferase [Eucalyptus globulus subsp. globulus]	ABG34280.1	38 829,9	2	6.29%	AIDCPYPYCDK	48.5	46.5	2	0	1	0	0	2	1 238,5189
41	peroxidase [Sesamum indicum]	ABB89209.1	35 838,4	2	5.45%	DHPDNLSLAGDGFDTVIK	59.9	45.3	14.6	0	0	1	0	2	1 913,9248
41	Probable non-specific lipid-transfer protein AKCS9 precursor [Vigna unguiculata]	Q43681.1	10 431,0	3	24.20%	KVLSNCGVITYPNC	61.6	45.7	15.9	0	1	0	0	2	1 511,6987
41	Probable non-specific lipid-transfer protein AKCS9 precursor [Vigna unguiculata]	Q43681.1	10 431,0	3	24.20%	VLSNCGVITYPNC	34.2	48.4	-14.2	0	1	0	0	2	1 383,6037
41	Probable non-specific lipid-transfer protein AKCS9 precursor [Vigna unguiculata]	Q43681.1	10 431,0	3	24.20%	VQEPCLCNVIK	59.2	47.5	11.7	0	1	0	0	2	1 423,6716
41	fasciclin-like arabinogalactan protein FLA8 [Arabidopsis thaliana]	AAG24276.1	43 044,2	1	2.62%	VGFGSAASGSK	64.6	46.1	18.5	0	1	0	0	2	967,4848
41	CYP1 (putative cyclophilin_ABH_like) [Vigna radiata]	BAB82452.1	18 188,7	5	23.80%	FADENFVK	40.3	45.8	-5.5	0	1	0	0	2	969,4682
41	CYP1 (putative cyclophilin_ABH_like) [Vigna radiata]	BAB82452.1	18 188,7	5	23.80%	FADENFVKK	42.5	45.5	-3	0	1	0	0	2	1 097,5632
41	CYP1 (putative cyclophilin_ABH_like) [Vigna radiata]	BAB82452.1	18 188,7	5	23.80%	IVFELFADTTTPR	85	46	39	0	1	0	0	2	1 408,7479
41	CYP1 (putative cyclophilin_ABH_like) [Vigna radiata]	BAB82452.1	18 188,7	5	23.80%	TAENFR	38.4	47.9	-9.5	0	1	0	0	2	737,3582
41	CYP1 (putative cyclophilin_ABH_like) [Vigna radiata]	BAB82452.1	18 188,7	5	23.80%	TSRPVAIADCGQLS	62.8	46.1	16.7	0	1	0	0	2	1 474,7326
41	alpha-galactosidase [Helianthus annuus]	BAC66445.1	47 103,4	1	3.50%	EVIANVQDLSLGVQGK	78.2	48.4	29.8	0	1	0	0	2	1 556,8285
41	peroxidase2 [Medicago sativa]	CAC38106.1	35 992,3	1	3.34%	IAINMDPTTTPR	78	46.5	31.5	0	2	0	0	2	1 228,6362
41	aldehyde reductase [Vigna radiata]	AAD53967.1	35 565,6	1	3.69%	DPQTELLDPAVK	60.4	47.6	12.8	0	1	0	0	2	1 325,6955
41	iron-superoxide dismutase precursor [Vigna unguiculata]	AAF28773.1	27 393,8	1	4.08%	LVSWDAVSSR	53.3	46.5	6.8	0	1	0	0	2	1 119,5798
41	ubiquitin [Arabidopsis thaliana]	ABH08753.1	59 877,8	2	4.87%	KTITLEVESSDTIDNVK	38	45.3	-7.3	0	0	1	0	2	1 891,9865
41	ubiquitin [Arabidopsis thaliana]	ABH08753.1	59 877,8	2	4.87%	TLADYNIQK	38.6	46.4	-7.8	0	7	0	0	2	1 065,5582
42	CYP1 (putative cyclophilin_ABH_like) [Vigna radiata]	BAB82452.1	18 188,7	5	39.00%	FADENFVK	37	45.8	-8.8	0	1	0	0	2	969,4682
42	CYP1 (putative cyclophilin_ABH_like) [Vigna radiata]	BAB82452.1	18 188,7	5	39.00%	IVFELFADTTTPR	76.4	46	30.4	0	1	0	0	2	1 408,7479
42	CYP1 (putative cyclophilin_ABH_like) [Vigna radiata]	BAB82452.1	18 188,7	5	39.00%	TAENFR	33.3	47.9	-14.6	0	1	0	0	2	737,3582
42	CYP1 (putative cyclophilin_ABH_like) [Vigna radiata]	BAB82452.1	18 188,7	5	39.00%	TSRPVAIADCGQLS	74.4	46.1	28.3	0	1	0	0	2	1 474,7326

42	CYP1 (putative cyclophilin_ABH_like) [Vigna radiata]	BAB82452.1	18 188,7	5	39.00%	VIPNFMCGQGGDFTAGNGTGGESIYG	77	43.7	33.3	0	0	1	0	2	2 748,2398
42	peroxidase [Sesamum indicum]	ABB89209.1	35 838,4	1	3.64%	VSCADILALATR	80.4	47.1	33.3	0	1	0	0	2	1 289,6889
42	alpha-galactosidase [Helianthus annuus]	BAC66445.1	47 103,4	1	3.50%	EIVAVNQDSLGVQGK	73	48.4	24.6	0	1	0	0	2	1 556,8285
42	Probable non-specific lipid-transfer protein AKCS9 precursor [Vigna unguiculata]	Q43681.1	10 431,0	4	35.40%	KVLSNCGVVTYPNC	56.2	45.7	10.5	0	1	0	0	2	1 511,6987
42	Probable non-specific lipid-transfer protein AKCS9 precursor [Vigna unguiculata]	Q43681.1	10 431,0	4	35.40%	LKVQEPLCLNYIK	46.3	45.4	0.9	0	0	1	0	2	1 664,8505
42	Probable non-specific lipid-transfer protein AKCS9 precursor [Vigna unguiculata]	Q43681.1	10 431,0	4	35.40%	QYVNSPGAK	35.4	47.7	-12.3	0	1	0	0	2	963.49
42	Probable non-specific lipid-transfer protein AKCS9 precursor [Vigna unguiculata]	Q43681.1	10 431,0	4	35.40%	VQEPCLCLNYIK	54	47.5	6.5	0	1	0	0	2	1 423,6716
42	peroxidase2 [Medicago sativa]	CAC38106.1	35 992,3	1	6.99%	IAINMDPTTPR	69.7	46.5	23.2	0	2	0	0	2	1 244,6311
42	peroxidase2 [Medicago sativa]	CAC38106.1	35 992,3	1	6.99%	VSCADILALATR	80.4	47.1	33.3	0	1	0	0	2	1 289,6889
42	aldehyde reductase [Vigna radiata]	AAD53967.1	35 565,6	3	10.80%	DPQTELLDPAVK	71	47.6	23.4	0	1	0	0	2	1 325,6955
42	aldehyde reductase [Vigna radiata]	AAD53967.1	35 565,6	3	10.80%	SLGIDYIPLEVSLK	59.4	47.4	12	0	1	0	0	2	1 546,8735
42	aldehyde reductase [Vigna radiata]	AAD53967.1	35 565,6	3	10.80%	TGLWYNLSK	51.1	45.9	5.2	0	1	0	0	2	1 081,5683
42	cyclophilin [Phaseolus vulgaris]	CAA52414.1	18 141,5	1	32.00%	VFFDMTIGGQPAGR	66.6	46	20.6	0	2	0	0	2	1 495,7370
42	cyclophilin [Phaseolus vulgaris]	CAA52414.1	18 141,5	1	32.00%	VIPNFMCGQGGDFTAGNGTGGESIYG	77	43.7	33.3	0	0	1	0	2	2 748,2398
42	Peroxidase 45 precursor [Arabidopsis thaliana]	Q96522.1	35 811,1	1	8.00%	VSCADILALATR	80.4	47.1	33.3	0	1	0	0	2	1 289,6889
42	Peroxioredoxin Q, chloroplast precursor (Thioredoxin reductase) [Sedum lineare]	Q9MB35.1	20 633,9	2	14.00%	GKPVVVVYFPADETPGCTK	47.8	44.9	2.9	0	0	1	0	2	1 280,0431
42	Peroxioredoxin Q, chloroplast precursor (Thioredoxin reductase) [Sedum lineare]	Q9MB35.1	20 633,9	2	14.00%	HIDETLK	42.7	45.7	-3	0	1	0	0	2	855.4578
43	Probable non-specific lipid-transfer protein AKCS9 precursor [Vigna unguiculata]	Q43681.1	10 431,0	2	22.20%	KVLSNCGVVTYPNC	51.6	45.7	5.9	0	1	0	0	2	1 511,6987
43	Probable non-specific lipid-transfer protein AKCS9 precursor [Vigna unguiculata]	Q43681.1	10 431,0	2	22.20%	QYVNSPGAK	33.6	47.7	-14.1	0	1	0	0	2	963.49
43	pepti (ISS) (putative Cyclophilin) [Ostreococcus tauri]	CAL57205.1	38 854,4	1	3.27%	IVLGLFGDDAPR	57.7	46.3	11.4	0	2	0	0	2	1 272,6955
43	unnamed protein product (putative Thaumatin family) [Vitis vinifera]	CAO62993.1	26 139,4	1	4.07%	GSDGSVIGCK	61.2	46.7	14.5	0	1	0	0	2	979.452
43	CYP1 (putative cyclophilin_ABH_like) [Vigna radiata]	BAB82452.1	18 188,7	2	10.50%	IVFELFADTTTPR	90	46	44	0	2	0	0	2	1 408,7479
43	CYP1 (putative cyclophilin_ABH_like) [Vigna radiata]	BAB82452.1	18 188,7	2	10.50%	TAENFR	40	47.9	-7.9	0	1	0	0	2	737.3582
43	ubiquitin/ribosomal protein 27a [Prunus avium]	AAG13985.1	85 258,5	1	1.18%	TLADYNIQK	57.2	46.4	10.8	0	20	0	0	2	1 065,5582
43	peroxidase2 [Medicago sativa]	CAC38106.1	35 992,3	2	5.47%	FDGLVSR	49.4	47.7	1.7	0	1	0	0	2	793.4209
43	peroxidase2 [Medicago sativa]	CAC38106.1	35 992,3	2	5.47%	IAINMDPTTPR	81.3	46.5	34.8	0	2	0	0	2	1 244,6311
43	aldehyde reductase [Vigna radiata]	AAD53967.1	35 565,6	1	3.69%	DPQTELLDPAVK	81.5	47.6	33.9	0	1	0	0	2	1 325,6955
43	putative glycine-rich RNA-binding protein [Dianthus caryophyllus]	BAF34340.1	16 872,1	1	5.68%	SITVNEAQRS	53.9	46.4	7.5	0	1	0	0	2	1 104,5649
43	cyclophilin [Phaseolus vulgaris]	CAA52414.1	18 141,5	1	11.60%	VFFDMTIGGQPAGR	79.2	45.7	33.5	0	2	0	0	2	1 511,7319
43	peroxidase [Spinacia oleracea]	CAA71493.1	33 435,5	1	4.85%	MGNISPLTGSSGEIR	75.2	45.8	29.4	0	1	0	0	2	1 534,7536
43	unnamed protein product [Populus trichocarpa]	ABK93386.1	83 612,9	1	0.92%	HIDETLK	63	45.7	17.3	0	2	0	0	2	855.4578
44	Os09g0537600 [Oryza sativa (japonica cultivar-group)]	NP_001063792.1	23 389,0	1	5.58%	IVIGLYGDVVPK	53.5	46.3	7.2	0	1	0	0	2	1 272,7570
44	oxidoreductase family protein [Arabidopsis thaliana]	NP_188715.2	38 560,4	1	3.94%	DVAVLEAMLESGAK	107	46.1	60.9	0	1	0	0	2	1 448,7308
44	CYP1 (putative cyclophilin_ABH_like) [Vigna radiata]	BAB82452.1	18 188,7	2	10.50%	IVFELFADTTTPR	72.9	46	26.9	0	2	0	0	2	1 408,7479
44	CYP1 (putative cyclophilin_ABH_like) [Vigna radiata]	BAB82452.1	18 188,7	2	10.50%	TAENFR	37.2	47.9	-10.7	0	1	0	0	2	737.3582
44	Cysteine proteinase inhibitor [Vigna unguiculata]	Q06445.1	10 740,0	1	16.50%	DVAGNQNSLEIDSLAR	63.4	45.2	18.2	0	1	0	0	2	1 701,8408
44	peroxidase2 [Medicago sativa]	CAC38106.1	35 992,3	2	5.47%	FDGLVSR	33.4	47.7	-14.3	0	1	0	0	2	793.4209
44	peroxidase2 [Medicago sativa]	CAC38106.1	35 992,3	2	5.47%	IAINMDPTTPR	65.2	46.5	18.7	0	1	0	0	2	1 244,6311
44	putative glycine-rich RNA-binding protein [Dianthus caryophyllus]	BAF34340.1	16 872,1	1	5.68%	SITVNEAQRS	56.6	46.4	10.2	0	1	0	0	2	1 104,5649
44	cyclophilin [Phaseolus vulgaris]	CAA52414.1	18 141,5	1	11.60%	VFFDMTIGGQPAGR	89.8	45.7	44.1	0	2	0	0	2	1 511,7319
44	peroxidase [Spinacia oleracea]	CAA71493.1	33 435,5	2	7.12%	MGASILR	49.8	47.7	2.1	0	2	0	0	2	763.4137
44	peroxidase [Spinacia oleracea]	CAA71493.1	33 435,5	2	7.12%	MGNISPLTGSSGEIR	56.4	45.8	10.6	0	1	0	0	2	1 534,7536
44	pterocarpan reductase [Lotus japonicus]	BAF34844.1	33 974,1	1	3.23%	AGHPTFALVR	59.6	46	13.6	0	0	1	0	2	1 068,5955
44	unnamed protein product [Populus trichocarpa]	ABK94155.1	77 435,5	1	1.28%	TCAQDEVLR	65.5	46.8	18.7	0	1	0	0	2	1 091,5157
44	Os01g0840100 [Oryza sativa (japonica cultivar-group)]	NP_001044757.1	71 715,0	1	1.99%	TTPSYVAFTDSER	67.2	45.9	21.3	0	2	0	0	2	1 473,6861
44	pterocarpan reductase [Lotus japonicus]	BAF34842.1	36 176,4	1	3.09%	VIIIGDGNPK	58.9	45.9	13	0	1	0	0	2	1 025,5998
45	unnamed protein product (putative Thaumatin family) [Vitis vinifera]	CAO62993.1	26 139,4	1	4.07%	GSDGSVIGCK	76.2	46.7	29.5	0	2	0	0	2	979.452
45	CYP1 (putative cyclophilin_ABH_like) [Vigna radiata]	BAB82452.1	18 188,7	1	6.98%	IVFELFADTTTPR	76.6	46	30.6	0	2	0	0	2	1 408,7479
45	peroxidase2 [Medicago sativa]	CAC38106.1	35 992,3	1	3.34%	IAINMDPTTPR	58.7	46.5	12.2	0	1	0	0	2	1 244,6311
45	putative glycine-rich RNA-binding protein [Dianthus caryophyllus]	BAF34340.1	16 872,1	1	5.68%	SITVNEAQRS	60.8	46.4	14.4	0	1	0	0	2	1 104,5649
45	Protein P21 (putative Thaumatin family) [Glycine max]	P25096.1	25 930,1	1	4.18%	TGCNFDGSGR	86	46	40	0	1	0	0	2	1 070,4326
45	cyclophilin [Phaseolus vulgaris]	CAA52414.1	18 141,5	1	8.14%	VFFDMTIGGQPAGR	90.1	45.7	44.4	0	2	0	0	2	1 511,7319
45	peroxidase [Spinacia oleracea]	CAA71493.1	33 435,5	1	4.85%	MGNISPLTGSSGEIR	87.1	45.8	41.3	0	1	0	0	2	1 534,7536

45	Os01g0840100 [Oryza sativa (japonica cultivar-group)]	NP_001044757.1	71 715,0	1	1.99%	ITPSYVAFTDSER	67.5	45.9	21.6	0	1	0	0	2	1 473,6861
46	CYP1 (putative cyclophilin_ABH_like) [Vigna radiata]	BAB82452.1	18 188,7	1	6.98%	IVFELFADTTTPR	76.5	46	30.5	0	1	0	0	2	1 408,7479
46	putative glycine-rich RNA-binding protein [Dianthus caryophyllus]	BAF34340.1	16 872,1	1	5.68%	SITVNEAQSR	73.2	46.4	26.8	0	1	0	0	2	1 104,5649
46	cyclophilin [Phaseolus vulgaris]	CAA52414.1	18 141,5	1	8.14%	VFFDMTIGGQPAGR	56.4	45.7	10.7	0	1	0	0	2	1 511,7319
46	peroxidase [Spinacia oleracea]	CAA71493.1	33 435,5	1	4.85%	MGNISPLTGSSGEIR	88.6	45.8	42.8	0	2	0	0	2	1 534,7536
47	Os08g0382400 [Oryza sativa (japonica cultivar-group)]	NP_001061695.1	53 596,5	1	4.73%	ESELTPSANILDR	68.6	45.5	23.1	0	1	0	0	2	1 615,7928
47	Heat shock 70 kDa protein [Zea mays]	P11143.1	70 586,9	1	2.02%	ITPSYVGFDTTER	68.2	45.9	22.3	0	1	0	0	2	1 473,6862
47	Peroxiredoxin Q, chloroplast precursor (Thioredoxin reductase) [Sedum lineare]	Q9MB35.1	20 633,9	2	10.20%	HIDETLK	51	45.7	5.3	0	2	0	0	2	855,4578
47	Peroxiredoxin Q, chloroplast precursor (Thioredoxin reductase) [Sedum lineare]	Q9MB35.1	20 633,9	2	10.20%	LPFTLLSDEGNK	78.6	46.4	32.2	0	1	0	0	2	1 333,7005
47	CYP1 (putative cyclophilin_ABH_like) [Vigna radiata]	BAB82452.1	18 188,7	1	6.98%	IVFELFADTTTPR	74	46	28	0	1	0	0	2	1 408,7479
47	putative glycine-rich RNA-binding protein [Dianthus caryophyllus]	BAF34340.1	16 872,1	1	5.68%	SITVNEAQSR	54.7	46.4	8.3	0	1	0	0	2	1 104,5649
47	cyclophilin [Phaseolus vulgaris]	CAA52414.1	18 141,5	1	8.14%	VFFDMTIGGQPAGR	84.5	45.7	38.8	0	3	0	0	2	1 511,7319
47	poly(A) polymerase [Pisum sativum]	AAC50041.1	50 217,5	1	7.27%	ADGFVVQTGDPEGPAEGFIDPSTEK	61.3	44.1	17.2	0	0	1	0	2	2 563,1842
47	peroxidase [Spinacia oleracea]	CAA71493.1	33 435,5	1	4.85%	MGNISPLTGSSGEIR	83.3	45.8	37.5	0	2	0	0	2	1 534,7536
47	unnamed protein product [Vitis vinifera]	CAO14784.1	49 165,4	1	3.35%	ESELTPSANILDR	68.6	45.5	23.1	0	1	0	0	2	1 615,7928
47	HSP70 (heat shock protein 70) [Arabidopsis thaliana]	NP_187864.1	71 085,2	1	2.00%	ITPSYVAFTDSER	73.1	45.9	27.2	0	1	0	0	2	1 473,6861
47	unknown [Populus trichocarpa]	ABK95873.1	28 122,0	2	4.96%	FVESTASSFSVA	34.2	46.5	-12.3	0	1	0	0	2	1 231,5846
47	unknown [Populus trichocarpa]	ABK95873.1	28 122,0	2	4.96%	KFVESTASSFSVA	56.1	45.9	10.2	0	1	0	0	2	1 359,6794
47	ubiquitin [Arabidopsis thaliana]	ABH08753.1	59 877,8	1	1.69%	TLADYNIQK	57.4	46.4	11	0	14	0	0	2	1 065,5582
48	Os06g0133800 [Oryza sativa (japonica cultivar-group)]	NP_001056711.1	80 012,2	1	1.88%	LAQLPGTISIEGVEK	78.5	46	32.5	0	1	0	0	2	1 441,7904
48	peroxidase2 [Medicago sativa]	CAC38106.1	35 992,3	2	5.47%	FDGLVSR	41.9	47.7	-5.8	0	1	0	0	2	793,4209
48	peroxidase2 [Medicago sativa]	CAC38106.1	35 992,3	2	5.47%	IAINMDPTTPR	95.9	46.5	49.4	0	1	0	0	2	1 244,6311
48	acetyl esterase [Vigna radiata]	AH004762.1	5 540,9	1	25.90%	VPVGITFVENAVAK	98.3	46.2	52.1	0	1	0	0	2	1 443,8211
48	putative xyloglucan endotransglycosylase [Cucumis sativus]	ABK55722.1	33 812,4	1	4.71%	IIENGNLITLSLDK	135	45.6	89.4	0	1	0	0	2	1 542,8746
48	glycerophosphoryl diester phosphodiesterase family protein [Arabidopsis thaliana]	NP_196420.1	42 865,7	2	4.30%	FVETLKK	45.5	47.4	-1.9	0	1	0	0	2	864,5196
48	glycerophosphoryl diester phosphodiesterase family protein [Arabidopsis thaliana]	NP_196420.1	42 865,7	2	4.30%	VVGILPEIK	40.2	46.9	-6.7	0	1	0	0	2	1 017,5986
48	putative secretory protein [Oryza sativa (japonica cultivar-group)]	AAG13529.1	28 687,5	1	3.85%	WDQGYDVTAR	83.6	46.4	37.2	0	1	0	0	2	1 210,5494
48	pectinacetyl esterase precursor [Vigna radiata var. radiata]	CAA67728.1	43 804,9	3	9.27%	AVGDWYYDR	78.1	46.3	31.8	0	1	0	0	2	1 144,5063
48	pectinacetyl esterase precursor [Vigna radiata var. radiata]	CAA67728.1	43 804,9	3	9.27%	IEEFGYSQVVQTHGSAK	49.9	45.4	4.5	0	0	1	0	2	1 282,8975
48	pectinacetyl esterase precursor [Vigna radiata var. radiata]	CAA67728.1	43 804,9	3	9.27%	VFAAVVDDLLAK	108	46.6	61.4	0	1	0	0	2	1 260,7204
48	endo-1,4-beta-mannanase [Glycine max]	ABG88068.1	44 105,4	1	2.55%	LLLSLVNNWK	70.7	46.2	24.5	0	1	0	0	2	1 199,7153
48	At5g07030 [Arabidopsis thaliana]	ABG25087.1	48 676,8	2	4.62%	SSLYYVNSLVAIR	87.5	45.8	41.7	0	1	0	0	2	1 397,7791
48	At5g07030 [Arabidopsis thaliana]	ABG25087.1	48 676,8	2	4.62%	SVVPIASGR	46.8	46.1	0.7	0	1	0	0	2	885,5157
48	hypothetical protein [Vitis vinifera]	CAN77531.1	33 023,8	1	4.39%	TDWSQAPFTASYR	61.2	45.8	15.4	0	1	0	0	2	1 529,7025
48	putative pectin methyl esterase 3 [Linum usitatissimum]	AAG17110.1	69 430,1	1	1.90%	DITFQNTAGPSK	72.4	46.6	25.8	0	1	0	0	2	1 278,6333
48	Os02g0698000 [Oryza sativa (japonica cultivar-group)]	NP_001047825.1	44 848,2	3	8.19%	ANDFDLMYEQVK	74.8	46.1	28.7	0	1	0	0	2	1 488,6681
48	Os02g0698000 [Oryza sativa (japonica cultivar-group)]	NP_001047825.1	44 848,2	3	8.19%	GVTALDPR	41.1	46.1	-5	0	1	0	0	2	828,4581
48	Os02g0698000 [Oryza sativa (japonica cultivar-group)]	NP_001047825.1	44 848,2	3	8.19%	LTSVFGGAAEPPK	82.4	46.9	35.5	0	1	0	0	2	1 273,6794
48	peroxidase 5 precursor [Phaseolus vulgaris]	AAD37430.1	35 496,7	1	2.69%	GFDVVDSIK	53.1	46.7	6.4	0	1	0	0	2	979,5102
49	peroxidase [Sesamum indicum]	ABB89209.1	35 838,4	2	9.09%	DHPDNLSLAGDGFDTVIK	58.9	45.3	13.6	0	0	1	0	2	1 913,9248
49	peroxidase [Sesamum indicum]	ABB89209.1	35 838,4	2	9.09%	VSCADILALATR	72.4	47.1	25.3	0	1	0	0	2	1 289,6889
49	acetyl esterase [Vigna radiata]	AH004762.1	5 540,9	1	25.90%	VPVGITFVENAVAK	97	46.2	50.8	0	1	0	0	2	1 443,8211
49	pectinacetyl esterase precursor [Vigna radiata var. radiata]	CAA67728.1	43 804,9	4	16.80%	AVGDWYYDR	64.9	46.3	18.6	0	1	0	0	2	1 144,5063
49	pectinacetyl esterase precursor [Vigna radiata var. radiata]	CAA67728.1	43 804,9	4	16.80%	NAQNAIISGCSAGGLAAILNCDR	60.5	44.4	16.1	0	0	1	0	2	2 346,1297
49	pectinacetyl esterase precursor [Vigna radiata var. radiata]	CAA67728.1	43 804,9	4	16.80%	VFAAVVDDLLAK	104	46.6	57.4	0	1	0	0	2	1 260,7204
49	pectinacetyl esterase precursor [Vigna radiata var. radiata]	CAA67728.1	43 804,9	4	16.80%	YPCDGSSTGDVEAVDPATNLHFR	65	44	21	0	0	0	1	2	2 558,1258
49	hypothetical protein [Vitis vinifera]	CAN77531.1	33 023,8	1	4.39%	TDWSQAPFTASYR	81.4	45.8	35.6	0	1	0	0	2	1 529,7025
49	pectin acetyl esterase [Eucalyptus globulus subsp. globulus]	ABG34280.1	38 829,9	2	6.29%	AEENPDDFNWNR	78.7	45.8	32.9	0	1	0	0	2	1 538,6663
49	pectin acetyl esterase [Eucalyptus globulus subsp. globulus]	ABG34280.1	38 829,9	2	6.29%	AIDCPCYCDK	56.4	46.5	9.9	0	1	0	0	2	1 238,5189
49	Fructose-bisphosphate aldolase, chloroplast precursor [Oryza sativa (japonica cultivar-group)]	ABA91632.2	42 913,5	1	3.26%	LASIGLENTEANR	82.7	46	36.7	0	1	0	0	2	1 387,7181
49	CYP1 (putative cyclophilin_ABH_like) [Vigna radiata]	BAB82452.1	18 188,7	1	6.98%	IVFELFADTTTPR	55.2	46	9.2	0	1	0	0	2	1 408,7479
49	unknown [Populus trichocarpa]	ABK94923.1	39 849,5	3	11.00%	LGNEASIK	49.6	47.1	2.5	0	1	0	0	2	831,4577
49	unknown [Populus trichocarpa]	ABK94923.1	39 849,5	3	11.00%	QGDMLLVPEGAYAVR	57.2	45.3	11.9	0	1	0	0	2	1 733,8897
49	unknown [Populus trichocarpa]	ABK94923.1	39 849,5	3	11.00%	SDDFSSLCGPVDDVK	96.4	45.4	51	0	1	0	0	2	1 739,7799

49	Polygalacturonase inhibitor 2 precursor [<i>Phaseolus vulgaris</i>]	P58822.1	37 086,3	1	4.09%	JSGAIPDSYGSFSK	53.2	45.8	7.4	0	1	0	0	2	1 428,7010
49	peroxidase2 [<i>Medicago sativa</i>]	CAC38106.1	35 992,3	2	9.12%	FDGLVSR	49.9	47.7	2.2	0	1	0	0	2	793.4209
49	peroxidase2 [<i>Medicago sativa</i>]	CAC38106.1	35 992,3	2	9.12%	IAINMDPTTPR	95.7	46.5	49.2	0	1	0	0	2	1 244,6311
49	peroxidase2 [<i>Medicago sativa</i>]	CAC38106.1	35 992,3	2	9.12%	VSCADILALATR	72.4	47.1	25.3	0	1	0	0	2	1 289,6889
49	unnamed protein product [<i>Vitis vinifera</i>]	CAO17011.1	42 507,9	1	2.04%	VINNLDER	56.6	46.7	9.9	0	1	0	0	2	972.5114
49	unnamed protein product [<i>Vitis vinifera</i>]	CAO62638.1	35 692,7	1	1.93%	LINLPK	52.1	45.2	6.9	0	1	0	0	2	697.4614
49	24 kDa seed coat protein [<i>Glycine max</i>]	AAS59524.1	24 551,8	1	5.94%	FNVIHDVGGANNVK	55.7	45.8	9.9	0	0	1	0	2	1 426,7441
49	unnamed protein product (putative Serine carboxypeptidase) [<i>Vitis vinifera</i>]	CAO68876.1	57 192,0	1	2.96%	NLEVGIPDLEEDGIK	58	45.3	12.7	0	1	0	0	2	1 624,8801
50	unnamed protein product [<i>Vitis vinifera</i>]	CAO15661.1	27 624,2	1	5.93%	MADLPTVLVTGAGGR	66.8	49.5	17.3	0	1	0	0	2	1 515,7843
50	unknown [<i>Populus trichocarpa</i>]	ABK95110.1	51 395,0	1	3.44%	AVANQPVSVAIEGGGR	58.3	45.7	12.6	0	1	0	0	2	1 524,8134
51	putative RuBisCo activase protein [<i>Zantedeschia hybrid cultivar</i>]	AAT12492.1	27 671,2	1	7.79%	IPVIVTGNDFSTLYAPLIR	66.4	44.6	21.8	0	0	1	0	2	2 089,1703
51	peroxidase [<i>Spinacia oleracea</i>]	CAA71493.1	33 435,5	1	4.85%	MGNISPLTGSSGEIR	70.3	45.8	24.5	0	1	0	0	2	1 534,7536
51	putative rubisco activase [<i>Vigna unguiculata</i>]	CAO02534.1	25 409,2	2	11.40%	FYWAPTR	32.1	45.5	-13.4	0	1	0	0	2	940.4681
51	putative rubisco activase [<i>Vigna unguiculata</i>]	CAO02534.1	25 409,2	2	11.40%	VPIIVTGNDFSTLYAPLIR	66.4	44.6	21.8	0	0	1	0	2	2 089,1703
51	unnamed protein product [<i>Vitis vinifera</i>]	CAO14784.1	49 165,4	1	3.35%	ESELTPSNANILDGR	68	45.5	22.5	0	1	0	0	2	1 615,7928
51	ATAMI1, amidase [<i>Arabidopsis thaliana</i>]	NP_563831.1	45 038,6	1	3.53%	LVDFSIGTDTGGSVR	114	45.8	68.2	0	1	0	0	2	1 523,7707
51	Peroxioredoxin Q, chloroplast precursor (Thioredoxin reductase) [<i>Sedum lineare</i>]	Q9MB35.1	20 633,9	2	7.53%	ETYVLDK	31.7	45.8	-14.1	0	1	0	0	2	867.4465
51	Peroxioredoxin Q, chloroplast precursor (Thioredoxin reductase) [<i>Sedum lineare</i>]	Q9MB35.1	20 633,9	2	7.53%	HIDETLK	54.7	45.7	9	0	1	0	0	2	855.4578

^a Numbers correspond to the numbers given in Fig. 3

^b Identities are based on sequence comparisons using the NCBI green plants protein database

^c Accession numbers are based on sequence comparisons using the NCBI green plants protein database

^d Molecular weights (MW) are based on sequence comparisons using the NCBI green plants protein database

^e Protein sequence coverage obtained with the peptides identified by mass spectrometry

		C1	
		1	60
FBP 1	(1)	-----VVGVVLGALPFSSDAQLDPSFYRNTCPVSHSIVREV	
P 49 (A.t.)	(1)	-----MARLTSFLLLSLFCVPLCLCDKSYGGKLFPGYAHSCPQVNEIVRSV	
PPOD	(1)	-----MGSAKFFVTLICIVPLASSFCSAQLSATFYASTCPNLQITVRNA	
VvPOD	(1)	-----MASHHSSSSVFTTFKLCFCLLLSFIGMASAQLTTNFYAKTCPNALSIIKSA	
VaPOD	(1)	MASISSNKNAIFSFLLLSIILSVSVIKVCEAQRPTVRGLSYTFYSKTCPTLKSIVRTE	
P 45 (A.t.)	(1)	-----MEKNTSQITIFSNFFLLLSLSSCVSAQLRTGFYQNSCPNVETIVRNA	
SoPOD	(1)	-----IILAYLACLNSAQLSSKHAYASSCPNLEKIVRKT	
SiPOD	(1)	-----MGQSSFLMTLFTLSLGVIVFSGSVSAQLKQNYANICPDVENIVRQA	
MsPOD	(1)	-----MGR-YNVILVWSLALTCLIPYTTFAQLSPNHYANICPNVQSVIRSA	
VuPOD		-----	
I Hdc2 C3 *****			
		61	120
FBP 1	(37)	IRNVSKSDPRMLASLIRLHFHDFVQGCDA SILLNNTDTIVSEQEALPNIN-SIRGLD VV	
P 49 (A.t.)	(50)	VAKAVARETRMAASLLRLHFHDFVQGCDSLLLDSSGRVATEKNSNPNSK-SARGFDV V	
PPOD	(45)	MTGAVNGQPRLAASILRLHFHDFVNGCDGSILLDDTATFTGEKNANPNRN-SARGFEV I	
VvPOD	(53)	VNSAVKSEARMGASLLRLHFHDFG--CDASILLDDTSNFTGEKTAGPNAN-SVRGYEV V	
VaPOD	(61)	LKKVFQSDIAQAAGLLRLHFHDFVQGCDSVLLDGSASGPEKDAPPNLTLEAEAFRII	
P 45 (A.t.)	(47)	VRQKFQQTFTVPATLRLHFHDFVRGCDASIMIASP----SERDHPDDMSLAGDGFDT V	
SoPOD	(34)	MKQAVQKEQRMGASILRLHFHDFVNGCDASLLDDTSTFTGEKTAISNRNNSVRGFEV I	
SiPOD	(48)	VTAKFKQTFVTVPATLRLYFHDFVSGCDASVIIASTPGNTAEKDHPDNL SLAGDGFDT V	
MsPOD	(47)	VQKKFQQTFTVPATLRLHFHDFVQGCDA SVLVASSGNNKA EKDPENLSLAGDGFDT V	
VuPOD		-----MGASILR-----DHPDNLSLAGDGFDT V	
			GYEVV
			GFEVI
C4 C5 II *****			
		121	180
FBP 1	(96)	NQIKTAVEN--ACPGV VSCADILTLAAEISSVLAQCPDWK VPLGRKDSL-TANRTLANQN	
P 49 (A.t.)	(109)	DQIKAELEK--QCPGT VSCADVTLAARDSSVLTGGPSWV VPLGRRDSR-SASLSQSNNN	
PPOD	(104)	DTIKTRVEA--ACNAT VSCADILALAARDGVVLLGGPSWTVPLGRRDAR-TASQSAANSQ	
VvPOD	(110)	DTIKSQLEA--SCPGV VSCADILAVAARD SVVALRGP SWVPLGRRDST-TASLSAANSN	
VaPOD	(121)	ERIRGLLEK--SCGRV VSCDITALAARDAVFLSGGPDYEIPLGRRDGLTFASRQVTLDN	
P 45 (A.t.)	(103)	VKAKQAVDSNPNCRNK VSCADILALATREVVVLTGGPSYPVELGRRDGR-ISTKASVQSQ	
SoPOD	(94)	DSIKTNVEA--SCKAT VSCADILALAARDGVFLLGGPSWK VPLGRRDAR-TASLTAATNN	
SiPOD	(108)	IKAKAAVDVPRCRNK VSCADILALATRDVINLAGGPSYPVELGRLDGL-KSTAASVNGN	
MsPOD	(107)	IKAKAALDAVPQCRNK VSCADILALATRDVINLAGGPSYTVELGRFDGL-VSRSSDVNGR	
VuPOD		IK-----VSCADILALATR-----FDGL-VSR-----	
		DTIK	
		DTIK	
III Hp C6 *****			
		181	240
FBP 1	(153)	LPAPFFNLTLKAAFAVQGLNTTDLVALSGAHTFGRAQCSTFVNRLYNFNTGNPDPTLN	
P 49 (A.t.)	(166)	IPAPNNTFQTI LSKFNROGLDITDLVALSGSHTIGFSRCTSFRQRLYNQSGNGSPDMTLE	
PPOD	(161)	IPSPASSLATLISMFSAGLSAGDMTALS GHTIGFARCTTFRNR IYN-----DTNID	
VvPOD	(167)	IPAPTLNLSGLISAF TNKGFNAREMVALSGSHTIGQARCTTFRTRIYN-----EANID	
VaPOD	(179)	LPPSSNTTILNLSLATKNLDPTDVVSLSGHTIGLSHCSEFNRLYP-----TQDPVMD	
P 45 (A.t.)	(162)	LPQPEFNLNQLNGMF SRHGLSQTDMI ALSGAHTIGFAHCGKMSKRIYNFSPTRIDPSIN	
SoPOD	(151)	LPPASSLSNLTTLENKGLSPKDMTALS GHTIGLARCVSFRHHIYN-----DTDID	
SiPOD	(167)	LPQPTFNLDQLNKMFASRGLSQADMIALSAGHTLGF SHCSKFSNR IYNFSRQNPVDPTLN	
MsPOD	(166)	LPQPSFNLNQLNTLFANNGLTQTDMI ALSGAHTSGF SHCDRFSNR IQ----T-PVDPTLN	
VuPOD		-----	
C7			
		241	300
FBP 1	(213)	TTYLQTLRAVCPNGG--GGTNLTNFDPTT PDKFDKNYYSNLQVHKGLLQSDQELFSTIGA	
P 49 (A.t.)	(226)	QSFAANLRQRCPKSG--GDQILSVLDII SAASFDNSYFKNLIENKGLLNSDQVLFSSNEK	
PPOD	(214)	ASFATRRRASC PASG--GDATLAPL DGT-QTRFDNYYTNLVARRGLLHSDQELFNGG SQ	
VvPOD	(220)	ASFKTSLQANCPSSG--GDNTLSPLDTQTPTTFDNAYYTNLVNKKGLLHSDQQLFNGG ST	
VaPOD	(234)	KTFGKNLRLTCPTNT--TDNTTVLDIRS PNTFDNKYYVDLMNRQGLFTSDQDLYTDKRT	
P 45 (A.t.)	(222)	RGYVVQLKQMCPIGVD--VRIAINMDP TSPRTFDNAYFKNLQQGKGLFTSDQILFTDQRS	
SoPOD	(204)	ANFEATRKNVNCPLSNNTGNTN LAPLDLQSP TKFDNSYKNI IAKRGLLHSDQELYNGG SQ	
SiPOD	(227)	KQYATQLQGMCPINVD--PRIAIDMDP TTPRKFDNAYFKNLVQGKGLFTSDQVLF TDTRS	
MsPOD	(221)	KQYAAQLQGMCPRNVD--PRIAIDMDP TTPRTFDNVYKNIQQGKGLFTSDQILFTDTRS	
VuPOD		-----IAINMDPTTPR-----GLFTSDQILFTDQR-	
		IAIDMDPTTPR	

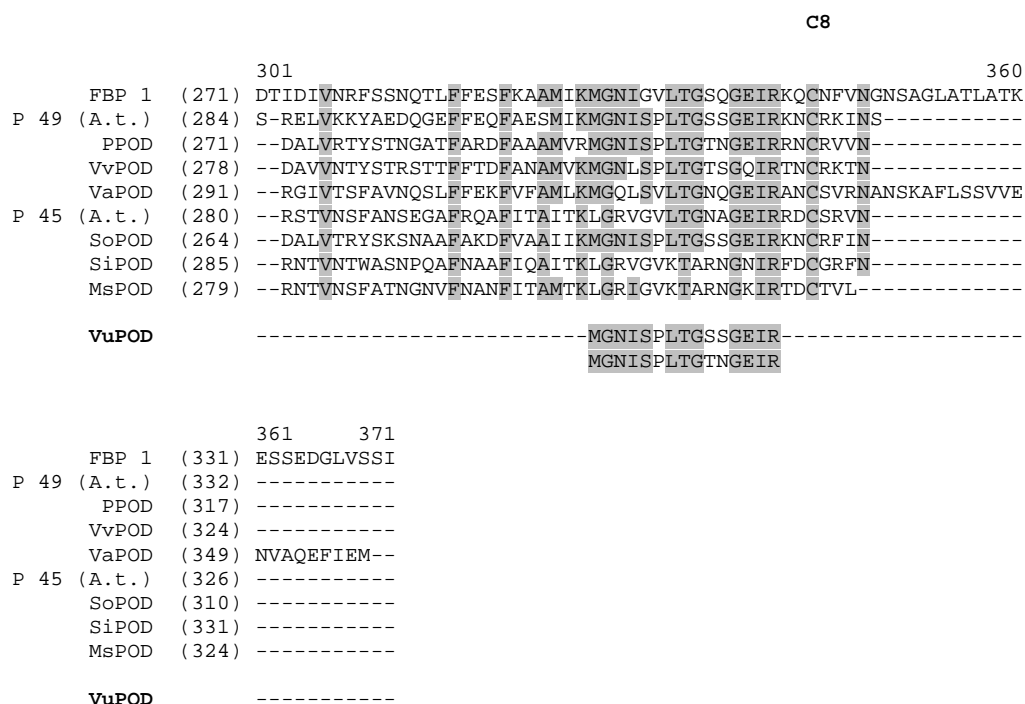


Fig. S1: Alignment of determined and deduced amino acid (aa) sequences of peroxidases of various plant species and all eleven nano LC-MS/MS-identified peroxidase peptide sequences from cowpea. Amino acid positions conserved in at least 50% of the sequences are underlayed in gray. Stars (*) indicate the conserved distal heme-binding domain (I), the central conserved domain of unknown function (II), and the proximal heme binding domain. The eight cysteines (C1-C8) and the distal (Hd) and proximal (Hp) histidines are indicated, too. Abbreviations: FBP1 French Bean Peroxidase 1 (Acc no.: AF149277), P49 (A.t.) POD isoenzyme 49 from *Arabidopsis thaliana* (Acc. no. O23237), PPOD from *Populus ssp.*(Acc. no.: AAX53172), VvPOD from *Vitis vinifera* (Acc. no.: CAO48839), VaPOD from *Vigna angularis* (Acc. no.: BAA01950), P45 (A.t.) POD isoenzyme 45 from *Arabidopsis thaliana* (Acc. no. Q96522), SoPOD from *Spinacia oleracea* (Acc. no.: CAA71493), SiPOD from *Sesamum indicum* (Acc. no.: ABB89209), MsPOD from *Medicago sativa* (Acc. no.: CAC38106), VuPOD POD peptide sequences of *Vigna unguiculata* (this study).

Supplementary material for Chapter IV.

Characterization of different leaf apoplastic proteome fractions in *Vigna unguiculata* in response to short term toxic manganese supply

Hendrik Führs¹, Mareike Vorholt¹, Sébastien Gallien², Dimitri Heintz³, Alain Van Dorsselaer², Hans-Peter Braun⁴ & Walter J. Horst¹

to be submitted

¹ Institute of Plant Nutrition, Faculty of Natural Sciences, Leibniz University Hannover, Herrenhäuser Str. 2, 30419 Hannover, Germany

² Laboratoire de Spectrométrie de Masse Bio-Organique, IPHC-DSA, ULP, CNRS, UMR7178 ; 25 rue Becquerel, 67 087 Strasbourg, France

³ Institut de Biologie Moléculaire des Plantes (IBMP) CNRS-UPR2357,ULP, 67083 Strasbourg, France

⁴ Institute of Plant Genetics, Faculty of Natural Sciences, Leibniz University Hannover, Herrenhäuser Str. 2, 30419 Hannover, Germany

Table S1: Peptide sequences of water-soluble and ionically-bound apoplastic cowpea proteins affected by 1 d of excess Mn.

Spot No. ^a	Acc.No. ^b	Identity ^c	Organism	Peptide sequence ^d	Coverage ^e
1	ABB89209/ Q96522 ^f	Peroxidase 45 precursor	<i>A. thaliana</i> / <i>Sesamum indicum</i>	MEKNTSQTIFSNFFLLLLLLSSCVSAQLRTGFYQNSCPNVETIVRNAVRQKFQQTFTVTA TLRLFFHDCFVRGCDASIMIASPSEDRHDDMSLAGDGFDTVVKAKQAVDSNPNCRNKVS CADILALATREVVVLTGGPSYPVELGRRDGRISTKASVQSQLPQPEFNLNLQNGMFSRHG LSQTDMIALSGAHTIGFAHCGKMSKRIYNFSPTTRIDPSINRGYVVQLKQMCPIGVDVRI AINMDPTSPRTFDNAYFKNLQQGKGLFTSDQILFTDQSRSTVNSFANSEGAFRQAFITA ITKLGRVGVLTGNAGEIRRDCSRVN	8% / 3,64%
	CAD11991	RubisCO small subunit	<i>Coffea arabica</i>	MASSMISSAAVATTTTRASPAQASMVAPFNGLKAASSFPISKKSVDITSLATNGGRVQCMQ VWPPRGLKKYETLSYLPDLTDEQLLKEIDYLIRSGWVPCLEFELEKGFVYREYHRSPGY DGRYWTMWKLPYMGCTDATQVLNEVGECLKEYPNCWVRIIGFDNVRQVQCISFIAAKPKG F	12.70%
2	ABB89209/ Q96522 ^f	Peroxidase 45 precursor	<i>A. thaliana</i> / <i>Sesamum indicum</i>	MEKNTSQTIFSNFFLLLLLLSSCVSAQLRTGFYQNSCPNVETIVRNAVRQKFQQTFTVTA TLRLFFHDCFVRGCDASIMIASPSEDRHDDMSLAGDGFDTVVKAKQAVDSNPNCRNKVS CADILALATREVVVLTGGPSYPVELGRRDGRISTKASVQSQLPQPEFNLNLQNGMFSRHG LSQTDMIALSGAHTIGFAHCGKMSKRIYNFSPTTRIDPSINRGYVVQLKQMCPIGVDVRI AINMDPTSPRTFDNAYFKNLQQGKGLFTSDQILFTDQSRSTVNSFANSEGAFRQAFITA ITKLGRVGVLTGNAGEIRRDCSRVN	8% / 3.64%
	CAD11991	RubisCO small subunit	<i>Coffea arabica</i>	MASSMISSAAVATTTTRASPAQASMVAPFNGLKAASSFPISKKSVDITSLATNGGRVQCMQ VWPPRGLKKYETLSYLPDLTDEQLLKEIDYLIRSGWVPCLEFELEKGFVYREYHRSPGY DGRYWTMWKLPYMGCTDATQVLNEVGECLKEYPNCWVRIIGFDNVRQVQCISFIAAKPKG F	8.84%
3	XP_001755457	predicted protein	<i>Physcomitrella</i> <i>patens</i> subsp. <i>patens</i>	RYALACALLASLNSTLLGYDIGVIAGAVLFIQEDLGISEFQEELLVGSLNLVSLIGAACA GRIADAVGRWMTMAIALFFLVGAGIMGVAPHFSLLMIGRLLLEGIGVGFALMIAPVYAE VAPASSRGLSLVSLPEIFINIGILLGYMVSYVFSGLPSNVNWRMLLGVGLPALVAVGL LMPESPRWLVMQNRKEAEIVLFKTSNDEAEANVRLQEIMDAAGIVSDGSGGTRSSLNSE GGVWKELLWPTSPVRRMLIVALGVQFFQQASGIDATVYSPVVFNHAGISGKSGVLLAT IAVGLTKTLFILVATIWLDRLRRLPLLLTSSIGMTVSLVLAIGFLFLNITPTDDIPAAP SDTSGPTVFAVLAILLSICSYVAFFSVGFGPIVWVLTSEIFPLRLRAQAMGLGIVNRLAS ATVALTFLSMARAMTIAGTFFLFSVMAFLSAIFVYIFTPETKGRSLEEIAKFFE	1.48%
	BAG09557	acetylcholinesterase	<i>Macroptilium</i> <i>atropurpureum</i>	MGSGAVFVGFVFLSCVVFVKVEPKTSPTCTFPALYNFGDSNSDTGGISASFVPIPAPYG EGFFHKPSGRDCDGRLLIDFIAEKLNLPLYLSAYLNSLGTNYRHGANFATGGSTIRRQNET IFQYGLSPFSLDIQIVQFNQFKARTKQLYEEAKTSFERSRLPVPEFAKALYTFDIGND LSVGFRKMNFDQIRESMPIILNQLANAVKNIYQQGGRSFWIHNTSPFGCMPVQLFYKHNI PSGYLDQYGCVKDQEMATEFNKQMKDRIKLRTELPEAAITYVDVYAAKYALISNTKTE GFVDPMKICCGYHVNDTHIWCNGLGSADGKDVFGSACENPSQYISWDSVHYAEANHWVA NRILNGSFTDPPTPIQACYKH	5.24%
	CAA03733	unnamed protein product	<i>Senna occidentalis</i>	MEKMMWAKVVLCLFVVLNASNCSGRLLNTIGNDHNNIHGRLLGNLGNTPPMGWNSWN HFQCDINEEMVRETADAMVSTGLASLGYEVNLLDCCWAEELNRDSKGNMVPASAKFP ALADYVHSGKGLKFGVYSDAGNQTCSKAMPGLGHEDQGAKTASWGVDFLKYDNCNNNDI SPRNYPKMSEALANSGRAIFFSMCEWGESDPALWAKSVGNSWRRTGDIEDKWEASMA IAQNDKWASVYAGPGGWNDDPDMLEVGNGGMTTEYRSHFSIWALAKAPLLIGCDVRSMDGAT	8.37%

	ABC55266	alpha-galactosidase 1	<i>Cucumis sativus</i>	YGLLSNKEVIAVNQDSLGVQKVKSDAGLEVWAGPLSDNRVAVVLWNRSSSKATVTASW SDIGLEKGGVVTAKDLWEHTTKASVSGQISADIDSHACKMYVLTTPN MECRSYCKAPAVVVVFLAFSLVLMLETTVSATSRMTEIASDGDLLRRNLLANGLGVTTPMG WNSWNHFACNINEKMIRETADALVSTGLSKLGYEYVNIDDCWAEIARDDKGNLVKPNSTF PSGMKALADYVHAKGLKIGIYSDAGYFTCSKTMPSGLGHEEQDAKTFAAWIDYLYKNDNC NNGNIKPTIRYPVMTALMKAGRP IFLSLCEWGDHLHPALWGDKLGNSWRRTTNDINDSWES MISRADLNEIYADYARPGGWNDPDMLEVGNGGMTKDEYIVHFSLWAI SKAPLLLGCDLRN LTKETKAIVTNTEVIAVNQDPLGVQAKKVRSEGDLEVWAGPLSGYRVAVVLLNRGPWRNA ISAQWDDIGIPPNSNVEARDLWEHTTLKTTFFVANLTATVD SHACKLYILKPI S	8.47%
	CAF34023	alpha-galactosidase 1	<i>Pisum sativum</i>	MGIKIEMMVVLTLLLICVTSSSLANNKNEEHLRRNLLANGLARTPPMGWNSWNHFA CQIDEKMIRETADALISTGLSKLGYTYVNIDDCWAE LNRRDDKGNLVAKNSTFPSPGIKALA DYVHSGKGLKGIYSDAGYFTCSKQMPGSLGHEFQDAKTFASWGIDYLYKNDNCFNGGSKPT KRYPVMTALVKAGRP IFFSLCEWGDHLHPALWGAKEVGNWRRTTGDISTWESMISKADTN EYVYAE LARPGGWNDPDMLEVGNGGMTKSEYIVHFSLWAI SKAPLLLGCDVRNVSQDMEI ISNKEVIAVNQDSLGVQAKKVRMEGDLEI WAGPLSGYRVAVVLLNKGAQRMAMTANWDDI GIPPKSVVEARDLWEHKTLEKHFVDKLSVTVESHACKMYVLPVA	22.00%
	CAN75822	hypothetical protein	<i>Vitis vinifera</i>	MGWNSWNHFNCKIDEKTIKETADALVATGLVKLGYEYVNIDDCWAEINRDEKGTLVAKKS TFPSGIKALADYVHSGKGLKGIYSDAGYFTCSKTMPSGLGHEEKDAKTFASWGIDYLYK NCNNDGSRPTDRYPVMTALMKAGRP IFFSLCEWGDHMPALWGSKVGNSWRRTTNDIADTW DSMMSRADMNDVYAQYARPGGWNDPDMLEVGNGGMTNDEYIVHFSI WAI SKAPLLIGCDV RNTTKETLDIIGNKEVIAVNQDPLGVQAKKVRSEGDQEI WAGPLSDYRVALLVNRGPWR YSVTANWDDIGLPXGTVVEARDLWEHKTLEKRFVGSLSXATMDSHACKMYILKPI S	14.50%
4	CAA03733	unnamed protein product	<i>Senna occidentalis</i>	MEKMMWAKVVLCLFVVLNANSCSRLNLTIGNDHNNIHGRLLNGNGLNTPPMGWNSWN HFQCDINEEMVRETADAMVSTGLASLGYEYVNLDDCWAE LNRRDSKGNMVP SAKFPSPGK ALADYVHSGKGLKFGVYSDAGNQTCSKAMPGSLGHEDQGAKTFASWGVDFLKYDNCNNDI SPRNRYPKMSEALANSGRAIFFSMCEWGEDPALWAKSVGNWRRTTGDIEDKWEASIA DQNDKWASYAGPGGWNDPDMLEVGNGGMTTEEYRSHFSI WALAKAPLLIGCDVRSMGAT YGLLSNKEVIAVNQDSLGVQKVKSDAGLEVWAGPLSDNRVAVVLWNRSSSKATVTASW SDIGLEKGGVVTAKDLWEHTTKASVSGQISADIDSHACKMYVLTTPN	3.69%
	ABK95990	unknown	<i>Populus trichocarpa</i>	MEICYRAALILAFALLDVGCQADALVPAIITFGDSAVDVGNNDYLPTIFKANYPPYGR DFVDQKPTGRFCNGKLATDITAETLGFKSYAPAYLSPDASGKNLLIGSNFASAASGYDEK AAALNHAIPLSQQLEYFKEYQGLAKVAGSKSASIKGALYILSAGSSDFLQNYVNPYL NKIYTVDQYGSYLVGSFTSFVKTLYGLGGRKLGVTSLPPLGCLPAARTIFGYHENGCVSR INTDAQQFNKINSAAATSLQKQLPGLKIVIFDIFQPLYDLVKSPSENGFQEARGCCGTG TVETTSLLCNPKSPGTCPNATEYVFWDSVHPSQAANQVLADALILQGISLIG	3.69%
	AAR92038	polygalacturonase-inhibiting protein	<i>Phaseolus vulgaris</i>	MTQFNIPVTMSSSLSIILVILVSLRALTALSEL CNPQDKQALLQIKKDLGNPTTSSWLPTT DCCNRTWLGVLCDTDTQTYRVNNDLDSGHNLPKPYPISSLANLPYLNFLYIGGINNLVG PIPPAI AKTLQLHYLYITHTNVSGAIPDFLSQIKTLVTLDFSYNALSGLTLPSSISLPLN GGITFDGNRISGAIPDSYGSF SKLFTAMTISRNLTKI PPTFANLNLA FVDLSRNMLEG DASVLFGSDKNTKKIHLAKNSLAFDLGKVLGSKNLNGLDLRNNRIYGTLPQGLAQLKFLQ SLNVSFNNLCGEIPQGGNLRKFDVSSYANNKCLCGSPLP SCT	7.02%
	BAC22609	41 kDa chloroplast nucleotide DNA-binding	<i>Nicotiana sylvestris</i>	MEHSLMATRSYFLLFSSTFLLILLSFPVEKSHALEAKETIESHFHTLQLTSLLPSSSCN TATKGKRRGASLEVVRQGPCTQLNQKGAAPTLEILAHDAQRVDSIQARVTDQSYDLF	4.58%

	NP_001062185	protein Os08g0505900	<i>Oryza sativa</i>	<p>KKKDKKSSNKKKSVDKSKANLPAQSGPLPLGTGNYIVNVGLGTPKKDLSLIFDFTGSDLTWT QCQPCVKSCYAQQQPIFDPSASKTYSNISCTSTACSGLKSATGNSPGCSSSSNCVYGIQYG DSSFTVGGFAKDTLTLTQNDVDFDGMFGCGQNNRGLFGKTAGLIGLGRDPLSIVQQTAKG FGKYFSYCLPTSRGSHGLTFGNGVVKTSKAVKNGITTFPFASQGGATFYFIDVLGISV GKGALSI SPMLFQNA GTIIDSGTVITRLPSTVYGLKSTFKQFMSKYPTAPALSLLDTCY DLSNYTISISPKISFNFNANVDLEPNGLITNGASQVCLAFAGNGDDDTIGIFGNIQQ QTLEVVYDVAGGQLGFGYKGC</p> <p>MASSPAPSPAAPPLLLAALAVVASASAAACSAGDRDALLAIRAALSEAHLGVFSSWT GTDCCTSWYGVSCDPTTGRVADLTLRGEADDPVMAPAGRPASGVMSGYISDAVCRLGRLS SLILADWKQISGPIPPCVATALPYLRILELPGNRLTGEIPRSIGLSRLTVLNLADNLIA GEIPSSITSLASLKHLDLTNNQLTGGIPDDVGDLTMLSRALLGRNKLTGAIPTSVGSLTR LADDLAENGLTGGIPDSLGGAHVLTSLYLGGNRVSGRIPASLLQNKGLGILNLSRNAVE GAIPDVFTAESYFMVLDLSRNRLTGAVPRSLSAAYVGHLDLSHNRLCGSIPAGPPFDHL DAASFASNSCLCGGPLGKCT</p>	2.63%
	CAF34023	alpha-galactosidase 1	<i>Pisum sativum</i>	<p>MGKIEEMVVLVTLILLICVTSSSLANNKNEEHLRRNLLANGLARTPPMGWNSWNHFA CQIDEKMIRETADALISTGLSKLGYTYVNIIDDCWAELENRDDKGNLVAKNSTFPSPGKAL DYVHSGKGLKGIYSDAGYFTCSKQMPGSLGHEFQDAKTFASWGDYLYKYNCFNGGSKPT KRYPVMTALVKAGRP IFFSLCEWGDHPALWGAKVGNWRRTTGDISDTWESMISKADTN EVYAEELARPGGWNDPDMLEVGNNGMTKSEYIVHFSLWAI SKAPLLGCDVRNVSKDTMEI ISNKEVIAVNQDSLGVQAKKVRMEGDLEIWAGPLSGYRVAVVLLNKGAQRMAMTANWDDI GIPKSVVEARDLWEHKTLEKHFVDKLSVTVESHACKMYVLKPVA</p>	4.20%
5	ABB89209	peroxidase	<i>Sesamum indicum</i>	<p>MGQSSFLMTLFTLSLGVIVFSGSVSAQLKQNYANICPDVENIVRQAVTAKFKQTFVTVP ATLRLYFHDCFVSGCDASV I IASTPGNTAEKDHPDNL SLAGDGFDTVIKAKAAVDVPRC RNKVSCADILALATR DVINLAGGPSYPVELGRLDGLKSTAA SVNGNLPQPTFNLDQLNKM FASRGLSQADMIALSAGHTLGF SHCSKFSNRIYNF SRQNPVDP TLNKQYATQLQGMCPIN VDPR I AIDMDPTTPRKFDNAYFKNLVQGGKGLFTSDQVLF TDTRSRTVNTWASNPAFNA AFIQAITKLRGVVKTARNGNIRFDCGRFN</p>	16.40%
	AAZ23955	GDSL-lipase 1	<i>Capsicum anuum</i>	<p>MGSEMRGWILVVQLVILGFMFSFYGANAAQQVPCYFIFGDSLVDNGNNNI QSLARANYLPY GIDFPGGPTGRFSNGKTTVDVIAEQLGFNNIPPYASARGRDLRGNVYASAAAGIREETG RQLGARIPFSGQVNNYRNTVQQVVQILGNENAAADYLKCKCIYSIGLSNDYLNMYFMPMY YSTRQFTPEQYANVLIQQYTQQLRILYNNGARKFALIGVQIGCSPNALAQNSPDGRTC VQRINVANQIFNNKALKALVDNFNGNAPDAKFIYIDAYGIFQDLIENPSAFGFRVTNAGCC GVGRNNGQITCLPFQRPCPNRNEYLFWDAFHPTAANIIVGRRSYRAQRSSDAYPFDISR LAQ</p>	13.20%
	CAC38106	peroxidase 2	<i>Medicago sativa</i>	<p>MGRYNVILVWSLALTLCLIPYTTFAQLSPNHYANICPNVQSI VRSAVQKFKQTFVTVPA TLRLFFHDCFVQGCDA SVLVASSGNNAEKDHPENLSLAGDGFDTVIKAKAALD VAPQCR NKVSCADILALATR DVINLAGGPSYTVELGRFDGLVSRSDVNGRLLPQPSFNLNQLNTLF ANNGLTQTDMIALS GAHTSGFSHCDRFSNRIQTPVDPTLNKQYAAQLQGMCPRNVDPRIA INMDPTTPRTFDNVYKNLQGGKGLFTSDQILFTDTRSRTVNSFATNGNVFNANFITAM TKLGRIGVKTARNKIRTDCTVL</p>	13.10%
	CAO71984	unnamed protein product	<i>Vitis vinifera</i>	<p>MGRFLLAIAMWSLSLVCVFPDTASAQLKQNYANICPNVENIVRGVVNTKFKQTFVTV PATLRLFFHDCFVQGCDA SVIISSTGSNTAEKDHPDNL SLAGDGFDTVIKAKAEVDKNPT CRNKVSCADILTMATR DVIALSGGPSYAVELGRLDGLSSTASVNGKLPQPTFNLDKLS LFAAKGLSQDMIALSAAHTLGF SHCSKFSANRIYNF SRENVPDPTLDKTYAAQLQSMCPK</p>	13.30%

	ABK94318	unknown	<i>Populus trichocarpa</i>	NVDPR IAIDMDPTTPKKFDNVYYQNLQQGKGLFTSDEVLF TDSRSKPTVNTWASSSTAFQ TAFVQAITKLG RVGVK TGNKGNIRDCSVFN MERSFSFKMMIDKALHPLVASLFFVIWFGGSLPYAYAQLTPTFYDGTCPNVSTIIRGVLA QALQTDPRIGASLIRLHFHDCFVDGCDGSILLDNTDTIESEKEAAPNNNSARGFDVVDNM KAAVENACPGIVSCADILAAEESVRLAGGPSWTVPLGRRDSL IANRSGANSSIPAPSE SLAVLKSKFAAVGLNTSSDLVALSGAHTFGRAQCLNFISRLYNFSGSGNPDP TLNTTYLA ALQQLCPQGGNRSVLTNLDRTTPDTFDGNYF'SNLQTNEGLLQSDQELFSTTGADTIAIVN NFSSNQTAFFESFVSMIRMGNISPLTGT DGEIRLNCRI VNNSTGSNALLVSSI	6.21%
	Q96522	Peroxidase 45 precursor	<i>A. thaliana</i>	MEKNTSQTIFSNFFLLLLLSSCVSAQLRTGFYQNSCPNVETIVRNAVRQKFQQTFFVTAPA TLRLFFHDCFVRGCDASIMIASP ERDHPDDMSLAGDGFDTVVKAKQAVDSNPNCRNKVS CADILALATREVVVLTGGPSYPVELGRRDGRISTKASVQSQLPQPEFNLNQLNGMFSRHG LSQTDMIALSGAHTIGFAHCGKMSKRIYNFSP TTRIDPSINRGYVVQLQMCPIGVDVRI AINMDPTSPRTFDNAYFKNLQQGKGLFTSDQILFTDQSRSTVNSFANSEGAFRQAFITA ITKLG RVGVLTGNAGEIRDCSRVN	8.00%

^a Numbers correspond to the spot numbers given in Figures 2 and 3 and in Table 1

^b Accession numbers correspond to the reference sequence at NCBI homepage

^c Identities are based on sequence comparisons using the NCBI green plants protein database

^d Amino acid sequences were identified by nanoLC MS/MS. Underlined residues are conserved within the proteins used for identification

^e Coverage of the peptides identified by mass spectrometry

^f reference sequence from accession no. Q96522

Tab S2. Data of evaluated protein spots from the strongly ionically-bound cell wall proteome of the sensitive cowpea cultivar TVu 91 after 1 day of elevated Mn supply.

No. ^a	Mean spot volume on individual gels ^b		Ratio ^c	<i>p</i> -value ^d	<i>pI</i> ^e	MW (kDa) ^e
	0.2 μ M Mn	50 μ M Mn				
1	0.746	1.337	1.792	<0.01	4.2	26
2	0.134	0.179	1.335	<0.01	4.45	45
3	0.312	0.460	1.476	<0.01	4.8	50
4	0.378	0.452	1.196	<0.01	5.4	26.5
5	0.290	0.427	1.473	<0.01	6.0	40
6	0.293	0.211	0.719	<0.01	6.4	52
7	0.298	0.517	1.732	<0.01	8.8	39.5

^a Numbers correspond to the spot numbers given in gels.

^b Values indicate mean % volume of the spots in relation to the total volume of all proteins calculated from three gel replicates.

^c Mean volumes of the proteins on the three independent gels in relation to the total volume of all proteins on the corresponding gels.

^d *p*-values were calculated using an algorithm incorporated into ImageMaster™ 2D Platinum Software 6.0.

^e *pI* (isoelectric point) and MW (molecular weight) values were estimated according to the spot position in the gels and “pH as function of distance” graphs (GE Healthcare)

Tab. S3: Peptide sequences and resulting identities of Mn induced strongly ionically-bound cell wall proteins.

Spot No. ^a	Acc.No. ^b	Identity ^c	Organism	Peptide sequence ^d	Coverage ^e
1	P00287	Plastocyanin	<i>Phaseolus vulgaris</i>	LEVLLGSGDGLVFPSEFSVPSGEKIVFKNNAGFPHNVFDEDEIPAGVDAVKISMPEE ELLNAPGETYVVTLDTKGTYSFYCSPHQAGMVGKVTVN	50.1%
2	CAA41023	28kDa ribonucleoprotein, chloroplast	<i>Spinacia oleracea</i>	CVAQTSEWEQEGSTNAVLEGESDPEGAVSWGSETQVSDEGGVEGGQGFSEPPEAKLFVG NLPYDVDSKLAGIFDAAGVVEIAEVIYNRETDRSRGFGFVTMSTVEEAEKAVELLNGYD MDGRQLTVNKAAPRGSPERAPRGDFEPSCRIVVGNLPPWDVTSRLEQLFSEHGKVVSVARV VSDRETGRSRGFGFVTMSESEVNDIAAALDGGTLDGRAVRVNVAAERPRRAF	23%
3	NP_198495	phosphoglycolate phosphatase, putative	<i>Arabidopsis thaliana</i>	MLSRVASAVTPVSSSSLLPNSKPIFCLKTLSGYRSSSFCGGCIRKINHKLPRMTSSNIT PRAMATQQLLENADQLIDSVETTFIFDCDGVWKGDKLIEGVPETLDMRLAKGKRLVFTNN STKSRKQYKGFETLGLNVNEEEIFASSFAAAAYLQSIINFPKDKVYVIGEEGILKELEL AGFQYLGPPDDGKRQIELKPGFLMEHDHVDGAVVVGFDYFNYKYIQYGLTCIRENPGCL FIATNRDAVTHLTDQAQEWAGGSMVGLVVGSTQREPLVVGKPSFMMDYLADKFGIQKSQ ICMVGDRLDTDILFGQNGGCKTLVLSGVTISISMLESPENKIQPDFYTSKISDFLSPKAA TV	49.1%
	BAA98057	4-nitrophenylphosphatase-like	<i>Arabidopsis thaliana</i>	MLSRVASAVTPVSSSSLLPNSKPIFCLKTLSGYRSSSFCGGCIRKINHKLPRMTSSNIT PRAMATQQLLENADQLIDSVETTFIFDCDGVWKGDKLIEGVPETLDMRLAKGKRLVFTNN STKSRKQYKGFETLGLNVNEEEIFASSFAAAAYLQSIINFPKDKVYVIGEEGILKELEL AGFQYLGPPDDGKRQIELKPGFLMEHDHVDGAVVVGFDYFNYKYIQYGLTCIRENPGCL FIATNRDAVTHLTDQAQEWAGGSMVGLVVGSTQREPLVVGKPSFMMDYLADKFGIQKSQ ICMVGDRLDTDILFGQNGGCKTLVLSGITNLQHFIFHFVVDLQSLCWLKALRTRYN QISTPARSPIFCLRKPQLYNLVSASITL	49.1%
	Q75GB0	Putative glyoxalase	<i>Oryza sativa</i>	MLHVYRVGDLDKTIKFYTECLGMKLLRKRDIPEERYTNAFLGYGPEDSHFVVELTYNYG VESYDIGTAFGHGFIAVEDVAKTVDLIKAKGGTVTREPDPVGGKSVIAFIEDPDGYKFE LIERGPTPEPLCQVMLRVGDLDAINFYKAFGMELLRKRDNQYKYTIAMMGYGPEDKN AVLELTNYNYGKEYDKGNAYAQIAISTDDVYKTAEVIRQNGGQITREPGLPGINTKITA CTDPDGWKTVFVDNVDFLKELEE	22.1%
4	Q95AH9	Putative thioredoxin m2	<i>Pisum sativum</i>	MATVQLESFSLIPSSQHPRTVASSLSRPIAARFPPTGLKLRPLAATSLRSRFAASRVV PRGGRVLCARDTAVEVASITDGNWQSLVIESDTPVLFVFWAPWCGPCRMMHPIDELAK EYVGKFKCYKLNTEDESPSTATRYGIRSIPTVIFFKDGEKKDAIGSVPKASLITITIEKFL	28,3%
5	AAP44537	cyclophilin-like protein	<i>Triticum aestivum</i>	MAATSSFATLAIARPAAGSAAQRALLASKAPSSALSRLRGRVSPALSASRQSRARFV ASASAEPYAPELQSKVTNKVYFDISIGNPVGKNVGRIVI GLYGDDVPQTVENFRALCTGE KGFYKGSFHRVIKDFMIQGGDFDKNGTGKSIYGRFTKDFENQVLVHTGPGVLSMANA GPNTNGSQFFICTVKTPLWDGRHVVFQVLEGMIVRMI ESSETDRGDRPKKVVISESG ELPVV	50,8%
6	AAO27260	putative malate dehydrogenase	<i>Pisum sativum</i>	MEAQAGANQRIARI SAHLHPSNFQEGGDVAINKANCRACKGAPGFKVAIILGAAGGIGQPL SLLKMNPLVSVLHLYDVVNTPGVTADVSHMDTGAVRFGFLGQPQLENALTGMDLVVI PA GVPRKPGMTRDDLKINAGIVRTLCEGVAKSCPNAIVNLISNPVNSTVPIAAEVFKKAGT YDPKRLLGVTTLDVVRANTFVAEVLGVDPREVDVPPVVGHGAGVTILPILLSQVKPSSFS EAEYLTNR IQNGGTEVVEAKAGAGSATLSMAYAAAKFANSCLHGLKGEAGVVECAFVDS QVTDLPFFATKVRVLRGGAEIYQLGPLNEYERAGLEKAKTELAGSIQGVVEFKK	32,59%
7	O48903	Malate dehydrogenase precursor	<i>Medicago sativa</i>	MEPNYSANSRITRIASHLNPPLKMNHEGGSSLTNVHCRAKGGTDPGFKVAIILGAAGGIGQ PLSMLKMNLLVSVLHLYDVVNTPGVTSDISHMDTSAVVRGFLGQNLQLEDALTMGLVVI PAGVPRKPGMTRDDLFINAGIVKTLCEAIAKRCPKAIVNLISNPVNSTVPIAAEVFKRA	18,2%

				GTYDPKRLLGVTMLDVVRANTFVAE <u>VMGLDPRD</u> VDPVVGGHAGITILPLLSQVKPPSSF TPKEI <u>EY</u> LDRIQNGGTEVVEAKAGAGSATLSMAYAAVKFADACLRAKGEADIIQCAVY DSQVTELPFF <u>ASKV</u> RLGRNGVEEFLPLGPLSDYERASLEKAKKELATSVEKGVSFIRK	
--	--	--	--	--	--

- ^a Numbers in the table represent numbers of the spots on gels (Fig.6)
- ^b The accession nos. correspond with proteins that showed sequence homology with cowpea proteins (protein database at NCBI).
- ^c Blastp Hit in the NCBI database
- ^d The amino acid sequences were determined by means of nanoLC MS/MS. Underlined amino acids are identical between cowpea and the database hit.
- ^e Coverage of the peptide from cowpea with the database hit.

Danke

Mein herzlicher Dank gilt Herrn **Prof. Dr. Walter J. Horst** nicht nur für die Bereitstellung des Themas, und für das in mich gesetzte Vertrauen. Danken möchte ich auch für die Ermöglichung von Aufenthalten in anderen Arbeitsgruppen und der Teilnahme an Tagungen, auch als Vortragender. Danke auch für die sehr große Unterstützung gerade gegen Ende der Dissertation.

Weiterhin möchte ich Herrn **Prof. Dr. Hans-Peter Braun** danken. Ich bedanke mich dafür, dass ich auch immer zur Arbeitsgruppe gehören durfte, die mich sehr herzlich aufgenommen hat. Außerdem habe ich ebenfalls in zahllosen Gesprächen eine Menge über Proteomics und auch physiologische und genetische Fragestellungen gelernt. Vielen Dank für die in mich investierte Zeit. Danke auch an die gesamte Arbeitsgruppe.

Dr. Joachim Kopka danke ich für die Übernahme des Gutachtens zu der Arbeit und für die freundliche Aufnahme in die Arbeitsgruppe in Golm. Dafür und für die viele Hilfe in Sachen Metabolomics möchte ich auch **Alexander Erban** und **Ines Fernes** danken.

Prof. Dr. Christoph Peterhänsel danke ich für die Übernahme des Prüfungsvorsitzes.

Prof. Dr. Alain Van Dorselaer, **Dr. Dimitri Heintz** und **Sébastien Gallien** möchte ich für die Sequenzierung und Identifizierung der vielen Proteinspots und den Erläuterungen dazu danken.

Außerdem möchte ich **André Specht** danken, für das Einbringen seiner Expertise in diese Arbeit, und weil er mir ein guter Freund geworden ist. Danke!

Ich danke auch **Tanja Frenzel**. Wir sind ebenfalls gute Freunde geworden, natürlich auch bei so einigen gemeinsam durchgeführten Ernten nicht nur von Cowpea sondern auch in Göttingen. Danke und Alles Gute!

Ich danke auch **Dr. Marion Fecht-Christoffers**. Ohne sie gäbe es diese Arbeit nicht, jedenfalls nicht aus meiner Feder. Danke, dass du mein Interesse geweckt und mich bei meiner Entscheidungsfindung unterstützt hast.

Natürlich danke ich auch **Ingrid Dusy**, für die viele Hilfe bei organisatorischen Fragen sowie die permanente Versorgung mit Zucker und Post.

Ich danke natürlich auch den Studenten, die mich begleitet haben: **Stefanie Götze**, für ihren unermüdlichen Einsatz zur Charakterisierung von Peroxidasen, **Christof Behrens** für seine riesige Einsatzbereitschaft und schöne Arbeit an Reis, **Moritz Hartwig** für seine transkriptomischen Arbeiten, **Katharina Bollig** ebenfalls für ihr großes Engagement, sich trotz Uni-Wechsels in die Pflanzenernährung und v.a. die Mn-Fragen einzuarbeiten, **Martin Duschyk** für seinen enormen Einsatz zur Charakterisierung der Buschbohne und **Mareike Vorholt** für ihre proteomischen Arbeiten. **Thore Fettköther** und **Markus Meier** danke ich für ihr Interesse am Thema Mn.

Außerdem habe ich auf ganz besondere Weise Herrn **Benjamin Klug**, meinem Büronachbarn aber natürlich v.a. Freund, zu danken. Ohne ihn wären einige Dinge bestimmt nicht mit so viel Spaß passiert. Außerdem hatte er immer ein offenes Ohr für private Dinge, und es gab Zeiten, in denen mir das sehr wichtig war. Danke dir!

Es gibt sehr viele liebe Menschen, denen ich danken muss. Leider würde dies aber den Rahmen sprengen, daher: Danke allen am Institut für Pflanzenernährung für das gute Miteinander und die Unterstützung, und allen Menschen, die mich in dieser nicht immer einfachen Zeit begleitet haben.

Bleibt meine Familie! Meinem Vater **Heinz** danke ich sehr. Er hat immer an mich geglaubt und wusste, dass ich es schaffe. Natürlich danke ich auch meinem Bruder **Michael** und meiner Schwägerin **Rabea** sowie auch **Finn Erik** und **Charlotte**. Es ist immer schön bei euch und mit euch! Danke Familie!

Der **Deutschen Forschungsgemeinschaft (DFG)** für die finanzielle Unterstützung.

Und dir **Anika**, dir danke ich ganz besonders. Von ganzem Herzen. Danke!

Lebenslauf

Persönliche Daten

Geburtsdatum: 10. März 1978
Geburtsort: Papenburg, Niedersachsen
Eltern: Heinz Führs und Erika Führs, geb. Mühring
Familienstand: ledig
Staatsangehörigkeit: deutsch

Ausbildung

1984 – 1988 Grundsule Völlenerfehn, Gemeinde Westoverledingen

1988 – 1990 Orientierungsstufe Michaelschule Papenburg

1990 – 1994 Realschule Michaelschule Papenburg
Abschluss: Erweiterter Sekundarabschluss II

1994 – 1997 Gymnasium Papenburg
Abschluss: Abitur

1997 – 1998 Zivildienst: Jugendheim Johannesburg GmbH, Papenburg

1998 – 2004 Studium der Gartenbauwissenschaften an der Universität Hannover
Abschluss: Dipl.-Ing. agr.

Seit September 2004 Wissenschaftlicher Mitarbeiter bei Prof. Walter J. Horst am Institut für Pflanzenernährung der Naturwissenschaftlichen Fakultät der Leibniz Universität Hannover